UNIVERSITY OF NOVI SAD
FACULTY OF TECHNOLOGY
NOVI SAD

ACTA PERIODICA TECHNOLOGICA

APTEFF, 52, 1-273 (2021)

ACTA PERIODICA TECHNOLOGICA (formerly Zbornik radova Tehnološkog fakulteta and Proceedings of Faculty of Technology) publishes articles from all branches of technology (food, chemical, biochemical, pharmaceutical), process engineering and related scientific fields.

Articles in Acta Periodica Technologica are abstracted by: Chemical Abstracts Service – Columbus, Ohio; Referativnyi zhurnal – Khimija, VINITI, Moscow; listed in Ulrich's International Periodical Directory, and indexed in the Elsevier Bibliographic databases – SCOPUS.

ISSN 1450-7188 (Print) CODEN: APTEFF
ISSN 2406-095X (Online) UDC 54:66:664:615

Publisher
University of Novi Sad, Faculty of Technology Novi Sad
Bulevar cara Lazara 1, 21000 Novi Sad, Serbia

For Publisher
Prof. Dr. Biljana Pajin, Dean

Editor-in-Chief
Prof. Dr. Sanja Podunavac-Kuzmanović

Editorial Board

From Abroad
Prof. Dr. Živko Nikolov
Texas A and M University, Biological and Agricultural Engineering Department, College Station, TX, USA
Prof. Dr. Erika Békássy-Molnár
University of Horticulture and Food Industry, Budapest, Hungary
Prof. Dr. Željko Knez
University of Maribor,
Faculty of Chemistry and Chemical Technology, Maribor, Slovenia
Dr. T.S.R. Prasada Rao
Indian Institute of Petroleum, Dehra Dun, India
Prof. Dr. Đerđ Karlović
Margarine Center of Expertise, Kruszwica, Poland
Dr. Szigmond András
Research Institute of Hungarian Sugar Industry, Budapest, Hungary
Dr. Andreas Reitzmann
Institute of Chemical Process Engineering, University Karlsruhe, Germany

From Serbia
Prof. Dr. Vlada Veljković
Prof. Dr. Gordana Ćetković
Prof. Dr. Ljubica Dokić
Prof. Dr. Jelena Dodić
Prof. Dr. Jonjaua Ranogajec
Prof. Dr. Lidija Petrović
Prof. Dr. Branka Pilić

CONTENT

APTEFF, 52, 1-273 (2021) UDC: 615.014.6:635.71+665.52]:547.63
DOI: https://doi.org/10.2298/APT2152001V BIBLID: 1450-7188 (2021) 52, 1-12
BY-NC-ND
Original scientific paper

ANTIOXIDANT AND ANTIMICROBIAL CAPACITY OF ENCAPSULATED THYME ESSENTIAL OIL IN ALGINATE AND SOY PROTEIN-BASED CARRIERS

Mina M. VOLIĆ[1,], Verica B. DJORDJEVIĆ[2], Maja S. VUKAŠINOVIĆ-SEKULIĆ[2], Nataša S. OBRADOVIĆ[1], Zorica D. KNEŽEVIĆ-JUGOVIĆ[2], Branko M. BUGARSKI[2]*

[1] University of Belgrade, Innovation Center of Faculty of Technology and Metallurgy, Karnegijeva 4, 11000 Belgrade, Serbia
[2] University of Belgrade, Faculty of Technology and Metallurgy, Karnegijeva 4, 11000 Belgrade, Serbia

Received: 21 October 2020 **Revised: 13 January 2021** **Accepted: 29 January 2021**

The aim of this study was to develop a stable hydrogel carrier system for thyme essential oil (TEO) that could protect its sensitive polyphenol compounds. The impact of wall material (soy protein and alginate) on encapsulation efficiency and thymol release in simulated gastrointestinal conditions, was investigated. The release of thymol was ~ 80 % and 20 % in simulated gastric and pancreatic solutions, respectively. Thyme essential oil plays an important role as an antimicrobial and antioxidant agent. Results indicated that encapsulated TEO inside the hydrogel matrix exhibited antioxidant activity demonstrated by CUPRAC and ABTS analysis, even after thermal treatment of the beads, indicating the metal chelate effect as dominant. In vitro antimicrobial activity of encapsulated TEO has been studied against several pathogenic microorganisms such as Escherichia coli, Staphylococcus aureus, Bacillus cereus and Candida albicans. Beads coded as Ca-A1.5/SP1.5 showed anti-Candida albicans activity, while modified bead formulations Ca-A1.5/SP1.5 and Ca-A1.5/SP0.25** showed bactericidal activity against Escherichia coli and Staphylococcus aureus.*

Keywords: encapsulation, hydrogel carriers, thymol release, antioxidant activity, antimicrobial activity.

INTRODUCTION

Essential oils (EOs) are odoriferous, highly volatile substances mainly identified with terpenoids, aromatic and aliphatic compounds, having a strong interest in food, pharmaceutical, and agricultural industries. EOs have been proposed as an alternative to antibiotic growth promoters, regarding their antioxidant, anti-inflammatory, and antimicrobial properties. Numerous studies have shown that EOs possess great antimicrobial activities against bacteria and fungi (1). In specific, EOs are particularly effective against *Candida albicans* (2). Gram-negative bacteria are less susceptible than Gram-positive bacteria (3), as they contain a lipopolysaccharide component (LPS) in the outer membrane of their cell wall, which protects them from hydrophobic compounds with antimicrobial properties, present in essential oils (4, 5). Therefore, it could be challenging to deliver oil concentration to the targeted place in the human body which will be effective in controlling different bacteria species.

Both, antioxidant and antimicrobial effects of many EOs, such as thyme (*Thymus vulgaris*) essential oil, are associated with the presence of the major polyphenol compounds: thymol and carvacrol (6). Nevertheless, EO components tend to be thermolabile and volatile, and may easily oxidize which leads to a decrease in their biological potential (7).

* Corresponding author: Mina Volić, Innovation Center of Faculty of Technology and Metallurgy, University of Belgrade, Karnegijeva 4, 11000 Belgrade, Serbia, e-mail: mvolic@tmf.bg.ac.rs

APTEFF, 52, 1-273 (2021)
DOI: https://doi.org/10.2298/APT2152001V
BY-NC-ND
UDC: 615.014.6:635.71+665.52]:547.63
BIBLID: 1450-7188 (2021) 52, 1-12
Original scientific paper

Recent strategies in the pharmaceutical and food industry have been focused on the design of bio-based carriers for entrapment and protection of essential oils (8, 9). Moreover, these essential oil-loaded polymer particles can be designed to carry bioactive substances to specific locations within the gastrointestinal tract (GIT) and release them at a controlled rate. During the last years, protein-based systems for encapsulation of bioactive agents have been studied due to their specific functional and nutritional properties (10, 11). Protein-based hydrogels have potential as controlled delivery systems due to their ability to produce a response to an environmental stimulus (e.g. changes in their physicochemical properties with a change in pH or temperature conditions) (12). For instance, protein unfolding and exposure of hydrophobic groups that lie on their surface make them potential surface-active molecules. Protein surface activity is related to the formation of a layer (i.e. adsorption) on a surface of oil droplets, thus providing oil stability and protection from droplets aggregation. Furthermore, proteins are known as oxidation inhibitors through free radical scavenging and chelation (13). However, high acidity in the stomach, as well enzymes presented in GIT which can initiate protein digestion; this poses a need for a combining with additional biopolymer to achieve protein hydrolysis at a slower rate and consequently slower oil release.

Blending natural biopolymers, protein and sodium alginate was found to be promising due to alginate's relatively slow degradation profile, which is related to shrinking in an acidic environment, thus providing protection from fast protein hydrolysis in simulated conditions of the stomach. According to the literature, this kind of blend has already been used for the preparation of microcapsules (14, 15). More precisely, the alginate/soy protein system for essential oil encapsulation has been partially characterized in our previous work (16).

This study represents the extension of our previous work (16) with the aim to investigate the potential of the encapsulation of thyme essential oil (TEO) in Ca-alginate/soy protein beads to achieve targeted release and protect its bioactive properties for application in food and pharmacy. Encapsulation efficiency (EE) and release profile of thymol, the main constituent of TEO, were calculated for different beads formulations by HPLC analysis. The ABTS and CUPRAC methods were used to confirm the antioxidant activity of prepared beads, as well test in suspension was carried out to confirm the antimicrobial activity of encapsulated oil against *Escherichia coli*, *Staphylococcus aureus*, *Bacillus cereus* and *Candida albicans*.

EXPERIMENTAL

MATERIALS

Sodium Alginate (sodium;3,4,5,6-tetrahydroxyoxane-2-carboxylate) was purchased from PanReac AppliChem, Germany. Commercial soy protein isolate powder (SPI) was purchased from Brenntag, Ireland. Thyme oil was supplied from local pharmaceutical shop Prima Cosmetics doo. Thymol (5-methyl-2-propan-2-ylphenol), analytical standard, was supplied from Dr. Ehrenstorfer GmbH. Pancreatin 4X USP grade (from porcine pancreas) was purchased from MP Biomedicals, LLC, France. Bile salts were obtained from Biolife, Italia. Pepsin (from porcine gastric mucosa), Neocuproine (2,9-Dimethyl-1,10-phenanthroline), Trolox (6-Hydroxy-2,5,7,8-tetramethylchromane-2-carboxylic acid) and ABTS (2,2'-

BY-NC-ND

azino-bis (3-ethylbenzthiazoline-6-sulfonic acid)diammonium salt), were obtained from Sigma-Aldrich, Germany. Calcium chloride dihydrate was purchased from Analytika, Ltd., Chech Republic. Methanol and acetonitrile (HPLC grade) were purchased from J.T. Baker, Netherlands. All reagents were used in accordance with the manufacturer's recommendations.

EMULSION AND BEADS PREPARATION

The Na-alginate/soy protein/thyme oil emulsions were prepared as follows. Na-alginate was dissolved and SPI was dispersed, both in water, after which protein solubility was enhanced by adjusting the SPI dispersion to pH 8.0. Finally, the protein denaturation step was carried out by heating the obtained SPI solution for 40 min at 80 °C. Both solutions (at room temperature) were mixed together, and thyme oil was added to the final Na-alginate/soy protein solution (polymer : thyme oil=5:1). The emulsion was homogenized with an UltraTurrax (IKA T25 digital, Germany) at 12,000 rpm for 3 min.

After preparation, the emulsion was extruded using a syringe pump (Razel, Scientific Instruments, Stamford, USA), for maintaining a constant flow rate, with an applied voltage of 5 kV (high voltage unit - Model 30R, Bertan Associates, Inc., New York). Thus formed droplets were trickled into a gelling bath solution containing $CaCl_2 \cdot 2H_2O$ (10 g/L), with gently stirring for the next 15 min to harden.

According to the Ca-alginate and SPI contents, obtained beads were coded as Ca-A1/SP1 (1 wt.% of Na-alginate and 1 wt.% of SPI), Ca-A1/SP1.5 (1 wt.% of Na-alginate and 1.5 wt.% of SPI), Ca-A1.5/SP1 (1.5 wt.% of Na-alginate and 1 wt.% of SPI), Ca-A1.5/SP1.5 (1.5 wt.% of Na-alginate and 1.5 wt.% of SPI), Ca-A2/SP1 (2 wt.% of Na-alginate and 1 wt.% of SPI) and Ca-A2/SP1.5 (2 wt.% of Na-alginate and 1.5 wt.% of SPI). Beads optimized for antimicrobial analysis were coded as Ca-A1.5/SP1.5* (1.5 wt.% of Na-alginate, 1.5 wt.% of SPI and 250 μL of TEO/4g of beads) and Ca-A1.5/SP0.25** (2 wt.% of Na-alginate, 0.25 wt.% of SPI and 250 μL of TEO/4g of beads).

CHARACTERIZATION OF THE BEADS

Size measurements of beads, wet and dry analogs, were evaluated under a digital light microscope (Motic BA210 Series), employing the image analyzer software (Motic Images Plus 2.0 ML). The shape of the beads was quantified by using the dimensionless shape indicator - Sphericity factor (SF), where the value zero of SF indicates a perfect sphere (17).

HPLC ANALYSIS

HPLC experiment was performed using a Nexera X2 with RID 20A detector (Shimadzu), with an ACE C18 (4.6 × 250 mm, 5 μm) column. UV-visible spectral properties were collected in the 200-900 nm range, extracting 274 nm for chromatograms. The mobile phase was an isocratic combination of acetonitrile (ACN):H_2O (50:50) with a flow rate of 1 ml/min. Stock solution of thymol (2 mg/ml) was prepared in ACN:H_2O (80:20) solvent, and different concentrations were made from stock solutions to plot the calibration curve of thymol.

APTEFF, 52, 1-273 (2021)
DOI: https://doi.org/10.2298/APT2152001V
BY-NC-ND
UDC: 615.014.6:635.71+665.52]:547.63
BIBLID: 1450-7188 (2021) 52, 1-12
Original scientific paper

ENCAPSULATION EFFICIENCY (EE)

The encapsulation efficiency of hydrogel beads was estimated after beads hardening in the $CaCl_2$ solution. Aliquots were taken from the gelling bath, and concentration thymol was obtained by the HPLC method. Encapsulation efficiency was then expressed as Eq. [1]:

$$\text{Encapsulation efficiency (\%)} = \frac{\text{actual amount of oil loaded in beads}}{\text{theoretical amount of oil loaded in beads}} \times 100 \qquad [1]$$

RELEASE OF THYMOL IN SIMULATED GASTROINTESTINAL CONDITIONS

The release of thymol from wet Ca-alginate/SPI beads was observed at 37 °C in solutions that simulated gastro-intestinal conditions. Solutions were freshly prepared before the analysis, according to the procedure described in our previous work (16). Firstly, the hydrogel beads (3 g) were kept in a flask containing gastric solution, under mild magnetic stirring, and aliquots of a sample were taken. After 1 h, the beads were filtered and transferred in the flask containing pancreatic solution, and sampling was continued until complete degradation of the beads. The release of thymol was analyzed using HPLC and results were expressed as the percentage of released thymol in SGF and SIF.

DETERMINATION OF FREE RADICAL - SCAVENGING ABILITY

The Trolox equivalent antioxidant capacity (TEAC) was estimated by the ABTS radical cation decolourisation assay. Free 2,2'-azino-bis(3-ethylbenzthiazoline-6-sulfonic acid) radical cation ($ABTS^{\bullet+}$), generated by chemical or enzymatic oxidation of ABTS, was produced according to the method published by Re *et al* (18). In order to test the TEAC of the beads, 1 g of freshly prepared beads were dissolved in 50 mL of 1% (w/v) Na-citrate solution and methanol (90:10). After complete degradation of the beads, a 30 µL aliquot of sample was added to 2.0 mL of the diluted $ABTS^{\bullet+}$ solution, and the absorbance readings were taken after exactly 6 min at 734 nm. The reagent blank was prepared by adding 30 µL of methanol to 2.0 mL of the diluted $ABTS^{\bullet+}$ solution. The results, obtained from triplicate analyses, were expressed as Trolox equivalents (µmol Trolox g_{beads}^{-1}) and derived from a calibration curve (62.5-1000 µmol L^{-1}) determined for this standard.

CUPRIC REDUCING ANTIOXIDANT POWER

The cupric reducing/antioxidant power (CUPRAC) assay was carried out according to a standard procedure by Apak *et al* (19). In brief, solutions of $CuCl_2$ (50 µL, 10 mM), neocuproine (50 µL, 7.5 mM) and CH_3COONH_4 buffer (60 µL, 1 M, pH 7.0) were prepared before the analysis. Around 3 g of hydrogel beads were degraded in Na-citrate solution and centrifuged at 700 rpm for 5 min. After complete degradation of the beads, a 400 µL aliquot of sample was mixed with reactive solutions and incubated for 1 h in a water bath at 30 °C. Absorbances were measured at 450 nm. A standard curve was prepared using different concentrations (31.25-250 µmol L^{-1}) of Trolox and results are expressed as µmol Trolox g_{beads}^{-1}.

APTEFF, 52, 1-273 (2021) UDC: 615.014.6:635.71+665.52]:547.63
DOI: https://doi.org/10.2298/APT2152001V BIBLID: 1450-7188 (2021) 52, 1-12
BY-NC-ND
Original scientific paper

EFFECT OF THERMAL TREATMENT ON THE ANTIOXIDANT ACTIVITY

In order to evaluate the change in antioxidant activity of the beads (Ca-A1.5/SP1.5) after thermal treatment, beads were undergone three different temperatures (50 °C, 75 °C and 100 °C) during 4 h. After heating at predetermined temperatures, 1 g of the beads were completely degraded in Na-citrate solution. The antioxidant activity of the supernatant was determined using the previously described methods (CUPRAC and ABTS assays). Absorbance was measured and compared with an absorbance of the non-heated beads.

DETERMINATION OF ANTIMICROBIAL ACTIVITY

Antimicrobial activity of wet encapsulated thyme oil beads was estimated against two Gram-positive strains *Staphylococcus aureus* ATCC 25923 *and Bacillus cereus* ATCC 11778, one Gram-negative strain *Escherichia coli* ATCC 25922 and yeast strain *Candida albicans* ATCC 10259, all obtained from American Type Culture Collection. Sterile freshly prepared wet alginate/oil/protein beads were aseptically added in each flask, in the amount of 4 g and mixed with 10 ml of sterile physiological saline solution (0.85% w/v NaCl) supplemented with Tween 80 (polysorbate 80) at a final concentration of 0.5% (v/v) to enhance thyme oil solubility. Content of flasks is gently mixed and inoculated with one of the tested microorganisms (overnight cultures, not older than 18h), and the initial number of cells in suspension was in the range 10^5–10^6 CFU/ml. Afterward, the flasks were incubated in a shaking water bath at 37 °C for 24 h At the same time, alginate/protein beads without thyme oil were used as the control. After 24h of incubation, 100 µl of the liquid sample was aseptically withdrawn from each flask and directly transferred to Petri dishes. From them, serial (10-fold) dilutions were made in a physiological saline solution prior to 100 µl of appropriate dilution was added in Petri dish. Content in the Petri dishes was homogenized with melted nutrient agar (1.5 wt. %, 55 °C) and incubated at 37 °C for 24 h. After incubation, all Petri dishes were visually analyzed and those with formed colonies were counted. The experiments were performed in duplicates and the number of viable cells is expressed as colony-forming units (CFU).

STATISTICAL ANALYSIS

All experiments were expressed as means with standard deviations (SD). The mean values were analysed using one-way ANOVA. All analyses were done using software Origin Pro 8.5 (OriginLab Corporation, Northampton, USA).

RESULTS AND DISCUSSION

SIZE AND SHAPE OF THE BEADS

In this work, the effect of alginate and protein concentration on the size and shape of the beads after oil encapsulation was determined and presented in Table 1. Sphericity factor (SF) was used in order to estimate the shape of the beads. Wet hydrogel beads can be considered as spherical (SF≤0.05) (17), with exception of Ca-A2/SP1 and Ca-A2/SP1.5, which showed deformation in form of the elongated drops, as well noticed by Levic *et al* (20).

APTEFF, 52, 1-273 (2021)
DOI: https://doi.org/10.2298/APT2152001V
BY-NC-ND
UDC: 615.014.6:635.71+665.52]:547.63
BIBLID: 1450-7188 (2021) 52, 1-12
Original scientific paper

Table 1. Dimensions (Maximum diameter and Minimum diameter), shape indicator (SF) and encapsulation efficiency of Ca-alginate/SPI complex beads with encapsulated thyme oil.

System code	Wet beads, µm		Dry beads, µm		$SF=(d_{max}-d_{min})/(d_{max}+d_{min})$		EE, %
	d_{min}	d_{max}	d_{min}	d_{max}	SF_w	SF_d	
Ca-A1/SP1	1561±12[a]	1688±34[a]	919±26[d]	1058±44[d]	0.040	0.070	70.04±0.1
Ca-A1/SP1.5	1601±17[b]	1769±42[b]	914±35[d]	958±15[b]	0.049	0.024	70.85±0.2
Ca-A1.5/SP1	1652±22[c]	1780±24[b]	729±36[a]	813±69[a]	0.037	0.054	72.90±0.4
Ca-A1.5/SP1.5	1679±45[c]	1838±31[c]	867±25[c]	960±29[b]	0.045	0.051	73.31±0.2
Ca-A2/SP1	1673±30[c]	1847±44[c]	837±28[b]	1002±28[c]	0.049	0.090	74.92±0.6
Ca-A2/SP1.5	1729±23[d]	1976±77[d]	868±37[c]	1144±64[e]	0.067	0.137	75.54±0.1

*Values with the same letter in each column showed no statistically significant difference.

The formulations were found to give an irregular shape of beads due to higher viscosity of blends with high polymer concentration. SPI concentration has shown no systematic influence on the shape of the beads. After drying, almost all beads showed irregular shape, probably due to intense shrinkage.

By using the electrostatic extrusion technique, the size of the hydrogel beads depends on many factors. Accordingly, beads were produced under the same conditions, thus the variation in their size dramatically depends on the concentration of polymers used for their production. The size of hydrogel beads ranged between ~1.56 mm and ~1.98 mm, while dried particles reduced in size compared to their hydrogel analogs (0.73 – 1.14 mm).

Both, alginate and protein content influenced the size of the beads. An increase in the bead size with an increase in polymer concentration has shown to be the most obvious by comparing the formulations Ca-A1/SP1 and Ca-A2/SP1.5. On the other side, a higher polymer concentration induced a higher amount of oil during bead preparation, making the matrix to be more pumped as more oil is inside.

ENCAPSULATION EFFICIENCY

The concentration of thymol encapsulated in the Ca-alginate/SPI beads was determined by HPLC analysis, and results were presented in Table 1. Depending on the content of alginate, SPI and consequently oil content, EE of thymol varied from 70.04 to 75.54 %. The concentration of both, alginate and SPI showed systematic dependence on encapsulation efficiency of the beads. Beads coded as Ca-A2/SP1.5 showed the highest EE, considering the alginate and protein concentration used for their production - in contrast to Ca-A1/SP1.

IN VITRO THYMOL RELEASE

As concerns the release kinetics of thymol from Ca-alginate/SPI delivery systems, Figure 1 shows the percentage of thymol released as a function of time. HPLC method was implemented in order to evaluate thymol concentration, and the impact of polymer concentration on thymol release was investigated (Ca-A1/SP1 vs. Ca-A2/SP1 and Ca-A2/SP1 vs. Ca-A2/SP1.5).

APTEFF, 52, 1-273 (2021)
DOI: https://doi.org/10.2298/APT2152001V
BY-NC-ND
UDC: 615.014.6:635.71+665.52]:547.63
BIBLID: 1450-7188 (2021) 52, 1-12
Original scientific paper

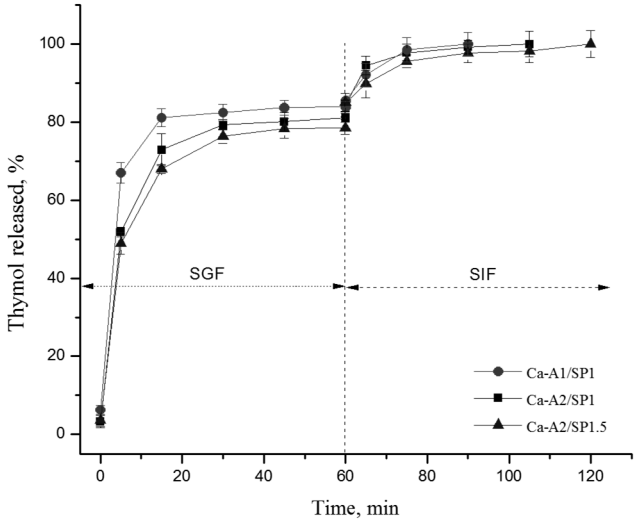

Figure 1. Release of thymol from Ca-alginate/protein beads in simulated SGF and SIF

ANOVA revealed a significant effect of polymer concentrations on thymol release (Figure 1) in simulated gastric conditions. The burst effect (in the first 10 min) was observed for all beads, which was characterized by the fast release of 'surface oil'. When the concentration of soy protein was 1.5 wt.%, in comparison to 1 wt.%, the release of thymol was lower. This could be due to changes in the density of the polymer matrix, resulted from the excess of protein in the continuous phase (non-adsorbed) (21). Moreover, a higher protein amount induces better emulsification (22), which leads to greater stability of emulsions and consequently of produced beads. However, the influence of alginate concentration was dominant. With an increase in alginate concentration (from 1 wt.% to 2 wt.%) polymer chains tend to be more densely packed, thus protecting the oil inside the matrix from fast leakage.

ANTIOXIDANT ACTIVITY

In this study, the antioxidant capacity of the beads with encapsulated thyme oil was determined using two analytical assays: (1) ABTS radical cation ($ABTS^{\bullet+}$) decolourisation assay and (2) Cupric (Cu^{2+}) reducing power activity.

According to the results of both tested assays (expressed per mass unit of beads), antioxidant activity was the lowest for the bead formulation with the lowest content of both alginate and protein (Ca-A1/SP1). In contrast, the highest Cu^{2+} reducing activity was achieved for the bead formulation with the highest network density (Ca-A2/SP1.5). According to cupric reducing power activity, an increase in protein content at the same concentration of alginate leads to higher antioxidant capacity; this is also true for ABTS radical cation scavenging activity, statistically significant for the formulations with 1 and 2 % alginate (Figure 2). It seems that antioxidant capacity correlates with the oil content (Table 1). However, it should have in mind that partially denatured proteins inside polymer matrix also express antioxidant activity (21).

APTEFF, 52, 1-273 (2021)
DOI: https://doi.org/10.2298/APT2152001V
BY-NC-ND
UDC: 615.014.6:635.71+665.52]:547.63
BIBLID: 1450-7188 (2021) 52, 1-12
Original scientific paper

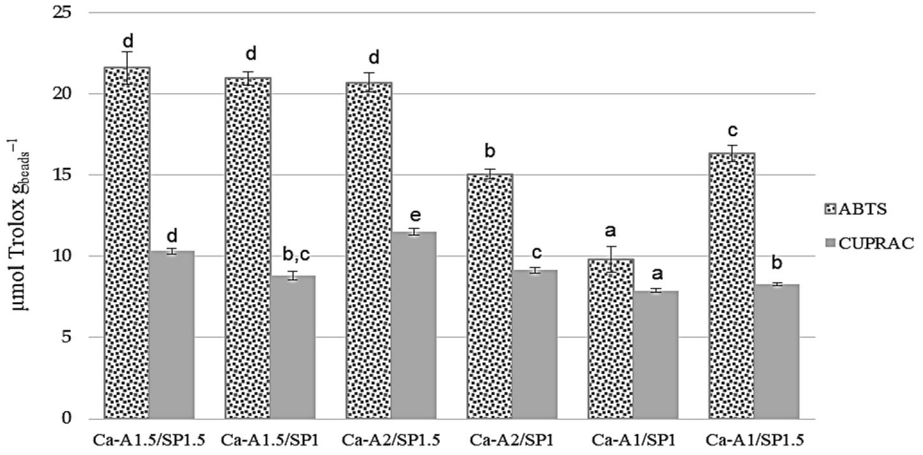

Figure 2. Comparison of the antioxidant activity of different beads formulations

The antioxidant activity of the beads has not been able to perform *in vivo,* probably due to enzyme interference in the applied method. Otherwise, enzymatic hydrolysis of proteins also increases the exposure of antioxidant amino acids, i.e. increases the antioxidant activity of the beads (23).

ANTIOXIDANT ACTIVITY OF THERMALLY TREATED BEADS

Initially, the air-dried beads were subjected to thermal treatment at 50 °C, 75 °C and 100 °C in order to evaluate the antioxidant capacity of beads after 4 h of heating. Both methods, CUPRAC and ABTS were applied in order to show the potential of a carrier (representative formulation Ca-A1.5/SP1.5) to preserve the antioxidant potential of encapsulated thyme essential oil.

Results are expressed as absorbance of compounds which has been interacted with free radicals, in comparison to the initial absorbance (non-treated beads), and presented in Figure 3.

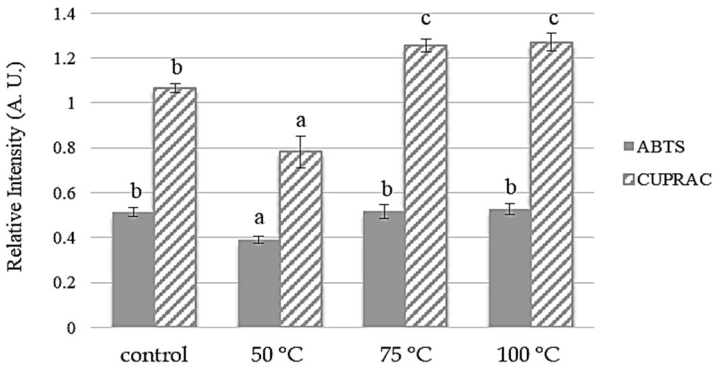

Figure 3. Antioxidant capacity of the heat-treated beads

APTEFF, 52, 1-273 (2021) UDC: 615.014.6:635.71+665.52]:547.63
DOI: https://doi.org/10.2298/APT2152001V BIBLID: 1450-7188 (2021) 52, 1-12
BY-NC-ND
Original scientific paper

After 4 h of treatment at 50 °C, the antioxidant capacity of the beads (according to both methods) was lower than the initial, which indicated a decrease in the biological potential of encapsulated thyme oil under the act of temperature. The decrease in antioxidant activities can be associated mainly to volatilization of polyphenols rather than degradation, since degradation process occurs at higher temperatures (24).

On the other hand, ABTS radical scavenging ability remained unchanged, while cupric reducing power activity even increased upon heating at 75 °C and 100 °C. At these temperatures, proteins undergo denaturation process and disruption of protein tertiary structure, which increases the accessibility of the amino acids with antioxidant potential. It is known, when proteins are used in order to stabilize o/w emulsions, one fraction of them absorb on the oil surface, while the rest remains in the continuous phase. According to Yang and Xiong (25), it is that interfacial proteins express antioxidant properties by inhibiting lipid oxidation, while Faraji *et al* (21) assigned this potential to soy proteins in a continuous phase of the emulsion. Soy protein isolate may act as an antioxidant by free radical scavenging and metal chelation activity, due to the presence of certain amino acids and other compounds, such as isoflavone (21).

The results obtained in our work, which are related to the antioxidant capacity of both, heated and non-heated beads, indicated that the metal chelate effect was dominant.

ANTIMICROBIAL ACTIVITY

Essential oils with a high percentage of phenolic compounds possess the strongest antimicrobial activity. Many authors have demonstrated thyme essential oil as a potential agent for the inhibition of various pathogens (26), thanks to the presence of thymol and carvacrol, the main compounds responsible for its antimicrobial effect (6). Thyme oil compounds manifest their antimicrobial activities through several possible mechanisms, and the hydrophobic character of EOs compounds, allows interaction with the lipids of the bacterial cells membrane, which enhances its permeability to potassium ions and protons, and consequently leads to inhibition of ATP synthesis and finally to cell death (27).

In order to demonstrate the potential utility of encapsulated thyme oil beads, antimicrobial activity of wet beads was studied in suspensions of *S. aureus, E. coli, B. cereus,* and *C. albicans* cells in physiological solution (0.85% w/v NaCl) with 0.5% (v/v) Tween 80 as a surfactant to allow better dissolution of thyme essential oil. The results of antimicrobial activity are presented for the representative formulation Ca-A1.5/SP1.5 which provides the actual concentration of thyme oil of 4.5 µl/ml (Table 2).

According to the results, the microbicidal effect was observed only on *C. albicans* (colonies were not detected in the medium after 24h), while on other species a reduction of total viable count happened to a greater (a fall in *E.coli* and *B. cereus* concentrations for two orders of magnitude) or lesser (*S. aureus*) degree. Therefore, another formulation (Ca-A1.5/SP1.5*) was made with the same matrix composition but a higher oil loading thus providing the actual concentration of thyme oil of 20 µl/ml. This one induced a more significant reduction in *S. aureus* (from 10^6 to 10^1 CFU/ml), and *E. coli* (10^4 to 10^1 CFU/ml) populations than Ca-A1.5/SP1.5. Here it should be emphasized that as opposed to thyme oil, released proteins promoted cell proliferation due to proteolytic activity of bacteria, as evidenced by a somewhat increase in cell number in control samples (blank beads without thyme oil). To optimize formulation which will have a microbicidal effect,

APTEFF, 52, 1-273 (2021) UDC: 615.014.6:635.71+665.52]:547.63
DOI: https://doi.org/10.2298/APT2152001V BIBLID: 1450-7188 (2021) 52, 1-12
BY-NC-ND
Original scientific paper

the content of protein was decreased (0.25 %) while keeping the same content of thyme oil and the new formulation (Ca-A1.5/SP0.25**) completely inactivated three of four tested pathogens. *B. cereus* strain appeared to be less sensitive than others although its initial inoculum size was the smallest.

Table 2. Antimicrobial activity of different bead formulations

	Initial number of cells (CFU/ml)			
	S. aureus	*E. coli*	*B. cereus*	*C. albicans*
Control	1.78×10^6	1.32×10^6	7.58×10^4	1.14×10^4
Ca-A1.5/SP1.5	1.78×10^6	1.32×10^6	7.58×10^4	1.14×10^4
Ca-A1.5/SP1.5*	3.30×10^5	1.90×10^6	7.60×10^3	n.d.
Ca-A1.5/SP0.25**	3.10×10^5	1.80×10^6	6.10×10^3	n.d.
	Number of cells after 24h incubation (CFU/ml)			
	S. aureus	*E. coli*	*B. cereus*	*C. albicans*
Control	8.20×10^6	8.60×10^6	3.60×10^7	1.00×10^4
Ca-A1.5/SP1.5	1.51×10^6	4.80×10^4	1.02×10^2	0
Ca-A1.5/SP1.5*	2.00×10^1	2.00×10^1	1.63×10^2	n.d.
Ca-A1.5/SP0.25**	0	0	9.40×10^2	n.d.

n.d.- not determined

CONCLUSION

The beads with higher polymer content exhibited higher encapsulation efficiency, which implies an increase in their antioxidative potential. A dose-related response required to significantly affect bacterial growth and survival was achieved using prepared biopolymer beads with encapsulated thyme essential oil. A combination of Na-alginate and soy protein isolate has enabled effective protection of thyme oil during heat treatment at 75 °C and 100 °C, as well as controlled release, up to 120 min, depending on the biopolymer concentration.

Acknowledgements

This work was supported by the Ministry of Education, Science and Technological Development of the Republic of Serbia (Contract No. 451-03-68/2020-14/200135).

REFERENCES

1. Swamy, M.K.; Akhtar, M. S.; Sinniah, U. R. Antimicrobial Properties of Plant Essential Oils against Human Pathogens and Their Mode of Action: An Updated Review. *Evid. Based Complementary Altern. Med.* **2016,** 2016, 1-21.
2. Tampieri, M.P.; Galuppi, R.; Macchioni, F.; Carelle, M.S.; Falcioni, L.; Cioni, P.L.; Morelli, I. The inhibition of Candida albicans by selected essential oils and their major components. *Mycopathologia,* **2005**, *159*, 339-345.

3. Trombetta, D.; Castelli, F.; Sarpietro, M.G.; Venuti, V.; Cristani, M.; Daniele, C.; Saija, A.; Mazzanti, G.; Bisignano, G. Mechanisms of antibacterial action of three monoterpenes. *Antimicrob. Agents Chemother*., **2005**, *49*, 2474-2478.
4. Nikaido, H. Prevention of drug access to bacterial targets: permeability barriers and active efflux. *Science,* **1994**, *264*, 382-388.
5. Nikaido, H. Molecular basis of bacterial outer membrane permeability revisited. *Microbiol. Mol. Biol. Rev*., **2003**, *67*, 593-656.
6. Guarda, A.; Rubilar, J.F.; Miltz, J.; Galotto, M.J. The antimicrobial activity of microencapsulated thymol and carvacrol. *Int. J. Food Microbiol.,* **2011**, *146*, 144-150.
7. Turek, C.; Stintzing, F.C. Stability of Essential Oils: A Review. *Compr. Rev. Food Sci. Food Saf.,* **2013**, *12*, 40-53.
8. De Oliveira, E.F.; Paula, H.C.B.; de Paula, R.C.M. Alginate/cashew gum nanoparticles for essential oil encapsulation. *Colloids Surf. B,* **2014**, *113*, 146-151.
9. El Asbahani, A.; Miladi, K.; Badri, W.; Sala, M.; Aït Addi, E.H.; Casabianca, H.; El Mousadik, A.; Hartmann, D.; Jilale, A.; Renaud, F.N.; Elaissari, A. Essential oils: from extraction to encapsulation. *Int. J. Pharm*., **2015**, *483*, 220-243.
10. Rajendran, S.; Udenigwe, C.C.; Yada, R.Y. Nanochemistry of protein-based delivery agents. *Front. Chem.,* **2016**, *4*, 31-39.
11. Abaee, A.; Mohammadian, M.; Jafari, S.M. Whey and soy protein-based hydrogels and nano-hydrogels as bioactivedelivery systems. *Trends Food Sci. Technol.,* **2017**, *70,* 69-81.
12. Martins, J.T.; Ramos, Ó. L.; Pinheiro, A.C.; Bourbon, A.I.; Silva, H.D.; Rivera, M.C.; Cerqueira, M.A.; Pastana, L.; Malcata, F.X.; González-Fernández, A.; Vicente, A.A. Edible bio-based nanostructures: delivery, absorption and potential toxicity. *Food Eng. Rev*., **2015**, *7*, 491-513.
13. Samaranayaka, A. G. P.; Li-Chan, E. C. Y. Food-derived peptidic antioxidants: A review of their production, assessment, and potential applications. *J. Funct. Foods,* **2011**, *3*, 229-254.
14. Déat-Lainé, E.; Hoffart, V.; Garrait, G.; Jarrige, J.F.; Cardot, J.M.; Subirade, M.; Beyssac, E. Efficacy of mucoadhesive hydrogel microparticles of whey protein and alginate for oral insulin delivery. *Pharm Res.,* **2013***, 30*, 721-734.
15. Tansaz, S.; Durmann, A.-K.; Detsch, R.; Boccaccini, A.R. Hydrogel films and microcapsules based on soy protein isolate combined with alginate. *J. App. Polym. Sci.,* **2016***, 134*, 44358-367.
16. Volić, M.; Pajić-Lijaković, I.; Djordjević, V.; Knežević-Jugović, Z.; Pećinar, I.; Stevanović-Dajić, Z.; Veljović, Đ.; Hadnađev, M.; Bugarski, B. Alginate/soy protein system for essential oil encapsulation with intestinal delivery. *Carbohydr. Polym.,* **2018***, 200*, 15-24.
17. Chan, E.-S.; Boon-Beng, L.; Ravindra, P.; Poncelet, D. Prediction models for shape and size of ca-alginate macrobeads produced through extrusion–dripping method. *J. Colloid Interface Sci.,* **2009***, 338,* 63-72.
18. Re, R.; Pellegrini, N.; Proteggente, A.; Pannala, A.; Yang, M.; Rice-Evans, C. Antioxidant activity applying an improved ABTS radical cation decolorization assay. *Free Radic. Biol. Med.,* **1999***, 26*, 1231-1237.
19. Apak, R.; Guclu, K.; Ozyurek, M.; Esin Celik, S. Mechanism of antioxidant capacity assays and the CUPRAC (cupric ion reducing antioxidant capacity) assay. *Microchim. Acta,* **2008***, 160*, 413-419.
20. Levic, S., Pajic-Lijakovic, I.; Djordjevic, V.; Rac, V.; Rakic, V.; Šolevic Knudsen, T.; Pavlović, V.; Bugarski, B.; Nedović, V. Characterization of sodium alginate/d-limonene emulsions and respective calcium alginate/d-limonene beads produced by electrostatic extrusion. *Food Hydro-coll.,* **2015***, 45*, 111-123.
21. Faraji, H.; McClements, D.J.; Decker, E.A. Role of continuous phase protein on the oxidative stability of fish oil-in-water emulsions. *J.Agric. Food Chem*., **2004**, *52,* 4558-4564.
22. Delahaije, R. J. B. M.; Gruppen, H.; Giuseppin, M.L.F.; Wierenga, P.A. Towards predicting the stability of protein-stabilized emulsions. *Adv. Colloid Interface Sci.,* **2015***, 219*, 1-9.

BY-NC-ND

23. Penta-Ramos, E.A.; Xiong, Y.L. Antioxidant Activity of Soy Protein Hydrolysates in a Liposomal System. J. Food Sci., 2002, 67, 2952-2956.
24. Majeed, H.; Bian, Y.-Y.; Ali, B.; Jamil, A.; Majeed, U.; Khan, Q.F.; Iqbal, K.J.; Shoemaker, C.F.; Fang, Z. Essential oil encapsulations: uses, procedures, and trends. *RSC Advances,* **2015***, 5*, 58449-58463.
25. Yang, J.; Xiong, Y.L. Inhibition of Lipid Oxidation in Oil-in-Water Emulsions by Interface-Adsorbed Myofibrillar Protein. *J. Agric. Food Chem*., **2015**, *63*, 8896-8904.
26. Burt, S.A.; Reinders, R.D. Antibacterial activity of selected plant essential oils against Escherichia coliO157:H7. *Lett. Appl. Microbiol.,* **2003***, 36*, 162-167.
27. Burt, S. Essential oils: their antibacterial properties and potential applications in foods - a review. *Int. J. Food Microbiol.,* **2004***, 94*, 223-253.

APTEFF, 52, 1-273 (2021) UDC: 691.51+661.332]:628.4.046:631.415.2
DOI: https://doi.org/10.2298/APT2152013A BIBLID: 1450-7188 (2021) 52, 13-24
BY-NC-ND
Original scientific paper

CHARACTERIZATION OF CARBIDE LIME WASTE: A COMPARATIVE STUDY FOR ACID SOIL STABILIZATION

Wafa ATMA[1], Fatiha SOUAHI[2]*

[1] Laboratory of Process Engineering and Chemistry of Solutions, Department of Process engineering, Faculty of sciences and technology, University of Mustapha Stambouli of Mascara, 29000, Algeria

[2] Department of Chemical Engineering, National Polytechnic School of Algiers, Algeria 10 Rue des Frères OUDEK, El Harrach 16200, Algeria

Received: 28 October 2020 **Revised: 14 February 2021** **Accepted: 17 February 2021**

The present work aims to study the physical, mineral and chemical properties of carbide lime residues for assessment as an acidic soil modification. Lime carbide waste is a byproduct of an acetylene generation plant located in Reghaia, east of Algiers, Algeria. This residue offers an effective and economical solution in the field of environmental protection, especially as raw materials for wastewater treatment and soil enrichment. Metallic content was studied using X-ray fluorescence (CubiX XRF/PANalytical). Toxic minerals was analyzed by atomic absorption spectroscopy (AAS).

According to the comparative study, the characterization and total concentrations of minerals are significantly low and do not exceed the limit values for hazardous wastes and are in line with the standard recommendations of the agricultural field. Lime can be used both environmentally and economically as an amendment to stabilize acidic soils.

Keywords: carbide lime waste, waste characterization, waste standards, heavy metals, acid soil enrichment, lime requirement.

INTRODUCTION

Carbide waste lime is produced in most major cities as a by-product from acetylene industry.

Carbide lime is a by-product of the reaction between calcium carbide in water that are produced during the fabrication of acetylene gas for welding.

The terms used for this by-product differ; It is often called “carbide lime” but the by-product of wet generation is also called “carbide sludge”, “lime sludge”, “acetylene generator sludge” or simply “generator sludge”, “acetylene (or generator) filter cake”, “lime cake”, “filter press cake”, “carbide lime residue”.

Calcium carbide (CaC_2) reacts with excess water (H_2O) to form gaseous acetylene (C_2H_2) and liquid calcium hydroxide ($Ca(OH)_2$) as follows:

$$CaC_2\ (s) + 2\ H_2O(l) \rightarrow C_2H_2 + Ca(OH)_2\ (aq) + 64\ kcal$$

The reaction of calcium carbide and water to form acetylene and calcium hydroxide is highly exothermic. Carbide for the production of acetylene is used in the following grain sizes (mm): (2 – 4), (4 – 7), (7 – 15), (15 – 25), (25 – 50) and (50 – 80).

* Corresponding author: Atma Wafa, Laboratory of Process Engineering and Chemistry of Solutions, Department of Process engineering, Faculty of sciences and technology, University of Mustapha Stambouli of Mascara, 29000, Algeria, e-mail: w.atma@univ-mascara.dz

BY-NC-ND

Calcium carbide produce 1.166 times its own weight of solid by-product; as obtained from wet generation, this means 2 to 3 tons per ton of carbide used. Production of each ton of acetylene is accompanied by the production of 3.5 to 4 tons of lime in a dry generator, or by 6 to 9 tons in a wet generator.

After this carbide lime is separated out of the 12 - 20 % aqueous slurry first obtained by settling or filtration (Cardoso et al, 2009; Pässler et al., 2011; Holzrichter et al., 2013). The carbide lime obtained in the wet generation process cannot be discharged into sewers, because of its high alkalinity and sulfur content and because it would cause calcium carbonates blockages. Moreover, the liquor may contain traces of cyanide also. Producers of acetylene in the world over have faced with the problem of dumping the by-product into waste lime pits because of the relatively high transportation costs. (Miller, 1965).

Carbide lime is the third largest weight of by product waste material in the world. Based on the statistics of the calcium carbide industry, the global production of calcium carbide was estimated to be 1370 million tons annually (Lam and Sin, 2019). With very few commercial uses of carbide lime and the unwillingness of producers to pay the treatment and disposal costs for neutralizing high pH, millions of plenty of carbide lime collected as a waste in lagoons, pits and heaps round the world, and therefore the quantity is increasing annually (Lilly et al., 2001, Cardoso et al, 2009).

Utilization of the carbide lime as a substitute for lime in construction, asphaltic paving mixes and other environmental problems have been documented (Alsayed et al. 1992; Ayeche and Hamdaoui 2012; Saldanha et al, 2018; Lam and Sin, 2019).

Moreover, they also can be used as alkaline chemicals for municipal sewage treatment in which they significantly reduced organic matter, suspended solids, nitrogenous, and phosphate compounds and also as an alternative to commercial CaO for acid mine drainage neutralization.

Carbide lime can be recycled because of its approving chemical and physical properties, and has the possible to be re-claimed for different requests, such as industrial processes, and water treatment plants, construction engineering applications, soil stabilization especially acid soil liming. These applications can reduce the undesirable environmental effect caused by disposal of Carbide lime agriculture soil.

There are a number of different materials which can be used for liming. The most common ones are calcium carbonate primarily as neutralizing and secondly as fertilizing agent.

Conversely, farmers now have access to several industrial by-products that may partially restore soil organic matter and nutrient content, and neutralize soil acidity (Lalande et al, 2008).

Among the most important causes of soil acidity are the natural sources of acidity, and carbonic acid, which consists of water and carbon dioxide, on top and inside the soil. Acid rain from industrial and urban activities affects the components of the acidification of the atmosphere in the atmosphere and is transported to the soil. In addition, “land use” and removal of plants harvested from calcium, magnesium and other excess cations. (Rowel and Wild, 1985; Gordon, 1997).

The important causes of soil acidity are the application of ammonium-based fertilizers and urea, elemental S fertilizer and the growth of legumes. Acidification can produces complex interactions of plant growth-limiting factors involving physical, chemical, and biological properties of soil.

APTEFF, 52, 1-273 (2021) UDC: 691.51+661.332]:628.4.046:631.415.2
DOI: https://doi.org/10.2298/APT2152013A BIBLID: 1450-7188 (2021) 52, 13-24
BY-NC-ND
Original scientific paper

Soil acidity is ameliorated by applying lime or other acid-neutralizing materials. 'Liming' (Goulding, 2016)

The English physicist Davy was the first to describe the effect of liming by the "neutralization of soil acidity" in 1813. The measurement of "lime requirement" (which is essential for land use of very acid soils) can be defined as the part of the charges that depend on pH between the natural soil pH and the pH required for a given crop. (Pansu and Gautheyrou, 2006).

Soil acidity can adversely affect crop production by increasing the availability of aluminum and manganese to toxic levels, and by reducing the availability of phosphorus (P).

Liming is the most effective solution for the problem of soil acidity (Beckie et al., 1995).

A major response of plants to liming is due to the neutralization of H, Al, and Mn, which if present in relatively high concentrations in the soil solution are toxic to plant growth. Toxic concentrations of H generally do not occur in soils except in certain organic soils when pH values are less than 4.5. In acid mineral soils with pH values less than 5.5 liming removes the negative effect of H on the absorption of Ca, Mg, and K.

The response of plants to liming is mainly due to the neutralization of exchangeable Al and its replacement on the exchange sites with Ca and/or Mg. Raising the pH of mineral soils to 6 has increased yield because of increased solubility of soil Mo, which is required by bacteria for N_2 fixation. Plant response to liming is due to neutralization of the toxic elements (Kamprath and Smyth, 2005; Mullen et al., 2007).

The objective of the present work is the possibility to use this waste by-product as a fertilizer and pH stabilizer according to a comparative study of results and prefectural order authorizing Linde company gas to process the spreading of lime in the Correze department in France and general standard recommendations.

Also, the study includes calculating the theoretical requirements of lime in order to raise the pH of agricultural soil.

MATERIALS AND METHODS

The Grain size (25-50 mm) of Calcium carbide (CaC_2) was used for wet generation of acetylene at Reghaia plant in Algiers. Carbide lime samples were collected from acetylene gas production plant, Algers (Algeria). Solid in milk of carbide lime represents 10 to 20 % of the total waste of the plant. After decantation and drying in the air for 24 hours, carbide lime was dried in an oven at 60 °C for 48 h to minimize the humidity content. Dried carbide lime was used for characterization in this study. Lime pH was measured in a 1:2.5 solid:water ratio and mineral content was studied using X-ray fluorescence (CubiX XRF/ PANalytical).

Heavy metals, were analyzed according to the aqua regia method, 1 g of dried and crushed sample was digested by a wet digestion method (aqua regia method) using an open system with a refluxing condenser.

The previously dried sample was weighed in the mineralization vessel and reagents (3 mL of concentrated hydrochloric acid, 1 mL of concentrated nitric acid,) were added. The mixture was boiled until a clear solution was obtained. Then the mixture was allowed to cool at laboratory temperature. (Hoeing et al. 1979). After cooling, the resulting solutions were quantitatively transferred into a calibrated flask and into a calibrated flask and com-

BY-NC-ND

pleted to 25 ml by adding distilled water and analysed by flame atomic absorption spectroscopy FAAS (Shimadzu AA6600). For reducing the number of analyses and the relative costs, toxic metals concentration sample obtained by mixing 12 samples (replications) for each part of lime pit.

NEUTRALIZING POWER AND NEUTRALIZING POWER BASE

The neutralizing power (NP) of calcium residues with an alkaline pH (>10) can be estimated by the following equation which has been empirically validated:

$$NP\ (\%\ ECC) = (\%\ Ca \times 2.5) + (\%\ Mg \times 4.17) + (\%\ K \times 1.20);$$

ECC CALCIUM CARBONATE EQUIVALENT

The alternative criteria “Neutralizing power base” are based on a minimum ratio to be observed between the neutralizing power (NP) of a fertilizing residual material and its content of inorganic trace elements (ITE).

MULTIPLE VALUATION INDEX

Multiple valuation index (MVI) is an index for quickly and objectively estimating whether a residue has an obvious minimum agricultural value concerning its properties as a fertilizer or soil amendment. The MVI equation and the criterion of 1 were according to the following equation:

$$MVI = (\text{dry matter } (\%) \div 100)\ X\ [(\text{organic matter } (\%\ d.b.) \div 15) + (\text{neutralizing power } (\%\ ECC\ d.b.) \div 25) + (N + P_2O_5 + K_2O\ (\%\ d.b.)) \div 2]$$ with: d.b : Dry base

ORGANIC MATTER

The CCE is a way to relate all liming materials to CaCO3 as a standard. The molecular weight of $CaCO_3$ is 100 (Ca = 40, C =12, and O =16 x 3). The CCE of $CaCO_3$ has been theoretically established at 100. When using materials other than $CaCO_3$, the molecular weight of $CaCO_3$ is divided by the other material’s molecular weight.

RESULTS AND DISCUSSION

CHEMICAL AND MINERALOGICAL ANALYSIS

Characterization by X-ray diffraction analysis (XRD) was performed on Carbide Lime waste to determine minerals, (table 1). Obtained results indicate the presence of calcium oxide as a dominant mineral.

Analyzes were compared and studied also by other researchers in the same field and the same subject.

APTEFF, 52, 1-273 (2021) UDC: 691.51+661.332]:628.4.046:631.415.2
DOI: https://doi.org/10.2298/APT2152013A BIBLID: 1450-7188 (2021) 52, 13-24
BY-NC-ND
Original scientific paper

X-ray fluorescence spectrometer (XRF) determined the primary chemical components of carbide lime in a significant proportion: 75.72% calcium oxide, 2.8% silicon oxide and less than 1% each of the metal oxides such as Al_2O_3, SiO_2, MgO, and Fe_2O_3.

Table 1 shows the results of the XRF obtained in this study and was compared with analyzes performed by other studies (Miller, 1965; Al Sayed et al., 1991; Sung et al., 2008; Sung et al., 2008: Ayeche and Hamdaoui, 2012, Saldanha et al. 2018)).

The chemical composition of carbide lime is similar in different studies (Table 1) by comparing the components and their percentages.

The amount of calcium oxide in the waste used in this study was 75.72%, and the other components were close to what it was founded by (Ayeche and Hamdaoui, 2012).

Saldanha et al. (2018) recommend more than 90% calcium oxide in lime for use in soil stabilization application, and therefore Carbide Lime in this study does not meet this condition. Other wastes that the researchers have evaluated are similar to carbide lime in terms of the main components that studies have proven can be reused in several areas (Sung et al., 2008; Al Sayed et al., 1991)

Table 1. X-Ray Fluorescence Spectrometry results of carbide lime waste

(Weight%)	Present study	Carbide lime (Miller, 1965)	Carbide lime (Al sayed et al.,1991)	Hydrated lime (Sung et al., 2008)	Recycled soda waste lime (Sung et al., 2008)	Carbide lime waste (Ayeche and Hamdaoui, 2012)	Carbide lime (Saltanha et al., 2018)
Al_2O_3	2.6	1.33	<1,22	0.79	1.81	2.14	0.46
CaO	75.72	96.30	65,05	65.34	47.72	67.03	74
Fe_2O_3	2.38	0.12	0,02	0.12	0.83	2.40	0.26
K_2O	0.014	ND	ND	0.02	0.38	ND	ND
MgO	0.48	<0.2	0,97	0.82	18.12	0.00	0.72
MnO	ND	ND	ND	0.01	0.08	ND	ND
Na_2O	0.14	ND	ND	0.19	3.00	ND	ND
P_2O_5	ND	ND	ND	0.02	0.07	ND	ND
SiO_2	2.28	1.41	<0,1	1.32	7.26	2.06	3.1
TiO_2	ND	ND	ND	0.01	0.05	ND	ND

ND = not defined

Algerian carbide lime differs from commercial lime in size and shape of grains, in its surface properties, and the nature and amount of impurities. According to Ayeche and Hamdaoui (2012), the characterization of lime carbide waste indicates that the waste is very similar to commercial lime (average particle size of 118 mm). X-ray diffraction analyzes showed that carbide lime waste can be compared in carbide lime metal compositions in other research. Miller's work (1965) indicates that the waste component is proportional to components of calcium carbide used in a reaction as its components are derived from minerals.

TOXIC HEAVY METALS ANALYSIS

Carbide lime has a strong alkaline pH plus a high calcium content with a copper content. In addition, there is a large amount of minerals. The results in Figure 1 and Table 2 indicate a copper content of 50 mg/kg and 7.8 mg/kg of chromium with traces of mercury, as well as 2.6 g/kg of aluminum, 2.3 g / kg of iron and 23 g/kg of calcium.

APTEFF, 52, 1-273 (2021) UDC: 691.51+661.332]:628.4.046:631.415.2
DOI: https://doi.org/10.2298/APT2152013A BIBLID: 1450-7188 (2021) 52, 13-24
BY-NC-ND
Original scientific paper

These results are smaller than the permissible marginal values in solid pollutants, and are permissible in relation to recommendations for fertilization.

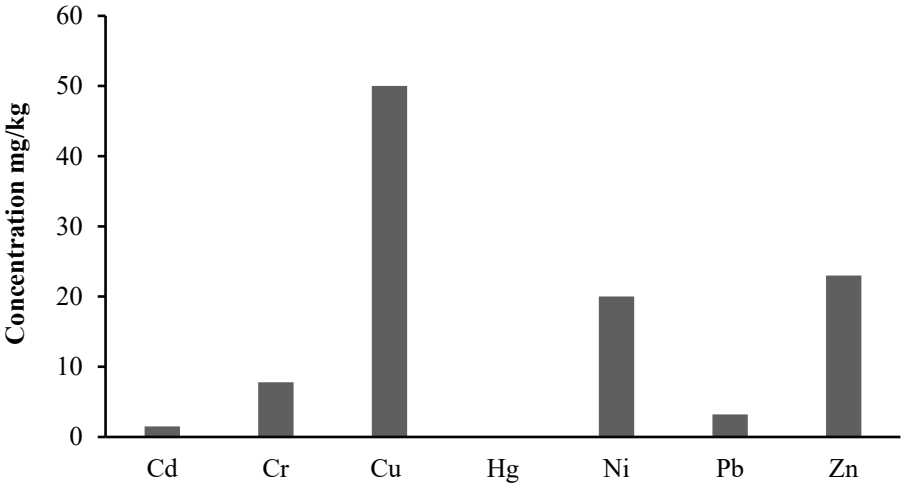

Figure 1. Heavy metals concentrations in carbide lime waste.

Table 2. Comparison between Algerian lime heavy metals analysis, limiting value and analysis of lime of Linde Allassac generator

	Analysis of Lime from Algeria generator (mg/kg) Present study	**Literature:** Analysis of Lime from Linde Allassac generator (mg/kg) (Linde gaz Allassac, 2005)	**Literature:** Carbide lime (Saltanha et al., 2018)(mg/kg)	Hazardous Waste limits (USEPA 2009)	Standard NF U44- 095 (mg/ kg)
Cd	1,5	0,35	0.33	20	3
Cr	7,8	8,95	3.8	100	120
Cu	50	20,62	21		300
Hg	0,065	0,23	0.02	4	2
Ni	20	94,94	0.115	11.5	60
Pb	3,2	5,54	1.8	100	180
Zn	23	8,17	-		600
Mg	530	972,76	-	-	-
Co	10	3,31	-	-	-
Fe	2300	2334,63	-	-	-

Lime analysis from the Linde Allassac generator indicates a significant zinc content of 825 mg/kg with traces of copper and nickel, and 1.1 g/kg of aluminum. The zinc and nickel

BY-NC-ND

content remains below the NFU 44041 standard (3000 mg/kg zinc and 200 mg/kg nickel) for fertilizers from urban wastewater treatment sludge and concentration limit values for heavy metals intended for use in agriculture (French Council Directive No. 86-278 of June 12, 1986) taking into account soil use with a pH lower than 6. (Lemordant, 2001).

The obtained results indicate that carbide contains impurities, about 20%, unincorporated and lime carbon, ferrous, silicon and metallic nodules (metallic mixtures of ore mixture with hard coal or iron carbide, tungsten, titanium, tantalum), active slag inert, water-soluble ammonia, hydrogen sulfide, and insoluble phosphorous hydrogen that develops with acetylene.

Since the same manufacturing method and the same waste have allowed this plant to use carbide limes to correct the acidity of the earth, compared to lime waste can be used and recycled.

As expected for Carbide Lime with high levels of $CaCO_3$, pH is adjacent to 12, heavy metals under high pH conditions are strongly held by precipitation/adsorption processes, and the amounts of soluble metals are insignificant in terms of their possibility to pose a risk to public health and the environment. Thus, Carbide Lime can be used as environmental-friendly amendment agent for applications in soil stabilization.

However, Carbide waste lime is comparable to commercial high -calcium hydrated lime in reducing soil plasticity and increasing soil strength. The worth of the slurry form of application is a secondary consideration, because it is a benefit for avoiding dusty powder, but a disadvantage with wet soils, which must be dehydrated prior to compaction (Wang and Handy, 1966). Obtained results presented in Table 2 where all the contents of the various elements, are below the limiting values fixed by the French regulation (Lemordant, 2001) and Hazardous Waste limits (USEPA, 2009).

Total metal concentrations are low and none exceeds the limits set for hazardous waste (USEPA, 2009) and analysis of Lime from Linde Allassac generator.

The liming of the carbide lime resulting from the manufacturing unit of acetylene from Regalia, Algeria on acid soils should make it possible to raise the pH to a level ensuring precipitation of heavy metals in of hydroxides form.

Results of Chukwudebelu et al (2013) confirm that the metal content of lime waste is still within the acceptable limit for discharge into the environment.

PROVISIONAL CRITERIA FOR THE VALUATION OF RESIDUAL LIME

Neutralizing power and Neutralizing power base

The neutralizing power (PN) of calcium residues with an alkaline pH (> 10) can be estimated:

$$PN\ (\%\ ECC) = (\%\ 23x\ 2{,}5) + (\%\ 5.3\ x\ 4.17) + (\%\ 0.028\ x\ 1.20);=79.63$$

The alternative criteria "Neutralizing power base" are based on a minimum ratio to be observed between the neutralizing power (PN) of a fertilizing residual material and its content of inorganic trace elements (ITE) are listed in Table 3.

APTEFF, 52, 1-273 (2021) UDC: 691.51+661.332]:628.4.046:631.415.2
DOI: https://doi.org/10.2298/APT2152013A BIBLID: 1450-7188 (2021) 52, 13-24
BY-NC-ND
Original scientific paper

Table 3. Alternative criteria based on neutralizing power

	Analysis of Lime from Algeria generator (mg/kg) Present study	Power base (agricultural soils only) Ratio NP/ITE (% E.C.C /mg/kg) regulated by the norm NQ 0419-090 (BNQ 1997). (Hébert, 2015)	Alternative criteria based on neutralizing power regulated by the norm NQ 0419-090 (BNQ, 1997). (Hébert, 2015)
Cd	1.5	53.09	≥2.5
Cr	7.8	10.21	≥0.047
Cu	50	1.6	≥0.066
Hg	0.065	1225.08	≥10
Ni	20	3.98	≥0.28
Pb	3.2	24.88	≥0.1
Zn	23	3.46	≥0.027
Mg	530	0.15	-
Co	10	7.96	> 0.33
Fe	2300	0.035	-

Multiple valuation index

MVI calculated by the equation:

$$MVI = (87\ (\%) \div 100)\ X\ [(13\ (\%\ d.b.) \div 15) + (79.64\ (\%\ ECC\ d.b.) \div 25) + (0 + 0 + 0.014\ (\%\ d.b.)) \div 2]$$

In this study MVI = 4.0096

From an agronomic point of view, this residue seems a priori to have a value because MVI ≥1.

MVI an index objectively estimates whether a residue has minimal agricultural value. The MVI equation and the criterion of 1 were established several years ago from the minimum reference fertilizer values. As an example, Wastewater often has an MVI <1 and ash of excellent quality can have an MVI of up to 7.

The alternative criteria "Neutralizing power base" are based on a minimum ratio to be observed between the neutralizing power (NP) of a residue and its ETI content adapted from the standards. The principle is that when the proportion of PR in the waste increases, it is recommended to reduce the dose of agricultural propagation, in order to avoid excessive soil irritation and reduce costs.

In practice, according to Heber (2015) the maximum long-term ITE load on the ground will remain very low, i.e. four times (400%) less than what the standard allows (BNQ, 1997). It will also be 2.5 to 8 times lower than the loads allowed by the criteria (Table 3), depending on the type of ETI. Alternative criteria can lead to contradictory choices; Thus, certain scientific studies showed that one could relax the permitted limit levels for several contaminants in order to minimize environmental and health risks.

Carbide lime has the properties of a fertilizing material and also meets environmental quality criteria. This means that it may be a recyclable residue.

APTEFF, 52, 1-273 (2021) UDC: 691.51+661.332]:628.4.046:631.415.2
DOI: https://doi.org/10.2298/APT2152013A BIBLID: 1450-7188 (2021) 52, 13-24
BY-NC-ND
Original scientific paper

LIME REQUIREMENT

The measurement of "lime requirement" can be defined as the part of the charges that depend on pH between the natural soil pH and the pH required for a given crop.

In the laboratory, lime requirement is expressed in milli-equivalents of $CaCO_3$ per kg of soil and in agronomy in tons of $CaCO_3$ per hectare (Pansu and Gautheyrou, 2006).

According to Goulding (2016) and Pansu and Gautheyrou (2006) the lime requirement could then be estimated from T – S (T: total cation exchange capacity in buffered solution at pH 7, S: sum of exchangeable cations) located the lime requirement between the exchangeable acidity extracted by a not buffered saline solution and the total acidity neutralized by a buffer solution adjusted to pH 8.1 and enables calculation of the quantity of calcium needed for the correction of acidity.

Lime requirements can also be evaluated by titration using techniques similar to those used for the measurement of exchange acidity.

These methods have been more or less abandoned because of the temporary excessive rise in pH they cause.

A method was proposed by Shoemaker, McLean and Pratt (SMP, 1962). A complex buffer is used with a pH close to neutral, that of carbonate-bicarbonate-CO_2 equilibrium of the soil atmosphere at normal pressure. The pH of a solution expresses the energy level of protons, the pH of a buffer measures potential acidity. Thus, theoretically, the Soil pH was measured after equilibration with a calcium acetate/p-nitrophenol/magnesium oxide buffer and the lime requirement was calculated by applying a factor to the difference between the measured and target pH.

The lime requirement (LR) is expressed in the laboratory by:

$$\text{LR in cmol (+)/kg} = 1.69\ (20\ \text{A}) - 0.86 = 33.8\ \text{A} - 0.86$$

And in field units at a depth of 20 cm:

$$\text{LR in ton/ha} = 45.5\ \text{A} - 1.16.\ \text{with}$$

The acidity (A) measured in mmol (H^+) for 5 g of soil is well described by Pansu and Gautheyrou (2006).

This method takes total H^+, and soluble and exchangeable aluminum into account. It is suitable for soils which require lime correction of more than 1 ton per hectare (soil depth of 20 cm) whose pH is lower than 5.8-6.0. The content of organic matter should not exceed about 15%. Very organic soils are only significantly improved by liming if their pH is lower than 5.3.

Actually, innovative methods are also used as rapid techniques, based on the analysis of many years showed a linear relationship between soil pH and lime requirement, with a slightly different relationship for each soil textural class. Lime requirement calculators have been accessible for many years.

Rothamsted constructed a lime requirement model RothLime (https://www.rothamsted.ac.uk/rothlime). Goulding et al. (1989) is used for deciding how much lime to add to raise a soil's pH under UK conditions. Soil pH refers to measurement made in water with a soil:water ratio of 1:2.5 (weight:volume)

BY-NC-ND

The Agricultural Lime Association (ALA), also has an online Lime Calculator (http://www.aglime.org.uk/lime_calculator.php).

The Lime Calculator allows to calculate a recommended liming rate (t/ha) based on the cropping (enterprise type), measured soil pH, soil type and liming material to be applied. (Goulding, 2016)

During liming, the increase in pH in soils is slowly decreasing in the range between pH 4 and pH 6 which is useful for agronomy (Pansu and Gautheyrou, 2006). The carbide lime, from its chemical characteristics, is relatively regarded as a rectifier of pH (calcic amendment) other than a fertilizer, because the results of analyses show that the carbide lime contains low contents of fertilizing elements (N, P and K).

According to Lippert et al. (1999) and Kamprath and Smyth (2005), and taking into account our comparative study, we propose three alternatives of use of lime:

- liming of the carbide lime in one single application of 50 kg/100 m2 without renewal. According to Beckie et al. (1995) one single liming, carried out in 1963, amounting up to 4-6 tons of carbide lime per hectare, gave more than 30 years later, led to an increase of soil pH of 0.5-1.1 units.
- liming in two separate applications of 25 kg/100 m^2 renewed every 10 -15 years.
- liming in several applications of 5 kg/100 m^2 renewed every 5 years.

This last approach can prove to be more effective because it can ensure obtaining a uniform rate of acidity at the depth of the vegetable roots.

Lime could be applied, at any time of the year, but advantageously just before abundant precipitations. However, Metals were often present in high concentrations in the alkaline by-product matrix, which had a high pH.

Dollhopf and Mehlenbacher (2002) were indicated that plant growth issues may have been mitigated when diluted in the soil profile at a typical application rate of 2 % to 10% (soil dry weight basis) or by an amended soil pH in the range of 7.0 – 8.4 when these metal contaminants were present at low concentrations in the soil solution. Treatment design risk was increased when alkaline by-products are used to amend soils.

CONCLUSIONS

In this study, a comparative study shows that carbide lime characterization indicates that this by-product was similar in chemical and mineralogical compositions to other industrial lime. Based on Prefectoral order authorizing the Linde company gas to the processing of lime milk in the department of Correze in France and the general standard recommenddations, the carbide lime has parallel characteristics with commercial lime.

The spreading of carbide lime from the acetylene plant on acid soils should make it possible to raise the pH of these to a level ensuring the precipitation of heavy metals in the form of hydroxides. Lime milk, by its chemical characteristics, is rather considered as a pH rectifier than a fertilizer (calcium amendment), because the results of analyzes indicate that lime milk contains low levels of nutrients (N, P and K).

With regard to the chemical composition of lime, the various analyzes performed show that all required substances have much lower concentrations than those identified.

However, we suggest that they be included in new analyzes campaigns related to PCBs and PAHs, for example. Finally, the process of correcting acidity relates to many founda-

BY-NC-ND

tions, sometimes when lands are close to streams and waterways. Under these conditions, the minimum distances to be observed must be specified.

Carbide lime waste can be applied at any time of the season before a period of abundant precipitation. Full results from this study indicate that carbide lime owns good proprieties and is environmentally efficient for use as an amendment for acid soil stabilization.

Acknowledgements

The authors express their gratitude to the engineers of the Algerian gas industry of Réghaia, for having provided important information, which contributed to the success of this study.

REFERENCES

1. Al-Sayed, M.; Ismail, H.; Madany, M. Properties of asphaltic paving mixes containing hydrated lime waste. *Waste Manage. Res.* **1992**, *10*, 183-194.
2. Ayeche, R; Hamdaoui, O. Valorization of carbide lime waste, a by-product of acetylene manufacture in wastewater treatment. *Desalin. Water Treat.* **2012**, *50*, 87-94.
3. Beckie, H. J.; Ukrainetz, H. Lime-amended acid soil has elevated pH 30 years later, *Can. J. Soil Sci*. **1995**, *1167*, 59-61.
4. BNQ. Amendements calciques ou magnesiens provenant de procédés industriels. NQ-0419-090. **1997**, 27 pp.
5. Cardoso, F., A.; Fernandes, H., C.; Pileggi, R. G.; Cincotto, M. A.; John, V. M. Carbide lime and industrial hydrated lime characterization, *Powder Technol*. **2009**, *195*, 143-149.
6. Chukwudebelu, J.A.; Igwe, C.C.; Taiwo, O.E.; Tojola, O.B. Recovery of pure slaked lime from carbide sludge: Case study of Lagos state, Nigeria, *Afr. J. Environ. Sci. Technol.* **2013**, *7*(6), 490-495. DOI: https://doi.org/10.5897/AJEST12.093
7. Dollhopf, D. J.; Mehlenbacher, J. T. Alkaline industrial by-product effects on plant growth in acidic-contaminated soil systems, Paper presented at the National Meeting of the American Society for Surface Mining and Reclamation, Lexington, KY, June 2002, 9-13.
8. French standards NF U 44-095 (2002). Organic soil improvers - Composts containing substances essential to agriculture, stanning from water treatment - Amendements organiques, AFNOR, France.
9. Gordon V. J. Causes and Effects of Soil Acidity. Oklahoma Cooperative Extension Service a Division of Agricultural Sciences and Natural Resources. **1997**, *2239*, 1,2. https://www.yumpu.com/en/document/read/25381599/f-2239-causes-and-effects-of-soil-acidity-plantstres-plantstresscom
10. Goulding, K. W. T. Soil acidification and the importance of liming agricultural soils with particular reference to the United Kingdom, *Soil Use and Management*, **2016**, *32*, 390-399. DOI: https://doi.org/10.1111/sum.12270
11. Heber, M. A Guide to Fertilizer Residue Recycling: Criteria References and regulatory standards - 2015 edition. Quebec. ISBN-978-2-550-72954-9, pp 73, 216 Pages. (translated from French)
12. Holzrichter, K.; Knott, A.; Mertschenk, B.; Salzinger, J. Calcium Carbide in: Ullmann's Encycl. Ind. Chem., Wiley-VCH Verlag GmbH & Co. KGaA, Weinheim, **2013**, 1-14. DOI: https://doi.org/10.1002/14356007.a04_533.pub2
13. Lalande, R.; Gagnon, B.; Royer, I. Impact of natural or industrial liming materials on soil properties and microbial activity. *Can. J. Soil Sci.* **2009,** *89,* 209222.

BY-NC-ND

14. Lam, S. M.; Sin J. C. Investigation of By products from Acetylene Manufacturing for Acid Mine Drainage Remediation, *Mine Water Environ*. **2019**, *38*(4), 757-766. DOI: https://doi.org/10.1007/s10230-019-00640-2
15. Lemordant, Y. Former lime deposit at the Linde Gas plant in Allasac. Opinion on the environmental impact and its valorization for calcium enhancement - Support to administrations'. 2001, Rap. BRGM RP-51085-EN. (translated from French)
16. Lilly M. J.; Meade, M. D.; Mortimer, J. Processing and use of carbide lime'; U. S. Pat. 2001, No.: US 6,310,129 B1. https://patentimages.storage.googleapis.com/ 31/6b/a0/2d99cb4cb750c9/US6310129.pdf
17. Linde gaz Allassac, Report authorizing the spreading of whitewash. Council of Health Department, France, 2005 (translated from French). http://infoterre.brgm.fr/rapports/RP-51085-FR.pdf
18. Miller, S. A. Acetylene its properties, manufacture and use, Vol. 1, Edition Ernest Benn Limited, London. 1965, 1-54.
19. Mullen, R.; Edwin, L.; and Maurice, W. Soil Acidity and Liming for Agronomic Production. The Ohio State University, *Extension fact Sheet*. **2007**, AGF-505-07.
20. Pansu M.; Gautheyrou J. Lime Requirement. In: Handbook of Soil Analysis. Springer, Berlin, Heidelberg. **2006**, 687-696. DOI: https://doi.org/10.1007/978-3-540-31211-6_24
21. Pässler, P.; Hefner, W.; Buckl, K.; Meinass, H.; Meiswinkel, A.; Wernicke, H.-J.; Ebersberg, G., Müller R., Bässler J., Behringer H., Mayer D., Acetylene, in: Ullmann's Encycl. Ind. Chem., Wiley-VCH Verlag GmbH & Co. KGaA, Weinheim, **2011**. 277- 326. DOI: https://doi.org/10.1002/14356007.a01_097.pub4
22. Rowel, D. L.; Wild, A. Causes of soil acidification: a summary, *Soil Use Manage*. **1985**, *1*(1), 32-33.
23. Saldanha, R. B.; Filho, H. C. S.; Mallmann, J. E. C.; Consoli, N. C.; Reddy, K. R. ASCE F. Physical-Mineralogical-Chemical Characterization of Carbide Lime: An Environment-Friendly Chemical Additive for Soil Stabilization, *J. Mater. Civ. Eng.* **2018**, *30*(6), 06018004. DOI: https://doi.org/10.1061/(ASCE)MT.1943-5533.0002283
24. Sung Do, H.; Park Hee Mun; Rhee Suk Keun. A study on engineering characteristics of asphalt concrete using filler with recycled waste lime. *Waste Manage*. **2008**, *28*, 191-199.
25. USEPA (U.S. Environmental Protection Agency). Waste characteristics, Materials Recovery and Waste Management Division in the Office of Resource Conservation and Recovery, 2009, Washington, DC.
26. Wang, J.W.H.; Handy, R. L; Evaluation of carbide waste lime for soil stabilization. Progress Report, 1966. Project 576-S, Iowa Highway Research Board Project HR-111, Engineering Experiment Station, Iowa State University, Ames, Iowa. http://publications.iowa.gov/id/eprint/17236
27. Kamprath, E.J.; Smyth, T.J.; LIMING, in Daniel Hillel, Encyclopedia of Soils in the Environment, 1st Ed., Academic Press, ISBN 978-0-12-348530-4, **2005**, 350-358. DOI: https://doi.org/10.1016/B0-12-348530-4/00225-3.

APTEFF, 52, 1-273 (2021) UDC: 582.28:663.26+628.042
DOI: https://doi.org/10.2298/APT2152025D BIBLID: 1450-7188 (2021) 52, 25-32
BY-NC-ND
Original scientific paper

IMPACT OF GRAPE POMACE AS A CULTIVATION SUBSTRATE ON THE *PLEUROTUS OSTREATUS* CHEMICAL AND BIOLOGICAL PROPERTIES

Ana DOROŠKI[1,], Anita KLAUS[1], Maja KOZARSKI[1], Biljana NIKOLIĆ[2], Jovana VUNDUK[1], Vesna LAZIĆ[1], Ilija DJEKIC[1]*

[1] University of Belgrade, Faculty of Agriculture, Institute for Food Technology and Biochemistry, Nemanjina 6, Belgrade 11080, Serbia
[2] University of Belgrade, Faculty of Biology, Studentski trg 16, Belgrade 11000, Serbia

Received: 10 November 2020 **Revised: 31 January 2021** **Accepted: 5 February 2021**

The objective of this study was to develop a single quality index of chemical characteristics of Pleurotus ostreatus extracts on 7th and 14th day of its shelf life, derived from the mushroom fruiting bodies. P. ostreatus was cultivated on four substrates containing different ratio of wine industry waste-grape pomace (P) and wheat straw (S): 100P, 80P20S, 50P50S, 20P80S. Four quality parameters of P. ostreatus mushroom extracts, i.e. antioxidative parameters: $ABTS^{+}$ and $DPPH^{\bullet}$ free radical scavenging capability, total phenolic compounds (TPC) and total polysaccharides (TPS) were used to define the final extract quality index. Analysis indicated 100P and 80P20S as the samples cultivated on the substrate with higher percent of grape pomace, as the best quality at the 7th day of its shelf life. On the other hand, final quality score indicated 50P50S and 20P80S, cultivated on a substrate with a lower percent of grape pomace, as the best quality samples at the 14th day of its shelf life. According to the results, samples cultivated on a higher pomace content substrate are of better quality in a shorter storage time period.

Keywords: *Pleurotus ostreatus*, food waste, quality index, grape pomace, mushroom.

INTRODUCTION

One of the most commonly cultivated and consumed mushrooms worldwide is *Pleurotus ostreatus* (Oyster mushroom). According to the Food and Agriculture Organisation of the United Nations data (FAOSTAT), total world production of mushrooms in 2018 was 9 million metric tons, with *P. ostreatus* holding the second place in industrial world production (1). Besides its specific pleasant taste and adaptibility to various cellulose substrates, scientific interest considering this mushroom species is also directed to its various bioactive compounds that improve defense mechanisms for cell oxidative damage (2). These components are also related to mushroom antioxidant, antimicrobial, antitumor, antiviral and immunomodulatory properties (1,3).

Apart from these positive properties, *P. ostreatus* belongs to "white-rot fungi" category. This is related to its ability to produce lignolytic enzymes, beside to its cellulose degradation capability. This feature gives the opportunity of using the wide range of agroindustrial and food production wastes for mushroom cultivation, instead of the ones ordinary used in global production (4). Considering *P. ostreatus*, it is usually cultivated on wheat straw (5), but the use of alternative substrates could be of great importance for increasing productivity and improving the properties of mushroom. Except the benefits of mushroom production,

* Correspoding author: Ana Doroški, University of Belgrade, Faculty of Agriculture, Institute for Food Technology and Biochemistry, Nemanjina 6, Belgrade 11080, Serbia, e-mail: ana.doroski@gmail.com

APTEFF, 52, 1-273 (2021) UDC: 582.28:663.26+628.042
DOI: https://doi.org/10.2298/APT2152025D BIBLID: 1450-7188 (2021) 52, 25-32
BY-NC-ND
Original scientific paper

agroindustrial waste recycling has the other adventages, such as solving of environmental global issues (6,7).

In this study quality of *P. ostreatus*, cultivated on grape pomace derived from the wine industry as a waste, was estimated by analyzing its chemical and biological properties at 7th and 14th day of its shelf life. *P. ostreatus* was cultivated on four substrates with different ratio of grape pomace and wheat straw. Four quality parameters, namely free radical scavenging capability determined in $ABTS^{+}$ and DPPH·assays and totals of phenolic compounds and polysaccharides, were involved in calculation of a single total quality index (TQI), in order to compare the quality of four mushroom extracts samples in two shelf life stages.

EXPERIMENTAL

SUBSTRATE PREPARATION

P. ostreatus extracts were derived from the fruiting bodies cultivated on four substrates containing different ratio of grape pomace and wheat straw, described in Table 1.

Table 1. Substrate composition used for *P. ostreatus* mycelium inoculation

No.	Substrate codes	Composition of substrate content
1	100S	100% wheat straw
2	100P	100% grape pomace
3	80P20S	80% grape pomace: 20% wheat straw
4	50P50S	50% grape pomace: 50% wheat straw
5	20P80S	20% grape pomace: 80% wheat straw

Grape pomace was collected during the summer 2018 from the grape variety Prokupac, originating from Aleksandrovačka Župa, Serbia. The tissue culture inoculation method described by Mondal et al. (8) was used, by isolation from fresh mushroom fruiting bodies of commercial strain A15.

Each substrate mixture was prepared in triplicates. The mixture was filled into polypropilene bags with filters (Microsac, PP75/BEH6/X37-53, Nevele, Belgium) and sterilized in autoclave for 2 h at 121 °C with 1.5 kg cm^{-2} pressure. Mushroom mother culture was added afterwards in sterile conditions to each substrate bag, and placed in an incubation room at 25 °C under 85% relative humidity. Mycelial growth was completed in approximately 20 days. Upon completion, each bag was opened and placed in a room with 80-85% relative humidity and the mycelium was in contact with external atmosphere, which enabled the growth of fruiting bodies in the next 5-7 days. Fresh mushrooms, harvested from the first flush, were selected to be of uniform size and shape. 50 g of mushrooms were individually packed in 85 μm thick (PA/PE/PE) bags (200mm x 300 mm) with transmission rates of 60 mL O_2, 12 mL N_2 and 180 mL CO_2 m^{-2} day^{-1} atm^{-1}, using HVC-510T/2A packaging machine; they were refrigerated under controlled conditions at 4 °C for 7 and 14 days.

APTEFF, 52, 1-273 (2021) UDC: 582.28:663.26+628.042
DOI: https://doi.org/10.2298/APT2152025D BIBLID: 1450-7188 (2021) 52, 25-32
BY-NC-ND
Original scientific paper

EXTRACT PREPARATION

In order to prepare mushroom extracts for further analysis, mushroom fruiting bodies were air-dried at 55 °C and powdered. The crude hot water extracts were prepared by adding 40 mg mL^{-1} of distilled water and heated at 75-85 °C for 2h. The samples were centrifuged for 10 min and supernatant was decanted and stored for further analysis.

CHEMICAL CHARACTERIZATION - TOTAL PHENOLIC AND POLYSACCHARIDE CONTENTS

Total phenolic content (TPC) was investigated by adapted Folin-Ciocalteu reaction method, previously described by Djekic et al. (9), with the same concentration range (0.625-40 mg mL^{-1}), using 96-well microplate reader (microplate reader ELx808, BioTek Instruments, Inc., SAD). Results were expressed as mg gallic acid equivalent (GAE) g^{-1} of the extract.

Determination of total polysaccharide content (TPS) was done by the phenol-sulfuric acid method with D-glucose [10], in a concentration range from 0.625-40 mg mL^{-1}.

ANTIOXIDATIVE POTENTIAL

Antioxidative potential was expressed by DPPH·and $ABTS^+$ free radical scavenging capability, expressed as EC_{50} (mg mL^{-1}) values, being defined as "the effective concentration of mushroom extract required to neutralize 50% of $ABTS^+$/DPPH·radicals". Higher antioxidant ability corresponds to lower EC_{50} value (2). DPPH·free radical scavenging activity assay was performed by the method of Ekanayake et al. (11), with catechin and Trolox as positive controls, in a concentration range of 0.03125 – 2 mg mL^{-1}. $ABTS^+$ free radical scavenging activity assay was performed by the method of [12], with catechin and BHA as positive controls, in the same concentration range of 0.03125 – 2 mg mL^{-1}. Concentrations ranging from 0.625 – 40 mg mL^{-1} for each extract were analyzed.

TOTAL QUALITY INDEX APPROACH AND STATISTICAL ANALYSIS

For calculating TQI of mushroom extracts, the following rules were applied for selected quality parameters: (a) rule "the smaller the value, the better the quality" has been applied for the EC_{50} values determined in ABTS+ and DPPH·assays; (b) rule "the higher the value, the better the quality" was applied for the TPC and TPS values. The final TQI score was calculated as previously described in the literature (13, 14). Interpretation of the final score is "the lower value of TQI, the better overall quality". Statistical analysis was obtained by two-way analysis of variance (ANOVA) and *Tukey's post hoc test* with statistical significance at the level $p<0.05$. SPSS Statistics 17.0 and Microsoft Excel 2010 were used for statistical data analysis.

RESULTS AND DISCUSSION

All obtained results are shown in Table 2 and 3. Our results indicate the growing values of TPC with prolonging of shelf life period. Namely, TPC of each extract was higher at the 14^{th} day compared to the 7^{th} day. Moreover, the growing trend was more extensive for the extracts

APTEFF, 52, 1-273 (2021) UDC: 582.28:663.26+628.042
DOI: https://doi.org/10.2298/APT2152025D BIBLID: 1450-7188 (2021) 52, 25-32
BY-NC-ND
Original scientific paper

with higher grape pomace substrate content. However, the highest value of TPC was shown for the 80P20S extract, not for the 100P, with the highest value determined after 14 days of growth, as well. Concerning TPS values, our results showed that they were approximately uniform for all the values determined at each day of shelf life (with exception of the value for the 100P extract determined at 7th day), but was slightly decreased in 14th day.

Table 2. The effects of grape pomace as a substrate on the *P. ostreatus* chemical properties

Chemical properties					
Day	**100P**	**80P20S**	**50P50S**	**20P80S**	**100S***
TPC (mg/g GAE)					
7th	19.83 ± 0.32^{A}	27.09 ± 0.56^{B}	21.10 ± 0.84^{A}	20.26 ± 1.01^{A}	19.40 ± 1.07
14th	25.11 ± 0.28^{A}	37.39 ± 2.42^{B}	24.9 ± 0.39^{A}	20.73 ± 0.59^{C}	
TPS (mg/g GLU)					
7th	110.06 ± 8.67	90.84 ± 1.05	114.93 ± 9.90	111.70 ± 2.64	107.44 ± 10.21
14th	69.27 ± 9.21^{A}	89.62 ± 2.60^{AB}	88.03 ± 2.70^{AB}	94.71 ± 3.40^{B}	

Means of ten replications ± standard deviation. Means in the same row with different capital letters are significantly different ($p<0.05$). Legend: 100P - 100% grape pomace substrate content; 80P20S - 80% grape pomace: 20% straw substrate content; 50P50S - 50% grape pomace: 50% straw substrate content; 20P80S - 20% grape pomace: 80% straw substrate content; 100S* - 100% wheat straw substrate content (control sample, day 0).
TPC - total phenolic compounds; TPS - total polysaccharides.

Mushrooms are well known for their antioxidant properties, being directly related to all tested extracts were characterized by some antioxidative activity, but generally higher potential was observed in $ABTS^{+}$ assay (Table 3.).

Table 3. The effects of grape pomace as a substrate on the *P. ostreatus* antioxidant properties

Antioxidant properties					
Day	**100P**	**80P20S**	**50P50S**	**20P80S**	**100S***
$ABTS^{+}$ EC_{50} (mg/mL)					
7	< 0.625^{A}	4.41 ± 0.05^{C}	4.96 ± 0.16^{C}	7.49 ± 0.01^{B}	8.42 ± 0.20
14	3.91 ± 0.11	3.68 ± 0.05	4.27 ± 0.21	3.59 ± 0.04	
DPPH·EC_{50} (mg/mL)					
7	2.66 ± 0.14^{A}	8.15 ± 0.21^{B}	13.21 ± 0.33^{C}	10.73 ± 0.04^{BC}	15.04 ± 0.08
14	8.08 ± 0.13^{A}	> 40^{B}	8.90 ± 0.23^{A}	8.11 ± 0.36^{A}	

Means of ten replications ± standard deviation. Means in the same row with different capital letters are significantly different ($p<0.05$). Legend: 100P - 100% grape pomace substrate content; 80P20S - 80% grape pomace: 20% straw substrate content; 50P50S - 50% grape pomace: 50% straw substrate content; 20P80S - 20% grape pomace: 80% straw substrate content; 100S* - 100% wheat straw substrate content (control sample, day 0).

The highest potential of both radicals neutralization was detected for the 100P extract prepared from 7th day of mushroom storage. On the other hand, control sample have shown the lowest potential of both radicals neutralization.

Figure 1. derived from TQI of four quality parameters of mushroom extracts analysis, shows that 100P was the extract with the best quality, followed by 80P20S, but only at the 7th day of their shelf life.

APTEFF, 52, 1-273 (2021)
DOI: https://doi.org/10.2298/APT2152025D
BY-NC-ND
UDC: 582.28:663.26+628.042
BIBLID: 1450-7188 (2021) 52, 25-32
Original scientific paper

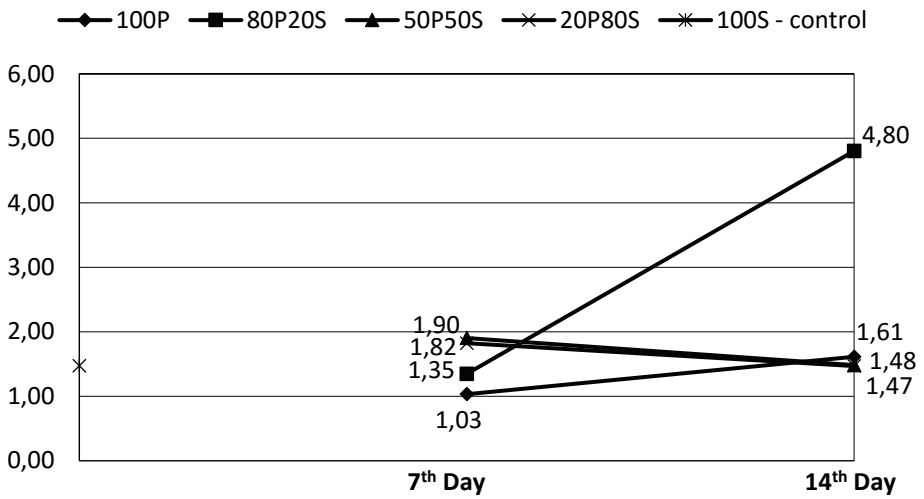

Legend: 100P - 100% grape pomace substrate content; 80P20S - 80% grape pomace: 20% straw substrate content; 50P50S - 50% grape pomace: 50% straw substrate content; 20P80S - 20% grape pomace: 80% straw substrate content

Figure 1. Total quality index (TQI) of parameters derived from measured values of mushroom extracts of the 7th and 14th day of its shelf life

The fact is that the chemical properties of the mushrooms are directly related to the substrate used for cultivation (15), and for that reason the variability of TPC and TPS values obtained for different extracts was expectable. With regard to the control sample, 100S, all other samples cultivated on the grape pomace substrate have shown higher TPC values, which can be related to the polyphenol content derived from the pomace. The growing trend of TPC values during shelf life period is in opposite with regard to Jiang T. et al. (16) and Jafri M. et al. (17), who reported decrease of phenolic content during mushroom storage, and explained this phenomenon as the enzymatic oxidation of phenolic compounds via polyphenol oxidase, which could be also associated with mushroom browning. Liu Z. and Wang X. (18) reported that the amount of polyphenolics increases with the influence of high oxygen conditions, but according to Gao M. et al. (19) additional phenolics in fruits could be formed as a defence mechanism. Vacuum-packaging applied in this study, as shelf life prolonging method, provides an anaerobic environment that suits to facultatively anaerobic bacteria: lactic acid bacteria, *Enterobacteriaceae* spp., etc. (20), with CO_2 present in the package as a metabolic by-product of microbial metabolism (21). Our results, indicating an increase of TPC during mushrooms storage, are in agreement with Karowe and Grubb (22), who reported that elevated CO_2 in the atmosphere may cause the increased levels of simple, complex and total phenolics of *Brassica rapa* (oilseed rape) under elevated CO_2.

Taking into account that Gąsecka et al. (23) reported 9.64 ± 0.33 mg g^{-1} polyphenols in *P. ostreatus* extract, being noticeable lower then the results of each analyzed extract, one could note that cultivation method that was used in our research favoured polyphenols

BY-NC-ND

production. Namely, Jiang et al. (16) used beech sawdust and flax shives, supplemented with wheat bran, corn flour, gypsum and wheat straw enriched with Se and Zn.

On the other hand, general trend was the drop of the TPS with the prolonging of shelf life, while substrate used (except the 100P sample) did not affect significantly this feature. Study by Li et al. (24) reported decrease of water-soluble crude polysaccharide content in shiitake mushroom (*Lentinus edodes*) after storage, which is justified by the sugar consumption caused by respiration of the mushrooms during the storage.

Scavenging of free radical in biological systems has a preventive role against arising of oxidative damage of DNA, cellular proteins and lipids and consequently could protect from many chronic diseases and carcinogenesis (25). Mushrooms are well known for their antioxidant properties, being directly related to phenolic compounds (26, 27). However, the correlation between phenolic compounds and antioxidant activity of the extracts is not noticed in this research, which concurs to the following finding (28). According to Antonić et al. (29), grape pomace is rich in mineral content, such as Fe and Zn, which could be directly related to mineral composition of the mushroom cultivated on grape pomace substrate (15). Namely, phenolic compounds have ability to make complexes with bioavailable minerals, such as Fe, Zn and Li, which could be present in mushroom chemical structure. This complexation process reduces scavenging activity of phenolic compounds and consequently leads to limited antioxidant ability.

Finally, in order to quantify the overall quality and to point out the best cultivation method, all obtained results were summarized in TQIs of all tested samples. The outcomes were changed during the shelf life period, especially for the 80P20S. However, this time-dependent changes in the quality of two extracts with the lower share of grape pomace in substrate (50P50S and 20P80S) were less pronounced. According to this feature, these two substrate modes can be considered as those that favor quality stability over extended storage times.

CONCLUSION

This investigation was meant to point out the benefits of using wine industry waste as a substrate for growing mushrooms, in the form of a total quality index (TQI). The advantage of this type of production is exploitation of food waste into the value-added new product. Additionally, the kind of waste used in the mushroom production distinctly affect nutritional profile of mushroom fruiting bodies, which concurs to this investigation outcome. Results indicated grape pomace as a valuable substrate for *P. ostreatus* cultivation. Lastly, this investigation pointed out the use of quality index approach as a useful tool for applied quality evaluation.

REFERENCES

1. Bellettini, M.B.; Fiorda, F.A.; Maieves, H.A.; Teixeira, G.L.; Ávila, S.; Hornung, P.S.; Júnior, A.M.; Ribani, R.H. Factors Affecting Mushroom Pleurotus Spp. Saudi. *J. Biol. Sci.* **2019,** *26*(4). 633-646.
2. Kozarski, M.; Klaus, A.; Niksic, M.; Jakovljevic, D.; Helsper, J.P.F.G.; Van Griensven, L.J.L.D. Antioxidative and Immunomodulating Activities of Polysaccharide Extracts of the Medicinal Mushrooms Agaricus Bisporus, Agaricus Brasiliensis, Ganoderma Lucidum and Phellinus Linteus. *Food Chem.* **2011,** *129*(4), 1667-1675.

3. Xu, X.; Yan, H.; Chen, J.; Zhang, X. Bioactive Proteins from Mushrooms. *Biotechnol. Adv.* **2011**, *29*(6), 667-674.
4. Tsujiyama, S.; Ueno, H. Performance of Wood-Rotting Fungi-Based Enzymes on Enzymic Saccharification of Rice Straw. *J. Sci. Food Agric.* **2013,** *93*(11), 2841-2848.
5. Kurt, S.; Büyükalaca, S. Yield Performances and Changes in Enzyme Activities of Pleurotus Spp. (P. Ostreatus and P. Sajor-Caju) Cultivated on Different Agricultural Wastes. *Bioresour. Technol.* **2010,** *101*, 3164-3169.
6. Djekic, I.; Miloradovic, Z.; Djekic, S.; Tomasevic, I. Household Food Waste in Serbia – Attitudes, Quantities and Global Warming Potential. *J. Clean. Prod.* **2019,** *229*, 44-52.
7. Djekic, I.; Operta, S.; Djulancic, N.; Lorenzo, J.M.; Barba, F.J.; Djordjević, V.; Tomasevic, I. Quantities, Environmental Footprints and Beliefs Associated with Household Food Waste in Bosnia and Herzegovina. *Waste Manag. Res.* **2019,** *37*(12), 1250-1260.
8. Mondal, S.; Rehana, J.; Noman, M.; Adhikary, S. Comparative Study on Growth and Yield Performance of Oyster Mushroom (Pleurotus Florida) on Different Substrates. *J. Bangladesh Agric. Univ.* **1970,** *8*(2), 213-220.
9. Djekic, I.; Vunduk, J.; Tomašević, I.; Kozarski, M.; Petrovic, P.; Niksic, M.; Pudja, P.; Klaus, A. Total Quality Index of Agaricus Bisporus Mushrooms Packed in Modified Atmosphere. *J. Sci. Food Agric.* **2017**, *97*(9), 3013-3021.
10. Dubois, M.; Gilles, K.A.; Hamilton, J.K.; Rebers, P.A.; Smith, F. Colorimetric Method for Determination of Sugars and Related Substances. *Anal. Chem.* **1956,** *28*(3), 350-356.
11. Ekanayake, M.P.; Park, G.T.; Kim, S.; Lee, Y.D.; Kim, S.J.; Jeong, S.C.; Lee, J. Antioxidant Potential of Eel (Anguilla japonica and Conger myriaster) Flesh and Skin. *Journal of food lipids*, **2005,** *12*(17), 34-47.
12. Arnao, M; Cano, A.; Acosta M. The Hydrophilic and Lipophilic Contribution to Total Anti-oxidant Activity. *Food Chem*. **2001**, *73*, 239-244.
13. Finotti, E.; Bersani, A.M.; Bersani, E. Total Quality Indexes for Extra-Virgin Olive Oils. *J. Food Qual.* **2007**, *30*(6), 911-931.
14. Djekic, I.; Tomic, N.; Bourdoux, S.; Spilimbergo, S.; Smigic, N.; Udovicki, B.; Hofland, G.; Devlieghere, F.; Rajkovic, A. Comparison of Three Types of Drying (Supercritical CO2, Air and Freeze) on the Quality of Dried Apple – Quality Index Approach. *Lwt.* **2018,** *94*, 64-72.
15. Oyetayo, O. V.; Ariyo, O.O. Micro and Macronutrient Properties of Pleurotus Ostreatus (Jacq : Fries) Cultivated on Different Wood Substrates. *Jordan J. Biol. Sci.*, **2013**, *6*(3), 223-226.
16. Jiang, T.; Feng, L.; Zheng, X. Effect of Chitosan Coating Enriched with Thyme Oil on Postharvest Quality and Shelf Life of Shiitake Mushroom (Lentinus Edodes). *J. Agric. Food Chem.* **2012**, *60*(1), 188-196.
17. Jafri, M.; Jha, A.; Bunkar, D.S.; Ram, R.C. Quality Retention of Oyster Mushrooms (Pleurotus Florida) by a Combination of Chemical Treatments and Modified Atmosphere Packaging. *Postharvest Biol. Technol.* **2013**, *76*, 112-118.
18. Liu, Z.; Wang, X. Changes in Color, Antioxidant, and Free Radical Scavenging Enzyme Activity of Mushrooms under High Oxygen Modified Atmospheres. *Postharvest Biol. Technol.* **2012**, *69*, 1–6.
19. Gao, M.; Feng, L.; Jiang, T. Browning Inhibition and Quality Preservation of Button Mushroom (Agaricus Bisporus) by Essential Oils Fumigation Treatment. *Food Chem.* **2014,** *149*, 107-113.
20. Doulgeraki, A.I.; Ercolini, D.; Villani, F.; Nychas, G.J.E. Spoilage Microbiota Associated to the Storage of Raw Meat in Different Conditions. *Int. J. Food Microbiol.* **2012**, *157*(2), 130-141.
21. Adams, K.R.; Niebuhr, S.E.; Dickson, J.S. Dissolved Carbon Dioxide and Oxygen Concentrations in Purge of Vacuum-Packaged Pork Chops and the Relationship to Shelf Life and Models for Estimating Microbial Populations. *Meat Sci.* **2015**,110, 1-8.
22. Karowe, D.N.; Grubb, C. Elevated CO2 Increases Constitutive Phenolics and Trichomes, but Decreases Inducibility of Phenolics in Brassica Rapa (Brassicaceae). *J. Chem. Ecol.* **2011**, *37*(12), 1332-1340.

BY-NC-ND

23. Gąsecka, M.; Mleczek, M.; Siwulski, M.; Niedzielski P. Phenolic Composition and Antioxidant Properties of Pleurotus Ostreatus and Pleurotus Eryngii Enriched with Selenium and Zinc. *Eur. Food Res. Technol.* **2016**, *242*(5), 723-732.
24. Li Y, Ishikawa Y, Satake T, Kitazawa H, Qiu X, Rungchang S. Effect of Active Modified Atmosphere Packaging with Different Initial Gas Compositions on Nutritional Compounds of Shiitake Mushrooms (Lentinus Edodes). *Postharvest Biol. Technol.* **2014**, *92*, 107-113.
25. Zhu, Q.; Hackman, R.; Ensunsa, J.; Holt, R.; Keen C. Antioxidative Activities of Oolong Tea. *J. Agric. Food Chem.* **2002**, *50*, 6929-6934.
26. Babu, D.R.; Pandey, M.; Rao, G.N. Antioxidant and Electrochemical Properties of Cultivated Pleurotus Spp. and Their Sporeless/Low Sporing Mutants. *J. Food Sci. Technol.* **2014**, *51*(11), 3317-3324.
27. Sudha, G.; Vadivukkarasi, S.; Shree, R.B.I.; Lakshmanan P. Antioxidant Activity of Various Extracts from an Edible Mushroom Pleurotus Eous. *Food Sci. Biotechnol.* **2012**, *21*(3), 661-668.
28. Fontes Vieira, P.A.; Gontijo, D.C.; Vieira, B.C.; Fontes, E.A.F.; Assunção, L.S. de.; Leite, J.P.V.; Oliveira, M.G. de A.; Kasuya, M.C.M. Antioxidant Activities, Total Phenolics and Metal Contents in Pleurotus Ostreatus Mushrooms Enriched with Iron, Zinc or Lithium. *LWT - Food Sci. Technol.* **2013**, *54*(2), 421-425.
29. Antonić, B.; Jančíková, S.; Dordević, D.; Tremlová, B. Grape Pomace Valorization: A Systematic Review and Meta-Analysis. *Foods* **2020,** *9*(11), 1627.

APTEFF, 52, 1-273 (2021) UDC: 66.067.8.081.3:582.542.1:667-12
DOI: https://doi.org/10.2298/APT2152033L BIBLID: 1450-7188 (2021) 52, 33-44
BY-NC-ND
Original scientific paper

REMOVAL OF METHYLENE BLUE BY BIOSORPTION ONTO *STIPA TENACISSIMA L.* (ALFA) PLANTS: KINETICS, EQUILIBRIUM AND THERMODYNAMIC STUDIES

Samir LADJALI[1,2], Nadjib DAHDOUH[1], Samira AMOKRANE[1], El hadj MEKATEL[1], Djamel NIBOU[1]*

[1] Laboratory of Materials Technology, Faculty of Mechanic and Engineering Processes (USTHB) BP 32, 16111, Algiers, Algeria
[2] Process Engineering Department, Faculty of Science and Technology, Mustapha Stambouli University-Mascara, Mascara, Algeria

Received: 27 September 2020 **Revised: 12 February 2021** **Accepted: 17 February 2021**

This study examines the ability of Stipa tenacissima L. (Alfa) to biosorb the Methylene Blue dye. Biosorption tests were performed in aqueous solution based on certain essential parameters such as solution's pH (2-12), solid/liquid ratio (1-6 g/L), initial dye concentration (25-125 mg/L) and contact time (0-300 min). The Langmuir, Freundlich, Temkin and Elovich models were applied. It was found that the equilibrium data could be fitted to the Langmuir isotherm for MB biosorption with a maximum capacity q_{max} 55, 95 mg/g. The kinetic study shows that the experimental data correspond to the pseudo-second order kinetic model. The negative Gibbs values free energy ΔG° reveal the spontaneity of MB biosorption at the surface of Stipa tenacissima L. The positive value of ΔH° reveals the endothermic nature of the process.

Keywords: *Stipa tenacissima L* (Alfa), methylene blue, biosorption, kinetic study and thermodynamic.

INTRODUCTION

Nowadays, environmental protection has become a major concern in all countries. Therefore, there is an urge for encouraging the development of processes for the improvement of waste-water treatment methods focusing on the reduction of pollution sources. However, industrial effluents from textile, tanning, or printing activities often have high colored pollutant loads which are difficult to biodegrade. The discharge of highly colored compounds such as dyes can block out sunlight penetration in surface waters, hence decreasing both photosynthetic activity and dissolved oxygen concentration and affecting aquatic life (1). Unfortunately, during the dyeing process, large fractions of reactive colors (10-50 percent) are wasted and an estimation is that over 7105 tons of dyes are produced each year (2). This is why many researchers within the water treatment field are interested in the removal of reactive dyes.

Several conventional treatments have proven ineffective in removing supplements and dyes due to their high-water solubility. Furthermore, various techniques have been used in the process of eliminating some soluble pollutants from industrial or domestic effluents. They are different from each other and can be cited for illustration purposes: adsorption (3), electrolysis (4), combined Adsorption/Photocatalysis (5), liquid-liquid extraction (6), mem-

* Corresponding author: Samir Ladjali, Process Engineering Department, Faculty of Science and Technology, Mustapha Stambouli University-Mascara, Algeria, e-mail: s.ladjali@univ-mascara.dz

BY-NC-ND

brane filtration (7), coagulation-flocculation (8), etc. The best prospect for dye removal tends to be adsorption on activated carbon. This adsorbent is costly and hard to recycle after use despite its efficiency. A wide variety of inexpensive adsorbent materials, such as clay minerals, have been identified in recent years (9) and biomasses (10). Most of the materials studied include wastes of aquatic and agro-industrial origin like seaweed, microbial biomass, pine bark, cotton, beet pulp, pine sawdust, sugarcane bagasse, jute fibers, olive kernel, coconut, and rice husks (11). The studies available in the scientific literature indicate that the biosorbents can be an alternative to the activated carbons in water treatment processes on an industrial scale (12). Thereby, this paper examines the treatment of water-containing dye such as methylene blue (MB) by following the adsorption process that is based on the retention of a pollutant by an adsorbent. In this case, it is a natural lignocellulosic material whose stems were chosen as the biosorbent. This study aims first and foremost to valorize this local resource which is abundant in Algeria and to determine its biosorption capacities regarding the dye. The fundamental investigations, mainly, include the characterization of biosorbents, biosorption equilibrium, kinetics and thermodynamics. Determination of biosorption kinetics is crucial in predicting the behavior of a biosorbent in practical applications (13).

Stipa tenacissima L. is also known as Alfa in the studied region (the Arabic name for the plant) like belongs to the grass family. It is widespread in arid regions in northwest Africa and southern Spain. This wild plant covers large areas of the Algerian highlands and usually blooms in the period time from April to June. However, it is a permanent plant that survives the winter. It grows up to approximately one-meter height in the form of a cylindrical rod. Like any lignocellulose/lingnocellulosic biomass, Alfa stems are hard, its Latin name is (*Stipa tenacissima L.*), low density, abundant in nature, renewable and 100% biodegradable. The untreated plant, namely *Stipa tenacissima L.,* is examined in this study. Methylene blue, a cationic dye, was used as a molecular model to study the biosorption properties for the removal of the typical dye (14).

EXPERIMENTAL

MATERIALS

Biosorbent preparation

The Alfa biomass stems were manually washed with tap water to remove debris, dust, and sand, and then it was thoroughly rinsed with distilled water, dried in the open air for 24 hours, and then warmed up in an oven at 80 °C for 48 hours. To grind the biosorbent, the biomass was immersed in liquid nitrogen for 15 minutes to harden and weaken the stems to facilitate the grinding process. Afterwards, they were easily crushed with a domestic mortar. Then, the ground powder was sieved (powder fraction <0.7mm). It is noteworthy to mention that the material did not undergo any chemical or physical treatment.

Adsorbate

Methylene blue (MB) is a cationic dye that can be used in many applications such as the textile industry. The aforementioned is one of the common pollutants in colored effluents.

APTEFF, 52, 1-273 (2021) UDC: 66.067.8.081.3:582.542.1:667-12
DOI: https://doi.org/10.2298/APT2152033L BIBLID: 1450-7188 (2021) 52, 33-44
BY-NC-ND
Original scientific paper

Several types of research were published on the possibility of removing the MB using different adsorbents (15).

Effect of pH: The effect of pH on the removal of MB dye was studied in the range from 2 to 12. The pH of the solution was adjusted to the desired value by micro-additions of HCl (0.1 M) or NaOH (0.1 M). The other parameters were kept constant: C_0 = 25 mg/L, contact time 90 min, R (S/L) of 6 g/L and at a temperature of 25 ± 2 °C. After the mixture was centrifuged and the adsorbate was analyzed by the spectrophotometer.

Effect of adsorbent dose: the mass of *Stipa tenacissima L* was determined by a series of experiments that contributed to the optimal biosorption by methylene blue. Consequently, a range from 1 to 6 g/L was selected.

Effect of initial methylene blue concentration: the MB concentrations were varied from 25 to 125 g/L while keeping the other operating conditions constant to determine the effect of the initial concentration of MB on the removal percentage.

Effect of contact time: The equilibrium time is an important parameter, it is determined following the achievement of a kinetic of MB biosorption at an initial concentration of 100 mg/L; R(S/L) of 6 g/L and the pH of the solution is 12. Several samples in time were taken, such as t = 5, 15, 30, 50, 60, 90, 120 and 180 min to determine the optimum time corresponding to the best MB biosorption yield. The removal percentage (%) of MB was determined using equation [1]:

$$Removal(\%) = \frac{(C_0 - C_e)}{C_0} \times 100 \quad [1]$$

The capacity q_e (mg/g) was calculated by the following expression (Eq. 2):

$$q_e = \frac{(C_0 - C_e)\,V}{m} \quad [2]$$

where, C_0 and C_e represent the initial and the equilibrium concentration (mg/L) of MB respectively, m is the mass of the biosorbent used (g) and V is the volume of the dye solution (L).

BIOSORPTION ISOTHERMS

Biosorption isotherms play a major role in determining maximum capacities and identifying the type of isotherm. Therefore, the four classical isothermal models (Langmuir, Freundlich, Temkin, and Elovich) were used to describe the removal mechanism of MB from biomass to establish the relationship between the amount of MB adsorbed and its equilibrium concentration in the solution. The Langmuir, Freundlich, Temkin and Elovich linearized equations are as follows [3], [4], [5], and [6], respectively (5, 16-19):

$$\frac{1}{q_e} = \frac{1}{q_m} + \frac{1}{K_L q_m C_e} \quad [3]$$

$$ln\, q_e = ln\, k_F + \frac{1}{n} ln\, C_e \quad [4]$$

APTEFF, 52, 1-273 (2021) UDC: 66.067.8.081.3:582.542.1:667-12
DOI: https://doi.org/10.2298/APT2152033L BIBLID: 1450-7188 (2021) 52, 33-44
BY-NC-ND
Original scientific paper

$$q_e = \frac{RT}{b_T} ln\, k_T + \frac{RT}{b_T} ln\, C_e \quad [5]$$

$$ln\left(\frac{q_e}{C_e}\right) = ln(K_E q_m) - \left(\frac{1}{q_m}\right) q_e \quad [6]$$

where, C_e (mg/L) is the equilibrium concentration; q_m (mg/g) is the maximum biosorption capacity; K_L (L/mg) is the Langmuir constant; K_F (mg $^{1-1/n}$ $L^{1/n}$ g^{-1}) is the Freundlich constant; n: the intensity of biosorption; K_T (L/mg) is the Temkin isothermal constant; b_T Variation in biosorption energy (J/mol); K_E (L/mg) represents the Elovich equilibrium constant.

BIOSORPTION KINETICS

The biosorption data obtained by experimental methods were fitted for pseudo-first order, pseudo-second order and intraparticle diffusion models (equations 7-9, respectively) to describe and interpret the biosorption process of MB on biomass and to calculate the various parameters that characterize the biosorption kinetics, as follows (16):

$$ln(q_e - q_t) = ln\, q_e - k_1 t \quad [7]$$

$$\frac{t}{q_t} = \frac{1}{k_2\, {q_e}^2} + \frac{1}{q_t} \quad [8]$$

$$q_t = k_{int} t^{0,5} + c \quad [9]$$

where, q_e (mg/g) and q_t (mg/g) are the adsorption capacities at equilibrium and at time t, respectively, while k_1(min^{-1}), k_2 (mg/g min) and K_{int} (mg/g min$^{0.5}$) are the biosorption rate constants of first-order, second-order kinetic and intraparticle diffusion models, and *c* is a constant related to the thickness of the boundary layer.

THERMODYNAMIC STUDY

The thermodynamic parameters of the biosorption process, namely free enthalpy (ΔG°), enthalpy (ΔH°), and entropy (ΔS°) explain the mechanism of the biosorption process of the cationic MB dye by Alfa biomass. The biosorption distribution coefficient (K_d) is given by the equation [10] (21):

$$K_d = \frac{(C_o - C_e)\ V}{C_e\ m} \quad [10]$$

The variation of enthalpy (ΔH^o) and entropy (ΔS^o) can be obtained from the slope and intercept of the ln K_d plot as a function of (1/T) equation [11]. The Gibbs free enthalpy of biosorption is calculated by the equation [12] (22):

$$ln\, K_d = \left(\frac{\Delta S^o}{R}\right) - \left(\frac{\Delta H^o}{RT}\right) \quad [11]$$

APTEFF, 52, 1-273 (2021)
DOI: https://doi.org/10.2298/APT2152033L
BY-NC-ND
UDC: 66.067.8.081.3:582.542.1:667-12
BIBLID: 1450-7188 (2021) 52, 33-44
Original scientific paper

$$\Delta G^o = \Delta H^o - T\Delta S^o \quad [12]$$

where, R (8.314 J /mol K) is the universal gas constant and T is the absolute temperature.

RESULTS AND DISCUSSION

EFFECT OF PH

Several studies have demonstrated that pH is an important factor to determine the biosorption capacity of organic cationic and anionic compounds (22) since it can influence both the adsorbent and adsorbate surface properties. In addition to the biosorption mechanism, it is highly observable that the removal percentage of MB and the biosorption capacity increase with the increase of pH (Fig. 1).

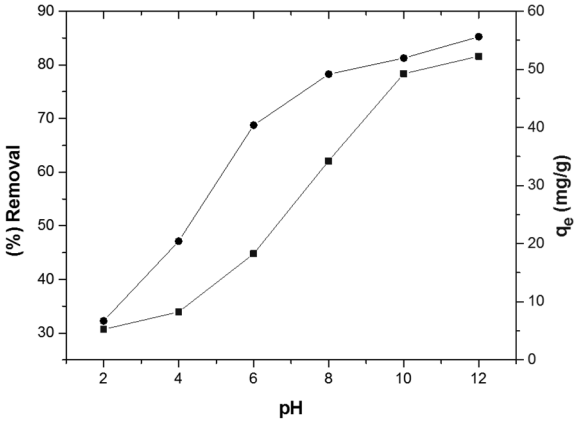

Figure 1. Effect of initial pH on MB removal and biosorption capacity (Co= 25 mg/L, R= 6 g/L, Time = 90 min and T= 298 ± 2 K).

The pKa of MB is 0.04, therefore, methylene blue is completely ionized at a pH above 0.04 and exists in a cationic form (22, 23). The surface of the biosorbent is negatively charged at pH values above pH_{ZPC}= 4.15 (14), which increases the electrostatic attraction of the positively charged dye cations, and hence it increases the biosorption of methylene blue (22, 24). A decrease of biosorption of methylene blue at low pH values was observed, besides, the highest removal percentage (85.54 %) and adsorbed amount (52.45 mg/g) were also obtained at pH=12.

That can be explained by the fact that the electrostatic repulsion between the cations and the positively charged biosorbent surface is present at low pH values, Moreover, the methylene blue cations can replace the ion on the surface of the biosorbent, resulting in an increased biosorption by the ion exchange mechanism (24). The biosorption might be explained by pure electrostatic interactions between the biosorbent negatively charged and the methylene blue positive charge (25). The dye's adsorption capacity depends on both the adsorbent's surface properties and the dye's structure (26-27).

APTEFF, 52, 1-273 (2021) UDC: 66.067.8.081.3:582.542.1:667-12
DOI: https://doi.org/10.2298/APT2152033L BIBLID: 1450-7188 (2021) 52, 33-44
BY-NC-ND
Original scientific paper

EFFECT OF BIOSORBENT DOSE

Fig.2 shows the effect of the Alfa biomass dose on the removal percentage of methylene blue and biosorption capacity. Therefore, it can be noted that the removal percentage of MB increases with the increase of Alfa biomass dose, while the opposite trend is observed for the biosorption capacity. The biosorption percentage of MB increased from 6.92 % to 92.25%, while the optimal dose of Alfa biomass is 6 g/L. The increase in the removal percentage of MB with an increasing ratio (S/L) is mainly due to the growing number of active sites available on the biosorbent surface. According to this curve, it is clear that the dose (S/L) of the biosorbent plays a very important role in the biosorption process.

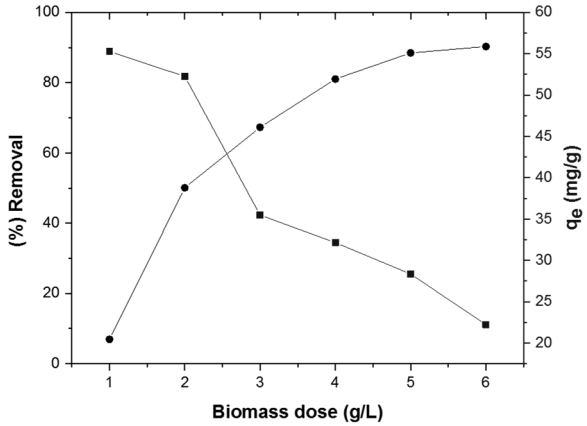

Figure 2. Influence of biosorbent dose on MB removal and biosorption capacity (Co= 25 mg/L, pH=12, R= 1-6 g/L, Time = 90 min and T= 298 ± 2 K).

Retrospectively, the adsorbed amount decreased from 55.27 to 22.43 mg/g. This can be explained by a large number of available active sites that are free in the biosorption medium making the MB cations difficult to approach the biosorption sites due to crowding. In addition, a large dose of biosorbent generates agglomerations of particles.

Furthermore, small quantities of biosorbent could be dispersed in the aqueous phase, facilitating the accessibility of the MB molecules to a large number of free sites of the material. A similar phenomenon was observed by Somasekhara Reddy et al. (2012) (28) in their study of Cango red adsorption on Jujube grains. Reddy attributed the decrease in the amount adsorbed on the adsorbent surface by increasing the initial dose to the establishment of adsorption sites during the process.

EFFECT OF INITIAL MB CONCENTRATION

Figure. 3 shows a rapid increase in biosorption for low concentrations, highest removal (92%) was obtained at C_o = 25 mg/L, and the best biosorption yields are 86.54 %, 81.6%, 75.25%, and 69.47 % for 50, 75, 100 and 125 mg/L respectively. Based on these results, it can be concluded that the optimal concentration was 25 mg/L for the best MB removal efficiency.

APTEFF, 52, 1-273 (2021)
DOI: https://doi.org/10.2298/APT2152033L
BY-NC-ND
UDC: 66.067.8.081.3:582.542.1:667-12
BIBLID: 1450-7188 (2021) 52, 33-44
Original scientific paper

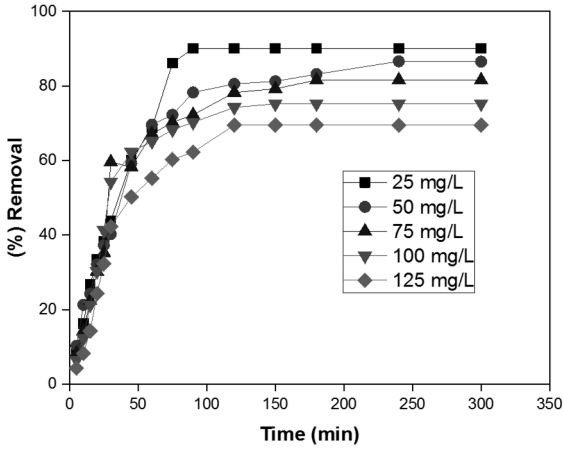

Figure 3. Effect of initial concentration on the removal of MB (R= 6 g/L, pH ~ 12 and T= 298 ± 2 K).

The fixation of the MB cations on the active sites of the biosorbent was rapid due to their low content at low concentration. The increase of the MB concentration can be explained by the rapid saturation of active sites resulting in a decrease in removal efficiency.

EFFECT OF CONTACT TIME

The analysis of the results observed in figure 4 shows that the biosorption kinetics of MB occurring in two phases. The first phase is fast at the beginning of the process due to the high availability of the biomass-free active sites, whereas the second phase becomes slower overtime to reach equilibrium.

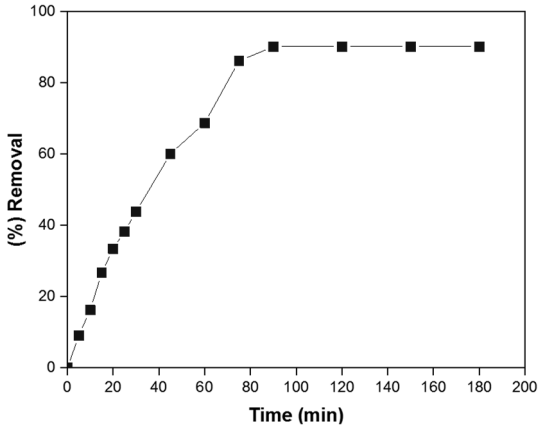

Figure 4. Effect of contact time on the removal of MB (Co= 25 mg/L, R= 6 g/L, pH ~ 12 and T=298 ± 2 K).

APTEFF, 52, 1-273 (2021) UDC: 66.067.8.081.3:582.542.1:667-12
DOI: https://doi.org/10.2298/APT2152033L BIBLID: 1450-7188 (2021) 52, 33-44
BY-NC-ND
Original scientific paper

The large number of free surface sites available is certainly responsible for the high adsorption efficiency at the beginning, while the subsequent deceleration is likely due not only to the decrease in available sites but also to repulsive forces among adsorbed dye molecules and those present in the solution (5). The equilibrium biosorption time is reached after 90 min and efficiency of 92%.

BIOSORPTION ISOTHERMS

The analyses of the results obtained from the biosorption of MB studied on the biomass Alfa (Table 1) demonstrates that the correlation coefficient value (R^2) of the Langmuir isotherm (0.99) is higher than that of Freundlich, Temkin and Elovich. This implies that Langmuir's model is better for the description of the biosorption process of MB on Alfa biomass. The dimensionless factor (R_L) was calculated to confirm that Langmuir's model corresponds to the experimental results and is presented in the form (29):

$$R_L = \frac{1}{1+K_L C_0} \quad [13]$$

The R_L factor was defined by Hall (1966) (29) as the separation factor whereK_L is the Langmuir constant and C_0 is the initial concentration of the MB cations (mg/L). The R_L value indicates the nature of the biosorption process:

- Unfavorable for R_L>1.
- Favorable for $0 < R_L < 1$.
- Irreversible ($R_L = 0$) and Linear ($R_L = 1$).

The R_L values of MB biosorption were $0.011<R_L<0.055$ (Table1), indicating that the biosorption process is favorable. Comparing the current study with other investigations, Table 2 demonstrates different adsorbent materials used in recent research that explains the removal of methylene blue and their adsorption capacities.

Table 1. Isotherms models parameters for the biosorption of MB by *Stipa Tenacissima* L. (Alfa)

Isotherm model	Parameters	Values	
Langmuir	q_m (mg/g)	55.95	
	b (L/mg)	0.68	
	R^2	0.997	
	R_L	$0.011<R_L<0.055$	$25<C_0<125$(mg/L)
Freundlich	K_F (mg $^{1-1/n}$ $L^{1/n}$ g^{-1})	22.87	
	n	4.43	
	R^2	0.842	
Temkin	K_T (L/mg)	3.10	
	b_T	315.61	
	R^2	0.943	
Elovich	q_m(mg/g)	28.23	
	K_E (L/mg)	0.65	
	R^2	0.873	

APTEFF, 52, 1-273 (2021) UDC: 66.067.8.081.3:582.542.1:667-12
DOI: https://doi.org/10.2298/APT2152033L BIBLID: 1450-7188 (2021) 52, 33-44
BY-NC-ND
Original scientific paper

Table 2. Comparison of adsorption capacities of some materials with *Stipa tenacissima* L. in MB removal

Adsorbents	Adsorption capacity (mg/g)	Reference
SW PMMA	97.09	(30)
Kaolin	52.76	(31)
Raz luffa cylindrical	49.46	(32)
Lignite	41.49	(33)
Stipa tenacissima L.	**55.95**	**This study**
Prunuscerasefera (PRUN)	143	(22)

BIOSORPTION KINETIC

Based on the results in Table 3, it can be stated that the pseudo-second order model is the best for describing the biosorption process of MB on the studied biomass since it provided a high value of correlation coefficient ($R^2 > 0.99$).

Table 3. Kinetic parameters for the MB biosorption by *Stipa tenacissima* L. (Alfa).

	Pseudo-first order				Pseudo-second order			Intraparticle diffusion		
C_o (mg/L)	q_e (exp) (mg/g)	q_e (cal) (mg/g)	k_1 (1/min)	R^2	q_e(cal) (mg/g)	k_2 (g /mg.min)	R^2	β	$K_{in} \cdot 10^2$ (mg/g.min$^{0.5}$)	R^2
25	48.49	8.26	0.054	0.815	27.26	0.072	0.997	5.22	12.47	0.799
50	34.27	10.25	0.048	0.824	34.89	0.039	0.994	7.36	31.51	0.825
75	41.58	28.25	0.031	0.789	41.38	0.028	0.997	8.47	58.25	0.902
100	49.89	22.95	0.044	0.799	49.58	0.010	0.998	11.03	76.58	0.858
125	54.25	1575	0.052	0.802	53.99	0.011	0.994	13.25	82.48	0.876

Similarly, it can be noted that the q_e values calculated by the pseudo-second order model are very close to those determined experimentally, which further justifies the fact that the biosorption kinetics are of the pseudo-second order.

Table 4 summarizes the values of free Gibbs enthalpy (ΔG^o), enthalpy (ΔH^o), and entropy (ΔS^o). The analysis of these thermodynamic parameters reveals that the removal of MB by Alfa biomass is a spontaneous reaction ($\Delta G°$). The decrease of $\Delta G°$ with increasing temperature shows that biosorption is more favorable at high temperature. The value of the variation in the entropy of MB biosorption is positive, which means that the molecules in the liquid phase are more organized than those in the solid-liquid interface (34). The positive value of $\Delta H°$ obtained shows that the biosorption process is endothermic.

Table 4. Thermodynamic parameters for the biosorption of MB onto *Stipa tenacissima* L. (Alfa).

ΔH° (kJ/mol)	ΔS° (J/mol K)	ΔG° (kJ/mol)			
T(K)		298	303	313	323
22.52	84.45	-25.73	-25.65	-26.41	-27.24

APTEFF, 52, 1-273 (2021) UDC: 66.067.8.081.3:582.542.1:667-12
DOI: https://doi.org/10.2298/APT2152033L BIBLID: 1450-7188 (2021) 52, 33-44
BY-NC-ND
Original scientific paper

The value of ΔH° indicates that the biosorption of MB on Alfa biomass was controlled by the physiosorption process, it is estimated below 40 kJ/mol. The biosorption process becomes chemical when ΔH° values are comprised between 40 and 120 kJ/mol (30).

CONCLUSION

Moreover, the natural biosorbent *Stipa tenacissima L.* was successfully used for the recovery of MB in an aqueous solution. In addition, optimal conditions for maximum MB removal were determined as follows: pH = 12, biosorbent dose = 6 g/L and initial MB concentrations = 25 mg/L. Optimization of these parameters resulted in a satisfactory removal efficiency and a 92% removal rate was achieved during 90 minutes. As a result, the Langmuir model provided a satisfactory correlation and proved to be the best for describing the biosorption of MB on the surface of the biomass which suggests the formation of a monolayer of the MB dye on the biosorbent surface. The R_L values for the biosorption of MB are less than 1, demonstrating that the biosorption process is favorable. Moreover, the biosorption kinetics of MB generally follows a pseudo-second order law.

The thermodynamic study shows that the biosorption of MB on the biomass used is spontaneous, endothermic and the biosorption process is physical. In summary, this work proves that the available biomass *Stipa tenacissima L.* is a promising biological material for the removal of cationic dyes like MB.

REFERENCES

1. Al-Degs, Y.S.; El-Barghouthi, M.I.; Khraisheh, M.A.; Ahmad, M.N.; Allen, S.J. Effect of surface area, micropores, secondary micropores, and mesopores volumes of activated carbons on reactive dyes adsorption from solution. *Sep. Purifi. Technol.* **2004**, *39*, 97-111.
2. Al-Duri, B.; Khader, K.; McKay, G. Prediction of binary compound isotherm for adsorption on heterogeneous surfaces. *J. Chem. Technol. Biotechnol*. **1992**, *53*, 345-352.
3. Abdel-Ghani, N.T.; El-Chaghaby, G.A.; Helal, F.S. Preparation, characterization and phenol adsorption capacity of activated carbons from African beech wood sawdust. *Global. J. Environ. Sci. Manag.* **2016**, *2*(3), 209-222.
4. Rana, P.; Mohan, N.; Rajagopal, C. Electrochemical removal of chromium from wastewater by using carbon aerogel electrodes. *Water Res*. **2004**, *38* (12), 2811-2820.
5. Mekatel, E.; Amorkrane, S.; Trari, M.; Nibou, D.; Ladjali, S. Combined adsorption/photocatalysis process for the decolorization of Acid Orange 61. *Arabian. J. Sci. Eng.* **2019**, *44*(6), 5311-5322.
6. Senol, A. Amine extraction of chromium (VI) from aqueous acidic solutions. *Sep. Purif. Technol*. 2004, *36* (1), 63-75.
7. Religa, P.; Kowalik-Klimczak, A.; Gieryc, P. Study on the behavior of nanofiltration membranes using for chromium (III) recovery from salt mixture solution. *Desalination.* **2013**, *315*, 115-123.
8. Prakash, N.B.; Sockan, V.; Jayakaran, P. Wastewater treatment by coagulation and flocculation. *Int. J. Eng. Sci. Innov. Techn.* **2014**, *3*(2), 479-484.
9. Toor, M.; Jin, b. isotherm, kinetics, and diffusion of modified natural bentonite for removing diazo dye. *Chem. Eng. J*. **2012**, *187*, 79-88.
10. Kumar, R.; Ahmad, R. Biosorption of hazardous crystal violet dye from aqueous solution onto treated ginger waste (TGW). *Desalination.* **2011**, *265*, 112-118.
11. Abramian, L.; El Rassy H. Adsorption kinetics and thermodynamics of azo-dye Orange II onto highly, porous titania aerogel. *Chem. Eng. J.* **2009**, *150*, 403-410.

BY-NC-ND

12. Yacoumi, S.; Tien, C. Kinetics of Metal Ion Adsorption from Aqueous Solutions. *Kluwer Academic Publisher*. **1995**.
13. Brdar, M. M.; Kukić, D. V.; Šćíban, M. B.; Vasić, V. M.; Prodanović, J. M. Comparison of the generalized and preset-order kinetic equations for description of biosorption data. *Acta Period. Technol.* **2018**, *49*, 11-20.
14. Ladjali, S.; Amokrane, S.; Mekatel, E.; Nibou,D. Adsorption of Cr (VI) on Stipa tenacissima L (Alfa): Characteristics, kinetics and thermodynamic studies. *Sep. Sci. Technol*. **2019**, *54*(6), 876-887.
15. Kannan, N.; Sundaram, M.M. Kinetics and mechanism of removal of methylene blue by adsorption on various carbons - comparative study. *Dye.Pigment*. **2001**, *51*, 25-40.
16. Rangabhashiyam, S.; Anu, N.; Nandagopal, M. G.; Selvaraju.; Environ. N. J. Relevance of isotherm models in biosorption of pollutants by agricultural byproducts. *Chem. Eng.* **2014**, *2* (1), 398-414.
17. Papegowda, P.K.; Syed, A.A. Isotherm, kinetic and thermodynamic studies on the removal of methylene blue dye from aqueous solution using Saw Palmetto spent. *Int. J. Environ. Res.* **2017**, *11*(1), 91-98.
18. Ratnamala, G.M.; Deshannavar, U.B.; Munyal, S.; Tashildar, K.; Patil, S.; Shinde, A. Adsorption of reactive blue dye from aqueous solutions using sawdust as adsorbent: optimization, kinetic, and Equilibrium studies. *Arab. J. Sci. Eng.* **2016**, *41*(2), 333-344
19. Elovich, S.Y.; Larinov, O.G. Theory of adsorption from solutions of non electrolytes on solid (I) equation adsorption from solutions and the analysis of its simplest form (II) verification of the equation of adsorption isotherm from solutions. *Izv. Akad. Nauk. SSSR Otd. Khim. Nauk.* **1962**, *2*(2), 209-216.
20. Gürses, A.; Hassani, A.; KıranYan, M.; AçıYlı, Ö. Karaca, S. Removal of methylene blue from aqueous solution using by untreated lignite as potential low cost adsorbent: Kinetic, thermodynamic and equilibrium approach. *J. Water Process Eng.* **2014**, *2*, 10-21.
21. Aid, A.; Amokrane, S.; Nibou, D.; Mekatel, E.; Trari, M.; Hulea, V. Modeling biosorption of Cr(VI) onto Ulvacompressa L. from Aqueous solution. *Water Sci. Technol.* **2017**, *77*(1), 60-69.
22. Ouldmoumna, A.; Reinert, L.; Benderdouche, N.; Bestani, B.; Duclaux, L. Characterization and application of three novel biosorbents “Eucalyptus globulus, Cynaracardunculus, and Prunus cerasefera” to dye removal. *Desalin. Water. Treat*. **2013**, *51*(16-18), 3527-3538.
23. Weng, C. H.; Lin, Y. T.; Tzeng, T. W. Removal of methylene blue from aqueous solution by adsorption onto pineapple leaf powder. *J. Haz. Mater*. **2009**, *170* (1) 417-424.
24. Seco, A.; Marzal, P.; Gabaldon, C. Study of the adsorption of Cd and Zn onto an activated carbon: influence of pH, cation concentration, and adsorbent concentration. *Sep. Sci. Technol*. **1999**, *34*(8), 1577-1593.
25. Rey-Castro, C.; Lodeiro, P.; Herrero, R.; Sastre de Vicente; Environ, M. E. Acid-base properties of brown seaweed biomass considered as a Donnan gel. A model reflecting electrostatic effects and chemical heterogeneity. *Sci. Technol*. **2003**, *37*(22), 5159-5167.
26. Lin, J. X.; Zhan, S. L.; Fang, M. H.; Qian, X. Q.; Yang, H. Adsorption of basic dye from aqueous solution onto fly ash. *J. Environ. Manage.* **2008**, *87*(1), 193-200.
27. Khattria, S. D.; Singh, M. K. Removal of malachite green from dye wastewater using neem sawdust by adsorption. *J. Hazard. Mater.* **2009**, *167*(1-3), 1089-1094.
28. Somasekhara Reddy, M.C.; Sivaramakrishna, L.; Varada Reddy, A. The use of an Agricultural waste material, Jujuba seeds for the removal of anionic dye (Congo red) from aqueous medium. *J. Hazar Mater.* **2012**, *203*, 118-127.
29. Hall, K.R.; Eagleton, L.C.; Acrivos, A.; Vermeule, T. Pore-and solid-diffusion kinetics in fixed-bed adsorption under constant-pattern conditions. *Ind. Eng Chemi Fundam*. **1966**, *5* (2), 212-223.
30. Dahdouh, N.; Amokrane, S.; Murillo, R.; Mekatel, E.; Nibou, D. Removal of Methylene Blue and Basic Yellow 28 Dyes from Aqueous Solutions Using Sulphonated Waste Poly Methyl Methacrylate. *J. Polym. Environ*. **2020**, *28*(1), 271-283.

BY-NC-ND

31. Mouni, L.; Belkhiri, L.; Bollinger, J. C.; Bouzaza, A.; Assadi, A.; Tirri, A.; Dahmoune, F.; Madani, K.; Remini, H. Removal of Methylene Blue from aqueous solutions by adsorption on Kaolin: Kinetic and equilibrium studies. *Appl. Clay. Sci.* **2018**, *153*, 38-45.
32. Boudechiche, N.; Mokaddem, H.; Sadaoui, Z.; Trari, M. Biosorption of cationic dye from aqueous solutions onto lignocellulosic biomass (Luffa cylindrica): characterization, equilibrium, kinetic and thermodynamic studies. *Int. J. Ind. Chem*. **2016**, *7*, 167-180.
33. Gürses, A.; Hassani, A.; KıranYan, M.; AçıYlı, Ö.; Karaca, S. Removal of methylene blue from aqueous solution using by untreated lignite as potential low cost adsorbent: Kinetic, thermodynamic and equilibrium approach. *J. Water Process Eng*. **2014**, *2*, 10-21.
34. Ho, Y.S. Review of second-order models for adsorption systems. *J. Hazard. Mater.* **2006**, *136*, 681-689.

APTEFF, 52, 1-273 (2021) UDC: 635.74:547.94]:616.252
DOI: https://doi.org/10.2298/APT2152045T BIBLID: 1450-7188 (2021) 52, 45-53
BY-NC-ND
Original scientific paper

IN VIVO AND *IN VITRO* ANTIDIABETIC PROPERTIES OF ALKALOIDS EXTRACT FROM *SALVIA CHUDAEI*

Mohammed Laid TLILI[1,2], Roukia HAMMOUDI[1], Mahfoud HADJ-MAHAMMED[3]*

[1] Department of Biological Sciences, Biogeochemistry of Desert Environments laboratory, Ouargla University, Algeria
[2] Department of Cellular and Molecular Biology, El Oued University, Algeria
[3] Department of Applied Sciences, Biogeochemistry of Desert Environments laboratory, Ouargla University, Algeria

Received: 7 January 2021 **Revised: 19 March 2021** **Accepted: 22 March 2021**

The aim of this study was to evaluate, for the first time, the antidiabetic effect of the alkaloids extract of Salvia chudaei Batt. & Trab. (Lamiaceae) on alloxan-induced diabetic rats. The alkaloids extract was prepared, and the in vitro inhibitory effect of key digesting enzymes related to postprandial hyperglycemia were determined. After acute toxicity test, the Swiss albino rats were induced with alloxan to get experimental diabetes animals. The fasting mean blood glucose, lipid profile, different liver and kidney function biomarkers and antioxidant biomarkers levels, after treatment for 30 days, diabetic untreated and diabetic rats treated with alkaloids extract were estimated. The alkaloids displayed remarkable in inhibiting α-glucosidase (IC50 = 248.25±2.61 µg/ml) than α-amylase (IC50 = 262.96±9.64 µg/ml) activities. In vivo, the results proved that alkaloids extract at dose of 500 mg/kg bw decreased significantly the blood glucose, lipid profile levels and improved the liver and kidney function biomarkers and increased the activities of antioxidant enzymes (superoxide dismutase and gluthatione reductase). This study demonstrates, that alkaloids are effective in inhibiting hyperglycemia and oxidative stress caused by diabetes.

Keywords: *Salvia chudaei*, alkaloids, antidiabetic, alloxan.

INTRODUCTION

Globally, a large number of Medicinal plants are the richest bio-resource of drugs and traditional systems of medicine, modern medicines, nutraceuticals, food supplements, folk medicines, pharmaceutical intermediates and chemical entities for synthetic drugs (1). The active principles responsible for the therapeutic effects of medicinal plants are phytochemicals, usually secondary metabolites, including alkaloids, steroids, flavonoids, terpenoids and tannins etc. (2). The alkaloids compounds have a wide range of biological activities such as antioxidant activity, protection against coronary heart diseases, antidiabetic, anti-inflammatory, anticancer, anti-Alzheimer and antimicrobial activities, which are caused by exposure to oxidative stress (3). Soxhlet extraction is the reference method for extraction of isoquinoline alkaloids, these groups of alkaloids have huge types of medicinal properties like antiviral, antifungal, anticancer, antioxidant, antispasmodic, antidiabetic, antiobesity and an enzyme inhibitor (4). Both the isoquinoline alkaloids extracts of *Fumaria capreolata* and *Fumaria bastardii* showed an antimicrobial, antimalarial, cytotoxic, and anti-HIV activities (5).

* Corresponding author: Mohammed Laid Tlili, Department of Biological Sciences, Ouargla University, BP 511, Ouargla 30 000, Algeria, e-mail: tlili-laid@univ-eloued.dz. https://orcid.org/0000-0003-4423-3992

APTEFF, 52, 1-273 (2021) UDC: 635.74:547.94]:616.252
DOI: https://doi.org/10.2298/APT2152045T BIBLID: 1450-7188 (2021) 52, 45-53
BY-NC-ND
Original scientific paper

Natural antioxidants from plants offer an alternative source of dietary ingredients. For example, α-amylase, α- glucosidase inhibitors are considered as one of the effective measures for regulating type II diabetes by controlling glucose uptake and increasing secretion of insulin hormone, their broad range of biological activities makes many alkaloids prominent starting point for chemical medicinal chemistry (6).

The genus *Salvia* is the largest member of Lamiaceae family comprising more than 1000 species distributed worldwide (7). *Salvia* species have been traditionally used as folk medicine for the management of various diseases and used in food industries such as flavor, spices and food preservation (8). *Salvia chudaei* Batt. & Trab. is an endemic specie, where it grows only in central Sahara, it is a perennial plant are used locally in folk medicine as antidiabetic, antituberculosis, antibronchitis, antipyretic, antirheumatic, insecticidal, cold improver, sexual enhancer, carminative, wound healer, mental and nervous system elevator. The aerial parts were pharmacologically proved to possess hypoglycaemic, antibacterial, and antidiarrhea effects (9, 10). Based on the ethno-medicinal importance and previously published works, this piece of research is designed to investigate the antidiabetic activities of alkaloids of *Salvia chudaei* growing in Algeria.

EXPERIMENTAL

PLANT MATERIAL

The aerial parts of *Salvia chudaei* were collected at full-flowering stage during the spring season of April 2017 from Tamanrasset region in the southern of Algeria, and identified by Dr. HAMMOUDI R. associate doctor, Department of Biological Sciences, University of Ouargla Algeria. A specimen of the plant was deposited in the herbarium (number PM/05) laboratory biogeochemistry desert environments, Ouargla University. The sample was dried in the shade at room temperature for two weeks. After drying, the sample was powdered until a fine powder used for the extraction of alkaloids.

PREPARATION OF THE EXTRACT

Extraction of the alkaloids from aerial part of *Salvia chudaei* was based on previously reported procedures (11). Briefly; 100 g of plant powder are defatted with 300 ml of petroleum ether and alkalized with a 30 ml ammonium hydroxide (0.5 M), the marc is extracted with dichloromethane (500 ml) in Soxhlet for 3 hours, the crude extract was taken up in (150 ml) sulfuric acid three times. The aqueous acid solution was adjusted to pH=9 with concentrated ammonium hydroxide and extracted with ethyl ether (3 x 150 ml). The extracts were dried over anhydrous sodium sulphate and the solvent evaporated to afford a crude extract of alkaloids. The final extract of alkaloids was detected by the Dragendorff reagent (potassium iodide potash) which produced orange precipitate.

IN VITRO ANTIDIABETIC CAPACITY

α-Amylase inhibitory assay

α-Amylase inhibition was assessed by methods described by Odeyemi *et al.,* (12). In brief 15 µl of extract was mixed with 5 µl α-amylase solution, the reaction mixture was pre-

BY-NC-ND

incubated at 37 °C for 10 min. Then, 20 µl water-soluble starch solution (2%) was added and reaction mixture was incubated at 37 °C for 30 min. After incubation, reaction was stopped by 10 µl of HCl (1 mM) and 75 µl iodine-potassium iodide reagent. The absorbance was taken at 580 nm. The negative control was prepared as above without any extract and the percent inhibition of α-amylase enzyme was calculated. As a positive control, acarbose was used.

α-Glucosidase inhibitory assay

Inhibition of α-glucosidase was carried out using the method of Asghari *et al.,* (13) with some modifications. 10 µl of extract was mixed with 20 µl α-glucosidase solution and volume made up to 150 µl with 0.1 M phosphate buffer (pH 6.9). The reaction mixture was pre-incubated at 25 °C for 5 min and then 20 µl p-nitrophenyl-α-D-glucopyranoside (5 mM) solution was added. After the incubation at 37 °C for 15 min, the reaction was stopped by adding 80 µl of sodium carbonate and absorbance was measured at 405 nm. The negative control was rendered in the same manner as the sample above without the extract. Acarbose was used as a positive control. On a percentage basis, α-glucosidase inhibition activity was estimated.

IN VIVO ANTIDIABETIC CAPACITY

Preparation of animals

Wistar male rats (supplied by "Pharmacie Centrale", Tunisia) weighting 180±20 g. All animals were kept in individual metal cages located in the animal laboratory of Sfax University, Faculty of Science at room temperature of 20-22 °C and at 45-55% relative humidity was calibrated for 12 h, for each dark and light period. A standard diet and a tap water were furnished. The experimental procedure was authorized by the Tunisian Ethical Committee for the treatment and use of laboratory animals.

Toxicity study

For the toxicity study, the rats were administered orally at the doses of 100, 200, 500, 1000 and 5000 mg/kg bw in a volume of 10 ml/kg of five groups of rats (n = 7) and the animals were kept under observation for mortality and behavioral changes (14).

Induction of hyperglycemia

The animals were given a single intraperitoneal injection of 150 mg/kg of alloxan monohydrate in isotonic saline and allowed to stabilize for 5 days before blood glucose levels were measured. rats were also given orally 5-10 ml of a 20% glucose solution after 6 h, fllowed by 5% glucose solution for the next 24 h on an as beverage to prevent too severe hypoglycaemia (15). Blood was drawn from a small cut in the tail and blood glucose level was measured at the end of each day with the aid of a one touch glucometer (Bionime, Pharmatec, Tunisia).

APTEFF, 52, 1-273 (2021) UDC: 635.74:547.94]:616.252
DOI: https://doi.org/10.2298/APT2152045T BIBLID: 1450-7188 (2021) 52, 45-53
BY-NC-ND
Original scientific paper

Experimental design

The male rats were divided into four groups, eight in each received the following treatment schedule. Group 1: (T) Normal rats, Group 2: (Alc *S. chudaei*) Normal rats received 500 mg/kg bw of alkaloids of *S. chudaei*, Group 3: (Allox) Alloxan-diabetic rats, Group 4: (Allox + Alc *S. chudaei*) Alloxan-diabetic rats received 500 mg/kg bw of alkaloids of *S. chudaei*. After 30 days, fasting blood glucose concentration was measured and animals were dissected. Blood and pancreas, were collected. Half of the organ were processed for histological examination while the remaining half were preserved for tissue antioxidant enzymes assays.

Body weight changes

Animals were observed for changes in their body weight before starting treatment (day 0) and at the end of study (day 30).

Determination of biochemical parameters

The analyses of serum aspartate transaminase (AST), alanine transaminase (ALT), lactate deshydrogenase (LDH), phosphatase alcaline (PAL), Acide urique, creatinine and urea as well as the levels of total cholesterol (TC), LDL-cholesterol (LDL-C), triglycerides (TG) were performed using the corresponding commercial kits (Biolabo, France) on an automatic biochemistry analyzer (Vitalab Flexor E, USA) at the biochemistry laboratory of Hedi chaker Hospital (Sfax, Tunisia).

About 1 g of excised pancreas was homogenized in 5 ml of phosphate bufer (pH 7.4) and centrifuged at 3500 rpm for 30 min at 4 °C. The supernatant was used for the determination of antioxidant enzymes activities. The activity of superoxide dismutase (SOD) was assayed by the method of Marklund and Marklund, (16). The catalase (CAT) activity was determined by measuring hydrogen peroxide decomposition at 240 nm according to the method described by Aebi, (17). The glutathione Peroxidase (GPx) activity was assayed by the subsequent oxidation of NADPH at 240 nm following the method described by Flohe and Gunzler, (18).

Statistical analysis

All the measurements of each indicator were repeated 3 times and the results were expressed as the mean ± standard deviation. The concentrations of the samples that provide 50% inhibition (IC_{50}) were obtained by interpolation from linear regression analysis. One-way analysis of variance (ANOVA) followed by P value adjustment for multiple comparisons were conducted using the Holm (sequential Bonferroni) correction method. $P<0.05$ was considered statistically significant.

APTEFF, 52, 1-273 (2021)
DOI: https://doi.org/10.2298/APT2152045T
BY-NC-ND
UDC: 635.74:547.94]:616.252
BIBLID: 1450-7188 (2021) 52, 45-53
Original scientific paper

RESULTS AND DISCUSSION

EXTRACTION YIELD

The extraction yield was 0.2%. Recently, modern alternative extraction methods, applied in environmental analysis and in phytochemistry: ultrasonification and microwave-assisted solvent extraction in closed and open systems, accelerated solvent extraction and supercritical fluid extraction (19, 20). The above methods have a stronger penetration of solvents into plant tissues or other solid matrix, are fast and save solvents.

IN VITRO ANTIDIABETIC ACTIVITY

The antidiabetic potential of alkaloids of *S. chudaei* extract were measured via α-amylase and α-glycosidase inhibition experiments. The results were presented in Figure 1.

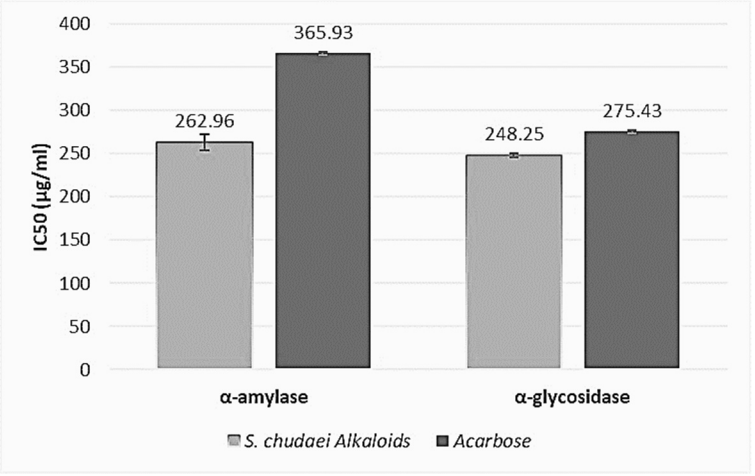

Figure 1. α-amylase and α-glucosidase inhibition potential of *S. chudaei* alkaloids and standard.

The extract of *S. chudaei* exhibited IC_{50} values of 262.96 ± 9.64 µg/ml for α-amylase. This value was found as 248.25 ± 2.61 µg/ml for α-glycosidase. Also, Acarbose was used as the standard antidiabetic drug (IC_{50} = 365.93 ± 1.7 µg/ml and 275.43 ± 1.59 µg/ml in α-amylase and αglucosidase assays, respectively).

The results obtained are in agreement with previous studies on *Salvia syriaca*, all of the tested extracts and essential oil showed strong α-glucosidase and α-amylase inhibitory activity (21). Our data suggest the use of S. chudaei extract, as viable alternatives to pharmaceutical inhibitors of the glycoside hydrolase enzymes. Since this plant extract is well tolerated, relatively inexpensive, and readily available, it has the potential to be used in many applications for glycemic control.

APTEFF, 52, 1-273 (2021) UDC: 635.74:547.94]:616.252
DOI: https://doi.org/10.2298/APT2152045T BIBLID: 1450-7188 (2021) 52, 45-53
BY-NC-ND
Original scientific paper

IN VIVO ANTIDIABETIC ACTIVITY

Acute toxicity test

The acute toxicity study showed that the administration of graded doses of alkaloids extract of *S chudaei* did not generate any observable signs of toxicity up to the dose of 5000 mg/kg. This was confirmed by the absence of significant changes in behaviours such asalertness, motor activity, weight loss, sluggishness, paralysis, breathing, restlessness, diarrhoea, convulsions, and coma. The result proves that the plant extracts had no observable adverse effect at the doses tested; implying that the medium lethal dose (LD_{50}) is greater than 5000 mg/kg.

The first priority in herbal research is an assessment of safety profile of herbal product and setting up a criterion for selecting a safe dose for human use (22). Therefore, $1/10^{th}$ of this dose i.e., 500 mg/kg and below were selected for further detailed studies.

Determination of biochemical parameters and weight gain

Alloxan-induced diabetic rats were treated with alkaloids extracts of *S. chudaei*, once a day orally, for 30 days. The effect of alkaloids extracts on biochemical parameters level is presented in Table 1. The present study was intended to examine the antidiabetic effects of the extract of *S. chudaei* leaves.

Our results showed, decrease in body weight a -70% in diabetic rats as compared to control rats, whereas, increase in body weight was observed in diabetic animals treated with extract (+122 %) for 30 days.

Table 1. shows that alloxan injection induced diabetes in the rats, which was evidenced by a significant increase in their blood glucose level (hyperglycemia) as compared to the controls. The co-treatment of diabetic rats with alkaloids extract was noted to significantly alleviate those high levels of blood glucose.

The treatment of *S. chudaei* extracts on alloxan-induced diabetic rats produced consistent reduction in the blood urea, creatinine and acid uric levels. the levels of total cholesterol, triglyceride and LDL-C levels in alloxan-induced diabetic rats were significantly increased by 72 % ($p<0.01$), 100 % ($p<0.001$) and 168 % ($p<0.001$) compared to the control rats, respectively. However, the TC, TG and LDL-C serum levels were significantly attenuated of the following the treatment with alkaloids extracts. The results of Table 1 shows that the activities of AST, ALT, PAL and LDH recorded for the alloxan-induced diabetic rats underwent significant increases of 130 % ($p<0.001$), 107 % ($p<0.001$), 53 % ($p<0.01$) and 60 % ($p<0.01$), respectively, in comparison with the control rats. The increases recorded for those markers in the diabetic rats were, however, noted to be attenuated to reach normal values following the treatment with *S. chudaei* extract.

The endogenous activities of antioxidant enzymes were determined**.** The findings indicated that, compared to control group of rats, the diabetic rats underwent significant decreases in the SOD (35.5 %), CAT (55 %), and GPx (34 %) activities. Those indicators were noted to be enhanced with alkaloids extracts of *S. chudaei.*

While the proper mechanism of action is still unidentified, earlier experiments have shown that the hypoglycemic effect of alkaloids is by blocking glucose spread across the enteric epithelium, which consequently reduces blood glucose levels (23, 24).

APTEFF, 52, 1-273 (2021) UDC: 635.74:547.94]:616.252
DOI: https://doi.org/10.2298/APT2152045T BIBLID: 1450-7188 (2021) 52, 45-53
BY-NC-ND
Original scientific paper

Table 1. Effect of the alkaloids extract of *S. chudaei* on biochemical parameters and weight gain of different experimental groups of rats.

Parameters	T	Alc *S. chudaei*	Allox	Allox + Alc *S. chudaei*
Weight gain (g)	31.01±0.12	31.1±2.12	9.4± 1.03*	20.9±1.05#
Blood glucose levels (mg/dl)	7.207±0.085	7.117±0.034	25.43±0.598*	15.48±0.626#
AST (UI/L)	52.62±1.37	60.32±0.23	121.1±1.02*	82.75±0.55#
ALT (UI/L)	30.65±0.47	30.3±0.11	63.41±0.75*	47.39±1.07#
PAL (UI/L)	120.3±0.14	123.4±0.33	184.3±0.14*	143.1±1.32#
LDH (UI/L)	201.3±0.19	203.6±1.12	321.6±0.32*	274.3±0.01#
Urea (mmol/l)	6.877±0.22	7.24±0.16	13.23±0.39*	10.11±0.26#
Creatinine (µmol/l)	30.7±0.50	35.37±0.7	43.13±1.2*	33.49±0.79#
Uric acid (µmol/l)	20.7±0.21	20.56±0.17	36.47±1.1*	29.6±0.79#
TC (mmol/L)	2.12±0.05	1.82±0.03	3.65±0.18*	2.21±0.05 #
TG (mmol/L)	1.27±0.03	0.94±0.01	2.54±0.07*	1.63±0.02 #
LDL-C (mmol/L)	0.82±0.08	0.74±0.03	2.2±0.02*	1.41±0.03 #
HDL-C (mmol/L)	1.27±0.09	1.36±0.03	0.69±0.01*	1.1±0.08 #
SOD (U/mg protein)	32.05±0.71	33.0 ± 0.56	20.7±0.51*	27.05±0.91#
CAT (µmol H_2O_2/min/mg protein)	19.15± 0.75	20.5±0.14	8.68±0.05*	15.2±1.83#
GPx (µmol GSH oxidized/min/mg protein)	43.25±2.75	42.4±0.14	28.5±0.14*	36.75±0.91#

Values represent means ± SD (and = 8 for each group).
Values differ significantly at $p<0.05$: ∗ $p<0.05$, compared with normal control rats.
# $p<0.05$, compared with diabetic rats

Lipids play an important role in the hyperglycemic condition. An elevated level of lipid in diabetes induces hypertriglyceridemia and excessive blood cholesterol levels. The level of serum lipid rises in diabetic rats such as cholesterol and triglycerides and therefore elicit coronary heart diseases (25). Insulin usually stimulates the enzyme lipoprotein lipase which metabolized triglycerides (26). The function of insulin is to enhance the deposition of fatty acid into adipose tissue which enhance triglycerides formation and also inhibit lipolysis.

Lipolysis is not prevented in diabetic patients, which usually leads to hyperlipidemia and elevated serum free fatty acid levels due to outflow of free fatty acid from adipose tissue and esterification–triglycerides lipolysis cycle is shift in favor of lipolysis (27). HDL is a lipoprotein that helps to prevent coronary heart disease by inhibiting atherogenesis and shifting cholesterol from peripheral tissues to the liver. The finding of current study revealed that administration of alkaloids extract showed significant improvement in blood lipids and also elevated the HDL-cholesterol level in diabetic rats further confirmed similar results with the previous reported findings (24).

Under normal conditions, hepatocytes possess a powerful antioxidant defence system, including enzymatic antioxidants such as SOD, CAT, and GPx (28). In consistence with these reports, our results showed that alloxane intoxication decreased the liver antioxidant enzymes activities, which could be attributed to the ROS depletion of the above antioxidants or to the suppression of the de novo protein synthesis. The impairment of the liver antioxidant status and overproduction of ROS associated to diabetes mellitus have been demonstrated to inhibit the tricarboxylic acid cycle activity and fatty acid oxidation, thus leading to the increase of serum cholesterol and triglycerides content (29).

APTEFF, 52, 1-273 (2021) UDC: 635.74:547.94]:616.252
DOI: https://doi.org/10.2298/APT2152045T BIBLID: 1450-7188 (2021) 52, 45-53
BY-NC-ND
Original scientific paper

CONCLUSION

From this experimental data, the alkaloids extract from aerial part of *Salvia chudaei* endowed significant blood glucose lowering and also ameliorate others diabetes associated complications. the alkaloids extract also proved effective in the protection of liver, kidney and pancreas tissues from the damages of alloxan induced diabetic rats. The encouraging results for such first antidiabetic effect study of *Salvia chudaei* lead us to enhance more specific investigations to isolate and identify the responsible bioactive molecules in the futuristic research.

Acknowledgements

The authors are grateful to CRBt (National Center of Biotechnology Research, Constantine, Algeria).

REFERENCES

1. Jamshidi-Kia, F.; Lorigooini, Z.; Amini-Khoei, H. Medicinal plants: Past history and future perspective. *Journal of Herbmed Pharmacology.* **2018**, *7*(1), 1-7.
2. Hussein, R.A.; El-Anssary, A.A. Plants Secondary Metabolites: The Key Drivers of the Pharmacological Actions of Medicinal Plants. In Herbal Medicine; Builders, P.F., Eds.; IntechOpen; **2019**; pp 11-30.
3. Shal, B.; Ding, W.; Ali, H.; Kim, Y.S.; Khan, S. Anti-neuroinflammatory Potential of Natural Products in Attenuation of Alzheimer's Disease. *Front. Pharmacol.* **2018***, 9*, 1-17.
4. Dey, P.; Kundu, A.; Kumar, A.; Gupta, M.; Lee, B.M.; Bhakta, T.; Dash, S.; Kim, H.S. Analysis of alkaloids (indole alkaloids, isoquinoline alkaloids, tropane alkaloids). In Recent Advances in Natural Products Analysis; Nabavi, M.S., Eds.; Elsevier; **2020**; pp 505-567.
5. Maiza-Benabdesselam, F.; Khentache, S.; Bougoffa, K.; Chibane, M.; Adach, S.; Chapeleur, Y.; Max, H.; Laurain-Mattar, D. Antioxidant activities of alkaloid extracts of two Algerian species of Fumaria: *Fumaria capreolata* and *Fumaria bastardii*. *Rec. Nat. Prod.* **2007,** *1,* 28-35.
6. Forni, C.; Facchiano, F.; Bartoli, M.; Pieretti, S.; Facchiano, A.; D'Arcangelo, D.; Norelli, S.; Valle, G.; Nisini, R.; Beninati, S.; Claudio Tabolacci, C.; Jadeja, R.N. Beneficial Role of Phytochemicals on Oxidative Stress and Age-Related Diseases. *BioMed Research International*. **2019,** *8748253*, 1-16.
7. Farimani, M.M.; Bahadori, M.B.; Koulaei, S.A.; Salehi, P.; Ebrahimi, S.N.; Khavasi, H.R.; Hamburgerd, M. New Ursane Triterpenoids from *Salvia Urmiensis* Bunge: Absolute Configuration and Anti-Proliferative Activity. *Fitoterapia.* **2015**, *106*, 1-6.
8. Eskandani, M.; Bahadori, M.B.; Zengin, G.; Dinparast, L.; Bahadori, S. Novel natural agents from Lamiaceae family: an evaluation on toxicity and enzyme inhibitory potential linked to diabetes mellitus. *Current Bioactive Compounds.* **2016**, *12*(1), 34-38.
9. Krimat, S., Dob, T.; Toumi, M.; Kesouri, A.; Noasri, A. Assessment of phytochemicals, antioxidant, antimicrobial and cytotoxic properties of *Salvia chudaei* Batt. et Trab. endemic medicinal plant from Algeria. *J. Mater. Environ. Sci.* **2015**, *6*(1), 70-78.
10. Hammoudi, R.; Dehak, K.; Tlili, M.L.; Khenfer, S.; Medjouel, M.; Hadj-Mahammed, M. Biological activities of phenolic extracts of a medicinal plant, endemic to the Algerian Sahara: *Salvia chudaei* Batt. & Trab. *International Journal of Biosciences.* **2017**, *11*(3), 108-115.
11. Zocoler, M.A.; de Oliveira, A.J.B.; Saragioto, M.H.; Grzesuik, V.L.; Vidohi, G.J. Quantitative determination of indole alkaloids of *Tabernaemontana fuchsiaefolia* Apocynaceae. *J. Brazilian Chem Soc.* **2005**, *16*(6B), 1372-77.

BY-NC-ND

12. Odeyemi, S.; Afolayan, A.; Bradley, G. *In vitro* anti-inflammatory and free radical scavenging activities of crude saponins extracted from *albuca bracteata* jacq Bulb. *Afr. J. Tradit Complement Altern Med.* **2015**, *12*(4), 34-40.
13. Asghari, B.; Zengin, G.; Bahadori, M.B.; Abbas-Mohammadi, M.; Dinparast, L. Amylase, glucosidase, tyrosinase, and cholinesterases inhibitory, antioxidant effects, and GC-MS analysis of wild mint *Mentha longifolia* var calliantha essential oil. A natural remedy. *European Journal of Integrative Medicine.* **2018**, *22*, 44-49.
14. Ben Younes, A.; Ben Salem, M.; El Abed, H.; Jarraya, R. Phytochemical Screening and Antidiabetic, Antihyperlipidemic, and Antioxidant Properties of *Anthyllis henoniana* (Coss.) Flowers Extracts in an Alloxan-Induced Rats Model of Diabetes. *Evidence-Based Complementary and Alternative Medicine.* **2018**, *8516302*, 1-14.
15. Jani, D.K.; Goswami, S. Antidiabetic activity of *Cassia angustifolia* Vahl. and *Raphanus sativus* Linn. leaf extracts. *Journal of Traditional and Complementary Medicine.* **2019**, *10*, 1-8.
16. Marklund, S.; Marklund, G. Involvement of the superoxide anion radical in the autoxidation of pyrogallol and a convenient assay for superoxide dismutase. *Eur J Biochem.* **1974**, *47*, 469-474.
17. Aebi, H. Catalase *in vitro*. Oxygen Radicals in Biological Systems*. Methods in enzymology.* **1984**, *105*, 121-126.
18. Flohe, L.; Gunzler, W.A. Assays of glutathione peroxidase. *Methods Enzymol.* **1984**, *105*, 114-121.
19. Djilani, A.; Legseir, B.; Soulimani, R.; Dickob, A.; Younos, C. New Extraction technique for alkaloids. *J Braz Chem Soc.* **2006**, *17*(3), 518-20.
20. Belwal, T.; Pandey, A.; Indra, D.; Bhatt, I.D.; Rawal, R.S. Optimized microwave assisted extraction (MAE) of alkaloids and polyphenols from Berberis roots using multiple-component analysis. *Scientific Reports*. **2020**, *917*, 1-10.
21. Bahadoria, M.B.; Dinparast, L.; Zenginc, G.; Sarikurkcu, C.; Bahadori, S.; Asghari, B.; Movahhedine, N. Functional components, antidiabetic, anti-Alzheimer's disease, and antioxidant activities of *Salvia syriaca* L. *International journal of food properties.* **2017**, *20*(8), 1761-72.
22. Yehya, A.H.S.; Asif, M.; Kaur, G.; Hassan, L.E.A.; Al-Suede, F.S.R.; Abdul Majid, A.M.S.; Oon, C.E. Toxicological studies of *Orthosiphon stamineus* (Misai Kucing) standardized ethanol extract in combination with gemcitabine. *Journal of Advanced Research.* **2018**, *15*, 59-68.
23. Shafi, T.; Sozio, S.M.; Plantinga, L.C. Jaar, B.G.; Kim, E.T.; Parekh, R.S.; Steffes, M.W.; Pow, N.R.; Coresh, J.; Selvin, E. Serum fructosamine and glycated albumin and risk of mortality and clinical outcomes in hemodialysis patients. *Diabetes Care*. **2013**, *36*(6), 1522-33.
24. Jan, N.U.; Ali, A.; Ahmad, B.; Iqbal, N.; Adhikari, A.; Rehman, I.; Ali, A.; Ali, S.; Jahan, A.; Ali, H.; Ali, I.; Ullah, A.; Musharraf, G.S. Evaluation of antidiabetic potential of steroidal alkaloid of *Sarcococca saligna*. *Biomedicine & Pharmacotherapy*. **2018**, *10,* 1-6.
25. Andallu, B.; Kumar, A.V.; Varadacharyulu, N.C. Lipid abnormalities in streptozotocin-diabetes: Amelioration by *Morus indica* L. cv Suguna leaves. *Int J Diab Dev Ctries.* **2009**, *29*(3), 123-128.
26. Andrade, J.M.C. Lipoprotein Lipase: A General Review. *Insights Enzyme Res.* **2018**, *2*(1), 1-14.
27. Trites, M.J.; Clugston, R.D. The role of adipose triglyceride lipase in lipid and glucose homeostasis: lessons from transgenic mice. *Lipids in Health and Disease.* **2019**, *18*, 1-9.
28. Sathya, A.; Siddhuraju, P. Protective effect of bark and empty pod extracts from *Acacia auriculiformis* against paracetamol intoxicated liver injury and alloxan induced type II diabetes. *Food Chem Toxicol.* **2013**, *56*, 162-170.
29. Farombi, E.O.; Ige, O.O. Hypolipidemic and antioxidant effects of ethanolic extract from dried calyx of *Hibiscus sabdariffa* in alloxan-induced diabetic rats. *Fundam Clinic Pharmacol.* **2007**, *21*, 601-609.

APTEFF, 52, 1-273 (2021) UDC: 628.312:551.468.6]:546.4/.8:639.2(72)
DOI: https://doi.org/10.2298/APT2152055R BIBLID: 1450-7188 (2021) 52, 55-62
BY-NC-ND
Original scientific paper

FIRST STUDY OF WATER QUALITY IN THE SAN CAMILO AND MOJAHUEVO ESTUARIES LOCATED IN GUAYAS FOR BEING USED IN AQUACULTURE

René Oscar RODRÍGUEZ-GRIMÓN[1], Juan Diego VALENZUELA-COBOS[1], Juan Carlos ERAZO-DELGADO[1], Ivanna Daniela TERAN NARVAEZ[1], María Fernanda GARCÉS-MONCAYO[2], Ana GRIJALVA-ENDARA[3], José Marcelo TIERRA-ARÉVALO[4]*

[1] Universidad Espíritu Santo - Ecuador
[2] Facultad de Ingeniería, Escuela Ingeniería Ambiental. Universidad Nacional de Chimborazo. Km 1/vía a Guano s/n, Riobamba, 060150. Ecuador
[3] Facultad de Ciencias Químicas, Universidad de Guayaquil- Ecuador
[4] Universidad Tecnológica Indoamérica; Ambato, Ecuador

Received: 24 January 2021 **Revised: 18 February 2021** **Accepted: 23 February 2021**

The water quality of the San Camilo and Mojahuevo estuaries was monitored in the months of April (rainy season) and June (dry season) of 2016. The water of the Mojahuevo estury presented in both seasons the lowest values of turbidity between 17.20 and 33.70 UNT, biochemical oxygen demand being in a range between 14.00 and 19.00 mg/L, zinc content (0.02-0.05 mg/L) and copper content (0.07 mg/L), ammonia content (0.21-0.35 mg/L), fats and oils (0.23-0.29 mg/L), phosphates (0.39-2.34 mg/L) and nitrates (0.84-2.29 mg/L), while the water of the two estuaries San Camilo and Mojahuevo (rainy season) showed similar phenolic content (0.019 mg/L). The results showed that the Mojahuevo estuary presented the high quality of water recommended for being used in productive process like aquaculture due to the low presence of pollutants.

Keywords: Aquaculture, estuaries, heavy metals, pollutants.

INTRODUCTION

Estuaries are bodies of water where the river mouth opens to a marine system, or where seawater dilutes significantly with the freshwater from underground drainage, and as a result, have a salinity between fresh and salty (3). In these ecosystems exist a great exchange of salinity, nutrients, sediments and living organisms; characteristics unique for a diversity of organisms (17). The water in the estuaries is impacted by the intense influence of anthropogenic activity, especially port activities. Estuary like The Gulf of Guayaquil represent 73% of the movement of international traffic ships in public ports of Ecuador (15, 34).

In natural bodies of water like estuaries, the contamination is the highest problem due to the industrial discharges from urban and periurban zones (26). Researches have indicated that in Guayaquil alone 94500 m^3/day were identified, drained directly to the Guayas and Daule rivers; these discharges proceed, for the most part, from the 542 companies in operation (24). The presence of heavy metals of the estuaries has a directly relation in the aquaculture due to the reutilization of this water during the productive cycles (20). The aquaculture is the second economic activity in Ecuador, and has has an average annual growth rate of 8.6% (25, 31). However, this increment in shrimp farms is affected for the

* Corresponding author: René Oscar Rodríguez-Grimón, Universidad Espíritu Santo – Ecuador, Samborondón, Guayas, Ecuador, e-mail: rrodriguez@uees.edu.ec

APTEFF, 52, 1-273 (2021) UDC: 628.312:551.468.6]:546.4/.8:639.2(72)
DOI: https://doi.org/10.2298/APT2152055R BIBLID: 1450-7188 (2021) 52, 55-62
BY-NC-ND
Original scientific paper

quality of the water used in the shrimp culture generating a decline in the economy of the country. Pollution generated by the city of Guayaquil has altered the physical, biochemical characteristics of the estuary such as: salinity, temperature, dissolved oxygen concentrations (DO), heavy metals, and the presence and distribution of benthonic macroinvertebrates (6, 16).

The water of the estuaries in periurban zones of Guayaquil has presented values of dissolved oxygen between 1 and 7 mg/L, with spatial and temporal gradients dependent on nearby population density and seasons (rainy and dry); a surface temperature ranged from 27 to 29 °C, with spatial differences depending on the presence of zones with mangroves or completely deforested and basic pH since 7 to 8, and a salinity rising up to 27% during dry season (5, 19). The reduction in the concentrations of methylmercury in estuary sediments between 2008 and 2014, as well as a spatial gradient of concentration, being greater in the mangroves zone when compared to a recreational beach spot (5). High concentrations of Cd and Pb in the water and sediments of the Salado estuary, exceeding the permissible limits established in the Ecuadorian environmental legislation (19). There are not studies about the quality of water of the estuaries such as: San Camilo and Mojahuevo that is used in different productive processes especially in the shrimp culture.

The aim of this research was evaluated the physical and chemical characteristics of the water of San Camilo and Mojahuevo estuaries during the rainy and dry seasons to determinate the estuary with the highest characteristics for being used in the aquaculture.

EXPERIMENTAL

STUDY AREA

The water quality was evaluated in the San Camilo and Mojahuevo estuaries located in Guayaquil, Ecuador (Table 1).

Table 1. Coordinates (X,Y) of the three sampling sites monitored during the rainy and dry seasons, along the microcuences of Mojahuevo and San Camilo estuaries in Guayaquil, Ecuador.

Treatments	Sites	Coordinates
Mojahuevo	1	0651621, 9751763
	2	0643222, 9753058
	3	0655525, 9751321
San Camilo	1	0632355, 9755797
	2	0631948, 9755905
	3	0630866, 9754852

SAMPLE COLLECTION

For both brackish water micro-basins three sampling sites were established, meeting with criteria of accessibility, representativeness of the soil type, and the closeness to industrial and domestic discharges. The samples were collected in the superficial region during low tide.

APTEFF, 52, 1-273 (2021) UDC: 628.312:551.468.6]:546.4/.8:639.2(72)
DOI: https://doi.org/10.2298/APT2152055R BIBLID: 1450-7188 (2021) 52, 55-62
BY-NC-ND
Original scientific paper

Sampling was made during the two first weeks of April (rainy season) and two last weeks of June (dry season) of 2016, accumulating a total of four campaigns, marking the end of the rainy season where the accessibility for sampling increased substantially after flooding decreased in the season of least precipitation.

PHYSICAL CHARACTERIZATION

The physical variables monitored for the superficial water quality evaluation and that were measured in situ with the use of a multiparameter meter brand HQd Portable were: temperature, turbidity, dissolved oxygen, pH, conductivity and biochemical oxygen demand (BOD) (8, 10, 14, 21).

CHEMICAL DETERMINATION

During the quantification of phosphate, the preparation and analysis of the sample followed the methodology described in Standard Methods 4500-P, sections B and C, using an AQUAMATE spectrophotometer with 100% recovery (30). In the case of ammonia, nitrate and phenols the UV-visible spectrophotometry technique, using HACH equipment and detection limits of 0.01, 2.30 and 0.02 mg/L, respectively (27). For the quantification of trace elements of chlorophenols, organochlorines and organophosphorus, a gas chromatographer coupled to a mass spectrometer (GC/MS) (28). The determinations of polychlorinated biphenyls (PCBs) and total petroleum hydrocarbons (TPH) were done using the gas chromatography technique, using an electron capture detector (GC/ECD) with technology ASTM D4059-00 (2010) for PCBs; and a flame ionization detector (GC/FID) with technology TNRCC (2010) for total petroleum hydrocarbons. Measurements of greases and oils were performed using the partition-gravimetric method with n-hexane as a solvent (29), with a quantification limit was of 0.3 mg/L and recovery of 93.5%. DBO5 was determined with the electrometric method, using Winkler flasks, a multiparameter HACH equipment (30).

HEAVY METALS DETERMINATION

The concentrations of the heavy metals Zn, Pb, Cd and Cu were determined using an ICP (Perkin Elmer Optimal Emission Spectrometer Optima 4300 DV) with an inductive coupling plasma technique, with quantification limits of 0.05, 0.0008, 0.005 and 0.006 mg/L for Zn, Pb, Cd and Cu, respectively. The recovering percentage maintained at 99.5% (12).

STATISTICAL ANALYSIS

In all analyzes, a completely randomized design and the results were studied using one-way analysis of variance (ANOVA) to determine the significance of individual differences at $p<0.05$ level, of the physical characteristics of the water of San Camilo and Mojahuevo estuaries during the rainy and dry seasons, when statistical differences were found, the Duncan Test with $\alpha = 0.05$ was applied. The analyses were carried out using statistical software (SPSS ver. 16).

APTEFF, 52, 1-273 (2021) UDC: 628.312:551.468.6]:546.4/.8:639.2(72)
DOI: https://doi.org/10.2298/APT2152055R BIBLID: 1450-7188 (2021) 52, 55-62
BY-NC-ND
Original scientific paper

RESULTS AND DISCUSSION

PHYSICAL CHARACTERIZATION

The physical variables of the water of the San Camilo and Mojahuevo estuaries during the rainy and dry seasons is presented in the Table 2.

Table 2. Physical characterization in the water of San Camilo and Mojahuevo estuaries located in Guayaquil, Ecuador during the rainy and dry seasons.

Variables	San Camilo		Mojahuevo	
	Rainy season	Dry season	Rainy season	Dry season
Temperature (°C)	29.50±1.04[a]	28.90±3.56[A]	29.50±0.91[a]	27.80±0.154[A]
Turbidity (UNT)	68.50±2.08[b]	128.40±4.94[B]	17.20±2.94[a]	33.70±0.65[A]
Disolved oxygen (mg/L)	3.06±0.04[a]	3.27±0.09[A]	5.84±0.68[a]	5.86±0.08[A]
pH	7.15±0.07[a]	7.38±0.26[A]	7.73±1.16[a]	7.88±0.93[A]
Biochemical oxygen demand (mg/L)	43.00±4.86[b]	47.00±1.49[B]	19.00±0.73[a]	14.00±1.10[A]

* All values are means ± standard deviation of three replicates. Uppercase letters indicate difference between the physical characteristics of the water of the two estuaries during the dry season, while lowercase letters indicate difference between the chemical characteristics of the water of the two estuaries during the rainy season according to Duncan's test ($p < 0:05$), $n = 3$.

The water of the Mojahuevo estuary presented the lowest values of turbidity in the rainy season (17.20 UNT) and in the dry season (33.70 UNT), while the water of the San Camilo estuary showed values of turbidity in the rainy season (68.50 UNT) and in the dry season (128.40 UNT). The water of the two estuaries showed similar statistical values of dissolved oxygen in the rainy season since 3.06 to 3.27 mg/L and in the dry season between 5.84 to 5.86 mg/L. In relation with the biochemical oxygen demand, the water of the of the Mojahuevo estuary presented the lowest values in the dry season (14.00 mg/L) and in the rainy season (19.00 mg/L), whereas the water of the San Camilo estuary exhibited highest values in the rainy season (43.00 mg/L) and in the dry season (47.00 mg/L). Studies have showed that high biochemical oxygen demand (BOD) levels in the water indicate pollution by organic matter, and also have pointed out that the presence of a high BOD is common when it derives from business anthropogenic sources, since industrial discharges from this establishments usually reduce biodegradability or the natural capacity of purification of the water (4, 23). The biodegradability of an industrial discharge is influenced by the presence of natural organic elements (7). The recommended conditions of the water for shrimp culture are: dissolved oxygen since 5.00 to 9.00 mg/L, temperature since 28 to 32 °C and pH values ranged from 7.00 to 8.30 (32). The water of the estuary of Mojahuevo in the two seasons presents the parameters for being used in the aquaculture process.

HEAVY METALS DETERMINATION

Table 3 presents the heavy metals determination of the water of the San Camilo and Mojahuevo estuaries during the rainy and dry seasons.

APTEFF, 52, 1-273 (2021) UDC: 628.312:551.468.6]:546.4/.8:639.2(72)
DOI: https://doi.org/10.2298/APT2152055R BIBLID: 1450-7188 (2021) 52, 55-62
BY-NC-ND
Original scientific paper

Table 3. Heavy metals present in the water of San Camilo and Mojahuevo estuaries located in Guayaquil, Ecuador during the rainy and dry seasons.

Variables	San Camilo		Mojahuevo	
	Rainy season	Dry season	Rainy season	Dry season
Zinc (mg/L)	0.12	0.06	0.02	0.05
Cadmium (mg/L)	<0.001	<0.001	<0.001	<0.001
Lead (mg/L)	0.002	0.005	0.002	0.005
Copper (mg/L)	0.008	0.008	0.007	0.007

The water of the estuary Mojahuevo presented the lowest content of heavy metals (zinc and copper), the content of zinc was 0.02 mg/L in the water during the rainy season and in the dry season was 0.05 mg/L, the content of copper was 0.007 mg/L in the water of the two seasons. For otherwise, the content of lead (0.002 mg/L) was similar in the water of the two estuaries during the rainy season, and the lead content was 0.05 mg/L in the water of the San Camilo and Mojahuevo estuaries in the dry season. The content of cadmium was <0.001 mg/L in water of the two estuaries during the rainy and dry seasons. Metals such as: zinc and copper have similar electron characteristics, but different chemical properties, ion radius, and affinities for biological (33). Cadmium, copper, lead, and zinc present in water may result in a major concern due to their toxicity and carcinogenicity which may cause damage to various systems of the human body (9, 22). Heavy metals present in the water causes multiple direct and indirect effects on practically all physiological processes in plants (18). The variation of concentration of heavy metal from locations to locations is correlated with the flow of the rivers and location of industries and their waste disposal system (1, 2). The maximum values of heavy metals of the water for shrimp culture are: zinc ≤ 100 ppb, lead ≤ 100 ppb, copper ≤ 25 ppb and cadmium ≤ 10 ppb (32). The content of the heavy metals (zinc and lead) is related with the rainy and dry seasons. The water of estuary Mojahuevo in the rainy and dry seasons shows the recommended quality for being used in the shrimp culture.

CHEMICAL CHARACTERIZATION

The chemical characterization of the water of two estuaries during the rainy and dry seasons is presented in the Table 4. Water of the estuary Mojahuevo showed the lowest content of ammonia (0.21 mg/L) in the water during the rainy season and in the dry season was 0.35 mg/L, while the water of the estuary San Camilo presented highest content of ammonia (0.53 mg/L) in the rainy season and in the dry season was 1.29 mg/L. Lowest content of fat and oils was showed in the water of the estuary Mojahuevo in the rainy season was 0.23 mg/L and in the dry season was 0.29 mg/L, whereas the content of fat and oils was presented in the water of the estuary San Camilo in the two seasons was between 0.30 and 0.32 mg/L. Phosphates present in the water of the estuary Mojahuevo showed value of 0.39 mg/L in the rainy season and in the dry season was 2.44 mg/L, while the content of phosphates in the water of the estuary San Camilo in the dry season was 0.77 mg/L in the rainy season and in the dry season was 5.43 mg/L. For otherwise, the lowest nitrates content in the water of the estuary Mojahuevo showed value of 0.84 mg/L in the rainy season and in the dry season was 2.29 mg/L, while the water of the estuary San Camilo presented highest content of ammonia (0.92 mg/L) in the rainy season and in the

BY-NC-ND

dry season was 2.32 mg/L. Phenols content was similar (0.019 mg/L) between the two estuaries in the dry season. The content of ammonia in the most Latin-American estuaries is related to pollution by industrial waters of urban or livestock origin due to is high concentration of organic matter and posterior aerobic bacterial decomposition (13). Studies have pointed out that there are other processes responsible for the presence of phenols in natural waters such as: production of brake linings, abrasive wheels, casting moulds, varnishes, thermic isolation, pesticides, plastics and adhesives (11). The highest levels of nitrates, hydrocarbons, phenols, phosphates and ammonia were found during the dry season in the San Camilo and Mojahuevo estuaries, however the quality of the water of the two estuaries is within the parameters for being used in the aquaculture process.

Table 4. Chemical characterization in the water of San Camilo and Mojahuevo estuaries located in Guayaquil, Ecuador during the rainy and dry seasons.

Variables	San Camilo		Mojahuevo	
	Rainy season	Dry season	Rainy season	Dry season
Phenols (mg/L)	0.006	0.019	0.013	0.019
Ammonia (mg/L)	0.53	1.29	0.21	0.35
Total organochlorines (µg/L)	0.005	<0.002	<0.002	<0.002
Chlorophenols (µg/L)	<0.01	<0.01	<0.01	<0.01
Polychlorinated biphenyls (µg/L)	<0.02	<0.02	<0.02	<0.02
Organophosphorus pesticides (µg/L)	<0.02	<0.02	<0.02	<0.02
Fats and Oils (mg/L)	0.32	0.30	0.23	0.29
Total petroleum hydrocarbons(mg/L)	0.11	0.34	0.05	0.34
Phosphates (mg/L)	0.77	5.43	0.39	2.44
Nitrates (mg/L)	0.92	2.32	0.84	2.29

CONCLUSION

The lowest content of heavy metals (zinc, cadmium, lead and copper) was found in the estuary Mojahuevo during the rainy and dry seasons.

Water of the estuary Mojahuevo presented high quality of water to the cultivation of white shrimp (*Litopenaeus vannamei*) for the lowest content of dissolved organic, content of heavy metals and chemical pollutants.

Acknowledgements

We would like to thank to the Research Center of the Universidad Espíritu Santo – Ecuador, for the financial support conceded for the realization of the project “Niveles de contaminación y aportes de descargas líquidas de los esteros San Camilo y Mojahuevo en la Provincia del Guayas”.

BY-NC-ND

REFERENCES

1. Alam, A.M.S.; Islam, M.A.; Rahman, M.A.; Siddique, M.N.; Matin, M.A. Comparative study of the toxic metals and non-metal status in the major river system of Bangladesh. *Dhaka Univ. J. Sci.* **2003,** *51,* 201-208.
2. Ahmad, M.K.; Islam, S.; Rahman, M.S.; Haque, M.R.; Islam, M. M. Heavy Metals in Water, Sediment and Some Fishes of Buriganga River, Bangladesh. *Int. J. Environ. Res.* **2010,** *4*, 321-332.
3. Bolaños, J.; Montero, N.; Rodríguez, N.; Sánchez, A. Calidad de aguas superficiales: estudio de la quebrada Estero, ubicada en el cantón de San Ramón, Costa Rica. Universidad de Costa Rica. *Rev. Pensamiento Actual.* **2015**, *15*, 61-76.
4. Caicedo, L.; Ortega, J. Evaluación de la calidad del agua del Estuario del Río Atacames en el sector Barrio Nueva Esperanza, para controbuir en la mejora de su potabilización. Tesis de Licenciatura. Universidad de Guayaquil. **2016**, p. 55.
5. Calle, P.; Monserrate, L.; Medina, F.; Calle-Delgado, M.; Tirapé, A.; Montiel, M.; Ruiz, O.; Alvarado, O.; Domínguez, G.; Alava, J. Mercury assessment, macrobenthos diversity and environmental quality conditions in the Salado Estuary (Gulf of Guayaquil, Ecuador) impacted by anthropogenic influences. *Mar. Pollut. Bull.* **2018,** *136*, 365-373.
6. Cárdenas-Calle, M.; Mair, J. Caracterización de macroinvertebrados bentónicos de dos ramales estuarinos afectados por la actividad industrial, Estero Salado-Ecuador. *Rev. Intropica*. **2014**, *9*, 118-128.
7. Cisterna, P.; Peña, D. Determinación de la relación DQO/DBO5 en aguas residuales de comunas con población menor a 25.000 habitantes en la VIII región, **2010**, pp. 1-19.
8. Chávez-Gutiérrez, M.C.; Pérez-Ortega, F.; Felisberti, M. I. Effects of the presence of cellulose and curaua fibers in the thermal and mechanical properties of eco-composites based on cellulose acetate. *Rev. Mex. Ing. Quim*. **2018**, *17*, 533-546.
9. Chungsying, L.; Huantsung, C. Adsorption of zinc (II) from water with purified carbon nanotubes. *Chem. Eng. Sci.* **2006**, *61*, 1138-1145.
10. Cornejo-Ramírez, Y.I.; Carvajal-Millán, E.; Brown-Bojórquez, F.; Sánchez-Villegas, J.A.; Rascón-Chu, A. Pectin hydrogels pH stability as affected by methacrylic grafting to low methoxyl pectin structure. *Rev. Mex. Ing. Quim.* **2019**, *18*, 531-542.
11. Covarrubias, H.; Sáenz, A.; Castañeda, A. Resinas termoestables de Fenol-Formaldehído. *Rev. Iberoam. Polim.* **2016**, *17*, 266-276.
12. Cruz, J.F.; Cruz, G.J.F.; Ainassaari, K.; Gómez, M.M.; Solís, J.L.; Keiski, R.L. Microporous activation carbon made of sawdust from two forestry species for adsorption of methylene blue and heavy metals in aqueous system – case of real polluted water. *Rev. Mex. Ing. Quim.* **2018**, *17*, 847-861.
13. Del Pezo, S.; Chiriguaya, N. Evaluación de la contaminación, físico-química y microbiológica de las aguas del estero salado, ciudadela universitaria de la ciudad de Guayaquil. Tesis de Licenciatura. Universidad de Guayaquil. **2015**, p. 87.
14. Espinosa-Rodríguez, M.A.; Ruiz-Sánchez, T.J.; Hidalgo-Millán, A.; Delgado-Delgado, R. Effect of the hydraulic load of a trickling filter in the nitrification process. *Rev. Mex. Ing. Quim.* **2019**, *18*, 107-113.
15. Félix, F. Organization and social structure of the bottlenose dolphin *Tursiops truncatus* in the Gulf of Guayaquil, Ecuador. *Aquat. Mamm.* **1997**, *23*, 1-16.
16. Fernández-Cadena, J.C.; Andrade, S.; Silva-Coello, C.L.; De La Iglesia, R. Heavy metal concentration in mangrove surface from the north-west coast of South América. *Mar. Pollut. Bull.* **2014**, *82*, 221-226.
17. Hutton, M.; Marrero, A.; Davyt, A.; Muniz, P.; Brugnoli, E. A zambullirse en los problemas de la costa. Facultad de Ciencias–Universidad de la República, Asociación Oceanográfica Uruguaya. Montevideo-Uruguay. **2012**.

BY-NC-ND

18. Kastori, R.; Petrović, M.; Petrović, N. Effect of excess lead, cadmium, copper, and zinc on water relations in sunflower. *J. Plant Nutr.* **1992**, *15*, 2427-2439.
19. Pernía, B.; Mero, M.; Cornejo, X.; Ramírez, N.; Ramírez, L.; Bravo, K.; López, D.; Muñoz, J.; Zambrano, J. Determinación de cadmio y plomo en agua, sedimento y organismos bioindicadores en el Estero Salado, Ecuador. *Enfoque UTE.* **2018**, *9*, 89-105.
20. Pozo-Miranda, F. Presencia de metales pesados cadmio y plomo en el estuario del río Chone-Manabí, Ecuador. *Rev. Ciencia UNEMI*. **2017**, *10*, 123-130.
21. Pradal-Velázquez, M.; Martínez-Trujillo, M.A.; Aguilar-Osorio, G. Cylanases and pectinases of *Aspergillus Flavus* CECT-2687 on different carbon sources and initial pH values. *Rev. Mex. Ing. Quim.* **2018**, *17*, 421-431.
22. Purdom, P.W. Environmental Health. Academic Press, New York. **1980**.
23. Raffo Lecca, E.; Ruiz Liza, E. Caracterización de las aguas residuales y la demanda bioquímica de oxígeno. *Industrial Data*. **2014**, *17*, 71-80.
24. Rivera, V.; Chalen, J. Estudio de las concentraciones por metales pesados e hidrocarburos en el ramal B del Estero Salado. Master Thesis. Universidad de Guayaquil. **2016**, p. 83.
25. Rivera, L.M.; Trujillo, L.E.; Pais-Chanfrau, J.M.; Núñez, J.; Pineda, J.; Romero, H.; Tinococo, O.; Cabrera, C.; Dimitrov, V. Functional foods as stimulators of the immune system of *Litopenaeus vannamei* cultivated in Machala, Province of El Oro, Ecuador. *Ital. J. Food Sci.* **2018**, 227-232.
26. Sousa, E.C.P.M.; Zaroni, L.P.; Gasparro, M.R.; Pereira, C.D.S. Review of ecotoxicological studies of the marine and estuarine environments of the Baixada Santista (São Paulo, Brazil). *Braz. J. Oceanogr*. **2014,** 62.
27. Suárez-García, L.C.; Cuervo-López, F.M.; Texier, A.C. Biological removal of mixtures of ammonium, phenol, cresol isomers, and sulfide in a sequencing batch reactor. *Rev. Mex. Ing. Quim.* **2019**, *18*, 1189-1202.
28. U.S. EPA. Method 8270d. Semivolatile organic compounds by Gas Chromatography/Mass Spectrometry (GC/MS). **1998a.**
29. U.S. EPA. Method 1664, Revision A N-Hexane Extractable Material (HEM; Oil and Grease) and Silica Gel Treated N-Hexane Extractable Material (SGT-HEM; Non-polar Material) by Extraction and Gravimetry. **1998b**.
30. U.S. EPA. Method 200.7 Trace Elements in Water, Solids, and Biosolids by Inductively Coupled Plasma-Atomic Emission Spectrometry. **2001**.
31. Valenzuela-Cobos, J.D.; Vargas-Farías, C.J. Study about the use of aquaculture binder with tuna attractant in the feeding of white shrimp (*Litopenaeus vannamei*). *Rev. Mex. Ing. Quim.* **2020,** *19*, 355-361.
32. Van Wyk, P.; Davis-Hodgkins, M.; Laramore, C.R.; Main, K.; Moutain, J.; Scarpa, J. Farming marine shrimp in recirculating freshwater production systems: a practical manual. FDACS Contract #4520. Florida Department of Agriculture Consumer Services, Tallahassee, FL. **1999**.
33. Woolhouse, H.W. Toxicity and tolerance in the responses of plants to metals, in: Lange, O.L.; Nobel, P. S.; Osmond, C.B.; Ziegler, H. (eds.) Physiologica Plant Ecology III. Encyclopedia of Plant Physiology III, New Series Vol. 12C. Springer-Verlag, New York, NY. **1983**. pp. 245-300.
34. Zografos, K.G.; Martinez, W. Improving the performance of a port system through service demand reallocation. *Transport Res. B-Meth.* **1990**, *24*, 79-97.

APTEFF, 52, 1-273 (2021) UDC: 502.17:542.943:632.951
DOI: https://doi.org/10.2298/APT2152063A BIBLID: 1450-7188 (2021) 52, 63-72
BY-NC-ND
Original scientific paper

DEGRADATION OF AN ORGANOPHOSPHORUS INSECTICIDE IN AQUEOUS MEDIUM BY ELECTRO-FENTON PROCESS

Mirvet ASSASSI[1], Farid MADJENE[2], Abdeltif AMRANE[3]*

[1] Université Mohamed El Bachir El Ibrahimi Bordj Bou Arreridj, Algérie
[2] Unité de Développement des Equipements Solaires, UDES, Centre de Développement des Energies Renouvelables, CDER, 42415, Tipaza, Algérie
[3] Université Rennes 1, Ecole Nationale Supérieure de Chimie de Rennes, CNRS, UMR 6226, 10 Avenue du Général Leclerc, CS 50837, 35708 Rennes Cedex 7, France

Received: 22 February 2021 **Revised: 18 April 2021** **Accepted: 21 April 2021**

This work proposes the remediation of toxic and/or refractory pollutants, such as the organophosphorus insecticide (Phosmet) which cannot be completely degraded by conventional methods like biological treatment, adsorption, flocculation, electro-flocculation, reverse osmosis, ultrafiltration, coagulation. However, these techniques have some disadvantages such as incomplete removal, therefore, the Electro-Fenton process was used. The major factors affecting the removal of Phosmet, namely the current intensity, catalyst concentration (Fe^{3+}), temperature solution, nature of the electrolytes and oxygenation duration of the solution were studied in this work. The optimal operating conditions appeared to be: current intensity 200 mA, 0.5 mmol L^{-1} of Fe^{3+}, T= 20 °C, pH =3 using Na_2SO_4 (50 mmol L^{-1}) as supporting electrolyte and an oxygen supply throughout all the experiments (120 min). Under these optimal conditions, the removal efficiency of the phosmet was 88%.

Keywords: advanced oxidation processes, COD abatement, Electro-Fenton, graphite felt electrode, organophosphorus insecticide, Phosmet

INTRODUCTION

The use of pesticides has improved yields and crop diversity to meet the nutritional demands of the increasing world population. However, this use has also caused indirect and harmful effects on the environment, which were quickly identified (1, 2). Studies have shown the presence of pesticide residues in food (3) and the contamination of groundwater and surface water (4). They are especially toxic for humans (1, 2). Estimating the effects on ecosystems of pesticide-related pollution is difficult because there are a thousand families of pesticides or tens of thousands of active ingredients. Their impact depends on both their mode of action (some are more toxic than others), their persistence over time (some are deteriorating much faster than others) and their by-products of degradation which sometimes are more toxic and degrade more slowly than the parent drug (5).

Some agricultural effluents can achieve high levels of pesticides in the range of 500 mg L^{-1} (6), while the limited concentration established by the fixed pesticide legislation concentration in water is 0.5 μg L^{-1}.

Therefore, it is necessary to treat these effluents containing pesticides before discharging them to the environment, for example, agricultural funds tank effluent and their rinse

* Corresponding author: Mirvet Assassi, Environmental Engineering Department, Faculty of Sciences and Technology, Mohamed El Bachir El Ibrahimi University, Bordj Bou Arreridj, Algeria, e-mail: mirvetassassi@yahoo.com

APTEFF, 52, 1-273 (2021) UDC: 502.17:542.943:632.951
DOI: https://doi.org/10.2298/APT2152063A BIBLID: 1450-7188 (2021) 52, 63-72
BY-NC-ND
Original scientific paper

water. Pesticides are now the source of diffuse pollution that contaminates all inland waters: rivers, groundwater and coastal areas.

When water is polluted with persistent toxic substances, adequate treatment is necessary for the protection of the environment. There are conventional techniques for the removal of pesticides such as physical mass transfer methods (decantation, precipitation, adsorption of pollutants on activated carbon, incineration, or the biological way). The use of traditional methods remains often inefficient in the case of persistent and or toxic pollutants such as pesticides (7).

Other alternatives to degrade recalcitrant organic pollutants are currently the subject of studies, particularly the Advanced Oxidation Processes (AOPs) which proved their efficiency for the removal of Persistent Organic Pollutants (POPs) (8, 9). These oxidative treatment processes can be classified into four categories: chemical oxidation processes in homogeneous phase, photocatalytic processes in homogeneous phase and/or heterogeneous phase, oxidation by sonochemical processes and electrochemical oxidation processes.

Electro-Fenton is an indirect electrochemical AOPs based on the Fenton's reaction, its particularity is to generate in situ hydroxyl radicals ($^{\bullet}OH$) which are powerful oxidizing and capable of breaking down most of the recalcitrant organic compounds into biologically degradable molecules or inorganic compounds such as CO_2 and H_2O. Hydrogen peroxide (H_2O_2) is electrochemically generated in the acid solution containing an amount of Fe^{2+} or Fe^{3+} as a catalyst.

This process is environmentally friendly for wastewater treatment and seems to be promising for the purification of water polluted by persistent and/or toxic organic pollutants including pesticides (10).

The objective of this work is to study for the first time the efficiency of the Electro-Fenton process on the degradation of an organophosphorus insecticide (Phosmet) and to determine the optimal conditions of degradation and mineralization of this latter in an aqueous solution by measuring the chemical oxidant demand (COD) abatement.

EXPERIMENTAL

MATERIALS AND METHODS

Materials

Phosmet (Imidan, $C_{11}H_{12}NO_4PS_2$), is an organophosphorus pesticide, was supplied by Sigma Aldrich (Lyon, France). It is in the form of a white solid crystal used as an insecticide on a large number of insects, which inhibits cholinesterase. Ferric (III) sulfate pentahydrate (> 98%, Fluka), sodium sulfate (anhydrous, 99%, Biochem) used as a supporting electrolyte, sulfuric acid (96%, Carlo Erba) for adjusting the pH of the solution.

Methods

The experiments were conducted at different temperatures (10-50 °C) in volumes of 0.5 L in individual reactors equipped with two electrodes. The cathode is graphite felt (area of 15 cm^2), the anode electrode is made of platinum (8 mm diameter) placed in the reactor

APTEFF, 52, 1-273 (2021) UDC: 502.17:542.943:632.951
DOI: https://doi.org/10.2298/APT2152063A BIBLID: 1450-7188 (2021) 52, 63-72
BY-NC-ND
Original scientific paper

center and in front of the cathode. Before electrolysis air was bubbled through the aqueous solutions for 10 minutes in the solution, which were stirred continuously by a magnetic stirrer (400 rpm), the iron was introduced into the solutions before electrolysis. The initial pH of the solutions was adjusted to 3 with H_2SO_4 (1M) to prevent the precipitation of iron. The pH of the solutions was measured by a pH meter type Sartorius professional meter PR-15.

The ionic strength was kept constant by adding Na_2SO_4 (50 mM). The current was supplied by a generator and displayed continuously throughout the electrolysis using a Multimetrix XA 3051 generator. For reproducibility of the results tests were duplicated.
The evolution of the degradation of Phosmet was analyzed by High-performance liquid chromatography (HPLC) (YL 9100). The samples were filtered before analysis by fiber-glass filters 0.45µm (Mini Sart GF prefilter glass). The HPLC system consisted of a pump 9111Binary YL, an apolar Teknokroma column (Tracer Excel 120 ODSA 5µm, 250 × 0.46 mm) and a UV detector (UV / Vis Detector YL 9120). The quantification takes place at the absorption maximum (230 nm). The column was eluted with a mixture of ultra-pure water-methanol 40:60 (v/v) with a flow rate of 0.9 mL min^{-1}. The COD expressed in mg of oxygen per liter of the sample was performed according to standard NF T90-101 (11).

RESULTS AND DISCUSSION

EFFECT OF THE CURRENT INTENSITY ON THE DEGRADATION OF PHOSMET

The effect of the current intensity on the degradation of organophosphorus insecticide (Phosmet) was investigated at a constant applied current ranging between 60 and 200 mA. Electrolysis reactions were performed in aqueous pesticide solution 25 mg L^{-1} in the presence of 0.5 mM of Fe^{3+}, pH ~ 3 at 20 °C, using Na_2SO_4 (50 mM) as supporting electrolyte.

The curves in Figure 1(a) show that the increase in the intensity of the current applied leads to an increase in the degradation kinetics rate. Indeed, the increase in the intensity of the current applied from 60 to 200 mA, results in an increase of Phosmet elimination rate from 44 to 60% after 60 minutes of electrolysis, indicating an improvement in treatment performance. The increased degradation rates due to the increase in the current intensity can be explained by the excess production of hydrogen peroxide and the increase of ferrous iron regeneration rate in the cathode via equation [1], which causes increased production of hydroxyl radicals according to the equation [2], and therefore increases the efficiency of Electro-Fenton treatment method.

$$Fe^{3+} + e^- \rightarrow Fe^{2+} \quad [1]$$

$$Fe^{2+} + H_2O_2 \rightarrow Fe^{3+} + OH^- + {}^{\bullet}OH \quad [2]$$

APTEFF, 52, 1-273 (2021)
DOI: https://doi.org/10.2298/APT2152063A
BY-NC-ND
UDC: 502.17:542.943:632.951
BIBLID: 1450-7188 (2021) 52, 63-72
Original scientific paper

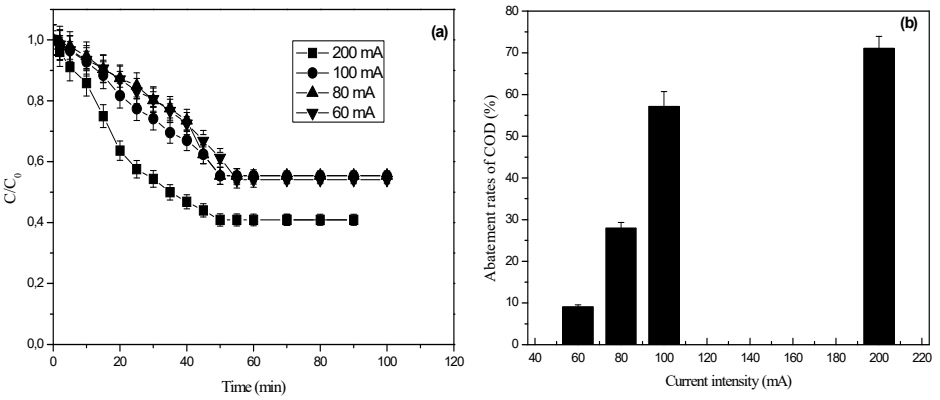

Figure 1. Effect of current applied: (a) on the degradation of Phosmet, (b) on the reduction of COD at pH=3, T=20°C, $[Na_2SO_4]$ =50.10^{-3} mol L^{-1}, $[Fe^{3+}]$ =0.5 mmol L^{-1}.

During the mineralization, for the higher currents, the efficiency of the apparent current decreases progressively with the electrolysis time, by progressive formation of products more difficult to be oxidized (12). Thus, weak currents indicated more for complete mineralization. The mass transfer of Fe^{3+} governs the regeneration of Fe^{2+} which comprises beyond a certain threshold, any additional current is unnecessary and overconsumption of electrical energy. More overabundance of current favors the evolution of H_2 and consequently it reduces the efficiency of current.

We also note that the degradation is not complete, it may be due to the formation of Fe^{2+} species that comes into competition with the radicals $^{\bullet}OH$ according to equation [3].

$$Fe^{2+} + {}^{\bullet}OH \rightarrow Fe^{3+} + OH^{-} \quad [3]$$

Due to this high reactivity, the reaction [3], which consumes hydroxyl radicals, should compete with other reactions, leading to the decrease of the degradation rate of Phosmet.

These results were confirmed by Figure 1 (b), where 200 mA current output gives better performance abatement of COD (71%).

Any additional power is unnecessary and electrical energy consumption. In addition, the current abundance promotes the production of H_2 (Equation 4) which reduces therefore the effectiveness of current.

$$2H_2O + 2e^{-} \rightarrow H_2 + 2OH^{-} \quad [4]$$

STUDY OF THE EFFECT OF THE INITIAL CONCENTRATION OF THE CATALYST

Another important factor affecting the Electro-Fenton process is the Fe^{3+} ions concentration. A series of experiments were therefore carried out to assess the optimal Fe^{3+} ions concentration by varying its concentration from 0.1 to 1 mmol L^{-1}. The experiments were carried out with 25mg L^{-1} of Phosmet, 200 mA, 25 °C, pH = 3 and 50 mmol L^{-1} of Na_2SO_4. The results are shown in Figures 2(a) and 2(b).

APTEFF, 52, 1-273 (2021)
DOI: https://doi.org/10.2298/APT2152063A
BY-NC-ND
UDC: 502.17:542.943:632.951
BIBLID: 1450-7188 (2021) 52, 63-72
Original scientific paper

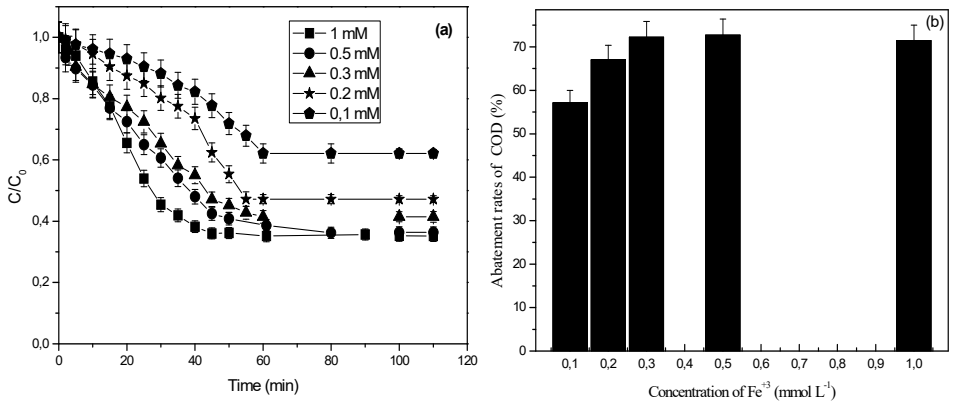

Figure 2. Effect of catalyst concentration: (a) on the degradation of phosmet, (b) on the reduction of COD at pH= 3, T= 20 °C, [Na_2SO_4] = 50 mmol L^{-1}, I= 200mA.

Figure 2(a) shows that the degradation yield of Phosmet increases with the increase of Fe^{3+} concentration. It reaches its maximum for a concentration of Fe^{3+} equal to 0.5 mmol L^{-1}. The fact that a higher rate of degradation of Phosmet is obtained at a higher concentration of catalyst is mainly attributed to the high production of hydroxyl radicals in the presence of a higher concentration of catalyst in the reaction medium (13, 14). An optimal degradation of pesticides can therefore be obtained by increasing in parallel with the concentration of the two reagents. However, too much excess of reagents can become a limiting factor, Fe^{2+} and H_2O_2 may act as radical traps and inhibit the reaction of Fenton, Chan and Chu,(14) explain this result by the fact that the radicals $^{\bullet}OH$ not consumed by the pesticide are then trapped by excess H_2O_2 rather than Fe^{2+}. The latter then remains available to produce the hydroxyl radicals. They also found that an excess of ferrous iron relative to hydrogen peroxide causes slow degradation, with iron becoming a major radical trap.

Furthermore, it is noted that the degradation efficiency decreases substantially when the catalyst concentration increases from 0.5 to 1 mmol L^{-1} after 60 minutes, a result confirmed by the COD values Figure 2(b). This is due to the excess Fe^{2+} which can consume hydroxyl radicals, according to equation [3] (13, 15, 16).

The implementation of a greater amount does not increase these yields. It indicates that we reach a threshold limit, in this procedure, beyond which hydrogen peroxide acts as a radical trap.

EFFECT OF TEMPERATURE ON THE DEGRADATION OF PHOSMET.

Several previous studies have shown the effect of temperature on the performance and efficiency of the Electro-Fenton process (17, 18). Experimental results of COD abatement evolution during treatment at various temperatures, namely, 10, 20, 30 and 50 °C are displayed in Figure 3.

APTEFF, 52, 1-273 (2021)
DOI: https://doi.org/10.2298/APT2152063A
BY-NC-ND
UDC: 502.17:542.943:632.951
BIBLID: 1450-7188 (2021) 52, 63-72
Original scientific paper

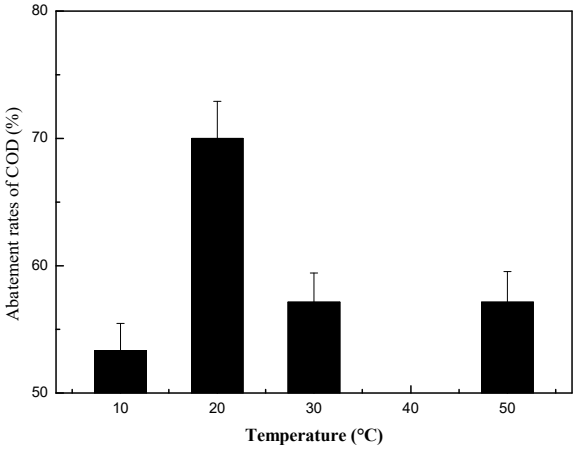

Figure 3. Effect of temperature on the reduction of COD at pH=3, $[Fe^{3+}]$ = 0.5 mmol L^{-1}, $[Na_2SO_4]$ = 50 mmol L^{-1}, I= 200mA.

From there, we will give only the results of the COD which are in our opinion a more relevant analysis than just follows the degradation of Phosmet (a global setting that gives an idea of degradation but also of mineralization).

Figure 3 shows that the degradation efficiency is promoted by raising the temperature from 10 to 20 °C then decreased after 20 °C. The rate of degradation increases from 53 to 70% when the temperature increases from 10 to 20 °C, this result shows that the oxidation reaction of Phosmet by hydroxyl radicals is promoted by increasing the temperature. Indeed, the temperature of the solution influences the electron transfer rate and the mass transfer rate and therefore affects the regeneration of the ferrous iron levels (13). However, we notice a decrease in the rate of reduction of COD at elevated temperature (> 20 °C). Wang et al, (16) have shown that an increase in the temperature affects negatively the production of hydrogen peroxide and consequently the efficiency of the Electro-Fenton process; they explained that this fact is due to low dissolved oxygen concentration and self-decomposition of hydrogen peroxide (19). Indeed, the concentration of hydrogen peroxide decreases with increasing temperature, due to the decreased solubility of oxygen (19).

Temperature variation has two opposing effects against Electro-Fenton reaction. From a certain value, any increase in temperature will have more adverse effects on the mineralization process than positive effects.

EFFECT OF OXYGENATION DURATION

The effect of oxygenation duration was also studied, the experiments were conducted under the following conditions: 25 mg L^{-1} of Phosmet, I = 200 mA, 0.5 mmol L^{-1} of Fe^{3+}, T= 20° C, pH = 3 and 50 mmol L^{-1} of Na_2SO_4. The amount of air (oxygen) added 10 min before the start of the electrolysis, is not sufficient; therefore, we can see in Figure 4 that bubbling air all over experience increases the yield of degradation up to 88%.

APTEFF, 52, 1-273 (2021)
DOI: https://doi.org/10.2298/APT2152063A
BY-NC-ND
UDC: 502.17:542.943:632.951
BIBLID: 1450-7188 (2021) 52, 63-72
Original scientific paper

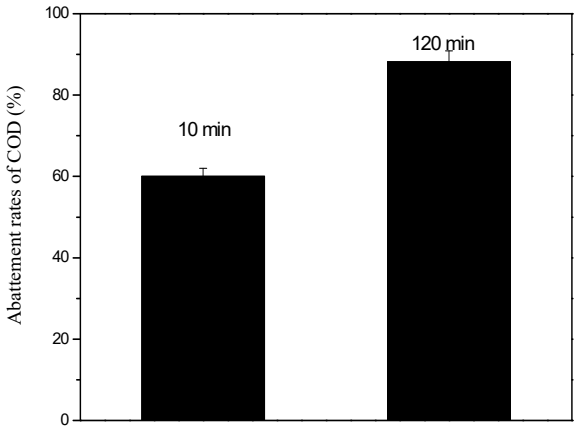

Figure 4. Effect of oxygenation duration on reduction of COD at pH= 3, T= 20 °C, $[Fe^{3+}]$ = 0.5 mmol L^{-1}, $[Na_2SO_4]$ = 50 mmol L^{-1}, I= 200mA.

In fact, oxygen is a limiting factor, which is responsible for the formation of H_2O_2 in the solution by reduction of oxygen at the cathode according to the following reaction:

$$O_2\,(g) + 2H^+ + 2e^- \rightarrow H_2O_2 \qquad [5]$$

EFFECT OF THE NATURE OF THE SUPPORTING ELECTROLYTE

The type of supporting electrolyte is also an important parameter in the Electro-Fenton process. Indeed, the addition of an electrolyte in a solution can affect the treatment because it changes the conductivity of the solution, facilitates the passage of electric current and reduces the energy cost of the process. The addition of the supporting electrolyte helps to improve the conductive properties of the solution. This results in increasing the amount of hydroxyl radicals formed and therefore increasing the process efficiency (20).

The effect of various electrolytes on the degradation of Phosmet such as Na_2SO_4, NaCl, $MgSO_4$, $CaCl_2$ has been examined at a concentration of 50 mmol L^{-1} and the other parameters are maintained at their optimal values. The results are shown in Figure 5.

We note that the rate of reduction of COD depends on the nature of the electrolyte, the yield pass from 19% when using $CaCl_2$ to 88% when using Na_2SO_4 as a supporting electrolyte.

In the presence of halide salts (Cl^-), the degradation rate decreases, whereas it is more pronounced with sodium sulfate. This can be explained because the electrolytes halides inhibit degradation by consumption of $^{\bullet}OH$ by chloride ions according to the equations [6] and [7].

$$OH + Cl^- \rightarrow ClOH^{\bullet-} \qquad [6]$$

After that, the radical anion $ClOH^{\bullet-}$ can be consumed according to the reaction:

$$ClOH^{\bullet-} + Fe^{2+} \rightarrow Cl^- + OH^- + Fe^{3+} \qquad [7]$$

APTEFF, 52, 1-273 (2021)
DOI: https://doi.org/10.2298/APT2152063A
BY-NC-ND
UDC: 502.17:542.943:632.951
BIBLID: 1450-7188 (2021) 52, 63-72
Original scientific paper

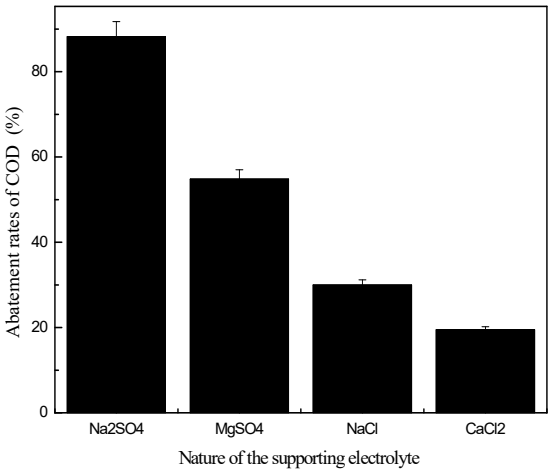

Figure 5. Effect of the nature of the supporting electrolyte in the COD at pH= 3, T= 20 °C, $[Fe^{3+}]$ = 0.5 mmol L^{-1}, I= 200 mA.

Also, El-Desoky et al. (21) showed that the degradation of organic material is more rapid in solutions containing Na_2SO_4, and that this may be due to the increased conductivity of the medium (22).

The higher degradation efficiency of Phosmet was obtained with Na_2SO_4. This result is consistent with those obtained by Gallegos-Alverez and Pletcher. (23) and Brillas et al. (24), who concluded that the sodium sulfate, in addition to increasing the conductivity of the medium accelerates the electron transfer that is beneficial to the Electro-Fenton reaction. This electrolyte salt is commonly used by different research teams working on the Electro-Fenton process (25). Thus, for all the reasons presented above and also to avoid the production of toxic and carcinogenic chlorinated species (26), Na_2SO_4 was chosen as a supporting electrolyte in our study.

CONCLUSION

The study of various parameters (current intensity, catalyst concentration, temperature, nature of the electrolytes and oxygenation duration) may influence the degradation of Phosmet by the Electro-Fenton process. The rise of the intensity of the applied current from 60 to 200 mA, results in an increase of Phosmet elimination rate from 44 to 60%. The degradation yield of Phosmet increases with the increase of Fe^{3+} concentration, it reaches its maximum for a concentration of Fe^{3+} equal to 0.5 mmol L^{-1}. The maximum of degradation (up to 88%) are obtained under optimal operating conditions: concentration of Fe^{3+} equal to 0.5 mmol L^{-1} at acidic pH (pH~ 3), T = 20 °C, 50 mmol L^{-1} of Na_2SO_4 and an oxygen supply throughout all the experiment (120 min). The temperature of 20 °C seems a suitable temperature for the Electro-Fenton treatment.

APTEFF, 52, 1-273 (2021) UDC: 502.17:542.943:632.951
DOI: https://doi.org/10.2298/APT2152063A BIBLID: 1450-7188 (2021) 52, 63-72
BY-NC-ND
Original scientific paper

REFERENCES

1. Meyer, A.; Chrisman, J.; Moreira, J.C.; Koifman, S. Cancer mortality among agricultural workers from Serrana Region, state of Rio de Janeiro. Brazil. *Environ Res*. **2003**, 93, 264-271.
2. Viel, J.F.; Challier, B.; Pitard, A.; Pobel, D. Brain cancer mortality among French farmers: the vineyard pesticide hypothesis. *Arch. Environ. Health*. **1998,** *53*, 65-70.
3. Cunnif, P. Official methods of analysis of AOAC International. 16th Edition. Editor: Arlington, V.A. AOAC international. **1995**, ISBN/ISSN 0935584544.
4. Di Corcia, A.; Marchetti, M. Method Development for Monitoring Pesticides in Environmental Waters: Liquid-Solid Extraction Followed by Liquid chromatography. *Environ. Sci. Technol*. **1992**, *26*, 66-74.
5. Forman, S.; Novák, J.; Tykva, R.; Kás, J.; Wimmer, Z.; Ruml, T. Evaluation of toxicity of pesticides and their biodegradation products using human cells. *Chemosphere*. **2002**, *46*, 209-217.
6. Chiron, S.; Fernandez-Alba, A.R.; Rodriguez, A.; and Garcia-Calvo, E. Pesticide chemical oxidation: state of the art. *Water Res*. **2000**, *34* , 366-377.
7. Oturan, M.A.; Brillas, E. Electrochemical advanced oxidation processes (EAOPs) for environmental applications. *Portugaliae Electrochimica Acta*. **2007**, *25*, 1-18.
8. Sirés, I.; Brillas, E. Remediation of water pollution caused by pharmaceutical residues based on electrochemical separation and degradation technologies. A review. *Environ.Int*. **2012**, *102*, 212-229.
9. Moreira, F.C.; Boaventura, R.A.R.; Brillas, E.; Vilar, V.J.P. Electrochemical advanced oxidation processes - A review on their application to synthetic and real wastewater. *Appl. Catal. B*. **2017**, *202*, 217-261.
10. Oturan, M.A.; Oturan, N.; Lahitte, C.; Trevin, S. Production of hydroxyl radicals by electrochemically assisted Fenton's reagent - application 279 to the mineralization of an organic micropollutant, pentachlorophenol. *J. Electroanal. Chem*. **2001**, *507* (1-2), 96-102.
11. Qualité de l'eau - Détermination de la demande chimique en oxygène (DCO). AFNOR NF T90-101 février 2001.
12. Oturan, M.A. An ecologically effective water treatment technique using electrochemically generated hydroxyl radicals for in situ destruction of organic pollutants: application to herbicide 2,4-D. *Journal of Applied Electrochemistry* . **2000**, *30* (4): 475-482.
13. Panizza, M.; Cerisola, G. Electro-Fenton degradation of synthetic dyes, *Water Res*. **2009**, *43*, 339-344.
14. Chan, K.H.; Chu, W. Modeling the reaction kinetcs of Fenton's process on the removal of atrazine. *Chemosphere*. **2003**, *51*, 305-311.
15. Sedlak, D.L.; Andren, A.W. Oxidation of chlorobenzene with Fenton's reagent. *Environ Sci Technol*. **1991**, *25*, 777-782.
16. Edelahi, M.C. Contribution à l'étude de dégradation in situ des pesticides par procédés d'oxydation avancés faisant intervenir le fer Application aux herbicides phénylurées, Thèse de Doctorat, Université de Marne-la-Vallée. **2004.**
17. Qiang, Z.; Chang, J.H., Huang, C.P. Electrochemical regeneration of Fe^{2+} in Fenton oxidation processes. *Water Res*. **2003**, *37*, 1308-1319.
18. Wang, C.T.; Hu, J.L.; Chou, W.L.; Kuo, Y.M. Removal of color from real dyeing wastewater by Electro-Fenton technology using a three-dimensional graphite cathode. *J Hazard Mater.* **2008**, *152*, 601-606.17.
19. Wang, C.T.; Chou, W.L.; Chung, M.H.; Kuo, Y.M. COD removal from real dyeing wastewater by electro-Fenton technology using an activated carbon fiber cathode. *Desalination*. **2010**, *253*, 129-134.
20. Wang, Y.R.; Chu, W. Degradation of 2,4,5-trichlorophenoxyacetic acid by a novel Electro-Fe(II)/Oxone process using iron sheet as the sacrificial anode. *Water Res*. **2011**, *45*, 3883-3889.

BY-NC-ND

21. El-Desoky, H.S.; Ghoneim, M.M.; Zidan, N.M. Decolorization and degradation of Ponceau S azo-dye in aqueous solutions by the electrochemical advanced Fenton oxidation. *Desalination*. **2010**, *264*, 143-150.
22. Kashefialasl, M.; Khosravi, M.; Marandi, R.; Seyyedi, K. Treatment of dye solution containing colored index acid yellow 36 by electrocoagulation using iron electrodes. *Int. J. Environ. Sci. Technol*. **2006**, *2*, 365-371.
23. Alverez-Gallegos, A.; Plecther, D. The removal of low-level organics via hydrogenperoxide formed in a reticulated vitreous carbon cathode cell. Part 2: The removal of phenols and related compounds from aqueous effluents. *Electrochem. Act.* **1999**, *44*, 2483-2492.
24. Brillas, E.; Banos, M.A.; Garrido, J. Mineralization of herbicide 3,6-dichloro-2-methoxybenzoic acid in aqueous media by anodic oxidation, electro-Fenton and photoelectro-Fenton. *Electrochim. Acta.* **2003**, *48* (12), 1697-1705.
25. Brillas, E.; Baños, M.Á.; Skoumal, M.; Cabot, P.L.; Garrido, J.A.; Rodríguez, R.M. Degradation of the herbicide 2,4-DP by anodic oxidation, electro-Fenton and photoelectro-Fenton using platinum and boron-doped diamond anodes. *Chemosphere*. **2007**, *2*, 199-209.
26. Malpass, G.R.P.; Miwa, D.W.; Mortari, D.A.; Machado, S.A.S.; Motheo A.J. Decolorisation of Real Textile Waste Using Electrochemical Techniques: Effect of the Chloride Concentration. *Water Research.* **2007**, *41*(13), 2969-77.

APTEFF, 52, 1-273 (2021) UDC: 628.316.12:66.021.3.081.3
DOI: https://doi.org/10.2298/APT2152073T BIBLID: 1450-7188 (2021) 52, 73-88
BY-NC-ND
Original scientific paper

CHARACTERIZATION OF NEW ADSORBENT PREPARED FROM APRICOT STONES ACTIVATED CARBON MIXED WITH AMORPHOUS SiO_2 FROM ALGERIAN DIATOMITE FOR REMOVAL OF *p*-NITROANILINE

Hayet TIZI[1], Tarek BERRAMA[1], Djamila HAMANE[1], Fatiha FERRAG-SIAGH[1,2], Zoubida BENDJAMA[1]*

[1] Laboratory of Industrial Process Engineering Sciences, University of Sciences and Technology Houari Boumediene BP 32, El-Alia, 16111, Bab-Ezzouar, Algiers, Algeria
[2] Faculty of Sciences, Department of Chemistry, University Mouloud Mammeri, Tizi-Ouzou 15000, Algeria

Received: 17 March 2021 **Revised: 30 April 2021** **Accepted: 04 May 2021**

This work aims to evaluate the adsorption efficiency of p-nitroaniline (PNA) onto apricot stones activated carbon (ASAC) mixed with treated extract of amorphous SiO_2 (TEAS), prepared from Algerian diatomite (AD). The best removal percentage (85%) is obtained for a ratio ASAC/TEAS (1/1). Adsorbent characteristics are investigated by the Brunauer-Emmett-Teller (BET), the scanning electron microscope (SEM), infrared spectroscopy (IR), X-ray fluorescence (XRF) and X-ray diffraction (XRD). The impregnation of TEAS and ASAC produces good adsorbent properties towards PNA especially in the ratio (1/1) and an increase in the specific surface. The isotherm data are well fitted by the Langmuir and Freundlich models. The maximum PNA uptake obtained is 94.34 mg g^{-1}. The performances of ASAC/TEAS for the PNA adsorption were compared with some adsorbents previously studied for the same purpose, and results show that the composite in the present work exhibit better performances. The adsorption behavior of the concerned material is explained on the basis of its chemical nature and porous texture.

Keywords: Low-cost adsorbents, adsorption, wastewater treatment, adsorption isotherm models, analysis of products, removal percent.

INTRODUCTION

p-Nitroaniline (PNA) is an important compound used as intermediate or precursor in the organic synthesis of azo dyes, antioxidants, fuel additives, corrosion inhibitors, pesticides, antiseptic agents and pharmaceuticals (1-5). However, the presence of PNA in water, even at very low concentrations, is extremely harmful to the aquatic life and human health in terms of hematoxicity, splenotoxicity and nephrotoxicity (6, 7). Many treatment processes, such as advanced oxidation process (8, 9), electrosorptive photocatalytic degradation (10) and biodegradation (11, 12) were used to remove PNA from industrial wastewaters. Unfortunately, they have proved to be inefficient at low concentrations, costly and usually cause secondary pollution. Indeed, due to the presence of nitro group in the aromatic ring, PNA is resistant to chemical and biological oxidation, and the anaerobic degradation by the microorganisms produces nitroso and hydroxylamines compounds which are known as carcinogenic (13). Therefore, the purification of water polluted with PNA is a great challenge to environmental scientists and engineers, and new cost-effective technologies for

* Corresponding author: Hayet Tizi, Laboratory of Industrial Process Engineering Sciences, USTHB, BP 32, El-Alia, 16111, Bab-Ezzouar, Algiers, Algeria, e-mail: thayet2@yahoo.fr

APTEFF, 52, 1-273 (2021) UDC: 628.316.12:66.021.3.081.3
DOI: https://doi.org/10.2298/APT2152073T BIBLID: 1450-7188 (2021) 52, 73-88
BY-NC-ND
Original scientific paper

PNA removal are crucial for the today's world. Adsorption process is widely used because of its simple design, easy operation, low cost, and relatively simple regeneration of the adsorbent. In this respect, varieties of adsorbents were tried to remove PNA from wastewaters (3, 6, 14, 15).

A large number of low-cost adsorbents were reported in the literature for the removal of undesirable organic and inorganic molecules. Among these adsorbents may be cited extracted chitin from shrimp shell (16), apricot stone (17-20), graphene and graphite nanoparticles (21), bentonite (22) and chitosan (23). Activated carbon prepared from agricultural by-product was the most widely used adsorbent in wastewater treatment because of its well-known adsorption capacity, hydrophobic property, high surface area and porous structure (17, 24). Also, due to its high porosity, high permeability, small particle size, abundant availability and low cost, the diatomite was used as adsorbent for organic and inorganic molecules removal from wastewater (24).

Very often, in adsorption process, only one type of adsorbent is used to remove pollutant, but no research works were dedicated to exploring the synergistic effect of adsorbents composite for this same focus.

In this framework, the two materials constituting the mixture are the activated carbon prepared from agricultural residue, and the treated extract of amorphous SiO_2 (TEAS) prepared from Algerian diatomite (AD). Both precursors of the adsorbents are locally available, which is an important advantage to implement an economic process to wastewater treatment contaminated by this type of pollutant.

The fact that the pollutant studied was never treated by adsorbent mixture prepared in this work, the adsorption in batch mode of PNA on a new mixture of two low-cost and available adsorbents, consisting of activated apricot stones carbon and treated extract of the amorphous Algerian diatomite SiO2, was considered as an interesting investigation area that must be developed.

EXPERIMENTAL

MATERIALS

All chemicals used in the experimental study were of analytical grade quality. The p-nitroaniline (PNA) (> 98% purity) was provided from Sigma Aldrich Co. H_3PO_4 (98%), HCl (37%), NaOH and $NaNO_3$ (> 99% purity) were purchased from Merck Company. The Silver nitrate (> 99% purity) was provided from Sigma Aldrich Co. Distilled water (0.9 MΩ cm) was used for preparing the stock and test solutions.

ANALYSIS METHODS

The chemical composition of prepared samples was examined by X-ray fluorescence (XRF, Bruker-Axs: SRS 3400). The morphology of the adsorbent composite ASAC/TEAS was obtained by scanning electronic microscopy (SEM) using a Philips XL 20 Welton Joanne, 1950. The X-ray diffraction (XRD) was performed with a Phillips PW 1710 diffractometer; FT-IR analyses were performed within the frequency range (400-4000 cm^{-1}) with Perkin Elmer Spectrum equipment. The Brunauer-Emmett-Teller (BET) (Quantachrome AS1Win^{TM}) method was used for specific surface area measurement, such as for the

APTEFF, 52, 1-273 (2021) UDC: 628.316.12:66.021.3.081.3
DOI: https://doi.org/10.2298/APT2152073T BIBLID: 1450-7188 (2021) 52, 73-88
BY-NC-ND
Original scientific paper

sorption phenomenon of nitrogen gas on the adsorbent surface at the temperature of liquid nitrogen (77 K). The moisture content was obtained by weighing the mixture before and after drying. The porosity was determined as the ratio between the volume of the voids and the total volume of a porous sample. The apricot stones were carbonized in a programmable electrical furnace (110 MCS, 75045/4). The residual PNA concentration was analyzed by a double beam spectrophotometer (UV-Visible, SAFAS, EASYPEC II 320 D) (λ_{max} = 380 nm).

PREPARATION OF ADSORBENTS

Preparation of apricot stone activated carbon (ASAC)

The apricot stones (Family: Rosacée), used as precursor, are originally from the area of Batna, located at East of Algeria. Several activation chemical agents were tested for the preparation of the apricot stone activated carbon. The best result is obtained with the phosphoric acid. The sample was mixed in 1:4 (wt) optimal ratio with H_3PO_4. The chemical treatment was performed in an agitated reactor (500 mL capacity), equipped with a cooling system to avoid any change in the acid concentration. The treatment duration is 2 hours. Then, the apricot stones treated were carbonized at 800 °C for 2 hours in a programmable electrical furnace, with a heating rate 5 °C·min^{-1}. The parameters of the activated carbon preparation such as carbonization temperature, carbonization time, concentration of H_3PO_4 and activation time were optimized (not presented in this study). The treated sample was repeatedly washed with water until getting neutral pH and dried at 105 °C for 24 hrs, after wards it was ground in an agate mortar and sieved. The grains less than 320 μm were stored in bottles (17).

Preparation of extract of amorphous SiO_2 (EAS)

The precursor used to produce the extract of amorphous SiO_2 (EAS) is the diatomite; originally from Sig (West of Algeria), it is a kind of natural low-cost mineral material. The extraction of silica was carried out based on optimization study of the solid-liquid ratio and settling time, both these parameters are essential for the elimination of crystalline silica. A weight of 200 g crude diatomite was soaked in distilled water at 100 °C in solid-liquid ratio of 1:30 (wt). The mixture was then subjected to a moderate stirring (1150 rpm, 1 hr). The supernatant was siphoned and centrifuged. This operation was repeated four times. The amorphous silica extract obtained was dried at 105 °C (25).

Preparation of treated extract of amorphous silica (TEAS)

The mineral impurities on the *EAS* surface were removed by thoroughly washing with (10% v/v) HCl and then washing to the neutrality (26). Leaching of amorphous silica extracted from crude diatomite was carried out with a solid-liquid ratio of 1:2 volumes; the amorphous silica was in contact with HCl (10%) at 100 °C for 3 hrs under moderate agitation (300 rpm), in an agitated vessel of 500 mL capacity, equipped with a reflux heating system to maintain the acid concentration constant. Then, the mixture was filtered and washed with distilled water at 60 °C until the disappearance of chloride ions from solution;

APTEFF, 52, 1-273 (2021) UDC: 628.316.12:66.021.3.081.3
DOI: https://doi.org/10.2298/APT2152073T BIBLID: 1450-7188 (2021) 52, 73-88
BY-NC-ND
Original scientific paper

this is achieved using silver nitrate solution. The obtained sample was dried at 105 °C, before characterizations (27).

pH_{PZC} DETERMINATION

The point of zero charge (pH_{PZC}) is the pH at which the surface has a neutral charge, is of fundamental importance in the surface chemistry. At pH values < pH_{PZC}, the adsorbent surface is positively charged, (attracting anions/repelling cations), conversely, at pH values > pH_{PZC}, the surface is negatively charged. pH_{PZC} was accurately determined according to the following method (28).

BATCH ADSORPTION

All adsorption tests were carried out in batch mode. 100 mL of PNA solution (100 mg L^{-1}, pH ~7) was mixed with ASAC/TEAS (1 g L^{-1}) and agitated at 300 rpm for 60 min, the temperature was maintained at 25 °C±0.2. The samples were withdrawn at regular times and subjected to vigorous centrifugation. The residual PNA concentration was analyzed using a double beam spectrophotometer at a wavelength of 380 nm. The removal efficiency (Y %) is calculated using Eq. [1].

$$Y(\%)=\frac{(C_{in}-C_t)}{C_{in}}\cdot 100 \quad [1]$$

where C_{in} is the initial concentration of the solution (mg L^{-1}) and C_t the concentration of the solution at time t (mg L^{-1}).

RESULTS AND DISCUSSION

CHARACTERIZATION OF PREPARED SAMPLES

The chemical composition of prepared powders (Crude Diatomite, EAS, TEAS, ASAC and ASAC/TEAS) is determined by X-ray fluorescence (XRF) analysis. Results (Table 1) are expressed in weight percentage; the phosphorus is the major element of ASAC powder with 11.6 wt %, this increase in the phosphorus results from the chemical treatment by H_3PO_4 applied to the precursor. The Algerian crude diatomite is rich in Si and Ca oxides and the treated extract amorphous silica (TEAS) is rich in SiO_2. The XRF spectra results show also that the main components of the natural raw diatomite are SiO_2 and CaO, with low amounts of the Al_2O_3, F_2O_3, and MgO. After the acid treatment, SiO_2 ratio increases, but CaO, Al_2O_3, MgO, F_2O_3, P_2O_5 and TiO_2 amounts decrease. The increase of SiO_2 ratio can be ascribed to the fact that the silica is relatively resistant to acid attack whereas the salts are more soluble in acidic media (29).

APTEFF, 52, 1-273 (2021)
DOI: https://doi.org/10.2298/APT2152073T
BY-NC-ND
UDC: 628.316.12:66.021.3.081.3
BIBLID: 1450-7188 (2021) 52, 73-88
Original scientific paper

Table 1. Chemical composition of solids.

Elements	Crude Diatomite	EAS	TEAS	ASAC	ASAC/TEAS (1:1)
SiO_2	72.30	81.09	92.14	0.05	20.34
Al_2O_3	2.27	1.59	0.47	<0.02	0.401
Fe_2O_3	0.88	0.74	0.05	0.005	0.188
CaO	6.24	3.14	0.01	0.40	1.085
MgO	1.48	0.53	< 0.02	0.10	0.21
MnO	0.020	0.026	0.021	<0.001	0.007
Na_2O	0.24	0.22	0.14	<0.03	0.07
K_2O	0.45	0.3	0.09	1.36	1.095
P_2O_5	0.100	0.072	<0.005	11.60	8.73
TiO_2	0.132	0.081	0.083	<0.001	0.02
$Cr2O_3$	0.038	0.039	0.044	<0.001	0.011
SO_3	0.06	0.06	0.03	0.045	<0.001
ZrO_2	< 0.005	0.01	0.01	<0.001	<0.001
SrO	0.0250	0.016	0.0004	<0.001	<0.001
Rb_2O	0.0011	< 0.001	< 0.001	-	-
PbO	<0.001	< 0.001	< 0.001	0.0170	0.012
ZnO	0.0164	0.0324	0.0025	0.0026	< 0.001
CuO	0.0143	0.0018	0.0014	0.0077	< 0.001
NiO	0.0039	0.001	<0.001	0.0037	< 0.001
BaO	0.0039	0.0181	0.014	-	< 0.001
Cl	0.067	-	-	<0.001	< 0.001
V	0.0038	-	-	-	-

The X-ray diffraction patterns of prepared powders (crude diatomite, EAS and TESA) collected over a diffraction angle (2θ) range from 3–32° (Figure 1); show that the samples are mainly composed of amorphous silica phase, revealed by a large peak between 18° and 27° (2θ). In addition, for crude diatomite, there are three other crystalline phases attributed to carbonate in the calcite ($CaCO_3$) at 2θ = 29.9°, carbonate in ankerite $Ca(Mg,Fe)(CO_3)_2$) at 2θ = 31° and quartz at 2θ = 27° (29), but for the EAS powder, the quartz and the carbonate in the ankerite disappear, and the peak of carbonate in the calcite is observed. For TESA sample, XRD analysis results show that calcite, initially presents as impurities in the natural diatomite have disappeared after acid treatment, and i.e. calcium is mainly in the form of carbonate, which can be decomposed easily in acidic media. This result agrees with literature data that acid treatment does not change the diatomite structure (29).

APTEFF, 52, 1-273 (2021)
DOI: https://doi.org/10.2298/APT2152073T
BY-NC-ND
UDC: 628.316.12:66.021.3.081.3
BIBLID: 1450-7188 (2021) 52, 73-88
Original scientific paper

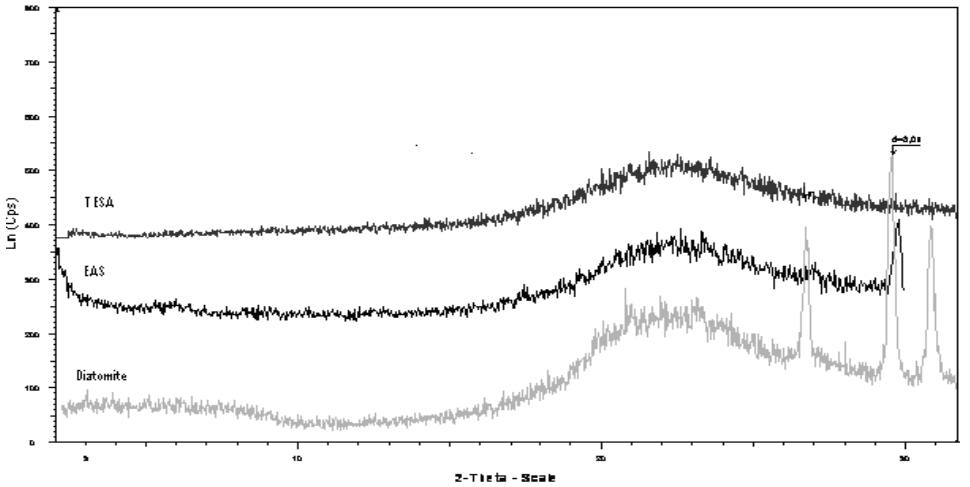

Figure 1. X-ray diffraction patterns of diatomite, EAS and TESA

XRD also gives evidence that the acid treatment is sufficient to eliminate calcite as already observed with XRF. Acid treatment permits the purification of raw diatomite (29).

EFFECT OF ASAC/TEAS RATIO ON THE PNA REMOVAL

The composite ASAC/TEAS ratio is an important parameter for the PNA removal. Batch adsorption tests were carried out with PNA concentration of 100 mg L^{-1} and mixed with ASAC/TEAS (1 g L^{-1}) at various ratios of ASAC/TEAS (0/1, 1/3, 1/1, 3/1 and 1/0). The effect of ASAC/TEAS ratio on the PNA removal is illustrated in Figure 2. The maximum removal percentage (85%) is obtained for a ratio of ASAC/TEAS (1/1), but elsewhere a decrease is observed. The Figure shows also that when each adsorbent is used alone (0/1 and 1/0), there is an elimination of PNA, it is more higher for the case of ASAC, this is obvious, because generally, the activated carbons are more efficiency, but the contribution of the TEAS may be not neglected for ratio (1/3, 1/1 and 3/1) because an improved of PNA elimination is observed in comparison with the TEAS, this implies the existence of a synergistic effect between ASAC and TEAS especially in the ratio (1/1), this also means that impregnation of TEAS and ASAC produces a good adsorbent properties towards PNA especially in the ratio (1/1). So, the ratio of 1/1 was chosen as optimum value for further experiments. The chemical composition of optimal ASAC/TEAS obtained by XRF is given in Table 1.

APTEFF, 52, 1-273 (2021)
DOI: https://doi.org/10.2298/APT2152073T
BY-NC-ND
UDC: 628.316.12:66.021.3.081.3
BIBLID: 1450-7188 (2021) 52, 73-88
Original scientific paper

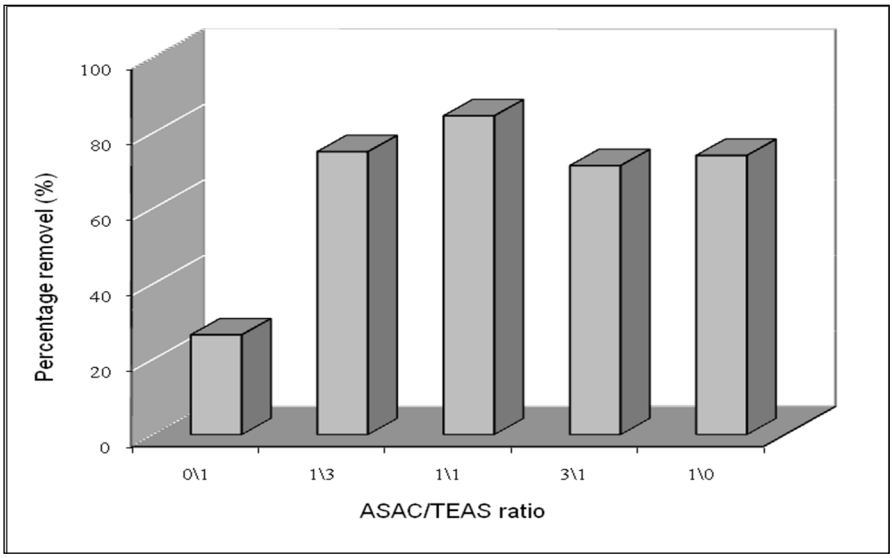

Figure 2. Percentage of PNA adsorption versus the mass ratio (C_{in} = 100 mg/L, ASAC/TEAS dose = 1 g/L, pH=7 , t=60min, 300rpm and T = 25 °C)

CHARACTERIZATION OF THE SORBENTS

Knowledge of the physicochemical properties of the optimal ASAC/TEAS mixture allows determining the behaviour of the adsorption capacity of the adsorbent. The results SEM/EDX**,** X-ray fluorescence, BET, and Fourier transform infrared (FTIR) were also investigated in order to interpret some results of PNA adsorption onto optimal ASAC/TEAS (1/1) composite. The main physical and chemical properties of the sorbents are given in Table 2.

Table 2. Physical and chemical characteristics of optimal ASAC/TEAS mixture

Sorbent / Characteristics	ASAC	TEAS	ASAC/TEAS
pHpzc	4.30	-	7.00
Porosity (%)	56.01	-	77.69
Moisture (%)	3.62	5.60	6.03
Total pore volume ($cm^3.g^{-1}$)	0.72	0.97	1.12
S_{BET} (m^2/g)	1160	111	1290
S_{mic} (m^2/g)	1050	39	770

SURFACE AREA DETERMINATION

The surface area of untreated apricot stones determined by BET method is $45m^2g^{-1}$ (17) while the surface area of the treated adsorbent is $1160m^2g^{-1}$. This analysis shows that phosphoric acid is effective in creating pores on the surface of the precursor.

BY-NC-ND

The results of the surface area analysis of the adsorbents are tabulated in Table 2. The BET surface area and total pore volume of composite ASAC/TEAS are higher than those of ASAC and TEAS. The larger surface area and total pore volume recorded for composite ASAC/TEAS with the porosity suggests that composite ASAC/TEAS might act as a better adsorbent in the uptake of PNA than ASAC and TEAS. This appears thanks to the mixture of two materials. So, this means that impregnation of TEAS and ASAC produces an increase in the specific surface, rendering a more developed texture.

Indeed, total pore volume and porosity of TEAS are higher than those of ASAC. On the other side, ASAC that has a large surface area, is essentially microporous, this being a good combination for the adsorption of PNA. Since the adsorptive properties of both materials are complementary, a mixture of both could be of high interest for some specific applications such as separation and purification purposes.

Analysis by SEM/EDX

In order to know the surface microstructure of the mixture, the morphological analysis is performed by SEM. Figure 3 (A) to (F) shows the surface morphology and structure of ASAC, Untreated apricot stones activated carbon, TEAS and ASAC/TEAS composite.

Figure 3 (A and B) shows the SEM micrographs of untreated and treated samples. It can be seen that the chemically treated adsorbent surface exhibits a homogenous type pores. It is revealed that chemically treated adsorbent is porous as compared to untreated adsorbent. As can be seen in Figure (C), diatomite morphology was clearly visible; its shape was mainly a disk structure. The SEM images (D), (E) and (F) show a highly porous morphology of the optimal ASAC/TEAS mixture with different shapes. Large pores in a honeycomb shape may be observed on the surface of the ASAC/TEAS mixture. The micrographs also reveal that the external surface display cavities which suggest that mixture ASAC/TEAS have a high internal surface area. It can be noted that this structure and surface morphology obtained is likely due to the impregnation of TEAS and ASAC and aggressive attack during the chemical treatment for ASAC (30). The mixture of two materials means that impregnation of TEAS and ASAC produces a rendering a more developed texture and porosity structure with regular distribution which gives a homogenous surface.

The energy dispersive X-ray (EDX) analysis (Figure 4C) indicates that ASAC has high carbon and phosphor amount. Phosphor is due to the activating agent (H_3PO_4) with promotes dehydration and depolymerization of the precursor. Figure 4B shows that TEAS has high silica content, which represents important characteristic of diatomite. The EDX of the optimal ASAC/TEAS mixture (Figure 4A) indicates mainly the presence of carbon and oxygen which come from TEAS and ASAC, silica from TEAS and phosphor from ASAC, along with some foreign atoms like as Ca, K and Mg.

APTEFF, 52, 1-273 (2021)
DOI: https://doi.org/10.2298/APT2152073T
BY-NC-ND
UDC: 628.316.12:66.021.3.081.3
BIBLID: 1450-7188 (2021) 52, 73-88
Original scientific paper

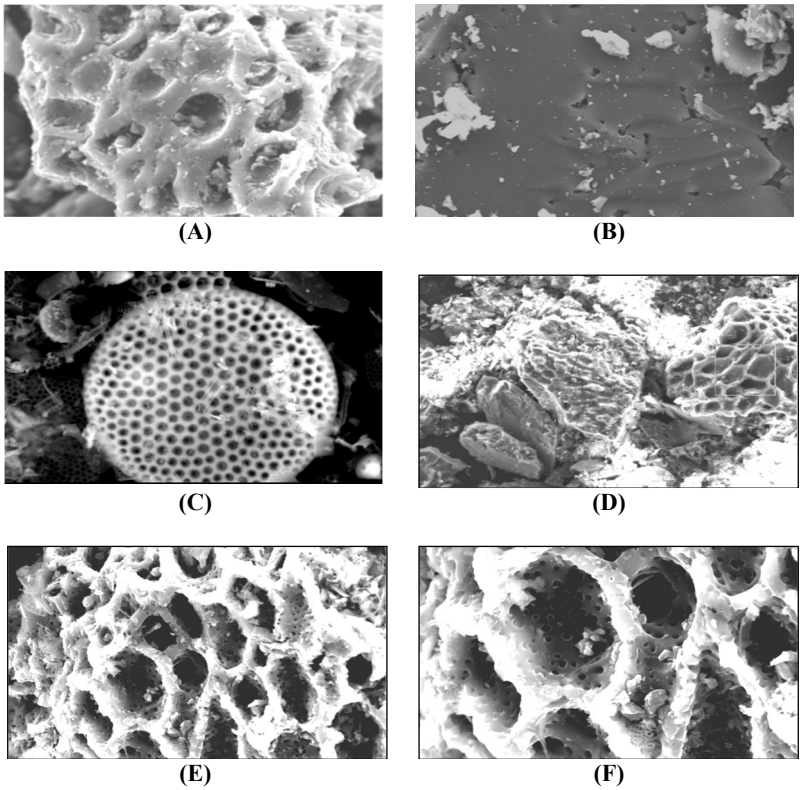

Figure 3. SEM images (magnification 1000 X) of (A)- ASAC, (B)-Untreated apricot stones activated carbon, (C)- TEAS (magnification 1500 X). (D), (E) and (F) - SEM of ASAC/TEAS at different magnifications (1000 X, 1200 X and 1500 X respectively)

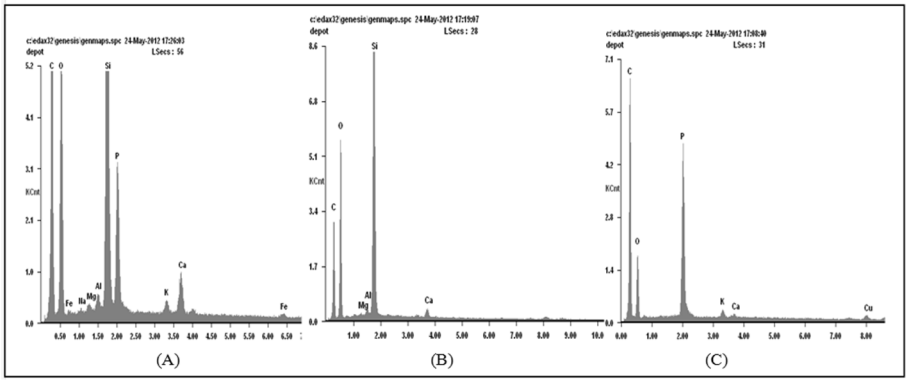

Figure 4. EDX pattern of (A) optimal ASAC/TEAS mixture, (B) TEAS and (C) ASAC

APTEFF, 52, 1-273 (2021)
DOI: https://doi.org/10.2298/APT2152073T
BY-NC-ND
UDC: 628.316.12:66.021.3.081.3
BIBLID: 1450-7188 (2021) 52, 73-88
Original scientific paper

x-Ray fluorescence analysis

The chemical composition of optimal ASAC/TEAS mixture was determined using XRF and listed in Table 1. The results obtained indicate mainly the presence of natural silica and phosphor and confirm the presence of Ca, Mg and K found in the SEM/EDX analysis. The elements Mn, Na, Zn, Ti, Cu, Ni and S also exist in small amounts.

FTIR analysis

In order to identify the functional group of chemical functions involved in the PNA adsorption, the FTIR analysis of the optimal ASAC/TEAS mixture, TEAS and ASAC are carried out. Figure 5 shows the FTIR spectra and the various functional groups corresponding to the vibrational absorption bands.

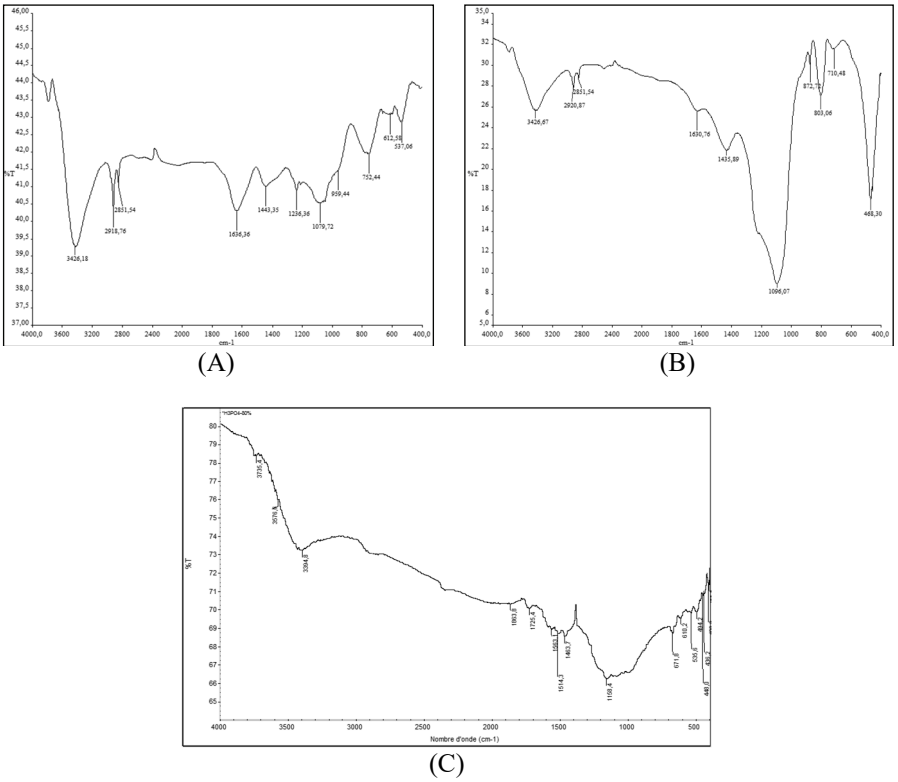

Figure 5. FT-IR spectrum of optimal ASAC/TEAS mixture (A), TEAS (B) and ASAC (C).

In the activated carbon spectra, the bands occurred at 3735, 3576 and 3394 cm^{-1} were assigned to the stretching vibration of hydroxyl (−OH). Five other peaks at 1863, 1725, 1563, 1514, and 1463 cm^{-1} were attributed to the -C=O, -C=O in the carboxylic group (31),

APTEFF, 52, 1-273 (2021) UDC: 628.316.12:66.021.3.081.3
DOI: https://doi.org/10.2298/APT2152073T BIBLID: 1450-7188 (2021) 52, 73-88
BY-NC-ND
Original scientific paper

-COO^- (24), -CH_2 (32), and C=C aromatic ring (33) respectively. The peaks at 1158, 671 and 536 cm^{-1} were the stretching vibrational bands of –C-O-C- (34), C-H aromatic ring (35) and phosphorus-containing groups respectively (36).

In the diatomite FTIR spectra, the broad band at 3426.67cm^{-1} suggests the presence of hydroxyl group (−OH) and silanol group (–Si–OH) (36, 37). The peaks at 1630, 1097, 710, 803 and 468 cm^{-1} were attributed to hydroxyl group (−OH) (29), asymmetric vibration of Si-O (36), symmetric vibration of Si–O (24, 36**),** vibration of Si–O–Si in the formed free silica (SiO_2) (27) and siloxane group Si-O-Si respectively. They are important characteristic peaks of diatomite (37). The bands at 2918 and 2851 cm^{-1} correspond to C–H in the methyl and methylene groups (38). At 1636 and 1443 cm^{-1} were ascribed to the C=C stretching vibrations in the aromatic rings. In the optimal mixture system, seven characteristic peaks of diatomite at 3426, 2918, 2851, 1636, 1443, 1097 and 710 cm^{-1} were preserved, and the peak at 3426 cm^{-1} were increased in intensity. This result is probably due to the abundant hydroxyl groups and silanol group in the optimal mixture system. New peaks appeared at 1236 cm^{-1} are probably caused by phosphorus-containing groups, such as the P=O bond in phosphate esters, O–C bond in P–O–C linkage, or P=OOH bond (39), and 959 cm^{-1} corresponds to Si–O stretching of silanol group. Other peaks at 537 cm^{-1} were attributed to the Si–O–Si bending vibration (40, 41).

According to the FTIR spectra and the pH dependency of the PNA adsorption, silanol is probably the functional group responsible for PNA molecules adsorption. However, the porosity of ASAC/TEAS plays an important role too in the retention in PNA molecules inside the pores of ASAC/TEAS. On basis of these considerations, two mechanisms can be proposed during the adsorption, (a) a π-π interaction was developed between the functional group of ASAC/TEAS surface and PNA and (b) a hydrogen bond was developed between silanol group of ASAC/TEAS and NH_2 group of PNA molecule (42) (Figure 6).

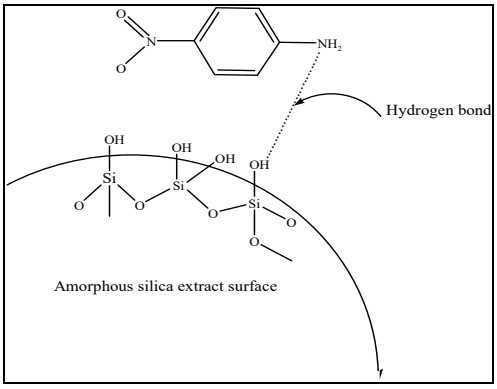

Figure 6. Representation of the adsorption by hydrogen bond of the optimal ASAC/TEAS mixture

MODELING ADSORPTION ISOTHERM

The isotherm plots show how the adsorbate is distributed between the liquid and solid phases at equilibrium. The analysis of the isotherm by fitting the experimental data to different models is an important step for the design purpose. Two known isotherms were

APTEFF, 52, 1-273 (2021) UDC: 628.316.12:66.021.3.081.3
DOI: https://doi.org/10.2298/APT2152073T BIBLID: 1450-7188 (2021) 52, 73-88
BY-NC-ND
Original scientific paper

applied, namely the Langmuir and Freundlich isotherms (17), given by their linear form in equations [3] and [4], respectively:

$$\frac{1}{Q_e} = \frac{1}{Q_o} + \frac{1}{b}.\frac{1}{Q_o C_e} \quad [3]$$

$$LnQe = LnK_F + \frac{1}{n} LnCe \quad [4]$$

where Q_0 is the maximum adsorption capacity (mg·g^{-1}), K_L (L g^{-1}) a binding constant in Langmuir equation, K_F and n are the Freundlich constants for the heterogeneous adsorbent (17). The corresponding values of the model's parameters are gathered in Table 3. Since the regression coefficients R^2 of Langmuir isotherm is higher (R^2=0.970), it is more suitable for the adsorption equilibrium modelling than the Freundlich one (R^2=0.870).

Table 3. Langmuir and Freundlich models parameters for PNA sorption on the optimal ASAC/TEAS mixture

Langmuir			Freundlich		
Q_o (mg g^{-1})	b (L mg^{-1})	R^2	K_F(mg g^{-1}(mgL^{-1})$^{-1/n}$)	1/n	R^2
94.339	0.188	0.970	40.593	0.181	0.870

From Table 3, the maximum adsorption capacity of PNA onto ASAC/TEAS mixture is more than 94 mg g^{-1} at initial PNA concentration of 100 mg L^{-1} at 25 °C. The maximum adsorption capacities (Q_0) of PNA compared to some other adsorbents previously studied for the removal of PNA (Table 4) show that the adsorbent of the present study (ASAC/TEAS) has the largest capacity for the removal of PNA.

Table 4. Values of Langmuir adsorption capacity (Q_0)

Sorbent	Q_0 (mg g^{-1})	References
Zeolitic adsorbent MgFZBFA	30.86	43
Zeolitic adsorbent MgMZBFA	12.72	43
Jatropha curcas Activated Carbon	38.76	44
Humic acid	1.8	45
Clinoptilolit	0.85	46
ASAC/TEAS	94.34	This work

Furthermore, the value of 1/*n* was found to be less than 1, indicating a favorable adsorption (47).

The above results suggest that the mixture ASAC/TEAS was an effective adsorbent for the PNA removal.

The Langmuir isotherm can be characterized by a dimensionless constant separation factor (R_L) (48; 49), given by equation [5]:

$$R_L = \frac{1}{(1+b \cdot C_{in})} \quad [5]$$

BY-NC-ND

R_L characterizes the shape of the isotherm: unfavorable ($R_L > 1$), linear ($R_L = 1$), favorable ($0 < R < 1$), or irreversible ($R_L = 0$); R_L values between 0 and 1 give a favorable adsorption. In the present investigation, $R_L = 0.050$, showing a favorable adsorption.

CONCLUSION

The present work was devoted to the adsorption in batch mode of p-nitroaniline on of the prepared adsorbent (ASAC/TEAS), consisting of activated apricot stones carbon and treated extract of the amorphous silica Algerian diatomite (SiO_2). The yield of PNA elimination achieved 85%. The activated carbons are more efficiency, but the contribution of the TEAS may be not neglected for ratio (1/3, 1/1 and 3/1) because an improved of PNA elimination is observed by comparing with the TEAS, this means that impregnation of TEAS and ASAC produces a good adsorbent properties towards PNA especially in the ratio (1/1) and an increase in the specific surface, this also implies the existence of a synergistic effect between ASAC and TEAS. The porosity of ASAC/TEAS plays an important role too in the retention in PNA molecules inside the pores of ASAC/TEAS. The characterization of the ASAC/TEAS adsorbent surface shows that its textural, morphology and composition constitute benefits allows ranking ASAC/TEAS among the competitive low-cost adsorbents.

The Langmuir equation shows good agreement with the adsorption isotherm data for the PNA on composite ASAC/TEAS at 25 °C. The maximum adsorption capacities of PNA compared to some other adsorbents previously studied for the removal of PNA show that the adsorbent of the present study (ASAC/TEAS) has the largest capacity for the removal of PNA.

Two mechanisms can be proposed during the PNA adsorption on ASAC/TEAS mixture, (a) a π-π interaction was developed between the functional group of ASAC/TEAS surface and PNA and (b) a hydrogen bond was developed between silanol group of ASAC/TEAS and NH_2 group of PNA. The application as material of cheap source for the PNA removal from contaminated water could be considered. After using scanning electron microscopy (SEM) and the gas adsorption techniques, it can be noticed that the prepared ASAC/TEAS is characterized by a very developed porous texture and high specific surfaces. All in all, ASAC/TEAS, is a novel adsorbent with the advantages of easy preparation, low cost and high adsorption performance for PNA removal.

Acknowledgements

This work was financially supported by the Directorate General of Scientific Research and Technological Development (DGRSDT).

REFERENCES

1. Şenlik K.; Gezici O.; Guven I.; Pekacar A.I. Adsorption of nitroaniline positional isomers on humic acid-incorporated monolithic cryogel discs: Application of ligand-exchange concept, *J. Envir. Chem. Eng.* **2017**, *5*, 2836-2844.

BY-NC-ND

2. Xiao G.; Wen R.; Wei D.; Wu D. Effects of the steric hindrance of micropores in the hyper-cross-linked polymeric adsorbent on the adsorption of p-nitroaniline in aqueous solution, *J. Hazar. Mater.* **2014**, *280,* 97-103.
3. Li K.; Zheng Z.; Feng J.; Zhang J.; Luo X.; Zhao G.; Huang X. Adsorption of p-nitroaniline from aqueous solutions onto activated carbon fiber prepared from cotton stalk, *J. Hazard. Mater.* **2009***, 166*, 1180-1185.
4. Gautam S.; Kamble S.P.; Sawant S.B.; Pangarkar V.G. Photocatalytic degradationof 4-nitro-aniline using solar and artificial UV radiation, *Chem. Eng. J.* **2005**, *110,* 129-137.
5. Sun J.H.; Sun S.P.; Fan M.H.; Guo H.Q.; Qia L.P.; Sun R.X. A kinetic study on the degradation of p-nitroaniline by Fenton oxidation process, *J. Hazard. Mater.* **2007**, *148,* 172-177.
6. Li K.Q.; Li Y.; Zheng Z. Kinetics and mechanism studies of p-nitroaniline adsorption on activated carbon fibers prepared from cotton stalk by $NH_4H_2PO_4$ activation and subsequent gasification with steam, *J. Hazard. Mater.* **2010**, *178*, 553-559.
7. Sun J.H.; Sun S.P.; Fan M.H.; Guo H.Q.; Lee Y.F.; Sun R.X. Oxidative decompositionof p-nitroaniline in water by solar photo-Fenton advanced oxidation process, *J. Hazard. Mater.* **2008**, *153*, 187-193.
8. Subbulekshmi N.L.; Subramanian E. Nano CuO immobilized fly ash zeolite Fenton-like catalyst for oxidative degradation of p-nitrophenol and p-nitroaniline, *J. Enviro. Chem. Eng.* **2017**, *5* (2), 1360-1371.
9. Zhao Y.S.; Sun C.; Sun J.Q.; Zhou R.; Kinetic modeling and efficiency of sulfate radical-based oxidation to remove p-nitroaniline from wastewater by persulfate/Fe_3O_4 nanoparticles process, *Separ. Purif. Tech*. **2015***, 142*, 182-188.
10. Wang Y.; Zhang Y.; Zhao G.; Wu M.; Li M.; Li D.; Zhang Y.; Zhang Y. Electrosorptive photocatalytic degradation of highly concentrated p-nitroaniline with TiO_2 nanorod-clusters/carbon aerogel electrode under visible light, *Separ. Purif. Tech.* **2013**, *104,* 229-237.
11. Silambarasan S.; Vangnai A.S. Biodegradation of 4-nitroaniline by plant-growth promoting *Acinetobacter* sp. AVLB2 and toxicological analysis of its biodegradation metabolites, *J. Hazard. Mater.* **2016**, *302,* 426-436.
12. Silambarasan S.; Vangnai A.; S.; Plant-growth promoting Candida sp. AVGB4 with capability of 4-nitroaniline biodegradation under drought stress, *Ecotox. Envir. Saf.* **2017**, *139*, 472-480.
13. Oturan M.A.; Peiroten J.; Chartrin P.; Acher A.J. Complete destruction of p-nitrophenol in aqueous medium by electro-Fenton method, *Environ. Sci. Technol.* **2000**, *34*, 3474–3479.
14. Zheng K.; Pan B.; Zhang Q.; Zhang W.; Pan B.; Han,Y.; Zhang Q.; Wei D.; Xu Z.; Zhang, Q. Enhanced adsorption of p-nitroaniline fromwater by a carboxylated polymeric adsorbent, *Sep. Purif. Technol.* **2007**, *57*, 250–256.
15. Wu, G.; Wu, G.; & Zhang, Q. Adsorptive removal of p-nitroaniline from aqueous solution by bamboo charcoal: kinetics, isotherms, thermodynamics, and mechanisms, *Desal. Wat. Treat.* **2016**, *57*(55), 26448-26460.
16. Naghizadeh A.; Ghafouri M.; Jafari A. Investigation of equilibrium, kinetics and thermodynamics of extracted chitin from shrimp shell in reactive blue 29 (RB-29) removal from aqueous solutions, *Desal. Wat. Treatm.* **2017**, *70***,** 355-363.
17. Tizi H.; Berrama T.; Kaouah F; Bendjama Z. Study of the conditions of activated carbon preparation from an agriculture by-product for 4BA elimination in aqueous solution using full factorial design, *Desal. Wat. Treat.* **2013***, 51*, 7286-7295.
18. Sekulić M.T.; Pap S.; Stojanović Z.; Bošković N.; Radonić J.; Knudsen T.Š. Efficient removal of priority, hazardous priority and emerging pollutants with Prunus armeniaca functionalized biochar from aqueous wastes : Experimental optimization and modeling, *Sci. Tot. Envir.* **2018**, 613-614, 736-750.
19. Šoštarić T.D.; Petrović M.S.; Pastor F.T.; Lončarević D.R.; Petrović J.T.; Milojković J.V.; Stojanović M.D. Study of heavy metals biosorption on native and alkali-treated apricot shells and its application in wastewater treatment, *J. Mol. Liq.* **2018**, 1-35.

BY-NC-ND

20. Fadhil A.B. Evaluation of apricot (Prunus armeniaca L.) seed kernel as a potential feedstock for the production of liquid bio-fuels and activated carbons, *Energ. Conv.Manag.* **2017**, 133, 307-317.
21. Naghizadeh A.; Ghasemi F.; Derakhshani E.; Shahabi H. Thermodynamic, kinetic and isotherm studies of sulfate removal from aqueous solutions by graphene and graphite nanoparticles, Desal. Wat. Treat.**2017**, *80,* 247-254.
22. Naghizadeh A.; Kamranifar M.; Yari A. R.; Mohammadi M. J. Equilibrium and kinetics study of reactive dyes removal from aqueous solutions by bentonite nanoparticles, *Desal. Wat. Treat.* **2017**, *97,* 329–337.
23. Naghizadeh A.; Ghafouri M. Synthesis and Performance Evaluation of Chitosan Prepared from Persian Gulf Shrimp Shell in Removal of Reactive Blue 29 Dye from Aqueous Solution (Isotherm, Thermodynamic and Kinetic Study), *Iran. J. Chem. Chem. Eng.* **2017**, *36* (3), 25-36.
24. Al-Ghouti M.A.; Al-Degs Y.S. New adsorbents based on microemulsion modified diatomite and activated carbon for removing organic and inorganic pollutants from waste lubricants, *Chem. Engin. J.* **2011**, *173*, 115-128.
25. Ferrag F.; Hadjadj-Aoul O.; Belkadi M.; Talamali R.; Canselier J.P. Extraction and characterization of amorphous silica in the Algerian diatomite, *Phys. Chem. News*, **2006**, *27,* 118-123.
26. Hadjadj-Aoul O.; Belabbes R.; Belkadi M.; Guermouche M.H. Characterization and performances of an Algerian diatomite-based gas chromatography support, *Applie. Surf. Sci.* **2005**, *240,* 131-139.
27. Boudriche L.; Calvet R.; Hamdi B.; Balardd H. Effect of acid treatment on surface properties evolution of attapulgite clay: An application of inverse gas chromatography, *Colloid. Surfa. A: Physicochem. Eng. Asp.* **2011***, 392,* 45-54.
28. Duman O.; Ayranci E. Structural and ionisation effects on the adsorption behaviours of some anilinic compounds from aqueous solution onto high area carbon cloth, *J. Hazar. Mater.* **2005**, *120*, 173-181.
29. Benkacem T.; Hamdi B.; Chamayou A.; Balard H.; Calvet R. Physicochemical characterization of a diatomaceous upon an acid treatment: a focus on surface properties by inverse gas chromatography, *Powd. Tech.* **2016**, *294*, 498-507.
30. Doufene N.; Berrama T.; Tahtat D.; Benredouane S.; Nekaa C. Combination of two experimental designs to optimize the dimethylphtalate elimination on activated carbon elaborated from Arundo donax, *Arab J. Sci. Eng.* **2019**, *44*, 5275-5287.
31. Budinova T.; Ekinci E.; Yardim F.; Grimm, A.; Björnbom, E.; Minkova, V.; Goranova, M. Characterization and application of activated carbon produced by H_3PO_4 and water vapor activation, *Fuel Proc. Tech.* **2006**, *87*, 899-905.
32. Abbas M.; Trari M. Kinetic, equilibrium and thermodynamic study on the removal of Congo Red from aqueous solutions by adsorption onto apricot stone, *Proc. Saf. Envir. Protec.* **2015**, *98*, 424-436.
33. Sun Y.; Webley P.A. Preparation of activated carbons from corncob with large specific surface area by a variety of chemical activators and their application in gas storage, *Chem. Engin. J.* **2010***, 162* (3), 883-892.
34. Zhao D.; Zhao L.; Zhu C.-S.; Shen X.; Zhang X.; Sha B. Comparative study of polymer containing β-cyclodextrin and –COOH for adsorption toward aniline, 1-naphthylamine and methylene blue, *J. Hazard. Mater.* **2009**, *171*, 241-246.
35. Derakhshani E.; Naghizadeh A. Optimization of humic acid removal by adsorption onto bentonite and montmorillonite nanoparticles, *J. Mol. Liq.* **2018**, *259,* 76-81.
36. Mu Y.; Cui M.; Zhang S.; Zhao J.; Meng C.; Sun Q. Comparison study between a series of new type functional diatomite on methane adsorption performance, *Microp. Mesop. Mater.* **2018**, *267*, 203-211.

BY-NC-ND

37. Song X.; Chai Z.; Zhu Y.; Li C.; Liang X. Preparation and characterization of magnetic chitosan-modified diatomite for the removal of gallic acid and caffeic acid from sugar solution, *Carbohyd. Polym.* **2019***, 219*, 316-327.
38. Deng H.; Li G.; Yang H.; Tang J.; Tang J. Preparation of activated carbons from cotton stalk by microwave assisted KOH and K_2CO_3 activation, *Chem. Eng. J.* **2010**, *163,* 373-381.
39. Puizy A.M.; Poddubnaya O.I.; Martínez-Alonso A.; Suárez-García F.; Tascón J.M.D. Synthetic carbons activated with phosphoric acid I. Surface chemistry and ion bonding properties, *Carbon*, **2002**, *40*, 1493–1505.
40. Rytwo G.; Tropp D.; Serban C. Adsorption of diquat, paraquat and methyl green on sepiolite: experimental results and model calculation. *Appl. Clay Sci.* **2002**, *20*, 273-282.
41. Hayakawa S.; Hench L.L. AM1 study on infra-red spectra of silica clusters modified byfluorine. *J. Non-Crystal Solid,* **2000**, *262,* 264-270.
42. Khraisheh M.A.M.; Al-Ghouti M.A.; Allen S.J.; Ahmad M.N. Effect of OH and silanol groups in the removal of dyes from aqueous solution using diatomite, *Water Res.* **2005***, 39*, 922-932.
43. Oluyinka, A.O.; Patel, A.V.; Shah B. A.; Bagia, M.I. Microwave and fusion techniques for the synthesis of mesoporous zeolitic composite adsorbents from bagasse fly ash: sorption of *p*-nitro-aniline and nitrobenzene, *Applied Water Sci.* **2020**, *236*, 1-20.
44. Azeez S.O.; Adekola, F. A. Sorption of 4-Nitroaniline on Activated Kaolinitic Clay and *Jatropha curcas* Activated Carbon in Aqueous Solution, *J. J. Chemis.* **2016**, *11*,128-145.
45. Wu Y.Q.; Zhou M.; Ma M.G.; ZHANG Y.; Chen H. Adsorption kinetics of p-nitroaniline on the insolubilized humic acid, *Tec.Water. Tr.* (Chinese), **2007**, 2, 14-17.
46. Ma M.G.; Wei Y.X.; Zhang Z.; Wu Y.; Guo H.; Chen H. Modify of clinoptilolit (from Baiyin) and its adsorption of p-nitroaniline, *J. Anhui Agri. Sci.* (Chinese), **2007**, 7, 2061-2062.
47. Gonzalez-Pradas E.; Ferna`ndez-Perez M.; Flores-Cespedes F.; Villafranca Sanchez M.; Urena-Amate M.D.; Socias-Viciana M.; Garrido-Herrera F. Effects of dissolved organic carbon on sorption of 3,4-dichloroaniline and 4-bromoaniline in a calcareous soil, *Chemosphere*, **2005**, 59, 721-728.
48. Subramani S.E.; Thinakaran N.; Isotherm, kinetic and thermodynamic studies on the adsorption behaviour of textile dyes onto chitosan, *Process. Saf. Environ*. **2017**, 106, 1-10.
49. Göçenoğlu Sarıkaya A.; Osman B.; Kara, A. Evaluation of the effectiveness of microparticle-embedded cryogel system in removal of 17 β-estradiol from aqueous solution, *Desalin. Water Treat.* **2016**, *57*, 15570-15579.

APTEFF, 52, 1-273 (2021) UDC: 582.282.23:634.8.077]:531.3:66.011
DOI: https://doi.org/10.2298/APT2152089S BIBLID: 1450-7188 (2021) 52, 89-110
BY-NC-ND
Original scientific paper

OPTIMIZATION OF BAKER`S YEAST PRODUCTION ON GRAPE JUICE USING RESPONSE SURFACE METHODOLOGY

Mahmood SAWSAN[1], Ali ALI[1], Darwesh AYHEM[1], Zam WISSAM[2]*

[1] Tartous University, Faculty of Technical Engineering, Tartous, Syria
[2] AL- Wade University, Faculty of Pharmacy, Homs, Syria

Received: 25 February 2021 **Revised: 06 May 2021** **Accepted: 07 May 2021**

There is an increasing interest in improving biological processes, including fermentation processes, improving fermentation conditions is difficult, as it requires the use of an appropriate improvement method that allows operating the biological fermenter under optimal conditions in order to obtain the largest possible amount of the final product. The aim of this work was to succeed in examples of fermentation conditions to produce the largest possible quantity of dry yeast biomass Saccharomyces cerevisiae using grape juice as the sole carbon source. The optimum values of five factors that have an effect on the production of dry biomass from baker`s yeast were determined. The design of the experiments was carried out using the central composite experimental design (CCD) and the number of experiments according to the design was (54) experiments, the response surface methodology method was used to determine the best possible amount of production of yeast, and has reached (41.44 g/L) after 12 hours of fermentation, under the following optimal conditions (temperature (30.11 °C), pH (4.75), sugar concentration (158.36 g/L), the ratio of carbon to nitrogen (an essential nutrient for yeast growth) is (11.9), initial concentration of yeasts (2.5 g/L), the amount of urea was 6.65 g/L and the amount of ammonium sulfate used was 6.65 g/L, so that the concentration of added urea and ammonium sulfate was (50-50)% and the required C/N ratio was achieved, and the used agitation speed was equal to 200 r.p.m during the fermentation process. The fermenter power of the obtained yeast was 470 ml. Three kinematic models (Monod, Verhulst, and Tessier) were also selected for the purpose of studying the kinetic performance of Saccharomyces cerevisiae yeast. Monod and Tessier`s models did not give satisfactory results, while the best results were according to the Verhulst model. Also, the Leudeking Piret model has also been successfully used to predict substrate consumption during fermentation time.

Keywords: *Saccharomyces cerevisiae,* response surface methodology, kinetic models, assumption, statistics.

INTRODUCTION

Fermentation is one of the oldest methods used by humans since ancient times for preserving foods and improving their organoleptic properties. More than 5.000 fermented foods and beverages are produced all over the world, from wine, beer, and vinegar to cheese, yogurt, sourdough bread, olives, sausages, kimchi, and miso (1).

Fermentation consists of the biochemical modification of raw materials, promoted by a complex and stable consortium of microorganisms, which mainly transform sugars into simple acids, alcohols, and carbon dioxide, improving flavor, texture, and aroma, prolonging the shelf-life of the fermented products. During fermentation, a wide range of secon-

* Corresponding author: Mahmood Sawsan, Tartous University, Faculty of Technical Engineering, Tartous, Syria, e-mail: sawsanmahmood480@gmail.com

BY-NC-ND

dary metabolites, including vitamins, antioxidants, and bioactive compounds are also produced by microbial communities, enhancing the nutritional and nutraceutical values of the final products (2).

There has also been a rapid and significant development in fermentation technologies in recent years after understanding the bio-physiology of microorganisms and controlling it. Among this biology is the yeast, which has received more attention after recent developments in understanding its physiology (3).

Yeasts are micro-organisms, single-celled, unicellular eukaryotes. Their shapes and structure differ from one species to another. They are spherical or oval in shape and their dimensions range between 5-30 μm in length and 3-10 m in width. The yeast multiplies quickly and grows well in the contained environment. On sugars where they multiply by budding or by division (4, 5). Yeasts play vital roles in food biotechnology, especially in fermented products (6).

Saccharomyces cerevisiae yeast is the most important type of yeast due to its use in many industrial fields. It is used in the production of food, bread, pastries, ethyl alcohol, beer, wine, and as well as in the production of single-cell protein and a number of medicinal foods (7, 8).

Saccharomyces cerevisiae yeast is considered to be the most important product of biotechnology due to its widespread use in the industrial field (9).

Saccharomyces cerevisiae biomass is produced by using bioreactors that contribute to controlling growth conditions and the production is carried out according to batch or fed-batch fermentation system (10).

Baker´s yeast is industrially produced according to different technologies: variations in the number of generations, duration and level of aeration in each phase, different types of bioreactors, and control in the last phase of the cultivation (11). It is an aerobic process based on propagating cells from pure culture to large bioreactors by increasing the volume in each propagation stage in a sugar-based medium (12).

Commercial bread yeast comes in three forms: (Pressed yeast that is sold in the form of pressed briquettes or cubes wrapped with wax paper or cellophane, and its shelf life does not exceed one week from the date of its production due to the speed of its corruption. Active dry yeast is sold in airtight containers and needs to be reactivated before use, its cells are about 8-10% moisture and its shelf life ranges from six months to a year depending on the storage temperature. The instant dry yeast contains 4-5% moisture and its shelf life reaches more than a year and is added to the dough directly without the need for revitalization) (13).

The global yeast market is estimated to be valued at USD 3.9 billion in 2020 and is projected to reach USD 6.1 billion by 2025 (14).

Molasses is the most used raw material in the production of Baker's yeast, and it may be sourced from sugar beet or sugar cane, and it contains about 50-55% of fermentable sugars, and some vitamins and minerals that are important in cell proliferation, also any substance containing fermentable sugars can be used such as the date and grape juices (15).

In the last years, the price of molasses has increased because of their use in other industrial applications such as animal feeding or bioethanol production (16), thus rendering the evaluation of new substrates for yeast biomass propagation a trending topic for biomass producers' research. New assayed substrates include molasses mixtures with corn steep liquor (20:80), different agricultural waste products (17), and other possibilities as date

BY-NC-ND

juice or agricultural waste sources, also called wood molasses that can be substrate only for yeast species capable of using xylose as a carbon source (18).

In this research, the possibility of using grape juice to produce a good yield from the yeast was studied in this study. Grape juice was chosen because it has a chemical composition similar to the chemical composition of molasses in terms of its good content of hexane-sugars and its richness with many important nutrients for the growth of yeast cells, in addition to the fact that grape cultivation is spread in various parts of the world, including Syria, which is one of the grape-producing countries.

During the last war period, Syria was exposed to difficult economic conditions and the suspension of the work of the only sugar factory in the country, and this was accompanied by the suspension of the yeast factory and the tendency to import yeast. So, the researchers went to study the possibility of an alternative or additional option for molasses that supports yeast production, and this is in line with the researchers' interest. In different parts of the world about studying the possibility of using available raw materials to support biotechnology industries and finding many options or alternatives that support any vital industry. The Syrian Arab Republic is the richest country in the Middle East in the cultivated varieties of grapes, and the number of varieties is about 100 varieties spread across the country where the most important varieties are spread, which are four varieties that represent 85% of the total grape production (Zaini 15%, Baladi 20% and Salti 20%, Heloani 30%). the main objective of the present work is to study the optimization of *Saccharomyces cerevisiae* biomass production, using grape juice as the only source of carbon, as grape juice is a good source of carbon and many important nutrients for the growth of yeast and it has a chemical composition close to the chemical composition of molasses (19).

The efforts of many researchers are directed towards improving various biological manufacturing processes (20), including fermentation processes, with the aim to determine the best conditions for the production of the required product, as well as with the aim to solve the problems that may face the required manufacturing process, reaching the highest possible production of the final product and reducing the costs of the manufacturing process as possible (21, 22).

Several statistical experimental design methods have been used to optimize biological processes (23, 24).

These methods, including the central composite experimental design (CCD), are characterized by reducing the number of experiments required, reducing financial and energy costs, reducing the time required, as well as reducing the reagents and materials required during work (25, 26).

The central composite experimental design (CCD) is one of the methods that contributed to the improvement of a number of biological processes such as the production of antibiotics, enzymes, organic acids, and ethanol (27, 28).

The present study was done according to the following: selecting the optimum conditions of five parameters (temperature; initial pH, sugar concentration in grape juice, the ratio of carbon to nitrogen, and initial concentration of yeasts) to obtain a high yield of *Saccharomyces cerevisiae* cells growth using a surface response methodology, then exploit the grape juice as the sole carbon source for the production of *Saccharomyces cerevisiae* at optimized conditions, and finally predict the biomass production process by three kinetic models.

APTEFF, 52, 1-273 (2021)
DOI: https://doi.org/10.2298/APT2152089S
BY-NC-ND
UDC: 582.282.23:634.8.077]:531.3:66.011
BIBLID: 1450-7188 (2021) 52, 89-110
Original scientific paper

EXPERIMENTAL

MATERIALS AND METHODS

Origin and reactivation of the yeast *Saccharomyces cerevisiae*

The yeast used in this study is a commercial yeast from the sigma company, it is a dry powder form of *Saccharomyces cerevisiae* (ATCC20408/S288c). This yeast needs to be reactivated before use with a suitable nutrient medium Yeast Peptone Glucose Agar (YPGA) consisting of 20 g/L agar, 10 g/L yeast extract, 10 g/L glucose, 10 g/L peptones with a pH 6, with incubated at 30 °C for 24 h.

Preparation of grape juice

The Baladi grape (Figure 1) was chosen and it is one of the varieties available in Syria. Its production reaches 20% of the grape production. It is a local variety that is distinguished by the size of its large clusters and has a single conical shape, and the grains are spherical in shape, with a large size, with a yellowish-white color, and a thin crust in a light pink color. The pulp is flaky, has a good taste, and has a distinctive flavor, one of the late-ripening varieties, and it is one of the famous and luxurious table varieties, suitable for remote transportation and long winter storage.

Figure 1. The Baladi grape

The grape is obtained from local markets. The grape berries were removed from their clusters and cleaned and washed with warm water. The juice was extracted by breaking and pressing in a doubly folded cloth, then the juice was pasteurized at 85 °C for 3 min.

Preparation of culture medium based on grape juice and inoculums

The obtained grape juice from the above preparation was supplemented by mineral salts: magnesium sulfate 0.44 g, urea 12.70 g, and ammonium sulfate 5.30 g. Finally, the medium was distributed in an Erlenmeyer of 250 mL with a ratio of 100 mL per flask and sterilized at 120 °C for 20 min. The pre-culture was obtained by inoculating two colonies of the yeast *Saccharomyces cerevisiae* in 250 mL shake flasks containing 100 mL of grape juice, mentioned above. The pre-culture was incubated at 30 °C for 3 h and used further as inoculums for the yeast biomass production (29).

APTEFF, 52, 1-273 (2021) UDC: 582.282.23:634.8.077]:531.3:66.011
DOI: https://doi.org/10.2298/APT2152089S BIBLID: 1450-7188 (2021) 52, 89-110
BY-NC-ND
Original scientific paper

Statistical design of experiments

Factor selection and organization of experiments

Five independent variables were selected (temperature, initial pH, concentration of sugars in grape juice, the ratio of carbon to nitrogen, initial concentration of yeasts).

In a previous study carried out by Naser and Abdelrahman (30) with the aim of determining the optimal conditions for producing baker`s yeast using sugar cane molasses and achieving the best yield and lowest production cost, and the best results were when using the concentration of sugars within the range (14-18) %, Yeast inoculum level 2 to 3 g/L, agitation speed between 150 r.p.m to 200 r.p.m, adding (40-50) % urea and ammonium sulfate at pH=5.

In another study by Muhammad et al. (31) the baker`s yeast production process was improved and the effect of various physical and chemical factors on the production of yeast cells was evaluated. The optimal conditions were determined to obtain the maximum possible growth of yeast cells at a concentration of sugars equal to 100 g/L, the agitation speed at 150 r.p.m, at pH = 4.5, and T = 28 °C.

Optimization of baker`s yeast production using date juice as the sole carbon source using response surface methodology method has been studied by Ali et al. (32) and the study showed the success of using date juice in obtaining a good yield of the yeast biomass at the initial conditions of the fermentation process (sugar concentration 70.93 g/L, temperature 32.9 °C and pH 5.35).

A study carried out by Taleb et al. (33) showed that the use of ammonium sulfate and urea as a source of nitrogen during the production of break`s yeast by 50-50 % contributed to improving production yield by more than 36%, and adding thiamine vitamin at a concentration of 0.6 had a positive role in improving production by more than 6%.

A study by Sokchea et al. (34) indicated that the best amount of biomass for yeast is obtained when the ratio between the concentration of glucose and nitrogen (C/N) used during the fermentation process is equal to 10.

After reviewing previous studies, the lower and upper levels of studied variables were selected, Table 1 shows the lower and upper levels of studied variables.

A program Minitab 19 software was used to optimize the Baker's yeast production The CCD matrix is composed of a complete factorial design, thirty-two cube points, eight center points in a cube, ten axial points, and four center points in axial of design variable at a distance of $\alpha = 2.366$ and two-level factorial. Each experiment was carried out twice and the average value is used.

Table 1. The lower and upper levels of studied variables

Variables	Lower level (-1)	Upper level (+1)
X1= Temperature (°C)	25	35
X2= Initial pH	3	6
X3= Concentration of sugars (g/L)	100	200
X4= The ratio of carbon to nitrogen	8:1	15:1
X5= Initial concentration of yeasts (g/L)	2	3

APTEFF, 52, 1-273 (2021) UDC: 582.282.23:634.8.077]:531.3:66.011
DOI: https://doi.org/10.2298/APT2152089S BIBLID: 1450-7188 (2021) 52, 89-110
BY-NC-ND
Original scientific paper

Effect estimation

The real values X have been calculated according to Equation [1].

$$X=(x-x_o)/\Delta x \quad [1]$$

where X, is the coded value for the independent variable, x, is the natural value, x_0, is the natural value at the center point and ΔX, is the step change value (the half of the interval (−1 +1)).

Regression equation in uncoded units:

$$Yi = \beta_0 + \beta_1X_1 + \beta_2X_2 + \beta_3X_3 + \beta_4X_4 + \beta_5X_5 + \beta_{11}X_1^2 + \beta_{22}X_2^2 + \beta_{33}X_3^2 + \beta_{44}X_4^2 + \beta_{55}X_5^2 + \beta_{12}X_1X_2 + \beta_{13}X_1X_3 + \beta_{14}X_1X_4 + \beta_{15}X_1X_5 + \beta_{23}X_2X_3 + \beta_{24}X_2X_4 + \beta_{25}X_2X_5 + \beta_{34}X_3X_4 + \beta_{35}X_3X_5 + \beta_{45}X_4X_5 \quad [2]$$

Yi is the predicted response (the Biomass production (g/L). The calculation of the effect of each variable and the establishment of a correlation between the response Yi and the variables X were performed using a Minitab 19 Statistical Software (Minitab, Inc., State College, PA, USA) (32).

Statistical Analysis

The statistical analysis was performed using (ANOVA), in order to validate the square model regression. It included the following parameters: coefficient of determination R^2; Fisher test (F); p-value and Student test (t); and the statistical significance test level was set at (probability < 0.05) (32).

Validation of Biomass Production in Optimum Medium

After completing the optimization of the production baker`s yeast on grape juice, the optimum values obtained and representative of the fermentation conditions were confirmed by conducting an experiment.

The experiment was carried out on 250 mL shake flasks and agitation speed was 200 r.p.m. To do this, 100 mL of grape juice was seeded with 11 mL of the yeast pre-culture and the pH of the medium was adjusted to the obtained value of 4.75. Shake flasks were sterilized at 120 °C for 20 min and incubated at 30 °C (optimum value) for 12 h.

Analytical Methods

*Determination of total reducing sugars.*1 ml of the sample is taken after filtering it and placed in a glass tube, then 98% sulfuric acid and 0.6 mL of 5% (w/v) phenol were added and mixed well after which it is left at room temperature for 30 minutes, the absorbance is measured using a spectrophotometer (Analytik Jena-Specord 200UV-VIS spec.) at a wave-length of 490 nm, the concentration of the reducing sugar is calculated depending on the

APTEFF, 52, 1-273 (2021) UDC: 582.282.23:634.8.077]:531.3:66.011
DOI: https://doi.org/10.2298/APT2152089S BIBLID: 1450-7188 (2021) 52, 89-110
BY-NC-ND
Original scientific paper

calibration curve, which was formed between different concentrations of standard solutions of glucose and between the absorbance values corresponding to each concentration (35).

Determination of biomass concentration. 1 ml of the sample is taken and subjected to a centrifugation process for 5 minutes at 5000 r.p.m., after which the supernatant is collected on the surface and washed twice with water and then placed in a drying oven at 105 °C, the drying continues until the weight is stable (36).

Determination of the fermentation power of the obtained yeast. 6.75 g of the sugar-phosphate mixture was mixed with 75 ml of calcium sulfate solution in the beaker. Then add 0.893 g of dry baker's yeast. Stir well to disperse the yeast. Then the fermentation power was measured using fermentometer (Rheo fermentometer F4) (37).

Modeling

In order to fit the experimental data, three kinetic models (Monod, Verhulst, and Tessier) were chosen.

Monod kinetic model is a substrate concentration-dependent, Verhulst kinetic model is an unstructured model depends on biomass, Tessier is an unstructured model for a substrate concentration-dependent (32).

The Kinetic parameters (μmax, Ks, and Xm), were determined after obtaining the curve fitting method of each model performed using Excel software (2016 Microsoft Corporation), and the results showed in Table 2 (38).

Table 2. Unstructured kinetic models to determine the kinetic parameters (32).

Kinetic Models	Equations	Linearized form	Symbols
Monod model	$\mu=\mu_{max}*(s/(s+k_s))$	$(1/\mu)=(k_s/\mu_{max})+(1/s)+ + (1/\mu_{max})$	μ: is the specific growth rate (h^{-1}). μ_{max}: is the maximum specific growth rate (h^{-1}). K_S: is the half-saturation constant (g/L). S: is the concentration in limiting substrate (g/L). X: is the biomass concentration (g/L). X_m: is the Maximum biomass concentration (g/L).
Verhulst model	$\mu=\mu_{max}*(1-x/x_m)$	$\mu= \mu_{max}-(\mu_{max}/x_m)*x$	
Tessier model	$\mu=\mu_{max}*(1-exp^{-k_s*s})$	$ln(\mu)=(1/k_s)*s+ ln(\mu_{max})$	

Profile Prediction of Biomass and Substrate Concentration

The integration of the Verhulst model was used (Equation 3), in order to predict the experimental profile of biomass of *Saccharomyces cerevisiae* during time (32).

$$X=(x_0* exp^{\mu_m*t}) / (1-(x_0/x_m)*(1- exp^{\mu_m*t})) \quad [3]$$

The substrate model (Leudeking Piret) as described below (Equation 4) was also applied to predict an experimental profile for total reducing sugars consumption by *Saccharomyces cerevisiae* during the time fermentation.

$$-ds/dt = p*(dx/dt) +q*x \quad [4]$$

APTEFF, 52, 1-273 (2021) UDC: 582.282.23:634.8.077]:531.3:66.011
DOI: https://doi.org/10.2298/APT2152089S BIBLID: 1450-7188 (2021) 52, 89-110
BY-NC-ND
Original scientific paper

where $p=1/y_{x/s}$ and q is a maintenance coefficient ($q=\mu_{max}/y_{x/x0}$). Equation [4] is rearranged as follows:

$$-ds=p*dx+ q \int x_{(t)}*dt \quad [5]$$

Substituting Equation [3] in Equation [5] and integrating with initial conditions ($S = S_0$; $t = 0$) give the following Equation:

$$S=s_0-p\ x_0\ \{exp^{\mu}{}_m{}^{*t}/1-(x_0/x_m)*(1- exp^{\mu_m*t})\}-q*(x_m/\mu_m)*ln\ (1-x_0/x_m)*(1-exp^{\mu_m*t}) \quad [6]$$

RESULTS AND DISCUSSION

The improvement of dry yeast biomass production was studied by determining the optimum values of the following factors (temperature, initial pH, concentration of sugars in grape juice, the ratio of carbon to nitrogen, initial concentration of yeasts) that have their influence on the production process using the central composite experimental design, and the results are shown in Table 3.

Ammonium sulfate and urea were added as a source of nitrogen in a ratio of 50-50 %, taking into account the achievement of the specified ratio between carbon and nitrogen for each experiment, and the agitation speed used during fermentation was 200 r.p.m.

Using the results obtained in diverse experiments, the correlation gives the influence of temperature (x_1), initial pH (x_2), total sugar concentration (x_3), the ratio of carbon to nitrogen (x_4), and initial concentration of yeasts (x_5) on the response. This correlation is obtained by Minitab 19 software and expressed by the following second-order polynomial (Equation 7).

$$Y=-261.1+8.96\ T+16.10\ pH + 0.353\ C+ 6.55\ C/N+49.8\ X- 0.1527\ T*T-1.769\ pH * pH-0.001414\ C*C-0.3025\ C/N*C/N-9.30\ X*X+0.0316T*\ pH+0.00096\ T*C+ 0.0206\ T*C/N- 0.117\ T*X+ 0.00414\ pH\ *C- 0.0390\ pH\ *C/N- 0.165\ pH\ *X+ 0.00163\ C*C/N+ 0.0096\ C*X- 0.016\ C/N*X \quad [7]$$

APTEFF, 52, 1-273 (2021) UDC: 582.282.23:634.8.077]:531.3:66.011
DOI: https://doi.org/10.2298/APT2152089S BIBLID: 1450-7188 (2021) 52, 89-110
BY-NC-ND
Original scientific paper

Table 3. The central composite design for biomass production

Run	Actual Values					(Yi): Biomass (g/L)	
	Temp. (°C)	Initial pH	Conc. of sugars (g/L)	The Carbon to Nitrogen ratio	Initial conc. of yeasts (g/L)	Experimental value	Predicted Value
01	35.00	6.000	200.0	8.000	2.000	22.41	23.0429
02	25.00	6.000	200.0	15.000	2.000	20.81	23.1708
03	25.00	3.000	100.0	15.000	2.000	20.01	19.6875
04	25.00	6.000	200.0	15.000	3.000	21.54	24.1742
05	25.00	3.000	200.0	8.000	2.000	19.18	18.5480
06	35.00	6.000	200.0	15.000	3.000	23.02	25.4896
07	25.00	6.000	200.0	8.000	2.000	20.02	21.9975
08	25.00	3.000	100.0	15.000	3.000	19.91	20.2285
09	30.00	4.500	150.0	11.500	2.500	40.45	38.5060
10	30.00	4.500	150.0	11.500	2.500	40.45	38.5060
11	35.00	3.000	200.0	8.000	3.000	18.91	19.0818
12	25.00	3.000	200.0	15.000	2.000	19.71	20.5400
13	35.00	3.000	100.0	15.000	2.000	18.84	20.2692
14	35.00	3.000	100.0	8.000	3.000	17.73	17.4531
15	30.00	4.500	150.0	11.500	2.500	40.45	38.5060
16	35.00	6.000	100.0	15.000	3.000	18.76	21.4784
17	35.00	3.000	200.0	8.000	2.000	17.79	18.6446
18	25.00	6.000	100.0	15.000	2.000	20.11	21.0771
19	35.00	6.000	100.0	8.000	2.000	20.23	21.1317
20	25.00	6.000	100.0	15.000	3.000	20.81	21.1218
21	35.00	6.000	100.0	8.000	3.000	20.91	20.1139
22	35.00	3.000	200.0	15.000	2.000	22.07	22.0803
23	25.00	6.000	100.0	8.000	2.000	21.06	21.0451
24	25.00	6.000	200.0	8.000	3.000	21.92	23.1122
25	35.00	6.000	200.0	15.000	2.000	23.07	25.6599
26	25.00	6.000	100.0	8.000	3.000	20.61	21.2010
27	35.00	3.000	200.0	15.000	3.000	21.41	22.4063
28	25.00	3.000	200.0	15.000	3.000	20.67	22.0397
29	30.00	4.500	150.0	11.500	2.500	40.45	38.5060
30	30.00	4.500	150.0	11.500	2.500	40.45	38.5060
31	30.00	4.500	150.0	11.500	2.500	40.45	38.5060
32	35.00	6.000	100.0	15.000	2.000	23.00	22.6074
33	35.00	3.000	100.0	8.000	2.000	21.11	17.9747
34	35.00	3.000	100.0	15.000	3.000	21.93	19.6364
35	25.00	3.000	200.0	8.000	3.000	20.27	20.1589
36	30.00	4.500	150.0	11.500	2.500	40.45	38.5060
37	30.00	4.500	150.0	11.500	2.500	40.45	38.5060
38	35.00	6.000	200.0	8.000	3.000	22.03	22.9839
39	25.00	3.000	100.0	8.000	2.000	20.17	18.8368
40	25.00	3.000	100.0	8.000	3.000	20.91	19.4890
41	30.00	4.500	150.0	11.500	2.500	40.45	43.9227
42	41.83	4.500	150.0	11.500	2.500	23.81	22.8190
43	30.00	4.500	150.0	11.500	3.683	33.02	31.1860
44	30.00	4.500	268.3	11.500	2.500	32.17	26.3327
45	30.00	4.500	150.0	11.500	1.317	31.56	30.6159
46	18.17	4.500	150.0	11.500	2.500	24.07	22.2828
47	30.00	4.500	150.0	11.500	2.500	40.45	43.9227
48	30.00	4.500	150.0	11.500	2.500	40.45	43.9227
49	30.00	8.049	150.0	11.500	2.500	30.94	24.7659
50	30.00	0.951	150.0	11.500	2.500	15.11	18.5059
51	30.00	4.500	150.0	11.500	2.500	40.45	43.9227
52	30.00	4.500	31.7	11.500	2.500	18.87	21.9291
53	30.00	4.500	150.0	3.219	2.500	19.11	21.1956
54	30.00	4.500	150.0	19.781	2.500	30.03	25.1663

APTEFF, 52, 1-273 (2021)
DOI: https://doi.org/10.2298/APT2152089S
BY-NC-ND
UDC: 582.282.23:634.8.077]:531.3:66.011
BIBLID: 1450-7188 (2021) 52, 89-110
Original scientific paper

Table 4 shows the coefficient regression corresponding with t and p-values for all the linear and the analysis of variance (ANOVA), quadratic, and interaction effects of parameters tested. A positive sign in the t-value indicates a synergistic effect, while a negative sign represents an antagonistic effect of the parameters on the biomass concentration (39).

Table 4. Estimated regression coefficients of t and p and Analysis of variance (ANOVA)

Term	DF	Adj SS	Adj MS	Coef	SE Coef	T-Value	P-Value	VIF	P-Value
T	1	0.55	0.555	0.113	0.447	0.25	0.802	1.00	0.802
pH	1	75.60	75.595	1.323	0.447	2.96	0.006	1.00	0.006
C	1	37.41	37.408	0.931	0.447	2.08	0.045	1.00	0.045
C/N	1	30.42	30.415	0.839	0.447	1.88	0.070	1.00	0.070
X	1	0.63	0.627	0.120	0.447	0.27	0.789	1.00	0.789
T*T	1	869.04	869.040	-3.818	0.381	-10.03	0.000	1.01	0.000
pH * pH	1	945.05	945.046	-3.981	0.381	-10.46	0.000	1.01	0.000
C*C	1	745.29	745.295	-3.536	0.381	-9.29	0.000	1.01	0.000
C/N*C/N	1	818.56	818.560	-3.705	0.381	-9.74	0.000	1.01	0.000
X*X	1	322.63	322.625	-2.326	0.381	-6.11	0,000	1.01	0.000
T* pH	1	1.80	1.800	0.237	0.519	0.46	0.651	1.00	0.651
T*C	1	1.84	1.838	0.240	0.519	0.46	0.648	1.00	0.648
T*C/N	1	4.17	4.169	0.361	0.519	0.69	0.492	1.00	0.492
T*X	1	2.76	2.755	-0.293	0.519	-0.56	0.576	1.00	0.576
pH *C	1	3.08	3.081	0.310	0.519	0.60	0.554	1.00	0.554
pH *C/N	1	1.34	1.341	-0.205	0.519	-0.39	0.696	1.00	0.696
pH *X	1	0.49	0.493	-0.124	0.519	-0.24	0.813	1.00	0.813
C*C/N	1	2.60	2.605	0.285	0.519	0.55	0.587	1.00	0.587
C*X	1	1.84	1.838	0.240	0.519	0.46	0.648	1.00	0.648
C/N*X	1	0.02	0.025	-0.028	0.519	-0.05	0.958	1.00	0.958

Model summary

S	R-sq	R-sq(adj)	R-sq(pred)
2.93825	92.85%	88.16%	69.22%

S represents the standard deviation of the distance between the data values and the fitted values, the lower the value of *S*, the better the model describes the response. *R-sq* (R^2) is the percentage of variation in the response that is explained by the model, the higher the R^2 value, the better the model fits your data. R^2 is always between 0% and 100%. *R-sq (adj)* (adjusted R^2) is the percentage of the variation in the response that is explained by the model. *R-sq (pred)* (predicted R^2) is calculated with a formula that is equivalent to systematically removing each observation from the data set, estimating the regression equation, and determining how well the model predicts the removed observation. The value of the predicted R^2 ranges between 0% and 100%. By referring to the values obtained in the current study for these parameters, we find that the current study model is acceptable.

The examination of Table 4 shows that all coefficient regression of the quadratic terms are statistically significant $p \leq 0.05$ and negatively affect the biomass production (Figure 2). In contrast, the interaction terms (T, C/N, X, T* pH, T*C, T*C/N, T*X, pH *C, pH *C/N, pH *X, C*C/N, C*X, C/N*X) are statistically not significant $p > 0.05$, and the interaction

APTEFF, 52, 1-273 (2021)
DOI: https://doi.org/10.2298/APT2152089S
BY-NC-ND
UDC: 582.282.23:634.8.077]:531.3:66.011
BIBLID: 1450-7188 (2021) 52, 89-110
Original scientific paper

terms (pH, C, T*T, pH * pH, C*C, C/N*C/N, X*X) are significant with $p < 0.05$ and have a synergistic effect on the response.

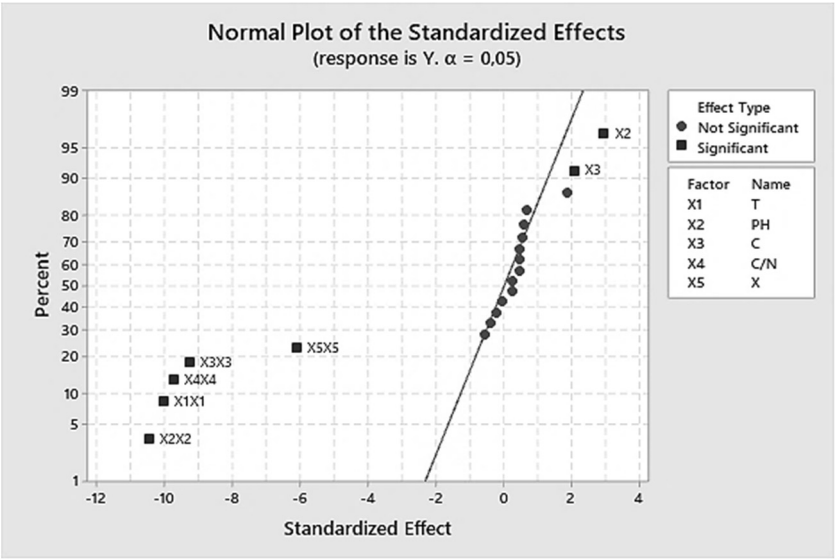

Figure 2. Variable effect signification on a biomass production.

It is known that the F-value with a low probability p-value indicates a high significance of the regression model (40).

Looking at the analysis of variance (ANOVA), the study shows that the model is important as the F-value had a low probability p-value ($p = 0.000$), and the resulting value of R^2 was equal to 92.9% and this indicates that only 7.1% of the variance is not explained by the model and therefore there is a good agreement between the model and the experimental data (41). Figure 3 shows the fit between the model and experimental data of cell growth.

By reviewing previous studies, Bennamoun et al. (42) use response surface methodology in order to improve and optimization of the medium components, which enhance the polygalacturonase activity of the strain Aureobasidium pullulans, and they got good results (a very low p-value (0.001) and a high coefficient of determination ($R^2 = 0.9421$), the results confirm the importance and success of using this method.

APTEFF, 52, 1-273 (2021)
DOI: https://doi.org/10.2298/APT2152089S
BY-NC-ND
UDC: 582.282.23:634.8.077]:531.3:66.011
BIBLID: 1450-7188 (2021) 52, 89-110
Original scientific paper

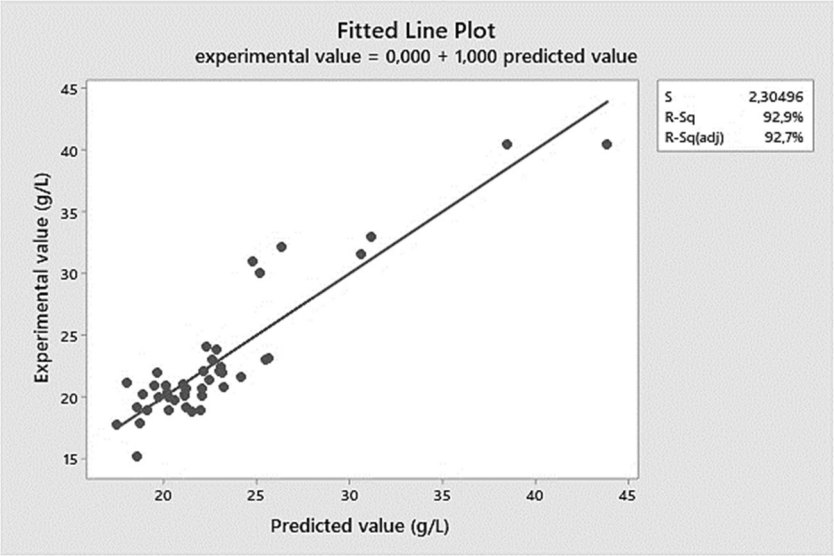

Figure 3. The fit between the model and experimental data of cell growth.

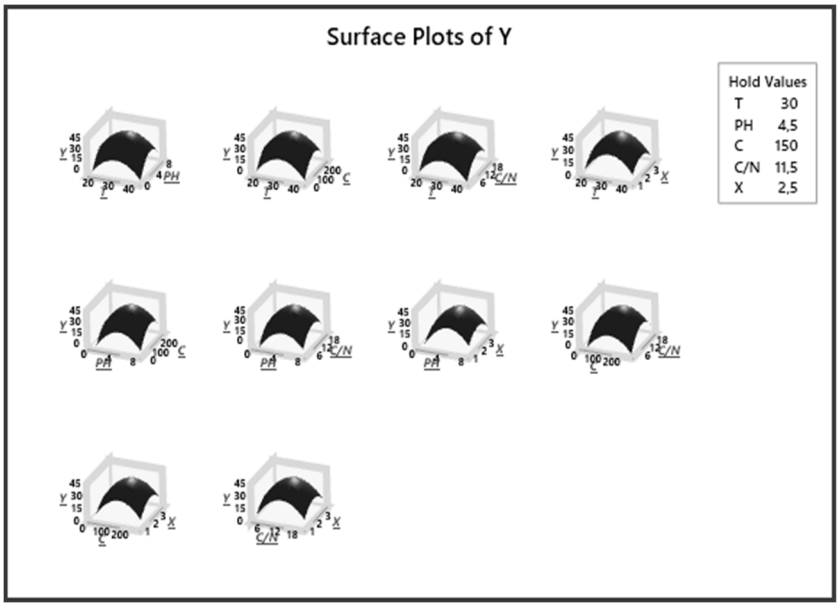

Figure 4. Surface plot for the effect of different parameters on biomass production.

APTEFF, 52, 1-273 (2021) UDC: 582.282.23:634.8.077]:531.3:66.011
DOI: https://doi.org/10.2298/APT2152089S BIBLID: 1450-7188 (2021) 52, 89-110
BY-NC-ND
Original scientific paper

A previous study by Boudjema, Fazouane-Naimi, and HellaL (27) showed the success of using the experimental design method in the study of production *Saccharomyces cerevisiae* DIV13-Z087°CVS using sweet cheese serum, as it confirmed a high significance of the regression model and the results showed a good agreement with experimental data (a low probability p-value ≤ 0.000 and a good correlation coefficient (R^2 = 0.914%).

The optimization of the response Yi (biomass production) and the prediction of the optimum levels of (temperature, initial pH, concentration of sugars in grape juice, the ratio of carbon to nitrogen, initial concentration of yeasts) were obtained. This optimization resulted in surface plots (Figure 4), the figure shows that there is an optimum, located at the center of the field of study.

In addition, the use of the Minitab optimizer will give exact values of the optimum operating conditions of the process (Figure 5).

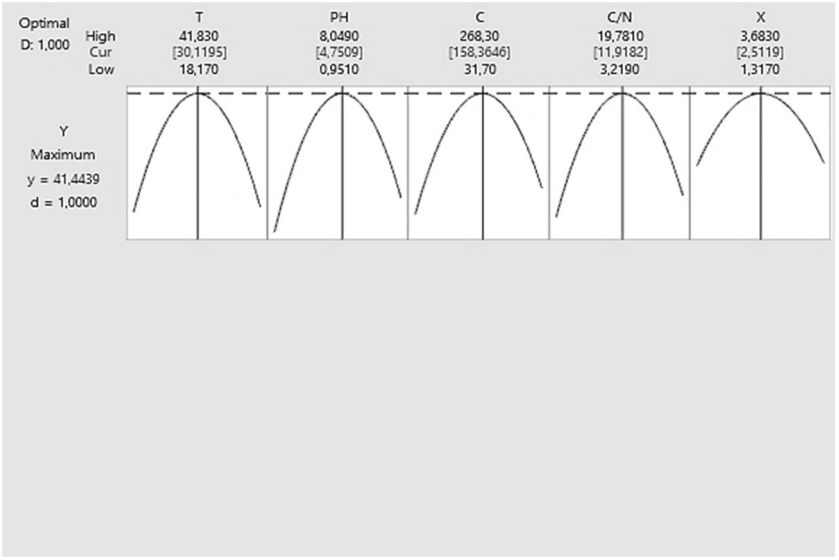

Figure 5. Values of optimal conditions on biomass production.

Figure 5 shows the maximum biomass production by *Saccharomyces cerevisiae* (41.444 g/L) corresponding to values of temperature (30.11 °C), pH (4.75), sugar concentration (158.36 g/L), the ratio of carbon to nitrogen (11.9), initial concentration of yeasts (2.5 g/L), The amount of urea was 6.65g/L and the amount of ammonium sulfate used was 6.65 g/L, so that the concentration of added urea and ammonium sulfate was 50-50% and the required C/N ratio was achieved, and the used agitation speed was equal to 200 r.p.m during the fermentation process. Jiménez-Islas et al (36) obtained the highest cell concentration of *Saccharomyces cerevisiae* ATCC 9763 (7.9 g/L) after 26 h when the strain grew at 30 °C and pH 5.5, so we note that our study gave a good result in achieving the greatest possible production of baker`s yeast.

The validation of the baker's yeast biomass concentration and total reducing sugar consumption, over time fermentation, at optimized conditions, are presented in Figure 6.

APTEFF, 52, 1-273 (2021)
DOI: https://doi.org/10.2298/APT2152089S
BY-NC-ND
UDC: 582.282.23:634.8.077]:531.3:66.011
BIBLID: 1450-7188 (2021) 52, 89-110
Original scientific paper

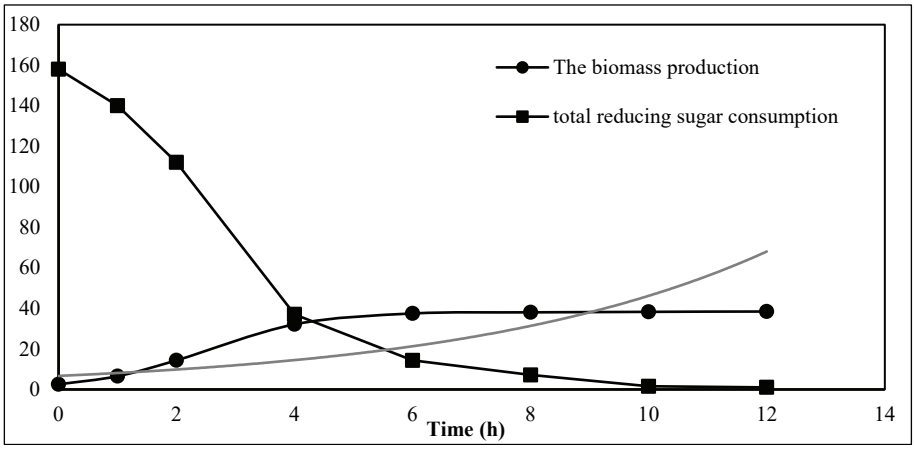

Figure 6. The biomass production, and total reducing sugar consumption overtime at optimized conditions.

At the beginning of the fermentation process, the concentration of the resulting biomass increases and is associated with the consumption of sugar. After 12 hours of the fermentation process, the sugar concentration has reached a very low level, and this is associated with a decrease in yeast production.

The same results were obtained by Ali et al. (32) where they study the optimization of Baker's Yeast Production on Date extract Using Response Surface Methodology (RSM), and the resulting yeast was equal to 40 g/L.

The measured fermentation power of the yeast obtained in this study from grape juice was 480 ml, so this is considered to have good fermentation capacity and is suitable for industrial use. The acceptable fermentation strength of yeast is not less than 350 ml according to the COFALEC (2012): General characteristics of dry baker's yeast.

Depending on the Monod model, the curve fitting of cell growth is formed (1/μ versus 1/S) and shown in Figure 7. Figure 8 shows the resulting graph according to the Verhulst model (μ versus X) and in Figure 9 the graphical curve is formed according to the growth of the Tessier model (μmax and Ks).

APTEFF, 52, 1-273 (2021)
DOI: https://doi.org/10.2298/APT2152089S
UDC: 582.282.23:634.8.077]:531.3:66.011
BIBLID: 1450-7188 (2021) 52, 89-110
Original scientific paper
BY-NC-ND

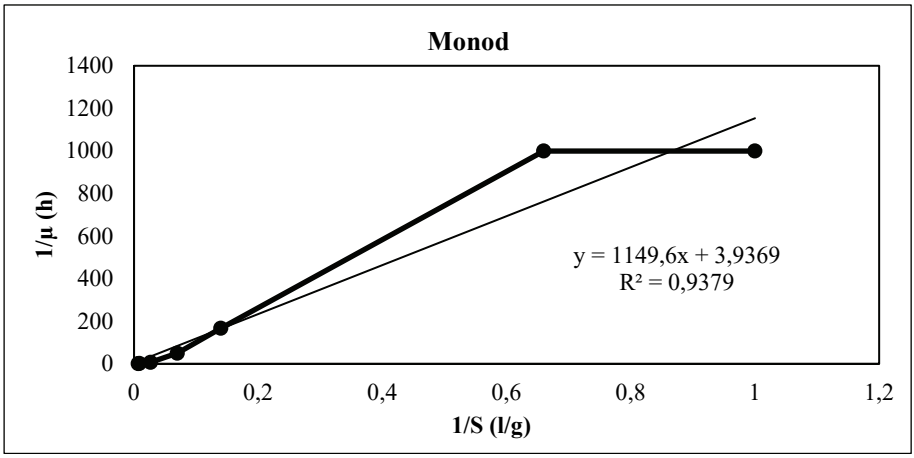

Figure 7. The Line Weaver Burk linear plot fitting the experimental data using the Monod kinetic model.

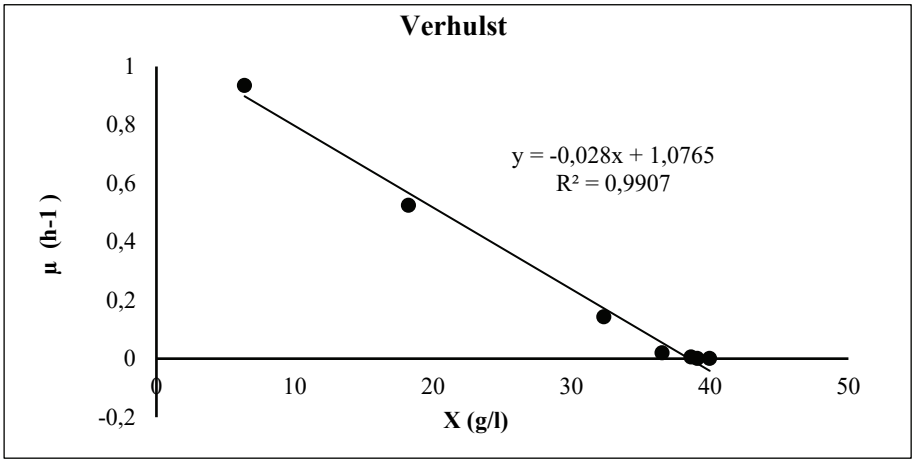

Figure 8. A plot fitting the experimental data using the Verhulst kinetic model.

APTEFF, 52, 1-273 (2021)
DOI: https://doi.org/10.2298/APT2152089S
BY-NC-ND
UDC: 582.282.23:634.8.077]:531.3:66.011
BIBLID: 1450-7188 (2021) 52, 89-110
Original scientific paper

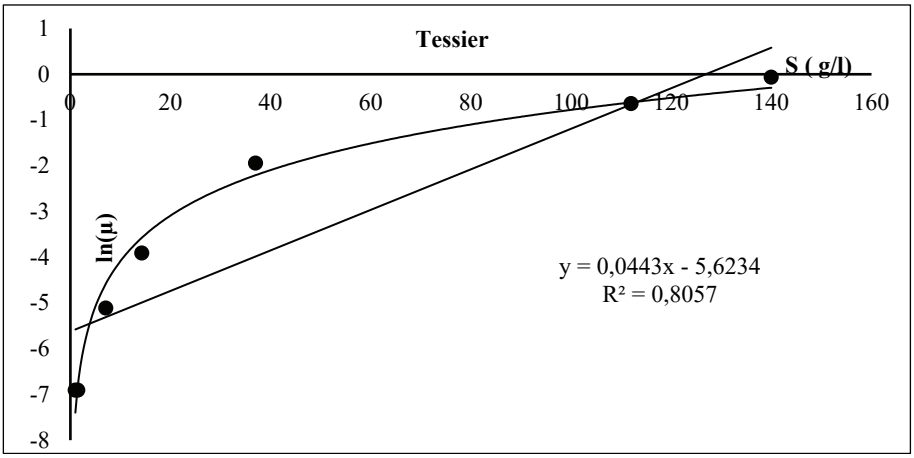

Figure 9. A plot fitting the experimental data using the Tessier kinetic model.

The results of the kinetic parameters of *Saccharomyces cerevisiae* growth with the different kinetic models based on the curve fitting method are presented in Table 5.

Table 5. Kinetic parameters of *Saccharomyces cerevisiae* growth and substrate utilization using unstructured models.

Kinetic models	Parameters of estimation			
	R^2	K_S (g/L)	μ_{max} (h^{-1})	X_m
Monod	0.94	291.99	0.254	-
Verhulst	0.99	-	1.0765	38.26
Tessier	0.81	22.7	0.0036	-

The results obtained from the modeling process appear as follows: the Monod model gave a good value for the parameter R^2 equal to 0.94, which indicates that it is an acceptable model for studying the kinetic performance of a strain *Saccharomyces cerevisiae* and the values of each of the maximum specific growth rate (μmax) and is the half-saturation constant (Ks) were evaluated as 0.254 h^{-1} and 291.99 g/L, respectively, which are good values indicating rapid growth of cells Yeast. Tessier`s model gave the lowest value for R^2 compared to the Monod and Verhulst models, where it was 0.81. Whereas, the Verhulst model gave the highest value for the parameter R^2 which reached 0.99, also gave a high value for the maximum specified growth rate reached 1.0765 h^{-1}, and the highest possible amount was obtained from the concentration of yeast according to the Tessier model reached 38.26 g/L. As a result, the Verhulst model is the best model for studying and controlling the kinetic behavior of a yeast strain *Saccharomyces cerevisiae*.

A residual plot is a graph that is used to examine the goodness of fit in regression. Examining residual plots helps determine whether the ordinary least squares assumptions are being met. If these assumptions are satisfied, then ordinary least squares regression will produce unbiased coefficient estimates with the minimum variance. The four-in-one residu-

APTEFF, 52, 1-273 (2021) UDC: 582.282.23:634.8.077]:531.3:66.011
DOI: https://doi.org/10.2298/APT2152089S BIBLID: 1450-7188 (2021) 52, 89-110
BY-NC-ND
Original scientific paper

al plot displays four different residual plots together in one graph window. This layout can be useful for comparing the plots to determine whether the Verhulst model meets the assumptions of the analysis. The residual plots in the graph include:

- Histogram - indicates whether the data are skewed or outliers exist in the data.
- Normal probability plot - indicates whether the data are normally distributed, other variables are influencing the response, or outliers exist in the data.
- Residuals versus fitted values - indicates whether the variance is constant, a nonlinear relationship exists, or outliers exist in the data.
- -Residuals versus order of the data - indicates whether there are systematic effects in the data due to time or data collection order.

Minitab provides the following residual plots in Figure 10.

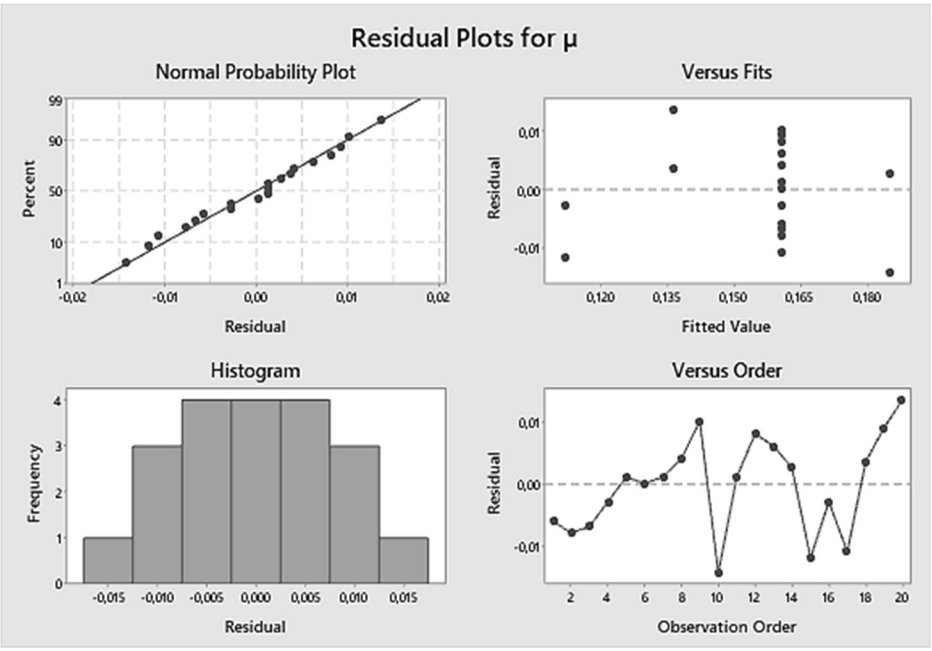

Figure 10. Residual plots for response.

In visually checking the residuals we can see that we have nothing to complain about. There does not seem to be any great deviation in the normal probability plot of the residuals. There's nothing here that is very alarming and it seems acceptable.

The kinematic models describe the growth rate of microorganisms based on biomass and substrate concentration and are useful because they help engineers design and control biological processes, including the Verhulst model which describes the experimental data obtained on the growth rate of yeast cells, where it describes the logarithmic growth of cells and shows that the first six hours of fermentation were during the initial cell growth phase, then the logarithmic growth phase began, which is characterized by a doubling of the number of yeast cells and an increase in the growth rate.

APTEFF, 52, 1-273 (2021)
DOI: https://doi.org/10.2298/APT2152089S
BY-NC-ND
UDC: 582.282.23:634.8.077]:531.3:66.011
BIBLID: 1450-7188 (2021) 52, 89-110
Original scientific paper

A profile of biomass and total reducing sugar concentration during fermentation time is compared to the values predicted by the equations model obtained in Figures 11 and 12.

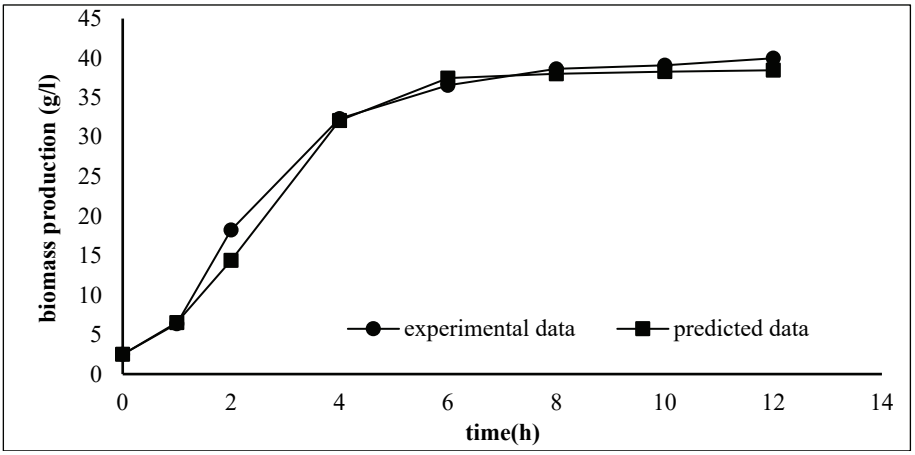

Figure 11. The comparison between predicted and experimental data for biomass production of baker`s yeast.

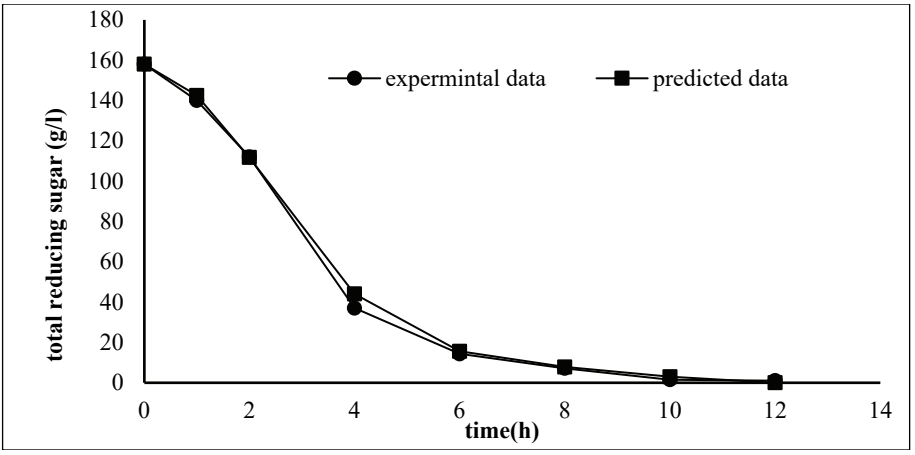

Figure 12. The comparison between predicted and experimental data for total reducing sugar consumption.

During the fermentation, values of biomass between predicted and experimental data were approximately the same. And for total reducing sugar concentration, the values obtained by the Leudeking Piret model were identical with predicted values, where the values ($p=1/y_{x/s}$, $q=\mu/y_{x/x0}$) were 3.81 g/g and 0.065 1/h, respectively.

On the basis of these results, good correlation coefficients showed that the proposed Verhulst model and the Luedeking Piret model were adequate to explain the development of the biomass production process on grape juice.

APTEFF, 52, 1-273 (2021) UDC: 582.282.23:634.8.077]:531.3:66.011
DOI: https://doi.org/10.2298/APT2152089S BIBLID: 1450-7188 (2021) 52, 89-110
BY-NC-ND
Original scientific paper

This study confirmed that the Logistic equation for the growth and the Leudeking Piret kinetic model for substrate utilization were able to fit the experimental data, and the same result was obtained by Kara Ali et al. (44) Where they used the logistic empirical kinetic model and Leudeking Piret model and they obtained good agreement with the experimental data.

Finally, what distinguishes this study from previous studies is the dependence on grape juice as a source of carbon with the aim of producing biomass from dry yeast, which researchers had not previously studied. The work has been done with a lot of numerical and experimental analysis.

This study will present an additional successful option for the production of yeast that commonly uses molasses. The improvement of the initial conditions of fermentation also contributed to the highest possible yield of yeast and good economic value. The fermentation power of the yeast was also good, so this study can be practically applied with the aim of producing a good mass of baker's yeast and using this yeast in various industrial and food fields.

CONCLUSION

The central composite design (CCD) proposed in this study seems pertinent to describe the optimum biomass production of *Saccharomyces cerevisiae*. A second-order polynomial model was developed to evaluate the quantitative effects of temperature, initial pH, and concentration of sugars in grape juice, the ratio of carbon to nitrogen, initial concentration of yeasts in order to discover the optimum conditions for the biomass production from grape juice. According to the experimental results, a maximum biomass concentration of (41.444 g/L) corresponding to values of temperature (30.11 °C), pH (4.75), sugar concentration (158.36 g/L), the ratio of carbon to nitrogen (11.9), initial concentration of yeasts (2.5 g/L), the amount of urea was 6.65g/L and the amount of ammonium sulfate used was 6.65 g/L, so that the concentration of added urea and ammonium sulfate was 50-50%, and the used agitation speed was equal to 200 r.p.m during the fermentation process. The fermenter power of the obtained yeast was 470 ml. In addition, among three unstructured kinetic models, the Verhulst model was the most suitable model to signify the baker’s yeast production on grape juice medium.

Acknowledgements

The authors are thankful to every one supported our work, and to every who collaboration and assistance to carry out this study.

Conflicts of interest

The authors declare no conflict of interest.

BY-NC-ND

REFERENCES

1. Palla, M.; Blandino, M.; Grassi, A.; Giordano, D.; Sgherri C.; Quartacci, M.F.; Reyneri, A.; Agnolucci, M.; Giovannetti, M. Characterization and selection of functional yeast strains during sourdough fermentation of different cereal wholegrain flours. *Scientific Reports.* **2020**, 10:12856. https://doi.org/10.1038/s41598-020-69774-6.
2. Tamang, J. P.: Watanabe, K.; Holzapfel, W. H. Diversity of microorganisms in global fermented foods and beverages. *Front. Microbiol*. **2016**, *7*, 377. https: //doi.org/10.3389/fmicb .2016.00377**.**
3. Gelinas, P.; McKinnon, C. Fermentation and microbiological processes in cereal foods, in handbook of cereal science and technology, 2nd Ed., Kulp K, Ponte JG. Jr.Ed. *Marcel Dekker Inc*. **2000**, 741-754.
4. Phaff, H.J. Isolation of yeasts from natural sources in Isolation of Biotechnological Organisms from Nature (Labeda, D. P., Ed.). *McGraw-Hill*, New York. **1990**.
5. Goffeau, A.; Barrell, B.G.; Bussey, H.; Davis, R.W.; Dujon, B.; Feldmann, H.; Galibert, F.; Hoheisel, J.D.; Jacq, C.; Johnston, M.; Louis, E.J.; Mewes, H.W.; Murakami, Y.; Philippsen, P.; Tettelin, H.; Oliver, S.G. Life with 6000 Genes. *Sci*. **1996**, *74*, 563-567.
6. Chris, T. H.; James, L. S.; David, S. R. Diverse yeasts for diverse fermented beverages and foods. *Elsevier Ltd*. **2018**, *49*,199-206. Doi: 10.1016/j.copbio.2018.10.004.
7. Sivasakthivelan, P.; Saranraj, P.; Sivasakthi, S. Production of bioethanol by *Zymomonas mobilis* and *Saccharomyces cerevisiae* using sunflower head wastes–A comparative study. *Int. J. Microb. Res*. **2014**, *5*(3), 208-216.
8. Prem Kumar, D.; Jayanthi, M.; Saranraj, P.; Kavi Karunya, S. Effect of Calcium propionate on the inhibition of fungal growth in Bakery products. *Indo-Asian J. Multidis. Res.* **2015**, *1*(3): 273-279.
9. Beudeker, F.R.; Van Dam, H.W.; Van der Plaat, J.B. ; Vellenga, K. Developments in baker's yeast production. In Yeast Biotechnology and Biocatalysis, ed. H Verachtert. New York: *Marcel Dekker, Inc.* **1990**.
10. Saranraj, P.; Sivasakthivelan, P.; Suganthi, K. Baker's Yeast:Historical Development, Genetic Characteristics, Biochemistry, Fermentation and Downstream Processing. *Journal of Academia and Industrial Research (JAIR)*. December **2017**, ISSN: 2278-5213.
11. Lisičar. J; Sedaghati. M; Barbe. S. Looking at baker´s yeast fermentation through new glasses: The neglected potential of vinasse for biotechnological applications. 31st Yeast Conference, Leuven (Belgium), **2018**.
12. Lisičar. J; Millenautzki. T; Scheper. T; Barbe .S. New trends in industrial baker's yeast fermentation: Recovery of key biomolecules and low-grade heat conversion. *Journal of Biotechnology*. **2018,** 280 (Suplement), S17-S18. DOI: 10.1016/j.jbiotec.2018.06.052.
13. Boyacıoğlu1, H.; Ertunç, S.; Hapoğlu1, H. Modelling of Baker's Yeast Production. *International Journal of Secondary Metabolite*. **2017**, 4(1), 10-17. DOI: 10.21448/ijsm.252053. https://dergipark.org.tr/tr/download/issue-file/2871.
14. Fadel, M.; Yousif, E.S.; Abdelfattah, A.; Ola S.S.; Sarra, E. Approach for Highly Active Baker`s Yeast Product from Distilled Yeast Biomass. *Current Science International*. **2020**, 321-334. DOI: 10.36632/csi/2020.9.2.27.
15. Reed, G. and Nagodawithana, T.W. Yeast Technology 2nd edition, Van Nostrand, New York. **2011**.
16. Arshadm, K.; Khalil, R.; Rajokam, I. Optimization of process variables for minimization of byproduct formation during fermentation of blackstrap molasses to ethanol at industrial scale. *Lett Appl Microbiol*. 475410414.**2018**.
17. Kopsahelis, N.; Nisiotou, A.; Kourkoutas, Y.; Panas, P.; Nychas, G. J.; Kanellaki, M. Molecular characterization and molasses fermentation performance of a wild yeast strain operating in an extremely wide temperature range. *Bioresour Technol*. **2009**, *100*, 4854-4862.

BY-NC-ND

18. Xandé ,X.; Archimède,H.; Gourdine, J. L.; Anais,C.; Renaudeau,D. Effects of the level of sugarcane molasses on growth and carcass performance of Caribbean growing pigs reared under a ground sugarcane stalks feeding system. *Trop Anim Health Prod*. 4211320.**2020**.
19. Makhoul, G.; Mahfoud, H.; Daoub, R. Morphological characterization of some grape types in the Sheikh Badr region of Tartous governorate. *Tishreen University Journal for Research and Scientific Studies - Biological Sciences Series* .**2018**, *4*(6), 8402.
20. Alexeeva, Y.V.; Ivanova, E.P.; Bakunina, I.Y.; Zvaygintseva, T.N.; Mikhailov, V.V. Optimization of glycosidases production by Pseudoalteromonasissachenkonii. KMM 3549T. *Lett. Appl. Microbiol*. **2002**, *35*, 343-346.
21. Patidar, P.; Agrawal, D.; Banerjee, T.; Patil, S. Chitinase production by Beauveriafelina. RD 101: Optimization of parameters under solid substrate fermentation conditions*. World J. Microbiol. Biotechnol*. **2005**, *21*, 93-95.
22. Rajendhran, J.; Krishnakumar, V.; Gunasekaran, P. Optimization of a fermentation medium for production of Penicillin G acylase from Bacillus sp. *Lett. Appl. Microbiol*. **2002**, *35*, 523-527.
23. Sayyad, S.A.; Panda, B.P.; Javed, S.; Ali, M. Optimization of nutrient parameters for lovastatin production by Monascus purpureus MTCC 369 under submerged fermentation using response surface methodology.*Appl. Microbiol. Biotechnol*. **2007**, *73*, 10541058.
24. Kennedy, M.; Krouse, D. Strategies for improving fermentation medium performance: *A review. J. Ind. Microbiol. Biotechnol*. **1999**, *23*, 456–475.
25. Chakravarti, R.; Sahai, V. Optimization of compaction production in chemically defined production medium by Penicilium citrinum using statistical methods. *Process Biochem***. 2002**, *38*, 481-486.
26. Kar, B.; Banerjee, R.; Bhattachaaryya, B.C. Optimization of physicochemical parameters for gallic acid production by evolutionary operation-factorial design techniques. *Process Biochem*. **2002**, *37*, 1395-1401.
27. Boudjema, K.; Fazouane-naimi, F.; HellaL, A. Optimization of the Bioethanol Production on Sweet Cheese Whey by Saccharomyces cerevisiae DIV13-Z087°CVS using Response Surface Methodology (RSM). *Rom. Biotech. Lett.* **2015**, *20*, 10814-10825.
28. Montgomery, D.C. Design and Analysis of Experiments, 5th ed.; *John Wiley & Sons, Inc.*: New York, NY, USA**, 2009**.
29. Kocher, G.S.; Uppal, S. Fermentation variables for the fermentation of glucose and xylose using Saccharomyces cerevisiae Y-2034 and Pachysolan tannophilus Y-2460. *Indian J. Biotechnol*. **2013**, *12*, 531-536.
30. Naser, F.N.; Abdelrahman, Z. Five major factors affecting the production of baker's yeast using sugar cane Molasses. Faculty of Agriculture, Cairo University. **2017**, https://www.researchgate.net/publication/315838486.
31. Muhammad, A.K.; Muhammad, M. J.; Qurat, A.; Sana, Z.; Kaleem, I. Process optimization for the production of Yeast Extract from fresh Baker's yeast (Saccharomyces cerevisiae). Department of Biotechnology, Virtual University, Lahore, Pakistan. **2020**, www.preprints.org.
32. Ali, M.; Outiti, N.; Kaki, A.; Cherfia, R.; Benhassine, S.; Benaissa, A.; Chaouche, N. Optimization of Baker's Yeast Production on Date Extract Using Response Surface Methodology (RSM). *MDPI. Foods* .**2017**, *6*, 64. DOI: 10.3390/foods6080064.
33. Taleb, T.; Khalid, A.; Abederhman, Kh.; Bhaskara, T. Optimization of Bakery Yeast Production Cultivated on Musts of Dates. *J. Appl. Sci. Res.***2007**, *3*(10), 964-971.
34. Sokchea, H.;Thi Hang,P.; Dinh Phung, L.; Duc Ngoan, L.; Thu Hong, T.; Borin ,K. Effect of Time, C/N Ratio and Molasses Concentration on Saccharomyces Cerevisiae Biomass Production. *J Vet Ani Res*. **2018**, 1, 104. http://article.scholarena.com/Effect-of-Time-Urea-and-Molasses-Concentration-on-Saccharomyces-Cerevisiae-Biomass-Production.pdf
35. Dubois, M.; Gilles, K.A.; Hamilton, J.K.; Rebers, P.A.; Smith, F. Colorimetric Method for Determination of Sugars and Related Substances. *Anal. Chem*. **1956**, *28*, 350-356.

BY-NC-ND

36. Jiménez-Islas, D.; Páez-Lerma, J.; Soto-Cruz, N.O.; Gracida, J. Modelling of Ethanol Production from Red Beet Juice by Saccharomyces cerevisiae under Thermal and Acid Stress Conditions. *Food Technol. Biotechnol*. **2014**, *52*, 93-100.
37. COFALEC **(2012)**: General characteristics of dry baker's yeast. 14 rue de Turbigo, 75001 Paris, France.
38. Juska, A. Minimal models of growth and decline of microbial populations. *J. Theor. Biol*. **2011**, *269*, 195-200.
39. LeMan, H.; Behera, S.K.; Park, H.S. Optimization of operational parameters for ethanol production from Korean food waste leachate. *Int. J. Environ. Sci. Tech.* **2010**, *7*, 157-164.
40. Rene, E.R.; Jo, M.S.; Kim, S.H.; Park, H.S. Statistical analysis of main and interaction effects during the removal of BTEX mixtures in batch conditions using wastewater treatment plant sludge microbes. *Int. J. Environ. Sci. Technol*. **2007**, *4*, 177-182.
41. Annuar, M.S.M.; Tan, I.K.P.; Ibrahim, S.; Ramachandran, K.B. A Kinetic Model for Growth and Biosynthesis of Medium-Chain-Length Poly-(3-Hydroxyalkanoates) in Pseudomonas putida. *Braz. J. Chem. Eng.* **2008**, *25*, 217-228.
42. Bennamoun, L.; Hiligsmann, S.; Dakhmouche, S.; Ait-Kaki, A.; Labbani, F.Z.K.; Nouadri, T.; Meraihi, Z.;Turchetti, B.; Buzziniand, P.; Thonart, P. Production and Properties of a Thermostable, PH-Stable Exo-Polygalacturonase Using Aureobasidium pullulans Isolated from Saharan Soil of Algeria Grown on Tomato Pomace. *Foods.* **2016**, *5*, 72.
43. Kara Ali, M.; Hiligsmann, S.; Outili, N.; Cherfia, R.; KacemChaouche, N. Kinetic models and parameters estimation study of biomass and ethanol production from inulin by Pichiacaribbica (KC977491). *Afr. J. Biotechnol*. **2017**, 16, 124–131.

APTEFF, 52, 1-273 (2021) UDC: 633.88+665.52]:579.84/.86:615.28
DOI: https://doi.org/10.2298/APT2152111R BIBLID: 1450-7188 (2021) 52, 111-121
BY-NC-ND
Original scientific paper

ESSENTIAL OIL AND ETHANOLIC EXTRACT COMPOSITION FROM *MYRTUS NIVELLEI* BATT. & TRAB. AND THEIR BIOLOGICAL EVALUATIONS

Farah RAMDANE[1,2], Oualid MEDJOUR[1], Abdel Karim BEN AOUN[1], Soumia HADJADJ[3], Messouda GUEMOUDA[1,4], Mounira KADRI[1,4], Mahfoud HADJ MAHAMMED[2]*

[1] Faculty of Nature Sciences and Life, El Oued University, PO Box 789, 39000 Algeria

[2] Biogeochemistry Laboratory in Desert Environments, Kasdi Merbah University, PO Box 511, 30000 Ouargla, Algeria

[3] Laboratory of Protection of Ecosystem in Arid and Semi-arid Area, Kasdi Merbah University, PO Box 511, 30000 Ouargla, Algeria

[4] Laboratory of Biology, Environment and Health. El Oued University, PO Box 789, 39000 Algeria

Received: 13 February 2021 **Revised: 10 April 2021** **Accepted: 14 April 2021**

This study aims to evaluate the chemical composition and biological effects of an endemic Algerian species Myrtus nivellei belonging to the Myrtaceae family. The aerial parts of the plant were submitted to hydrodistillation and analysed with gas chromatography - mass spectrometry (GC-MS). This oil was yielded 0,75% (w/w). The GC-MS revealed that 1,8 cineole is the most abundant component (53,44%) while other compounds were present in high contents: 2,2,6,7-tetramethyl-10-oxatricyclo [4.3.0.1(1,7)]-decan-5-one (11,73%), trans ocimene (7,54%), linalyl propirionate (6,81%) and lavandulyl acetate (5,24%). In addition ethanolic extract of studied plant was prepared. Total phenol, tannin, flavonoid, and condensed tannin's contents were determined using Folin-Ciocalteu, aluminum chloride and vanillin colorimetric methods, respectively. Three tests were used for the investigation of antioxidant activity of both extract and oil. Strong antioxidant activity was shown mainly by crude extract. Antibacterial screening was evaluated against Gram positive and Gram negative bacteria. Ethanolic extract and oil were active especially against Staphylococcus aureus.

Keywords: *Myrtus nivellei*, antioxidant activity, antimicrobial activity, essential oil, ethanolic extract.

INTRODUCTION

In recent years, an increasing interest has been observed regarding the use of medicinal plants owing to their therapeutic purpose and the little or no side effects (1). For this reason, a large number of plant species have received much attention to be tested for their potential biological, therapeutic effects (2). The Myrtaceae is one of the large family of dicotyledonous woody plants containing over 5,650 species with various genres and interesting pharmacological activities, including *Sizygium*, *Eucaluptys* and *Myrtus* (3). In Algeria the genus *Myrtus* (M) is represented by two species *M. communis* L. commonly known as common myrtle (4; 5) and *M. nivellei* commonly known as Sahara myrtle (5, 6). *M. nivellei* Bath. & Trab. is a one the most aromatic species used in popular culture medicine for treatment of many diseases in south part of Algeria (7, 8). Previous biological and pharmacological investigations on Sahara myrtle were connected its efficiency to the presence of effective phytochemicals including phenolic and volatile compounds (7, 8, 9, 10, 11).

* Corresponding author: Farah Ramdane, Faculty of Nature Sciences and Life, el Oued University. PO Box 789, 39000 Algeria. Email: ramdane-farah@univ-eloued.dz

APTEFF, 52, 1-273 (2021) UDC: 633.88+665.52]:579.84/.86:615.28
DOI: https://doi.org/10.2298/APT2152111R BIBLID: 1450-7188 (2021) 52, 111-121
BY-NC-ND
Original scientific paper

These latter are evenly characterized largely aromatic species (12, 13) to gather with phenolic compounds (14, 15); which can play important roles in health care as antioxidant (15, 16) and as antimicrobial agents (17). In addition, essential oils are widely used in flavouring and aromatherapy for centuries (18). Recent investigations have documented their beneficial and positive effect in decreasing incidence of many diseases (19). Furthermore, consumers need always natural sources to cover their demands (20), and to combat reactive oxygen species (ROS) in the case of over production in body (21). Therefore, the goal of this study is to continue our occurring works on essential oil composition, total phenols, flavonoids, and tannins contents of ethanolic extract obtained from Sahara myrtle and evaluate their antioxidant and antibacterial activities.

EXPERIMENTAL

PLANT COLLECTION

Myrtus nivellei aerial parts were harvested in Oued Isakarasane; Ideless, South Algeria (23° 25′ 13,7″ N, 005° 45′ 47,8″ E. Altitude: 1952m) in 2015. Sahara myrtle was ground to a fine green powder and stored at room temperature till its use.

ESSENTIAL OIL AND EXTRACT PREPARATION

Hydro-distillation was used for extraction of essential oils by Clevenger-type apparatus according to Ramdane et al. (13). The extracted oil was dried using anhydrous sodium sulfate and stored at 4 °C. One millilitre of diluted sample was charged into a sampler flask for GC-MS analysis. Further, 10 g sample was extracted with ethanol according to Svetaz et al (22). Extract was evaporated by a vacuum rotary evaporator (Büchi Rotavapor R-200) and the crude extract was used for dosage.

CHEMICAL COMPOSITION OF ESSENTIAL OIL

Essential oil was analysed by an Agilent 6890 gas chromatography, coupled to a quadruple mass spectrometer 5973 MSD (Agilent Technologies, Hewlett-Packard, CA, USA) as described in Ramdane et al. (b) (13). The identification of volatile compounds was done by comparing their retention indices with those of reference compounds in the literature (23) and confirmed by GC-MS by comparison of their mass spectra with those of reference compounds in Wiley Registry 9th Edition/NIST 2011 edition mass spectral library.

DETERMINATION OF PHENOLIC CONTENT

Total phenolic was evaluated by the method described in Bahramikia et al. (24). Optical density was determined at 765 nm by the UV–VIS spectrophotometer. The concentration of the total phenolic was calculated in terms of gallic acid equivalent µg/ mg of plant extract after reaction for 30 min of 200 µl of extract and 1 ml FCR (diluted 1:10, v/v) followed by 0.8 ml of Na_2CO_3 (7.5%, v/v).

APTEFF, 52, 1-273 (2021) UDC: 633.88+665.52]:579.84/.86:615.28
DOI: https://doi.org/10.2298/APT2152111R BIBLID: 1450-7188 (2021) 52, 111-121
BY-NC-ND
Original scientific paper

DETERMINATION OF FLAVONOID CONTENT

$AlCl_3$ method was used for the estimation of total flavonoid. The absorbance of samples was determined at 420 nm after one hour of reaction between 1.5 ml of extract + 1.5 ml of $AlCl_3$ solution (2%) at room. Rutin was used standard sample. Estimation of total flavonoids was repeated three times and represented in μg of rutin equivalent/mg of plant extract (25).

DETERMINATION OF CONDENSED TANNIN CONTENT

Condensed tannin was evaluated according to the following method of vanillin/HCl assay (26). Sample tubes contain approximately 50 μL extract, 3 ml methanol vanillin solution and 2.5 mL HCl were placed at room temperature for 20 min. The absorbance was measured at 500 nm and results were expressed as μg catechin equivalents per mg of extract.

DETERMINATION OF TOTAL TANNIN

To determine total tannin, the technique described by Aroke et al. (27) was used. First, tannin must be precipitating by mixing extract with gelatin (200 mg) at 4° C (15 min), after that the supernatant (150 μL) were added to water in tubes and non-tannin phenolics were determined following the same method of phenolic content as above. Calculated values were subtracted from total phenolic content to determine total tannin.

EVALUATION OF ANTIOXIDANT ACTIVITY BY PHOSPHOMOLYBDENUM, DIPHENYL-PICRYLHYDRAZYL AND FERRIC-REDUCING ANTIOXIDANT POWER TESTS (PM, DPPH AND FRAP)

To estimate the antioxidant activity three colorimetric assays were used: firstly, total antioxidant capacity of crude extract was evaluated by the method of Dung et al. (28). Initially 0.1 mL of samples were combined with 3 mL of reagent solution prepared by solubilizing of 28 mM sodium phosphate, 4 mM ammonium molybdate and 0.6 M sulphuric acid. Tests tubes were put at 95 °C for 90 min after that optical density was determined at 695 nm. Method of Jaitak et al. (29) was used for the ferric reducing antioxidant power assay (FRAP). The FRAP reagent was freshly prepared before analysis. Tubes containing extract 300μL (1 mg/mL) of samples were added to 2.7 mL of the FRAP reagent. The absorbance of the combination was reported at 593 nm after 4 min. The antioxidant activity was expressed as the number of equivalents of ascorbic acid in this method and the above. The 2,2-diphenyl-2-picrylhydrazyl (DPPH) radical techniques was used for free radical-scavenging activity: 50 μL of extract concentrations was supplemented to 1 mL of 100 μM methanolic DPPH·solution on reaction tubes. These later were deposed at laboratory for 30 min until determination of absobance at 517nm.

The percentage of free radical-scavenging activity was determined using the equation below (30):

$$\% \text{ inhibition} = \frac{(\text{methanolic solution absorbance - extract absorbance}) \times 100}{\text{methanolic solution absorbance}}$$

APTEFF, 52, 1-273 (2021)
DOI: https://doi.org/10.2298/APT2152111R
BY-NC-ND
UDC: 633.88+665.52]:579.84/.86:615.28
BIBLID: 1450-7188 (2021) 52, 111-121
Original scientific paper

ANTIBACTERIAL ACTIVITY

Biological activity of both ethanolic extract and essential oil against bacteria strains was determined by employing agar disc diffusion method (31). Suspensions containing bacteria *Escherichia coli* ATCC 25922, *Pseudomonas aeruginosa* ATCC 27853, Staphylococcus aureus ATCC 25923, and clinic isolates *Salmonella sp.*, *Vibrio sp.* (0.1 ml of 10^8 cells per ml) spread on Muller Hinton Agar (MAH). Filter paper discs (6 mm in diameter) were impregnated with 20 µL of extract (50 mg/mL), to achieve a final amount 1mg/disc and placed on the inoculated MAH. These plates, after remaining at ambient temperature for 30 min, were incubated at 37 °C for overnight to allow bacterial growth.

RESULTS and DISCUSSION

CHARACTERISTIC OF ESSENTIAL OIL

Yellowish oil from aerial parts of Sahara myrtle was obtained (Figure 1), yielded 0.75% of volatile distillate fractions (w/w). Analysis result by GC/MS from the DB-5 capillary column is shown in Table 1.

Figure1. Essential oil of Sahara Myrtle

This species belonging to the Myrtaceae family yielded important mixture of volatile compounds. The Chemical characterization of the volatile fraction showed the presence of 23 different terpenes, revealing about 93.79 % of total oil components. This oil contains mostly oxygenated (68.38 %) and hydrocarbon monoterpenes (10.02 %). The mainly monoterpenes of *M. nivellei* oil were 1,8-cineole (53.44%) followed by 2,2,6,7-tetramethyl-10-oxatricyc-lo[4.3.0.1(1,7)]decan-5-one (11.73%), *trans*-ocimene (7.54%), linalyl propirionate (6.81%) and lavandulyl acetate (5.24%). α-pinene, vetiverol, 1,2-benzenediol, 3,5-bis(1,1-dimethyl-ethyl), cyclohexene, 2 butyl-1,3,3-trimethyl were up to 1%. Oxygenated sesquiterpenes (1.44%) and sesquiterpene hydrocarbon (0.77 %) were represented by low percentage. This oil contains phenolic compounds with 13.18%: 1,2-benzenediol, 3,5-bis(1,1-dimethylethyl (1.45%) and 2,2,6,7-tetramethyl-10-oxatricyclo [4.3.0.1(1,7)]decan-5-one (11.73 %). In this

BY-NC-ND

present investigation it was revealed that the chemical composition and percentage of amount of Sahara myrtle essential oil were considerably different to ones reported by Bouzabata et al. (7), in which 1,8-cineole, limonene, α-terpinyl acetate, geranyl acetate, α-terpineol, 1-hydroxy-1-(3-methyl-2-butenoxy)-2-acetoxy-3,5,5-trimethyl-3-cyclopentene were the most abundant compounds in leaves *M. nivellei* essential oil from Tassili and Tamanresset origin respectively (43.9-39.0%), (20.5-19.9%), (5.7-4.00%), (5.1-3.6%), (4.4-5.0%) and (3.7-6.7%) (7). These could be associated to several factors such as genetic, geographic and, edaphic factors (32). It was before documented that 1,8-cineole has been the mainly constituent in several species of *Eucalyptus* belong to the same family Myrtaceae (33). Few papers on the composition of *M. nivellei* essential oil have been reported, however several reports on the composition of *M. communis* essential oil from many localities were documented with major similar components found to be in all these chemotypes, which were α-Pinene, 1,8-cineole and limonene (34 - 41).

Table 1. The essential oil composition of Sahara myrtle

No	Volatile components	RT	percentage
1.	α-Pinene	6.42	1.69±0.15
2.	2-β-Pinene	7.62	0.11±0.01
3.	*p*-cymene	9.12	0.68±0.10
4.	1,8-cineole	9.38	53.44±2.15
5.	Linalool	11.61	0.85±0.11
6.	α-terpineol	13.87	0.23±0.031
7.	4-terpineol	14.25	0.66±0.09
8.	Linalyl propionate	14.808	6.81±0.68
9.	Piperitone	17.29	0.35±0.03
10.	Vetiverol	17.44	1.15±0.12
11.	Methyl citronellate	17.62	0.23±0.025
12.	Endo-Acetoxy-1,8-cineole	20.21	0.33±0.02
13.	*trans*-Ocimene	20.458	7.54±0.47
14.	Citronellyl propionate	20.58	0.06±0.00
15.	Nerol acetate	20.895	0.18±0.01
16.	Lavandulyl acetate	21.43	5.24±0.31
17.	Humulene	23.208	0.45±0.01
18.	1,2-Benzenediol, 3,5-bis(1,1-dimethylethyl)-	24.275	1.45±0.03
19.	Aromandendrene	25.108	0.19±0.00
20.	Selina-3,7(11)-diene	25.25	0.13±0.01
21.	Aromadendrene oxide	26.137	0.18±0.00
22.	Caryophyllene oxide	26.47	0.11±0.01
23.	2,2,6,7-Tetramethyl-10-oxatricyclo[4.3.0.1(1,7)] decan-5-one	26.57	11.73±1.35

APTEFF, 52, 1-273 (2021)
DOI: https://doi.org/10.2298/APT2152111R
BY-NC-ND
UDC: 633.88+665.52]:579.84/.86:615.28
BIBLID: 1450-7188 (2021) 52, 111-121
Original scientific paper

PHENOLIC CONTENT OF ETHANOLIC EXTRACT

The extract yielded 6.21 ± 1.28 % (w/w) with green pale colour, pasty aspect. Phenolic content of ethanol extracts showed a value of 119.65 ± 9.10 µg eqGA/mg E, flavonoid was order 41.88 ±1.91 µg eq rutin/ mg of extract, total and catechic tannin displayed a values of 47.82 ± 9.18 µg eqGA/mg E and 3.90 ± 0.14 µg eq c/mg E respectively.

Table 2. Phenolic quantification of ethanolic extract from *M. nivellei*

Phenolic	Flavonoid	Total tannin	Condensed tannin
119,65±9,10	41,88 ±1,91	47,82±9,18	3,90±0,14

Phenolic and total tannins contents were as µg AGE /mg of extract
Flavonoid content was as µg RE/ mg of extract
Condensed tannin content was µg eq c/mg of extract

The previous report has showed that aerial parts of *M. nivellei* contain polyphenols, flavonoids, alkaloids, terpenoids and saponins (8). Which potentially contributed to its biological activities in vitro and in vivo (8,11). The content of phenolics flavonoids and total tannin of ethanolic extract was approximately the same when comparing with the aqueous fraction in our previous work within 128.03 ± 1.87 µg eqGA/mg of extract, 22.42 ± 6.92 µg rutin equivalent/mg and 55.45 ± 6.00 µg eqGA/mg E of extract respectively (8) but the results were less from those demonstrated in our recent report within 204.64 ± 1.87 µg eqGA/mg of extract, 85.32 ± 13.67µg rutin equivalent/mg and 190.62 ± 1.11 µg eqGA/mg of extract (11). It was reported that solubility of the phenolic compounds increases with solvent polarity (42). Phenolic component have already displayed by Mansour et al. (10) which reported that myricetin 3-*O*-β-D-(6'-galloyl)glucopyranoside, isomyricitrin and myricitrin were identified as the major constituents, roseoside, myricetin 3-*O*-β-D-(6'galloyl)glucopyranoside, 1,2,3,6-tetra-*O*-galloyl glucose, quercetin 3-*O*-β-D-(6'-galloyl) glucopyranoside, and 3-oxo-α-ionol-9-*O*-β-D-glucopyranoside were identified for the first time in this plant.

ANTIOXIDANT ACTIVITY

The antioxidant potency of *M. nivellei* extract was tested using three test systems. The DPPH free radical scavenging, ferric reducing power and total antioxidant capacity (molybdenum assay) were presented in table 3. Several antioxidant techniques were different in system process and structure reactions (43) so it is interest to study more than one technique of antioxidant capacity to determine the various mechanisms of antioxidant action (44). Essential oil displayed important antioxidant activity may be linked to its content on some phenolic compounds (10). Which were well known to reduce free radicals as has already described (45). Major constituents of volatile oil possessed remarkable antioxidant effect; nevertheless, the existence of little amount of other interesting chemical compounds can react with strong potential effect (4).

The essential oil showed a higher antioxidant activity through DPPH assays than ethanolic extract, however, this latter was more able in comparison with the essential oil to reduce the ferric iron to ferrous iron. This feature would indicate effective antioxidant activity

APTEFF, 52, 1-273 (2021)
DOI: https://doi.org/10.2298/APT2152111R
BY-NC-ND
UDC: 633.88+665.52]:579.84/.86:615.28
BIBLID: 1450-7188 (2021) 52, 111-121
Original scientific paper

of myrtle extract; the results of the present work are in good agreement with our previous study (8) which mentioned significantly higher antioxidant effect of extract, generally related to their abundance on phenolic compounds, which are precious constituents in the management of ROS (8).

Table 3. Antioxidant activities of *M.nivellei* ethanolic extract, essential oil and standard

Extract	PM	FRAP	DPPH assay IC_{50} (mg/ml)
Ethanolic extract	443.18 ± 11.56	215.21 ± 3.01	24.79 ± 1.03
Essential oil	ND	210.86 ± 4.78	2.25 ± 0.21
Ascorbic acid	ND	ND	8.25 ± 0.88

PM and FRAP values were quantified as µg AAE/mg of extract
ND: not determined

ANTIBACTERIAL ACTIVITY

Antibacterial activity

The *in vitro* antimicrobial potential of *M. nivellei* essential oil and ethanol extract against the employed strains was quantitatively assessed by measurement of inhibition zones. The results are summarised in Table 4.

Table 4. Antibacterial activity of essential oil, ethanolic extract and gentamicin

Bacteria strains	Inhibition zones (mm)		
	Essential oil	Ethanolic extract	Gentamicin
E. coli ATCC 25922	8.55±0.35	14.02±1.41	21.07±6.83
P. aeruginosa ATCC 27853	NA	NA	25.36±0.04
S. aureus ATCC 25923	18.02±1.37	15.17±1.16	20.5±0.7
Vibrio sp.	9.71±0.96	10.52±0.1	23.36±0.56
Salmonella sp.	8.87±0.71	8.09±0.01	22.13±1.60

NA: not active

It was clearly demonstrated that the essential oil and extract exhibited antibacterial effect less than that of gentamicin with different zone of inhibition 8.55-18.02 mm, 8.09-15.17 mm and 20.05-23.13 mm respectively.

Djenane et al (46) have revealed that the essential oils of *Eucalyptus globulues* and *M. communis* possessed vigorous antibacterial effects against *E. coli* O157:H7 and *S. Aureus* which was the more sensitive to Eucalyptus oil. The phenolic composition of *M. nivellei* was already been studied with the existence of myricetin 3-*O*-β-D-(6'-galloyl) glucopyranoside, isomyricitrin and myricitrin as the most abundant constituents of extract (10). 1,8-Cineol was the major oxygenate monoterpenes of essential oil in this present study. These major components may be responsible to exhibit antibacterial effects. Phenolic compounds of essential oils can also exhibit a strong antibacterial activity (46). We cannot however, exclude the possibility that other minor compounds participate in the inhibitory effect (46,

BY-NC-ND

47). Essential oil and alcohol extract were more active on *S. aureus* than other strains with zone of inhibition 18,02 and 15,17 mm respectively. This activity could be explained that gram-positive bacteria were more sensitive in comparison with gram-negative bacteria. These results were confirmed with those of many scientific papers (48, 49, 50). Essential oil can disorder the cell structures of bacteria (47).

CONCLUSION

This paper demonstrates the antioxidant and antibacterial activities of the volatile fraction and ethanolic extract of the endemic species *M. nivellei*. Both essential oil and ethanolic extract have showed high antioxidant activity. However, moderate antibacterial effect was obtained. The volatile oil has revealed 1,8-cineole as the most abundant constituent with the presence of a small amount of phenolic compounds. Ethanolic extract has demonstrated its richness in phenolic content, these results were considerable, and encourage us for its future thorough analysis and application in therapeutic drugs.

Acknowledgements

The authors recognize Professor Ferid Limam for his help on volatil oil analysis (Tunisia) and the botanist El Ouassis Dahmane at INRF Algeria (Plant collection).

REFERENCES

1. Oladeji, O.S; Adelowo, F.E; Ayodele, D.T; Odelade, K.A. Phytochemistry and pharmacological activities of *Cymbopogon citratus* : A review. *Scientific African*. **2019**, 6 e00137, 1-11.
2. Nguyen, T. D; Jung, M. Kim; Sun, C. K. Chemical composition, antimicrobial and antioxidant activities of the essential oil and the ethanol extract of Cleistocalyx operculatus (Roxb.) Merr and Perry buds. *Food Chem. Toxicol.* **2008**, *46*, 3632-3639.
3. Grattapaglia, D; Vaillancourt, R.E; Shepherd, M; Thumma, B. R; Foley, W; Külheim, C; Potts, B. M; Myburg, A. A. Progress in Myrtaceae genetics and genomics: *Eucalyptus* as the pivotal genus. *Tree Genet. Genomes*. **2012**, *8*, 463-508
4. Lim, T.K. *Myrtus communis*. In Edible Medicinal And Non-Medicinal Plants. Springer Netherlands, **2012**, *3*, 642-654.
5. Wahid, N. Perspectives de la valorisation de l'usage et de la culture du *Myrtus communis* L. au Maroc. *Phytothérapie,* **2013**, *11*, 237-243.
6. Migliore, J; Baumel, A; Juin, M; Médail, F. From Mediterranean shores to Central Saharan Mountains: key phylogeoraphic alinsights from the genus Myrtus. *J. Biogeogr.* **2012**, 39, 942-956.
7. Bouzabata, A.; Bazzali, O.; Cabral, C.; Gonçalves, M. J.; Cruz, M.T.; Bighelli, A.; Cavaleiro, C.; Casanova, J.; Salgueiro, L.: Tomi, F. New compounds, chemical composition, antifungal activity and cytotoxicity of the essential oil from *Myrtus nivellei* Batt. &Trab. an endemic species of Central Sahara. *J. Ethnopharmacol*. **2013**, *149*, 613-620.
8. Ramdane, F.; Essid, R.; Fares, N.; El Ouassis, D.; Aziz, S.; Hadj Mahammed, M.; Ould Hadj, M.D.; Limam, F. Antioxidant antileishmanial cytotoxic and antimicrobial activities of a local plant *Myrtus nivellei* from Algeria Sahara. *Asian Pac. J. Trop. Biomed*. **2017a**, *7*(8) , 702-707.
9. Touaibia, M.; Chaouch, F. Z. Anti-inflamatory effect of *Myrtus nivellei* Bath & Trab (Myrtaceae) methanolic extract. *J. Fundam. Apppl. Sci.* **2017**, *7*(1), 77-82.

BY-NC-ND

10. Mansour, M.; Celano, R.; Mencherini, T.; Picerno, P.; Piccinelli, A.L.; Cherif, Y.F.; Csupor, D.; Rahili, G.; Yahi, N.; Nabavi, S.M.; Aquino, R. P.; Rastrelli. L. A new cineol derivative, polyphenols and norterpenoids from Saharan myrtle tea (*Myrtus nivellei*): Isolation, structure determination, quantitative determination and antioxidant activity. *Fitoterapia.* **2017**, *119*, 32-39.
11. Ramdane, F.; Sobti, A.; Hrizat, N. H.; Hadj Mahammed, M. Blood Biochemical Parameters Effect of Sahara Myrtle on Diabetic Rats. *Pharmacophore.* **2019**, *10* (1), 71-77.
12. Hassiotis, C.N. Chemical compounds and essential oil release through decomposition process from *Lavandula stoechas* in Mediterranean region. *Biochem. Syst. Ecol.* **2010**, *38*, 493-501.
13. Ramdane, F.; El Ouassis, D.; Hammami, M.; Essid, R.; Sobti, A.; Hrizat, N. H.; Ben Amara, S.; Fares, N.; Hadj Mahammed, M.; Ould Hadj, M. D.; Limam, F. Chemical composition and biological effects of essential oil of *Artemisia judaica* an endemic plant from central Sahara of Algeria Hoggar. *Int. J. Biosci.* **2017b**, *10* (1), 16-23.
14. Chew, Y.L.; Ling Chan, E.W.; Tan, P.L.; Lim, Y.Y.; Stanslas, J.; Goh, J.K. Assessment of phytochemical content, polyphenolic composition, antioxidant and antibacterial activities of Leguminosae medicinal plants in Peninsular Malaysia. *BMC Complement. Altern. Med.* **2011**, *11* (12), 1-10.
15. Gonçalves, S.; Gomes, C. P.; Romano, A. The phenolic content and antioxidant activity of infusions from Mediterranean medicinal plants. *Ind. Crops. Prod.* **2013**, *43*, 465-471.
16. Do, Q.D.; Angkawijaya, A. E.; Tran-Nguyen, P.L.; Huynh, L.H.; Soetaredjo, F.E.; Ismadji, S.; Ju. Y.H. Effect of extraction solvent on total phenol content, total flavonoid content, and antioxidant activity of *Limnophila aromatica*. *J Food Drug Anal*. **2014**, *22*, 296-302.
17. Rguez, S.; Essid, R.; Adele, P.; Msaada, K..; Hammami, M.; Mkadmini, K..; Fares, N.; Tabbene, O.; Elkahoui, S.; Portelli, D.; Ksouri, R.; Hamrouni Sellami. I. Towards the use of *Cupressus sempervirens* L. organic extracts as a source of antioxidant, antibacterial and antileishmanial biomolecules. *Ind. Crops. Prod.* **2019**, *131*, 194-202.
18. Hamid, A.A.; Aiyelaagbe, O.O.; Usman, L.A. Essential oils: its medicinal and pharmacological uses. *Int J Curr Res.* **2011**, *3* (2), 086-098.
19. Riahi, L.; Elferchichi, M.; Ghazghazi, H.; Jebali, J.; Ziadi, S.; Aouadhie, C.; Chogranif, H.; Zaoualif, Y.; Zoghlami N.; Mliki, A. Phytochemistry, A. antioxidant and antimicrobial activities of the essential oils of *Mentha rotundifolia* L. in Tunisia", *Ind. Crops. Prod*. **2013**, *49*, 883-889.
20. Nithiyananthama, S.; Siddhurajua, P.; Francis,G. A promising approach to enhance the total phenolic content and antioxidant activity of raw and processed Jatropha curcas L. kernel meal extracts. *Ind. Crops. Prod.* **2012**, 43, 261-269.
21. Ksouri, A.; Dob, T.; Belkebir, A.; Lamari, L.; Krimat, S.; Metidji, H. Total Phenolic, Antioxidant, Antimicrobial Activities and Cytotoxicity Study of Wild *Anethum graveolens* L. *Int. J. Pharmacogn. Phytochem. Res.* **2015**, *7* (6), 1025-1032.
22. Svetaz, L.; Zuljan, F.; Derita, M.; Petenatti, E.; Tamayo, G.; Cáceres, A.; Filho, V. C.; Giménez, A.; Pinzon, R.; Zacchino, S. A.; Gupta. M. Value of the ethnomedical information for the discovery of plants with antifungal properties. A survey among seven Latin American countries. *J. Ethnopharmacol.* **2010**, *127*,137-158.
23. Adams, R.P. Identification of essential oils components by gas chromatography/quadrupole mass spectroscopy. Allured Publishing Corporation, Carol. Stream, IL, USA. **2001**, 456p.
24. Bahramikia, S.; Ardestani, A.; Yazdanparast, R. Protective effects of four Iranian medicinal plants against free radical-mediated protein oxidation. *Food Chem.* **2009**, *115*, 37-42.
25. Nićiforović, N.; Mihailović, V.; Mašković, P.; Solujić, S.; Stojković, A.; Pavlović Muratspahić, D. Antioxidant activity of selected plant species; potential new sources of natural antioxidants. *Food Chem. Toxicol.* **2010**, *48*, 3125-3130.
26. Aidi Wannes, W.; Mhamdi, B.; Sriti, J.; Ben Jemia, M.; Ouchich, O.; Hamdaoui, G.; Kchouk, E.; Marzouk, B. Antioxidant activities of the essential oils and methanol extracts from myrtle *(Myrtus communis* var. *italica* L.) leaf, stem and flower. *Food Chem. Toxicol.* **2010**, *48*, 1362-1370.

BY-NC-ND

27. Aroke, S.A.; Elgorashi, E.; Moodley, N.; McGaw, L.J.; Naidoo, V.; Eloff, J. N. The antimicrobial, antioxidative, anti-inflammatory activity and cytotoxicity of different fractions of four South African Bauhinia species used traditionally to treat diarrhoea. *J. Ethnopharmacol.* **2012**, *143*, 826-839.
28. Dung, N. T.; Kim, J. M.; Kang, S. C. Chemical composition, antimicrobial and antioxidant activities of the essential oil and the ethanol extract of Cleistocalyx operculatus (Roxb.) Merr and Perry buds. *Food Chem. Toxicol.* **2008**, *46*, 3632-3639.
29. Jaitak, V.; Sharma, K.; Kalia, K.; Kumar, N.; Singh, H.P.; Kaul, V.K.; Singh, B. Antioxidant activity of Potentilla fulgens: An alpine plant of western Himalaya. *J. Food. Compos. Anal.* **2010**, *23*, 142-147.
30. Kintzios, S.; Papageorgiou, K.; Yiakoumettis, L.; Baričević, D.; Kušar. A. Evaluation of the antioxidants activities of four Slovene medicinal plant species by traditional and novel biosensory assays. *J. Pharm. Biomed. Anal*. **2010**, 53,773-776
31. Ruban, P.; Gajalakshmi, K. In vitro antibacterial activity of Hibiscus rosa-sinensis flower extract against human pathogens. *Asian Pac. J. Trop. Biomed*. **2012**, 399-403.
32. Nyamador, S. W.; Ketoh, G.K.; Koumaglo, H.K.; Glitho, I. A. Activités Ovicide et Larvicide des Huiles Essentielles de *Cymbopogon giganteus* Chiov. et de *Cymbopogon nardus* L. Rendle sur les stades immatures de *Callosobruchus maculatus* F. et de *Callosobruschus subinnotatus* Pic. (Coleoptera:Bruchidae). J. Soc. Ouest-Afr. Chim. **2010**, 29, 67-79.
33. Djibo, A.K.; Samaté, A.D.; Nacro, M. Composition chimique de l'huile essentielle de *Ocimum americanum* Linn.syn., *O. canum* Sims du Burkina Faso. *C. R. Chim.* **2004**, *7*,1033-1037.
34. Curini, M.; Bianchi, A.; Epifano, F.; Bruni, R.; Torta, L.; Zambonelli, A. Composition and *in vitro* antifungal activity of essential oils of *Erigeron canadensis* and *Myrtus communis* from France. Chem. Nat. Compd. **2003**, *39* (2), 191-194.
35. Flamini, G.; Cioni, P. L.; Morelli, I.; Maccioni, S.; Baldini, R. Phytochemical typologies in some populations of *Myrtus communis* L. on caprione promontory (East Liguria, Italy). *Food Chem.* **2004**, *85*, 599-604.
36. Jamoussi, B.; Romdhane, M.; Abderraba, A.; Ben Hassine, B.; EL Gadri, A. Effect of harvest time on the yield and composition of Tunisian myrtle oils. *Flavour Fragr J.* **2005**, *20*, 274-277.
37. Tuberoso, C. I.; Barra, A.; Angioni, A.; Sarritzu, E.; Piris, F. M. Chemical composition of volatiles in Sardinaian myrtle (*Myrtus communis* L) alcoholic extracts and essential oils. *J. Agric. Food Chem.* **2006**, *54*, 1420-1426.
38. Gardeli, C.; Papageorgiou, V.; Mallochos, A.; Theodosis, K.; Komaitis, M. Essential oil composition of *Pistacia lentiscus* L. and *Myrtus communis* L. evaluation of antioxidant capacity of methanolic extract. Food Chem. **2008**, *107*, 1120-1130.
39. Aidi Wanes, W.; Mhamdi, B.; Marzouk, B. Variations in essential oil and fatty acid composition during *Myrtus communis* var.*italica* fruit maturation. *Food Chem.* **2009**, *112,* 621-626.
40. Barboni, T.; Venturini, N.; Paolini, J.; Desjobert, J. M.; Chiaramonti, N.; Costa, J. Characterisation of volatiles and polyphenols for quality assessment of alcoholic beverages prepared from Corsican *Myrtus communis* berries. *Food Chem.* **2010**, *122*, 1304-1312.
41. Bouzabata, A.; Cabral, C.; Goncalves, M. J.; Cruz, M. T.; Bighelli, A.; Cavaleiro, C.; Casanova, J.; Tomi, F.; Salgueiro, L. *Myrtus communis* L. as source of a bioactive and safe essential oil. Food Chem. Toxicol. **2015**, 75, 166-172.
42. Tongpoothorn, W.; Chanthai, S.; Sriuttha, M.; Saosang, K.; Ruangviriyachai, C. Bioactive properties and chemical constituents of methanolic extract and its fractions from Jatropha curcas oil. *Ind. Crops. Prod.* **2012**, *36*, 437-444
43. Matkowski, A. Plant in vitro culture for the production of antioxidants - A review Biotechnol. Adv. **2008**, 26, 548-560.

BY-NC-ND

44. Costa, P.; Grevenstuk, T.; Costab, A.R.; Gonçalves, S.; Romanoa, A. Antioxidant and anti-cholinesterase activities of Lavandula viridis L'Hér extracts after in vitro gastrointestinal digestion. *Ind. Crops. Prod.* **2014**, 55, 83-89.
45. Barkat, M., Laib, I. Antioxidant activity of the essential oil from the flowers of *Lavandula stoechas* . *J. Pharmacognosy Phytother.* **2012**, *4* (7), 96-101.
46. Djenane, D.; Aïder, M.; Yangüela, J.; Idir, L.; Gomez, D.; Roncales, P. Antioxidant and antibacterial effects of Lavandula and Mentha essential oils in minced beef inoculated with E. coli O157:H7 and S. aureus during storage at abuse refrigeration temperature. *Meat Sci.* **2012**, *92*, 667-674.
47. Riahi, L.; Elferchichi, M.; Ghazghazi, H.; Jebali, J.; Ziadi, S.; Aouadhi, C.; Chograni, H.; Zaouali, Y.; Zoghlami, N.; Mliki, A. Phytochemistry, antioxidant and antimicrobial activities the essential oils of Mentha rotundifolia L. in Tunisia. *Ind. Crops. Prod.* **2013**, *49*, 883- 889.
48. Tadeg, H.; Mohammed*, E.*; Asres*,* K.; Gebre-Mariam, T. Antimicrobial activities of some selected traditional Ethiopian medicinal plants used in the treatment of skin disorders. *J. Ethnopharmacol.* **2005**, *100*, 168-175.
49. Oussalah, M.; Caillet, S.; Saucier, L.; Lacroix, M. Inhibition effects of selected plant essential oils on the growth of four pathogenic bacteria: *E. coli* O157: H 7, *Salmonella Typhimurium*, *Staphylococcus aureus* and *Listeria manocytogense*. *Food Control.* **2007**, *18*, 414-420.
50. Deba, F.; Xuan, T. D.; Yasuda, M.; Tawata, S. Chemical composition and antioxidant, antibacterial and antifungal activities of the essential oils from *Bidens pilosa Linn*. Var. *Radiata*. *Food Control.* **2008**, *19*, 346-352.

APTEFF, 52, 1-273 (2021) UDC: 582.998.16+665.52]:543.544(497.11)
DOI: https://doi.org/10.2298/APT2152123A BIBLID: 1450-7188 (2021) 52, 123-132
BY-NC-ND
Original scientific paper

THE QUANTITATIVE STRUCTURE-RETENTION RELATIONSHIP OF THE GC-MS PROFILE OF YARROW ESSENTIAL OIL

Milica AĆIMOVIĆ[1], Lato PEZO[2], Jovana STANKOVIĆ JEREMIĆ[3], Marina TODOSIJEVIĆ[4], Milica RAT[5], Vele TEŠEVIĆ[4], Mirjana CVETKOVIĆ[3]*

[1] Institute of Field and Vegetable Crops, Maksima Gorkog 30, 21000 Novi Sad, Serbia
[2] Institute of General and Physical Chemistry, University of Belgrade, Studentski trg 12-16, Belgrade, Serbia
[3] Institute of Chemistry, Technology, and Metallurgy, University of Belgrade, Njegoševa 12, 11000 Beograd, Serbia
[4] Faculty of Chemistry, University of Belgrade, Studentski trg 12-16, Belgrade, Serbia
[5] Faculty of Science, University of Novi Sad, Trg Dositeja Obradovića 3, Novi Sad, Serbia

Received: 21 March 2021 **Revised: 09 May 2021** **Accepted: 13 May 2021**

In the essential oil of yarrow (Achillea millefolium L. sensu lato) collected from natural population on Mt. Rtanj (Serbia) and distilled by Clevenger apparatus 104 compounds were detected, and the most abundant were camphor (9.8%), caryophyllene oxide (6.5%), terpinen-4-ol (6.3%) and 1,8-cineole (5.6%). The quantitative structure-retention relationship (QSRR) model was employed to predict the retention indices, using four molecular descriptors selected by factor analysis and a genetic algorithm. The coefficients of determination reached the value of 0.862, demonstrating that this model could be used for prediction purposes.

Keywords: *Achillea millefolium* L., retention indices, molecular descriptors, factor analysis, genetic algorithm, coefficients of determination.

INTRODUCTION

Genus *Achillea* (Asteraceae family), commonly known as yarrow, includes more than 100 perennial species, which mostly grow spontaneously throughout Europe and Asia. There are 19 species reported in Serbia (1). *Millefolium* group is characterized by a wide morphological, cytological and chemical diversity (2). Furthermore, these species have the tendency to hybridize and to vary in phenotype according to the environmental conditions (3). Common yarrow (*Achillea millefolium* L. *sensu lato*) is considered to be aggregate. In the Flora of Serbia, three subspecies are reported: subsp. *pannonica*, subsp. *millefolium* and subsp. *collina* with two forms (f. *colina* with white flowers and f. *rubriflora* with pink flowers) (1). Yarrow with white flowers (*Millefolii herba*) has been used in traditional medicine since the ancient times. Throughout Euro-Asian region it is widely used for treating gastrointestinal complaints as a bitter aromatic and to stimulate the secretion of bile, as well as an antispasmodic, emenagogue and febrifuge (4). Yarrow has been used in Serbian traditional medicine for treating hemorrhoids and to improve wound healing (external application). These applications are mentioned in other traditional medicine as well (5), corroborated by experiments (6). Modern scientific investigations show that it possesses anti-inflammatory (7), antioxidant and antibacterial activities (8, 9), as well as antican-

* Corresponding author: Milica AĆIMOVIĆ, Institute of Field and Vegetable Crops Novi Sad, Serbia, e-mail: milica.acimovic@ifvcns.ns.ac.rs

APTEFF, 52, 1-273 (2021) UDC: 582.998.16+665.52]:543.544(497.11)
DOI: https://doi.org/10.2298/APT2152123A BIBLID: 1450-7188 (2021) 52, 123-132
BY-NC-ND
Original scientific paper

cer properties (10). The aim of this investigation is to determine essential oil composition of *A. millefolium sensu lato* from Mt Rtanj and to develop a QSRR model for predicting the retention times of chemical compounds from the essential oil.

MATERIAL AND METHODS

The aerial parts of *A. millefolium* (~35 cm) was collected on 7th July 2018, from natural population on Mt. Rtanj at full flowering stage. Voucher specimens were deposited in the Herbarium of the University of Novi Sad (BUNS) under the acquisition number 2-1449.

A total of 20.0 g of cut *A. millefolium* aerial parts was placed in a 1000 mL round-bottomed flask and 500 mL of water was added and the flask was then connected to Clevenger apparatus. The distillation was done at a rate of 2-3 mL/min for 2h. At the end of the process 0.16% of pale yellow essential oil was obtained, which was analyzed by GC (HP 5890) coupled to an MS (HP 5973 MSD) and fitted with a capillary column HP-5MS. Terms and conditions are described in detail in the previous paper (11).

Obtained results of GC-MS analysis of *A. millefolium* essential oil were used for quantitative structure retention relationship (QSRR) analysis, artificial neural network (ANN) modeling as well as for global sensitivity analysis (12). The determination of molecular descriptors (MDs) was performed using the PaDel-descriptor software (13). The most relevant MDs for RIs prediction by factor analysis and genetic algorithm (GA), using Heuristic Lab software. Statistical investigation of the data was performed by the Statistica 10 software. Multi-layer perceptron architecture (MLP) was used to build the ANN for prediction of RIs for compounds found in *A. millefolium* essential oil. Broyden–Fletcher–Goldfarb–Shanno (BFGS) algorithm was used to speed-up the calculation of weight coefficients of the ANN (11). The observed data were randomly separated to 60%, 20% and 20% of data used for training, testing and validations, respectively (12). Yoon's global sensitivity equation was used to calculate the relative impact of the chosen MDs on RIs, according to weight coefficients of the developed ANN (14).

RESULTS AND DISCUSSION

In the *A. millefolium* essential oil, a total of 104 compounds were detected, which represented 96.4% of the total oil composition (Table 1). Among these compounds, 20 were not identified compounds (NI), which compromised 15.3%. However, relative intensity of molecular ions peaks (m/z) for all NI compounds were given in Table 1. As it can be seen from the table, the most abundant compounds in *A. millefolium* essential oil were camphor (9.8%), caryophyllene oxide (6.5%), terpinen-4-ol (6.3%) and 1,8-cineole (5.6%). Oxygenated monoterpenes and sesquiterpenes with 28.1% and 23.6%, respectively, were dominant in the chemical composition, followed by monoterpene and sesquiterpene hydrocarbons with 14.2% and 11.2%, respectively.

APTEFF, 52, 1-273 (2021)
DOI: https://doi.org/10.2298/APT2152123A
BY-NC-ND
UDC: 582.998.16+665.52]:543.544(497.11)
BIBLID: 1450-7188 (2021) 52, 123-132
Original scientific paper

Table 1. Chemical composition of *A. millefolium* aerial parts and molecular descriptors

No	Compound	RI[a]	RI[b]	$RI_{pred.}$	%	GATS5e	Mv	VE1_Dt	MWC9
1	α-Thujene	928	924	866.121	0.2	0.562	0.551	0.203	10.807
2	α-Pinene	935	932	1284.488	0.7	0.762	0.551	0.005	10.594
3	Camphene	949	946	1334.457	0.4	0.431	0.551	0.084	10.543
4	Sabinene	974	969	949.974	2.8	0.594	0.551	0.203	10.807
5	β-Pinene	978	974	1283.501	1.5	0.766	0.551	0.005	10.594
6	dehydro-1,8-Cineole	991	988	1131.366	0.2	0.145	0.557	0.066	10.521
7	α-Terpinene	1015	1014	1128.345	0.4	0.757	0.551	0.165	9.434
8	p-Cymene	1022	1020	987.050	0.9	0.876	0.575	0.165	9.434
9	Limonene	1027	1024	928.663	0.1	0.666	0.551	0.165	9.434
10	1,8-Cineole	1028	1026	1143.515	5.6	0.132	0.538	0.066	10.521
11	γ-Terpinene	1052	1054	1098.075	1.1	0.745	0.551	0.165	9.434
12	cis-Sabinene hydrate	1060	1065	1136.628	0.4	0.633	0.531	0.203	10.807
13	Terpinolene	1080	1086	893.172	0.3	0.646	0.551	0.165	9.434
14	Linalool	1092	1095	1018.278	4.2	0.489	0.538	0.110	9.125
15	n-Nonanal	1096	1100	1105.060	0.2	0.835	0.521	0.000	8.043
16	NI-1	1107	-	-	2.5	-	-	-	-
17	cis-p-Menth-2-en-1-ol	1113	1118	1308.579	0.2	0.473	0.538	0.112	9.795
18	Chrysanthenone	1116	1124	923.006	0.2	2.406	0.580	0.002	10.827
19	trans-Pinocarveol	1132	1135	1304.882	0.1	0.775	0.557	0.020	10.750
20	trans-p-Menth-2-en-1ol	1133	1136	1296.376	0.1	0.813	0.531	0.165	9.434
21	Camphor	1138	1141	1372.125	9.8	1.300	0.557	0.078	10.917
22	NI-2	1150	-	-	0.3	-	-	-	-
23	Pinocarvone	1155	1160	1301.057	0.7	0.838	0.580	0.020	10.750
24	Borneol	1159	1165	1510.630	1.6	1.148	0.538	0.078	10.917
25	NI-3	1160	-	-	0.2	-	-	-	-
26	cis-Pinocamphone	1167	1172	1316.178	0.1	0.727	0.557	0.020	10.750
27	Terpinen-4-ol	1173	1174	1186.422	6.3	0.209	0.538	0.242	9.931
28	Thuj-3-en-10-al	1179	1181	1079.573	0.1	0.768	0.538	0.245	9.795
29	α-Terpineol	1186	1190	1088.580	1.3	1.277	0.557	0.042	10.667
30	Myrtenol	1189	1194	1247.659	0.2	1.426	0.580	0.042	10.667
31	Myrtenal	1191	1195	1223.580	0.4	0.900	0.567	0.084	9.992
32	cis-Carveol	1226	1226	1334.126	0.1	0.751	0.557	0.132	9.732
33	trans-Chrysanthenyl acetate	1231	1235	1129.230	0.2	1.430	0.572	0.018	10.994
34	Cumin aldehyde	1235	1238	1348.877	0.1	0.858	0.607	0.117	9.560
35	cis-Chrysanthenyl acetate	1257	1261	1129.230	0.4	1.430	0.572	0.018	10.994
36	Bornyl acetate	1282	1287	1235.626	0.4	0.996	0.554	0.012	11.061
37	Thymol	1288	1289	1372.639	0.6	2.548	0.580	0.119	9.756
38	Carvacrol	1298	1298	1252.284	1.1	0.942	0.580	0.132	9.732
39	p-Mentha-1,4,-dien-7-ol	1325	1325	1428.156	0.2	0.853	0.557	0.117	9.560
40	trans-Carvyl acetate	1334	1339	1254.619	0.1	0.815	0.572	0.009	10.022
41	Eugenol	1354	1356	1493.266	0.1	1.230	0.612	0.046	9.735
42	cis-Carvyl acetate	1359	1365	1254.619	0.1	0.815	0.572	0.009	10.022
43	α-Copaene	1373	1374	1504.613	0.1	1.007	0.551	0.098	11.349
44	β-Bourbonene	1382	1387	1507.414	0.1	0.932	0.551	0.095	11.355
45	cis-Jasmone	1395	1392	1322.328	0.1	1.226	0.573	0.046	9.773
46	Methyl eugenol	1401	1403	1428.597	0.1	1.485	0.601	0.058	9.856
47	trans-Caryophyllene	1418	1417	1320.696	4.7	0.963	0.551	0.032	10.671
48	cis-β-Farnesene	1441	1440	1548.775	0.1	0.841	0.551	0.012	9.162
49	α-Humulene	1451	1452	1537.107	0.7	0.930	0.551	0.084	9.783
50	trans-β-Farnesene	1455	1454	1548.775	0.1	0.841	0.551	0.012	9.162
51	9-epi-trans-Caryophyl-lene	1459	1464	1320.696	0.4	0.963	0.551	0.032	10.671
52	γ-Muurolene	1473	1478	1586.163	0.3	0.984	0.551	0.109	10.550
53	Germacrene D	1480	1484	1562.301	2.9	0.941	0.551	0.103	9.733
54	β-Selinene	1484	1489	1573.418	0.2	0.884	0.551	0.109	10.651

APTEFF, 52, 1-273 (2021)
DOI: https://doi.org/10.2298/APT2152123A
BY-NC-ND
UDC: 582.998.16+665.52]:543.544(497.11)
BIBLID: 1450-7188 (2021) 52, 123-132
Original scientific paper

Table 1. Continuation.

No	Compound	RI[a]	RI[b]	$RI_{pred.}$	%	GATS5e	Mv	VE1_Dt	MWC9
55	trans-Muurola-4(14),5-diene	1490	1493	1591.800	0.1	1.077	0.551	0.109	10.550
56	epi-Cubebol	1493	1493	1567.126	0.5	0.856	0.555	0.109	11.652
57	γ-Cadinene	1512	1513	1586.163	1.1	0.984	0.551	0.109	10.550
58	α-Calacorene	1540	1544	1600.514	0.3	1.100	0.583	0.109	10.550
59	Elemol	1546	1548	1532.135	0.7	0.703	0.542	0.132	10.623
60	trans-Nerolidol	1560	1561	1428.523	0.1	0.467	0.542	0.085	9.517
61	NI-4	1565	-	-	0.2	-	-	-	-
62	NI-5	1571	-	-	0.4	-	-	-	-
63	ar-Tumerol	1575	1582	1621.097	0.6	2.104	0.570	0.257	9.954
64	Caryophyllene oxide	1580	1582	1331.415	6.5	0.579	0.555	0.015	11.141
65	NI-6	1584	-	-	0.2	-	-	-	-
66	Viridiflorol	1587	1592	1416.937	0.5	0.921	0.542	0.067	11.406
67	Ledol	1596	1602	1416.937	0.1	0.921	0.542	0.067	11.406
68	Humulene epoxide II	1603	1608	1474.255	0.6	0.626	0.555	0.072	10.652
69	NI-7	1605	-	-	0.2	-	-	-	-
70	NI-8	1622	-	-	0.3	-	-	-	-
71	γ-Eudesmol	1626	1630	1114.227	1.5	0.580	0.542	0.185	10.789
72	Caryophylla-4(12), 8(13)-dien-5-α-ol	1631	1639	1376.326	1.8	0.691	0.555	0.035	10.758
73	α-Muurolol (=Torreyol)	1636	1640	1547.839	3.3	0.839	0.542	0.076	10.772
74	NI-9	1641	-	-	0.2	-	-	-	-
75	β-Eudesmol	1646	1649	1365.178	2.4	0.699	0.542	0.185	10.789
76	α-Cadinol	1648	1652	1547.839	1.2	0.839	0.542	0.076	10.772
77	NI-10	1653	-	-	0.3	-	-	-	-
78	NI-11	1664	-	-	4.3	-	-	-	-
79	NI-12	1667	-	-	0.5	-	-	-	-
80	NI-13	1670	-	-	0.2	-	-	-	-
81	α-Bisabolol	1678	1685	1590.963	0.3	0.961	0.542	0.205	10.136
82	Germacra-4(15),5, 10(14)-trien-1-α-ol	1681	1685	1377.912	1.7	0.733	0.555	0.098	9.930
83	NI-14	1686	-	-	4.0	-	-	-	-
84	NI-15	1700	-	-	0.2	-	-	-	-
85	NI-16	1707	-	-	0.3	-	-	-	-
86	Curcuphenol	1711	1717	1534.119	0.2	1.952	0.570	0.148	10.041
87	2Z,6E-Farnesol	1715	1713	1845.951	0.2	1.186	0.542	0.010	9.240
88	Chamazulene	1724	1730	1512.019	0.1	1.048	0.611	0.057	10.419
89	6R,7R-Bisabolone	1739	1740	1600.565	1.2	1.979	0.555	0.148	10.041
90	β-Costol	1761	1765	1535.495	0.3	0.841	0.555	0.152	10.695
91	NI-17	1779	-	-	0.2	-	-	-	-
92	2-Pentadecanone, 6,10,14-trimethyl-	1840	1847	2133.804	0.2	0.643	0.518	0.000	9.459
93	NI-18	1903	-	-	0.3	-	-	-	-
94	Heptadecanal	1913	1922	1929.535	0.1	0.704	0.518	0.000	8.883
95	NI-19	1945	-	-	0.2	-	-	-	-
96	Heneicosane	2100	2100	2148.124	0.2	0.973	0.506	0.000	9.076
97	Phytol	2123	2122	2404.862	0.1	1.057	0.517	0.007	9.594
98	9,12-Octadecadienoic acid (Z,Z)-	2148	2132	1961.330	0.1	0.736	0.535	0.029	9.103
99	trans-Geranylgeraniol	2172	2181	1576.040	0.3	1.108	0.544	0.007	9.594
100	NI-20	2226	-	-	0.3	-	-	-	-
101	Tricosane	2301	2300	2216.401	0.6	0.975	0.507	0.000	9.187
102	Pentacosane	2497	2500	2277.141	0.4	0.978	0.508	0.000	9.287
103	Heptacosane	2701	2700	2627.325	0.2	0.000	1.000	0.000	9.377
104	Nonacosane	2909	2900	2626.827	0.3	0.000	1.000	0.000	9.460
Monoterpene hydrocarbons					14.2				
Oxygenated monoterpenes					28.1				

APTEFF, 52, 1-273 (2021) UDC: 582.998.16+665.52]:543.544(497.11)
DOI: https://doi.org/10.2298/APT2152123A BIBLID: 1450-7188 (2021) 52, 123-132
BY-NC-ND
Original scientific paper

Table 1. Continuation.

No	Compound	RI[a]	RI[b]	$RI_{pred.}$	%	GATS5e	Mv	VE1_Dt	MWC9
Sesquiterpene hydrocarbons					11.2				
Oxygenated sesquiterpenes					23.6				
Oxygenated diterpenes					0.3				
Other[c]					2.5				
NI					15.3				
Total identified					**96.4**				

RI[a] – Retention Index calculated; RI[b] – Retention Index from the NIST webbook database; $RI_{pred.}$ – Retention Index obtained usig QSRR model; GATS5e – Autocorrelation descriptor (Geary autocorrelation - lag 5 / weighted by Sanderson electronegativities); Mv – Constitutional descriptor (Mean atomic van der Waals volumes; scaled on carbon atom); VE1_Dt – Detour matrix descriptor (Coefficient sum of the last eigenvector from detour matrix); MWC9 – Walk counts descriptor (Molecular walk count of order 9 (ln(1+x)); Other[c] – aliphatic hydrocarbons, aliphatic aldehydes and alcohols, aliphatic acids, their esters and aldehydes, aromatic esters with aliphatic acids, alkyl-aromatic alcohols, or aryl esters of aromatic acids; NI[d] – Not Identified compound

***Mass spectrum of NI compounds, m/z (intensity):**

NI-1: 41.05 (43.0), 67.05 (51.0), 69.10 (39.0), 79.00 (39.0), 81.05 (100.0), 91.05 (60.0), 95.00 (44.0), 107.05 (65.0), 109.10 (84.0), 121.10 (86.0)

NI-2: 41.05 (33.0), 55.05 (27.0), 67.05 (70.0), 79.05 (48.0), 81.00 (100.0), 82.05 (23.0), 95.00 (44.0), 96.05 (39.0), 109.00 (43.0), 123.00 (25.0), 152.15 (3.0)

NI-3: 41.10 (20.0), 59.00 (30.0), 67.05 (29.0), 69.05 (24.0), 79.00 (19.0), 81.10 (44.0), 93.10 (19.0), 108.05 (51.0), 109.05 (100.0), 123.10 (14.0), 152.00 (3.0)

NI-4: 43.05 (31.0), 67.05 (23.0), 79.00 (36.0), 80.05 (39.0), 81.05 (24.0), 91.00 (26.0), 93.05 (100.0), 94.05 (23.0), 107.05 (27.0), 121.10 (30.0)

NI-5: 41.05 (62.0), 69.05 (70.0), 77.05 (39.0), 79.05 (54.0), 91.05 (59.0), 93.05 (43.0), 107.05 (41.0), 133.05 (44.0), 134.05 (100.0), 135.05 (53.0), 218.00 (3.0)

NI-6: 41.05 (60.0), 67.05 (56.0), 79.05 (85.0), 91.05 (95.0), 93.05 (100.0), 94.05 (78.0), 105.05 (73.0), 107.00 (67.0), 121.05 (65.0), 159.05 (75.0), 220.10 (47.0)

NI-7: 41.10 (30.0), 55.10 (17.0), 69.05 (100.0), 93.05 (30.0), 94.05 (21.0), 109.10 (23.0), 119.10 (58.0), 137.05 (20.0), 161.10 (17.0), 207.15 (53.0), 222.10 (5.0)

NI-8: 41.05 (30.0), 43.05 (25.0), 79.05 (30.0), 81.05 (25.0), 95.05 (28.0), 105.05 (43.0), 119.05 (100.0), 159.10 (39.0), 161.10 (63.0), 204.15 (31.0), 220.15 (2.0)

NI-9: 79.05 (53.0), 81.05 (59.0), 82.05 (63.0), 91.05 (57.0), 105.05 (63.0), 107.05 (46.0), 119.05 (67.0), 123.05 (100.0), 161.10 (56.0), 177.05 (67.0), 220.15 (13.0)

NI-10: 41.05 (28.0), 55.05 (20.0), 79.05 (23.0), 91.05 (78.0), 93.05 (25.0), 105.05 (28.0), 107.05 (23.0), 119.05 (65.0), 132.05 (100.0), 133.05 (75.0)

NI-11: 67. 10 (21.0), 91.05 (39.0), 121.05 (25.0), 135.05 (58.0), 145.05 (24.0), 147.05 (34.0), 159.05 (49.0), 173.05 (57.0), 201.05 (82.0), 216.10 (100.0)

NI-12: 41.10 (83.0), 79.00 (100.0), 91.05 (93.0), 92.00 (77.0), 93.10 (93.0), 95.05 (81.0), 105.05 (76.0), 107.05 (94.0), 109.05 (87.0), 131.05 (78.0), 220.15 (4.0)

NI-13: 79.05 (30.0), 91.05 (43.0), 93.05 (43.0), 105.05 (39.0), 107.05 (29.0), 109.05 (31.0), 121.05 (42.0), 133.05 (73.0), 159.05 (100.0), 176.10 (100.0), 220.15 (21.0)

NI-14: 67.05 (27.0), 91.05 (44.0), 121.05 (27.0), 135.05 (61.0), 145.05 (25.0), 147.05 (36.0), 159.10 (45.0), 173.10 (59.0), 201.05 (82.0), 216.10 (100.0)

NI-15: 41.05 (46.0), 77.05 (41.0), 81.05 (39.0), 91.05 (84.0), 93.05 (100.0), 105.00 (61.0), 107.05 (46.0), 119.05 (49.0), 133.05 (79.0), 189.05 (58.0), 220.15 (4.0)

NI-16: 41. 00 (89.0), 43.10 (94.0), 55.05 (86.0), 57.05 (100.0), 69.10 (58.0), 82.05 (97.0), 93.05 (88.0), 96.05 (60.0), 107.05 (95.0), 135.05 (84.0)

NI-17: 41.05 (49.0), 43.05 (35.0), 69.05 (55.0), 82.05 (52.0), 91.0 0 (49.0), 93.10 (70.0), 109.05 (35.0) 119.05 (100.0), 121.00 (40.0), 233.10 (35.0), 248.15 (12.0)

NI-18: 41. 00 (51.0), 55.00 (29.0), 69.00 (44.0), 109.05 (45.0), 111.00 (39.0), 125.05 (100.0), 126.05 (27.0), 151.05 (87.0), 153.05 (36.0), 236.15 (34.0)

NI-19: 41.05 (44.0), 43.00 (43.0), 69.05 (49.0), 95.00 (35.0), 108.0 0 (38.0), 109.05 (56.0), 121.05 (39.0) 135.05 (100.0), 136.10 (30.0), 148.05 (32.0), 236.15 (17.0)

NI-20: 41.05 (50.0), 43.05 (38.0), 55.05 (65.0), 67.05 (43.0), 69.05 (50.0), 81.05 (74.0), 93.00 (49.0), 95.05 (100.0), 107.05 (40.0), 109.05 (40.0)

In order to develop a QSRR model for prediction of RIs, PaDel-descriptor software was used. A large set of MDs were calculated, and only the most important descriptors were selected to build the predictive RIs model (12). The four most significant molecular descriptors selected by GA were shown in Table 1. Subsequently, the used MDs were appro-

APTEFF, 52, 1-273 (2021) UDC: 582.998.16+665.52]:543.544(497.11)
DOI: https://doi.org/10.2298/APT2152123A BIBLID: 1450-7188 (2021) 52, 123-132
BY-NC-ND
Original scientific paper

priate to foresee the RIs of compounds in *A. millefolium* by multivariate ANN model. Table 2 represents the correlation matrix among these descriptors.

Table 2. Correlations between molecular descriptors

	Mv	VE1_Dt	MWC9
GATS5e	-0.207	-0.007	0.090
	p=0.061	p=0.954	p=0.416
Mv		-0.169	-0.091
		p=0.128	p=0.412
VE1_Dt			0.081
			p=0.465

In order to investigate the nonlinear relationship between RIs of compounds in and MDs selected by GA, ANN modelling tool was used. The neural network MLP 4-8-1 was constructed to predict the retention time of compounds isolated from *A. millefolium* essential oil. The coefficients of determination during the training cycle was 0.862, indicating that this model could be used for prediction of RIs, due to low prediction error and high r^2. The statistical results of the ANN model are shown in Table 3.

Table 3. ANN model summary (performance and errors), for training, testing and validation cycles

Net. name	Performance			Error			Train. algor.	Error funct.	Hidden activat.	Output activat.
	Train.	Test.	Valid.	Train.	Test.	Valid.				
MLP 4-8-1	0.862	0.884	0.973	14496.458	32524.903	6374.756	BFGS 72	SOS	Logistic	Identity

*Performance term represent the coefficients of determination, while error terms indicate a lack of data for the ANN model. ANN cycles: Train. – training, Test. – testing, Valid. – validation, algor. –algorythm, funct. – function, activat. – activation.

The predicted RIs are presented in Fig. 1, confirming the good quality of the constructed ANN, by showing the relationship between the predicted and experimental RIs values. Graphical comparison between: experimentally obtained retention indices of *A. millefolium* essential oil essential oils composition (RI^a), and the retention time indices predicted by the four ANN models ($RI_{pred.}$) were presented in Fig. 2. The obtained results presented in Fig. 1 and Fig. 2 show the good reliability of the ANN models for predicting the RIs of compounds in *A. millefolium* essential oil obtained by GC-MS analysis. The influence of four most important input variables, identified using genetic algorithm on RIs was studied. According to the Fig. 3, MWC9 was the most important MD for chemical compounds in *A. millefolium* essential oil. The positive influence was observed for GATS5e descriptor, while the two negative influential MDs with almost equally importance were: Mv and VE1_Dt.

APTEFF, 52, 1-273 (2021)
DOI: https://doi.org/10.2298/APT2152123A
BY-NC-ND
UDC: 582.998.16+665.52]:543.544(497.11)
BIBLID: 1450-7188 (2021) 52, 123-132
Original scientific paper

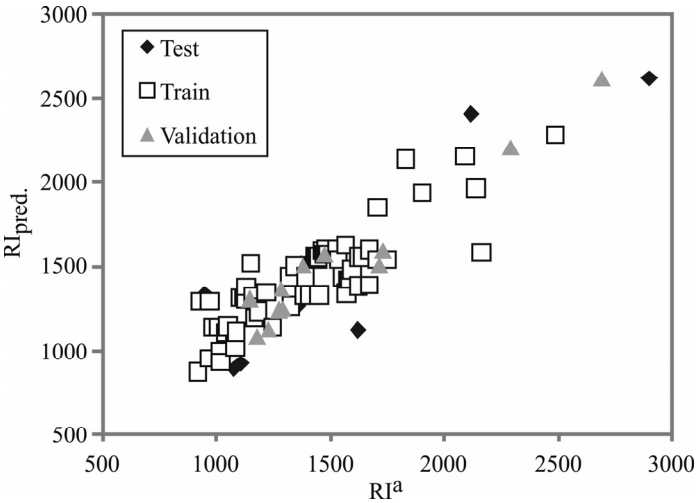

Figure 1. Retention time indices of the *A. millefolium* essential oil composition, from: experimentally obtained GC-MS data (RI^a) and predicted by the ANN ($RI_{pred.}$).

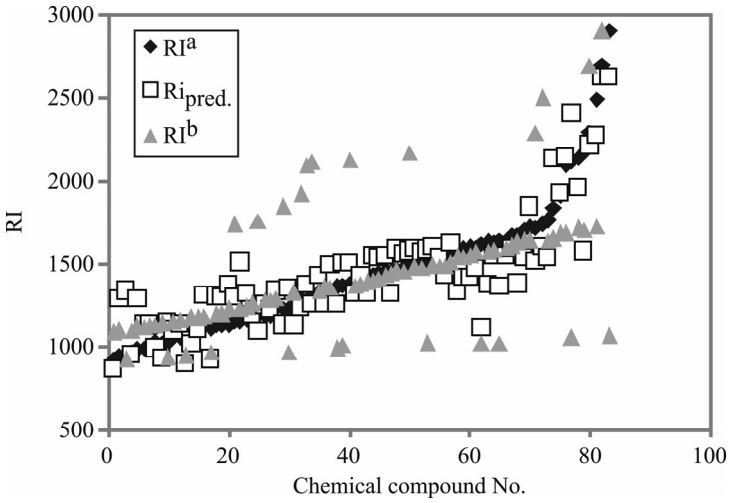

Figure 2. Comparison of experimentally obtained RIs with ANN predicted values

APTEFF, 52, 1-273 (2021)
DOI: https://doi.org/10.2298/APT2152123A
BY-NC-ND
UDC: 582.998.16+665.52]:543.544(497.11)
BIBLID: 1450-7188 (2021) 52, 123-132
Original scientific paper

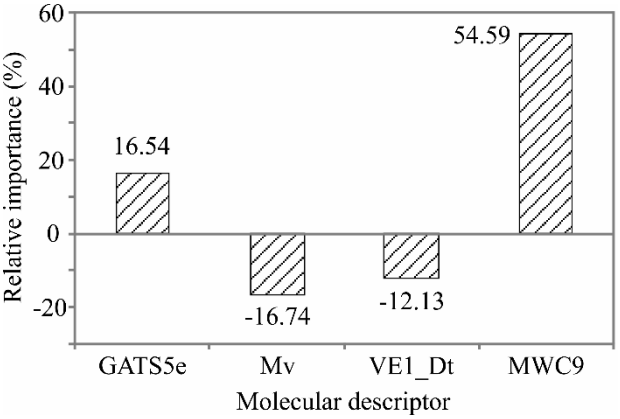

Figure 3. The relative importance of the molecular descriptors on RI, determined using Yoon interpretation method

Investigations of *A. millefolium* composition from different countries showed that the quantitatively most important components of the oil were chamazulene, *β*-pinene, sabinene, bornyl acetate, *β*-caryophyllene, *E*-nerolidol, 1,8-cineole and germacrene D (15). The most frequently identified compound among the monoterpenes was 1,8-cineole, found in almost every essential oil, followed by compounds with bornane skeleton such as camphor and borneol (16). The basic chromosome number of *Achillea* species is x=9, but the diversity in chromosome numbers and ploidy levels occurs frequently in this genus. Consequently, there are diploid, tetraploid, hexaploid and octaploid accessions (15; 17). However, diploid and tetraploid accessions contain chamazulene and their essential oil is blue, while the accessions with high percentage of oxygenated monoterpenes and absence of azulene in the essential oil are characterized by being pale yellow (hexaploid and octaploid) (15; 18). Furthermore, population developed by hybridization and polyploidy exhibits great variation and ecological divergence (19). The color of essential oil of *A. millefolium* from Rtanj Mt. indicated that it could be hexaploid or octaploid accession. However, hexaploid accessions of *A. millefolium* aggregate have the widest range of spreading, usually as a weed throughout Europe and Asia (17). Furthermore, oxygenated monoterpenes as the dominant class (28.1%) with compounds such as camphor, terpinen-4-ol and 1,8-cineole could be eco-geographical characters of accessions from this specific mountain. Further cytogenetic investigation need to be done to confirm this.

CONCLUSION

In the essential oil from the *A. millefolium sensu lato* collected in Rtanj Mt. 104 compounds were detected, and the most abundant were camphor, caryophyllene oxide, terpinen-4-ol and 1,8-cineole. The results showed that the selected four molecular descriptors were adequate in predicting the retention indices of the observed chemical compounds. The coefficients of determination for training cycle were 0.862 (for compounds found in *A. millefolium* essential oil.

BY-NC-ND

Acknowledgements

This research was supported by the Ministry of Education, Science and Technological Development of the Republic of Serbia, grant number: 451-03-9/2021-14/200032.

REFERENCES

1. Josifović, M. Flora SR Srbije. Vol 7. Srpska akademija nauke i umetnosti, Beograd, Serbia, **1975**.
2. Pljevljakusic, D.; Ristic, M.; Savikin, K. Screening of yarrow (*Achillea millefolium* Agg.) populations in Serbia for yield components and essential oil composition. *Lekovite Sirovine*. **2017**, *37*, 25-32.
3. Orth, M.; Czygan, F.C.; Dedkov, V. Variation in essential oil composition and chiral monoterpenes of *Achillea millefolium* S.L. from Kaliningrad. *Journal of Essential Oil Research*. **1999**, *11*, 681-687.
4. Tucakov, J. Lečenje biljem: fitoterapija. Rad, Beograd, Srbija, **2006**.
5. Hashempur, M.H.; Khademi, F.; Rahmanifard, M.; Zarshenas, M. An evidence-based study on medicinal plants for hemorrhoids in Medieval Persia. *Journal of Evidence-Based Complementary and Alternative Medicine*. **2017**, *22*, 969-981.
6. Nirmala, S.; Karthiyayini, T. Wound healing activity on the leaves of *Achillea millefolium* L. by excision, incision, and dead space model on adult Wistar albino rats. *International Research Journal of Pharmacy*. **2011**, *2*, 240-245.
7. Mohamed, D.; Hanfy, E.; Fouda, K. Evaluation of antioxidant, anti-inflammatory and anti-arthritic activities of yarrow (*Achillea millefolium*). *Journal of Biological Sciences*. **2018**, *18*, 317-328.
8. Mazandarani, M.; Mirdeilami, S.Z.; Pessarakli, M. Essential oil composition and antibacterial activity of *Achillea millefolium* L. from different regions in North east of Iran. *Journal of Medicinal Plants Research*. **2013**, *7*, 1063-1069.
9. Aćimović, M.; Zorić, M.; Zheljazkov, V.D.; Pezo L.; Čabarkapa, I.; Stanković Jeremić J.; Cvetković, M. Chemical characterization and antibacterial activity of essential oil of medicinal plants from Eastern Serbia. Molecules. **2020**, *25*, 5482; doi:10.3390/molecules25225482
10. Acar, M.B.; İbiş, E.K.; Şimşek, A.; Vural, C.; Tez, C.; Özcan, S. Evaluation of *Achillea millefolium* essential oil compounds and biological effects on cervix cancer HeLa cell line. *The EuroBiotech Journal*. **2020**, *4*, 17-24.
11. Aćimović, M.; Pezo, L.; Stanković Jeremić, J.; Cvetković, M.; Rat, M.; Čabarkapa, I.; Tešević, V. QSRR model for predicting retention indices of geraniol chemotype of *Thymus serpyllum* essential oil. *Journal of Essential Oil Bearing Plants*. **2020**, *23*, 464-473.
12. Aćimović, M.; Pezo, L.; Tešević, V.; Čabarkapa, I.; Todosijević, M. QSRR Model for predicting retention indices of *Satureja kitaibelii* Wierzb. ex Heuff. essential oil composition. *Industrial Crops and Products*. **2020**, *154*, 112752.
13. Yap, C.W. PaDEL-descriptor: An open source software to calculate molecular descriptors and fingerprints. *Journal of Computational Chemistry*. **2011**, *32*, 1446-1474.
14. Yoon, Y.; Swales, G.; Margavio, T.M. A comparison of discriminant analysis versus artificial neural networks. *Journal of the Operational Research Society*. **2017**, *44*, 51-60.
15. Raal, A.; Orav, A.; Arak, E. Essential oil content and composition in commercial *Achillea millefolium* L. herbs from different countries. *Journal of Essential Oil Bearing Plants*. **2012**, *15*, 22-31.
16. Turkmenoglu, F.P.; Agar, O.T.; Akaydin, G.; Hayran, M.; Demirci, B. Characterization of volatile compounds of eleven *Achillea* species from Turkey and biological activities of essential oil and methanol extract of *A. hamzaoglui* Arabaci & Budak. *Molecules*. **2015**, *20*, 114432-11458.

BY-NC-ND

17. Guo, Y.P.; Saukel, J.; Ehrendorfer, F. AFLP trees versus scatterplots: evolution and phylogeography of the polyploidy complex *Achillea millefolium* agg. (Asteraceae). *Taxon*. **2008**, *57*, 153-169.
18. Bozin, B.; Mimica-Dukic, N.; Bogavac, M.; Suvajdzic, Lj.; Simin, N.; Samojlik, I.; Couladis, M. Chemical composition, antioxidant and antibacterial properties of *Achillea collina* Becker ex Heimerl s.l. and *A. pannonica* Scheele essential oils. *Molecules*. **2008**, *13*, 2058-2068.
19. Ma, J.X.; Li, Y.N.; Vogl, C.; Ehrendorfer, F.; Guo, Y.P. Allopolyploid specification and ongoing backcrossing between diploid progenitor and tetraploid progeny lineages in the *Achillea millefolium* species complex: analyses of single-copy nuclear genes and genomic AFLP. *BMC Evolutionary Biology*. **2010**, *10*, 100.

APTEFF, 52, 1-273 (2021) UDC: 544.526.5:546.47-31:667.5.03
DOI: https://doi.org/10.2298/APT2152133A BIBLID: 1450-7188 (2021) 52, 133-145
BY-NC-ND
Original scientific paper

MODELING AND OPTIMIZATION OF THE PHOTOCATALYTIC DEGRADATION OF TARTRAZINE IN AQUEOUS SOLUTION

Mirvet ASSASSI[1], Farid MADJENE[2], Sara HARCHOUCHE[2], Hind BOULFIZA[2]*

[1] Mohamed El Bachir El Ibrahimi University, Bordj Bou Arreridj, Algeria
[2] Unité de Développement des Equipements Solaires, UDES, Centre de Développement des Energies Renouvelables, CDER, 42415, Tipaza, Algérie

Received: 23 April 2021 **Revised: 21 May 2021** **Accepted: 31 May 2021**

The application of heterogeneous photocatalysis process using ZnO photocatalyst for the degradation of Tartrazine (TRZ) dye in aqueous solution was investigated in a batch reactor. The estimation, the comparison of the parameter's effects and the optimization of the removal yield of TRZ were realized by using Box–Behnken experimental design (BBD). The results suggested that the most influential factor on the photocatalytic degradation of the dye was the initial TZR concentration with an effect of (-23.24), the second in the order was the amount of the catalyst with an effect of (+18.09), the third was the reaction time with an effect of (+15.38) and the fourth was stirring speed with a positive effect of (+4.41). The model obtained by BBD led to the following optimal conditions for degradation yield of TRZ: initial concentration of TZR equal to 20.035 mg/L, reaction time equal to 88.635 min, 0.6409 mg/L of ZnO amount and 404.9 rpm for the stirring speed, which gave 98.576% of degradation efficiency. The study of irradiation type effect shows that a solar irradiation gave higher yield than photocatalysis by UV lamp. The $O_2^{\bullet-}$ radicals were the principal active species responsible of the degradation of TRZ. The BOD_5/COD ratio increased from 0.26 to 0.41 after 60 minutes of photocatalysis under solar light, indicating the feasibility of coupling the photocatalysis process to biological treatment for the removal of TRZ.

Keywords: Heterogeneous photocatalysis, ZnO, UV light, solar light, tartrazine, Box-Behnken design, biodegradability.

INTRODUCTION

Water is the central element of all socio-economic processes, regardless of the degree of development of society. The increase in industrial activities is putting increasing pressure on the world's fresh water reserves. Indeed, these activities generate a great diversity of chemicals discharged in aquatic ecosystems endangering the fragile natural balance, which allowed life to develop on earth. Often the chemicals in wastewater are difficult to biodegrade and the lack or inadequacy of treatment systems leads to their accumulation in the aquatic environment. Better production and less pollution are the challenges of manufacturers in all sectors. The constraints in legislative and normative form are more and more drastic. Industries diverse chemicals, petrochemicals, textiles, stationery and tanneries, produce a wide variety of effluents which require new investigations and development of specific processes.

* Corresponding author: Mirvet Assassi, Environmental Engineering Department, Faculty of Sciences and Technology, Mohamed El Bachir El Ibrahimi University, Bordj Bou Arreridj, Algeria,
e-mail: mirvetassassi@yahoo.com

APTEFF, 52, 1-273 (2021) UDC: 544.526.5:546.47-31:667.5.03
DOI: https://doi.org/10.2298/APT2152133A BIBLID: 1450-7188 (2021) 52, 133-145
BY-NC-ND
Original scientific paper

Tartrazine is one of anionic azo dye utilized in the textile industry, cosmetics and for coloring food (1). Therefore, due to his stability and toxicity this dye has become a severe environmental and health problem. The presence of dye molecules in the effluent is very toxic to biotic life, even at low concentrations (2,3). Thus, to solve the environmental problem, it is very important to remove these dyes from effluents by decomposing into non-toxic components. Conventional methods for removing dyes including biological methods (4), flocculation (5), reverse osmosis (6), ultrafiltration membranes (7), adsorption (8) and chemical oxidation methods are either expensive or do not often reach the threshold set up by the water standards. Simple and inexpensive solutions are then strongly required to fulfill the required conditions. During the last decade, a lot of research has focused on a new class of oxidation techniques: Advanced Oxidation Processes (AOPs) (9-11).

These technologies have already shown their potential in the treatment of toxic and "biologically recalcitrant" organic pollutants. AOPs include photocatalytic process as an environmentally friendly process and has considerable advantages over some existing technologies; usually leads to complete mineralization of organic pollutants into CO_2 and H_2O by using atmospheric oxygen as oxidant and solar light as light source (12). For the degradation of persistent organic compounds contained in wastewater, several studies recommend integrated processes, especially the coupling of AOPs and biological treatment (13-16). The innovation of this study was to investigate the degradation mechanism of TRZ and to test the feasibility of combining photocatalytic process treatment with biological process, this approach was scarcely investigated in the treatment of toxic and recalcitrant organic compounds.

Conventional and classical methods to analyze a process by maintaining other factors involved at an unspecified constant level does not depict the combined effects of all the involved operating factors. This method is also time consuming and requires many experiments to determine optimal levels. One of the most important and widely used experimental design methods is the Response Surface Methodology (RSM) (17-19). RSM is a statistical method, has many advantages in terms of cost and time because of the reduced number of experimental studies required to interpret multiple parameters and their interactions. The Box–Behnken experimental design (BBD) is amongst the most RSM commonly used in various experiments, it is useful in avoiding experiments performed under extreme conditions, for which unsatisfactory results might occur (20-22).

The main objectives of this work are:

I) to investigate the individual and the interactive effects of four operating parameters, mainly: initial concentration of TRZ, irradiation time, ZnO amount and stirring speed, on the yield of degradation of TRZ by photocatalytic process using the Box–Behnken experimental design; and to optimize those process variables;
II) to investigate the effect of irradiation type (UV-Light and solar light) on the removal efficiency of TRZ;
III) to investigate the degradation mechanism of TRZ and
IV) to investigate the possibility to enhance the biodegradability of TRZ with photocatalytic process and the feasibility of combining photocatalytic process treatment with biological process.

APTEFF, 52, 1-273 (2021) UDC: 544.526.5:546.47-31:667.5.03
DOI: https://doi.org/10.2298/APT2152133A BIBLID: 1450-7188 (2021) 52, 133-145
BY-NC-ND
Original scientific paper

MATERIALS AND METHODS

CHEMICALS

The photocatalyst used in this study was zinc oxide (ZnO) (99.9%, purity), obtained from Aldrich chemical company. The anionic dye Tartrazine (TRZ) ($C_{16}H_9N_4Na_3O_9S_2$, 534.3 g/mol, purity 62%) was purchased from Sigma Aldrich, its chemical structure is given below (Figure 1).

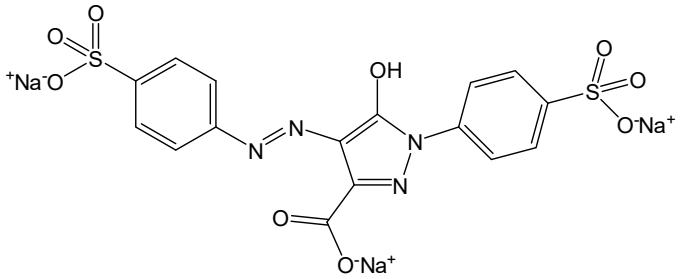

Figure 1. Chemical structure of Tartrazine.

PHOTOCATALYTIC ACTIVITY EXPERIMENTS

To evaluate the efficacy of ZnO on the degradation of Tartrazine, a series of experiments were carried out in a batch photoreactor, represented by 250 ml opened beaker, under UV PHILPS PL-L 24W / 10 / 4P U.V. lamps with a maximum emission of 365 nm. The lamp irradiance (18 W/m^2) received by the dye solution was determined by using DALE40 Phototherapy Radiometer. The experiments under solar irradiation were carried out in Bou-Ismail, Algeria, in summer 2020 (latitude 36°.39′; longitude 2°.42′), the solar ultraviolet radiation (UV) was measured by global UV radiometer (KIPP & ZONZN, CMP11).The degradation tests were carried out while keeping the same operating procedure for all degradation experiments. Three solutions of different concentrations (10, 55 and 100 mg/L) were prepared, and then the catalyst was added to the solution. The suspension was stirred in order to homogenize it well.

TARTRAZINE ANALYSIS

The samples were withdrawn at regular time intervals, centrifuged and the supernatants were analyzed for residual dye concentration by the measurement of the solution absorbance using a UV-visible double beam spectrometer (SHIMADZU UV 1800) at λ_{max}=425 nm.

COD AND BOD_5 MEASUREMENTS

The COD was analyzed by using potassium dichromate in hot and acidic medium (AQUALYTIC AL 200COD Vario), Biochemical oxygen demand (BOD_5) was measured using OXITOP IS 12 (WTW) equipment.

APTEFF, 52, 1-273 (2021) UDC: 544.526.5:546.47-31:667.5.03
DOI: https://doi.org/10.2298/APT2152133A BIBLID: 1450-7188 (2021) 52, 133-145
BY-NC-ND
Original scientific paper

EXPERIMENTAL DESIGN, MODEL FITTING AND STATISTICAL ANALYSIS

Box-Behnken Design of twenty-four experiments consisting of three replicates experiments at the central points was used and the results were evaluated by RSM. The behavior of photocatalytic degradation system was related by the following empirical second-order polynomial equation given in Eq. [1]:

$$Y = b_0 + \sum_{i=1}^{k} b_i x_i + \sum_{i=1}^{k} b_{ii} x_i^2 + \sum_{i=1}^{k-1} \sum_{j=2}^{k} b_{ij} x_i x_j + \varepsilon \quad [1]$$

where, Y is the predicted value of response, x_i, x_j,…, x_k are the input variables; x_i^2, x_j^2,…, x_k^2 are square effects and $x_i x_j$, $x_j x_k$ and $x_i x_k$ are the interaction effects. b_0, b_i, b_{ii}, b_{ij} and ε represent the linear coefficients, the quadratic effect coefficients, the interaction effect coefficients (for i, j = 1, 2, …, k) and a random error, respectively.
The response was expressed as the percent of TRZ degradation as follow Eq. [2]:

$$Y_{TRZ}(\%) = \frac{C_0 - C}{C_0} 100 \quad [2]$$

The initial TRZ concentration (x_1), irradiation time (x_2), ZnO amount (x_3) and stirring speed (x_4) were chosen as the most influential study factors on the photocatalytic degradation of the TRZ. The levels selected for each factor were presented in Table 1.

Table 1. The main factors and their levels in the BBD during the TZR dye degradation process

Operating factors	Levels		
	-1	**0**	**+1**
x_1: [TRZ] (mg/L)	10	55	100
x_2: Time (min)	30	75	120
x_3: [ZnO] (g/L)	0.1	0.55	1
x_4: Stirring speed (rpm)	100	350	600

All other parameters of the reaction such as: free pH of the solution (~ 7), lamp irradiance (18 W m^{-2}), ambient temperature (~ 25 °C) and volume of the solution (200 ml) have been fixed during the experiments. The range of variables was determined on the basis of the pre-experimental results. Each experiment was repeated three times and average values were used for optimization. The experimental conditions and results of the designed experiments were presented as TRZ dye degradation percentage in Table 2.

In the present study, MODDE 6.0 software was used to fit the experimental data and in regression analysis. Three-dimensional plots were obtained based on the fitted polynomial function.

APTEFF, 52, 1-273 (2021)
DOI: https://doi.org/10.2298/APT2152133A
BY-NC-ND
UDC: 544.526.5:546.47-31:667.5.03
BIBLID: 1450-7188 (2021) 52, 133-145
Original scientific paper

Table 2. Box-Behnken design and TZR dye removal yield

Run n°	Coded values of parameters				Y_{TRZ} (%)
	x_1	x_2	x_3	x_4	
1	-1	-1	0	0	100
2	1	-1	0	0	32.18
3	-1	1	0	0	100
4	1	1	0	0	85.12
5	0	0	-1	-1	37.57
6	0	0	1	-1	85.93
7	0	0	-1	1	54.19
8	0	0	1	1	99.83
9	-1	0	0	-1	100
10	1	0	0	-1	51.41
11	-1	0	0	1	100
12	1	0	0	1	59.34
13	0	-1	-1	0	30.54
14	0	1	-1	0	77.12
15	0	-1	1	0	76.47
16	0	1	1	0	100
17	-1	0	-1	0	100
18	1	0	-1	0	19.68
19	-1	0	1	0	100
20	1	0	1	0	73.46
21	0	-1	0	-1	62.03
22	0	1	0	-1	99.55
23	0	-1	0	1	75.99
24	0	1	0	1	99.65
25	0	0	0	0	100
26	0	0	0	0	100
27	0	0	0	0	99.88

RESULTS AND DISCUSSION

ELABORATION AND ANALYSIS OF THE MODELS

The data analysis results presented in Table 2 were used to obtain a quadratic polynomial equation taking into account the interaction between the dependent variable and the independent parameters. The significance of each parameter was determined from p-value of that parameter (Table 3**)**. The second-order models obtained according to a BBD after discarding the insignificant effects were as follows:

$$y_{TRZ} = 99.84 - 23.24\ x_1 + 15.38\,x_2 + 18.09\,x_3 + 4.41\,x_4 + 13.23\,x_1x_2 + 13.44\,x_1x_3 - 10.62\,x_1^2 - 8.4\,x_2^2 - 18.92\,x_3^2 - 10.04\,x_4^2 \quad [3]$$

A good adjustment of Eq. [3] to the experimental data was checked through the high correlation coefficient values obtained of R^2= 0.972 and $R^2_{adjusted}$= 0.939. A comparison of the experimental and calculated responses (Figure 2-a) shows a clear agreement between the observed values and those predicted by the model (Eq. 3). Figure 2-b shows the points moved from straight line revealed normal distribution of residuals, which indicates the normality of data.

APTEFF, 52, 1-273 (2021)
DOI: https://doi.org/10.2298/APT2152133A
BY-NC-ND
UDC: 544.526.5:546.47-31:667.5.03
BIBLID: 1450-7188 (2021) 52, 133-145
Original scientific paper

Table 3. The effect of each parameter on TZR degradation revealed statistically by MODDE 6.0 software

Coefficients	Coefficient estimate	P-value
b_0	99.84	4.16E-12*
b_1	-23.24	2.97E-8*
b_2	15.38	2.63E-6*
b_3	18.09	4.77E-7*
b_4	4.41	0.036*
b_{12}	13.23	0.001*
b_{13}	13.44	0.001*
b_{11}	-10.62	0.002*
b_{22}	-8.4	0.010*
b_{33}	-18.92	1.84E-5*
b_{44}	-10.04	0.003*

(*) - significant coefficient; R^2 - 0.972; Adjusted R^2 - 0.939;

According to the regression equation (Eq. 3), the initial TZR concentration (x_1) has the strongest effect on the response with a negative effect (b_1 = -23.24), the negative sign of the b_1 coefficient suggests that the removal yield of TZR decreased with increasing initial TZR concentration. The second in the order was the amount of the catalyst with a positive effect (b_3 = 18.09). The third was the reaction time with a positive effect (b_2 = 15.38). The fourth in order was stirring speed with a positive effect (b_4 = 4.41). The positive sign of these coefficients indicates that there is a direct relation between removal yield of TZR and those factors. All significant interactions found by the model were displayed in Figure 3. According to the interaction graphs (see Fig. 3), the strongest interaction was between the initial TZR concentration (x_1) and reaction time (x_2) (Figure 3-a) and between the initial TZR concentration (x_1) and the amount of ZnO (x_3) (Figure 3-b).

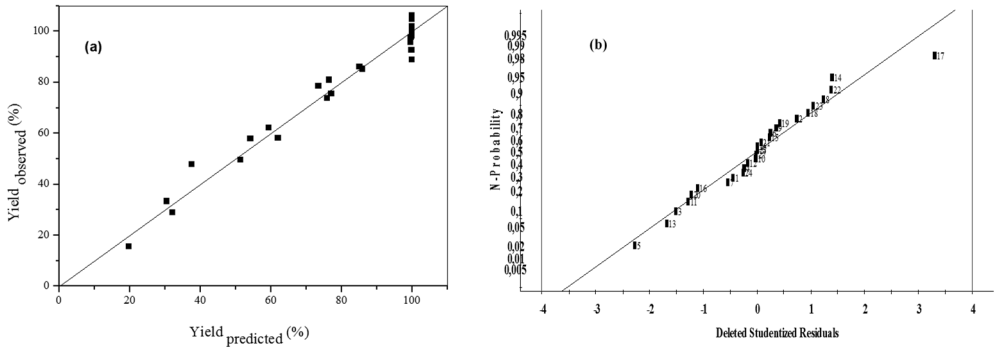

Figure 2. (a): Comparison of experimental and predicted responses, **(b):** Normal probability plot of studentized residuals

APTEFF, 52, 1-273 (2021) UDC: 544.526.5:546.47-31:667.5.03
DOI: https://doi.org/10.2298/APT2152133A BIBLID: 1450-7188 (2021) 52, 133-145
BY-NC-ND
Original scientific paper

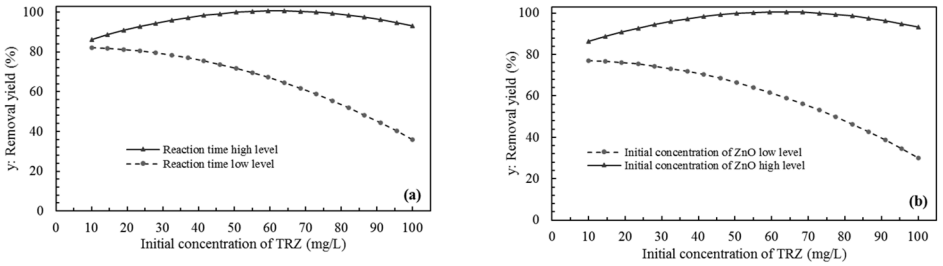

Figure 3. Interaction graphs obtained by the model

OPTIMIZATION OF THE OPERATING VARIABLES

To calculate the conditions for the maximization of removal yield of TZR, we have set the partial derivatives of the function to zero with respect to the corresponding variables. The maximum of response is the solution of the following system of equations:

$$\frac{dy}{dx_i}=0 \Leftrightarrow \begin{cases} \frac{dy}{dx_1}=-21.24x_1+13.23x_2+13.44x_3-23.24=0 \\ \frac{dy}{dx_2}=13.23x_1-16.8x_2+15.38=0 \\ \frac{dy}{dx_3}=\&13.44x_1-37.84x_3+18.09=0 \\ \frac{dy}{dx_4}=-20.08x_4+4.41=0 \end{cases}$$

The resolution leads to: $x_1 = -0.777$, $x_2 = 0.303$, $x_3 = 0.202$ and $x_4 = 0.2196$ corresponding respectively to the real variables 20.035 mg/L of TZR, 88.635 min of reaction time, 0.64 mg/L of ZnO and 405 rpm of stirring speed.

Figures 4-a to 4-f represented the results of the interaction between the 4 input variables and the process response in form of 3-D response surfaces (a). According to this figures the following conclusions can be drawn:

- Figure 4-a shows any rise in reaction time and for 31.42 mg/L≤ TZR ≤ 96.895 mg/L can lead to improvements in removal yield of TZR from 40.95 to 94.096%.
- Figure 4-b shows that any rise in concentration of ZnO from 0.9568 to 1 g/L and any decline in initial concentration of TZR from 91 to 10 mg/L can lead to improvements in removal yield of TZR from 30.83 to 93.083%.
- Figure 4-c shows that any rise in stirring speed and decline in initial concentration of TZR from 100 to 38.35 mg/L can lead to improvements in removal yield of TZR from 68.205 to 96.82%.
- Figure 4-d shows that any rise in concentration of ZnO and reaction time can lead to improvements in removal yield of TZR from 74.457 to 97.446%.
- Figure 4-e shows that any rise in stirring speed and reaction time can lead to improvements in removal yield of TZR from 85.765 to 98.576%.

APTEFF, 52, 1-273 (2021)
DOI: https://doi.org/10.2298/APT2152133A
BY-NC-ND
UDC: 544.526.5:546.47-31:667.5.03
BIBLID: 1450-7188 (2021) 52, 133-145
Original scientific paper

- Figure 4-f shows that any rise in stirring speed and concentration of ZnO from 0.2233 to 1 g/L can lead to improvements in the removal yield of TZR from 73.857 to 97.386%.

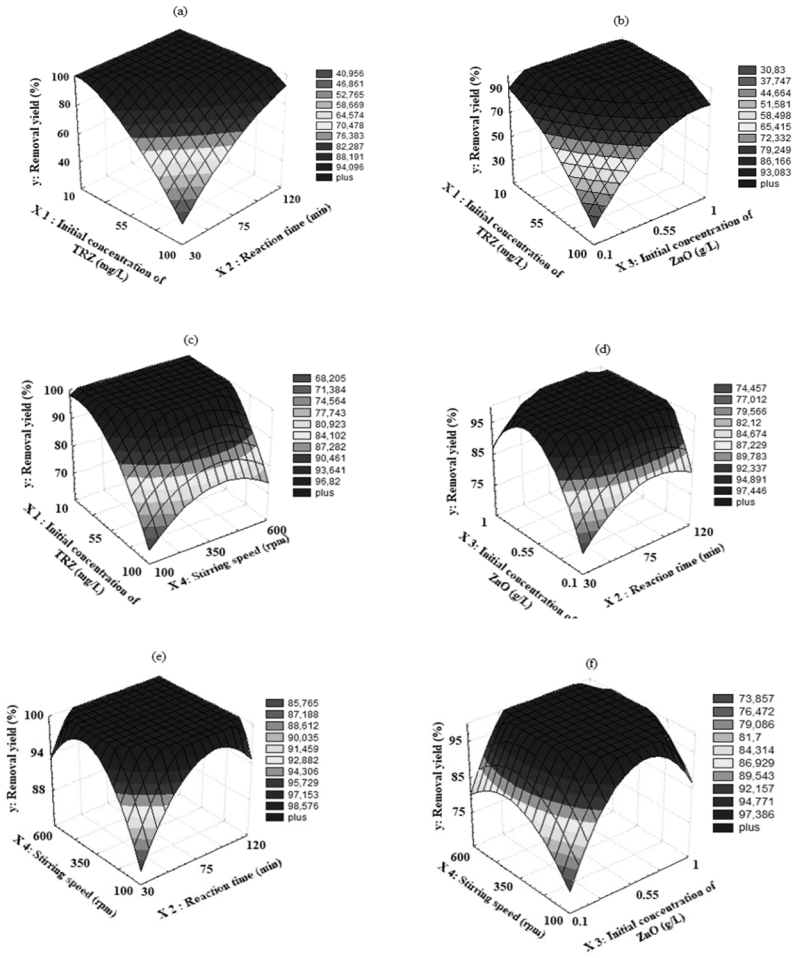

Figure 4. 3D response surfaces

(a): Showing the effect of initial concentration of TZR (x_1) and reaction time (x_2) on the removal yield of TZR. Conditions: T= 25°C, ZnO =0.64 g/L, stirring speed = 405 rpm and free pH of the solution (7)

(b): Showing the effect of initial concentration of TZR (x_1) and initial concentration of ZnO (x_3) on the removal yield of TZR. Conditions: T= 25°C, $t_{reaction}$=88.635 min, stirring speed= 405 rpm and free pH (7)

(c): Showing the effect of initial concentration of TZR (x_1) and stirring speed (x_4) on the removal yield of TZR. Conditions: T= 25°C, $t_{reaction}$ = 88.635 min, ZnO =0.64 g/L and free pH of the solution (7)

(d): Showing the effect of reaction time (x_2) and initial concentration of ZnO (x_3) on the removal yield of TZR. Conditions: T= 25°C, TZR = 20.035 mg/L, stirring speed = 405 rpm and free pH (7)

(e): Showing the effect of reaction time (x_2) and stirring speed (x_4) on the removal yield of TZR. Conditions: T= 25°C, TZR = 20.035 mg/L, ZnO =0.64 g/L and free pH of the solution (7)

(f): Showing the effect of initial concentration of ZnO (x_2) and stirring speed (x_4) on the removal yield of TZR. Conditions: T= 25°C, TZR = 20.035 mg/L, $t_{reaction}$ = 88.635 min and pH of the solution (7)

APTEFF, 52, 1-273 (2021) UDC: 544.526.5:546.47-31:667.5.03
DOI: https://doi.org/10.2298/APT2152133A BIBLID: 1450-7188 (2021) 52, 133-145
BY-NC-ND
Original scientific paper

EFFECT OF IRRADIATION TYPE

To determine the effect of the type of irradiation on the degradation rate of TRZ by the photocatalysis process, the degradation of TZR using solar (758 W/m^2) and UV irradiations (18 W/m^2) was studied under the optimal conditions obtained by Box-Behnken Design except for the initial concentration of TZR (100 mg/L) and reaction time (120 min).

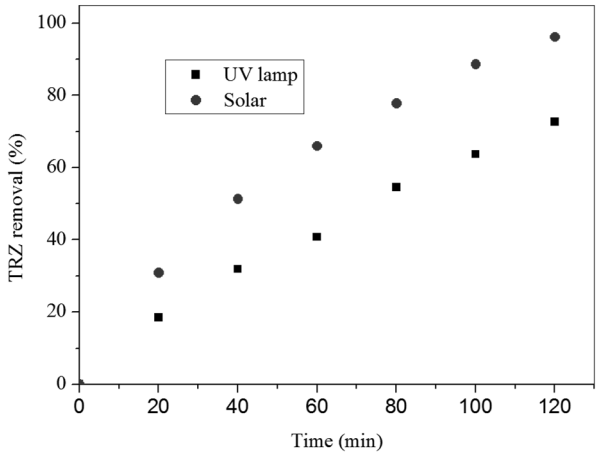

Figure 5. TZR degradation for solar irradiation and UV irradiation
TZR = 100 mg/L, [ZnO]= 0.65 g/L and stirring speed= 405 rpm

According to the Figure 5, the use of a solar irradiation gave higher yields (up to 96%) than photocatalysis by UV lamp. Similar results were also observed by Tassalit et al. (23) for tartrazine degradation and by Madjene et al. for Rhodamine degradation (24).

MECHANISM OF THE TZR DEGRADATION

Scavengers which are specifically trapping active species have been used to assess the photocatalytic reaction mechanism of the pollutant studied since they can modify the kinetic profile of the reaction, providing information on the participation of different active species. Tert-butanol, ammonium oxalate and the benzoquinone were used to show the role in the oxidation mechanism of hydroxyl radicals ($OH^{\bullet}$), holes (t^{+}), and superoxide anion ($O_2^{\bullet -}$) respectively (25).

APTEFF, 52, 1-273 (2021)
DOI: https://doi.org/10.2298/APT2152133A
BY-NC-ND
UDC: 544.526.5:546.47-31:667.5.03
BIBLID: 1450-7188 (2021) 52, 133-145
Original scientific paper

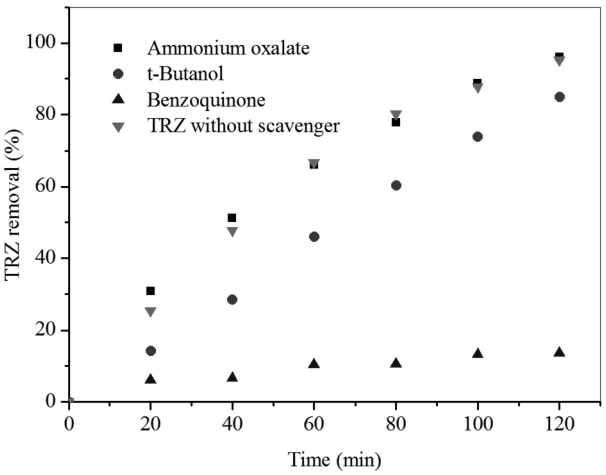

Figure 6. Degradation mechanism of Tartrazine
[Dye]= 100 mg/L, [ZnO]= 0.64 g/L, stirring speed= 405 rpm

As seen in Figure 6, with the addition of benzoquinone ($O_2^{\bullet}$ scavenger), the photocatalytic degradation rates of the dye decreased, indicating that the oxidation groups ($O_2^{\bullet-}$) were the main active species for the degradation of this pollutant. On the other hand, no significant change was observed with the addition of ammonium oxalate (hole scavenger) and t-butanol ($OH^{\bullet}$ scavenger).

The TRZ could be degraded using a strong oxidation power of $O_2^{\bullet-}$ according to the following mechanism:

$$TRZ + h\nu \rightarrow TRZ^{\bullet+} + e^-_{cb} \quad [4]$$

$$e^-_{cb} + O_2 \rightarrow O_2^{\bullet-} \quad [5]$$

$$TRZ^{\bullet+} + O_2^{\bullet-} \rightarrow \text{degradation product} \quad [6]$$

Dye was degraded by the oxidative action of $O_2^{\bullet-}$ produced in the medium to be treated. These radicals are produced only in the UV and solar system. The $O_2^{\bullet-}$ radicals are capable of degrading almost all of the persistent organic pollutants because of their very high oxidizing power, their reactivity and their non-selectivity towards organic substances.

BIODEGRADABILITY TESTS

The biodegradability study of Tartrazine was considered non-biodegradable ($BOD_5/COD = 0.26$) < 0.4 (24). After 60 minutes of photocatalytic pretreatment of TZR, an increase in the BOD_5/COD ratio from 0.26 initially to 0.41 was observed indicating the biodegradability of the treated Tartrazine solution. This result proved the efficiency of photocatalytic process for improved the biodegradability of organic compounds in the wastewater.

APTEFF, 52, 1-273 (2021) UDC: 544.526.5:546.47-31:667.5.03
DOI: https://doi.org/10.2298/APT2152133A BIBLID: 1450-7188 (2021) 52, 133-145
BY-NC-ND
Original scientific paper

COMPARATIVE REVIEW

We have compared the TRZ removal efficiency by photocalaysis process in the presence of ZnO under solar light to other water treatment process found in the literature (Table 4). However, due to the difference in experimental conditions and the process used it is difficult to make an objective comparison. Nevertheless, it appears from a qualitative point of view, that the observed removal yields were similar to or greater than those reported in other findings.

Table 4. Comparison of our results with others wastewater treatments technologies

Authors	TRZ Concentration	Treatment methods	Reaction time (min)	Removal efficiency (%)
Petruta Oancea and Viorica Meltzer. (26)	1.035×10^{-5} M	Photo-Fenton	2h	80
Tu and Tuan. (27)	50 mg/L^{-1}	Heterogeneous Fenton-like reaction on Fe_2O_3/SiO_2 composite	80 min	98.5%
Vaiano et al. (28)	10 mg/L $^{-1}$	Photocatalysis FeO_3/ZnO	4h	84
Elsayed and Gobara. (29)	100 mg/L^{-1}	Photocatalysis TiO_2-decorated PANI	120 min	99
Present study	55 mg/L^{-1}	Photocatalysis ZnO	90 min	100

CONCLUSION

The present work deals with modeling and optimization of the photocatalytic degradation of tartrazine in aqueous solution. From the results presented in this study, the following conclusions can be drawn:

- A quadratic model showing the functional relationship between degradation efficiency of Tartrazine and four independent variables was established by using Box-Behneken factorial design, the model has been validated by various statistical analyses. The optimal conditions giving 98.576 % degradation yield of TRZ were: initial concentration of TZR equal to 20.035 mg/L, reaction time equal to 88.635 min, 0.6409 mg/L of ZnO and 404.9 rpm for the stirring speed.
- A solar irradiation gave higher yield than photocatalysis by UV lamp.
- The study of the TRZ degradation mechanism indicate that degradation of dye was carried out by the oxidative action of the $O_2^{\bullet-}$ radicals.
- An increase in the BOD_5/COD ratio after 60 minutes from 0.26 initially to 0.41 indicates an enhancement in the biodegradability of the treated Tartrazine solution by photocatalysis.

BY-NC-ND

REFERENCES

1. Goscianska, J. and Pietrzak, R. Removal of tartrazine from aqueous solution by carbon nanotubes decorated with silver nanoparticles. Catal. Today. **2015,** 249, 259-264.
2. Fulekar, M.H., Wadgaonkar, S.L. and Singh, A. Decolourization of Dye Compounds by Selected Bacterial Strains isolated from Dyestuff Industrial Area. Intern. J. Advan. Res. Technol. **2013,** 2, 182-192.
3. Basu, A. and Kumar, G.S. Binding and Inhibitory Effect of Dyes Amaranth and Tartrazine on Amyloid Fibrillation in Lysozyme. J. Phys. Chem. B. **2017,** 121, 1222-1239.
4. Bhatia, D., Sharma, N.R., Singh, J. and Kanwar, R.S. Biological methods for textile dye removal from wastewater: A review. Crit. Rev. Environ. Sci. Technol. **2017,** 47, 1836-1876.
5. Zonoozi, M.H., Moghaddam, M.R.A. and Arami, M. Removal of acid red 398 dye from aqueous solutions by coagulation/flocculation process. Environ. Eng. Manag. J. **2008,** 7, 695-699.
6. AL-Nakib, N.M.H. Reverse Osmosis Polyamide Membrane for the Removal of Blue and Yellow Dye from Waste Water. Iraqi J. Chem. Petrol. Eng. **2013,** 14, 49-55.
7. Hidalgo, A.M., Gómez, M., Murcia, M.D., Serrano, M., Rodríguez-Schmidt R. and Escudero, P.A. Behaviour of polysulfone ultrafiltration membrane for dyes removal. Water Sci. Technol. **2018,** 77, 2093-2100.
8. Vargas, V.H., Paveglio, R.R., Pauletto, P., Salau, N.P.G. and Dotto, L.G. Sisal fiber as an alternative and cost-effective adsorbent for the removal of methylene blue and reactive black 5 dyes from aqueous solutions. Chem. Eng. Comm. 2019, **207,** 523-536.
9. Yahya, F., El-Rassy, H., Younes, G. and Al-Oweini, R. Synthesis and characterisation of mesoporous hybrid silicapolyoxometalate aerogels for photocatalytic degradation of rhodamine B and methylene blue. Intern. J. Environ. Anal. Chem. **2019,** 1375-1396.
10. Drumm, F.C., de Oliveira, J.S., Foletto, E.L., Dotto, G.L., Flores, E.M.M., Enders, M.S.P., Müller, E.I. and Janh, S.L. Response surface methodology approach for the optimization of tartrazine removal by heterogeneous photo-Fenton process using mesostructured Fe_2O_3-suppoted ZSM-5 prepared by chitin-templating. Chem. Eng. Comm. **2018,** 205, 445-455.
11. Konyar, M., Yildiz, T., Aksoy, M., Yatmaz, H.C. and Öztürk, K. Reticulated ZnO Photocatalyst: Efficiency Enhancement in Degradation of Acid Red 88 Azo Dye by Catalyst Surface Cleaning. Chem. Eng. Comm. **2017,** 204, 705-710.
12. Madjene, F. and Yeddou-Mezenner, N. *Design* and optimization of a new photocatalytic reactor with immobilized ZnO for water purification. *Sep. Sci. Technol.* **2018**, 53, 364-373.
13. Yahiaoui, I., Yahia Cherif, L., Madi, K., Aissani-Benissad, F., Fourcade F. and Amrane, A. The feasibility of combining an electrochemical treatment on a carbon felt electrode and a biological treatment for the degradation of tetracycline and tylosin - Application of the experimental design methodology. *Sep. Sci. Technol.* **2018**, *53*, 337-348.
14. Yahiaoui, I., Aissani-Benissad, F., Fourcade F. and Amrane, A. Enhancement of the biodegradability of a mixture of dyes (Methylene Blue and Basic Yellow 28) using the electrochemical treatment on a glassy carbon electrode. *Desalin. Water Treat.* **2016**, *57*, 12316-12323.
15. Aissani, T. Yahiaoui, I. Boudrahem, F. Ait Chikh, S. Aissani-Benissad, F. and Amrane, A. The combination of photocatalysis process (UV/ TiO_2 (P25) and UV/ZnO) with activated sludge culture for the degradation of sulfamethazine. *Sep. Sci. Technol.* **2018**, *35*, 1423-1424
16. Aissani, T., Yahiaoui, I., Boudrahem, F., Yahia Cherif, L., Fourcad, F., Amrane, A. and Aissani-Benissad, F. Sulfamethazine degradation by heterogeneous photocatalysis with ZnO immobilized on glass plate using heat attachment method and its impact on the biodegradability. *Reac Kinet Mech Cat.* **2020**, *131*, 471-487.
17. Rahman, S.H.A., Choudhury, J.P., Ahmad, A.L. and Kamaruddin, A.H. Optimization studies on acid hydrolysis of oil palm empty fruit bunch fiber for production of xylose. *Biores. Technol.* **2007,** *98*, 554-559.

BY-NC-ND

18. Catalkaya, E.C. and Kargi, F. Response Surface Analysis of Photo-Fenton Oxidation of Simazine. *Water Environ. Res.* **2009,** *81*, 735-742.
19. Dibene, K., Yahiaoui, I., Aitali, S., Khenniche, L., Amrane, A. and Aissani-Benissad, F. Central composite design applied to paracetamol degradation by heat-activated peroxydisulfate oxidation process and its relevance as a pretreatment prior to a biological treatment. *Environ. Technol.* **2021**, *42*, 905-913.
20. Ferreira, S.L.C., Bruns, R.E., Ferreira, H.S., Matos, G.D., David, J.M., Brandao˜, G.C., da Silva, E.G.P., Portugal, L.A., dos Reis, P.S., Souza, A.S. and dos Santos, W.N.L. Box-Behnken design: An alternative for the optimization of analytical methods. *Analytica Chimica Acta.* **2007,** 597, 179-186.
21. Ay, F., Catalkaya, E.C. and Kargi, F. A statistical experiment design approach for advanced oxidation of Direct Red azo dye by photo-Fenton treatment. *J. Hazard. Mater.* **2009,** 162, 230-236.
22. Zhang, H., Li, Y., Wu, X., Zhang, Y. and Zhang, D. Application of response surface methodology to the treatment landfill leachate in a three-dimensional electrochemical reactor. *Waste Manag.* **2010,** *30*, 2096-20102.
23. Tassalit, D., Lebouachera, S., Dechir, S., Chekir, N., Benhabiles, O. and Bentahar, F. Comparison between TiO_2 and ZnO Photocatalytic Efficiency for the Degradation of Tartrazine Contaminant in Water. *Intern. J. Environ. Sci.* **2016,** ***1,*** 357-364.
24. Madjene, F., Assassi, M., Chokri, I., Enteghar, T. and Lebik, H. Optimization of photocatalytic degradation of Rhodamine B using Box Behnken experimental design: mineralization and mechanism. *Water Environ. Res.* **2020**, *92*, 112-122.
25. Madjene, F., Assassi, M. and Yeddou-Mezenner, N. Degradation of atenolol in rectangular staircase photocatalytic reactor with immobilized ZnO. Chem. Eng. Techno. **2021,** *44*, 140-147.
26. Oancea, P., Meltzer,V. Photo-Fenton process for the degradation of Tartrazine (E102) in aqueous medium. *J. Taiwan Inst. Chem. Engrs.* **2013,** *44*, 6990-6994.
27. Tu, V., Tuan, V. Degradation of Tartrazine dye from aqueous solution by heterogeneous Fenton-like reaction on Fe_2O_3/SiO_2 composite. *Vietnam Journal of Chemistry.* **2017,** *55*, 470-477.
28. Vaiano, V., Iervolino, G., Sannino, D. Photocatalytic Removal of Tartrazine Dye from Aqueous Samples on FeO_3/ZnO Photocatalysts. *Chem. Eng. Trans.* **2016**, *52*, 847-852.
29. Elsayed, M. A., Gobara, M. Enhancement removal of Tartrazine dye using HCl-doped polyaniline and TiO_2 decorated PANI particles. *Mater. Res. Express*. **2016**, 085301.

APTEFF, 52, 1-273 (2021) UDC: 543.544:544.722.123:547.92
DOI: https://doi.org/10.2298/APT2152147K BIBLID: 1450-7188 (2021) 52, 147-158
BY-NC-ND
Original scientific paper

THE ANALYSIS OF CHROMATOGRAPHIC BEHAVIOR OF HOMOANDROSTANE DERIVATIVES IN REVERSED-PHASE ULTRA-HIGH PERFORMANCE LIQUID CHROMATOGRAPHY

Strahinja KOVAČEVIĆ[1], Milica KARADŽIĆ BANJAC[1,], Jasmina ANOJČIĆ[2], Lidija JEVRIĆ[1], Sanja PODUNAVAC-KUZMANOVIĆ[1], Slobodan GADŽURIĆ[2], Marina SAVIĆ[2], Ivana KUZMINAC[2], Andrea NIKOLIĆ[2], Marija SAKAČ[2]*

[1] University of Novi Sad, Faculty of Technology Novi Sad, Department of Applied and Engineering Chemistry, Bulevar cara Lazara 1, 21000 Novi Sad, Serbia
[2] University of Novi Sad, Faculty of Sciences, Department of Chemistry, Biochemistry and Environmental Protection, Trg Dositeja Obradovića 3, 21000 Novi Sad, Serbia

Received: 18 May 2021 **Revised: 03 June 2021** **Accepted: 07 June 2021**

Homoandrostane derivatives, as compounds with significant bioactivity, were studied in terms of their chromatographic behavior in reversed-phase ultra-high performance liquid chromatography (RP-UHPLC). In the present study, five androstane derivatives from the series of homoandrostanes were analyzed, including: 3β-hydroxy-17-oxa-17a-homoandrost-5-en-16-one, 3β,5α-dihydroxy-17-oxa-17a-homoandrostane-6,16-dione, 17-oxa-5β,6β-epoxy-17a-homoandrostane-3,16-dione, 5α-hydroxy-17-oxa-17a-homoandrostane-6,16-dione-3β-yl acetate and 3β-hydroxy-17-oxa-5α,6α-epoxy-D-homoandrostan-16-one. The compounds were analyzed by applying methanol-water mobile phases with different volume fractions of methanol, as a polar protic solvent, and $\log k_0$ parameters of each compound were determined. The outstanding correlations between in silico logP descriptors and $\log k_0$ parameters were obtained, as well as between in silico logD descriptors and $\log k_0$ parameters. The $\log k_0$ parameters are very well correlated with polar surface area (PSA) descriptor as well. The studied compounds and lipophilicity descriptors (including the chromatographic lipophilicity parameters – $\log k_0$) were clustered applying hierarchical cluster analysis (HCA) in the form of clustered heat map known as double dendrogram. Furthermore, the sum of ranking differences (SRD) method was used for the ranking of the lipophilicity measures of the analyzed homoandrostane derivatives so the most suitable lipophilicity measures of this series of compounds can be selected.

Keywords: Androstanes, chromatography, lipophilicity, sum of ranking differences, steroids.

INTRODUCTION

As one of the essential parameters of biologically active compounds, lipophilicity has a very important role in biological behavior of drug candidates (1). Lipophilicity has the influence on passive transport of compounds through biological membranes, as well as their binding to receptors and different proteins (2). Generally, lipophilicity can be defined as the affinity of a compound or a moiety towards lipophilic environment (2, 3). It is usually expressed in the form of partition coefficient (*P*) or in more often its logarithmic form (log*P*). The partition coefficient is known as intrinsic lipophilicity and refers to the equilibrium of a non-ionized compound between aqueous and organic phase (3). A pH-dependent lipophili-

* Corresponding author: Milica KARADŽIĆ BANJAC, University of Novi Sad, Faculty of Technology Novi Sad, Department of Applied and Engineering Chemistry, Bulevar cara Lazara 1, 21000 Novi Sad, Serbia, e-mail: mkaradza@uns.ac.rs

APTEFF, 52, 1-273 (2021)
DOI: https://doi.org/10.2298/APT2152147K
BY-NC-ND
UDC: 543.544:544.722.123:547.92
BIBLID: 1450-7188 (2021) 52, 147-158
Original scientific paper

city descriptor is distribution coefficient (D) or log$D$ which describes lipophilicity of ionizable solutes. It presents the contribution of all ionic forms existing at certain pH value (3):

$$D = f^{N} \cdot P^{N} + \Sigma\,(f^{I} \cdot P^{I}) \qquad [1]$$

where f^{N} and f^{I} are the molar fractions of neutral (N) and ionized (I) form of the compound.

The determination of lipophilicity of compounds is a complex task by the means of selection the most suitable approach. One of the most used methods in lipophilicity determination of various compounds is liquid chromatography. Thin-layer chromatography (TLC) and high performance liquid chromatography (HPLC) on reversed phases (RP) are one of the most used chromatographic techniques in lipophilicity estimation of biologically active compounds (4-8). The retention parameters obtained by using these chromatographic techniques, such as R_M or R_M^0 and log$k$ or logk_0, were proven to be good predictors of lipophilicity. This lipophilicity is known as anisotropic lipophilicity since it is determined by using chromatographic system as an anisotropic system (3).

Molecular polarity is a molecular property of a significant relevance in the prediction of molecular permeability (9). It is a consequence of the presence of the atoms with different electronegativity. Practically, the polar surface area (PSA) descriptor quantifies molecular polarity. It presents the surface area of a molecule that comes from nitrogen or oxygen atoms plus hydrogen atoms connected to nitrogen or oxygen atoms (9). Generally speaking, the PSA is the ability of a molecule to form hydrogen bonds due to the presence of oxygen or nitrogen atoms (9).

Generally, chromatographic methods have numerous advantages over classical shake-flask method in terms of lipophilicity determination (9). The consumption of chemicals is significantly low and the time of the analysis is much shorter than in the case of shake-flask method (10). In HPLC technique small amounts of analytes are required and wider range of log$P$ can be estimated. In ultra-high performance liquid chromatography (UHPLC) shorter columns are usually used with smaller particle size (less than 2 μm), so it provides a better resolution than traditional HPLC (11). Also, in UHPLC system much higher pressures can be achieved by using specialized pumps.

Homoandrostane derivatives, investigated in the present study, are the group of androstane derivatives which possess significant biological activity (12-18). The preliminary biological screening of oxygen-containing D-homo lactone androstane derivatives (12-18) showed that the further biological investigations are worthy to be done, so their characterization in terms of their physicochemical properties is desirable.

The main aim of the present study is to experimentally determine the lipophilicity of five androstane derivatives, including 3β-hydroxy-17-oxa-17a-homoandrost-5-en-16-one, 3β,5α-dihydroxy-17-oxa-17a-homoandrostane-6,16-dione, 17-oxa-5β,6β-epoxy-17a-homoandrostane-3,16-dione, 5α-hydroxy-17-oxa-17a-homoandrostane-6,16-dione-3β-yl acetate and 3β-hydroxy-17-oxa-5α,6α-epoxy-D-homoandrostan-16-one, applying RP-UHPLC technique. Chromatographic lipophilicity of the analyzed derivatives, expressed as logk_0 parameter obtained by extrapolation of the dependence between volume fraction of methanol in mobile phase (φ) and log$k$ parameter, is further correlated with *in silico* lipophilicity measures (log$P$ and log$D$), as well as with polar surface area (PSA). The determined experimental and *in silico* lipophilicity parameters are clustered by hierarchical cluster analysis

APTEFF, 52, 1-273 (2021)
DOI: https://doi.org/10.2298/APT2152147K
BY-NC-ND
UDC: 543.544:544.722.123:547.92
BIBLID: 1450-7188 (2021) 52, 147-158
Original scientific paper

(HCA) and ranked by sum of ranking differences (SRD) chemometric methods in order to select the most suitable lipophilicity descriptors of the analyzed series of homoandrostane derivatives.

MATERIAL AND METHODS

THE SERIES OF HOMOANDROSTANE DERIVATIVES

The set of analyzed homoandrostane derivatives included five compounds. Their IUPAC names are given in Table 1. The compounds were synthesized at Department of Chemistry, Biochemistry and Environmental Protection, Faculty of Sciences, University of Novi Sad (12-18).

Table 1. The IUPAC names of the studied homoandrostane derivatives

No.	the IUPAC name
1	3β-Hydroxy-17-oxa-17a-homoandrost-5-en-16-one
2	3β,5α-Dihydroxy-17-oxa-17a-homoandrostane-6,16-dione
3	17-Oxa-5β,6β-epoxy-17a-homoandrostane-3,16-dione
4	5α-Hydroxy-17-oxa-17a-homoandrostane-6,16-dione-3β-yl acetate
5	3β-Hydroxy-17-oxa-5α,6α-epoxy-D-homoandrostan-16-one

The 2D structures of the studied compounds are presented in Figure 1.

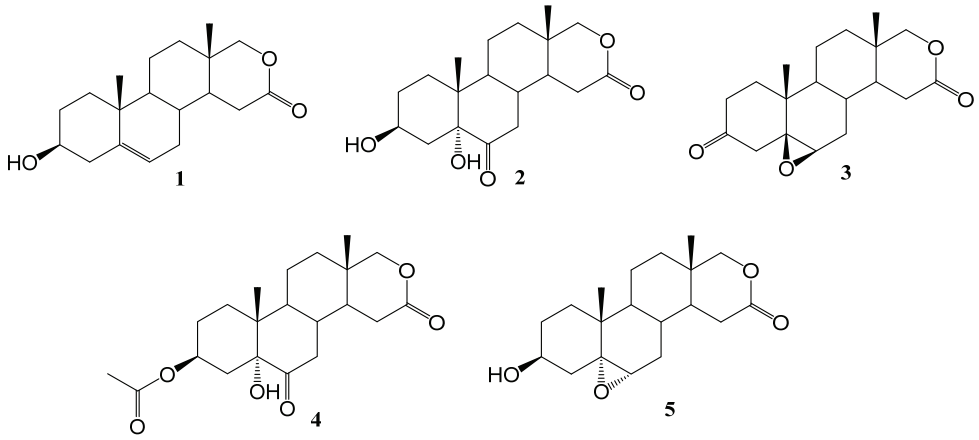

Figure 1. The molecular structures of the analyzed homoandrostane derivatives

The analyzed homoandrostane derivatives contain various substituents in their structures, including hydroxy, epoxy and acetoxy groups.

APTEFF, 52, 1-273 (2021) UDC: 543.544:544.722.123:547.92
DOI: https://doi.org/10.2298/APT2152147K BIBLID: 1450-7188 (2021) 52, 147-158
BY-NC-ND
Original scientific paper

RP-UHPLC ANALYSIS OF HOMOANDROSTANE DERIVATIVES

The RP-UHPLC analysis was carried out on UHPLC Agilent 1290 Infinity LC System with Diode Array Detector with the column ZORBAX Eclipse C18, 95Å, 2.1 × 50 mm, 1.8 μm (1200 bar pressure limit, LC Platform, Low Dispersion UHPLC). The analytes were dissolved in acetone in concentration of 1 mg/mL. The analytes solutions were submerged into ultrasonic bath and filtered through Captiva Econofilter with nylon membrane (25 mm diameter, 0.45 μm pore size, 1000/pk). The column temperature was maintained at 25 ºC and the pressure varied in the range 540–580 bar. The injection volume of the sample was 10 μL and the flow was set at 0.3 mL/min. The mobile phases used in the isocratic chromatographic analysis were a mixture of methanol and water. The volume fractions of methanol, as a polar protic solvent, varied from 0.80 to 0.40 v/v. The chromatographic peaks were recorded at λ_1 = 210 nm. The chemicals used in analysis are methanol (HPLC gradient grade, Baker), acetone (for HPLC analysis, Carlo Erba) and double distilled water.

Determination of chromatographic lipophilicity is achieved by variation of volume fraction of methanol in the mobile phase and measuring the retention of the compounds in each mobile phase. Afterwards, the capacity factors (k) are calculated based on retention time (t) and dead time (t_0) and presented in logarithmic form (log$k$):

$$\log k = \log((t - t_0)/t) \quad [2]$$

Dead time was defined as the first disturbance on the chromatogram.

HIERARCHICAL CLUSTER ANALYSIS (HCA) AND SUM OF RANKING DIFFERENCES (SRD)

The HCA was carried out by NCSS 2021 program (NCSS, LLC. Kaysville, Utah, USA, ncss.com/software/ncss). The results are presented in the form of clustered heat map (double dendrogram) which shows the grouping of both compounds and lipophilicity parameters. The clustering was done based on the Euclidean distances and Ward's algorithm.

The SRD analysis was performed in program formed in Excel. The method was introduced by Héberger (19, 20). It is a robust and non-parametric method which is applied in this study to rank the lipophilicity measures of homoandrostane derivatives. The SRD method is based on calculation of absolute differences of ranks between defined reference ranking known as benchmark or "golden standard" and each lipophilicity parameter (19). The row-average (consensus ranking) was used as the reference ranking. The results of SRD analysis were validated by comparison of ranks by random numbers (CRRN) (19). The detailed description of the SRD methodology can be find elsewhere (19-21).

The data used in HCA were scaled by Z-scores method. In the SRD analysis the data were scaled by *min-max* normalization approach in the range 0.01-0.99.

CALCULATION OF LIPOPHILICITY DESCRIPTORS

Lipophilicity parameters (log$P$) and distribution coefficients (log$D$) were calculated by using ChemBioDraw v. 12 program ($\log P_{ChDr}$, $\mathrm{Clog}P_{ChDr}$), MarvinSketch v. 14.9.15.0 program ($\log P_{Mrv}$, $\log Dvg_{Mrv}$, $\log Dklop_{Mrv}$, $\log Dphys_{Mrv}$) and Molinspiration program ($\mathrm{milog}P_{Mol}$). Based on log$P$ and log$D$ values, the average values were calculated (Av.logP, Av.logD).

APTEFF, 52, 1-273 (2021)
DOI: https://doi.org/10.2298/APT2152147K
BY-NC-ND
UDC: 543.544:544.722.123:547.92
BIBLID: 1450-7188 (2021) 52, 147-158
Original scientific paper

Polar surface area (PSA) was calculated applying MarvinSketch v. 14.9.15.0 program. Log*D* values were calculated considering tautomerization and resonance at pH = 7.4.

RESULTS AND DISCUSSION

CHROMATOGRAPHIC BEHAVIOR OF HOMOANDROSTANE DERIVATIVES IN THE RP-UHPLC SYSTEM

The retention behavior of the series of five homoandrostane derivatives was determined by using different mobile phases. After the determination of the retention time, the logk values of each compound in each applied mobile phase was determined. The values of determined log*k* parameters (isocratic log*k*) and volume fraction of methanol in mobile phase are presented in Table 1. Based on the relationships between logk and volume fraction of methanol in mobile phase the logk_0 parameters were determined for each compound. The experimental determination of logk_0 parameters applying pure water is not practically possible due to potential collapse of side-chains which are hydrophobic and due to quite long elution times (22). Those relationships are presented in Figure 2, while in Table 2 the polynomial equations of each relationship are provided. The obtained relationships are characterized by very high determination and correlation coefficients, as well as by the quite low standard deviation (SD).

Table 1. The retention parameters (log*k*) of the studied compounds determined by using various mobile phases with different volume fractions of methanol (φ)

Compound	φ (MeOH)								
	0.80	**0.75**	**0.70**	**0.65**	**0.60**	**0.55**	**0.50**	**0.45**	**0.40**
1	-	-0.023	0.154	0.341	0.550	1.030	-	-	-
2	-	-	-	-	-0.138	0.029	0.248	0.489	0.734
3	0.265	0.444	0.704	0.967	1.276	-	-	-	-
4	-	-	0.210	0.410	0.617	0.876	1.167	-	-
5	-	-	0.093	0.199	0.293	0.530	-	-	-

The logk_0 values are given in Table 3 together with *in silico* log*P* and log*D* values. The compound **2** is the compound with the lowest logk_0 value. By comparing the compound **2** with other compounds from the series, it can be seen that it has the highest number of highly polar functional groups so the interactions between the compound **2** and the mobile phase are considered to be the strongest. On the contrary, the compound with the highest logk_0 is the compound **1**. The compound **1** possess the highest lipophilicity compared to other molecules from the series and consequently the highest retention parameter. The compounds **3** and **5** have similar structural characteristics as well as similar logk_0 values. The compound **5** in position 3 has a polar hydroxy group, while the compound **3** has less polar oxo group. Therefore, the compound **5** is slightly more polar than the compound **3** and it has smaller logk_0 parameter. The differences between the chromatographic behavior between the compounds **2** and **4**, which differ only in a substituent in position 3, are reflec-

APTEFF, 52, 1-273 (2021)
DOI: https://doi.org/10.2298/APT2152147K
BY-NC-ND
UDC: 543.544:544.722.123:547.92
BIBLID: 1450-7188 (2021) 52, 147-158
Original scientific paper

ted in the fact that the compound **2** in the position 3 possesses a hydroxy group unlike the compound **4** which has an acetoxy group. Acetoxy group is less polar than the hydroxy group. Therefore, the compound **4**, as more lipophilic, has higher logk_0 parameter than the compound **2**.

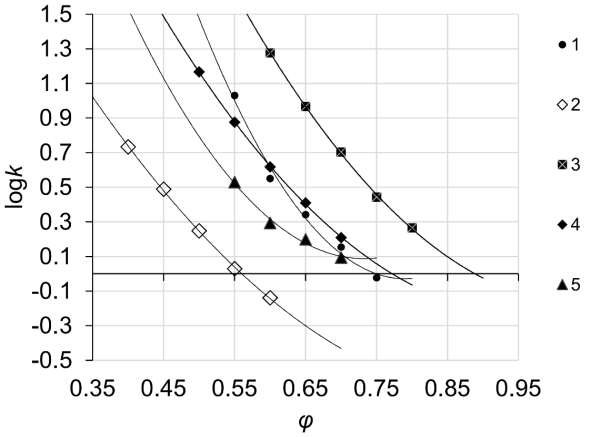

Figure 2. The polynomial relationships between log$k$ and volume fractions of methanol in mobile phase (φ)

Since the relationships between volume fraction of organic modifier and log$k$ values of the studied homoandrostane derivatives are described by polynomial functions, it was not possible to calculate alternative lipophilicity parameters such as the slope of the linear relationship (S) between log$k$ and φ and C_0 as the ratio between logk_0 and S. Therefore, in the present study the chromatographic retention of the analyzed homoandrostane derivatives is depicted only in the form of logk_0 parameter.

Table 2. The equations of the polynomial relationships between log$k$ and volume fractions of methanol in mobile phase

Compound	Equation	R^2	R	SD
1	$\log k = 17.942 \cdot \varphi^2 - 28.33 \cdot \varphi + 11.154$	0.9885	0.9942	0.023
2	$\log k = 5.0874 \cdot \varphi^2 - 9.4959 \cdot \varphi + 3.7228$	0.9995	0.9997	0.005
3	$\log k = 7.493 \cdot \varphi^2 - 15.98 \cdot \varphi + 7.9283$	0.9995	0.9997	0.007
4	$\log k = 6.617 \cdot \varphi^2 - 12.699 \cdot \varphi + 5.8603$	0.9998	0.9999	0.004
5	$\log k = 13.091 \cdot \varphi^2 - 19.17 \cdot \varphi + 7.1051$	0.9888	0.9944	0.011

Considering the log$P$ values presented in Table 3, the analyzed compounds can be described as lipophilic. The covered range of average lipophilicity (log$P$) is between 0.91 (compound **2**) and 2.84 (compound **1**). Average log$P$ and average log$D$ values of the studied compounds are slightly different, however highly correlated. Their log$D$ values are constant in wide pH range, as it was predicted by MarvinSketch program. The range of ave-

APTEFF, 52, 1-273 (2021)
DOI: https://doi.org/10.2298/APT2152147K
BY-NC-ND
UDC: 543.544:544.722.123:547.92
BIBLID: 1450-7188 (2021) 52, 147-158
Original scientific paper

rage log*D* values is between 1.22 (compound **2**) and 2.56 (compound **1**). Since the lipophilicity measures of the compounds are between 0 and 6, the isocratic elution used in the present study is justified (22).

Table 3. The determined logk_0 values and *in silico* log*P* and log*D* parameters and polar surface area (PSA) of the analyzed homoandrostane derivatives

Compound	logk_0	logP_{ChDr}	ClogP_{ChDr}	logP_{Mrv}	milogP_{Mol}	Av.logP	logDvg_{Mrv}	log$Dklop_{Mrv}$	log$Dphys_{Mrv}$	Av.logD	PSA_{Mrv} (Å^2)
1	11.154	2.88	2.52	2.56	3.36	2.84	2.47	2.32	2.88	2.56	46.53
2	3.7228	1.06	-0.29	1.22	1.50	0.91	1.21	1.25	1.19	1.22	83.83
3	7.9283	2.19	0.95	2.25	2.61	2.04	2.24	2.43	2.09	2.25	55.90
4	5.8603	1.29	0.66	1.66	2.20	1.42	1.64	1.76	1.57	1.66	89.90
5	7.1051	1.87	0.81	1.82	2.79	1.83	1.53	1.92	1.99	1.81	59.06

RELATIONSHIP BETWEEN LIPOPHILICITY MEASURES AND CHROMATOGRAPHIC PARAMETERS OF HOMOANDROSTANE DERIVATIVES

The relationships between logk_0 and average log*P*, average log*D* and PSA are presented in Figures 3–5. Taking into account very high determination coefficients of the relationships between logk_0 and log*P* (R^2 = 0.9977), as well as between logk_0 and log*D* (R^2 = 0.9454), it can be concluded that logk_0 parameter can be considered to be an outstanding lipophilicity measure of the studied series of homoandrostane derivatives.

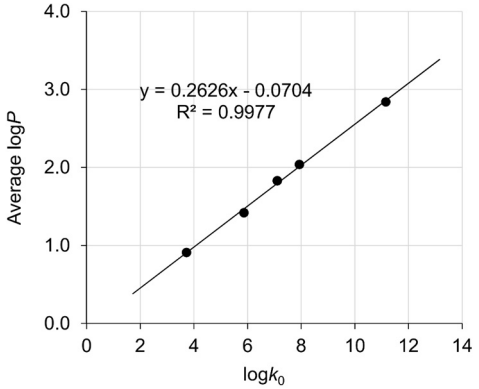

Figure 3. The relationship between logk_0 parameters and average log*P* values of the analyzed compounds

The relationship between PSA and logk_0 is described by significant determination coefficient (R^2 = 0.7417), as it is shown in Figure 5. PSA is the parameter which represents the part of the molecular surface which has polar characteristics. It is one of the most signifi-

APTEFF, 52, 1-273 (2021)
DOI: https://doi.org/10.2298/APT2152147K
BY-NC-ND
UDC: 543.544:544.722.123:547.92
BIBLID: 1450-7188 (2021) 52, 147-158
Original scientific paper

cant features in characterization of transport properties of biologically active compounds and provides significant correlations with intestinal absorption (23).

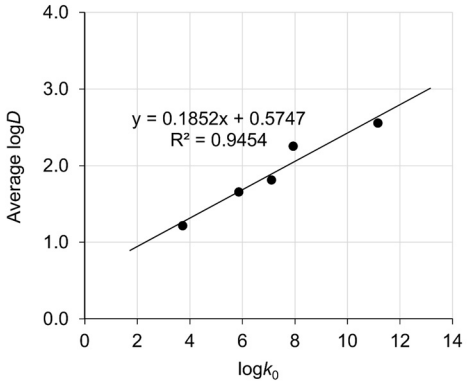

Figure 4. The relationship between logk_0 parameters and average log$D$ values of the analyzed compounds

High relationships between PSA and logk_0 imply that logk_0 parameter can possibly be used as a predictor of intestinal absorption however for definite conclusion further investigations must be carried out. The compounds with PSA < 60 Å^2 are more than 90% absorbed, while the compounds which have PSA > 140 Å^2 are absorbed less than 10% (23). Among the analyzed homoandrostane derivatives, the compounds **1**, **3** and **5** have PSA < 60 Å^2 and none of them crosses the limit of 140 Å^2. The compounds **2** and **4** have PSA parameter between 80 and 90 Å^2 so their intestinal absorption will be less than 90%. Therefore, the majority of the analyzed compounds will probably be easily absorbed in intestinal tract.

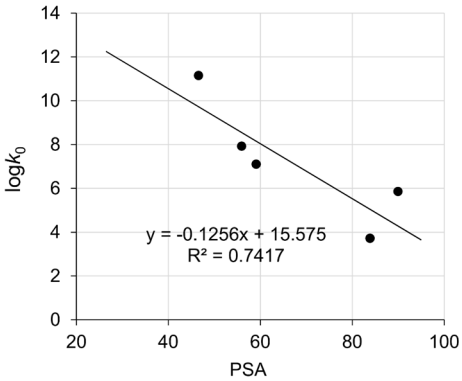

Figure 5. The relationship between polar surface area (PSA) and logk_0 parameters of the analyzed compounds

The significant relationship between PSA descriptor and average log$P$ (R^2 = 0.7812), as shown in Figure 6, is another confirmation of intercorrelation between lipophilicity, polarity and retention behavior of compounds in reversed-phase liquid chromatography.

APTEFF, 52, 1-273 (2021)
DOI: https://doi.org/10.2298/APT2152147K
BY-NC-ND
UDC: 543.544:544.722.123:547.92
BIBLID: 1450-7188 (2021) 52, 147-158
Original scientific paper

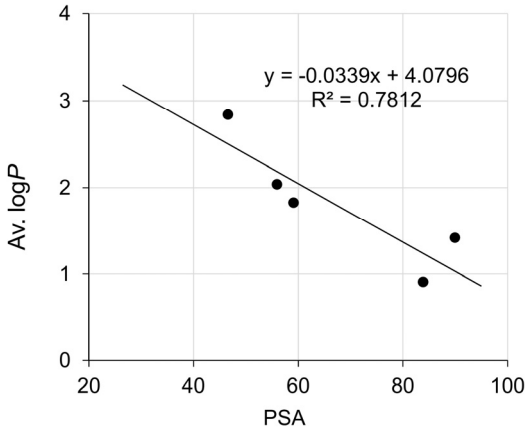

Figure 6. The relationship between polar surface area (PSA) and average log*P* values of the analyzed compounds

CLASSIFICATION AND RANKING OF EXPERIMENTAL AND *IN SILICO* LIPOPHILICITY PARAMETERS

In order to gain an overview about similarities and dissimilarities among the studied homoandrostane derivatives in terms of their lipophilicity measures, the hierarchical cluster analysis and sum of ranking differences approach were applied.

The results of the HCA are presented in Figure 7 in the form of double dendrogram which reveals the clustering of both the compounds and the variables. The HCA confirmed statistically significant similarities between the compounds **2** and **4** since they are put together in one main cluster. The other main cluster contains the compounds **1**, **3** and **5** and among them the compounds **3** and **5** are the most similar. The obtained results of HCA are in agreement with the conclusions drawn earlier. The clustering of the scaled lipophilicity parameters indicated significant similarity between logk_0 parameter and average log*P* descriptor since they are placed in the same subcluster. Also, the descriptor logDphys$_{Mrc}$ belongs to the same cluster as logk_0 and average log*P*.

The results of SRD analysis are presented in Figure 8. The SRD graph indicates that there are two main groups of lipophilicity measures of homoandrostane derivatives. The closest to the reference (consensus) ranking is the group which contains the following descriptors: logk_0, logP$_{ChDr}$, ClogP$_{ChDr}$, logP$_{Mrv}$, Av.logP, logDphys$_{Mrv}$ and Av.logD. This group has the same ranking as the reference ranking (SRD = 0). The second group, placed further from the reference ranking contains milogP$_{Mol}$, logDvg$_{Mrv}$ and logDklop$_{Mrv}$ descriptors. The second group is placed closer to the random number distribution than the first one; thus, the lipophilicity measures placed in the first group can be considered to be more suitable than the descriptors in the second group. It must be emphasized that the chromatographically determined lipophilicity parameter logk_0 has the same rank (SRD = 0) as the majority of lipophilicity parameters placed in the first group.

APTEFF, 52, 1-273 (2021)
DOI: https://doi.org/10.2298/APT2152147K
BY-NC-ND
UDC: 543.544:544.722.123:547.92
BIBLID: 1450-7188 (2021) 52, 147-158
Original scientific paper

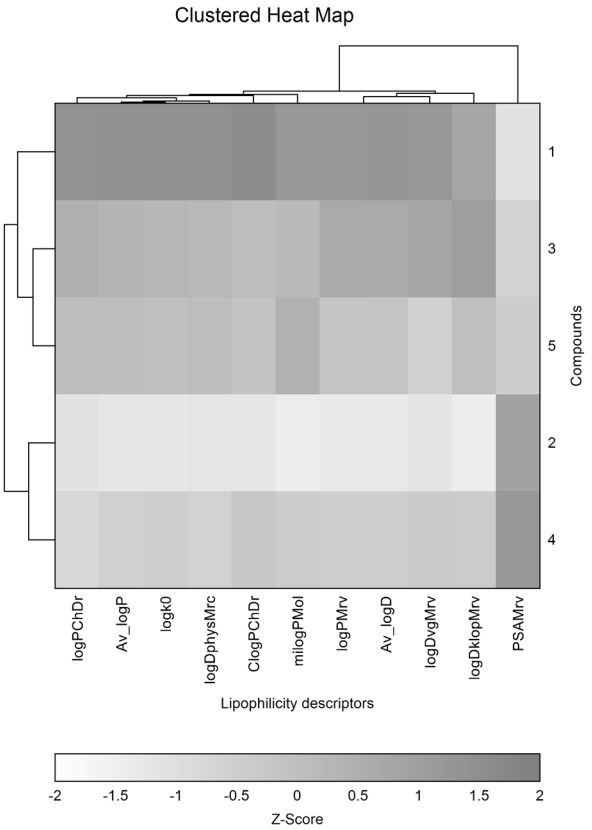

Figure 7. The double dendrogram of the hierarchical cluster analysis of the lipophilicity measures of the studied homoandrostane derivatives

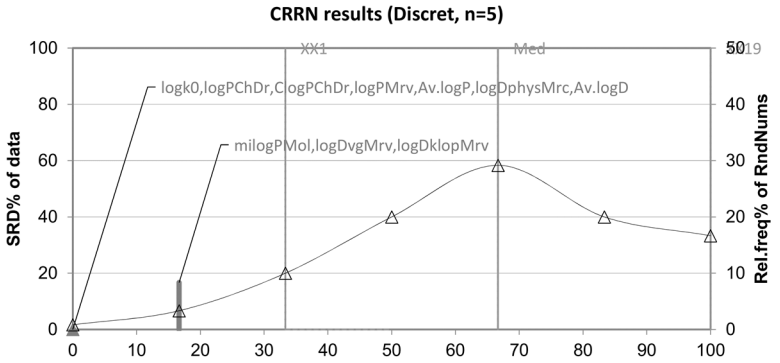

Figure 8. The ranking of lipophilicity measures of homoandrostane derivatives obtained by CRRN-SRD approach. The statistical characteristics of the theoretical distribution function are the following: first icosaile (5%), XX1 = 4; first quartile, Q1 = 6; median, Med = 8; last quartile, Q3 = 10; last icosaile (95%), XX19 = 12.

APTEFF, 52, 1-273 (2021) UDC: 543.544:544.722.123:547.92
DOI: https://doi.org/10.2298/APT2152147K BIBLID: 1450-7188 (2021) 52, 147-158
BY-NC-ND
Original scientific paper

CONCLUSION

In the present study the chromatographic lipophilicity of five homoandrostane derivatives was determined by using RP-UHPLC system with methanol/water mobile phase and correlated with their *in silico* lipophilicity measures (log*P*, log*D* and PSA). As a chromatographic lipophilicity measure of the analyzed compounds the logk_0 parameter was proposed on the basis of an outstanding correlation of this parameter with average log*P* values. Based on the calculated polar surface area descriptor, as a good predictor of intestinal absorption, and its correlation with logk_0 values it was assumed that the logk_0 parameter may possibly be the predictor of intestinal absorption of homoandrostane derivatives, however further studies are required to confirm this assumption. The HCA indicated certain similarities among the compounds based on their lipophilicity measures. The CRRN-SRD analysis indicated that according to the proximity to the reference ranking, the logk_0 parameter can be considered suitable lipophilicity descriptor of the analyzed homoandrostane derivatives.

Acknowledgements

The present research is financed in the framework of the projects of Ministry of Education, Science and Technological Development of the Republic of Serbia (Project No. 451-03-9/2021-14/200134 and 451-03-9/2021-14/200125).

REFERENCES

1. Ciura, K.; Fedorowicz, J.; Andrić, F.; Žuvela, P.; Ewa Greber, K.; Baranowski, P.; Kawczak, P.; Nowakowska, J.; Baczek, T.; Saczewski, J. Lipophilicity determination of antifungal isoxazolo[3,4-b]pyridin-3(1H)-ones and their N1-substituted derivatives with chromatographic and computational methods. *Molecules,* **2019**, *24*, 1-22.
2. Andrić, F.; Bajusz, D.; Racz, A.; Šegan, S.; Heberger, K. Multivariate assessment of lipophilicity scales-computational and reversed phase thin-layer chromatographic indices. *J. Pharm. Biomed. Anal.,* **2016**, *127*, 81-93.
3. Caron, G.; Ermondi, G. Lipophilicity: Chemical nature and biological relevance. In *Molecular drug properties, Measurement and prediction;* Mannhold, R., Ed.; Wiley-VCH: Weinheim, Germany, **2008**; pp 315-329.
4. Ciura, K.; Fedorowicz, J.; Andrić, F.; Greber, K.E.; Gurgielewicz, A.; Sawicki, W.; Sączewski, J. Lipophilicity Determination of Quaternary (Fluoro)Quinolones by Chromatographic and Theoretical Approaches. *Int. J. Mol. Sci.* **2019**, *20*, 5288.
5. Sobanska, A. W. Application of planar chromatographic descriptors to the prediction of physicochemical properties and biological activity of compounds. *J. Liq. Chromatogr. Relat. Technol*. **2018**, *41*, 255-271.
6. Kovačević, S.Z.; Podunavac-Kuzmanović, S.O.; Jevrić, L.R.; Jovanov, P.T.; Djurendić, E.A.; Ajduković, J.J. Comprehensive QSRR modeling as a starting point in characterization and further development of anticancer drugs based on 17α-picolyl and 17(E)-picolinylidene androstane structures. *Eur. J. Pharm. Sci*. **2016**, *93*, 1-10.
7. Ranušová, P.; Nemeček, P.; Lehotay, J.; Čižmárik, J. QSRR modelling aimed on the HPLC retention prediction of dimethylamino- and pyrrolidino-substitued esters of alkoxyphenylcarbamic acid. *Chem. Pap*. **2021**, *75*, 2525-2535.
8. Baranowska, I.; Zydroń, M. Quantitative Structure-Retention Relationships (QSRR) of Biogenic Amine Neurotransmitters and their Metabolites on RP-18 Plates in Thin-Layer Chromatography. *JPC-J Planar Chromat* **2003**, *16*, 102-106.

BY-NC-ND

9. Caron, G.; Ermondi G. Molecular descriptors for polarity: the need for going beyond polar surface area. *Future Med. Chem*. **2016**, *8*, 2013-2016.
10. Lončar, E. Molekulska struktura i retencija u tečnoj hromatografiji – monografija. Tehnološki fakultet Novi Sad, Univerzitet u Novom Sadu, **2010**.
11. Nováková, L.; Svoboda, P.; Pavlík, J. Ultra-high performance liquid chromatography. In *Liquid Chromatography (Second Edition)*; Fanali, S.; Haddad, P. R.; Poole, C. F.; Riekkola, M. L., Eds.; Elsevier, **2017**; pp 719-769.
12. Savić, M. P.; Kuzminac, I. Z.; Škorić, D. Đ.; Jakimov, D. S.; Rárová, L.; Sakač, M. N.; Djurendić, E. A. New oxygen-containing androstane derivatives: Synthesis and biological potential. *J. Chem. Sci.*, **2020**, *132*, 98.
13. Kuzminac, I. Z.; Jakimov, D. S.; Bekić, S. S.; Ćelić, A. S.; Marinović, M. A.; Savić, M. P.; Raičević, V. N.; Kojić, V. V.; Sakač, M. N. Synthesis and anticancer potential of novel 5,6-oxygenated and/or halogenated steroidal D-homo lactones. *Bioorg. Med. Chem.* **2021**, *30*, 115935.
14. Kovačević, S. Z.; Podunavac-Kuzmanović, S. O.; Jevrić, L. R.; Vukić, V. R.; Savić, M. P.; Djurendić, E. A. Preselection of A- and B- modified D-homo lactone and D-seco androstane derivatives as potent compounds with antiproliferative activity against breast and prostate cancer cells – QSAR approach and molecular docking analysis. *Eur. J. Pharm. Sci.* **2016**, *93*, 107-113.
15. Penov-Gaši, K.; Cvjetićanin, S.; Stojanović, S.; Kuhajda, K.; Stupavský, Lj.; Čanadi, J.; Molnár-Gábor, D.; Mijačević, Lj.; Sakač, M. Chemical transformations of 3β,17β-dihydroxy-16-oximino-5-androstene. *Acta Period. Technol.* **2000**, *31* (B), 675-683.
16. Djurendić, E. A.; Zaviš, M. P.; Sakač, M. N.; Čanadi, J. J.; Kojić, V. V.; Bogdanović, G. M.; Penov Gaši, K. M. Synthesis and antitumor activity of new D-seco and D-homo androstane derivatives. *Steroids*, **2009**, *74*, 983-988.
17. Đurendić, E.; Sakač, M.; Zaviš, M.; Gaković, A.; Čanadi, J.; Andrić, S.; Klisurić, O.; Kojić, V.; Bogdanović, G.; Penov Gaši, K. Synthesis and biological evaluation of some new A,B-ring modified steroidal D-lactones, *Steroids*, **2008**, *73*, 681-688.
18. Nikolić, A. R.; Kuzminac, I. Z.; Jovanović-Šanta, S. S.; Jakimov, D. S.; Aleksić, L. D.; Sakač, M. N. Anticancer activity of novel steroidal 6-substituted 4-en-3-one D-seco dinitriles. *Steroids*, **2018**, *135*, 101-107.
19. Héberger, K. Sum of ranking differences compares methods or models fairly. *TRAC-Trends Anal. Chem.* **2010**, *29*, 101-109.
20. Héberger, K.; Kollár-Hunek, K. Sum of ranking differences for method discrimination and its validation: comparison of ranks with random numbers. *J. Chemometr*. **2011**, *25*, 151-158.
21. Kollár-Hunek, K.; Héberger, K. Method and model comparison by sum of ranking differences in cases of repeated observations (ties). *Chemom. Intell. Lab. Syst*. **2013**, *127*, 139-146.
22. Martel, S.; Guillarme, D.; Henchoz, Y.; Galland, A.; Veuthey, J. L.; Rudaz, S.; Carrupt, P. A. Chromatographic approaches for measuring Log P. In *Molecular drug properties, Measurement and prediction;* Mannhold, R., Ed.; Wiley-VCH: Weinheim, Germany, **2008**; pp 331-355.
23. Ertl, P. Polar Surface Area. In *Molecular drug properties, Measurement and prediction;*Mannhold, R., Ed.; Wiley-VCH: Weinheim, Germany, **2008**; pp 111-126.

APTEFF, 52, 1-273 (2021) UDC: 356.22:355.231.1]:613.2
DOI: https://doi.org/10.2298/APT2152159S BIBLID: 1450-7188 (2021) 52, 159-171
BY-NC-ND
Original scientific paper

FOOD SAFETY KNOWLEDGE AMONG CADETS OF MILITARY ACADEMY IN REPUBLIC OF SERBIA

Nada SMIGIC[1], Sladjana JOVANOVIC[2], Ilija DJEKIC[1], Srboljub NIKOLIC[2]*

[1] Department of Food Safety and Quality Management, University of Belgrade - Faculty of Agriculture, Nemanjina 6, Belgrade, Republic of Serbia
[2] Department of Defence Logistics, University of Defence – Military Academy, Pavla Jurisica Sturma Street 33, Belgrade, Republic of Serbia

Received: 06 June 2021 **Revised: 31 July 2021** **Accepted: 06 September 2021**

The purpose of this study was to evaluate the level of food safety knowledge among cadets of Military Academy in the Republic of Serbia. For that purpose, a structured, self-administrative questionnaire was designed and used to assess the level of food handling practices and food safety knowledge. In total, 120 cadets were involved in the study. For each participating cadet, the food handling practice score (FHPS) and food safety knowledge score (FSKS) was calculated by dividing the sum of correct answers by the total number of correct responses. Additionally, knowledge gaps were identified for each question.

Our results indicated that on the average FHPS among Serbian cadets was 44.5%, while FSKS was 50.5%. Female cadets showed better scores compared to males, although this was not statistically significant. Better FHPS scores were determined among cadets living with parents (48.7%), compared to cadets living with roommates (43.6%, $p \leq 0.05$), while an opposite was determined for FSKS. In total, 95.8% of cadets apply good practice of hand hygiene before preparing food, 90.8% of them knew that is not safe to consume food when the shelf-life is expired, and 89.2% knew that the opened sterilized milk should not be stored outside the refrigerator. Also, 91.7% of cadets knew that content of blown can is not safe for the consumption. Almost 64.2% of all cadets could successfully make association between meat and Trichinella, while merely 27.5% of them knew that Escherichia coli O157 is the most important pathogen for raw minced meat, and only 13.3% of cadets knew that Listeria monocytogenes is associated with ready-to-eat meat products. Finally, only 10% of cadets knew that Campylobacter is food-borne pathogen mostly associated with raw and undercooked chicken meat. Also, our cadets were not aware that color, smell or appearance of food would not give any indication of food contamination, as only 6.7% of cadets knew this. Results obtained in this study pointed out some food safety areas which need further improvement via educational program, but also via media and internet courses, material or short clips.

Keywords: Cadets, Military Academy, food handling practices, food safety knowledge.

INTRODUCTION

Food-borne diseases include a number of illnesses ranging from mild gastrointestinal issues to life threatening illnesses such as botulism, hemolytic–uremic syndrome, Guillain-Barre syndrome, etc. (1). Despite numerous projects and studies performed in the field of food safety and various preventive and control measures defined for the food industry, the number of reported food-borne cases remains at an unacceptable high level (2–4). World

* Corresponding author: Nada Smigic, Department of Food Safety and Quality Management, University of Belgrade, Faculty of Agriculture, Nemanjina 6, 11080 Belgrade, Republic of Serbia,
e-mail: nadasmigic@agrif.bg.ac.rs

BY-NC-ND

Health Organization (WHO) has estimated the burden of food-borne diseases, with more than 420 000 millions of people fall ill, and 230 000 dies every year from diarrheal diseases, caused by consumption of contaminated food and/or water (5). Although the majority of cases occurs in developing countries, a great number of people in developed countries still experience some food-borne diseases (6, 7). In the European Union (EU), more than 43 000 cases of food-borne illnesses, with 4 541 hospitalizations and 33 deaths occurred only in 2017. Among these cases, almost 34.2% occurred at home, 30% cases occurred at restaurants, pubs, street vendors and take away places and 16% of them took place in different institutions, such as canteen or catering, school, hospital, residential institutions (nursing home or prison or boarding school) where food was prepared and/or served by catering services (6).

Institutional food services include entities that serve food to people who are members of particular institution such as hospital, schools, nursing homes, prisons, military or industry (8). Mostly, army and military establishments have their own food procurement systems which are dedicated to the prevention of both unintentional and intentional contamination of food. Nevertheless, foods consumed at military institutions have been also identified as an important source of food-borne outbreaks (9), including outbreaks caused by viruses, such as Norovirus or Hepatitis A (10–13), bacteria, such as *Salmonella* spp., *Staphylococcus aureus* (14–17), but also toxins such as histamine (18) or scromboine (19) associated with eating yellow fin tuna (*Thunnus albacares*). Despite the fact that military staff usually includes health people in good physical condition, they still constitute a high risk group for food poisoning due to the community kitchen practice and common meals (20–22). Great number of preventive and control measures have been identified for military food services, including the application of adequate sanitary procedures during food processing and preparation, personal hygiene practices, prevention of cross contamination, adequate time-temperature control, etc. (23). Along with these pre-requisite programs, the food safety management system should be also implemented to ensure that safe food is being manufactured, distributed, and consumed in military food services.

The great number of food-borne outbreaks occurs due to bad food handling practices (24, 25), and it is assumed that this is also the case in military food services. The knowledge and practices of food handlers are essential, either when food handlers are professionals working in the food industry or institutional food services, such as military establishments, or when they are casually preparing food at home environments (26, 27). Food handlers may contaminate food due to hand contact with food (by bear hands or gloves), improper hand hygiene, inadequate cleaning of processing or preparation equipment, inadequate food preparation, etc. (6, 28). Many authors have investigated the level of food safety knowledge and self-reporting food handling practices among students of different background (29–37). Nevertheless, only one study has investigated these issues among military students (23) and to our best knowledge no study has been performed among Serbian cadets. Therefore, it was the aim of this study to evaluate food safety knowledge and handling practices among cadets of the final year of Military Academy, in the Republic of Serbia.

APTEFF, 52, 1-273 (2021) UDC: 356.22:355.231.1]:613.2
DOI: https://doi.org/10.2298/APT2152159S BIBLID: 1450-7188 (2021) 52, 159-171
BY-NC-ND
Original scientific paper

MATERIAL AND METHODS

SELECTION OF STUDENTS

This study involved 120 cadets from the Military Academy in the Republic of Serbia. Cadets that participated in this study were inscribed in different modules in the Military Academy and they have participated on voluntary and anonymous basis. Cadets were asked to fill the questionnaire during class, and it took approximately 15 min to finalize it.

QUESTIONNAIRE

For the purpose of this study, a structured questionnaire was designed based on the previously published articled (30, 31, 34, 36, 37). The questionnaire consisted of different types of questions such as true/false, yes/no and multiple choice answers. Additionally, cadets had the possibility to circle "I don't know" for each question, to minimize the possibility to select the correct answer randomly.

The questionnaire consisted of three separate parts; first one consisted of questions related to demographic characteristics of cadets, such as gender, age, residential area, and involvement in cooking, information on food safety issues, estimated food safety knowledge and previous experience with food borne illnesses. Second part of the questionnaire was related to food handling practices and it included 13 questions, covering those related to cross-contamination (3), temperature regime (2), food preparation and manipulation (8). Finally the third section focused on food safety knowledge and included 28 different questions, comprising of questions related to cross-contamination (7), temperature regime (8), food handling (9), and food poisoning (4).

DATA ANALYSIS

For each cadet, the food handling practice score (FHPS) and food safety knowledge score (FSKS) was calculated as a percentage of correct answers for a given section. Each multiple-choice question had only one correct answer. Calculated scores were analyzed using an independent sample t-test (for two groups, such as gender, age, previous food poisonings) or analysis of variance (ANOVA) with post-hoc Tukey test (for more than two groups, such as type of faculty, living, eating, information of food safety issues, estimated food safety knowledge, etc. (SPSS Statistics 17.0)). Values with a $p<0.05$ were considered statistically significant.

RESULTS AND DISCUSSION

SAMPLE CHARACTERISTICS

For the purpose of this study, 120 cadets studying at the Military Academy have been interviewed. In total, 19.2% females and 80.8% males participated (Table 1). The majority of cadets declared that they were living with roommates 97 (80.8%), while 23 (19.2%) of them were living with their parents. Again, majority of them were eating in the canteen 107 (89.2%), only 6 (5.0%) of them were preparing food by themselves, while 7 (5.8%) cadets

APTEFF, 52, 1-273 (2021) UDC: 356.22:355.231.1]:613.2
DOI: https://doi.org/10.2298/APT2152159S BIBLID: 1450-7188 (2021) 52, 159-171
BY-NC-ND
Original scientific paper

were eating with their parents. Only 54 (15%) cadets stated that they experienced a personal food poisoning incident in the past. The major source of food safety information for 19 cadets (40.8%) was Internet, for 25 cadets (20.8%) it was family/friends, while only 19 cadets (15.8%) declared that the major source of food safety information was education and faculty. It is of note that 11 cadets (9.2%) indicated that they did not inform themselves on food safety at all.

Table 1. Demographic characteristics of cadets participating in this study and their food hygiene practices (FHPS) and food safety knowledge (FSKS) (n=120)

		N (%)	FHPS (%)[x]	Within[y] p-value	FSKS (%)[x]	Within[y] p-value
Gender	Female	23 (19.2%)	47.83	0.13	54.19	0.06
	Male	97 (80.8%)	43.81		49.63	
Living	With roommate	97 (80.8%)	43.59	0.05*	50.99	0.18
	With parents	23 (19.2%)	48.76		48.45	
Eating	Preparing food alone	6 (5.0%)	41.67	0.68	48.81	0.35
	In the canteen	107 (89.2%)	44.46		50.71	
	At home with parents	7 (5.8%)	48.98		57.14	
Information on food safety issues	Via friends/family	25 (20.8%)	45.14	0.32	$46.71^{a,b}$	0.005*
	Via education/faculty	19 (15.8%)	47.74		$55.82^{b,c}$	
	Via public media	16 (13.3%)	46.87		$56.02^{b,c}$	
	Via internet	49 (40.8%)	44.31		$50.65^{a,b}$	
	I do not inform myself	11 (9.2%)	35.7		41.23^{a}	
Estimated food safety knowledge	Excellent	25 (20.8%)	39.85	0.423	$46.05^{a,b}$	0.016*
	Very good	47 (39.2%)	42.28		$53.57^{a,b}$	
	Good	22 (18.3%)	46.80		$49.84^{a,b}$	
	Satisfactory	7 (5.8%)	47.07		55.52^{b}	
	Sufficient	19 (15.8%)	42.85		40.30^{a}	
Previous food safety poisoning	Yes	12 (10.0%)	42.85	0.343	55.35	0.08
	No	108 (90.0%)	44.77		49.96	

*statistical significance $p < 0.05$
[x] knowledge score, relative percentage which is based on valid values
[y] differences within the characteristics of cadets
Items denoted with the same small letter are not significantly different within the group

FOOD HYGIENE PRACTICES AND FOOD SAFETY KNOWLEDGE SCORES

The average value for food handling practice score (FHPS) was 44.5% and for food safety knowledge score (FSKS), was 50.5% (Table 1). As expected, cadets who were informed about food safety issues via classical education and courses obtained better FHPS scores (47.74%) compared to other cadets that were getting information thought public media (46.87%), family/friends (45.14%), and internet (44.31%), although this was not statistically significant ($p>0.05$, Table 1). Results on FSKS scores showed higher values for cadets who were informed via classical education (55.82%) and via public media (56.02%), compared to their colleges that were informed via internet (50.65%) and friends and family (46.71%, $p<0.05$, Table 1) Surprisingly, cadets who experienced some previous food poiso-

APTEFF, 52, 1-273 (2021) UDC: 356.22:355.231.1]:613.2
DOI: https://doi.org/10.2298/APT2152159S BIBLID: 1450-7188 (2021) 52, 159-171
BY-NC-ND
Original scientific paper

ning obtained lower FHPS than their colleagues without that experience, although it may be expected that they are more careful and interested in food safety.

It is of note that 11 participating cadets (9.2%) indicated that they do not inform themselves on food safety issues at all, and these cadets presented the lowest FHPS and FSKS scores (35.7% and 41.2%, respectively). Most of them are aware of this, as they estimated their overall food safety knowledge as poor or only sufficient (data not shown). This is very worrying, as these young people might be still involved in food preparations in their private lives or professional activities. Cadets studying at the module Defence Logistics, might be also responsible for different operations related to food services, logistics, and organization, both in the canteen level or at the terrain exercises. They might be involved in creating diet plans based on the scientific, medical, nutritional and culinary bases, for all military staff, taking into account the diversity of tasks they perform. As persons in charge of nutrition, they are responsible for the application of all sanitary and hygienic measures during the reception of food, storage, preparation and distribution of food. In addition, they hold trainings for people who are preparing and distributing food.

KNOWLEDGE GAPS

To identify the major gaps in cadets' practices and knowledge, percentage of correct answer for each question was calculated, and obtained results for food handling practices and food safety knowledge were presented in Table 2 and Table 3, respectively.

Table 2. Frequencies of correct answers to food hygiene practices for cadets participating in this study (n=120).

Question	% correct answers
Using the same cutting board for raw and ready-to-eat food.	60.8
Using knife for vegetables, after it was used for raw meat.	63.3
Storage of raw and ready-to-eat food in cooling units.	22.5
Cut on the hand and food preparation.	14.2
Habit of checking temperature in the fridge.	47.5
Keeping cooked meal at room temperature.	53.3
Checking when the chicken is cooked.	5.8
Duration of the reheating bolognaise spaghetti, prepared the day before.	19.2
Habit of eating/preparing cakes with raw egg white.	37.5
Habit of washing cabbage used for salad preparation.	84.2
Defrosting food.	6.7
Hand washing practice.	95.8
Duration of hand washing.	47.5
Jewelry and food preparation.	65.8

Majority of cadets involved in this study knew how to correctly handle cutting board or knife, to avoid cross contamination (Table 2). Similarly, 61.6% of students from Jordan

BY-NC-ND

correctly handle cutting board (31), and 74.3% of Lebanese students correctly handle cutting knife, when used for fresh produce and raw meat (36). The good practice of thawing food includes leaving frozen foods overnight in the refrigerator, and only 6.7% of all Serbian cadets perform this in everyday life, which is lower than reported in Lebanon, being 28.1% (36). Serbian cadets usually defrost food by keeping it at room temperature (Table 2), which is the least safe way of doing this. In line with this, only 25.8% of cadets knew this fact (Table 3).

Cold storage of food should be organized in a way to prevent cross contamination between ready-to-eat and raw foods, to keep fridge hygiene and to assure that fridge is operating at correct temperature (38, 39). Almost 70% of participating cadets knew that ready-to-eat and raw food should be kept separately in the fridge, to avoid possible cross-contamination (Table 3). Nevertheless, questions on food handling practices showed that only 22.5 % of cadets participating in this study would place potato salad (ready-to-eat food) above the raw meat in the fridge (Table 2). In addition, half of all participants (50.0 %) indicated that they would leave prepared food, where there is available place in the fridge, showing insufficient awareness for the proper food arrangements. These results suggest that the knowledge itself is not a sufficient guarantee for food safety, and it should be complemented with adequate food handling practices, which are often driven by other determinants (40–42).

What seems to be important is the fact that 65 % of participating cadets knew what is the required temperature for the cold storage of food, which is greater than 56 % reported for consumers in Belgrade (43). Additionally, 47.5 % of all cadets had a habit of checking the temperature in the refrigerator (Table 2), while Janjic et al. (2016) reported that only 25% of all Belgrade consumers knew, or regularly measured the temperature of their refrigerators. The great number of domestic refrigerators operate at approx. 9-10 °C (39, 43), which is capable of supporting the growth of some food-borne pathogens including *Staphylococcus aureus, Bacillus cereus, Escherichia coli* O157, *Salmonella* spp. Our results indicated that only 47.5 % of cadets knew that some microorganisms might slowly grow in the fridge, while 18.3 % of them thought that microorganisms could not initiate growth under refrigerator conditions. Even correctly adjusted refrigerator temperature of 4 °C, might support the growth of pathogens such as *Listeria monocytogenes* and *Yersinia enterocolitica,* in foods stored for the extended period of time (38). Almost 60 % of our participants knew that most food-borne pathogens would optimally grow at room temperature. Still, our cadets were not aware that color, smell or appearance of food would not give any indication of food contamination, as only 6.7% of cadets knew this (Table 3). Similar was reported elsewhere (44–47). When foods have bad smell, taste or appearance, it is mostly contaminated with spoilage microorganisms, while the presence of food-borne pathogens would leave no obvious sign of contamination. Therefore, the knowledge of the temperature profile, cross-contamination, growth characteristics of important food-borne pathogens and good handling habits are of ultimate importance for managing food safety risks.

According to data obtained through the official Serbian reporting system, the most frequently identified causative agent of food-borne outbreaks in Serbia has been *Salmonella* spp. (48). In line with this official report, this pathogen is the most often seen in media, as usually great number of mostly vulnerable people, such as kids in the kindergarten and elderly in orderly homes, is involved in *Salmonella* outbreak. However, it seems that this food safety risk is not completely acknowledged by Serbian cadets, as almost 62.5% of them said that they consume cakes prepared with raw egg white.

APTEFF, 52, 1-273 (2021) UDC: 356.22:355.231.1]:613.2
DOI: https://doi.org/10.2298/APT2152159S BIBLID: 1450-7188 (2021) 52, 159-171
BY-NC-ND
Original scientific paper

Table 3. Frequencies of correct food safety answers for all cadets participating in this study (n=120)

Question	% correct answers
Optimal temperatures for bacterial multiplication.	60.8
Identification of food contaminated with pathogens.	6.7
Identification of most common cause of food-borne illness.	1.7
Food often associated with *Listeria monocytogenes.*	13.3
Food often associated with *Campylobacter spp.*	10.0
Food often associated with *Trichinella*	64.2
Consequences of eating meat contaminated with *Escherichia coli* O157	27.5
Common symptoms of food-borne diseases.	52.5
Association between abortion and mental disorders in newborn and food-borne disease	24.2
The least risky group of people for the food poisoning	51.7
Identification of diseases that can be transmitted by food.	34.2
Required temperature inside refrigerator.	65.0
Required temperature inside freezer	54.2
Bacterial behavior at chilled temperatures.	47.5
Separation of cooked and raw food.	70.0
The least safe practice of food thawing.	25.8
Is it safe to eat food with expired used by date?	90.8
Is it safe to keep open sterile milk outside of fridge?	89.2
Is it safe to consume content of the blown can?	91.7
Minimal required temperature for cooking poultry meat?	20.8
Degustation of food during preparation is the best way to check if the food is done?	52.5
The same cutting board can be used for different meats (red, poultry, fish).	54.2
Washing hands is mandatory after…	
...touching face	63.3
...potteries washed in the machine	76.7
…fresh fruits	54.2
...cloths	85.8
…potteries used for food preparation	54.2
Washing hands with soap may decrease chances of food poisoning.	71.7

Our results showed that 95.8% of all respondents report washing hands with water and soap (Table 2), while only 2.5% of all respondents report washing their hands only with water. Similar was also reported by other researchers. A total of 96.8% of Greek students, 80.7% of Lebanese students (36), 51% of students in Jordan (31) reported that they properly wash their hands. It is however important to note that all these results, as well as those found in this study, were self-reported and sometimes they may differ from actual hygiene

BY-NC-ND

practices (49). Almost 95% of Malaysian food sellers declared that they wash their hands after using toilet, while merely 4.7% of them actually did this (50). In addition, some studies have shown that food handlers might be aware of some safe food handling practices, but they do not perform them in everyday life. For example, 85.1% Spanish students declared that washing hands with water and soap before and during food preparation is very important for preventing cross-contamination, but only 13.5% of them performed proper hand hygiene (51). Our results showed also that only 47.5% of all cadets report washing their hands for at least 20 s, as it is recommended (52). It is worth noting that this study was performed before the onset of novel Coronavirus disease (Covid-19) outbreak, which is currently continuing at the time of writing this paper. The hand hygiene knowledge and handling practices will be certainly better in future, due to great number of published instructions, guidelines and videos that have been issued during this worldwide outbreak (53, 54).

When cadets were asked which food is most commonly contaminated with *Trichinella*, 64.2% of them responded correctly, despite the relatively low prevalence of *Trichinella* contamination in Serbian meat nowadays (55). It seems that cadets are well aware of risks related to protozoa in raw meat, as a result of great public interest for this matter in the past and the well-known need for *post mortem* veterinary inspection of meat when pigs are traditionally slaughtered at home arrangements (56). On the other side, *E. coli* O157 is also pathogen most commonly associated with raw (minced) meat (57), and merely 27.5% of all cadets knew this. In addition, only 13.3% of cadets knew that *Listeria monocytogenes* is associated with ready-to-eat meat products (58, 59), and almost 60.0% of cadets circled "I do not know", indicating low level of knowledge in this field. Finally, only 10% of cadets knew that *Campylobacter* is food-borne pathogen mostly associated with raw and under-cooked chicken meat. Obtained results showed insufficient knowledge on pathogens associated with meat and meat products, except for *Trichinella*. This is in line with results presented elsewhere (30, 31, 34, 60). It is of note that cadets involved in this study do not have any course covering food microbiology topic in their education, and therefore it is to be expected that cadets will show limited knowledge in this field.

Desired elimination of pathogenic microorganisms in ground or minced meat can be achieved through heat treatment, that should comprise temperature of at least 74 °C in the center of the product, and only 20.8% of cadets knew this (Table 3), while 50.8% of them indicated that they do not know the answer. In addition, almost half of all participants would check if meat is done, by using a fork and checking if there are bloody juices coming from the meat (49.2%), while only 5.8% of cadets use thermometer (Table 2). Similar was seen in other studies, only 7.4% of Lebanese students (36) and 1.1% of Greek students (34) was using thermometer for this purpose. It is of note that 51.4% of Canadian students indicated that the best way to check the readiness of meat is to use thermometer (33). The obtained difference seen in the study performed in Canada might be related to the fact that they have asked a question related to knowledge, not a practice as it was in this study.

What seems to be promising is the fact that Serbian cadets are aware of labeling instructions given by food producers, as 90.8% of them knew that it is not safe to consume food when the shelf-life is expired, and 89.2% knew that the opened sterilized milk should not be stored outside the refrigerator (Table 3). Finally, 91.7% of cadets are familiar with the fact that content of blown can is not safe for the consumption, due to possible outgrowth of anaerobic bacteria *Clostridium botulinum* (61).

APTEFF, 52, 1-273 (2021) UDC: 356.22:355.231.1]:613.2
DOI: https://doi.org/10.2298/APT2152159S BIBLID: 1450-7188 (2021) 52, 159-171
BY-NC-ND
Original scientific paper

The symptoms of food poisoning usually involve diarrhea, vomiting and fever (1), and 52.5% of cadets were able to recognize them. Nevertheless, food poisoning might include more serious symptoms, such as meningitis, septicemia, spontaneous abortion, still birth or fetal death in patients with listeriosis (62) and only 24.2% of cadets knew this. Not only listeriosis, but other food-borne illnesses may result in very serious conditions, which can be life treating, particularly for vulnerable population (YOPI group including young, old, pregnant and immune-compromised). The population which is mostly resistant to food poisonings includes young people/teenagers and 51.7% of Serbian cadets were aware of this. Other studies have reported better results, as 66.2% of Lebanese (36) and 82% of Jordan students knew about the most resistant population.

Our results showed that cadets possess relatively low level of knowledge and bad handling practices, as it was also noticed in other similar studies. Nevertheless, some differences could be seen, and they are most probably related to the university curriculum. Some studies involved only students from food/health related faculties (63, 64), other involved students also from non-food/health related faculties (30, 34, 36). In general, better knowledge was seen among students who had a chance to participate in some food safety courses during their education. Participants in this study involved also cadets studying at the module Logistic Defence, at Military Academy in Serbia. It is of note, that students of this module have only few elective courses in which some aspects of food safety have been covered. These courses are Food products, Food technology and Nutrition organization. Cadets studying at other modules at Military Academy, such as Management in Defense, Military Mechanical Engineering, Military Electronic Engineering, Military Chemical Engineering, Military Aviation do not have any of food related courses in their curriculum. Therefore, it is assumed that cadets' food safety knowledge mainly originates from the previous education, as well as from private home, family and friends, media, Internet, etc. (34, 49). This might explain the lack of some important food safety facts, related to food microbiology. Having in mind that these young people might be also active in some military food services, it is important that during their education they should be provided with adequate information. Additionally, this knowledge must be complemented with practical things, using the means of social media (65).

CONCLUSION

In conclusion, our results indicated that Serbian cadets have shown relatively good knowledge for some food safety issues, including prevention of cross contamination in the kitchen, hand and personal hygiene, labeling instructions. On the other side, areas such as food microbiology, behavior and manifestation of food pathogens, the seriousness of the food-borne disease and its symptoms, seems to be inadequately understood and recognized by Serbian cadets. Information obtained in this study could be helpful for improving their knowledge, designing various educational programs and courses within their university curriculum. Finally, media and internet courses, material or short clips could also help in improving knowledge and practices among young people in order to prevent food poisonings in future.

BY-NC-ND

REFERENCES

1. Bari, M.L.; Yeasmin, S. Foodborne Diseases And Responsible Agents. In: Food Safety and Preservation. Elsevier. pp. 195–229.
2. Newell, D.G.; Koopmans, M.; Verhoef, L.; Duizer, E.; Aidara-Kane, A.; Sprong, H.; Opsteegh, M.; Langelaar, M.; Threfall, J.; Scheutz, F.; der Giessen, J. van; Kruse, H. Food-Borne Diseases - The Challenges Of 20 Years Ago Still Persist While New Ones Continue To Emerge. *Int. J. Food Microbiol*. **2010**, *139*(SUPPL. 1), S3–S15.
3. Havelaar, A.H.; Brul, S.; de Jong, A.; de Jonge, R.; Zwietering, M.H.; ter Kuile, B.H. Future Challenges To Microbial Food Safety. *Int. J. Food Microbiol*. **2010**, *139*(SUPPL. 1), S79-94.
4. Nyachuba, D.G. Foodborne Illness: Is It On The Rise? *Nutr. Rev*. **2010**, *68*(5), 257–269.
5. Kirk, M.D.; Pires, S.M.; Black, R.E.; Caipo, M.; Crump, J.A.; Devleesschauwer, B.; Döpfer, D.; Fazil, A.; Fischer-Walker, C.L.; Hald, T.; Hall, A.J.; Keddy, K.H.; Lake, R.J.; Lanata, C.F.; Torgerson, P.R.; Havelaar, A.H.; Angulo, F.J. World Health Organization Estimates Of The Global And Regional Disease Burden Of 22 Foodborne Bacterial, Protozoal, And Viral Diseases, 2010: A Data Synthesis. PLoS Med. 2015, 1–21.
6. EFSA. The European Union One Health 2018 Zoonoses Report. *EFSA J.* **2019**, *17*(12), 1–109.
7. Painter, J.A.; Hoekstra, R.M.; Ayers, T.; Tauxe, R. V.; Braden, C.R.; Angulo, F.J.; Griffin, P.M. Attribution Of Foodborne Illnesses, Hospitalizations, And Deaths To Food Commodities By Using Outbreak Data, United States, 1998-2008. *Emerg. Infect. Dis.* **2013**, *19*(3), 407–415.
8. Schmidt, R.H.; Rodrick, G.E.; Puckett, R.P. Institutional Food Service Operations. In: Food Safety Handbook. John Wiley & Sons, Inc. pp. 523–547.
9. Mullaney, S.B.; Hyatt, D.R.; Salman, M.D.; Rao, S.; McCluskey, B.J. Estimate Of The Annual Burden Of Foodborne Illness In Nondeployed Active Duty US Army Service Members: Five Major Pathogens, 2010–2015. *Epidemiol. Infect.* **2019**, 147.
10. Mayet, A.; Andréo, V.; Bédubourg, G.; Victorion, S.; Plantec, J.Y.; Soullié, B.; Meynard, J.B.; Dedieu, J.J.; Polvèche, P.Y.; Migliani, R. Food-Borne Outbreak Of Norovirus Infection In A French Military Parachuting Unit, April 2011. *Eurosurveillance* **2011**, *16*(30), 1.
11. Warner, R.D.; Carr, R.W.; McCleskey, F.K.; Johnson, P.C.; Elmer, L.M.G.; Davison, V.E. A Large Nontypical Outbreak Of Norwalk Virus: Gastroenteritis Associated With Exposing Celery To Nonpotable Water And With Citrobacter Freundii. *Arch. Intern. Med.* **1991**, *151*(12), 2419–2424.
12. Rubertone, M.; DeFraites, R.; Krauss, M.; Brandt, C. Outbreak Of Hepatitis A During A Military Field Training Exercise. *Mil. Med.* **1993**, *153*(1), 37–41.
13. Wadl, M.; Scherer, K.; Nielsen, S.; Diedrich, S.; Ellerbroek, L.; Frank, C.; Gatzer, R.; Hoehne, M.; Johne, R.; Klein, G.; Koch, J.; Schulenburg, J.; Thielbein, U.; Stark, K.; Bernard, H. Food-Borne Norovirus-Outbreak At A Military Base, Germany, 2009. *BMC Infect. Dis*. **2010**, *10*(1), 30.
14. Jadhav, S.L.; Sinha, A.K.; Banerjee, A.; Chawla, P.S. An Outbreak Of Food Poisoning In A Military Establishment. *Med. J. Armed Forces India* **2007**, *63*(2), 130–133.
15. Lee, V.J.; Ong, A.E.; Auw, M. Salmonella Outbreak In Military Camp. *Ann Acad Med Singap*. **2009**, *38*(3), 207-211.
16. Teague, N.S.; Grigg, S.S.; Peterson, J.C.; Gómez, G.A.; Talkington, D.F. Outbreak Of Staphylococcal Food Poisoning From A Military Unit Lunch Party - United States, July 2012. *Morb. Mortal. Wkly. Rep.* **2013**, *62*(50), 1026–1028.
17. Kasper, M.R.; Lescano, A.G.; Lucas, C.; Gilles, D.; Biese, B.J. Diarrhea Outbreak During U.S. Military Training In El Salvador. *PLoS One* **2012**, *7*(7), 1–8.
18. Velut, G.; Delon, F.; Mérigaud, J.P.; Tong, C.; Duflos, G.; Boissan, F.; Watier-Grillot, S.; Boni, M.; Derkenne, C.; Dia, A.; Texier, G.; Vest, P.; Meynard, J.B.; Fournier, P.E.; Chesnay, A.; Pommier de Santi, V. Histamine Food Poisoning: A Sudden, Large Outbreak Linked To Fresh Yellowfin Tuna From Reunion Island, France, April 2017. *Eurosurveillance* **2019**, 24(22).

BY-NC-ND

19. Demoncheaux, J.P.; Michel, R.; Mazenot, C.; Duflos, G.; Iacini, C.; Delaval, F.; Saware, E.M.; Renard, J.C. A Large Outbreak Of Scombroid Fish Poisoning Associated With Eating Yellowfin Tuna (Thunnus Albacares) At A Military Mass Catering In Dakar, Senegal. *Epidemiol. Infect.* **2012**, *140*(6), 1008–1012.
20. Marlow, M.A.; Luna-Gierke, R.E.; Griffin, P.M.; Vieira, A.R. Foodborne Disease Outbreaks In Correctional Institutions-United States, 1998-2014. *Am. J. Public Health* **2017**, *107*(7), 1150-1156.
21. Guo, W.; Cronk, R.; Scherer, E.; Oommen, R.; Brogan, J.; Sarr, M.; Bartram, J. A Systematic Scoping Review Of Environmental Health Conditions In Penal Institutions. *Int. J. Hyg. Environ. Health* **2019**, *222*(5), 790–803.
22. Mustafa, M.S.; Jain, S.; Agrawal, V.K. Food Poisoning Outbreak In A Military Establishment. *Med. J. Armed Forces India* **2009**, *65*(3), 240–243.
23. Lee, H.Y.; Chik, W.N.W.; Bakar, F.A.; Saari, N.; Mahyudin, N.A. Sanitation Practices Among Food Handlers In A Military Food Service Institution, Malaysia. *Food Nutr. Sci.* **2012**, *03*(11), 1561–1566.
24. Todd, E.C.D.; Greig, J.D.; Bartleson, C.A.; Michaels, B.S. Outbreaks Where Food Workers Have Been Implicated In The Spread Of Foodborne Disease. Part 4. Infective Doses And Pathogen Carriage. *J. Food Prot.* **2008**, *71*(11), 2339–2373.
25. Clayton, D.A.; Griffith, C.J.; Price, P.; Peters, A.C. Food Handlers' Beliefs And Self-Reported Practices. *Int. J. Environ. Health Res.* **2002**, *12*(1), 25–39.
26. Redmond, E.C.; Griffith, C.J. Consumer Food Handling In The Home: A Review Of Food Safety Studies. *J. Food Prot.* **2003**, *66*(1), 130–161.
27. Taché, J.; Carpentier, B. Hygiene In The Home Kitchen: Changes In Behaviour And Impact Of Key Microbiological Hazard Control Measures. *Food Control* **2014**, *35*(1), 392–400.
28. Patil, S.R.; Cates, S.; Morales, R. Consumer Food Safety Knowledge, Practices, And Demographic Differences: Findings From A Meta-Analysis. *J. Food Prot.* **2005**, *68*(9), 1884–1894.
29. Medeiros, L.C.; Hillers, V.N.; Chen, G.; Bergmann, V.; Kendall, P.; Schroeder, M. Design And Development Of Food Safety Knowledge And Attitude Scales For Consumer Food Safety Education. *J. Am. Diet. Assoc.* **2004**, *104*(11), 1671–1677.
30. Smigic, N.; Lazarov, T.; Djekic, I. Does The University Curriculum Impact The Level Of Students' Food Safety Knowledge? *Br. Food J.* **2020**, ahead-of-p(ahead-of-print).
31. Osaili, T.M.; Obeidat, B.A.; Abu Jamous, D.O.; Bawadi, H.A. Food Safety Knowledge And Practices Among College Female Students In North Of Jordan. *Food Control* **2011**, *22*(2), 269–276.
32. Luo, X.; Xu, X.; Chen, H.; Bai, R.; Zhang, Y.; Hou, X.; Zhang, F.; Zhang, Y.; Sharma, M.; Zeng, H.; Zhao, Y. Food Safety Related Knowledge, Attitudes, And Practices (KAP) Among The Students From Nursing, Education And Medical College In Chongqing, China. *Food Control* **2019**, *95*, 181–188.
33. Courtney, S.M.; Majowicz, S.E.; Dubin, J.A. Food Safety Knowledge Of Undergraduate Students At A Canadian University: Results Of An Online Survey. *BMC Public Health* **2016**, *16*(1), 1–16.
34. Lazou, T.; Georgiadis, M.; Pentieva, K.; McKevitt, A.; Iossifidou, E. Food Safety Knowledge And Food-Handling Practices Of Greek University Students: A Questionnaire-Based Survey. *Food Control* **2012**, *28*(2), 400–411.
35. Stratev, D.; Odeyemi, O.A.; Pavlov, A.; Kyuchukova, R.; Fatehi, F.; Bamidele, F.A. Food Safety Knowledge And Hygiene Practices Among Veterinary Medicine Students At Trakia University, Bulgaria. *J. Infect. Public Health* **2017**, *10*(6), 778–782.
36. Hassan, H.F.; Dimassi, H. Food Safety And Handling Knowledge And Practices Of Lebanese University Students. *Food Control* **2014**, *40*(1), 127–133.
37. Al-Shabib, N.A.; Husain, F.M.; Khan, J.M. Study On Food Safety Concerns, Knowledge And Practices Among University Students In Saudi Arabia. *Food Control* **2017**, *73*(B), 202–208.
38. Jackson, V.; Blair, I.S.; McDowell, D.A.; Kennedy, J.; Bolton, D.J. The Incidence Of Significant Foodborne Pathogens In Domestic Refrigerators. *Food Control* **2007**, *18*(4), 346–351.

BY-NC-ND

39. Vegara, A.; Festino, A.R.; Di Ciccio, P.A.; Costanzo, C.; Pennisi, L.; Ianieri, A. The Management Of The Domestic Refrigeration: Microbiological Status And Temperature. *Br. Food J.* **2014**, *116*(6), 1047–1057.
40. Shapiro, M.A.; Porticella, N.; Jiang, L.C.; Gravani, R.B. Predicting Intentions To Adopt Safe Home Food Handling Practices. Applying The Theory Of Planned Behavior. *Appetite* **2011**, *56*(1), 96–103.
41. Wilcock, A.; Pun, M.; Khanona, J.; Aung, M. Consumer Attitudes, Knowledge And Behaviour: A Review Of Food Safety Issues. *Trends Food Sci. Technol.* **2004**, *15*(2), 56–66.
42. Da Cunha, D.T.; Stedefeldt, E.; de Rosso, V.V. The Role Of Theoretical Food Safety Training On Brazilian Food Handlers' Knowledge, Attitude And Practice. *Food Control* **2014**, *43*, 167–174.
43. Janjic, J.; Katic, V.; Ivanovic, J.; Boskovic, M.; Starcevic, M.; Glamoslija, N.; Baltic, M.Z. Temperatures, Cleanliness And Food Storage Practises In Domestic Refrigerators In Serbia, Belgrade. *Int. J. Consum. Stud.* **2016**, *40*(3), 276–282.
44. Djekic, I.; Tomic, N.; Smigic, N.; Tomasevic, I.; Radovanovic, R.; Rajkovic, A. Quality Management Effects In Certified Serbian Companies Producing Food Of Animal Origin. *Total Qual. Manag. Bus. Excell.* **2014**, *25*(3–4), 383-396.
45. Carbas, B.; Cardoso, L.; Coelho, A.C. Investigation On The Knowledge Associated With Foodborne Diseases In Consumers Of Northeastern Portugal. *Food Control* **2013**, *30*(1), 54–57.
46. Martins, R.B.; Hogg, T.; Otero, J.G. Food Handlers' Knowledge On Food Hygiene: The Case Of A Catering Company In Portugal. *Food Control* **2012**, *23*(1), 184–190.
47. Smigic, N.; Antic, D.; Blagojevic, B.; Tomasevic, I.; Djekic, I. The Level Of Food Safety Knowledge Among Meat Handlers. *Br. Food J.* **2016**, *118*(1), 9–25.
48. Serbia. Health Statistical Yearbook Of Republic Of Serbia 2018, Institute Of Public Health Of Serbia (In Serbian).
49. Byrd-Bredbenner, C.; Maurer, J.; Wheatley, V.; Cottone, E.; Clancy, M. Observed Food Safety Behaviours Of Young Adults. *Br. Food J.* **2007**, *109*(7), 519–530.
50. Tan, S.L.; Cheng, P.L.; Soon, H.K.; Ghazali, H.; Mahyudin, N.A. A Qualitative Study On Personal Hygiene Knowledge And Practices Among Food Handlers At Selected Primary Schools In Klang Valley Area, Selangor, Malaysia. *Int. Food Res. J.* **2013**, *20*(1), 71–76.
51. Garayoa, R.; Córdoba, M.; García-Jalón, I.; Sanchez-Villegas, A.; Vitas, A.I. Relationship Between Consumer Food Safety Knowledge And Reported Behavior Among Students From Health Sciences In One Region Of Spain. *J. Food Prot.* **2005**, *68*(12), 2631–2636.
52. WHO. WHO Guidelines On Hand Hygiene In Health Care: A Summary First Global Patient Safety Challenge Clean Care Is Safer Care.
53. WHO. Coronavirus Disease (COVID-19) Outbreak - World Water Day 2020 Highlights The Essential Role Of Handwashing. 2020.
54. UNICEF. Everything You Need To Know About Washing Your Hands To Protect Against Coronavirus (COVID-19). 2020.
55. Sofronic-Milosavljevic, L.; Djordjevic, M.; Plavsic, B.; Grgic, B. Trichinella Infection In Serbia In The First Decade Of The Twenty-First Century. *Vet. Parasitol.* **2013**, *194*(2–4), 145–149.
56. Buncic, S.; Mirilovic, M. Trichinellosis In Wild And Domestic Pigs And Public Health: A Serbian Perspective. In: Game meat hygiene in focus. Wageningen Academic Publishers. pp. 143–156.
57. Nobili, G.; Franconieri, I.; La Bella, G.; Basanisi, M.G.; La Salandra, G. Prevalence Of Verocytotoxigenic Escherichia Coli Strains Isolated From Raw Beef In Southern Italy. *Int. J. Food Microbiol.* **2017**, *257*, 201–205.
58. Churchill, K.J.; Sargeant, J.M.; Farber, J.M.; O'connor, A.M. Prevalence Of Listeria Monocytogenes In Select Ready-To-Eat Foods—Deli Meat, Soft Cheese, And Packaged Salad: A Systematic Review And Meta-Analysis. *J. Food Prot.* **2019**, *82*(2), 344–357.
59. Kramarenko, T.; Roasto, M.; Meremäe, K.; Kuningas, M.; Põltsama, P.; Elias, T. Listeria Monocytogenes Prevalence And Serotype Diversity In Various Foods. *Food Control* **2013**, *30*(1), 24–29.

BY-NC-ND

60. Farahat, M.F.; El-Shafie, M.M.; Waly, M.I. Food Safety Knowledge And Practices Among Saudi Women. *Food Control* **2015**, *47*, 427–435.
61. Lund, B.M.; Peck, M.W. Clostridium Botulinum. *Guid. to Foodborne Pathog.* **2013**, (June), 91–111.
62. Gandhi, M.; Chikindas, M.L. Listeria: A Foodborne Pathogen That Knows How To Survive. *Int. J. Food Microbiol.* **2007**, *113*(1), 1–15.
63. Giritlioglu, I.; Batman, O.; Tetik, N. The Knowledge And Practice Of Food Safety And Hygiene Of Cookery Students In Turkey. *Food Control* **2011**, *22*(6), 838–842.
64. Lange, M.; Göranzon, H.; Marklinder, I. Self-Reported Food Safety Knowledge And Behaviour Among Home And Consumer Studies Students. *Food Control* **2016**, *67*, 265–272.
65. Bramlett, A.; And, M.; Harrison, J.A. Safe Eats: An Evaluation Of The Use Of Social Media For Food Safety Education. *J. Food Prot.* **2012**, *75*(8), 1453–1463.

APTEFF, 52, 1-273 (2021) UDC: 661.7:577.114:547.426.1
DOI: https://doi.org/10.2298/APT2152173Z BIBLID: 1450-7188 (2021) 52, 173-187
BY-NC-ND
Original scientific paper

THE EFFECT OF CULTIVATION TIME ON XANTHAN PRODUCTION BY *Xanthomonas* spp. ON GLYCEROL CONTAINING MEDIUM

Ida E. ZAHOVIĆ[1], Jelena M. DODIĆ[1], Jovana A. GRAHOVAC[1], Mila S. GRAHOVAC[2] and Zorana Z. TRIVUNOVIĆ[1]*

[1] University of Novi Sad, Faculty of Technology Novi Sad, Department of Biotechnology and Pharmaceutical Engineering, Novi Sad, Serbia
[2] University of Novi Sad, Faculty of Agriculture, Department of Phytomedicine and Environmental Protection, Novi Sad, Serbia

Received: 19 July 2021 **Revised: 06 September 2021** **Accepted: 08 September 2021**

In this study, the influence of cultivation time on xanthan biosynthesis by different Xanthomonas strains, reference strain and crucifers' and pepper leaves' isolates, was examined. Biopolymer was produced by submerged cultivation of fourteen producing strains on medium with glycerol as a sole carbon source. Each experiment was performed at a laboratory level under aerobic conditions at 30°C and 150 rpm for 168 h and 240 h. Bioprocess efficacy was estimated based on the xanthan quantity and its average molecular weight that was selected as quality parameter. According to the obtained results, it can be concluded that all applied strains have a statistically significant effect on xanthan concentration in medium and on its average molecular weight, while cultivation time significantly affect the bioprocess efficacy only when biosynthesis is performed by Xanthomonas strains isolated from crucifers. Further, when only Xanthomonas strains isolated from crucifers are observed, statistically obtained data suggest that the largest amount of the best quality xanthan in applied experimental conditions can be accomplished by the cultivation of CB strain for 240 h. On the other hand, when it comes to Xanthomonas strains isolated from pepper leaves, the highest productivity is shown by PL 2, PL 4 and PL 5 strains regardless of the cultivation time, while the PL 3 strain was responsible for the synthesis of biopolymers with the highest average molecular weight. The results obtained in this study represent valuable information for development of biotechnological process for xanthan production on glycerol containing media using new producing strain.

Keywords: Biotechnological production, biopolymer, xanthan, *Xanthomonas* strains, cultivation time

INTRODUCTION

Xanthan is one of the most widely investigated microbial polysaccharides (1). Because of its non-toxicity and biocompatibility, xanthan has been approved by the United States Food and Drug Administration (FDA) as a food additive without any specific quantity limitations (2, 3). Besides the food industry, xanthan is extensively used in cosmetics, pharmaceutical, paper, paint, textile and other industries due to its exceptional rheological properties (4). Rheological properties of xanthan solution are greatly influenced by structure of its macromolecule (5). The primary structure of xanthan is composed of repeating units consisting of two glucose units, two mannose units and one glucuronic acid unit in the molar ratio 2.8:2.0:2.0. Xanthan molecular weight distribution depends on the association between structural chains and it ranges from around $2 \cdot 10^5$ to $5 \cdot 10^7$ g/moL (6, 7).

* Corresponding author: Ida E. Zahović, University of Novi Sad, Faculty of Technology Novi Sad, Department of Biotechnology and Pharmaceutical Engineering, Bulevar cara Lazara 1, 21000 Novi Sad, Serbia, e-mail: ida.zahovic@uns.ac.rs

APTEFF, 52, 1-273 (2021) UDC: 661.7:577.114:547.426.1
DOI: https://doi.org/10.2298/APT2152173Z BIBLID: 1450-7188 (2021) 52, 173-187
BY-NC-ND
Original scientific paper

Many types of bacteria of the genus *Xanthomonas* such as *Xanthomonas campestris*, *Xanthomonas phaseoli*, *Xanthomonas malvacearum* and *Xanthomonas carotae* have the ability to biosynthesize xanthan, but *Xanthomonas campestris* is the most widely used for its production (8). All *Xanthomonas campestris* strains are known as phytopathogens due to the fact that they cause infections of a large number of plants that are important for agriculture, such as cabbage, tomato and pepper (9-11). Commercially, xanthan is produced by aerobic submerged cultivation of reference strain *Xanthomonas campestris* ATCC 13951 on glucose or sucrose containing medium under optimal conditions. However, high cost of glucose and sucrose indicates the need for more economical carbon sources in order to reduce xanthan production costs (12). Among various alternative substrates of lower market value that have been considered as a suitable feedstock in the recent past, glycerol proved to be one of the most promising for xanthan production (13, 14).

Several studies suggest that certain strains of bacteria of the genus *Xanthomonas* possess the ability to biosynthesize xanthan on a medium with glycerol as a sole carbon source (15, 16). Research related to the xanthan biosynthesis on glycerol containing media is still in initial stages, probably by reason of impaired metabolic activity of the applied producing strains (17). This implies that there is a need for isolation of new *Xanthomonas* strains that are able to metabolize glycerol and produce xanthan. According to the latest research, cultivation time directly affect the xanthan quantity and quality, including its chemical composition. So, there is also a need to determine the optimal cultivation time for new producing strains (18) in order to achieve successful efficacy of examined biotechnological process. The usual fermentation time for xanthan production is from 72 h to 120 h (15, 19, 20), and in one study, xanthan biosynthesis was performed on glycerol containing medium up to 168 h (7). The results from the available literature where xanthan biosynthesis was performed on glycerol containing media show that the applied producing strains did not metabolize all available amount of glycerol during the cultivation of 96 h (15) and 120 h (20), and glycerol conversion was about 50% or less. This is probably due to lack of time for the applied strains to adapt to glycerol and produce xanthan in a sufficient amount. Taking into account all of these, there is a need for increase of cultivation time during the xanthan production on glycerol containing media in order to achieve higher productivity and higher degree of glycerol conversion.

The aim of this study was to investigate the effect of cultivation time on xanthan production by different *Xanthomonas* strains, reference strain and vegetable crop isolates, on medium with glycerol as a sole carbon source. Bioprocess efficacy was estimated based on the selected quantity and quality parameters, i.e. xanthan concentration in medium at the end of biosynthesis and its average molecular weight.

EXPERIMENTAL

PRODUCING MICROORGANISMS

The reference strain *Xanthomonas campestris* ATCC 13951, eight *Xanthomonas* strains isolated from crucifers (Am, CF, CB, KA, Xp 3-1, Xp 7-2, Mn 7-2, 12-2) and five *Xanthomonas* strains isolated from pepper leaves (PL 1, PL 2, PL 3, PL 4, PL 5) were used as the

APTEFF, 52, 1-273 (2021) UDC: 661.7:577.114:547.426.1
DOI: https://doi.org/10.2298/APT2152173Z BIBLID: 1450-7188 (2021) 52, 173-187
BY-NC-ND
Original scientific paper

producing microorganisms in these experiments. All strains were stored at 4°C on agar slant (YMA®, HiMedia, India) and subcultured every four weeks.

CULTIVATION MEDIA

The commercial medium (YMB®, HiMedia, India) was used for inoculum preparation, while xanthan production was performed on semi-synthetic medium with commercial glycerol (HiMedia, India) in a quantity of 20.0 g/L. The production medium also contained yeast extract (3.0 g/L), $(NH_4)_2SO_4$ (1.5 g/L), K_2HPO_4 (3.0 g/L) and $MgSO_4 \cdot 7H_2O$ (0.3 g/L). The pH value of glycerol containing medium was adjusted to 7.0±0.2. All media were sterilized by autoclaving (121°C, 2.1 bar, 20 min) and stored at 4°C until use.

INOCULUM PREPARATION

Xanthomonas strains were subcultured on agar slant and incubated at 25°C for 48 h. Further, in inoculum preparation procedure was included the suspending of producing microorganism cells in liquid medium. The prepared suspension was then incubated in aerobic conditions at 25°C and 150 rpm (laboratory shaker KS 4000i control, Ika® Werke, Germany) for 48h.

XANTHAN PRODUCTION

The xanthan production was carried out in 300 mL Erlenmeyer flasks with 100 mL of the glycerol containing medium. Inoculation was performed by adding 10% (v/v) of inoculum prepared as previously described. The biosynthesis was performed under aerobic conditions at 30°C and 150 rpm (laboratory shaker KS 4000i control, Ika® Werke, Germany) for 168 h and 240 h.

XANTHAN SEPARATION

At the end of biosynthesis, the xanthan was separated from the supernatant of cultivation medium by precipitation with cold 96% (v/v) ethanol in the presence of the potassium-chloride as electrolyte as described in previous research (7). The concentration of the produced biopolymer was evaluated by determining the weight of the dry product per litre of cultivation medium.

DETERMINATION OF XANTHAN MOLECULAR WEIGHT

The average molecular weight of the separated xanthan was estimated based on the intrinsic viscosity of its solution in 0.1 M sodium chloride using the Mark-Houwink type equation (21):

$$[\eta] = 1{,}7 \cdot 10^{-7} \cdot {M_W}^{1{,}14} \quad [1]$$

APTEFF, 52, 1-273 (2021) UDC: 661.7:577.114:547.426.1
DOI: https://doi.org/10.2298/APT2152173Z BIBLID: 1450-7188 (2021) 52, 173-187
BY-NC-ND
Original scientific paper

DATA ANALYSIS

All experiments were carried out in triplicate and the results were averaged. The experimental data were processed by two-way analysis of variance (Two-Way ANOVA). Significant differences between the means were determined by Duncan's multiple range test at the significance level of α=0.05 using Statistica 13.2 software (Dell Inc., USA).

RESULTS AND DISCUSSION

In order to examine the effect of applied *Xanthomonas* strains and cultivation time on xanthan quantity and quality, statistical analysis of experimental data was carried out. The results of Two-Way ANOVA analysis, as well as results of post hoc analysis by Duncan's multiple range for xanthan concentration in media and its average molecular weight are further discussed.

EFFECT OF *XANTHOMONAS* STRAINS AND CULTIVATION TIME ON XANTHAN CONCENTRATION

The results of statistical analysis of the effect of applied *Xanthomonas* strains, isolated from crucifers and pepper leaves, on xanthan concentration in media obtained for different cultivation time are shown in Table 1 and Table 2.

Two-Way ANOVA results, which are presented in Table 1, show that the *p*-values for the analysed parameters and their interaction are much lower than 0.05 for *Xanthomonas* strains isolated from crucifers, which indicates that the applied *Xanthomonas* strains and cultivation time as well as their combination have a statistically significant effect on xanthan concentration in cultivation media, as reported in other researches (6, 17, 22).

Table 1. Analysis of variance (Two-Way ANOVA) of the effect of the different *Xanthomonas* strains and cultivation time on xanthan concentration in media

Xanthomonas strain	Variability	SS	DF	MS	F-value	*p*-value
Isolates from crucifers	Strain	222.491	8	27.811	129.98	< 0.000001
	Cultivation time	35.785	1	35.785	167.24	< 0.000001
	Strain and cultivation time	26.645	8	3.331	15.57	< 0.000001
	Error	7.703	36	0.214		
Isolates from pepper leaves	Strain	49.262	4	12.315	40.102	< 0.000001
	Cultivation time	0.643	1	0.643	2.094	0.163398
	Strain and cultivation time	0.160	4	0.040	0.130	0.969717
	Error	6.142	20	0.307		

SS – sum of squares; DF – degrees of freedom; MS – mean square

However, if attention is paid to the mean square values presented in the same table, it can be concluded that the cultivation time (35.785) has a much greater effect on this group of results, while the effect of *Xanthomonas* strain (27.811) is lower. The obtained results

APTEFF, 52, 1-273 (2021) UDC: 661.7:577.114:547.426.1
DOI: https://doi.org/10.2298/APT2152173Z BIBLID: 1450-7188 (2021) 52, 173-187
BY-NC-ND
Original scientific paper

suggest that cultivation time is of great importance for efficacy of bioprocesses performed by *Xanthomonas* strains isolated from crucifers. On the other side, the *p*-values for the analysed parameters and their interaction for *Xanthomonas* strains isolated from pepper leaves show different behaviour. Considering that the *p*-values for *Xanthomonas* strains is much lower than 0.05, it is evident that this parameter has statistically significant effect on xanthan concentration in cultivation media. However, the *p*-values for cultivation time (0.163398) and interaction of *Xanthomonas* strains and cultivation time (0.969717) are much higher than 0.05. This indicates that the cultivation time and combination of *Xanthomonas* strains isolated from pepper leaves and cultivation time have insignificant effect on xanthan concentration in cultivation media.

The results of statistical analysis of the effect of the different *Xanthomonas* strains on the xanthan concentration in media regardless of the cultivation time are presented graphically by Box & Whisker Plots in Figure 1, and the results of statistical analysis of the effect of cultivation time on the xanthan concentration in media regardless of the producing strain are presented in Figure 2.

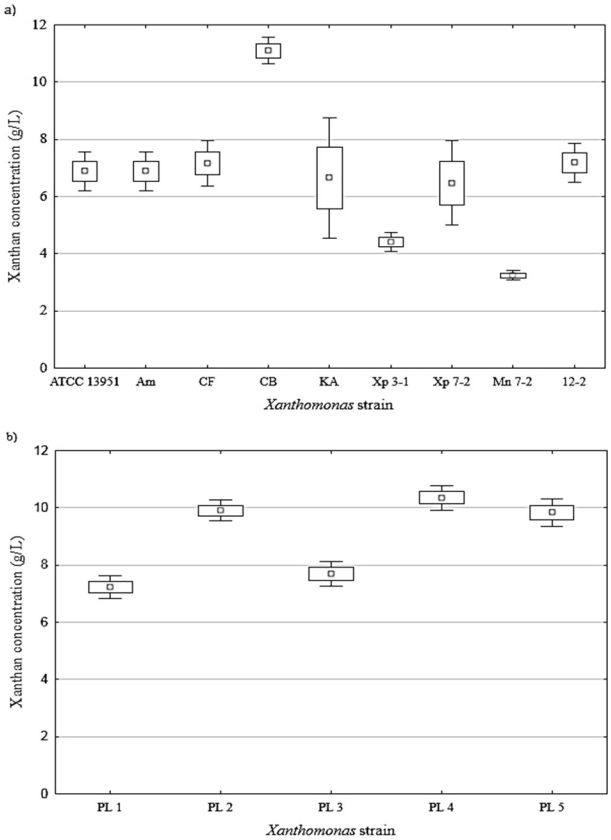

Figure 1. Effect of different *Xanthomonas* strains isolated from crucifers (a) and pepper leaves (b) on xanthan concentration in media regardless of the cultivation time

APTEFF, 52, 1-273 (2021)
DOI: https://doi.org/10.2298/APT2152173Z
BY-NC-ND
UDC: 661.7:577.114:547.426.1
BIBLID: 1450-7188 (2021) 52, 173-187
Original scientific paper

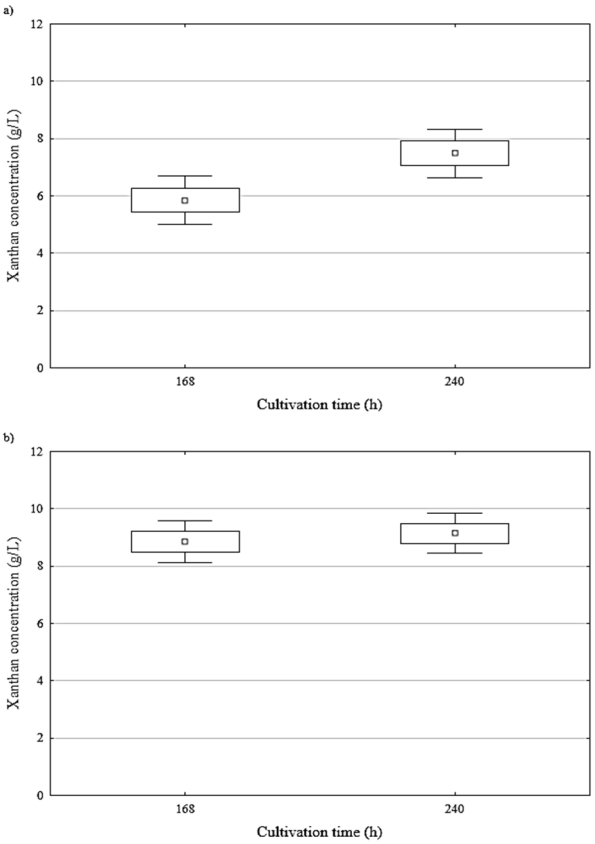

Figure 2. Effect of cultivation time on xanthan concentration in media obtained by *Xanthomonas* strains isolated from crucifers (a) and pepper leaves (b)

The results presented in Figure 1 indicate that there is statistically significant difference in xanthan concentration in media when different *Xanthomonas* strains were used. According to the results presented in Figure 1a, it is evident that the CB strain proved to be the best strain for xanthan production in applied experimental conditions among *Xanthomonas* strains isolated from crucifers. Also, it can be noted that there is no statistically significant difference in the xanthan concentration in media when reference strain, Am, CF, KA, Xp 7-2 or 12-2 strains were used. In this group of producing microorganisms, the lowest concentration of xanthan in media was achieved by Mn 7-2 strain. On the other hand, results represented in Figure 1b suggest that PL 4 strain is the best strain for xanthan production in applied experimental conditions among *Xanthomonas* strains isolated from pepper leaves. However, as it can be seen from the graphically presented results, there is no statistically significant difference in the xanthan concentration in media when PL 2, PL 4 or PL 5 strains were used. The results for *Xanthomonas* strains isolated from pepper leaves pre-

APTEFF, 52, 1-273 (2021) UDC: 661.7:577.114:547.426.1
DOI: https://doi.org/10.2298/APT2152173Z BIBLID: 1450-7188 (2021) 52, 173-187
BY-NC-ND
Original scientific paper

sented in Figure 1b also show that the lowest xanthan concentration in media was achieved by using PL 1 and PL 3 strains, and it is evident that there is no statistically significant difference in the xanthan concentration in media when these strains were used.

The results presented in Figure 2a indicate that there is statistically significant difference in xanthan concentration in media when *Xanthomonas* strains isolated from crucifers were cultivated for different time. As it can be seen from the graphically presented results, higher xanthan concentration in media was obtained after 240 h of cultivation of *Xanthomonas* strains isolated from crucifers on glycerol containing medium in applied experimental conditions. This is probably due the fact that producing microorganisms need more time to adapt to the medium with glycerol (23). According to the results presented in Figure 2b, the values for xanthan concentration in media obtained for both examined cultivation time are at the same level of significance, i.e. the amount of xanthan produced after 240 h is not significantly higher than the amount of xanthan produced after 168 h using the selected strains. In comparison with the previously discussed results (Figure 2a), it can be concluded that *Xanthomonas* strains isolated from pepper leaves adapt to glycerol in a shorter time.

In order to select the combination of *Xanthomonas* strain and cultivation time for which the highest xanthan quantity can be achieved, the experimental data were also analysed using Duncan's multiple range test whose results are given in Table 2.

Table 2. Duncan's multiple range test: mean ± standard deviation for xanthan concentration in media obtained by cultivation of *Xanthomonas* strains isolated from crucifers and pepper leaves for 168 h and 240 h

Isolates from crucifers			Isolates from pepper leaves		
Strains	**Cultivation time (h)**	**Xanthan (g/L)***	**Strains**	**Cultivation time (h)**	**Xanthan (g/L)***
Mn 7-2	168	3.13 ± 0.12^{a}	PL 1	168	7.04 ± 0.55^{a}
Mn 7-2	240	3.36 ± 0.23^{ab}	PL 1	240	7.41 ± 0.51^{a}
Xp 3-1	168	4.11 ± 0.29^{bc}	PL 3	168	7.42 ± 0.36^{a}
KA	168	4.28 ± 0.28^{c}	PL 3	240	7.95 ± 0.64^{a}
Xp 3-1	240	4.71 ± 0.24^{c}	PL 5	168	9.73 ± 0.56^{b}
Xp 7-2	168	4.83 ± 0.18^{c}	PL 2	168	9.86 ± 0.51^{b}
ATCC 13951	168	6.19 ± 0.32^{d}	PL 5	240	9.94 ± 0.71^{b}
Am	168	6.25 ± 0.54^{d}	PL 2	240	9.96 ± 0.49^{b}
CF	168	6.36 ± 0.35^{d}	PL 4	168	10.22 ± 0.63^{b}
12-2	168	6.51 ± 0.44^{d}	PL 4	240	10.48 ± 0.51^{b}
Am	240	7.53 ± 0.49^{e}			
ATCC 13951	240	7.58 ± 0.48^{e}			
12-2	240	7.87 ± 0.43^{e}			
CF	240	7.97 ± 0.64^{e}			
Xp 7-2	240	8.11 ± 0.65^{e}			
KA	240	9.02 ± 0.72^{f}			
CB	168	11.01 ± 0.61^{g}			
CB	240	11.18 ± 0.60^{g}			

*Values in the same column marked with the same letter are not significantly different at $\alpha=0.05$

BY-NC-ND

The results for *Xanthomonas* strains isolated from crucifers show that the highest xanthan content was accomplished when the cultivation of CB strain was performed for 240 h (11.18±0.60 g/L). It can be also seen that there is no statistically significant difference in xanthan concentration in media obtained when CB was cultivated for 168 h (11.01±0.61 g/L) which is confirmed by the *p*-value of 0.660510. However, the obtained results from Table 2 show that significantly higher amount of xanthan was produced when the cultivation of *Xanthomonas* strains isolated from crucifers lasted 240 h, except of strain CB, when the cultivation lasted 168 h. This may be due the fact that different strains need different time to adapt to the glycerol (17). The results for *Xanthomonas* strains isolated from crucifers show that the lowest concentration of xanthan in media (3.13±0.12 g/L) was achieved when strain Mn 7-2 was cultivated for 168 h. According to the same results, there is insignificant difference in the xanthan concentration in media when strain Mn 7-2 was cultivated for 168 h and 240 h (3.36±0.23 g/L), which is statistically confirmed by *p*-value of 0.546502. Comparing to the results from earlier study where xanthan biosinthesis was performed by *Xanthomonas* strains isolated from the infected leaves of several different cruciferous plants on glycerol containing medium and where xanthan was produced in the range from 1.68 g/L to 7.44 g/L (20), it can be noted that productivities of the examined strains obtained in this study (from 3.13±0.12 g/L to 11.18±0.60 g/L) are much higher.

From the results of Duncan's multiple range test for *Xanthomonas* strains isolated from pepper leaves presented in the same table, it can be seen that the highest xanthan content was accomplished when the cultivation of PL 4 strain was performed for 240 h (10.48±0.51 g/L). The presented results also indicate that there is no statistically significant difference between this result and the results obtained when PL 4 strain was cultivated for 168 h (10.22±0.63 g/L), PL 2 strain for 168 h (9.86±0.51 g/L) and 240 h (9.96±0.49 g/L) and PL 5 strain for 168 h (9.73±0.56 g/L) and 240 h (9.94±0.71 g/L). This is confirmed by the *p*-values of 0.573068, 0.235221, 0.289609, 0.154375 and 0.287271, respectively. The results presented in Table 2 indicate that the lowest xanthan concentration was achieved when strains PL 1 and PL 3 were used among *Xanthomonas* strains isolated from pepper leaves. There is no statistically significant difference between xanthan concentration when cultivation of PL 1 and PL 3 was performed for 168 h and 240 h, which is confirmed by *p*-values of 0.423322, 0.435666 and 0.079448, respectively. Values of xanthan concentration obtained in this study are much higher comparing to the results from literature data (0.157±0.04 g/L and 0.186±0.01 g/L) obtained when *Xanthomonas* isolates from Brazil were cultivated on glycerol-based media (15) and results from aforementioned study (1.68-7.44 g/L) when xanthan biosinthesis was performed by *Xanthomonas* strains isolated from the infected leaves of several different cruciferous plants on glycerol containing medium (20). Comparing to the previously discussed group of *Xanthomonas* isolates, it can be noted that *Xanthomonas* strains isolated from pepper leaves generally produce xanthan in higher concentration for shorter cultivation time (168 h).

Considering all these it can be concluded that *Xanthomonas* strains isolated from pepper leaves greatly affect xanthan production in applied experimental conditions. The difference in productivity among two groups of *Xanthomonas* isolates used in this research is probably due the fact that different *Xanthomonas* species possess different metabolic pathways and cycles (24) and that different strain need different time to adapt to the medium with glycerol (23).

APTEFF, 52, 1-273 (2021) UDC: 661.7:577.114:547.426.1
DOI: https://doi.org/10.2298/APT2152173Z BIBLID: 1450-7188 (2021) 52, 173-187
BY-NC-ND
Original scientific paper

EFFECT OF *XANTHOMONAS* STRAINS AND CULTIVATION TIME ON XANTHAN MOLECULAR WEIGHT

The results of statistical analysis of the effect of applied *Xanthomona*s strains, isolated from crucifers and pepper leaves, on average molecular weight of xanthan biosynthesized for different cultivation time are shown in Table 3 and Table 4.

Two-way ANOVA results given in Table 3 show that the *p*-values for the analysed parameters and their interaction for *Xanthomonas* strains isolated from crucifers are much lower than 0.05, which indicates that the applied *Xanthomonas* strains and cultivation time as well as their combination have a statistically significant effect on the average molecular weight of xanthan, as previously reported in other researches (6, 22). The mean square values presented in the same table suggest that *Xanthomonas* strains ($1.454113 \cdot 10^{11}$) have a much greater effect on this group of results, while the effect of cultivation time ($3.542870 \cdot 10^{10}$) is considerably lower. This indicates that selection of *Xanthomonas* crucifers' isolates has important effect on quality of synthesized biopolymer. Additionally, from the results presented in Table 3 it can be seen that the *p*-values for the analysed parameters for *Xanthomonas* strains isolated from pepper leaves show different behaviour. Hence, the *p*-value for the *Xanthomonas* strains is much lower than 0.05, which indicate that the applied *Xanthomonas* pepper leaves' isolates have a statistically significant effect on the average molecular weight of xanthan. This result is in agreement with results from earlier research where it is shown that producing strains have an effect not only on the yield but on the properties of xanthan too (25). On the other side, the *p*-values for cultivation time and combination of *Xanthomonas* strains and cultivation time are much higher than 0.05, which indicates that both of these parameters have insignificant effect on the average molecular weight of xanthan. Therefore, it can be concluded that different *Xanthomonas* strains isolated from pepper leaves have great effect on the molecular weight of xanthan produced in applied experimental conditions.

Table 3. Analysis of variance (Two-Way ANOVA) of the effect of the different *Xanthomonas* strains and cultivation time on the average molecular weight of xanthan

Xanthomonas strain	Variability	SS	DF	MS	F-value	*p*-value
Isolates from crucifers	Strain	$1.163290 \cdot 10^{12}$	8	$1.454113 \cdot 10^{11}$	327.081	< 0.000001
	Cultivation time	$3.542870 \cdot 10^{10}$	1	$3.542870 \cdot 10^{10}$	79.692	< 0.000001
	Strain and cultivation time	$2.305973 \cdot 10^{10}$	8	$2.882466 \cdot 10^{9}$	6.484	0.000032
	Error	$1.600461 \cdot 10^{10}$	36	$4.445725 \cdot 10^{8}$		
Isolates from pepper leaves	Strain	$1.976730 \cdot 10^{12}$	4	$4.941826 \cdot 10^{11}$	825.22	< 0.000001
	Cultivation time	$1.436183 \cdot 10^{9}$	1	$1.436183 \cdot 10^{9}$	2.40	0.137150
	Strain and cultivation time	$8.868970 \cdot 10^{8}$	4	$2.217243 \cdot 10^{8}$	0.37	0.826987
	Error	$1.197692 \cdot 10^{10}$	20	$5.988462 \cdot 10^{8}$		

SS – sum of squares; DF – degrees of freedom; MS – mean square

The results of statistical analysis of the effect of the different *Xanthomonas* strains on the average molecular weight of xanthan regardless of the cultivation time are presented graphically by Box & Whisker Plots in Figure 3, and the results of statistical analysis of the

APTEFF, 52, 1-273 (2021) UDC: 661.7:577.114:547.426.1
DOI: https://doi.org/10.2298/APT2152173Z BIBLID: 1450-7188 (2021) 52, 173-187
BY-NC-ND
Original scientific paper

effect of cultivation time on the same biopolymer quality parameter regardless of the producing strain are presented in Figure 4.

The results presented in Figure 3 indicate that there is statistically significant difference in xanthan quality when different *Xanthomonas* strains were applied.

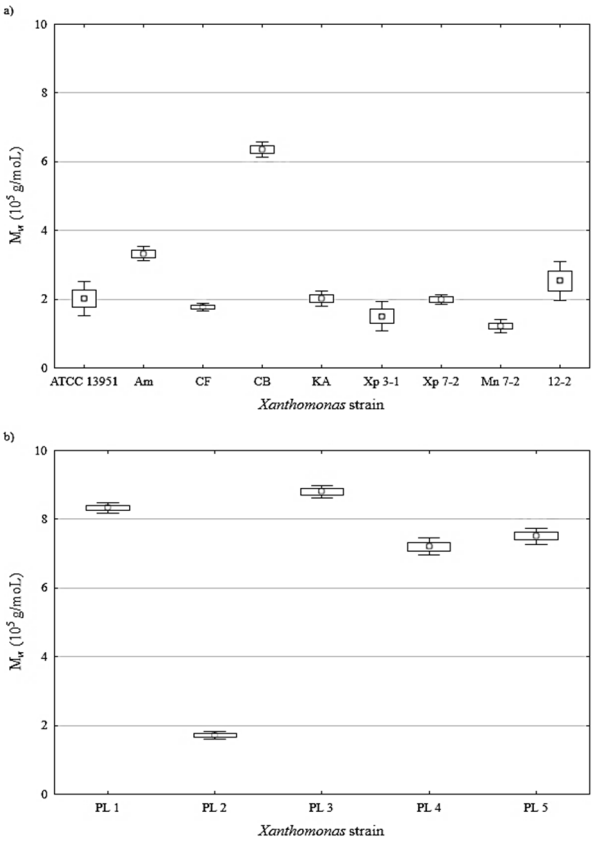

Figure 3. Effect of different *Xanthomonas* strains isolated from crucifers (a) and pepper leaves (b) on the average molecular weight of biosynthesized xanthan regardless of the cultivation time

According to the graphically represented results (Figure 3a), xanthan with the highest average molecular weight was achieved when using CB strain. As it can be seen from the Figure 3a, the other strains in applied experimental conditions produced xanthan with significantly lower average molecular weight. The obtained results show that the xanthan of the lowest average molecular weight was achieved by Xp 3-1 and Mn 7-2 strains and that there is no statistically significant difference between the values of average molecular weight of xanthan when these strains were used. The graphically presented results in Figure 3b suggest that xanthan with the highest average molecular weight was achieved by PL 3

APTEFF, 52, 1-273 (2021) UDC: 661.7:577.114:547.426.1
DOI: https://doi.org/10.2298/APT2152173Z BIBLID: 1450-7188 (2021) 52, 173-187
BY-NC-ND
Original scientific paper

strain. Xanthan of high molecular weight was also achieved when strain PL 1 was cultivated in applied experimental conditions. According to the obtained results, there is no statistically significant difference between the values of average molecular weight when PL 4 and PL 5 were used. Xanthan of the lowest average molecular weight was achieved by PL 2 strain among *Xanthomonas* strains isolated from pepper leaves. The results presented in Figure 3b suggest that molecular weight of xanthan produced by the PL2 strain is much lower comparing to the molecular weight of xanthan produced by other *Xanthomonas* strains isolated from pepper leaves.

The results presented in Figure 4a indicate that there is no statistically significant difference in molecular weight of xanthan obtained when different *Xanthomonas* strains isolated from crucifers were cultivated for different time.

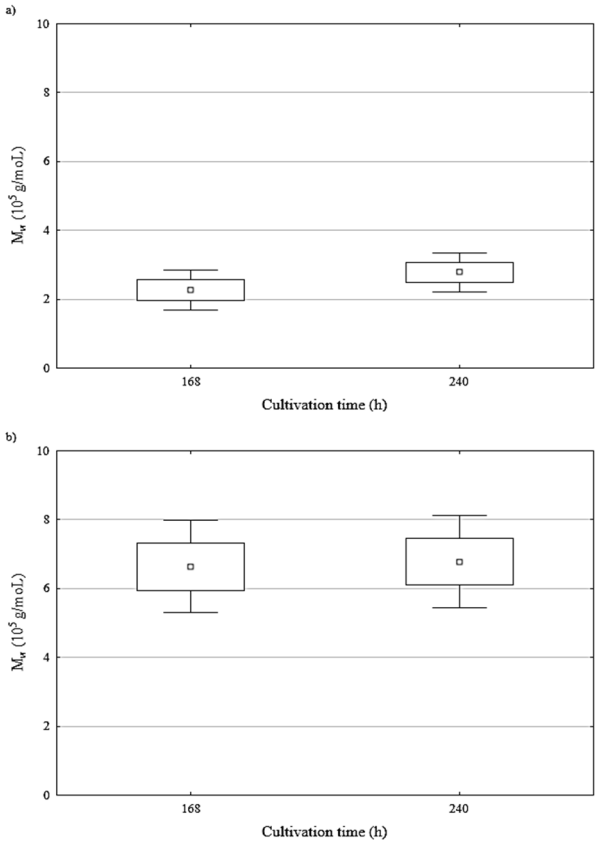

Figure 4. Effect of cultivation time on average molecular weight of xanthan obtained by *Xanthomonas* strains isolated from crucifers (a) and strains isolated from pepper (b)

According to the obtained results, *Xanthomonas* strains isolated from crucifers produce xanthan of higher molecular weight on glycerol containing medium for 168 h of cultivation,

APTEFF, 52, 1-273 (2021)
DOI: https://doi.org/10.2298/APT2152173Z
BY-NC-ND
UDC: 661.7:577.114:547.426.1
BIBLID: 1450-7188 (2021) 52, 173-187
Original scientific paper

under the applied experimental conditions. Considering the results presented in Figure 4b, the results for both examined cultivation time are at the same level of significance, i.e. quality of xanthan produced after 240 h is not significantly higher than the quality of xanthan produced after 168 h on glycerol containing media using the tested strains.

Aiming to select the combination of *Xanthomonas* strain and cultivation time for which the xanthan with the highest quality can be biosynthesized, the experimental data was further analysed using Duncan's multiple range test whose results are given in Table 4.

Table 4. Duncan's multiple range test: mean ± standard deviation for the average molecular weight of xanthan obtained by 168 h and 240 h of cultivation of *Xanthomonas* strains isolated from crucifers and pepper leaves

Isolates from crucifers			Isolates from pepper leaves		
Strains	**Cultivation time (h)**	M_w [10^5 g/moL]*	**Strains**	**Cultivation time (h)**	M_w [10^5 g/moL]*
Xp 3-1	168	1.05 ± 0.16^{a}	PL 2	168	1.65 ± 0.16^{a}
Mn 7-2	168	1.08 ± 0.18^{a}	PL 2	240	1.76 ± 0.14^{a}
Mn 7-2	240	$1.36\pm0.21^{a,b}$	PL 4	168	7.03 ± 0.32^{b}
ATCC 13951	168	$1.48\pm0.24^{b,c}$	PL 4	240	$7.38\pm0.22^{b,c}$
CF	168	$1.73\pm0.2^{c,d}$	PL 5	168	7.48 ± 0.19^{c}
CF	240	$1.81\pm0.1^{c,d}$	PL 5	240	7.54 ± 0.4^{c}
Xp 7-2	168	1.9 ± 0.16^{d}	PL 1	168	8.31 ± 0.2^{d}
12-2	168	1.92 ± 0.28^{d}	PL 1	240	$8.36\pm0.21^{d,e}$
KA	168	1.96 ± 0.31^{d}	PL 3	168	$8.75\pm0.29^{e,f}$
Xp 3-1	240	1.96 ± 0.21^{d}	PL 3	240	8.87 ± 0.29^{f}
KA	240	2.08 ± 0.3^{d}			
Xp 7-2	240	2.08 ± 0.2^{d}			
ATCC 13951	240	2.55 ± 0.16^{e}			
Am	168	$3.15\pm0.2^{f,g}$			
12-2	240	3.15 ± 0.2^{f}			
Am	240	3.5 ± 0.2^{g}			
CB	168	6.16 ± 0.18^{h}			
CB	240	6.54 ± 0.2^{i}			

*Values in the same column marked with the same letter are not significantly different at $\alpha=0.05$

The results of Duncan's multiple range test for the average molecular weight of xanthan, obtained by cultivation of different *Xanthomonas* strains for 168 h and 240 h, are given in Table 4. Analysing the values of average molecular weight of xanthan produced by *Xanthomonas* strains isolated from crucifers it can be observed that the highest average molecular weight of xanthan was obtained when the cultivation of CB strain was performed for 240 h ($6.54\pm0.2\cdot10^5$ g/moL). Additionally, it is evident that high value of average mole-

BY-NC-ND

cular weight of xanthan was also obtained when CB strain was cultivated for 168 h ($6.16\pm0.18\cdot10^5$ g/moL). These results and results for xanthan concentration in medium suggest that CB strain is the most suitable *Xanthomonas* strain isolated from crucifers for xanthan production in applied experimental conditions. The results presented in Table 4 indicate that xanthan with the lowest average molecular weight ($1.05\pm0.16\cdot10^5$ g/moL) was achieved when Xp 3-1 strain was cultivated for 168 h among *Xanthomonas* strains isolated from crucifers. The obtained results show that there is no statistically significant difference between this result and result achieved when Mn 7-2 strain was cultivated for 168 h ($1.08\pm0.18\cdot10^5$ g/moL) and 240 h ($1.36\pm0.21\cdot10^5$ g/moL), which is confirmed by *p*-values of 0.873551 and 0.100488, respectively. When it comes to the values of examined quality indicator for xanthan biosynthesized by *Xanthomonas* strains isolated from pepper leaves presented in the same table it is obvious that the xanthan with the highest average molecular weight was obtained when the cultivation of PL 3 strain was performed for 240 h ($8.87\pm0.29\cdot10^5$ g/moL). Also, it can be noticed that there is no statistically significant difference between this result and result obtained when PL 3 strain was cultivated for 168 h ($8.75\pm0.29\cdot10^5$ g/moL). This is confirmed by the *p*-value of 0.569389. The results presented in Table 4 ssuggest that average molecular weight of xanthan produced by cultivation of strain PL 1 for 240 h and 168 h was also high ($8.36\pm0.21\cdot10^5$ g/moL and $8.31\pm0.2\cdot10^5$ g/moL, respectively) and that there is no statistically significant difference between obtained values of average molecular weight of xanthan for different cultivation time. This is confirmed by the *p*-value of 0.794531. Additionally, the obtained results indicate that xanthan with the lowest average molecular weight ($1.65\pm0.16\cdot10^5$ g/moL) was achieved when PL 2 strain was cultivated for 168 h among *Xanthomonas* strains isolated from pepper leaves. There is no statistically significant difference between obtained values of average molecular weight of xanthan when this strain is cultivated for 168 h and 240 h (1.76±0.14 g/moL). This is confirmed by the *p*-value of 0.582609. Previously discussed results suggest that PL 3 strain is the most suitable strain isolated from pepper leaves for the production of xanthan, with the highest average molecular weight, on glycerol containing media in applied experimental conditions. The values of molecular weight obtained in this research are higher comparing to the results obtained in previous research ($2.64\text{-}3.17\cdot10^5$ g/moL) when reference strain *Xanthomonas campestris* ATCC 13951 was cultivated on media with different concentration of glycerol (7). According to the obtained results, xanthan with the highest molecular weight can be achieved by *Xanthomonas* strains isolated from crucifers after 240 h of cultivation and by *Xanthomonas* strains isolated from pepper leaves after 168 h of cultivation. The observed differences in the values of average molecular weight of xanthan obtained by different *Xanthomonas* strains can be explained by the influence of medium composition, *Xanthomonas* strains and their metabolic pathways and behaviours during xanthan production and the operational conditions, which have a significant impact on the synthesized molecular structure of xanthan (18, 26).

CONCLUSIONS

In accordance with the defined aim, in this study the influence of cultivation time on xanthan biosynthesis by different *Xanthomonas* strains, reference strain and crucifers' and

BY-NC-ND

pepper leaves' isolates, on glycerol containing medium was examined. Based on the obtained results it can be concluded that selection of *Xanthomonas* strains have a statistically significant effect on xanthan concentration in cultivation media and its average molecular weight for both groups of *Xanthomonas* isolates. On the other side, cultivation time has significant effect on analysed indicators of xanthan quantity and quality only when bioprocess is performed by *Xanthomonas* strains isolated from crucifers. The results obtained in this research may be a suitable background for the future optimization of the economically justified production of xanthan on glycerol-based media using new producing microorganism.

Acknowledgements

This study is part of the project (451-03-9/2021-14/200134) funded by the Ministry of Education, Science and Technological Development of the Republic of Serbia.

REFERENCE

1. Petri, D. F. S. Xanthan gum: A versatile biopolymer for biomedical and technological applications. *J. Appl. Polym. Sci.* **2015**, *132* (23), 42035.
2. Pooja, D.; Panyaram, S.; Kulhari, H.; Rachamalla, S.S.; Sistla, R. Xanthan gum stabilized gold nanoparticles: characterization, biocompatibility, stability and cytotoxicity. *Carbohydr. Polym*. **2014**, *110*, 1-9.
3. Kumar, A.; Rao, K.M.; Han, S.S. Application of xanthan gum as polysaccharide in tissue engineering: A review. *Carbohydr. Polym*. **2018**, *180*, 128-144.
4. Kumara, S.M.; Khan, B.A.; Rohit, K.C.; Purushotham, B. Effect of carbon and nitrogen sources on the production of xanthan gum from *Xanthomonas campestris* isolated from soil. *Arch. Appl. Sci. Res*. **2012**, *4* (6), 2507-2512.
5. Klaic, P.M.A.; Nunes, A.M.; Moreira, A.dS.; Vendruscolo, C.T.; Ribeiro, A.S. Determination of Na, K, Ca and Mg in xanthan gum: sample treatment by acid digestion. *Carbohydr. Polym*. **2011**, *83* (4), 1895–1900.
6. Papagianni, M.; Psomas, S.K.; Batsilas, L.; Paras, S.V.; Kyriakidis, D.A.; Liakopoulou-Kyriakides, M. Xanthan production by *Xanthomonas campestris* in batch cultures. *Process Biochem*. **2001**, *37*, 73–80.
7. Rončević, Z.; Bajić, B.; Grahovac, J.; Dodić, S.; Dodić, J. Effect of the initial glycerol concentration in the medium on the xanthan biosynthesis. *Acta Period. Technol*. **2014**, *45*, 239-246.
8. Sujithra, B.; Deepika, S.; Akshaya, K.; Ponnusami, V. Production and optimization of xanthan gum from three-step sequential enzyme treated cassava bagasse hydrolysate. *Biocatal. Agric. Biotechnol*. **2019**, *21*, 101294.
9. García-Ochoa, F.; Santos, V.E.; Casas, J.A.; Gómez, E. Xanthan gum: production, recovery, and properties. *Biotechnol. Adv*. **2000**, *18* (7), 549-579.
10. Ciardi, J.A.; Tieman, D.M.; Lund, S.T.; Jones, J.B.; Stall, R.E.; Klee, H.J. Response to *Xanthomonas campestris* pv. *vesicatoria* in Tomato Involves Regulation of Ethylene Receptor Gene Expression. *Plant Physiol*. **2000**, *123* (1), 81-92.
11. Sherley, K.I.; Priyadharshini, R.D. Review on production of Xanthan gum in batch and continuous reactors. *Int. J. ChemTech Res*. **2015**, *8* (2), 711-717.
12. Demirci, A.S.; Palabiyik, I.; Apaydın, D.; Mirik, M.; Gumus, T. Xanthan gum biosynthesis using *Xanthomonas* isolates from waste bread: Process optimization and fermentation kinetics. *LWT - Food Sci. Technol*. **2019**, *101*, 40–47.

BY-NC-ND

13. Ozdal, M.; Kurbanoglu, E.B. Valorisation of chicken feathers for xanthan gum production using *Xanthomonas campestris* MO-03. J. *Genet. Eng. Biotechnol*. **2018**, *16*, 259-263.
14. Trindade, R.A.; Munhoz, A.P.; Burkert, C.A.V. Impact of a carbon source and stress conditions on some properties of xanthan gum produced by *Xanthomonas campestris* pv. *mangiferaeindicae*. *Biocatal. Agric. Biotechnol*. **2018**, *15*, 167-172.
15. Reis, E.C.; Almeida, M.; Cardoso, J.C.; Pereira, M.A.; de Oliveira, C.B.Z:, Venceslau, E.M.; Druzian, J.I.; Mariano, R.; Padilha, F.F. Biopolymer synthesized by strains of *Xanthomonas* sp. isolate from Brazil using biodiesel-waste. *Macromol. Symp*. **2010**, *296* (1), 347-353.
16. Trindade, R.A.; Munhoz, A.P.; Burket, C.A.V. Raw Glycerol as an Alternative Carbon Source for Cultivation of Exopolysaccharide-Producing Bacteria. Journal of Applied Biotechnology. **2015**, *3* (2), 61-73.
17. Wang, Z.; Wu, J.; Zhu, L.; Zhan, X. Activation of glycerol metabolism in *Xanthomonas campestris* by adaptive evolution to produce a high-transparency and low-viscosity xanthan gum from glycerol. *Bioresour. Technol*. **2016**, *211*, 390-397.
18. Miranda, A.L.; Costa, S.S.; Assis, D.dJ.; de Jesus, C.S.; Guimarães, A.G.; Druzian, J.I. Influence of strain and fermentation time on the production, composition, and properties of xanthan gum. *J. Appl. Polym. Sci.* **2020**, *137* (15), 48557.
19. Psomas, S.K.; Liakopoulou-Kyriakides, M.; Kyriakidis, D.A. Optimization study of xanthan gum production using response surface methodology. Biochem. Eng. J. 2007, 35, 273-280.
20. Bajić, B.Ž.; Rončević, Z.Z.; Dodić, S.N.; Grahovac, J.A.; Dodić, J.M. Glycerol as a carbon source for xanthan production by *Xanthomonas campestris* isolates. *Acta Period. Technol*. **2015**, *46*, 197-206.
21. Milas, M.; Rinaudo, M; Tinland, B. The viscosity dependence on concentration, molecular weight and shear rate of xanthan solutions. *Polym. Bull*. **1985**, *14* (2), 157- 164.
22. Gumus, T.; Demirci, A.S.; Mirik, M.; Arici, M.; Aysan, Y. Xanthan gum production of *Xanthomonas* spp. isolated from different plants. *Food Sci. Biotechnol*. **2010**, *19* (1), 201-206.
23. Crosse, A.J.; Brady, D.; Zhou, N.; Rumbold, K. Biodiesel's trash is a biorefineries' treasure: The use of "dirty" glycerol as an industrial fermentation substrate. World J. Microbiol. Biotechnol. **2020**, *36*, 2.
24. Saddler, G.S.; Bradbury, J.F. The Proteobacteria. In Bergy's Manual of Systematic Bacteriology; Brenner, D.J., Krieg, N.R., Staley, J.T., Eds.; New York: Springer; **2004**: pp 63-91.
25. Demirci, S.; Palabiyik, I.; Altan, D.D.; Apaydın, D.; Gumus, T. Yield and rheological properties of exopolysaccharide from a local isolate: *Xanthomonas axonopodis* pv. *vesicatoria*. *Electron. J. Biotechnol.* **2017**, *30*, 18–23.
26. Brandão, L.V.; Assis, D.J.; López, J.A.; Espiridião, M.C.A.; Echevarria, E.M.; Druzian, J.I. Bioconversion from crude glycerin by Xanthomonas campestris 2103: xanthan production and characterization. *Braz. J. Chem. Eng.* **2013**, *30* (4), 737-746.

APTEFF, 52, 1-273 (2021) UDC: 615.281/.282:546.62'284:577.67
DOI: https://doi.org/10.2298/APT2152189B BIBLID: 1450-7188 (2021) 52, 189-201
BY-NC-ND
Review paper

ANTIMICROBIAL ACTIVITIES OF DIFFERENT AGENTS INCLUDING PYROPHYLLITE AGAINST FOODBORNE PATHOGENS: A BRIEF REVIEW

Aleksandra S. BOČAROV-STANČIĆ[1], Jelena A. KRULJ[2], Marijana M. MASLOVARIĆ[1], Marija I. BODROŽA-SOLAROV[2], Rade D. JOVANOVIĆ[1], Radmila B. BESKOROVAJNI[1], Milan J. ADAMOVIĆ[3]*

[1] Institute for Science Application in Agriculture, 11000 Belgrade, Bulevar despota Stefana 68B, Serbia
[2] University of Novi Sad, Institute of Food Technology Novi Sad, 21000 Novi Sad, Bulevar cara Lazara 1, Serbia
[3] Institute for Technology of Nuclear and Other Mineral Raw Materials, Bulevar Franše d'Eperea 86, 11000 Belgrade, Serbia

Received: 11 August 2021 **Revised: 21 September 2021** **Accepted: 22 September 2021**

There has been worldwide an increasing interest and more strict criteria for food/feed safety including absence or reduction of the total number of microorganisms (bacteria, moulds and yeasts). Besides heavy metals, materials of biological origin (plant extracts, bio waste, chitosan etc.), some mineral adsorbents also have antimicrobial properties. There is much information about the antibacterial activity of the modified bentonite, montmoriollonite, smectute, zeolites and antifungal activity of various metal ion-exchanged zeolites and natural mineral clay, but there is almost no information about the antimicrobial properties of pyrophyllite, a monoclinic mineral from the group of phyllosilicates. This work summarizes the recent developments of antimicrobial agents and their application, current research, and trends in the area, highlighting pyrophyllite and its potential applications. Pyrophyllite, an unexploited mineral, possesses antimicrobial properties such as antibacterial and antifungal activities against foodborne pathogens which contributes to the protection of consumer's health and preservation of the environment. Results from preliminary investigations indicate that pyrophyllite showed antibacterial properties against Escherichia coli, Staphylococcus aureus, Enterococcus faecalis, and antifungal properties against fungal pathogens (Fusarium oxysporum, Phoma glomerata and Rhizoctonia solani). This mineral can also be used for biological control of F. oxysporum in the soil for growing potato.

Keywords: antimicrobial agents, pyrophyllite, foodborne pathogens

INTRODUCTION

The increase in standard and education of the human population affects the establishment of strict criteria on food/feed safety and quality, including the absence of microorganisms, mycotoxins, heavy metals and other harmful substances. Therefore, in recent decades, studies and looking for solutions that will contribute to the protection of food/feed from various types of contamination, increasing the quality of animal products, protecting consumer's health and preserving the environment were undertaken.

Today, antibiotic-resistant bacteria became ubiquitous in hospitals, food processing plants and animal breeding facilities as a consequence of the spreading of antibiotic resistance through selective pressure. To overcome that problem the need for different approaches for keeping pathogenic microorganisms away has risen. One such alternative is the use

* Corresponding author: Jelena A. Krulj, Institute of Food Technology Novi Sad, University of Novi Sad, Bulevar Cara Lazara 1, 21000 Novi Sad, Serbia, e-mail: jelena.krulj@fins.uns.ac.rs

BY-NC-ND

of copper, not only in hygiene-sensitive areas but also the use of copper vessels to render drinkable water as a low-cost alternative for developing countries (1). The use of copper instead of aluminium in air-conditioned systems showed that copper can offer an antifungal surface that can prevent subsequent germination of presented spores, so it can be used in different air-conditioning systems, particularly in the hospital environment (2).

Pathogenic fungi, the main infectious plant agents, in some cases are indirectly responsible for allergic or toxic disorders among consumers as the result of the production of allergens or toxic metabolites (mycotoxins). The increasing demand for production and regulations on the use of agrochemicals justifies the search for new control strategies based on plant extracts (3, 4), waste biomass (5), chitosan (6, 7, 8).

Having in mind a worldwide increase in antibiotic resistance, besides heavy metals, natural mineral clays have lately received particular scientific attention as antibacterial agents against a variety of multidrug-resistant bacterial (MDR) and two major fungal pathogens (9). Several studies have reported that some raw clays have bactericidal activity against both Gram-positive and Gram-negative bacteria (10-14). Clays and clay mineral clays, either as such or after modification, are recognized as valuable materials due to their abundant, inexpensive and environmentally friendly. Modified mineral materials based on bentonite, montmorillonite, smectite or zeolite possesses antibacterial and antifungal properties against some microbiota (15-18). Contrary to these minerals and their antimicrobial activity there is almost no information about the same properties of pyrophyllite, a monoclinic mineral from the group of phyllosilicates, a mineral whose rich deposits are found in the Western Balkans region. This review attempts to describe the several points relating to antimicrobial activities of different agents highlighting pyrophyllite and its potential applications that have been discovered so far. The information obtained is still very incomplete, additional research is needed, especially those related to the use of pyrophyllite in the food/feed safety sector.

ANTIMICROBIAL AGENTS IN GENERAL

METALS

Antimicrobial properties of metals/metal complexes have become increasingly attractive because of acting strongly against a broad spectrum of bacterial and fungal species. The antimicrobial effects of noble metals such as silver have been widely explored. The silver complexes of chelating copolymers of butyl acrylate-co-itaconic acid (BuA/IA)Ag and butyl acrylate-co-maleic acid (BuA/MA)Ag were fungicidal for *Aspergillus flavus*, *Botrytis allii* and *Fusarium oxysporum.* Also, (BuA/IA) Ag had the fungicidal effect on *Trichoderma reseei*, and (BuA/MA)Ag compound acter as a fungicidal agent of *Aspergillus terreus* and *Helminthosporium turcicum*. On the other hand, these copolymers showed the fungistatic effect to *A. niger*, *Diplodia oryzae*, *Macrophomina phaseoli* and *Mucor rouxii* (19).

The United States Environmental Agency (EPA) recognized in 2008 copper as the first metallic antimicrobial agent. Besides antiviral and antibacterial activity this heavy metal possess antifungal activity against filamentous fungi *Alternaria alternata*, *Aspergillus flavus, R. solani* and *Penicillium chrysogenum* and yeasts such as *Candida* species (20). Antifungal effect of silver nanoparticles (0.1, 1.0, 10 and 100 μg/ml) on two *Aspergillus* species

BY-NC-ND

isolated from raw and wastewater (*A. niger* and *A. terreus*) was more expressed against *A. terreus* as the higher fungal growth reduction of this species was observed compared to *A. niger* (21). Antimicrobial effects of metal/metal complexes can be referred to the increase of their lipophilic affinity which in turn deactivates enzymes responsible for respiratory processes and probably other cellular enzymes, which play a vital role in various metabolic pathways of the tested bacteria. Also, it is expected that the activity of the toxicant is the denaturation of one or more cell proteins and this impairs normal cellular process.

MATERIALS OF BIOLOGICAL ORIGIN

Plant, as sources of bioactive compounds have continued to play a dominant role in the maintenance of human health since ancient times. A wide range of plants species possess different medicinal properties against microbes. Studies of application of natural antifungal plant extracts of *Cassia alata* (Canicro bush), *Azadiraghta indica* (Neem), *Ocimum sanctum* (Tuls) and *Cassia obtusifolia* (Moneu bush) and natural antifungal-metal ferrocyanide complexes tested against *A. niger* found that ferrocyanides complexes had more antifungal properties than natural antifungals alone. It was found that the complexes of mercury ferrocyanide with Neem and copper ferrocyanide with Canicro bush had the highest and lowest antifungal activity, respectively (3). From extracts of 10 plant species used in traditional Uruguayan medicine extracts of *Salvia sclarea*, *S. officinalis* and *Rosmarinus officinalis* could be considered as antifungal compounds against phytopathogenic fungi *Alternaria* spp. (4). Nanocomposite adsorbent based on *Apocynaceae* leaf waste activated carbon by cobalt ferrite nanoparticles showed antimicrobial activity against *Staphylococcus aureus*, *Escherichia coli* and *Candida albicans* (inhibitory zone ranged from 11 to 17.56 mm) (5). Chitosan is a modified, natural biopolymer obtained by chitin acetylation. Its antimicrobial properties, besides other characteristics, make it a potential source of food and feed preservative (22). The antifungal activities of the chitosan derivatives against *Alternaria alternata* and *Phomopsis asparagi* increased with the molecular weight increase, concentration or the degree of substitution (6). According to the results of Guerra-Sánchez et al. (23) all types of chitosan investigated expressed antifungal activity and significantly increased glucose consumption and the release of compounds in 3 isolates of *Rhizopus stolonifer*.

Films and solutions based on chitosan with different molecular weights and different concentrations showed different antifungal activity against *A. niger*, *A. alternata* and *Rhizopus oryzae* (7). Chitosan films were significantly more effective on *A. niger* than the solution treatments, while solution treatments were more effective when applied against *A. alternata* (up to 97%) and *R. oryzae.*

Mohamed and Fekry (8) investigated antimicrobial activities of both chitosan and its Schiff's base towards *E. coli*, *S. aureus*, *A. niger* and *C. albicans*. They concluded that chitosan Schiff's base showed higher activities. Chitosan, prepared from shrimp shell waste by deacetylation of chitin, showed inhibition of *Xanthomonas* sp. growth in a liquid medium (24). Bacteriostatic effect of chitin was observed on Gram-negative bacteria such as *E. coli* ATCC 25922, *Vibrio chole*rae, *Shigela dysenteriae* and *Bacteroides fragilis* (25). Lactic acid bacteria (LAB) produce a large spectrum of metabolites that inhibit fungal growth (26).

APTEFF, 52, 1-273 (2021) UDC: 615.281/.282:546.62'284:577.67
DOI: https://doi.org/10.2298/APT2152189B BIBLID: 1450-7188 (2021) 52, 189-201
BY-NC-ND
Review paper

MINERAL MATERIALS

A variety of mineral materials as active substance show chemical inertness and low or zero toxicity for the humans and animals and therefore, are used as active principles or excipients in pharmaceutical formulations. Adamović et al. (27) examined, besides others, the antibacterial and antifungal activity of pelleting agent based on bentonite (Bentopel) applied in feed mixtures for laying hens. Total bacteria count (39.000/g) was much higher in the control (pelleted mixture without addition of Bentopel) compared to sample with the addition of 2% Bentopel (5.000/g), as well as total yeasts and moulds count (30/g and 10/g, respectively). Also compared to 8 fungal species identified in the control only 3 species were found in the sample where Bentopel was added (*Aspergillus fumigatus, Fusarium verticillioides* and *Mucor mucedo*). According to (15) (manganese oxide/bentonite nanocomposites showed greater antibacterial properties against *S. aureus* then *Pseudomonas aeruginosa.* These authors recorded vigorous antifungal behaviour against *C. albicans* that could be useful for biomedical applications. Das et al. (16) observed significant antibacterial activity of copper nanoparticle-decorated organically modified montmorillonite against ubiquitous Gram-negative bacteria *Klebsiella pneumonia* and Gram-positive bacteria *S. aureus.* Antibacterial potential of raw montmoriollonite clay modified with Ag nanoparticles for water disinfection was confirmed by the reduction of bacterial growth of *S. aureus*, *E. coli* and *P. aeruginosa*, by 64%, 39% and 70%, respectively (28).

Modified Laponite®RD (smectite, trioctahedrals) with Ag and Cu cations, investigated for their antibacterial activity against *E. coli*, *S. aureus* NCIMB6571 and *P. aeruginosa* NCIMB8295 reduced the growth of all tested bacterial species (17). The results of Demirici et al. (18) indicate that various metal ion-exchanged zeolites can get antibacterial (*E. coli, P. aeruginosa, Bacillus cereus, S. aureus*), antifungal (*Aspergillus niger, Penicillium vinaceum*) and anticandidal (*C. albicans, C. glabrata*) properties. Investigations of antifungal activity against *Fusarium graminearum* of zeolite 4A and its ion-exchange forms with Zn^{+2}, Li^{+}, Cu^{+2} and Co^{+2} showed significant antifungal activities that could be explained by the interaction with free metal cations (29). Hybrid MCM-41 (mesoporous material with a hierarchical structure from a family of silicate and alumosilicate) was an inhibitor of Gram-negative bacteria (*E. coli* ATCC 25922, *P. aeruginosa* ATCC 27853), Gram-positive bacteria (*S. aureus* ATCC 25932 and ATCC 43300), and yeast *C. albicans* ATCC10231 (30). Behroozian et al. (9) reported about broad-spectrum of antimicrobial and biofilm activity of a mineral natural clay (Kisameet clay-KS). Besides the known spectrum of antibacterial activities of KS, it was efficient against two major fungal pathogens *C. albicans* and *Cryptococcus neoformans.*

OTHER MATERIALS

A hydrophilic polypropylene fibre comprising polypropylene with added effective amount of at least one Cs to C2 fatty acid monoglyceride has antimicrobial activity against Gram-positive bacteria to the surface of the fibre such as *Klebsiella pneumoniae* (31). Short pyrrole tetra amides series are described with submicromolar DNA binding whose submicromolar DNA binding affinity provided strong antibacterial activity (32). Antifungal activity of mineral trioxide aggregate (MTA) formulated from commercial Portland cement, a class of materials covering a range of compositions (between silica-alumina and calcium),

APTEFF, 52, 1-273 (2021) UDC: 615.281/.282:546.62'284:577.67
DOI: https://doi.org/10.2298/APT2152189B BIBLID: 1450-7188 (2021) 52, 189-201
BY-NC-ND
Review paper

combined with bismuth oxide powder for radio-opacity was investigated by (33). These authors concluded that freshly prepared MTA was effective after 24 h of contact against *C. albicans*.

PYROPHYLLITE

PHYSICOCHEMICAL CHARACTERISTICS

Pyrophyllite is a monoclinic mineral from the group of phyllosilicates, with the chemical formula $Al_2[Si_4O_{10}](OH)_2$, and is considered to be the simplest mineral in this group of phyllosilicates (34). It became by the hydrothermal metamorphosis of underground lava that turned into clay by interaction with groundwater, steam and pressure. The colour varies depending on the oxide content and ranges from white, grey-white, purple-white, to grey-green. It usually appears in lamellar, fibrous or dense aggregates in shale rocks rich in silicon and aluminium (Figure 1), which is why it belongs to the group of non-metallic aluminosilicate mineral raw materials.

It contains electrolytes (sodium, potassium, calcium, magnesium, iron, etc.) and free ions that give it the ability to be a detoxicant and antioxidant. The following minerals prevail in pyrophyllite shale: pyrophyllite, sericite and kaolinite, and to a lesser extent, it also contains quartz, calcite, magnesite, dolomite, illite and montmorillonite. As adsorption and absorption clay with a combination of ring-shaped tetrahedral molecules, it resembles the shape of red blood cells (RBCs), representing the most appropriate geometric shape for the uptake and/or delivery of nutrients (35).

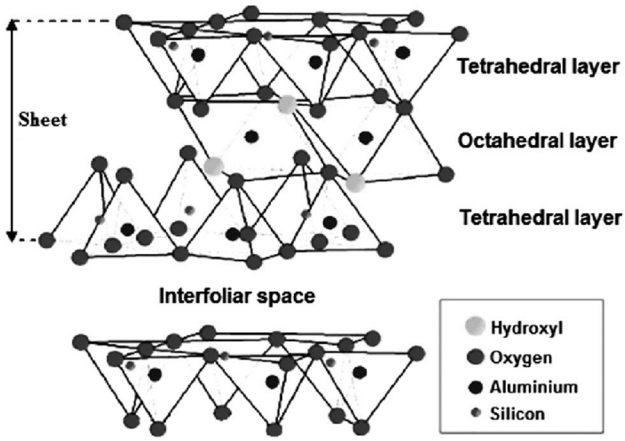

Figure 1. Structure of pyrophyllite (36)

The price of pyrophyllite and its applications are highly dependent on its Al_2O_3 and impurity contents. Recently, resources of high-grade pyrophyllite are limited due to the continuous use of high-grade pyrophyllite with low impurity contents. Therefore, techniques such as flotation, electrification, and electrolysis are required to improve the purity of low-grade pyrophyllite and remove Fe, Ti, Cl, and S (37).

APTEFF, 52, 1-273 (2021) UDC: 615.281/.282:546.62'284:577.67
DOI: https://doi.org/10.2298/APT2152189B BIBLID: 1450-7188 (2021) 52, 189-201
BY-NC-ND
Review paper

According to recent analyses of Harbinja et al. (38) pyrophyllite from the mine Parsovići site, Konjic, AD Harbi Ltd., Sarajevo, Bosnia and Herzegovina is composed of 64.15% SiO_2, 15.10% Al_2O_3, 0.64% K_2O, 0.31 % Na_2O, 1.06% MgO, 6.65% CaO, 1.57% Fe_2O_3, 0.37% FeO, <0.02% SO_3, <0.17% TiO_2, 0.64% K_2O, 0.18 % P_2O_5, <0.001% BaO, 5.18% H_2O. Loss on ignition was found to be 9.46%, and the pH value of pyrophyllite determined in distilled water (10 g per 100 ml) was 9. This source and quality of pyrophyllite were used in the researches (39-42). Stotzky (43) investigated respiration of *Agrobacterium radiobacter* by clay minerals of the 2:1 type and 1:1 type. Contrary to most 2:1 mineral types pyrophyllite had relatively little influence on respiration and it did not maintain favourable pH for sustained respiration in either buffered or nonbuffered systems. Many clays, including pyrophyllite, showed cytotoxicity to several macrophage cell types and had haemolytic activity towards several RBCs. Larger and longer particle sizes and longer fibres caused more adverse effects. A dose-dependent effect on cytotoxicity or lysis was recorded (44).

Although fibrosis and pneumoconiosis were observed in workers involved in the mining and processing of kaolin, montmorillonite, pyrophyllite, zeolite and different types of silicates, (44) concluded that these minerals are safe for use in cosmetic products.

World Health Organisation (45) represented Health Criteria 231 for Bentonite, kaolin, and other selected mineral clays. According to Paoletti et al. (46), 17 different mineral types were identified in the lung parenchyma of 10 deceased subjects' resident in urban areas and no occupational exposure to dust. Among 70% of minerals consisted of phyllosilicates pyrophyllite was found in 10 cases.

USE IN COSMETICS AND OTHER INDUSTRIES

In terms of better understanding pyrophyllite, its characteristics, possibilities of modification and application in the industry, several papers were published (38, 47-51). According to Wenninger et al. (52) pyrophyllite is used in cosmetics as an adsorbent, colourant, and opacifying agent. Under the Code of Federal Regulations (21CFR73.1400) (53) as a naturally occurring colour additive, it must follow the specification: Pb not more than 20 ppm and As not more than 3 ppm. Pyrophyllite can also be for externally applied cosmetics (21CFR73.2400) (54). Other applications of pyrophyllite are also in refractories, rubber, ceramics, insecticides, plastics, paint, roofing, bleaching powder, textiles, cordage, and wall boar (44).

Naturally, hydrophobic pyrophyllite modified to hydrophilic by treatment with pre hydrolyzed *N*-(2-aminoethyl)-3-aminopropyltrimethoxysilane (APEO) coupling agent was efficient for the removal of 4-nitrophenol from aqueous solution (55). Pyrophyllite modified by coating with aminosilane 3-(2-aminoethylamino) propyl-methyldimetoxysilane (APMDS) eliminated 90% of Fe (III) from aqueous medium compared to 54% by natural pyrophyllite, and in the case of Cu (II) removed 60% of this metal compared to 18% in the case of natural pyrophyllite (56). The adsorption of cationic Methylene Blue (MB) and anionic Procion Crimson H-EXL (PC) dyes from an aqueous medium on pyrophyllite was investigated in the study of Gücek et al. (2005) (57). Pyrophyllite showed good sorptive properties for the versatile removal of cationic and anionic dyes. El Gaidoumi et al. (36) used copper-impregnated pyrophyllite (Cu/RC) as the catalyst for wet peroxide oxidation (CWPO) of phenol. The CWPO catalyst had a good activity after five successive runs at

APTEFF, 52, 1-273 (2021) UDC: 615.281/.282:546.62'284:577.67
DOI: https://doi.org/10.2298/APT2152189B BIBLID: 1450-7188 (2021) 52, 189-201
BY-NC-ND
Review paper

optimized conditions. Murtić et al. (42) investigated the use of pyrophyllite as the soil conditioner. The results of their study showed that the substitution of fertilizers with the pyrophyllite in the amount of 25% and 50%, respectively of the recommended fertilizer rate increased lettuce yield and total antioxidant activity compared to the control treatment that supports the hypothesis that pyrophyllite could be used as remediation material in soils polluted with heavy metals (Cu, Zn, Pb and Mn). Adamović et al. (35) investigated the effect of pyrophyllite on the quality of maize plant silage, primarily on the production of organic acids, pH value, quality assessment and microbiological safety. These authors found that the addition of 0.5 and 1.0 % pyrophyllite to chopped corn green mass resulted in first-class silages based on the content and interrelationship of lactic, acetic and butyric acid, as well as the pH values.

ANTIMICROBIAL ACTIVITY

The antimicrobial activity of pyrophyllite is still insufficiently analysed and examined, but recent studies have shown that the mineral pyrophyllite possesses an antibacterial one. The specific capability of the pyrophyllite against several of the most important foodborne pathogens is detailed in Table 1. Park et al. (58) found that pyrophyllite was effective in bacteriophage MS2 removal under flow-through conditions with higher removal capacity (8.17×10^6 pfu/g) with no fluoride present. A study by Kang et al. (59) demonstrated that pyrophyllite could be used as adsorptive filter materials in the removal of bacteria (*E. coli*). The results of research conducted by Monsif et al. (60) showed that the epoxy/crude clay nanocomposites, which content pyrophyllite, exhibited a high inhibition action against *E. coli* and *S. aureus*. In recent research conducted at the Faculty of Technology and Metallurgy in Belgrade (39), it was determined that pyrophyllite (from the mine Parsovići site, Bosnia and Herzegovina) can inhibit the development of gram-negative bacteria *Escherichia coli* (67.20-84.80%) and gram-positive bacteria *Enterococcus faecalis* (74.42-81.33%). Better results were achieved by using finer granulation of pyrophyllite. In contrast, no inhibition of *Staphylococcus aureus* development was found, probably due to the pronounced defence mechanism of this bacterium. Faculty of Agriculture in Banja Luka (40) performed *in vitro* testing of the influence of fractions of modified, microalloyed and micronized pyrophyllite of different granulations added in different concentrations to the nutrient medium PDA on the growth of fungal phytopathogens *Fusarium oxysporum*, *Phoma glomerata* and *Rhizoctonia solani*. The best results were obtained with growth restriction of *P. glomerate* (microgelated granulation <100 μm and mechanically modified granulation <45 μm). In *F. oxysporum*, the best effect on fungal growth *in vitro* was exerted by microgelated fractions 0-2 mm, as well as mechanically modified fractions 0-2 mm and <45 μm, while the weakest results were achieved in *R. solani*.

The effect of mechanically modified pyrophyllite fractions of <45 μm and 0-2 mm (10%) on the control of potato infection by the phytopathogenic fungus *F. oxysporum* Schlecht was investigated by Faculty of Agriculture in Banja Luka (41). Based on the obtained results of *in vivo* experiments, it was seen that pyrophyllite, and especially the mechanically modified fraction 0-2 mm, significantly reduced the symptoms of wilting of plants and thus reduced the loss of potato yield in soil inoculated with *F. oxysporum*. The obtained results indicated the possibility of using pyrophyllite in the biological control of soil contaminated with *F. oxysporum*, which would greatly contribute to the production of

BY-NC-ND

food. Adamović et al. (35) recorded that the number of aerobic mesophilic bacteria, as well as the number of yeasts, was lower in the whole corn plant silages with the addition of 0.5 and 1.0% pyrophyllite than in the control (without the addition of pyrophyllite). The concentration of added pyrophyllite did not affect the number of aerobic mesophilic bacteria that was 3.7 x 10^6 cfu/g in both cases. The presence of yeast was significantly higher in silage without the addition of pyrophyllite (0%) and decreased with increasing dose of pyrophyllite from 0.5% to 1.0% and according to the order of treatment was 1.3 x 10^5, 1.1 x 10^5 and 0.69 x 10^5 cfu/g, respectively. The presence of moulds in all three tested silages was negligible (<100 cfu/g) and could not be related to the tested doses of pyrophyllite in the silage. Aluminium as the major component of pyrophyllite allows bacteria removal due to their adhesion to the surfaces of this clay (59). Nevertheless, it was found that aluminium is, also, able to attach to a bacterial surface envelope, interfering with the influx of nutrients or efflux of waste from bacteria.

Table 1. Antimicrobial activities of pyrophyllite

Pyrophyllite form	Microorganism	Effect	References
Pyrophyllite	Aerobic mesophilic bacteria Yeasts	Growth inhibition (reduction in CFU/g)	35
Pyrophyllite	Bacteriophage MS2	Decrease in MS2 concentration	58
Washed pyrophyllite	*E. coli*	Bacteriostatic effect	59
Epoxy/clay nanocomposites	*E. coli* *S. aureus*	Bacteriostatic effect	60
Ag/nanocomposite (pyrophyllite based)	*E. coli* *S. aureus* *Acinetobacter baumannii* *Pseudomonas aeruginosa*	Growth inhibition (after exposure 24h)	61

CURRENT ACTIVITY

Besides heavy metals (19-21), plant extracts (3, 4), waste biomass (4, 5), chitin and its modification chitosan (6-8, 22-25) lactic acid bacteria (26) and other substances that have antiviral, antibacterial and antifungal properties, some mineral adsorbents also possess antimicrobial activity.

Examples of that are mineral adsorbents like preparations based on bentonite (15, 27), montmorillonite (16, 28), smectite (17), zeolites (18, 29) hybrid McM-14 (30) as well as pyrophyllite (monoclinic mineral from monoclinic phyllosilicates) that also possesses antibacterial properties (35, 39) and antifungal properties against plant fungal pathogens *F. oxysporum*, *P. glomerata* and *R. solani* (40, 41).

To date, only a few reports about the safety of using pyrophyllite in different aspects has been published. According to Elmore (44), pyrophyllite and similar types of minerals are safe for use in cosmetic products, although fibrosis and pneumoconiosis were observed

BY-NC-ND

in workers involved in the mining and processing of kaolin, montmorillonite, pyrophyllite, zeolite and different types of silicates. Also, The Code of Federal Regulations of the United States of America (21 CFR573900) (62), allows the use of pyrophyllite as the complete meals additive for animal nutrition up to 2%. The development of novel technological ingredients with antimicrobial potential and different food/feed protection functions is of great scientific importance and technological interest.

CONCLUSION

One of the insufficiently tested mineral compounds that have antimicrobial activity is certainly pyrophyllite (the monoclinic mineral from the group of phyllosilicates). Based on the published results of such pyrophyllite, as an antibacterial agent (against *E. coli*, *E. faecalis* and *S. aureus*), antifungal agent (against *F. oxysporum*, *P. glomerata* and *R. solani*) as well as for biological control of *F. oxysporum* in the soil for growing potato, it would be necessary to continue research of its antimicrobial activity against a wider range of fungal and bacterial pathogens. A particularly interesting subject of new research is going to be the possibility of pyrophyllite modification and its more appropriate physical form (different particle granulation) to improve the efficient application of this mineral in practical conditions. Pyrophyllite as advanced antimicrobial material is also worth considering as a future option for its increasing applicability in the food/feed safety sector.

Acknowledgements

The paper is within the contract on the implementation and financing of scientific researches in 2021 between the Institute for Science Application in Agriculture, Belgrade and the Ministry of Education, Science and Technological Development of the Republic of Serbia, contract number: 451-03-9/2021-14/ 200045.

REFERENCES

1. Grass, G.; Rensing, C.; Solioz, M. Metallic copper as an antimicrobial surface. *Appl. Environ. Microbiol*. **2011**, *77*(5), 1541-1547.
2. Weaver, L.; Michels, H. T.; Keevil, C. W. Potential for preventing of fungi in air-conditioning systems constructed using copper instead of aluminium. *Lett. Appl. Microbiol.* **2010***, 50*(1), 18-23.
3. Tewari, B. B.; Sing, S. Studies of medical application of natural antifungals – metal hexacyanoferrate(ii) complexes. *Rev. Soc. Quím. Perú*. **2006**, *72*(4), 197-204.
4. Dellavalle, P. D.; Cabrera, A.; Alem, D.; Larrañaga, P.; Ferreira, F.; Rizza, M. D. Antifungal activity of medicinal plant extracts against phytopathogenic fungus *Alternaria* spp. *Chil. J. Agric. Res.* **2011***, 71*(2), 231-239.
5. Suba, V.; Rathika, G.; Ranjith Kumar, E.; Saravanabhavan, M.; Nayak Badavath, V.; Thangamani, K. S. Enhanced adsorption and antimicrobial activity of fabricated *Apocynaceae* leaf waste activated carbon by cobalt ferrite nanoparticles for textile effluent treatment. *J. Inorg. Organomet. Polym. Mater.* **2019**, *29*, 550-563.
6. Zhong, Z.; Chen, R.; Xing, R. Synthesis and antifungal properties of sulfanilamide derivatives of chitosan. *Carbohydr. Res.* **2007***, 34*, 2390-2395.

BY-NC-ND

7. Ziani, K.; Fernández-Pan, I.; Royo, M.; Mate, J.I. Antifungal activity of films and solutions based on chitosan against typical seed fungi. *Food Hydrocoll.* **2009***, 23*, 2309-2314.
8. Mohamed, R. R.; Fekry, A. M. Antimicrobial and anticorrosive activity of adsorbents based on chitosan schiff's base. *Int. J. Electrochem. Sci.*. **2011***, 6*, 2488-2508.
9. Behroozian, S.; Svensson, S. L.; Li, L. Y.; Davies, J. E. Broad-Spectrum Antimicrobial and Antibiofilm Activity of a Natural Clay Mineral from British Columbia, Canada. *mBio*, **2020**, *11*(5), 1-14, e02350-20.
10. Morrison, K. D.; Underwood, J. C.; Metge, D. W.; Eberl, D. D.; Williams, L. B. Mineralogical variables that control the antibacterial effectiveness of a natural clay deposit. *Environ. Geochem. Health*. **2014**, *36*(4), 613-631.
11. Morrison, K. D.; Misra, R.; Williams, L. B. Unearthing the antibacterial mechanism of medicinal clay: a geochemical approach to combating antibiotic resistance. *Sci. Rep*. **2016**, *6*(1), 1-13.
12. Otto, C. C.; Haydel, S. E. Exchangeable ions are responsible for the in vitro antibacterial properties of natural clay mixtures. *PLoS One*. **2013**, *8*(5), e64068.
13. Williams, L. B.; Metge, D. W.; Eberl, D. D.; Harvey, R. W.; Turner, A. G.; Prapaipong, P.; Poret-Peterson, A. T. What makes a natural clay antibacterial? *Environ. Sci. Technol.* **2011**, *45*(8), 3768-3773.
14. Williams, L. B.; Haydel, S. E. Evaluation of the medicinal use of clay minerals as antibacterial agents. *Int*. *Geol. Rev*. **2010**, *52*(7-8), 745-770.
15. Krishnan, B.; Mahalingam, S. Facile synthesis and antimicrobial activity of manganese oxide/bentonite nanocomposites. *Res. Chem. Intermed.* **2017***, 43*, 2351–2365.
16. Das, G.; Dutta Kalita, R.; Gogoi, P.; Buragohain, A. K.; Karak, N. Antibacterial activities of copper nanoparticle-decorated organically modified montmorillonite/epoxy nanocomposites. *Appl. Clay Sci.* **2014**, *90*, 18-26.
17. Ituah, F. A. The modification of Laponite®RD with silver and copper and investigation of their antibacterial activity. PhD Thesis, University of Wolverhampton, UK, June 2012.
18. Demirci, S.; Ustaoğlu, Z.; Gonca, G. A.; Sahin, F.; Nurcan Baç, N. Antimicrobial Properties of Zeolite-X and Zeolite-A Ion-Exchanged with Silver, Copper, and Zinc Against a Broad Range of Microorganisms. *Appl. Biochem. Biotechnol.* **2013***, 172(3),* 1652-1662.
19. Kansoh, A. L.; Youssef, E. A. M.; Abd-El-Ghaffar, M. A. Studies on the antifungal activities of the novel synthesized chelating co-polymer emulsion lattices and their silver complexes. *Biotechnol. Agron. Soc. Environ*. **2008***,12*(3), 231-238.
20. Vincent, M.; Duval, R. E.; Hartemann, P.; Engels-Deutsch, M.. Contact killing and antimicrobial properties of copper. *Appl. Microbiol.* **2017***, 124*, 1032-1046.
21. Alananbeh, K. M.; Al-Refaee, W. J.; Al-Qodah, Z. Antifungal effect of silver nanoparticles on selected fungi isolated from raw and wastewater. *Indian J. Pharm. Sci.,* 2017*, 79*(4), 559-567.
22. Hernandez-Patlan, D.; Solis-Cruz, B.; Hargis, B. M.; Tellez, G. Chitoneous materials for control of foodborne pathogens and mycotoxins in poultry. In *Chitin-Chitosan - Myriad Functionalities in Science and Technology,* 1st Edition (Ed. Rajendra Sukhadeorao Dongre) Intech-Open Publishers, London, UK, 2018; pp 261-282.
23. Guerra-Sánchez, M. G.; Vega-Pérez, J.; Velázquez-del Valle, M. G.; Hernández-Lauzardo, A. N. Antifungal activity and release of compounds on *Rhizopus stolonifer* (Ehrenb.:Fr.) Vuill. by effect of chitosan with different molecular weights. *Pestic. Biochem. Physiol.* **2009***, 93*(1), 18-22.
24. Mohanasrinivasan, V.; Mishra, M.; Singh Peliwal, J.; Singh, S. Kr.; Selvarajan, E.; Suganthi, V.; Subathra Devi, C. Studies on heavy metal removal efficiency and antibacterial activity of chitosan prepared from shrimp shell waste. *3 Biotech.* **2014***, 4*(2), 167-175.
25. Benhabiles, O. M. S.; Salah, R.; Lounici, H.; Drouiche, N.; Goosen, M. F. A.; Mamer, I. N. Antibacterial activity of chitin, chitosan and its oligomers prepared from shrimp shell waste. *Food Hydrocoll.* **2012**, *29*(1), 48-56.

BY-NC-ND

26. Sadiq, F. A.; Yan, B.; Tian, F.; Zhao, J.; Zhang, H.; Chen, W. Lactic acid bacteria as antifungal and anti-mycotoxigenic agents: A comprehensive review. *Compr. Rev. Food Sci. Food Saf.* **2019***, 18*(5), 1403-1436.
27. Adamović, M.; Bočarov-Stančić, A.; Pantić, V.; Vukić-Vranješ, M.; Jovanović, R.; Panić, M. Effect of a pelleting agent on microbiological and mycotoxicological safety of feed mixtures. *Biotechnol. Anim. Husb*. **2011**, *27*(3), 1209-1217.
28. Stevanović, M.; Bajić, Z. J.; Veličković, Z. S.; Karkalić, R. M.; Pecić, Lj., Otřísal, O.; Marinković, A. D. Adsorption performances and antimicrobial activity of the nanosilver modified montmorillonite clay. *Desalin. Water Treat.* **2020***, 187*, 345-369.
29. Savi, G. D.; Cardoso, W. A.; Furtado, B. G.; Bortolotto, T. Antifungal activities against toxigenic Fusarium species and deoxynivalenol adsorption capacity of ion-exchanged zeolites. *J. Environ. Sci. Health B*. **2017***, 53*(3), 1-7.
30. Bouchikh, N.; Adjdir, M.; Bendeddouche, K. C.; Bouazza, Dj.; Mokhtar, A.; Bennabi, F.; Tabti, H. A.; Sehmi A.; Miloudi, H. Enhancement of adsorption capacity of low cost mesoporous MCM-41 and their antibacterial and antifungal activities. *Mater. Res. Express*. **2020**, *6*, 125oj7.
31. Klun, T. M.; Dunshee, W. K.; Schaffer, K. R.; Andrews, J. F.; Neu, D. M.; Scholz, M. T. Hydrophilic polypropylene fibres having antimicrobial activity. United States Patent No. US 7,879,746 B2, Feb. 1, 2011.
32. Dyatkina, N. B.; Roberts, C. D.; Keicher, J. D.; Dai, Y.; Nadherny, J. P.; Zhang, W.; Schmitz, U.; Kongpachith, A.; Fung, K.; Novikov, A. A.; Lou, L.; Velligan, M.; Khorlin, A. A.; Chen, M. S. Minor groove DNA binders as antimicrobial agents. 1. Pyrrole tetraamides are potent antibacterials against vancomycin resistant *Enteroccoci* and methicillin resistant *Staphylococcus aureus. J. Med. Chem.* **2002***, 45*(4), 805-817.
33. Al-Nazhan, S.; Al-Judai, A. Evaluation of antifungal activity of mineral trioxide aggregate. *J. Endod.* **2003**, *29*(12), 826-827.
34. Essalhi, A.; Essalhi, M.; Toummite, A.; Mostadi, A. El.; Raddi, Y. Mineralogical and textural arguments for a metasomatic origin of the Ougnat pyrophyllite, Eastern Anti-Atlas, Morocco. *J. Mater. Environ. Sci*. **2017**, *8*(1), 22-32.
35. Adamović, M. J.; Stojanović, M. D.; Harbinja, M. M.; Maslovarić, M. D.; Bočarov-Stančić, A. S.; Pezo, L. L. Efficiency investigation of the use of pyrophyllite in ensiling maize plant. *Food Feed Res*. **2020**, *47*(2) 109-118.
36. El Gaidoumi, A.; Doña-Rodrigues, J. M.; Palido Melián, E.; González-Diaz, O. M.; Mavio, J. A.; El Bali, B.; Kherbeche, A. Catalytic Efficiency of Cu-supported Pyrophyllite in heterogeneous catalytic oxidation of phenol. *Arab. J. Sci. Eng.* **2019***, 44*(7), 6313-6325.
37. Kim, B. J.; Cho, K. H.; Chang, B.; Kim, H. S.; Lee, S. G.; Park, C. Y.; Lee, S.; Choi, N. C. Sequential microwave roasting and magnetic separation for removal of Fe and Ti impurities in low-grade pyrophyllite ore from Wando mine, South Korea. *Miner. Eng.* **2019**, *140*, 105881.
38. Harbinja, M.; Hodžić, A.; Kaljanac, A.; Selman, F.; Radulović, D.; Andrić, Lj.; Stojanović, J.; Petrović, M. *Pyrophyllite - the mineral of the future for use in agriculture* [Unpublished monograph in Bosnian]. **2019**. AD Harbi, Sarajevo, Bosnia and Herzegovina.
39. Faculty of Technology and Metallurgy in Belgrade. Report on testing the potential antimicrobial activity of pyrophyllite samples [Research report in Serbian]. 2018. AD Harbi Ltd. Sarajevo, Bosnia and Herzegovina.
40. Faculty of Agriculture in Banja Luka. Report of investigation of mechanically and microgelated modified pyrophyllite on suppression of mycelial growth of phytopathogenic fungi and its possible application as active substances in plant protection products [Research report in Serbian]. 2019. AD Harbi Ltd. Sarajevo, Bosnia and Herzegovina.
41. Faculty of Agriculture in Banja Luka. *In vivo* investigations of pyrophyllite effect on *Fusarium oxysporum* infection on the potato [Research report in Serbian]. 2020. AD Harbi Ltd. Sarajevo, Bosnia and Herzegovina.

BY-NC-ND

42. Murtić, S.; Zahirović, Ć.; Karić, L.; Jurković, J.; Čivić, H.; Sijahović, E. Use of pyrophyllite as soil conditioner in lettuce production. *Nat. Environ. Pollut. Technol.* **2020***, 19*(1), 355-359.
43. Stotzky, G. Influence of clay minerals on microorganisms: II. Effect on various clay species, homoionic species, and other particles on bacteria. *Can. J. Microbiol.* **1966***, 12*, 831–848.
44. Elmore, A. R. Final Report on the Safety Assessment of Aluminum Silicate, Calcium Silicate, Magnesium Aluminum Silicate, Magnesium Silicate, Magnesium Trisilicate, Sodium Magnesium Silicate, Zirconium Silicate, Attapulgite, Bentonite, Fuller's Earth, Hectorite, Kaolin, Lithium Magnesium Silicate, Lithium Magnesium Sodium Silicate, Montmorillonite, Pyrophyllite, and Zeolite. *Int. J. Toxicol.* **2003***, 22*(1), 37–102.
45. World Health Organization. Environmental Health Criteria 231 for bentonite, kaolin, and other selected mineral clays, EHC 231, Geneva, 2005; pp 1-196.
46. Paoletti, L.; Batisti, D.; Caiazza, S.; Petrelli, M. G.; Taggi, F.; De Zorzi, L.; Dina, M. A.; Donelli, G. Mineral particles in the lungs of subjects resident in the Rome area and not occupationally exposed to mineral dust. *Environ. Res.* **1987***, 44*, 18–28.
47. Keren, R.; Sparks, D. L. Effect of pH and ionic strength on boron adsorption by pyrophyllite. *Soil. Sci. Soc. Am. J.* **1994***, 58*, 1095-1100.
48. Sánchez-Soto, P. J.; Justo, A., & Pérez-Rodríguez, J. L. Grinding effect on kaolinite-pyrophyllite-illite natural mixtures and its influence on mullite formation. *J. Mater. Sci.* **1994***, 29*(5), 1276-1283.
49. Erdemoglu, M.; Erdemoglu, S.; Sayılkan, F.; Akarsu, M.; Sener., S.; Sayılkanc, H. Organo-functional modified pyrophyllite: preparation, characterisation and Pb (II) ion adsorption property. *Appl. Clay Sci.* **2004***, 27*, 41 – 52.
50. Adamović, M., Stojanović, M. *Pyrophyllite (natural and modified-refined) - functional food for plants and animals* [Research report in Serbian]. **2019**, AD Harbi Ltd., Sarajevo, Bosnia and Herzegovina.
51. Adamović, M. *Program of research and development of products based on pyrophyllite in animal husbandry and veterinary medicine, grain storage, fisheries and mushroom growing* [Unpublished program in Serbian]. **2019**. AD Harbi Ltd., Sarajevo, Bosnia and Herzegovina.
52. Wenninger, J. A.; Canterbury, R. C.; McEwen, Jr., G. N. *International Cosmetic Ingredient Dictionary and Handbook*, 8th ed., vols. 1–3, Washington, DC: CTFA, 2000.
53. Code of Federal Regulations – CFR. Title 21 – Food and Drugs, Chapter I - Food and Drug Administration, Department of Health and Human Services, Subchapter A – General, Part 73 – Listing of colour additives exempt from certification, Subpart B – Drugs*, Sec. 73.140 Pyrophyllite,* 2020. (https://www.accessdata.fda.gov/scripts/cdrh/cfdocs/cfcfr/CFRSearch.cfm?fr=73.1400).
54. Code of Federal Regulations – CFR. 21 – Food and Drugs, Chapter I - Food and Drug Administration, Department of Health and Human Services, Subchapter A – General, Part 73 – Listing of colour additives exempt from certification, Subpart C – Cosmetics, *Sec. 73.240 Pyrophyllite,* 2020. (https://www.accessdata.fda.gov/scripts/cdrh/cfdocs/cfcfr/CFRSearch.cfm?fr=73.2400).
55. Sayilkan, H.; Erdemoğlu, S.; Şener, Ş.; Sayilkan, F.; Akarsu, M.; Erdemoğlu, M. Surface modification of pyrophyllite with amino silane coupling agent for the removal of 4-nitrophenol from aqueous solution. *J. Colloid Interface Sci.* **2004***, 275*(2), 530-538.
56. Talidi, A.; Ibnghazala, M.; Chakir, A.; Elkacemi, K.; Bouachrine, M. Characterisation and modification of Maroccan clay by an organic molecule and its application to the removal of iron and copper in aqueous medium. *Int. J. Innov. Res. Sci. Eng. Technol.* **2017***, 6*(7), 13743-13753.
57. Gücek, A.; Şener, S.; Bilgen, S.; Mazmancı, M. A. Adsorption and kinetic studies of cationic and anionic dyes on pyrophyllite from aqueous solutions. *J. Colloid. Interface Sci*. **2005**, *286*(1), 53-60.
58. Park, J.; Kim, J. H.; Lee C. G.; Kim, S. B. Pyrophyllite clay for bacteriophage MS2 removal in the presence of fluoride. *Water Sci. Technol.: Water Supply.* **2014***, 14*(3), 485.

BY-NC-ND

59. Kang, J. K.; Lee, C. G.; Park, J. A.; Kim, S. B.; Choi, N. C.; Park, S. J. Adhesion of bacteria to pyrophyllite clay in aqueous solution. *Environ. Technol.* **2013**, *34*(6), 703-710.
60. Monsif, M.; Zerouale, A.; Kandri, N. I.; Bertani, R.; Bartolozzi, A.; Bresolin, B. M.; Zorzi, F.; Tateo, F.; Zappalorto, M.; Quaresimin, M.; Sgarbossa, P. Multifunctional Epoxy/Nanocomposites Based on Natural Moroccan Clays with High Antimicrobial Activity: Morphological, Thermal and Mechanical Properties. *J. Nanomater*. **2019,** *2019,* 1-12.
61. Šmitran, A.; Božić, L.; Đermanović, M.; Bojanić, L.; Jelić, D. Nanocomposite (clay based) as suitable carriers for bioactive molecules: stability and antimicrobial aspect. *J. Hyg. Eng. Des.*, **2021**, *34*, 46-51.
62. Code of Federal Regulations – CFR. Title 21 – Food and Drugs, Chapter I - Food and Drug Administration, Department of Health and Human Services, Part 573 - Food additives permitted in feed and drinking water of animals. Subpart B – Food Additive Listing, *Sec. 573.900 Pyrophyllite,* 2020. (https://www.accessdata.fda.gov/scripts/cdrh/cfdocs/cfcfr/CFRSearch.cfm?fr=573.900).

APTEFF, 52, 1-273 (2021) UDC: 628.4.02:628.477.6]:502.1(497.6)
DOI: https://doi.org/10.2298/APT2152203G BIBLID: 1450-7188 (2021) 52, 203-216
BY-NC-ND
Original scientific paper

SUSTAINABLE MANAGEMENT OF WASTE-TO-ENERGY IN REPUBLIC OF SRPSKA

Brankica B. GEGIĆ, Bojana Ž. BAJIĆ, Damjan G. VUČUROVIĆ, Jovana D. GUCUNSKI, Siniša N. DODIĆ*

University of Novi Sad, Faculty of Technology, Department of Biotechnology and Pharmaceutical Engineering, Bulevar Cara Lazara 1, 21000 Novi Sad, Republic of Serbia

Received: 01 September 2021 **Revised: 30. September 2021** **Accepted: 1. October 2021**

Republic of Srpska (RS) is one of the two entities in Bosnia and Herzegovina (BiH). It is located in South-eastern Europe, in the western part of the Balkan Peninsula. As in most developing countries, waste management is based on landfilling. The constant increase in waste generation creates a growing burden on the existing waste management system and the environment. Comparing the amount of waste with GDP, despite a much lower standard, RS/BiH residents, compared to EU residents, generate far more waste for the same amount of money. All generated waste is disposed of in landfills, which causes greenhouse gas emissions and has a negative effect on the environment. On the other side, untreated waste deposited in landfills represents the loss of potential of waste as a renewable energy source. In this study, an attempt has been made to represent the possibilities of sustainable waste-to-energy management in RS with the goal to provide reliable support to decision-makers to direct waste management in a sustainable framework.

Keywords: Republic of Srpska, waste management, renewable energy, waste-to-energy, sustainable waste management

INTRODUCTION

The Republic of Srpska (RS) is one of the two entities in Bosnia and Herzegovina (BiH). It is located in South-eastern Europe, in the western part of the Balkan Peninsula, with an area of 24,857 km^2. According to the census data from 2013, the RS has a population of 1,170,342, which generate 316 kg/person/year of waste on average (1). As in most developing countries, waste management is based on landfilling. Untreated waste deposited in landfills disenables the exploitation of resources from waste and represents a considerable loss of potential revenue and an environmental threat (2).

Worldwide, 2.01 billion tons of municipal waste is generated per year, or in average 0.74 kg of waste per capita per day (3). The latest studies shows that by the end of 2025 it is expected that 4.3 billion people from urban areas will generate around 1.42 kg per capita per day or a total of 2.2 billion tons of waste annually (4), and that by the end of 2050 global waste is expected to grow to 3 billion of tons annually (3).

There is a general understanding that waste quantities will substantially increase. The drivers are increased consumption of goods in growing urban populations, changes in lifestyle, and increasing wealth of the rising middleclass (5). The constant increase in the amount of generated waste creates a growing burden on existing systems of waste manage-

* Corresponding author: Bojana Ž. Bajić, University of Novi Sad, Faculty of Technology, Bul. Cara Lazara 1, Novi Sad 21000, Republic of Serbia, e-mail: baj@uns.ac.rs

APTEFF, 52, 1-273 (2021)
DOI: https://doi.org/10.2298/APT2152203G
BY-NC-ND
UDC: 628.4.02:628.477.6]:502.1(497.6)
BIBLID: 1450-7188 (2021) 52, 203-216
Original scientific paper

ment and the environment. If this trend continues without adequate solutions in the field of waste management, the basic principles of sustainable development will be brought to question. The data shows that the rate of municipal waste generation in most cases has a larger increase compared to the degree of urbanization of society and economic development of a certain country expressed through gross domestic product (GDP) (4). However, it should be noted that developed countries, despite the fact that greater amounts of waste are generated in relation to other countries, have a highly developed waste management system with adequate facilities for its treatment, together with a strong institutional and legal framework that regulates this area. Underdeveloped and developing countries have a lower rate of waste generation, but possess a poorly developed system of waste management. The lack of appropriate waste treatment plants, as well as weak legislation, makes the negative impacts on the environment caused by waste generation more significant (6).If we compare the ratio of GDP and the amount of waste produced per capita for RS/BiH and the EU average, it can be concluded that a resident of BiH generates 0.068 kg of waste for 1 EUR, while an EU resident generates 0.018 kg of waste for the same amount of money (7, 8). Despite a much lower standard, BiH residents compared to EU residents generate far more waste for 1 EUR. This may be an indication of a lack of population awareness on waste prevention and reuse or inadequate implementation of laws and regulations that govern the field of waste.

In addition to the current trend of growing waste production, the various options of its treatment determine the degree of impact on the environment to a large extent. Given that in the RS the only way of waste disposal is landfilling, which causes a negative impact on the environment through emissions of greenhouse gases, it is estimated that emissions of greenhouse gases (GHG) resulting from the treatment of municipal waste contribute to nearly 5% of total global GHG emissions.

Methane (CH_4) emissions from landfills account for 12% of total CH_4 emissions on a global level (9). Table 1 provides an overview of GHG emissions from waste in the RS in the period 2010-2018 (10).

Table 1. Greenhouse gas emissions from waste in Republic of Srpska

Emissions CH_4 from waste landfills, Gg CO_2 equivalent*								
2010	**2011**	**2012**	**2013**	**2014**	**2015**	**2016**	**2017**	**2018**
273	301	287	256	346	275	286	303	316

*Equivalent mass of carbon dioxide (CO_2), expressed in gigagrams (1 Gg=1,000 t)

Although the developed part of Europe is of the opinion that waste is a resource and use waste for material and energy recovery, recent data shows that in the EU approximately 23% of municipal waste goes to landfills, 48% is recycled and 29% sent to waste-to-energy, with large differences between the Member States. Although, recycling and waste-to-energy are growing simultaneously in the EU, still almost half of the EU member states sent to landfills more than 40% of their municipal waste (11).The high-income countries have rigorous landfill taxes, while in low-income countries landfilling is still the cheapest option for waste disposal.The total price for the disposal of one ton of municipal waste in landfills in EU countries ranges from € 17.50 in Lithuania to € 155.50 in Sweden (12). Waste managers and decision makers in developing countries have to respond to these new challenges,

APTEFF, 52, 1-273 (2021) UDC: 628.4.02:628.477.6]:502.1(497.6)
DOI: https://doi.org/10.2298/APT2152203G BIBLID: 1450-7188 (2021) 52, 203-216
BY-NC-ND
Original scientific paper

and in recent times waste-to-energy (WtE) has been increasingly viewed as a solution to the problems derived from rising waste quantities in expanding cities as well as rapidly growing energy demands.

The objective of this study was to indicate the possibility of sustainable waste-to-energy management in RS, through reviews of legislation, data on amount and composition of municipal waste as well as a review of biochemical technology for converting waste into energy.

THE LEGAL FRAMEWORK

Due to specific structure of BiH as a country, the competence in the waste and energy sector is on the entity level. Relevant regulations governing the field of waste-to-energy management are presented in Figure 1 by the scheme of legislative framework structuring for waste and renewable energy in the EU and in RS.

The revised Waste Framework Directive 2008/98/EC sets the basic concepts and definitions regarding waste management – what is waste, what is recycling, use, etc. (13). The basic principles this Directive lays down that waste should be managed without endangering human health and the environment, and especially without the risk of impacts on water, air, soil, plants or animals, without causing undesirable noise or odours, and without any negative effects on the environment or places of special interest. This Directive introduces the principle in which the polluter pays a fee and defines the term extended responsibility of the producer. The Waste Framework Directive from 2008 unified rules on a number of issues that have previously been the content of several regulations and directives, which simplified EU legislation on waste. The Waste Framework Directive, i.e. Directive 2008/98/EC, modified by Directive (EU) 2018/851, as part of the Circular Economy Waste Package. Directive 2018/851 makes amendments to Directive 2008/98/EC on waste (The Waste Framework Directive) and adds the new targets: by 2025 the preparation for re-use and recycling of municipal waste shall be increased to a minimum of 55%, by 2030 minimum of 60% and by 2035 a minimum of 65% by weight; by the end of 2023, bio-waste must be separated and recycled at source, or must be collected separately and not mixed with other types of waste.

Promoting renewable forms of energy is one of the goals of the EU energy policy. That goal is pursued by Directive (EU) 2018/2001 of the European Parliament and of the Council on the promotion of the use of energy from renewable sources (14).Directive (EU) 2018/2001 replaced Directive 2009/28/EC, which established a common legal framework and in a unique manner regulates the encouragement for the use of electricity produced from renewable sources in the internal market and promoting the use of biofuels or other renewable fuels for transport. While in the old Directive, i.e. 2009/28/EC, the target for the share of electricity produced from renewable energy sources was 20% for 2020, Directive (EU) 2018/2001established a binding Union target of a share of at least 32 % of renewable energy for 2030.

In the RS, the Law on Waste Management (15) is harmonized with Directive 2008/98/EC. The aim of this Law is to provide and ensure the conditions for waste management in a way that does not endanger human health and the environment. According to the waste hierarchy, a top priority is waste prevention, in particular by developing clean technologies and rational use of natural resources. The next priority is reuse and recycling, separation of secondary raw

APTEFF, 52, 1-273 (2021)
DOI: https://doi.org/10.2298/APT2152203G
BY-NC-ND
UDC: 628.4.02:628.477.6]:502.1(497.6)
BIBLID: 1450-7188 (2021) 52, 203-216
Original scientific paper

materials from waste and the use of waste as an energy source. The law established procedures and methods for waste disposal, remediation of uncontrolled landfills, monitoring existing and newly established landfills and raising awareness on waste management.

Figure 1. The scheme of legislative framework structuring for Waste and Renewable Energy in EU and in Republic of Srpska

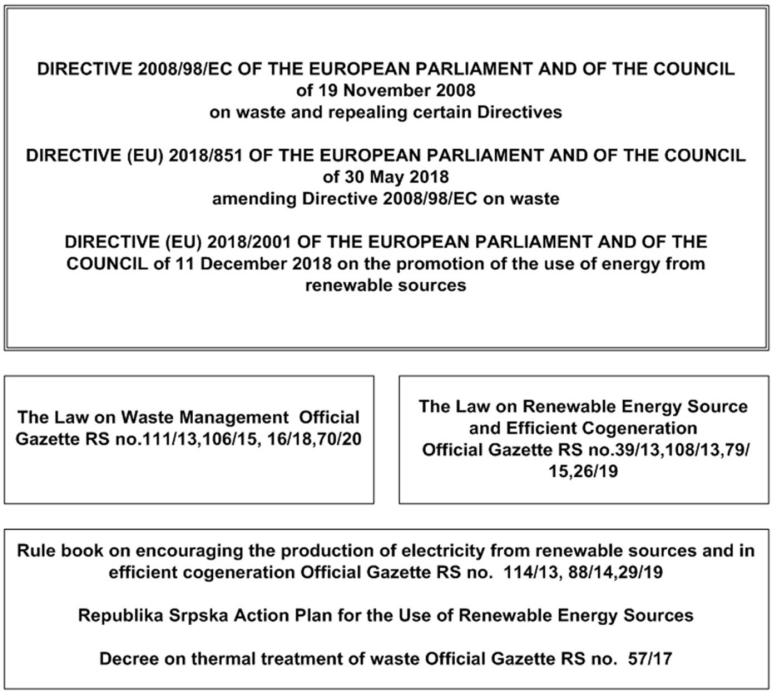

The adoption of the Law on Renewable Energy Sources and Efficient Cogeneration(16) in 2013 fully defined the legislative framework and enabled the functioning of the system of incentives for all energy sources prescribed by law and thus created conditions for unobstructed fulfilment of obligations under the Energy Community Treaty (17) in terms of meeting the defined targets on the participation of energy from renewable sources in gross final energy consumption. The Law governs the planning and encourages the production and consumption of energy from renewable sources and efficient cogeneration, technologies for renewable energy use, incentive measures for the production of electricity using renewable energy sources and efficient cogeneration, implementation of the system of subsidies for energy production from renewable sources and construction of plants for the production of electricity from renewable energy sources and other issues of importance for this area. In addition, the aim of this Law is the realization of the energy policy in terms of achieving binding targets of energy from renewable energy sources compared to the final energy consumption in RS, contribution to environmental protection, supporting the objectives to mitigate climate change, contributing to sustainable development, rational use of

APTEFF, 52, 1-273 (2021)
DOI: https://doi.org/10.2298/APT2152203G
BY-NC-ND
UDC: 628.4.02:628.477.6]:502.1(497.6)
BIBLID: 1450-7188 (2021) 52, 203-216
Original scientific paper

primary energy sources, increasing energy security, improving the diversification of sources, etc.

According to the Law, the Energy Regulatory Commission of the RS has enacted a number of bylaws governing and stimulating of electricity production from renewable energy sources and its efficient cogeneration, licensing, issuing of certificates for production facilities that produce electricity from renewable energy sources or efficiently use cogeneration and issuing a guarantee on the origin of the electricity and decision making on the value of guaranteed purchase prices and premiums for electricity produced from renewable energy sources or its efficient cogeneration. The costs of renewable energy sources charges are borne by the final consumers, through the electricity bill, to which a unit renewable energy sources fee was added. For 2021, based on the Decision of the Regulatory Commission, the amount of the fee for encouraging the production of electricity from renewable sources is regulated and amounts to 0.0033 EUR / kWh (18)

OVERVIEW OF THE WASTE AND RENEWABLE ENERGY SECTOR

In Europe, as in the world, the share of electricity produced from renewable energy sources is gradually increasing, thanks to energy policies, a new social paradigm and the affordable price of technology. In 2019, renewable energy represented 19.7 % of the energy consumed in the EU-27, only 0.3 % short of the 2020 target of 20 %. With more than half of energy from renewable sources in its gross final consumption of energy, Sweden (56.4 %) had by far the highest share among the EU Member States in 2019, ahead of Finland (43.1 %), Latvia (41.0 %), Denmark (37.2 %) and Austria (33.6 %). At the opposite end of the scale, the lowest proportions of renewables were registered in Luxembourg (7.0 %), Malta (8.5 %), the Netherlands (8.8 %) and Belgium (9.9 %) (19).The waste management and resource management sectors provided about 3 million jobs in the EU in 2016 and employment has increased by 79 % since the year 2000 (20).

In the BiH Framework Energy Strategy until 2035 (agreed with the entities), one of the strategic priorities for achieving security of supply and creating sustainable development and a competitive energy sector is to use the potential of renewable energy sources. Most of the energy produced in the RS comes from non-renewable energy sources. These are mainly domestic coal, and also oil and natural gas which are imported. All these fuels represent significant sources of pollution and emissions of greenhouse gases (21). Combustion of fossil fuels is the largest cause of global warming due to CO_2, sulfur, and nitrogen compounds emissions. The problem with non-renewable energy sources is in their quantity and prevalence. Fossil fuels reserves are limited and are quickly disappearing, and due to the concentration of energy sources in few areas around the world, the use of non-renewable fuels has created a system of interdependence, so the countries that import fossil fuels are in a subordinated position (22). In contrast to the non-renewable, RES represents energy sources used to produce electricity or heat, or any useful work, and whose reserves are constantly or cyclically renewed.

According to the Report on the work of the Energy Regulatory Commission, an overview of the realized electricity production in RS in the period 2015-2019 is presented in Figure 2. The realized electricity production by technologies in RS in 2019 is shown in Figure 3 (23).

APTEFF, 52, 1-273 (2021)
DOI: https://doi.org/10.2298/APT2152203G
BY-NC-ND
UDC: 628.4.02:628.477.6]:502.1(497.6)
BIBLID: 1450-7188 (2021) 52, 203-216
Original scientific paper

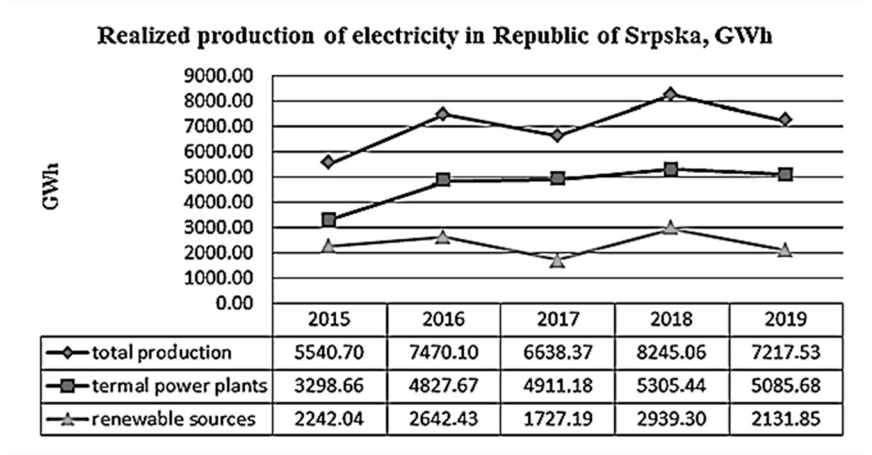

	2015	2016	2017	2018	2019
total production	5540.70	7470.10	6638.37	8245.06	7217.53
termal power plants	3298.66	4827.67	4911.18	5305.44	5085.68
renewable sources	2242.04	2642.43	1727.19	2939.30	2131.85

Figure 2. Realized electricity production in the period 2015-2019

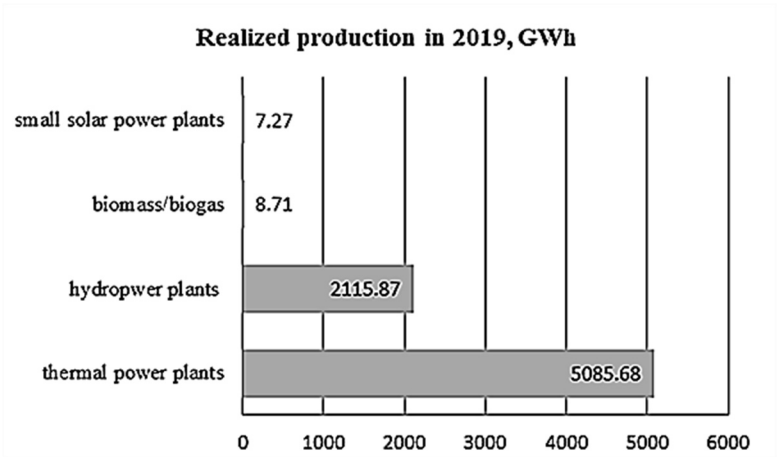

Figure 3. Realized electricity production by technologies

In the process of EU integration, BiH/RS has provided harmonization of legislation with EU legislation in the field of waste management. Also, BiH committed to becoming part of the internal EU energy market through the Energy Community Treaty, signed in 2005. By the Treaty, in 2012, the Council of Ministers adopted a Decision on the implementation of Directive 2009/28 on the production of electricity from renewable energy sources. The provisions of the agreement contain the requirements of the EU and BiH's international obligations in the field of the energy sector. Alignment of legislation with the European acquis is a complex task, as it involves extensive and substantial changes in the waste sector, as well as a comprehensive reform of the energy sector. According to the obligations assumed by signing the contract, the state goal of BiH was to achieve a share in renewable energy sources in the gross final energy consumption of 40% until 2020 (24). In submitted Annual implementation report for BiH it is registered a 35.97% renewable share in 2019 (25).

APTEFF, 52, 1-273 (2021)
DOI: https://doi.org/10.2298/APT2152203G
BY-NC-ND
UDC: 628.4.02:628.477.6]:502.1(497.6)
BIBLID: 1450-7188 (2021) 52, 203-216
Original scientific paper

The Framework Energy Strategy of BiH (26) provides a vision of the development of RES contributions in the electricity sector. The Figure 4 shows contribution of RES technologies in the electricity sector in percent (GWh)

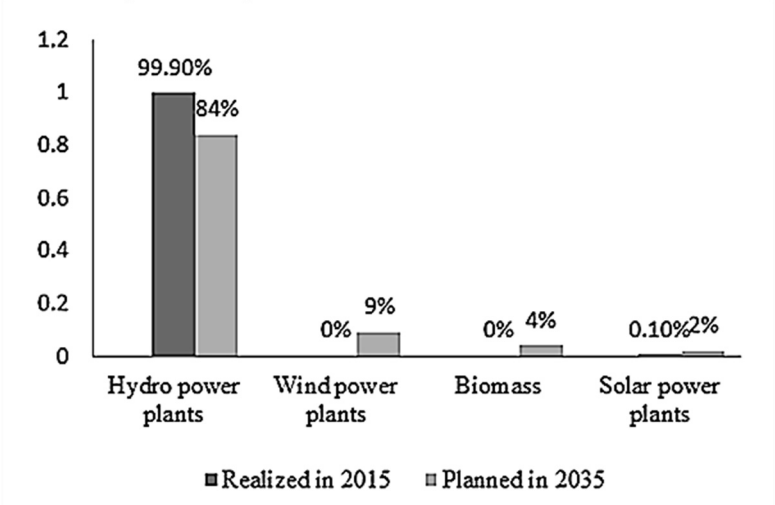

Figure 4. Contribution of RES technologies in the electricity sector in percent (GWh)

Therefore, the largest contribution to the total share of RES will be made by hydropower plants and it is assumed that it will amount to approximately 84%. However, their relative share will decrease, due to the increase in the share of other renewable energy sources. In order to achieve the estimated contribution of biomass, which is ~ 4%, it is necessary to encourage the use solid biomass in cogeneration plants.

WASTE-TO-ENERGY TECHNOLOGIES

The new concept of improved waste management (Enhanced Waste Management) sets the disposal of waste in the context of sustainability (27). This concept offers the possibility to choose the appropriate waste-to-energy technology. As shown in Figure 5, there are numerous available technologies for the conversion of waste into thermal and electrical energy, transportation fuels, chemicals or materials. These technologies are generally divided into three categories: biochemical, thermochemical, and physicochemical.

Waste-to-energy technologies are promising technologies, especially for developing countries, to turn waste into a useable form of energy (28). The success of this new concept depends not only on technological progress and achievements, but also on a variety of socio-economic barriers, such as legislation, social acceptability, economic viability, and feasibility of certain technologies in such a way as to prevent emissions of CO_2 and other pollutants into the environment (29).

APTEFF, 52, 1-273 (2021)
DOI: https://doi.org/10.2298/APT2152203G
BY-NC-ND
UDC: 628.4.02:628.477.6]:502.1(497.6)
BIBLID: 1450-7188 (2021) 52, 203-216
Original scientific paper

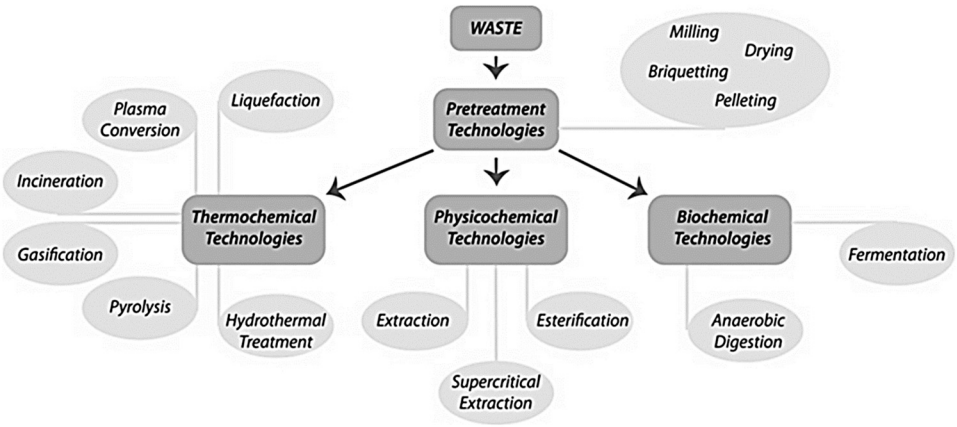

Figure 5. The scheme of the waste to energy conversion technologies

Currently, proven facilities in practice are the ones with conventional thermal treatment of waste (incineration), but there are alternative technologies for thermal treatment which are mostly in the development stage, so there is not enough data on their effectiveness and operating costs. Coupling the energy potential of waste, depending on the type and characteristics of the waste, with the strict requirements of environmental protection and public health can result in a sustainable system in both economic and environmental terms (30).

Biological treatment technologies are designed and engineered for natural biological process working with the organic rich fraction of municipal solid waste (28). These treatments include fermentation process and anaerobic digestion process.

Anaerobic digestion is natural process in which bacteria existing in oxygen-free environments decompose organic matter. The chemical composition of raw biogas includes 50-75% methane (CH_4), 25-50% carbon dioxide (CO_2). The rest of biogas makes water vapour (H_2O), and traces of oxygen (O_2), nitrogen (N_2) and hydrogen sulphide (H_2S). The main product of anaerobic digestion is a biogas, mixture of methane (50-70%) and carbon dioxide (30-50%), along with a nutrient rich effluent (digestate) (31). Biogas is an ecological fuel with a thermal power of 6-7 kWh/m^3 and can be used for commercial purposes for the production of electricity or as an energy source in households (12). Many papers present the importance of biogas produced by anaerobic digestion as a safe and environmentally friendly technology for converting waste into energy and useful products. Energy production from the anaerobic digestion of organic waste is widely recognized as a social and environmental opportunity, since it allows the reduction of waste disposal and makes waste management economically profitable. However, the profitability of these plants is strongly affected by the quantity and the quality of wastes, as well as by the availability of local subsidies (32). In many countries, the focus has been on diverting organic waste from landfills, and subsidies for construction are used very widely in order to support the installation of new capacity for treatment. In some countries electricity produced from the gas is subsidized (e.g. Germany) while in others a tax relief is provided for upgrading the gas to car fuel (e.g. Sweden). Such differences in subsidies have a significant impact on the development of technology. The energy content in biogas is significant and usually exceeds the amount of

APTEFF, 52, 1-273 (2021) UDC: 628.4.02:628.477.6]:502.1(497.6)
DOI: https://doi.org/10.2298/APT2152203G BIBLID: 1450-7188 (2021) 52, 203-216
BY-NC-ND
Original scientific paper

energy used in running the anaerobic digestion process (33). Biogas can be burned on-site to produce electricity or upgraded and used as a fuel for vehicles or as natural gas. The internal combustion engine can potentially convert the generated heat energy to electricity. Approximately 25% of the power produced from this process can be utilized for the functioning of plant and approximately 75% can be used for other purposes or sold to the local grid station (34).

Cabbai et al. (35) state that biogas is a renewable energy source and a key factor for a future fossil fuels independent society. In comparison with fossil fuels anaerobic digestion technology can reduce greenhouse gas emissions by utilizing locally available sources (36). Biogas production is growing in the European energy market and offers an economical alternative for bioenergy production (37). The latest data stated that total biogas production in Europe corresponds to about 14 billion m^3 in natural gas equivalent (36). Biogas is mainly used for electricity and heat generation. The European Union is the world leader in biogas electricity production with more than 10 GW in 2015 installed and a number of 17,400 biogas plants. In the European Union, biogas delivered 127 TJ of heat and 61 TWh of electricity in 2015(38). These data support the fact that biogas production is a great solution for two issues, energy generation and waste management (36)

WASTE GENERATION IN REPUBLIC OF SRPSKA

Based on data for the period 2010-2019 presented in Table 2, RS generates an average 406,000 tons of municipal waste per year ie. 0.97 kg of municipal waste per capita per year. According to data in the Waste management plan for RS, the composition of municipal waste in average is presented in Table 3 and Figure 6 shows the composition of municipal waste for four regional landfills in RS. In Figure 6 can be seen the composition of municipal waste at landfills in Banja Luka, Prijedor, Bijeljina, and Zvornik as well as the average for RS. According to available data on the waste composition, the organic component accounts for over 40% of total municipal waste (39). In addition to the composition of waste, an important parameter for choosing the waste-to-energy technology is the moisture content, which in this case is about 43% (12).

Table 2. Indicators regarding municipal waste

INDICATOR	2010	2011	2012	2013	2014[1]	2015	2016	2017	2018	2019
Total amount of generated municipal waste (tons)	392891	381185	376438	388767	….	403352	425962	391186	395737	399826
Average annual amount of municipal waste per capita (tons)	0.27	0.27	0.26	0.27	….	0.35	0.37	0.34	0.35	0.35
Average daily amount of municipal waste per capita (kg)	0.74	0.74	0.71	0.74		0.96	1.01	0.93	0.96	0.96

As a rule, the poor and middle-income countries have a higher share of organic components in municipal waste, which generally ranges from 40% to 85%, which is confirmed in this case. Waste categories such as paper, cardboard, plastic, glass, and metal are more present in highly developed countries.

APTEFF, 52, 1-273 (2021)
DOI: https://doi.org/10.2298/APT2152203G
BY-NC-ND
UDC: 628.4.02:628.477.6]:502.1(497.6)
BIBLID: 1450-7188 (2021) 52, 203-216
Original scientific paper

Table 3. Composition of municipal waste in RS

WASTE COMPONENTS	%W/W AVERAGE
Organic waste	40.3
Wood	2.83
Textile	3.84
Glass	4.43
Construction waste	4.3
Electronic waste	<1%
PET packaging	3.34
Foil	7.1
Gum	0.81
Plastic	5.92
Cans	1.48
Metal	2.18
Paper and paperboard	14.66
Animal waste	1.44
Other	6.91

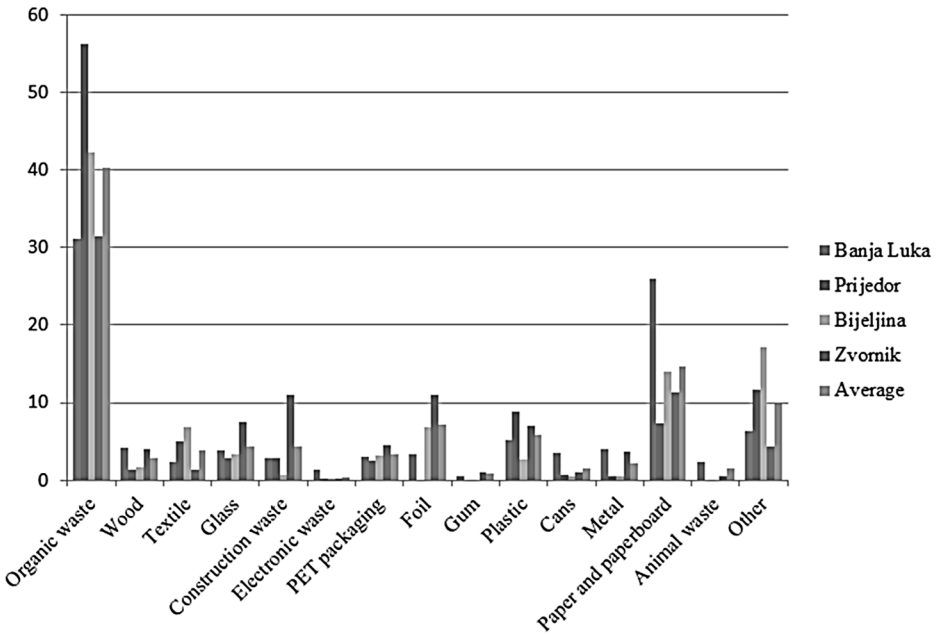

Figure 6. The composition of municipal waste in RS, %w/w

In addition to the composition of waste, an important parameter for choosing the technology of converting waste into energy is the moisture content and calorific value, which in this case are about 43% and 10,000 J/kg, respectively. Such data on waste characteristics

BY-NC-ND
UDC: 628.4.02:628.477.6]:502.1(497.6)
BIBLID: 1450-7188 (2021) 52, 203-216
Original scientific paper

gives preference to biological waste treatment. Uncontrolled and irresponsible disposed waste endangers human health and the environment, and there are numerous examples in which the damage to human health resulting from irresponsible waste management has been proven. By analyzing the available data on the amount and composition of waste in RS, which indicates a significant share of the organic component in the total amount of municipal waste, the preferred waste conversion technology could be anaerobic digestion. Waste treatment by anaerobic digestion reduces GHG emission, diverts waste from landfills, and produced biogas that can be used for energy generation. The methane content in the biogas determines the energy value of the biogas. According to literature data, biogas yield from municipal waste is 101 m^3/t, while the average methane content is 55-60% (36). Using literature data and data on the annual amount of waste in the RS, it is possible to give an estimate of the annual amount of biogas generated from municipal waste. The estimated annual amount of biogas from waste in RS is about 41 million m^3. Based on the assessment of the amount of biogas, it could be pointed out there is a need for a more detailed examination of the potential of the waste for the application of the waste-to-energy concept in RS.

As previously mentioned, different technologies are applied in energy recovery from MSW and to select the appropriate WTE technology, a comprehensive study needs to be done. The selection of the most beneficial WTE technology should be based on considering the sustainability aspects of each alternative as well as all related advantages and disadvantages in terms of environmental, economic, and social aspects. The selection of appropriate WTE technology is a multivariable complex problem that includes diverse criteria. Diverse criteria are partially or completely conflicting, so for assessing different technologies multicriteria decision-making (MCDM) methods are used as appropriate techniques (40). For analyzing decision problems in various disciplines such as waste management and renewable energy, the analytical hierarchy process is the most popular MCDM method that is widely adopted (41, 42). Since this paper aims to draw attention to the neglected potential of waste as a renewable energy source in RS, further research could apply an analytical hierarchy process to select the appropriate technology.

CONCLUSION

It is clear that population growth inevitably leads to an increase in the amount of waste as well as energy and product consumption demands of society. Thanks to its geographical position in Europe, RS (and BiH in general) has significant hydropower potential and is well placed to generate renewable energy from wind power plants, biomass, and solar energy. A series of legislative measures enabled progress in the use of renewable energy, mainly hydro potential. Other renewable energy sources are still not adequately included in the share of production from renewable energy sources. In order to achieve the estimated contribution of biomass for BiH in 2035, which is ~ 4%, it is necessary to encourage the use of solid biomass and promote biochemical technology for waste-to-energy. Waste as part of biomass used as a renewable energy source puts the system of waste management in the framework of sustainable development. Using waste as a renewable energy source would reduce greenhouse gas emissions from landfills and create the conditions for the production of energy from waste to depreciate part of the cost for waste disposal. The paper sought to draw attention to the neglected potential of waste as a renewable energy resource. The facts presented in this study should be the starting point for further comprehensive analysis of

BY-NC-ND

waste potential for energy generation and directing competent decision makers towards sustainable waste management.

Acknowledgements

This work was supported by the Ministry of Education, Science and Technological Development of the Republic of Serbia (Grant no. 451-03-9/2021-14/200134).

REFERENCES

1. Institute of Statistics of the Republic of Srpska.Census of Population, Households and Dwellings in BiH (2013), http://www2.rzs.rs.ba/static/uploads/bilteni/popis/PreliminarniRezultati_Popis2013-drugo_izdanje_sa_kartama_Final.pdf (accessed 24.06.21).
2. Bajić, B.; Dodić, S.; Gegić, B.; Puskas, V.; Dodić, J. The potential of landfill gas utilization for energy production in the region of South East Europe. 41th IAEE International Conference, 10-13th June, Groningen, Netherlands. **2018**.
3. Kaza, S.; Yao, L.; Bhada-Tata, P.; VanWoerden, F. What a Waste 2.0: A Global Snapshot of Solid Waste Management to 2050. Urban Development, DC: World Bank, Washington, USA. **2018**.
4. Hoornweg, D.; Bhada-Tata, P. What a waste – A global review of solid waste management, World Bank, Washington, USA, **2012.**
5. Mutz, D.; Hengevoss, D.; Hugi, C.; Gross T. Waste-to-Energy Options in Municipal Solid Waste Management - A Guide for Decision Makers in Developing and Emerging Countries, GIZ, Bonn, Germany, **2017.** https://www.giz.de/en/downloads/GIZ_WasteToEnergy_Guidelines_2017.pdf (accessed 24.06.21).
6. Kumar, S. Integrated waste management –Volume I, InTechOpen, **2011.**
7. http://www.eurostat.com/ (accessed 24.06.21).
8. https://www.statista.com/statistics/453971/gross-domestic-product-gdp-per-capita-in-bosnia-herzegovina (accessed 24.06.21).
9. USEPA Solid waste management and greenhouse gases – A Life-Cycle Assessment of Emission and Sinks Report 3rd Edition, Washington, USA, **2006.** https://nepis.epa.gov/ (accessed 23.07.21).
10. Institute of Statistics of the Republic of Srpska. Environment Statistics Annual Release No. 374/19. https://www.rzs.rs.ba/static/uploads/saopstenja/zastita_zivotne_sredine/emisija_gasova_sa_efektom_staklene_baste/2017/Emisija_gasova_sa_efektom_staklene_baste_2017.pdf (accessed 23.07.21).
11. Clean Technologies for Sustainable Waste Mnagement https://www.eswet.eu/how-does-the-eu-treat-its-municipal-waste/ (accessed 23.07.21).
12. Bjelić, D. Razvoj optimalnog modela upravljanja komunalnim otpadom za Banjaluku primjenom procjene životnog ciklusa. Ph.D. Thesis, University of Banja Luka, October **2017**.
13. Directive 2008/98/EC of the European Parliament and of the Council, Official Journal, 2008. http://data.europa.eu/eli/dir/2008/98/oj (accessed 21.08.21).
14. Directive (EU) 2018/2001 of the European Parliament and of the Council, Official Journal, 2018. http://data.europa.eu/eli/dir/2018/2001/oj (accessed 21.08.21).
15. Official Gazette of the Republic of Srpska No. 111/13 106/15, 16/18, 70/20, 63/21; http://www.vladars.net/sr-SP-Cyrl/Vlada/Ministarstva/mgr/Documents/Zakon-o-upravljanju-otpadom_028820936.pdf› (accessed 21.08.21).
16. Official Gazette of the Republic of Srpska No. 39/13,108/13, 79/15, 26/19; https://reers.ba/wp-content/uploads/2019/05/Zakon_OIE_39_13.pdf (accessed 21.08.21).

BY-NC-ND

17. Energy Community Treaty Bosnia and Herzegovina, https://www.energy-community.org/implementation/Bosnia_Herzegovina.html (accessed 21.08.21).
18. https://reers.ba/wp-content/uploads/2021/01/Odluka-o-visini-naknade-za-podsticanje-proizvodnje-elektricne-energije-iz-obnovljivih-izvora-energije-i-u-efikasnoj-kogeneraciji-cirilica.pdf (accessed 21.08.21).
19. Renewable energy statistics https://ec.europa.eu/eurostat/statistics-explained/index.php?title=Renewable_energy_statistics (accessed 21.08.21).
20. Waste and resources in a circular economy, https://www.eea.europa.eu/publications/soer-2020/chapter-09_ (accessed 21.08.21).
21. Regional Development Agencies, Central BiH. Report on Environmental Technologies & Renewable Energies in the Balkan Area, Zenica, BiH, 2012. https://www.rez.ba/wp-content/uploads/2017/12/Publ-016-RES-Report-Eng.pdf (accessed 21.08.21).
22. Dodić, S.N.; Zekić, V.N.; Rodić, V.O.; Tica, N.Lj.; Dodić, J.M.; Popov, S.D. Situation and perspectives of waste biomass application as energy source in Serbia, *Renew.Sust.Energy Rev*. **2010**, *14*, 3171-3177.
23. Energy Regulatory Commission, Work report 2019. https://reers.ba/wp-content/uploads/2020/12/Izvjestaj_RERS_2019_LAT_2_dio.pdf (accessed 21.08.21).
24. Akcioni plan zakorišćenje obnovljivih izvora energije u BiH, **2016.** http://www.sluzbenilist.ba/page/akt/wgztz5k76kjn45hGk0gztz5k76kjn45hRkyQ8 (accessed 21.08.21).
25. Energy Community Secretariat, Annual implementation report BiH, November 2020. https://energy-community.org/news/Energy-Community-News/2020/11/23.html (accessed 21.08.21).
26. http://www.mvteo.gov.ba/data/Home/Dokumenti/Energetika/Okvirna_energetska_strategija_Bosne_i_Hercegovine_do_2035._HR_FINALNA.PDF (accessed 21.08.21).
27. Van Oost, G.; Hrabovsky, M.; Kopecky, V.; Konrad, M.; Hlina, M.; Kavka, T.; Chumak, O.; Beeckman, E.; Verstraeten, J. Pyrolisis of waste using a hybrid argon-water stabilized torch. *Vacuum*. **2006**, *80* (11-12), 1132-1137.
28. Moya, D.; Aldas, C.; Lopez, G.; Kaparaju P. Municipal solid waste as valuable renewable energy resource: a worldwide opportunity of energy recovery by using Waste-To-Energy Technologies. *Energy Procedia.* **2017**, *134*, 286-295.
29. Jones, P.T.; Geysen, D.; Rossy, A.; Bienge, K. Enhanced landfill mining (ELFM) and enhanced waste management (EWM), essential components for the transition to sustainable materials management (SMM). In Proceedings of the First International Symposium on Enhanced Landfill Mining, Houthalen-Helchteren, Belgium, **2010**.
30. Dodić, S.M.; Vučurović, D.G.; Popov, S.D.; Dodić, J.M.; Ranković, J.A. Cleaner bioprocesses for promoting zero-emission biofuels production in Vojvodina. *Renew Sust Energy Rev.* **2010,** *14*, 3242-3246.
31. Dhanya, B.S.; Mishra, A.; Chandel, A.K.; Verma, M.L. Development of sustainable approaches for converting the organic waste to bioenergy. *Science of the Total Environment*, **2020.** 723, 138109.
32. Massaro, V.; Digiesi, S.; Mossa, G.; Ranieri, L. The sustainability of anaerobic digestion plants: a win-win strategy for public and private bodies. *Journal of Cleaner Production*, **2015,** *104*, 445-459.
33. Christensen, T.H. Solid Waste Technology, Volume II, John Wiley & Sons Ltd, Publication, United Kingdom. **2011**.
34. Guiot, S.R.; Frigon, J.C. Biomethane production from starch and lignocellulosic crops: a comparative review. *Biofuels Bioproducts&Biorefining*, **2010**, *4*(4), 447-458.
35. Cabbai, V.; Ballico, M.; Aneggi, E.; Goi, D. BMP tests of sources selected OFMSW to evaluate anaerobic codigestion with sewage sludge, *Waste Management*, **2013**, *33*, 1626-1632.

BY-NC-ND

36. Katinas, V.; Marčiukaitis, M.; Perednis, E.;.Dzenajavičiene, E.F. Analysis of biodegradable waste use for energy generation in Lithuania. *Renewable and Sustainable Energy Reviews*, **2018,** *101*, 559-567.
37. Achinas, S.; Achinas, V.; Euverink, G.J.W. A Technological Overview of Biogas Production from Biowaste. *Engineering*, **2017,** *3*, 299-307.
38. Scarlat, N.; Dallemand, J.F.; Fahl, F. Biogas: Development and perspecives in Europe. *Renewable Energy*, **2018,** *129*, 457-472.
39. Republički plan upravljanja otpadom za Republiku Srpsku (2019) http://www.mvteo.gov.ba/data/Home/Dokumenti/Energetika/Okvirna_energetska_strategija_Bosne_i_Hercegovine_do_2035._HR_FINALNA.PDF
40. Kurbatova, A.; Abu-Qdais, H.A. Using Multi-Criteria Decision Analysis to Select Waste to Energy Technology for a Mega City: The Case of Moscow. *Sustainability*, **2020,** *12*, 9828.
41. Khoshand, A.; Kamalan, H.; Razaei, H. Application of analytical hierarchy process (AHP) to assess options of energy recovery from municipal solid waste: a case study in Tehran, Iran. *Journal of Material Cycles and WasteManagement*, **2018,** *20*, 1689-1700.
42. Qazi, W.A.; Abushammala, M.F.M.; Azam, M.-H. Multi-criteria decision analysis of waste-to-energy technologies for municipal solid waste management in Sultanate of Oman. *Waste Management&Research*, **2018,** *36(7)*, 594-605.

APTEFF, 52, 1-273 (2021) UDC: 664.683.6:543.92:366.62/.63
DOI: https://doi.org/10.2298/APT2152217P BIBLID: 1450-7188 (2021) 52, 217-227
BY-NC-ND
Original scientific paper

FUNCTIONAL HANDMADE MINIONS – CONSUMERS AND EXPERIENCED TASTERS SENSORY EVALUATION OF THE NEW PRODUCT

Jovanka POPOV RALJIĆ[1], Ivana BLEŠIĆ[2,3,], Milan IVKOV[2], Marko PETROVIĆ[3,4], Tamara GAJIĆ[3,4], Milica ALEKSIĆ[5]*

[1] Faculty of Tourism and Hospitality Management, University Singidunum, Danijelova 32, 11000 Belgrade, Serbia
[2] Department of Geography, Tourism and Hotel Management, Faculty of Sciences, University of Novi Sad, Trg Dositeja Obradovića 3, 21000 Novi Sad, Serbia
[3] Institute of Sports, Tourism and Service, South Ural State University, Sony Krivoy street 60, 454080 Chelyabinsk, Russia
[4] Geographical Institute "Jovan Cvijić", Serbian Academy of Sciences and Arts (SASA), Đure Jakšića 9, 11000 Belgrade, Serbia
[5]University of Business Studies, Faculty of Tourism and Hotel Management, Banja Luka 78000, Republic of Srpska, Bosnia and Herzegovina

Received: 06 September 2021 **Revised: 22 September 2021** **Accepted: 24 September 2021**

The study examines consumer sensory preferences of 12 different handmade pastry products in the form of minions, made of rice and flaxseed flour, tapioca starch with natural taste ingredients and with addition of prebiotic (inulin), herbs and other ingredients. The sensory evaluation was performed by professionals (experienced tasters). Preferred minion flavour was tested at group of 324 consumers (hotel guests) of different nationality. ANOVA and t-test were performed to reveal differences in attitudes related to socio-demographic characteristics of the consumers. Also, determination of taste preferences according to consumer nationality was examined as an additional consumer care aspect. The evaluation of equality of the samples' average rates, as well as the groups of minions, is done by parametric or nonparametric model of variance analysis. Principal component analysis (PCA) was applied in order to group the investigated minions regarding their sensory properties, while the sum of ranking differences (SRD) was used to determine the minions with the best sensory properties. Consumers and experienced tasters have almost the same opinion about the sensory quality of minions, which indicates that assessment of the consumer can be considered as a representative opinion in the near future. Such functional food – minions could be widely used as a substitute for the most common commercial sweets rich in sugar and fat.

Keywords: Handmade minions, sensory evaluation, consumer preferences, functional food.

INTRODUCTION

Pastry products are very important food product group and therefore it is crucial for food industry to know consumer preferences. Defining their sensory quality properties (appearance, texture, odour, taste and packaging) has the interest for scientific, professional and consumer population (1, 2).

Confectionery, including sugar-based confectionery and chocolate, is typically consumed for enjoyment, and there is probably no such thing as a healthy confectionery product (3). Therefore, the main aim of the reserach of the study was to determine consumer sensory preferences of a potentially new market product – rice and flaxseed flour handmade pastry products with addition of prebiotic.

* Corresponding author: Ivana Blešić, University of Novi Sad, Faculty of Sciences, Department of Geography, Tourism and Hotel Management, Trg Dositeja Obradovića 3, 21000 Novi Sad, Serbia.
e-mail: ivana.blesic@gmail.com

APTEFF, 52, 1-273 (2021) UDC: 664.683.6:543.92:366.62/.63
DOI: https://doi.org/10.2298/APT2152217P BIBLID: 1450-7188 (2021) 52, 217-227
BY-NC-ND
Original scientific paper

Rice flour was applied in order to produce gluten free product, since rice flour is non-wheat flour (4, 5, 6). Flaxseed flour is used in the production of pastry products because it has properties of functional foods. Flaxseed contains important substances such as vitamins A, B and E, magnesium, calcium, zinc, selenium, phosphorus, and it is also an excellent source of fibres and one of the best sources of ω-3 fatty acid that must be present in the food and ingested as the body cannot synthesize it and lignan (phytoestrogens with antioxidant effects) (7, 8, 9). Furthermore, due to its composition, flaxseed has a numerous health benefits such as reduction in the risk of occurrence of breast cancer, various cardiovascular and gastrointestinal diseases, diabetes and osteoporosis (10, 11, 12). Benefits of consuming ω-3 fats resulted in high consumer interest in food that contains ω-3 fatty acids (13).

The enhancement of pastry products could be achieved by adding functional ingredients such as inulin (non-digestible fermentable food ingredient – dietary fiber), due to its neutral taste and minimal influence on the sensory characteristics of the product, reduced energy value, increased level in fiber and as a replacement for fat and sugar (14,15,16,17).

The specific herbs (liquorice, eucalyptus and mint) are also used in minion production due to their positive effects on health. Liquorice (*Glycyrrhiza glabra*) is one of the most popular and widely consumed herbs in the world, the second most prescribed herb in China. In addition, many know this herb for its flavoring in pastry and confectionery products, and many health benefits - positive effects on digestive and respiratory organs and exhibition of anti-inflammatory, anti-viral, anti-allergenic, anti-ulcer and anti-oxidative properties (18, 19). Further, liquorice extracts and bioactive ingredients have shown beneficial effects in preventing and treating oral diseases (20).

There are many studies that report positive effect of eucalyptus (*Eucalyptus* spp.) on human health as a remedy for abscess, arthritis, asthma, boils, bronchitis, burns, flu, inflammation, rhinitis, worms, and wounds (21) and it also has antioxidant and antibacterial characteristics (22, 23). Therefore, there is an increasing interest in its application as a natural additive for food (24). Similarly, mint/menthol (*Mentha* spp.) is widely used as a natural antioxidant in food production (25, 26). Lastly, during the production *Stevia Rebaudiana* could be used, instead of sugar, as a natural sweetener which has positive health effects (27, 28).

MATERIALS AND METHODS

SENSORY EVALUATION BY CONSUMERS

The survey among consumers was carried out from March 1, 2019 to June 15, 2019 in Belgrade (Serbia) in three 4* and 5* hotels. The target group consisted of hotel guests who stayed at least four days at the hotel in the period of the research, and who are not allergic to any type of food. The self-administered questionnaire was distributed to guests' rooms in print, along with the selection of 12 different handmade pastry products in the form of small minions, packed in appropriate packaging material and classified into four groups (Table 1). The minions were handmade in restaurant kitchen with the following ingredients: rice and flaxseed flour, tapioca starch, sugar, Stevia with addition of prebiotic (inulin) and other natural flavour ingredients such as fruits, herbs, chocolate, etc. Each sample had a declaration on the package containing the name of the product group, product composition, storage conditions with appropriate temperatures and shelf life.

APTEFF, 52, 1-273 (2021)
DOI: https://doi.org/10.2298/APT2152217P
BY-NC-ND
UDC: 664.683.6:543.92:366.62/.63
BIBLID: 1450-7188 (2021) 52, 217-227
Original scientific paper

Table 1. Minions groups

Groups	Dominant minion aroma	Composition
Fruit Minions (A)	A1– nf strawberry/yogurt	Eggs, sugar, rice flour, tapioca starch, lyophilized strawberries, yogurt, butter, caster sugar, lemon juice
	A2 – nf cherry	Eggs, sugar, rice flour, tapioca starch, lyophilized cherry, butter, caster sugar, lemon juice
	A3 – nf orange	Eggs, sugar, rice flour, tapioca starch, lyophilized oranges, butter, caster sugar, lemon juice
	A4 – nf apple	Eggs, sugar, rice flour, tapioca starch, lyophilized apples, butter, caster sugar, lemon juice
Herbal Minions (B)	B5 – nf anethole	Eggs, sugar, rice flour, tapioca starch, butter, caster sugar, lemon juice, anise oil (85% anethole)
	B6 with eucalyptus and menthol	Eggs, sugar, rice flour, tapioca starch, butter, caster sugar, lemon juice, eucalyptus and menthol oil
	B7 with Philippine lemon and menthol	Eggs, sugar, rice flour, tapioca starch, lyophilized Philippine lemon, butter, caster sugar, lemon juice, menthol oil
	B8 with liquorice	Eggs, sugar, rice flour, tapioca starch, butter, caster sugar, lemon juice, sweet liquorice oil
Minions with coffee and chocolate (C)	C9 with espresso coffee	Eggs, sugar, rice flour, tapioca starch, butter, caster sugar, espresso coffee
	C10 with dark chocolate	Eggs, sugar, rice flour, tapioca starch, butter, caster sugar, dark chocholate
Diet Minions (D)	D11 with *Stevia Rebaudiana* and natural vanilla flavor	Aquafaba, rice flour, flaxseed flour, tapioca starch, butter, *Stevia Rebaudiana*, xanthan (E410), vanilla pulp, inulin
	D12 milk minions with *Stevia Rebaudiana*	Eggs, rice flour, flaxseed flour, tapioca starch, powdered lactose free milk, coconut butter, *Stevia Rebaudiana*, xanthan (E410), inulin

Consumers were asked to evaluate sensory properties (appearance, texture, odour, taste and package) of each minion type and the groups in general, using 5-point Hedonic scale (1 = dislike extremely, 5 = like extremely). A total of 400 questionnaires were distributed and 324 (81%) were returned. The collected data were analyzed using software SPSS 23.

APTEFF, 52, 1-273 (2021) UDC: 664.683.6:543.92:366.62/.63
DOI: https://doi.org/10.2298/APT2152217P BIBLID: 1450-7188 (2021) 52, 217-227
BY-NC-ND
Original scientific paper

SENSORY QUALITY EVALUATION BY EXPERIENCED TASTERS

The same handmade minions (Table 1) have been tested for their sensory characteristics (appearance, texture, odour, taste and package) by the Commission consisting of experienced tasters (n=20) according to ISO 8586:2015 and ISO 8589:2015 (29, 30, 31) in the appropriate accredited laboratory.

The following dominant sensory properties of the quality were evaluated: appearance (surface, breading/coating, size, shape, colour), texture (hardness, fragility, plasticity, chewability, gumminess and adhesiveness), odour, taste and packaging. For each of the above properties, the description of sensory properties is given by marks (1.00 – extremely pronounced error, 2.00 – clearly visible errors, 3.00 –excessive deviation, 4.00 – slight deviation, 5.00 – fully meets quality requirements) with the possibility of assigning one half and one quarter of points. For each selected quality property, the importance factor (FI) is assigned and used for corrections of the given marks (by multiplying). Importance factors are selected according to the influence of an individual property onto the overall quality and they are balanced so that their sum is 20. The addition of individual marks provides a complex indicator that represents the overall sensory quality and it is expressed as "% of the maximum possible quality".

A sample of minions that receives a mark < 2.50 does not meet the requirements for sensory quality, that is, it is considered as unacceptable; the mark from 2.50 to 3.50 corresponds to good quality; from 3.50 to 4.50 is very good quality and the range of marks from 4.50 to 5.00 is excellent quality. Also, it is worth mentioning that none of the ratings was below 2.50, the level that is considered unacceptable.

Principal component analysis (PCA) is used in order to reduce the amount of data when there is presence of correlation. Using PCA, the grouping of similar objects into clusters is possible. The result of PCA analysis is shown through scores and loadings plots (32). Sum of ranking differences (SRD) is a relatively novel non-parametric ranking approach (33, 34) successfully used in different branches of food industry (35, 36). Usually, in SRD analysis, the closer SRD value to zero is, the better is the sample. SRD is validated using a comparison of ranks by random numbers (CRRN) (33, 34). PCA analysis of experimental results was performed using STATISTICA (Statsoft, Inc., Tulsa, USA) and SRD analysis was carried out using Microsoft Excel visual basic macros: http://aki.ttk.mta.hu/srd/.

RESULTS AND DISCUSSION

The sample included 170 (52.5%) females and 154 (47.5%) males among the 324 respondents. The main age groups were 31-40 and it represented 45.4% of respondents followed by age group 41-50 representing 39.2% and the smallest share was of the groups over 51 years, representing 12%, and 18-30, representing 3.4%. Most of the respondents finished graduate studies (49.9%) or postgraduate studies (36.4%).

Regarding the general sensory quality of the minion groups, the herbal minions (Group B) obtained the best marks. It received the highest score regarding appearance (M=4.28, SD=1), odour (M=4.49, SD=0.72), taste (M=4.39, SD=0.75) and package (M=4.33, SD=0.79) and the second highest regarding texture (M=4.2, SD=1.16). It is worth of mentioning that herbs used for production of minions from Group B, especially liquorice, have many health benefits (21, 24) which add the value to these products. Moreover, healthy lifestyle is becoming an important factor for consumers (37).

APTEFF, 52, 1-273 (2021)
DOI: https://doi.org/10.2298/APT2152217P
BY-NC-ND
UDC: 664.683.6:543.92:366.62/.63
BIBLID: 1450-7188 (2021) 52, 217-227
Original scientific paper

The consumers evaluated coffee and dark chocolate minions (Group C) with the highest mark (M=4.32, SD=0.87) for the sensory property texture and with the second highest marks for odour (M=4.24, SD=1.01) and taste (M=4.31, SD=1.03). The results of sensory evaluation by consumers (inexperienced tasters) are presented in Figures 1-5.

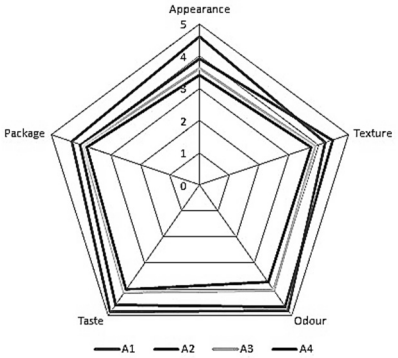

Figure 1. Sensory evaluation by consumers: Group A

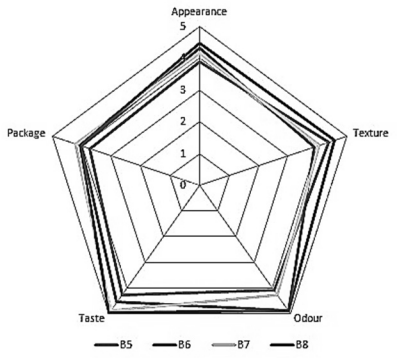

Figure 2. Sensory evaluation by consumers: Group B

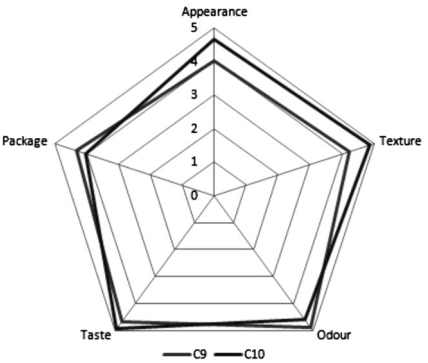

Figure 3. Sensory evaluation by consumers: Group C

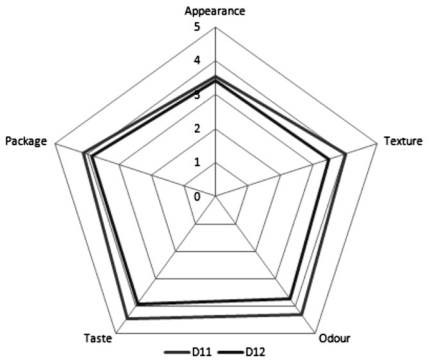

Figure 4. Sensory evaluation by consumers: Group D

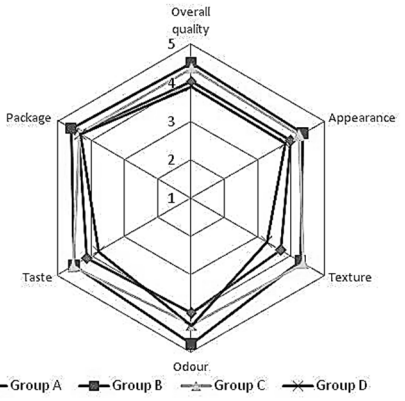

Figures 5. Sensory evaluation by consumers: Comparative view of four groups

APTEFF, 52, 1-273 (2021) UDC: 664.683.6:543.92:366.62/.63
DOI: https://doi.org/10.2298/APT2152217P BIBLID: 1450-7188 (2021) 52, 217-227
BY-NC-ND
Original scientific paper

The independent sample t-test showed that females had significantly lower mean ratings toward appearance and taste (M=3.74; t=14.913, and M=3.80, t=15.201, p<0.001); compared to males' mean ratings (M=4. 33; M=4.40,). This finding could be supported by the fact that females eat more sweet food than males (38), they pay more attention to aesthetics, and that they have superior sense of taste to men (39). Moreover, it is found that highly educated women give statistically significantly higher ratings to minions in Group D (M=4.5532, SD=0.81442, p<0.001), compared to other women (p<0.01) and men (p<0.001). The results point out to the fact that the level of education can affect the perception and choice of pastry products in relation to sensory or nutrition quality aspects. This can be explained by the lack of information and the quality of life of respondents with lower education. The similar effect of education on food choice was found by (40). Also, it was found that minions in group D is awarded much higher marks by respondents older than 51 years (M = 5.3103, SD = 1.07942, p< 0.001) in relation to younger respondents. This can be explained by the fact that older people take much more care about healthy food choices.

Further analysis included determination of taste preferences according to consumer nationality. It is well-known that food and taste preferences vary a lot among different cultures and nationalities, which is also mentioned by (41). However, articles published so far do not examine pastry products extensively. The results of statistical analysis of taste preference are shown in Table 2.

Table 2. Preferred minion taste by consumer nationality

Country of origin	Number of consumers	Preferred minion taste
Serbia	52	Lemon and menthol
Russia	40	Eucalyptus and menthol
Germany	39	Coffee
Italy	38	Liquorice
China	24	Liquorice
Austria	22	Chocolate
France	20	Strawberry / yoghurt
Hungary	20	Cherry
Romania	19	Chocolate
Turkey	18	Lemon and menthol
*Others	32	/

Note: The presented preferred taste refers to a taste with the highest obtained score by each nationality.
*Small number of consumers per country, less than 5.

The results indicate that consumers and professional tasters have almost the same opinion about the sensory quality of pastry products, especially regarding the liquorice minions. However, professional tasters gave lower marks to all examined samples. As stated by (42), the line between professional and consumer panels will continue to disappear. It is good to know the expert opinion but personal preferences and buying decisions are still made by consumers. Additionally, food suppliers must focus on both intrinsic and extrinsic attributes since consumers' food choice is a complex phenomenon (43).

The results of sensory evaluation by experienced tasters of different types of minions, including % of maximum possible quality are presented in Figure 6.

APTEFF, 52, 1-273 (2021)
DOI: https://doi.org/10.2298/APT2152217P
BY-NC-ND
UDC: 664.683.6:543.92:366.62/.63
BIBLID: 1450-7188 (2021) 52, 217-227
Original scientific paper

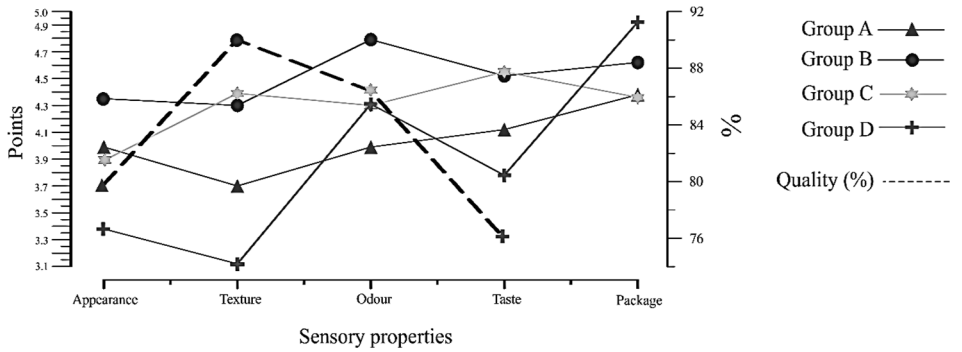

Figure 6. Statistical indicators of sensory quality for the four groups of minions and realised percentage out of maximum possible quality

The second group of samples (B) is comprised of herbal minions. According to sensory properties (appearance and texture), this group can be classified as very good quality while sensory attributes: odour, taste and packaging, can be classified as excellent quality. The weighted average mark is 4.50, that is, 90.00%. It should be pointed out that odour and taste are highly marked mainly due to the addition of herbs which contributes to the classification of these samples into excellent (the best) quality in relation to other groups (A, C and D).

The obtained PCA model is shown through two principal components (Figure 7). These two principal components describe 70.45% of the total variance. PC1 contributes with 48.81% and PC2 with 21.64% of the total variance. From loadings plot (Fig. 7A), it can be noticed that on the position of the investigated minions on the scores, taste has the greatest influence with positive coefficient of latent variable, regarding PC1. From the scores plot (Fig. 7B), it can be noticed that the investigated minions are grouped according to their taste on the positive and negative end of PC1 axis. On the positive end of PC1 axis minions with higher taste mark (≥ 4.31) are positioned and minions with lower taste mark (≤ 4.19) are positioned on the negative and of PC1 axis.

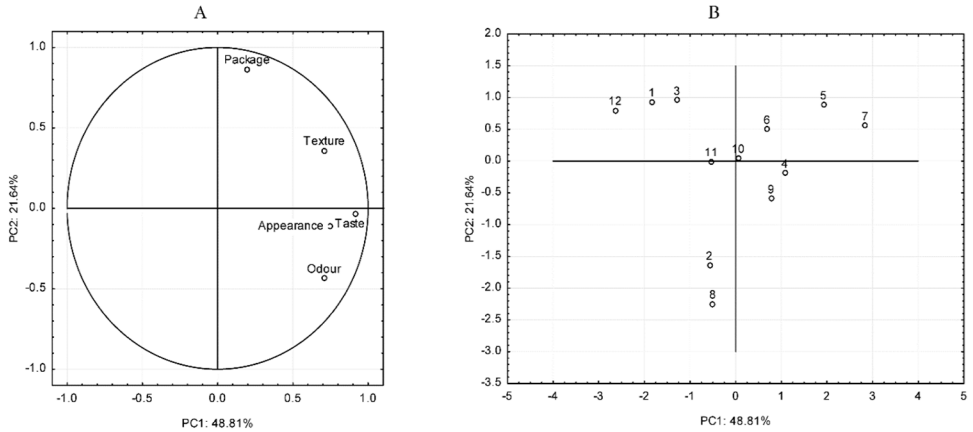

Figure 7. PCA analysis results (loadings plots – A and scores plots – B)

APTEFF, 52, 1-273 (2021) UDC: 664.683.6:543.92:366.62/.63
DOI: https://doi.org/10.2298/APT2152217P BIBLID: 1450-7188 (2021) 52, 217-227
BY-NC-ND
Original scientific paper

SRD analysis of 12 different types of minions gave results presented in Figure 8. In Fig. 8A reference ranking was defined as maximum row values while in Fig. 8B reference ranking was defined as average row values. The results of SRD analysis (Fig. 8A) indicate that sample 9 (minions with espresso coffee from group C – Minions with coffee and dark chocolate) have the highest SRD value that implies the highest deviation from the ideal (reference) ranking. According to the proximity to the reference ranking sample 7 (Philippine lemon and menthol from group B – Herbal minions) has the smallest SRD value and it can be considered as the best one. In the second case (Fig. 8B) again sample 9 occurs as the worst one with the highest SRD value regarding its sensory characteristics. In this case, sample 6 (eucalyptus and menthol) was chosen as the best one while having the smallest SRD value. This sample is also from the group B – Herbal minions same as sample 7.

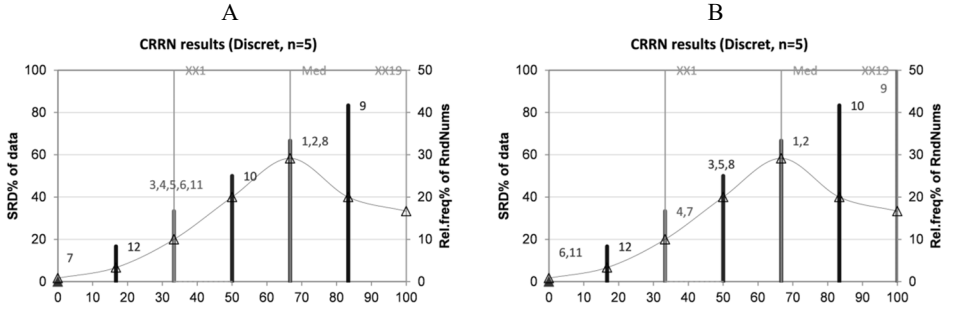

Figure 8. The order of 12 different types of caramels obtained by sum of ranking differences

Note: The reference ranking was defined as maximum row values (A) and average row values (B). The statistical characteristics of the theoretical distribution function are following: first icosaile (5%), XX1 = 32; first quartile, Q1 = 42; median, Med = 48; last quartile, Q3 = 54; last icosaile (95%), XX19 = 62.

CONCLUSIONS

The pressure on food companies to offer healthy products is evident, especially for "sensitive" consumer groups (children, people with health issues/on diet, etc.). According to the PCA method, the best discrimination factor between the investigated minions according to their sensory characteristics is their taste. Applying SRD analysis, Herbal minions were distinguished as the best choice of minions according to their sensory characteristics. Concerning this, herbal pastry products, due to the highest obtained marks and positive health effects of used herbs and *Stevia Rebaudiana*, could be a good choice for a small personal attention/gift, e.g. at public places such as hotels, banks, medical and dental care offices, post offices, etc. They can also be an integral part of the desserts in hospitality establishments, at least in terms of taste. The producers might want to launch a new functional product – handmade minions with reduced energy value by substituting sugar with Stevia and additionally fit into concept of "light" rational nutrition. On the other hand, it is very important to know customer preferences and to continuously explore expectations and needs of consumers accompanied by simultaneous assessment of sensory quality in order to create a competitive product and positive emotions among consumers.

BY-NC-ND

As for the study limitations, it should be certainly mentioned the study sample composition and its size. Therefore, we suggest for future in-depth studies to include respondents from different social areas and market sectors.

REFERENCES

1. Popov Raljić, J.; Mastilović, J.; Laličić Petronijević, J.; Kevrešan, Ž.; Demin, M. Sensory and colour properties of dietary cookies with different fiber sources during 180 days of storage. *Chem. Ind.***2013**, *67*, 123-134.
2. Janković, V.; Lakičević, B.; Đorđević, V.; Spirić, D.; Petronijević, R.; J. Popov Raljić, J. Soybean and gluten in meat products – consumer protection strategy. *Agro Food Ind. Hi-Tech*. **2016**, *27*, 30-32.
3. Wolf, B. *Confectionery and Sugar-Based Foods*. In: Reference Module in Food Science, **2016**.
4. Jeong, S.; Kim, H.W.; Lee, S. Rheological and secondary structural characterization of rice flour-zein composites for noodles slit from gluten-free sheeted dough. *Food Chem.***2017**, *221*, 1539-1545.
5. Chiş, M.S.; Păucean, A.; Man, S.M.; Bonta, V.; Pop, A.; Stan, L.; Pop, C.R.; Mureşan, V.; Muste, S. Effect of Rice Flour Fermentation with Lactobacillus spicheri DSM 15429 on the Nutritional Features of Gluten-Free Muffins. Foods. **2020**, *9*, 822.
6. Das, A.B.; Bhattacharya, S. Characterization of the batter and gluten-free cake from extruded red rice flour. *LWT- Food Sci. Technol*. **2019**, *102*, 197-204.
7. Filipović, J.; Filipović, V.; Pezo, L.; Krulj, J. The effects of ω 3 fatty acids and inulin addition to spelt pasta quality. *LWT - Food Sci. Technol*. **2015**, *63*, 43-51.
8. Parikh, M.; Maddaford, T.G.; Austria, J.A.; Aliani, M.; Netticadan, T.; Pierce, G.N. Dietary flaxseed as a strategy for improving human health. *Nutrients*. **2019**, *11*, 1171.
9. Biao, Y.; Jiannan, H.; Yaolan, C.; Shujie, C.; Dechun, H.; Mcclements, D.J.; Chongjiang, C. Identification and characterization of antioxidant and immune-stimulatory polysaccharides in flaxseed hull. *Food Chem.***2020**, *315*, 126266.
10. Rubilar, M.; Gutiérrez, C.;Verdugo, M.; Shene, C.; Sineiro, J. Flaxseed as a source of functional ingredients. *J. Soil Sci. Plant Nutr.***2010,** *10*, 373-377.
11. Lowcock, E.C.; Cotterchio, M.; Boucher, B.A. Consumption of flaxseed, a rich source of lignans, is associated with reduced breast cancer risk. *Cancer Cause Control*. **2013**, *24*, 813-816.
12. Hu, T.; Linghu, K.; Huang, S.; Battino, M.; Georgiev, M.I.; Zengin, G.; Li, D.; Deng, Y.; Wang, Y.T.; Cao, H. Flaxseed extract induces apoptosis in human breast cancer MCF-7 cells. *Food Chem. Toxicol.***2019**, *127*, 188-196.
13. Fuchs, R. H. B.; Ribeiro, R. P.; Matsushita, M.; Tanamati, A.A.C.; Bona, E.; de Souza, A.H. P. Enhancement of the nutritional status of Nile tilapia (Oreochromis niloticus) croquettes by adding flaxseed flour. *LWT - Food Sci. Technol*. **2013**, *54*, 440-446.
14. Roberfroid, M. Functional food concept and its application to prebiotics. *Dig. Liver Dis.* **2002**, *34*, 105-110.
15. Estruch, R.; Vendrell, E.; Ruiz-León; A.M., Casas; R., Castro-Barquero, S.; Alvarez, X.. Reformulation of Pastry Products to Improve Effects on Health. *Nutrients.***2020,**12, 1709.
16. Shoaib, M.; Shehzad, A.; Omar, M.; Rakha, A.; Raza, H.; Sharif, H.R.; Shakeel, A., Ansari, A.; Niazi, S. Inulin: Properties, health benefits and food applications. *Carbohyd. Polym*. **2016**, *147*, 444-454.
17. de Souza Paglarini, C.; Vidal, V.A.; Ribeiro, W.; Badan Ribeiro, A.P.; Bernardinelli, O.D.; Herrero, A.M.; Ruiz-Capillas, C.; Sabadini, E.; Rodrigues Pollonio, M.A. Using inulin-based emulsion gels as fat substitute in salt reduced Bologna sausage. *J. Sci. Food Agr.***2020**, *101*, 505-517.

BY-NC-ND

18. Al-Bachir, M.; Lahham, G. The effect of gamma irradiation on the microbial load, mineral concentration and sensory characteristics of liquorice (Glycyrrhiza glabra L). *J. Sci. Food Agr.***2003**, *83*, 70-75.
19. Castangia, I.; Caddeo, C.; Manca, M.L.; Casu, L.; Latorre, A.C.; Díez-Sales, O.; Ruiz-Saurí, A.; Bacchetta, G.; Fadda, A.M.; Manconi, M. Delivery of liquorice extract by liposomes and hyalurosomes to protect the skin against oxidative stress injuries. *Carbohydr. Polym*. **2015**, *134*, 657-663.
20. Sidhu, P.; Shankargouda, S.; Rath, A.; Ramamurthy, P.H.; Fernandes, B.; Singh, A.K. Therapeutic benefits of liquorice in dentistry. *J. Ayurveda Integ. Med.***2020**,11, 82-88.
21. Bachir, R.G.; Benali, M. Antibacterial activity of the essential oils from the leaves of Eucalyptus globulus against Escherichia coli and Staphylococcus aureus. *Asian Pac. J. Trop. Biomed.***2012***, 2*, 739-742.
22. Luís, Â.; Duarte, A.; Gominho, J.; Domingues, F.; Duarte, A.P. Chemical composition, antioxidant, antibacterial and anti-quorum sensing activities of Eucalyptus globulus and Eucalyptus radiata essential oils. *Ind. Crop. Prod.***2016**, *79*, 274-282.
23. Vecchio, M.G.; Loganes, C.; Minto, C. Beneficial and healthy properties of Eucalyptus plants: A great potential use. *Open Agric. J.***2016**, *10,* 52-57.
24. Goldbeck, J.C.; do Nascimento, J.E.; Jacob, R.G.; Fiorentini, Â.M.; da Silva, W.P. Bioactivity of essential oils from Eucalyptus globulus and Eucalyptus urograndis against planktonic cells and biofilms of Streptococcus mutans. *Ind. Crops Prod*.**2014**, *60*, 304-309.
25. Biswas, A.K.; Chatli, M.K.; Sahoo, J. Antioxidant potential of curry (Murrayakoenigii L.) and mint (Mentha spicata) leaf extracts and their effect on colour and oxidative stability of raw ground pork meat during refrigeration storage. *Food Chem*. **2012**, *133*, 467-472.
26. Stringaro, A.; Colone, M.; Angiolella, L. Antioxidant, antifungal, antibiofilm, and cytotoxic activities of Mentha spp. essential oils. *Medicines*. **2018**, *5*, 112.
27. Lemus-Mondaca, R.; Vega-Gálvez, A.; Zura-Bravo, L.; Ah-Hen, K. Stevia rebaudianaBertoni, source of a high-potency natural sweetener: A comprehensive review on the biochemical, nutritional and functional aspects. *Food Chem*. **2012**, *132*, 1121-1132.
28. Hossain, M.F.; Islam, M.T.; Islam, M.A.; Akhtar, S. Cultivation and uses of stevia (Stevia rebaudiana Bertoni): A review. *African J. Food, Agric. Nutr. Dev*. **2017**, 17, 12745-12757.
29. SRPS EN ISO 8586, Sensory analysis - General guidelines for the selection, training and monitoring of selected assessors and expert sensory assessors.
30. SRPS EN ISO 8589, Sensory analysis - General guidance for the design of test rooms.
31. Popov Raljić, J.; Stojšin, Lj. *Confectionery technology*; Faculty of Agriculture: Belgrade, Serbia, **2007**.
32. Trifković, J.; Andrić, F.; Ristivojević, R.; Andrić, D.; Tešić, Ž.Lj.; Milojković Opsenica, D.M. Structure-retention relationship study of arylpiperazines by linear multivariate modeling. *J. Sep. Sc.***2010**, *33*, 2619-2628.
33. Héberger, K.; Kollár-Hunek, K. Sum of ranking differences for method discrimination and its validation: Comparison of ranks with random numbers. *J. Chem.***2001**, *25*, 151-158.
34. Héberger, K. Sum of ranking differences compares methods or models fairl", *TRAC-Trend. Anal. Chem.***2010**, *29*, 101-109.
35. Kovačević, S.Z.; Tepić, A.N.; Jevrić, L.R.; Podunavac-Kuzmanović, S.O.; Vidović, S.S.; Šumić, Z.M.; Ilin, Ž.M. Chemometric guidelines for selection of cultivation conditions influencing the antioxidant potential of beetroot extracts. *Comput. Electron. Agr.* **2015**, *118*, 332-339.
36. Jevrić, L.R.; Karadžić, M.Ž.; Podunavac-Kuzmanović, S.O.; Tepić Horecki, A.N.; Kovačević, S.Z.; Vidović, S.S.; Šumić, Z.M.; Ilin, Ž. M. New guidelines for prediction of antioxidant activity of Lactuca sativa L. varieties based on phytochemicals content and multivariate chemometrics. *J. Food Process. Pres.***2018**, 42, 1–11.
37. Vicentini, A.; Liberatore, L.; Mastrocola, D. Functional Foods: Trends and Development of the Global Market. *Ital. J. Food Sci*. **2016,** *28*, 338-351.

BY-NC-ND

38. Katou, Y.; Mori, T.; Ikawa, Y. Effect of age and gender on attitudes towards sweet foods among Japanese. *Food Qual. Pref*. **2005**, *16*, 171-179.
39. Wright, L.T.; Nancarrow, C.; Kwok, P.M. Food taste preferences and cultural influences on consumption. *Brit. Food J*. **2001**, *103*, 348-357.
40. Allen, K.N.; Taylor, J.S.; Kuiper, R. Effectiveness of Nutrition Education on Fast Food Choices in Adolescents. *J. Sch. Nurs*. **2007,** *23*, 337-341.
41. Macbeth, H. *Food preferences and taste*; Berghahn Books: New York, United States, **2006**.
42. Meiselman, H. The future in sensory/consumer research: evolving to a better science. *Food Qual. Pref*. **2013**, *27*, 208-214.
43. Topcu, Y. Turkish Consumer Decisions Affecting Ice Cream Consumption, *Ital. J. Food Sci*. **2015**, *27*, 29-39.

APTEFF, 52, 1-273 (2021) UDC: 582.973+665.52]:543.544.3
DOI: https://doi.org/10.2298/APT2152229V BIBLID: 1450-7188 (2021) 52, 229-237
BY-NC-ND
Original scientific paper

CHEMICAL COMPOSITION OF ESSENTIAL OILS OF ELDERBERRY (*SAMBUCUS NIGRA* L.) FLOWERS AND FRUITS

Milena D. VUJANOVIĆ[1], Saša D. ĐUROVIĆ[2], Marija M. RADOJKOVIĆ[1]*

[1] University of Novi Sad, Faculty of Technology Novi Sad, Bulevar cara Lazara 1, 21 000 Novi Sad, Serbia
[2] Institute of General and Physical Chemistry, Studentski trg 12/V, 11158 Belgrade, Serbia

Received: 07 September 2021 **Revised: 18 September 2021** **Accepted: 20 September 2021**

The majority of essential oils obtained from medicinal plants have been demonstrated to be effective in the treatment of different kinds of diseases, and they are increasingly used in the diet. Due to their chemical composition, essential oils are a very interesting product of the secondary metabolism of plants, for both consumers and researchers. Among others, elderberry (Sambucus nigra L.) is mostly a woody plant, while it can rarely be found as a herbaceous perennial plant. This plant species has been used in traditional medicine because it is a very rich source of phytochemicals. The aim of this study was to identify and compare the composition of essential oils obtained from flowers and fruits of this plant, collected from the Balkan Peninsula. The oils were obtained using the Clevenger apparatus, and their composition was evaluated by gas chromatography - mass spectrometry (GC-MS). The oil composition was affected by the part of the plants used: the most abundant bioactive compounds in the essential oil of air-dried elderberry fruits were β-damascenone (35.70%) and linalyl anthranilate (24.15%). β-damascenone was the dominant compound in the essential oil of lyophilized elderberry fruits (38.64%), while linalool was detected in the concentration of 32.80%. In the essential oil of air-dried elderflowers, the most abundant compound was carane (13.19%). The essential oils of S. nigra shown substantial chemical composition and could be used as a potential source of natural products in the cosmetics and food industry.

Keywords: essential oils, *Sambucus nigra* L., chemical composition, hydrodistillation.

INTRODUCTION

The pace of modern life has influenced the development of various diseases that have become the primary concern of contemporary society. The scientific community has focused its research on the treatment of diseases of modern society by using plants. Plant species that grow on the Balkan Peninsula are very available and cheap sources of biopotent molecules and have been used for centuries in traditional medicine. Essential oils are recognized as a very promising product of secondary plant metabolism (1). The use of essential oils in herbal medicine dates back to the early development of civilization. The essential oil has found its application in various cosmetic, pharmaceutical, and food products. Also, in aromatherapy the essential oil is used in pure or diluted form. Plant raw materials are recognized as a source of anti-inflammatory, antimicrobial and antitumor agents, therefore metabolites that are produced in plant metabolism have biological and pharmacological potential in the prevention and treatment of diseases of modern society (2).

One of the unutilized plant species in our region is elderberry (*Sambucus nigra* L). Elderberry is a wild-growing plant species that belongs to the Adoxaceae family. This plant species is characterized by whitish flowers and small dark purple fruits. Of the 30 species

* Corresponding author: Milena D. Vujanović, University of Novi Sad, Faculty of Technology Novi Sad, Bulevar cara Lazara 1, 21 000 Novi Sad, Serbia, e-mail: milenavujanovic@uns.ac.rs

APTEFF, 52, 1-273 (2021)
DOI: https://doi.org/10.2298/APT2152229V
BY-NC-ND
UDC: 582.973+665.52]:543.544.3
BIBLID: 1450-7188 (2021) 52, 229-237
Original scientific paper

named in the world, nine have use-value, while only two species, *S. nigra* L. (black elderberry) and *S. canadensis* L. (Canadian, American elderberry), are used for commercial purposes. Three species grow in the Balkans: *Sambucus nigra* L., *Sambucus ebulus* L., and *Sambucus racemosa* L. (3). Black elderberry is widespread in western and central Europe, it can grow at an altitude of 1200 meters, it is also present in the south of Europe, in Sicily, and in the continental regions of Greece. The natural limit for the growth of the plant species *Sambucus nigra* is Scotland and southern Scandinavia. In addition to the European continent, elderberry also grows in Asia, North Africa, and North America. For the suitable growth of the elderberry, fertile humus and moist soil rich in nitrogen are needed, so it can be found in villages, fields, thickets, on the banks of rivers, in lighter forests (4).

Since the development of civilization, it has been used in traditional medicine and nutrition. Elderberry flowers and fruit were used to treat flu and colds, while in traditional nutrition they were used to make syrups, juices, jams, jellies. Numerous studies have shown that elderberry has pronounced biological properties if they are antioxidant, anti-inflammatory, neuroprotective, antimicrobial (5). Based on data from the literature, it was determined that that research focused on methods for isolation of elderberry essential oil is scarce. The studies that have dealt with the isolation and characterization of essential oil from elderberry are Najar et al., 2021 (6) and Agalar et al., 2014 (7). A special contribution and novelty within this research were based on the application of drying techniques, especially lyophilization as a modern drying technology, with the idea of preserving the chemical composition of elderberry, in order to obtain quality products that are not yet available on the market. Hence, the aim of this study was to identify the chemical composition of essential oil, of air-dried elderflowers and elderberry fruits, and lyophilized elderberry fruits collected on the Balkan Peninsula, using the gas chromatography-mass spectrometry (GC-MS) technique.

EXPERIMENTAL

The fresh elderberry flowers and fruits used in this research were collected in June and August 2017 in mountain Ljubišnja, Pljevlja (Montenegro). After collection, part of fresh elderberry flowers and fruits were dried by traditional drying technique and part fresh fruits were dried using lyophilization, as a modern drying technique at the industrial level. Traditional drying was performed in an area that is protected from sunlight and without the influence of temperature, and the drying process lasted 5 days at temperature 22 °C, while lyophilization lasted 48 hours. The dried plant material was prepared for hydrodistillation process. The specimen's voucher (*Sambucus nigra* L., No. 2-1512) was prepared and identified by Milica Rat, Ph.D., and deposited at the Herbarium of the Department of Biology and Ecology (BUNS Herbarium), University of Novi Sad, Faculty of Sciences, Republic of Serbia.

HYDRODISTILLATION OF PLANT MATERIAL

The essential oil was isolated from the air-dried fruits and flowers and the lyophilized elderberry fruits, in an apparatus according to Clavenger (1928). The weighed plant material was transferred to a distillation flask, the flask was placed on a heating pad and water was added as a solvent. The ratio of plant material to solvent was 1:10 (g/mL). The distilla-

APTEFF, 52, 1-273 (2021)
DOI: https://doi.org/10.2298/APT2152229V
BY-NC-ND
UDC: 582.973+665.52]:543.544.3
BIBLID: 1450-7188 (2021) 52, 229-237
Original scientific paper

tion process lasted 4 hours, and the essential oil was isolated in 1 ml of n-hexane. The hexane layer was dropped into a beaker and dried over anhydrous sodium sulfate. After 24 hours, the hexane solution was filtered and the filtrate was transferred to a previously measured flask. The residual solvent was evaporated on a vacuum evaporator. The content of easily volatile components in the essential oil is expressed as a relative percentage (%, m/m).

CHEMICAL ANALYSIS OF THE ESSENTIAL OIL OF *SAMBUCUS NIGRA*

The analysis of the essential oils of *S. nigra* included the qualitative and quantitative composition of the oil of air-dried flowers and fruits and lyophilized fruits, which was determined by GC/MS (gas chromatography/mass spectrometry) method (Thermo Fisher, USA). TR WAX-MS (30m x 0.25 mm, 0.25 μm) capillary column was used, while the analyzed samples were dissolved in methylene chloride and injected into GC through TriPlus AS autosampler (2 μL). The temperature program was: initial temperature 45 °C (8 min), then 8.0 °C/min to 230 °C (10 min). Injector, MS transfer line and ion source temperatures were 250 °C, 200 °C and 220 °C, respectively. The compounds were identified combining the NIST 08 MS database and MS spectra of authenticated standards. The final results were expressed as a relative percentage (%) (9).

RESULTS AND DISCUSSION

The results of the research are presented in the tables in the paper.

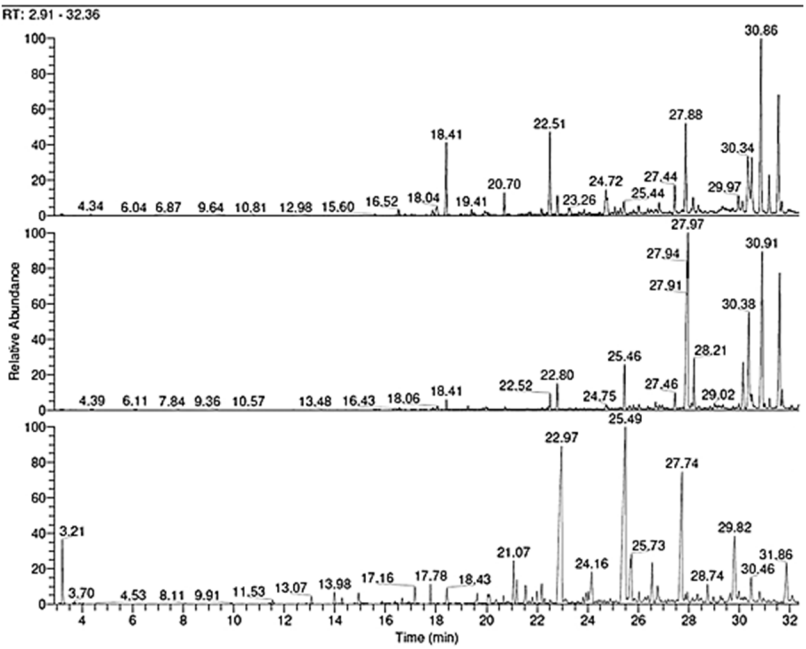

Figure 1. Chromatogram of elderberry and elderflowers essential oils. The numbers refer to those in Tables 1, 2, and 3.

APTEFF, 52, 1-273 (2021)
DOI: https://doi.org/10.2298/APT2152229V
BY-NC-ND
UDC: 582.973+665.52]:543.544.3
BIBLID: 1450-7188 (2021) 52, 229-237
Original scientific paper

Table 1. The chemical composition of the essential oil obtained from air-dried elderberry fruits

Retention time	Isolated compounds	Content (%, m/m)
6.12	2-hexenol	5.19±0.21
7.09	4-heptyn-3-ol	0.10±0.01
7.89	isopentyl acetate	0.24±0.01
11.82	2-pentylfuran	0.33±0.02
11.93	E)-ocimene	0.13±0.01
12.73	*p*-cymene	0.10±0.01
14.47	α-lonene	0.53±0.01
14.73	*cis*-rose oxide	0.41±0.01
15.04	*trans*-rose oxide	0.20±0.01
15.60	β-cyclocitral	1.63±0.06
16.46	ethil caprylate	3.22±0.26
16.57	β-lonene	4.46±0.17
17.93	2,5,5,8a-tetramethyl-3,4,4a,5,6,8a-hexahydro-2H-chromene	5.20±0.16
18.44	linalyl anthranilate	24.15±2.31
20.74	α-terpineol	5.71±0.28
22.06	methyl hydrocinnamate	1.66±0.07
22.55	β-damascenone	35.70±3.41
24.01	indane-4-carboxaldehyde	2.45±0.15
25.82	5-methyl-2-phenyl-2-hexenal	8.58±0.26

Table 2. The chemical composition of the essential oil obtained from lyophilized elderberry fruits

Retention time	Isolated compounds	Content (%, m/m)
10.50	limonene	0.04±0.01
11.77	2-pentylfuran	0.03±0.01
11.87	*cis*-β-ocimene	0.04±0.02
12.33	*trans*-β-ocimene	0.11±0.01
12.98	terpinolene	0.12±0.01
14.40	α-lonene	0.25±0.03
14.68	*cis*-rose oxide	0.12±0.01
14.98	*trans*-rose oxide	0.04±0.01
15.54	*trans-p*-mentha-2,8-dien ol	0.19±0.01
16.52	β-lonene	3.25±0.16
18.04	α-lonone	6.87±0.21
18.41	linalool	32.80±3.23
18.98	β-lonone	1.07±0.05
20.70	α-terpineol	9.59±0.18
22.51	β-damascenone	38.64±3.80
31.68	phytol	6.84±0.27

APTEFF, 52, 1-273 (2021) UDC: 582.973+665.52]:543.544.3
DOI: https://doi.org/10.2298/APT2152229V BIBLID: 1450-7188 (2021) 52, 229-237
BY-NC-ND
Original scientific paper

In the essential oil of air-dried fruits, 19 components were identified, which represented 99.99% of the essential oil. The main components of the essential oil of air-dried elderberry fruits were: β-damascenone (35.70%), linalyl anthranilate (24.15%), 5-methyl-2-phenyl-2-hexenal (8.58%) and α-terpineol (5.71%).

In the essential oil of lyophilized elderberry fruits, 16 components were identified, which represented 100% of the composition of the essential oil. The dominant compound in the essential oil of lyophilized fruits was also β-damascenone (38.64%), with a slightly lower percentage of linalool (32.80%). α-Terpineol was present in the percentage of 9.59%, while α-lonone and phytol were recorded in the percentage of 6.87% and 6.84%, respectively. Comparing the obtained results with previous studies, it was noticed that elderberry oil contains the same groups of easily volatile compounds, but in a different percentage. Namely, the essential oil of air-dried elderberry in study (6) as a dominant compound were contained linalyl acetate (26.30%) and linalool (10.20%), while these compounds have not been identified in the essential oil of air-dried elderberry, tested in this paper. However, linalool was detected in the essential oil of lyophilized elderberries in a concentration of 32.80%, which is significantly higher, compared to the research of Najar et al., 2021 (6). These results could be explained by the influence of the drying process on the content of certain components, especially because lyophilization ensures the preservation of the chemical composition of plant materials. Also, the process of hydrodistillation affected the content of easily volatile compounds, but also the composition of the soil on which the plant grew.

In the essential oil of air-dried and lyophilized fruits, the dominant components belong to rose ketones. Damascenones and lonones are compounds found in various essential oils, including rose oil. They significantly contribute to the aroma of roses, despite the relatively low concentration, and are important chemical substances used in the perfumery, and are obtained by the decomposition of carotenoids (10).

Seven of the same components have been identified in the essential oil of air-dried and lyophilized elderberry fruits (2-pentylfuran, α-lonene, *cis*-rose oxide, *trans*-rose oxide, β-lonone, α-terpineol and β-damascenone). With the exception of α-terpineol and β-damascenone, the other compounds identified were in a higher percentage presented in the essential oil of air-dried elderberry fruits compared to the chemical composition of the essential oil of lyophilized elderberry fruits.

The difference in the content of individual components in the essential oils of air-dried and lyophilized elderberry is probably due to the influence of the hydrodistillation process itself, as well as the conditions under which the processes took place. The highest yield of essential oil is expected at the beginning of hydrodistillation until the temperature becomes constant and until equilibrium is established (11). The mechanism of hydrodistillation is closely related to the anatomy of berry fruits and their degree of fragmentation. The process of drying berry fruits affects the chemical composition of the fruits. Air-drying removes water from the plant material, but the dried material is more susceptible to contamination in this case. On the other hand, lyophilization provides the preservation of the chemical composition and quality of dried material. In the process of lyophilization, the anatomy of the berry fruits is more uniform, while air drying does not enable the uniform anatomy of the fruits. Drying and preservation of the plant material are also associated with the process of hydrodistillation. Higher degrees of fragmentation afford a larger contact area and easier isolation of more volatile compounds. During hydrodistillation, the boiling temperature

APTEFF, 52, 1-273 (2021)
DOI: https://doi.org/10.2298/APT2152229V
BY-NC-ND
UDC: 582.973+665.52]:543.544.3
BIBLID: 1450-7188 (2021) 52, 229-237
Original scientific paper

could lead to disturbances or degradation of the chemical structure of thermolabile metabolites, which is directly related to the chemical composition being analyzed. The berry fruits contain essential oil in their structure, and by crushing, the structure of the fruit is destroyed and the essential oil is released on the surface of the particle of plant material. The oil that has reached the surface of the particle is quickly carried away by the steam that is formed during distillation, and that period in hydrodistillation is marked as fast hydrodistillation. The isolation of essential oil from the inner parts of the plant material is not completely ensured by crushing the berries, so the diffusion of the essential oil is difficult and this period of hydrodistillation is marked as slow hydrodistillation (12).

The difference in the content of aromatic components of essential oil also stems from the impossibility of temperature regulation. Thermolabile aromatic compounds are subject to degradation due to the influence of boiling temperature, in addition to hydrodistillation, the composition of the essential oil is also affected by the chosen technique of drying the plant material. The components present in the essential oil of air-dried elderberry fruits were presented in a higher percentage compared to the components found in the essential oil of lyophilized fruits, except α-terpineol and β-damascene which were the most abundant in the essential oil of lyophilized elderberries. Comparison of the drying techniques clearly shows the difference and efficiency of lyophilization in relation to the traditional method of drying, as well as the higher share of compounds in the essential oil of lyophilized fruits. Lyophilization affects the preservation of the structure of fruits, and thus their chemical composition, which is related to the quality of dried raw materials.

In addition to the fruit, for the production of essential oil within this scientific paper, a traditionally dried elderflower was used, and the results of the research are shown in Table 3.

The presence of 35 compounds was determined in the essential oil of the elderflowers, where the basic components of the oil are monoterpenes and sesquiterpenes. The most common compounds in the essential oil of elderflowers were: caran (13.19%), α-limonene diepoxide (7.23%), methyl salicylate (7.00%), caryophyllene (6.55%), benzopyran (5.89%), cis-geraniol (5.78%), and linalyl anthranilate (5.48%), while other aromatic components are presented in a smaller percentage. Compared with the chemical composition of the essential oil of the elderberry fruits, it was noted that monoterpenes cis-rose oxide and trans-rose oxide, as well as linalyl anthranilate belonging to the terpene family, are presented in the essential oil of both the fruits and the flowers of *Sambucus nigra*. Qualitative analysis of the oil showed that monoterpene cis-rose oxide and trans-rose oxide were detected in a higher percentage in the essential oil of the flowers, while linalyl anthranilate was identified four times higher in the essential oil of air-dried elderberry fruits. Based on the conducted examination of the essential oil from the fruits and flowers of *S. nigra*, it could be noticed that the dominant compounds in the essential oil of the fruit were present in a higher percentage, while the components present in the essential oil of the elderflower are identified in up to three times in a lower percentage. The composition and yield of essential oil in different organs of the same plant species depends on biotic and abiotic factors, the genetics of the plant itself, and the influence of the environment (13). In the families, Lamiaceae, Apiaceae, Asteraceae, Rutaceae, Lauraceae, Myrtaceae, plant species rich in essential oil are represented. The isolation of essential oil from the fruits of berries is not particularly interesting, as evidenced by the small number of studies. The essential oil of the elderberry fruits was not the subject of scientific publications, and it is assumed that the main reason is

BY-NC-ND

the low content of essential oil in the plant species of the genus Sambucus. Essential oil as a product of secondary metabolism of plants has a number of pharmacological activities, fungicidal, antirheumatic, as well as antiseptic effects.

Table 3. The chemical composition of the essential oil obtained from the traditionally dried elderflower

Retention time	Isolated compounds	Content (%, m/m)
8.44	α-pinene	0.01±0.01
8.94	3-penten-2-ol	0.03±0.01
10.94	2-pentylfuran	0.06±0.02
13.07	4-pentyn-2-ol	2.93±0.02
13.98	*cis*-rose oxide	4.20±0.05
14.28	*trans*-rose oxide	2.09±0.02
14.78	1.2-methyl-1.4-pentadiene	0.39±0.01
14.94	1-undecyn	4.78±0.04
15.86	linalool oxide	0.84±0.02
16.37	3.6-dihydro-4-methyl pyran	0.84±0.02
16.45	1.3-isopentyl-cyclopentene	0.31±0.01
17.16	benzopyran	5.89±0.07
17.78	linalyl anthranilate	5.48±0.05
18.43	caryophyllene	6.55±0.10
20.05	α-terpinol	2.97±0.04
20.67	epoxy-linalool	2.30±0.03
20.80	α-farnesene	0.50±0.02
20.88	β-cadinene	0.18±0.01
21.07	carane	13.19±0.27
21.20	methyl salicylate	7.00±0.37
21.54	α-limonene diepoxide	7.23±0.41
21.81	β-damascenone	1.68±0.12
22.00	6-methyl-5-nonadiene-2-on	3.99±0.23
22.18	*cis*-geraniol	5.78±0.30
22.29	*cis*-geranylacetone	1.39±0.15
23.81	γ-elemene	1.74±0.19
23.93	α-caryophyllene oxide	2.91±0.21
24.02	1-benzyl-1,2,3-triazole	2.51±0.17
24.42	*trans*-2-caren-4-ol	0.86±0.08
24.64	β- caryophyllene oxide	0.93±0.08
24.77	α-copaen-11-ol	0.58±0.03
24.89	β-methyl ionone	1.57±0.10
26.39	methyl-2-hydroxy-1,6-dimethyl cyclohexane carboxylate	2.22±0.15
28.34	α- hexyl cinnamaldehyde	2.18±0.18
29.64	3-*p*-menthen	3.88±0.26

BY-NC-ND

In the food industry, the essential oil is increasingly used as a natural preservative and a potential alternative to synthetic preservatives to improve the taste of products, but also to protect products from oxidation and microorganisms during packaging (14). The obtained results indicate that the essential oils of elderberry are a good source of biopotential aromatic compounds. The presence of rose ketones and terpene molecules as dominant components in the analyzed essential oils provides an opportunity to continue research in this area in the direction of their potential application in the food industry as natural agents for maintaining product freshness and shelf life.

CONCLUSION

The results obtained in this paper showed that elderberry essential oils have a high content of volatile molecules belonging to rose ketones. In this regard, the further work and development of this research could be based on the application of modern technologies in order to isolate the dominant compounds in larger quantities. The dominant compounds detected in the analyzed essential oils are characterized by exceptional biological activity, especially linalool, terpineol, limonene, caryophyllene, which have antihypertensive, anticancer, antimicrobial, antioxidant, and sedative effects. In addition, future research could be based on testing the biological activity of the oil obtained, in order to apply it to existing food or cosmetic products, with the idea of ensuring a better quality of products.

REFERENCES

1. Koné, A. P.; Desjardins, Y.; Gosselin, A.; Cinq-Mars, D.: Guay, F.; Saucier, L. Plant extracts and essential oil product as feed additives to control rabbit meat microbial quality. *Meat sci.* **2019,** *150*, 111-121.
2. Rathod, N. B.; Kulawik, P.; Ozogul, F.; Regenstein, J. M.; Ozogul, Y. Biological activity of plant-based carvacrol and thymol and their impact on human health and food quality. *Food Sci. Technol*. **2021,** *116*, 733-748.
3. Jabbari, M.; Hashempur, M. H.; Razavi, S. Z. E.; Shahraki, H. R.; Kamalinejad, M.; Emtiazy, M. Efficacy and short-term safety of topical Dwarf Elder (*Sambucus ebulus* L.) versus diclofenac for knee osteoarthritis: a randomized, double-blind, active-controlled trial. *J. Ethnopharmacol.* **2016**. *188*, 80-86.
4. Tucakov, J. Lečenje biljem. **2010.** Beograd. Zapis
5. Domínguez, R.; Zhang, L.; Rocchetti, G.; Lucini, L.; Pateiro, M.; Munekata, P. E.: Lorenzo, J. M. Elderberry (*Sambucus nigra* L.) as potential source of antioxidants. Characterization, optimization of extraction parameters and bioactive properties. *Food Chem.* **2020**, *330*, 127266.
6. Najar, B.; Ferri, B.; Cioni, P. L.; Pistelli, L. Volatile emission and essential oil composition of *Sambucus nigra* L. organs during different developmental stages. *Plant Biosyst.* **2021**. *155*(4), 721-729.
7. Ağalar, H. G.; Demirci, B.; Başer, H. C. The volatile compounds of elderberries (*Sambucus nigra* L.). *Nat. Vol. & Essent. Oils*. **2014**. *1*(1), 51-54.
8. Clevenger, J. F. Apparatus for the determination of volatile oil. *J. Am. Pharm. Assoc.* **1928**. *17*(4), 345-349.

BY-NC-ND

9. Mićić, D.; Ostojić, S.; Pezo, L.; Blagojević, S.; Pavlić, B.; Zeković, Z.; Đurović, S. Essential oils of coriander and sage: Investigation of chemical profile, thermal properties and QSRR analysis. *Ind. Crops Prod*. **2019**. *138*, 111438.
10. Leffingwell, J. C.; Alford, E. D. Volatile constituents of perique tobacco. *Elec. J. Env. Agricult. Food Chem*. **2005**. *4*(2), 899-915.
11. Milojević, S. Ž.; Stojanović, T. D.; Palić, R.; Lazić, M. L.; Veljković, V. B. Kinetics of distillation of essential oil from comminuted ripe juniper (*Juniperus communis* L.) berries. *Biochem. Eng. J.* **2008**, *39*(3), 547-553.
12. Milojević, S. Ž. Kinetika hidrodestilacije, karakterizacija i frakcionisanje etarskog ulja ploda kleke *(Juniperus communis L.)* **2011**. Doktorska disertacija, Univerzitet u Beogradu, Tehnološko-metalurški fakultet.
13. Simões, C.M.O.; Schenkel, E.P.; Gosmann, G.; Mello, J.C.P.; Mentz, L.A. Farmacognosia: da planta ao medicamento. **2010**. 6. ed. Porto Alegre: UFRGS.
14. Ju, J.; Xu, X.; Xie, Y.; Guo, Y.; Cheng, Y.; Qian, H.; Yao, W. Inhibitory effects of cinnamon and clove essential oils on mold growth on baked foods. *Food Chem.* **2018***. 240*, 850-855.

APTEFF, 52, 1-273 (2021) UDC: 635.64:547.56+547.979.8]:616.34-002
DOI: https://doi.org/10.2298/APT2152239S BIBLID: 1450-7188 (2021) 52, 239-252
BY-NC-ND
Original scientific paper

SIMULATED GASTROINTESTINAL DIGESTION AND STORAGE STABILITY OF TOMATO WASTE ENCAPSULATES

Slađana M. STAJČIĆ, Jasna M. ČANADANOVIĆ-BRUNET, Gordana S. ĆETKOVIĆ, Vesna T. TUMBAS ŠAPONJAC, Jelena J. VULIĆ, Vanja N. ŠEREGELJ*

University of Novi Sad, Faculty of Technology Novi Sad, Bulevar cara Lazara 1, 21 000 Novi Sad, Serbia

Received: 19 September 2021 **Revised: 07 September 2021** **Accepted: 08 October 2021**

The application of bioactive antioxidant compounds is limited because of their instability. To overcome this drawback, different protection systems including encapsulation have been developed. In this study, for the stabilisation of bioactive compounds (carotenoids and phenolics) extracted from tomato waste, encapsulation with carbohydrate (inulin and gum arabica) and protein (soy protein and pea protein) wall materials by freeze drying method was applied. Content of bioactive compounds and antioxidant properties (determined by DPPH, reducing power and β-carotene bleaching assay) of encapsulates before and after in vitro digestion was investigated. Also, in obtained encapsulates carotenoid stability during storage at ambient (25 ± 5 °C) light and dark conditions for four weeks was assessed. The results indicated that release behavior of bioactive compounds and antioxidant activity after digestion of encapsulates varied according to the type of wall material. Protein carriers showed better ability to preserve phenolic compounds through in vitro gastrointestinal digestion in comparison to carbohydrate wall materials. Pea protein showed best carrier properties for delivery of carotenoids, while differently to other used carriers, gum arabica showed minor ability to release carotenoids after in vitro gastrointestinal digestion. During storage higher content of carotenoids was preserved in encapsulates prepared with carbohydrate carriers. All encapsulates retained higher amount of carotenoids under dark conditions. The results of this study showed that assessment of the behavior of encapsulates during digestion and storage is necessary in order of selection appropriate delivery system of bioactive compounds in powder form which can be used as ingredient in functional food products.

Keywords: tomato waste, bioactive compounds, encapsulation, gastrointestinal digestion, stability study

INTRODUCTION

Epidemiological studies have suggested the strong association of consumption of tomato and tomato-based products with reduced risk of chronic diseases such as cardiovascular disease and certain types of cancer (1). These protective effects are mainly attributed to the presence of antioxidant bioactive compounds, such as carotenoids, vitamins and polyphenols, which probably interact synergistically (2).

Tomato (*Solanum lycopersium* L.) is one of the vegetable crops most widely produced in the world (3). It is consumed as fresh or processed into a wide range of products (such as paste, juice, puree, sauce, soup, ketchup, whole dried tomatoes and tomato powder) (1, 3). With growing importance on a global scale, worldwide production of processing tomato recently reached approximately 40 million tons annually (3). During the processing of tomatoes,

* Corresponding author: Slađana M. Stajčić, University of Novi Sad, Faculty of Technology Novi Sad, Bulevar cara Lazara 1, 21 000 Novi Sad, Serbia, e-mail: sladja@uns.ac.rs

APTEFF, 52, 1-273 (2021) UDC: 635.64:547.56+547.979.8]:616.34-002
DOI: https://doi.org/10.2298/APT2152239S BIBLID: 1450-7188 (2021) 52, 239-252
BY-NC-ND
Original scientific paper

the main waste generated is the tomato pomace, a mix of tomato skin and seeds and a small fraction of the pulp (3). The amount of pomace produced can vary from one way of processing to the other, due to the raw material characteristics and processing conditions, and has been reported in range from 1.5% up to 40% of the initial weight of tomatoes (3, 4). This waste is mainly used for animal feed or turn into compost, thus representing costs and environmental concerns for the tomato processing industry (1, 3). Although these wastes have no commercial value, they can be used as a rich source of highly biologically active compounds, including phenolics and carotenoids (1, 5). Considering that tomato processing industry is present worldwide, tomato waste is available in large quantity in many countries (3).

Since bioactive compounds are highly unstable, they can be degraded during food processing, storage and gastrointestinal tract (6-9). One of the ways of increasing the stability of sensitive compounds is encapsulation. In the food industry, encapsulation is implemented by trapping active compounds into coatings (9). This process results in preventing the destruction of bioactive compounds by environmental factors and during digestion, to improve the shelf life of the final product, reduce evaporation, decomposition or reaction with other food ingredients during the process. Also, controlled release of compounds can be achieved (9).

Although freeze-drying is an effective method for encapsulation of bioactive compounds and suitable for the preservation of heat-sensitive components, stability of bioactive compounds in prepared encapsulates during storage need to be assessed (10).

In view of the instability of bioactive compounds during digestion, their content and antioxidant activity in different food samples before the digestion is not a real reflection of their beneficial effects on health (2). Therefore, the simulation of gastrointestinal condition by means of *in vitro* digestion methods using digestive enzymes (pepsin and pancreatin) is recommended to mimic the physiological release of food bioactive compounds and to evaluate their antioxidant capacity (2).

Due to the production of huge amounts of tomato waste and high content of antioxidant bioactive compounds in it, encapsulation of valuable compounds extracted from tomato waste is of importance for investigation. The aim of this study was evaluation of stability of bioactive compounds content and antioxidant activity in prepared tomato waste encapsulates during simulated gastrointestinal digestion. Also, stability of bioactive compounds (carotenoids) during storage was examined.

EXPERIMENTAL

CHEMICALS AND INSTRUMENTS

Pancreatin, pepsin, Folin-Ciocalteu reagent, 2,2-diphenyl-1-picrylhydrazyl radical (DPPH•), β-carotene, trichloroacetic acid and Trolox, were purchased from Sigma Chemical Co. (St Louis, MO, USA), and ferric chloride was obtained from J.T. Baker (Deventer, Holland). Soy protein isolate were purchased from Olimp Laboratories (Debica, Poland), gum arabica from Carlo Erba (Val de Reuil, France), pea protein from Beyond d.o.o. (Niš, Serbia) and inulin from Elephant Co. (Belgrade, Serbia). All other chemicals and solvents used were of the highest analytical grade. Spectrophotometric measurements were done with a Multiskan GO microplate reader (Thermo Fisher Scientific Inc., Waltham, MA, USA). Lyophilization was carried out using a freeze dryer, model Christ Alpha 2-4 LSC (Martin Christ, Osterode am Harz, Germany).

APTEFF, 52, 1-273 (2021) UDC: 635.64:547.56+547.979.8]:616.34-002
DOI: https://doi.org/10.2298/APT2152239S BIBLID: 1450-7188 (2021) 52, 239-252
BY-NC-ND
Original scientific paper

PLANT MATERIAL AND DRIED TOMATO WASTE PREPARATION

Fresh tomato waste was obtained after pressing of pulp as by-product from the fruit and vegetable processing industry (Zdravo Organic d.o.o., Selenča, Serbia). Waste material was freeze-dried, ground, packed in vacuumed plastic bags and stored at -20 °C for further analysis (11).

EXTRACTION PROCEDURE

Freeze-dried tomato waste was extracted three times using acetone:ethanol mixture (36:64 v/v) in solid to solvent ratio 1:20 w/v, with the same volume of solvents. The extraction was performed using a laboratory shaker (Unimax 1010, Heidolph Instruments GmbH, Kelheim, Germany) at 300 rpm for 10 min, at room temperature and under light protection. The obtained three extracts were combined, filtered (Whatman paper No.1, Sigma-Aldrich, St. Louis, MO, USA), and kept in dark bottles at -20 °C for further analysis.

ENCAPSULATION PROCESS

Freeze dried encapsulates were prepared following the method described by Stajčić et al. (11). Briefly, 28 g of wall material (inulin, gum arabica, pea protein or soy protein) was dissolved in 42 ml of water at 60 °C and kept under stirring until the temperature reached 30 °C. Separately, 160 ml of tomato waste extract was combined with sunflower oil (6 ml), concentrated under reduced pressure on a rotary evaporator set at 40 °C to remove the organic solvent, and immediately mixed with 0.1 g of Tween 80 and with previously prepared carrier solution. The mixtures were homogenized (Heidolph DIAX 900, Heidolph Instruments GmbH, Kelheim, Germany) at 11000 rpm for 5 min at room temperature and freeze dried.

IN VITRO SIMULATED GASTROINTESTINAL DIGESTION

In vitro digestion of encapsulates was investigated by simulation of digestion in gastric and intestinal fluid, according to the method of Vaštag et al. (12), with modifications. In the gastric phase of digestion, encapsulate (2.5% water suspension) was treated with pepsin at pH 2.0 and 37 °C, during 1 h. After gastric, in the intestinal phase of digestion the pH of the solution was adjusted to 7.5, pancreatin was added and by keeping the same conditions solution was stirred for 2 h. Before and at the end of digestion, the sample aliquots were concentrated on a rotary evaporator, dissolved in acetone:ethanol mixture (36:64 v/v) and analyzed for the content of bioactive compounds and antioxidant activity.

CONTENT OF ENCAPSULATED BIOACTIVE COMPOUNDS AND ANTIOXIDANT ACTIVITY BEFORE AND AFTER *IN VITRO* SIMULATED GASTROINTESTINAL DIGESTION

The content of bioactive compounds (phenolics and carotenoids) and antioxidant activity before and after digestion were measured spectrophotometrically. The analysis of total phenolics (TPh) was performed by Folin-Ciocalteau method (13), adapted to microscale. The results were expressed as a gallic acid equivalent (GAE) per 100 g of encapsulates (DW). Spectrophotometric analysis of total carotenoids (TCar) was performed by the

APTEFF, 52, 1-273 (2021) UDC: 635.64:547.56+547.979.8]:616.34-002
DOI: https://doi.org/10.2298/APT2152239S BIBLID: 1450-7188 (2021) 52, 239-252
BY-NC-ND
Original scientific paper

method of Nagata and Yamashita (14) and the results were expressed as mg of carotenoids (lycopene and β-carotene) per 100 g of encapsulates (DW). The antioxidant activity was determined by three methods: 2,2-diphenyl-1-picrylhydrazyl (DPPH) method described by Girones-Vilaplana et al. (15), reducing power (RP) by the Oyaizu (16), and β-carotene bleaching assay (BCB) by Al-Shaikan et al. (17). The results of antioxidant activity were expressed as mmol Trolox equivalent (TE) per 100 g of encapsulates (DW).

STORAGE STABILITY OF ENCAPSULATED CAROTENOIDS

The tomato waste encapsulates were stored at ambient temperature (25±5 °C) in glass and amber bottles for 28 days to determine the effects of time and light exposure on the stability of bioactive compounds (carotenoids). For that purpose, total carotenoids in encapsulates were determined by previously described method every 7 days. Retention of carotenoids was calculated by the formula:

$$\text{Retention (\%)} = (\text{TCar at } t / \text{ TCar at } t_0) \times 100;$$

where TCar at t and TCar at t_0 were content of total carotenoids at different times, and at zero time of storage, respectively.

Rate constant (k) and half-life time ($t_{1/2}$) were calculated by the method of Cai and Corke (18) using the regression analysis of ln (Retention, %) against storage time when plotted on a natural logarithmic scale (19).

STATISTICAL ANALYSIS

All experiments were run in triplicate and results were represented as means ± standard deviation. Statistical analyses were carried out using Origin 8.0 SRO software package and Microsoft Office Excel 2010. Significant differences were calculated by ANOVA ($p<0.05$).

RESULTS AND DISCUSSION

Stability of encapsulates depends on the type and properties of wall materials utilized for encapsulation (9). Actually, the behavior of encapsulates through simulated digestion depends on the composition of their surrounding medium, sensitivity to digestive enzymes and pH of simulated environment (20). Therefore, chemical transformations that occur during gastrointestinal transit may change the content of bioactive compounds and bioactivity of food components (21). For evaluation of these possible changes, content of bioactive antioxidant compounds (carotenoids and phenolics) was determined before and after simulated *in vitro* gastrointestinal digestion of encapsulates EIN, EGA, EPP and EPS, prepared using inulin, gum arabica, pea protein and soy protein as wall materials, respectively (Figure 1).

APTEFF, 52, 1-273 (2021)
DOI: https://doi.org/10.2298/APT2152239S
BY-NC-ND
UDC: 635.64:547.56+547.979.8]:616.34-002
BIBLID: 1450-7188 (2021) 52, 239-252
Original scientific paper

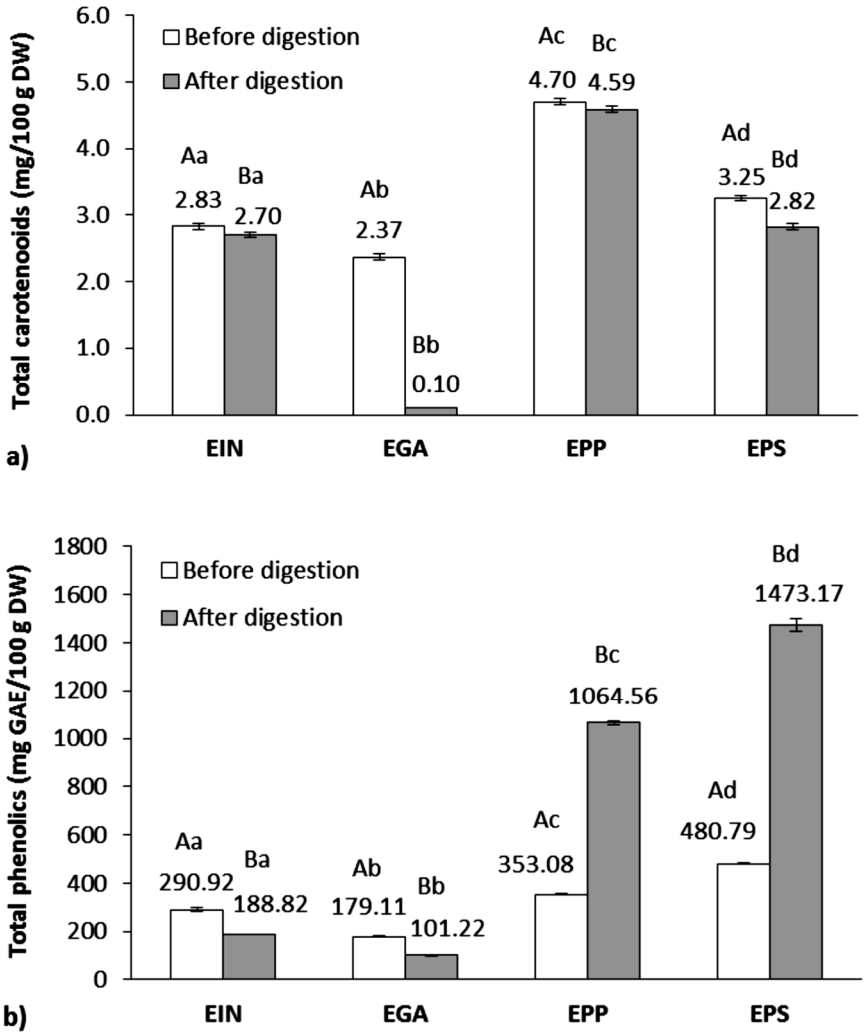

Figure 1. Total carotenoids (a) and phenolic (b) content before and after *in vitro* gastrointestinal digestion of encapsulates (EIN, EGA, EPP and EPS)

The bars represent the mean of three replicates and the error bars represent the standard deviations. Different capital letters for each encapsulate indicate significant differences ($p<0.05$) between mean values before and after digestion, different lowercase letters indicate significant differences ($p<0.05$) between mean values of different encapsulates at the same phase of digestion.

After simulated *in vitro* gastrointestinal digestion, the content of total carotenoids decreased for all encapsulates, compared to samples before this treatment. The highest content of total carotenoids before *in vitro* digestion was determined in the case of encapsulated tomato waste extract with pea protein as a carrier, and the lowest in the case of encapsulation

BY-NC-ND

with gum arabic as a carrier. After simulated gastrointestinal digestion, highest content of total carotenoids was released by encapsulate with pea protein as a carrier, while lowest content of total carotenoids was released in the case of gum arabic as a carrier. The encapsulate with pea protein as a carrier released 97.66% of the total carotenoid content, i.e. the content of total carotenoids after simulated digestion was 4.59 mg/100 g of encapsulate. During digestion of encapsulate prepared with gum arabic as a carrier only 4.22% of the initial content of total carotenoids was released, and carotenoid content determined after digestion was 0.10 mg/100 g of encapsulate. It may be that carotenoids remained trapped within undigested lipid droplets in the beads (22, 23). Previously, it was observed that main difference between gum arabic and protein (i.e. whey protein) is in the extent of degradation (24). Structurally, gum arabic is a complex heteropolysaccharide with small protein content, with main and side chains linked by β-glycosidic bonds (24). In simulated digestive fluids, which usually contain α-amylases and α-glucosidases, gum arabic is minimally digested (24). Therefore, the indigestibility of gum arabic can explain low release of carotenoids in our study. In accordance to our study, Szabo et al. (25) encapsulated carotenoids extracted from tomato processing by-products (tomato peels) by spray drying technology with linseed oil as carrier, and a binary blend of gum arabic and maltodextrin (1:1 w/ w) as wall materials and at end point of the simulated digestion the results showed low amount of total carotenoids and undetectable quantities of β-carotene. Nevertheless, most proteins can be easily digested by the human gastrointestinal tract (26). Similarly as in our study, it was reported that along with the digestion of proteins (nanocarriers), encapsulated β-carotene in the nanocomplex was progressively released during the whole gastric and intestinal digestion, and at the end of digestion (180 min), the amount of β-carotene transferred to the aqueous phase reached almost 100% (relative to the total β-carotene amount) (27). Degradation of carotenoids during *in vitro* digestions in the presence or not of digestive enzymes and dietary pro-oxidants were investigated by Kopec et al. (28). They reported a decrease in the remaining β-carotene, lutein and lycopene of around 40%, 40% and 20%, respectively, after *in vitro* digestion with digestive enzymes without pro-oxidants (28, 29). In the study of Toor et al. (30), after *in vitro* digestion method of fresh tomatoes of three cultivars (Excell, Tradiro and Flavourine) only 3.2 - 4.5% of the total lycopene was released. Tommonaro et al. (2) estimated bioactive metabolite contents of different tomato hybrids after the *in vitro* digestion with the aim to evaluate the effect of this physiological process on the bioactive compounds stability, and reported that the presence of carotenoids, lycopene and β-carotene was still detectable and in some case the amount of these carotenoids was higher than that before the digestion process. After gastrointestinal digestion of the purple tomato extract, carotenoids were significantly affected with an approximate 72% decrease (31).

The content of phenolics in encapsulate with inulin as carrier after digestion was 188.82 mg GAE/100 g of encapsulate, which is 64.90% of the determined initial content. Using gum arabic as a carrier, the content of phenolics after digestion was 101.22 mg GAE/100 g of encapsulate, i.e. 56.51% of the content determined before digestion. In contrast, in encapsulates with protein carriers, a significant increase in the content of total phenolics was observed. The content of total phenolics determined after simulated digestion of encapsulate with soy protein as carrier was 1473.17 mg GAE/100 g of encapsulate, while in the encapsulate with pea protein as carrier 1064.56 mg GAE/100 g of encapsulate was found. From the above results arise that protein carriers showed a greater ability to preserve phenolic compounds. In our study phenolic losses during *in vitro* gastrointestinal digestion of

BY-NC-ND

encapsulated tomato waste extract with carbohydrate carriers could be explained by the physicochemical transformations, such as oxidation or the interactions with other components, like polysaccharides in the digestion mixture (32). Our results for the encapsulated extracts with protein carriers are in accordance with the results of Flores et al. (33), where they studied the *in vitro* release properties of encapsulated blueberry extracts with whey protein isolate via spray drying and found that phenolic contents increased after digestion. Ahmadian et al. (9) studied simulated gastrointestinal digestion of saffron by-product (petal) encapsulates prepared by spray and freeze drying with different amount of wall materials (i.e. maltodextrin from 10% to 12%, and pectin from 0 to 2% in the final feed system), and reported that spray-dried and freeze-dried samples, containing highest pectin in wall composition, indicated highest release (79.74% and 76.54%, respectively) of polyphenols in simulated digestion. The behaviour of encapsulates in a simulated gastrointestinal medium is always dependent on the surrounding matrix composition and their resistance or susceptibility to digestive enzymes as well as on the gastrointestinal conditions like pH range (34). Toor et al. (30) reported that from 71% to 77% of the total phenolics were released from tomatoes of three cultivars during digestion. In the study of Li et al. (31), during gastrointestinal digestion of the purple tomato extract phenolics were reduced by approximately 37% and 39% in total phenolic content and total anthocyanin contents, respectively. The causes of degradation of these phytochemical groups remained unclear as they are unlikely to be destroyed by the enzymes used in the model system (31). In the study of Pasli et al. (35), the effect of *in vitro* gastrointestinal digestion on total phenolic content of 13 dried vegetable samples were determined and the reduction in post gastric values of total phenolic content was observed for all except for dried tomato sample. Total content of phenolic compound of dried tomato in the initial, post gastric, post intestine coded as IN (i.e. in the dialysis bags; representing material that entered the serum) and post intestine coded as OUT (i.e. outside the dialysis bags; representing material that remained in the gastrointestinal tract) samples was 4.73, 5.21, 1.18 and 2.95 mg GAE/g sample, respectively (35). The differences in bioaccessibility among different samples could be due to several factors such as possible interactions with other food components, the chemical state of the compound and its release from the food matrix (35). In accordance with our study, Flores et al. (24) found that after simulated digestion whey protein microcapsules yielded higher phenolics contents, and reported that this could be attributable to interactions between whey proteins and polyphenols.

Beside the content of bioactive compounds (carotenoids and phenolics), antioxidant activity was also determined before and after simulated *in vitro* gastrointestinal digestion of encapsulates (Figure 2). Since determination of antioxidant activity depends on different mechanisms of the assays, combination of at least two antioxidant activity assays was recommended by several authors to provide a more reliable result of the antioxidant activity of a food product or some other sample (35). For this reason, in the present work three different antioxidant activity assays were performed. The influence of simulated gastrointestinal digestion on antioxidant activity of encapsulates (EIN, EGA, EPP and EPS) was determined by using DPPH, RP and BCB assay (Figure 2).

APTEFF, 52, 1-273 (2021)
DOI: https://doi.org/10.2298/APT2152239S
BY-NC-ND
UDC: 635.64:547.56+547.979.8]:616.34-002
BIBLID: 1450-7188 (2021) 52, 239-252
Original scientific paper

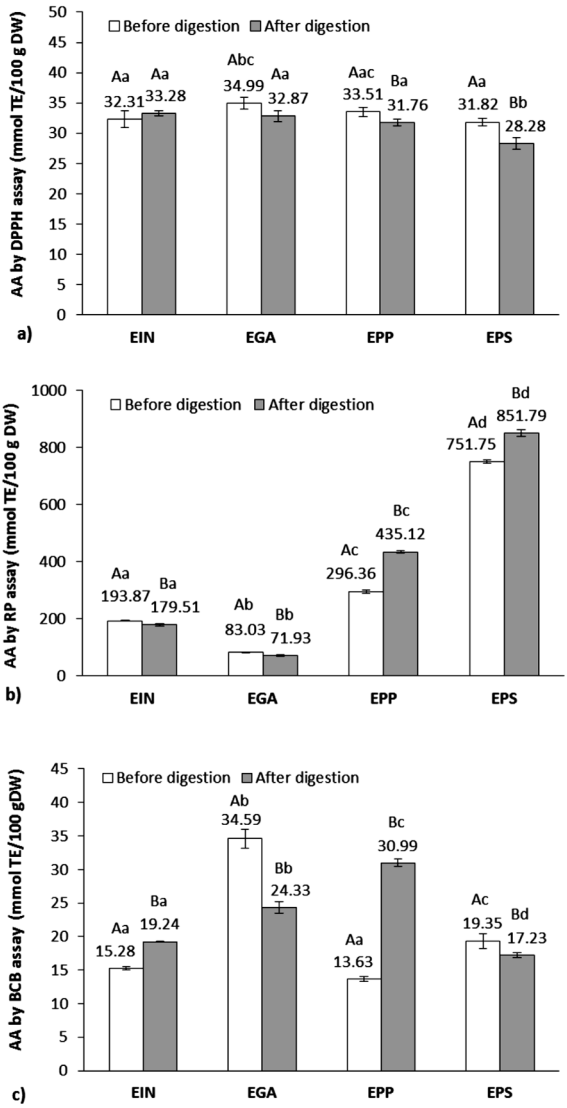

Figure 2. Antioxidant activity (AA) by using DPPH (a), RP (b) and BCB assay (c) before and after *in vitro* gastrointestinal digestion of encapsulates (EIN, EGA, EPP and EPS)

The bars represent the mean of three replicates and the error bars represent the standard deviations. Different capital letters for each encapsulate indicate significant differences ($p<0.05$) between mean values before and after digestion, different lowercase letters indicate significant differences ($p<0.05$) between mean values of different encapsulates at the same phase of digestion.

The decrease in antioxidant activity determined by DPPH assay (of 5.22% and 11.14%) was recorded in encapsulates with pea and soy protein as carriers in relation to antioxidant activity determined before digestion. Antioxidant activity by DPPH assay after digestion in

encapsulates with inulin and gum arabic as carriers did not change significantly ($p<0.05$). According to Gullon et al. (36), the increment in antioxidant activity could be attributed to higher release of bioactive compounds, with scavenging properties, from the samples under the acidic conditions of gastric digestion. Furthermore, the antioxidant properties of bioactive compounds might change due to the chemical transformations resulting from different mechanisms during the gastrointestinal digestion (32). It is well-known that the chemical structure of phenolics (i.e. number and position of hydrogen-donating hydroxyl groups on the aromatic rings of the phenolic molecules) plays an important role in the free radical-scavenging activity, in this sense the aglycone compounds possess higher antioxidant power than their glycosides (37). In the study of Ydjedd et al. (32), the antioxidant activities tested by DPPH assay of encapsulated and nonencapsulated phenolic carob pulp extracts decreased strongly after the digestion process in comparison to the raw material. They stated that this reduction in activity could be due to the decrease in phenolics after the digestive process. In the study of Li et al. (31), *in vitro* digestions affected the antioxidant activities in a similar manner as they affected the phytochemical contents (carotenoids, phenolics and anthocyanins), i.e. the digestive process significantly reduced the antioxidant activities. For the lipophilic extracts containing mainly carotenoids, after gastric digestion the DPPH and ORAC-L antioxidant activities were reduced by 63% and 67%, respectively, while intestinal digestion caused 64% and 69% reduction in antioxidant activities, respectively (31). Total antioxidant capacity by DPPH assay of dried tomato in the initial, post gastric, post intestine IN and post intestine OUT samples was 1.82, 4.01, 1.07 and 2.02 mg TEAC/g sample, respectively (35).

The results of the reducing power test showed that the antioxidant activity of encapsulates with carbohydrate carriers after digestion decreased by 7.41% for encapsulates with inulin and 13.37% for encapsulates with gum arabic as a carrier. However, with protein carriers used for encapsulation, the antioxidant activities increased by 46.82% in encapsulate with pea protein and by 13.31% in encapsulate with soy protein as carrier. In the study of Ydjedd et al. (32), the decrease of antioxidant activity tested by FRAP assay of encapsulated and nonencapsulated phenolic carob pulp extracts after the digestion process in comparison to the raw material was attributed to the decrease in phenolics. Flores et al. (33) showed that ferric reducing power increased after digestion for the encapsulated blueberry extracts with whey protein isolate as wall material. Similar was observed in our study, reducing power also increased after digestion of tomato waste encapsulates prepared with protein carriers. In the study of Li et al. (31), the digestions caused significant decrease in ORAC-H and FRAP values for the hydrophilic extracts (containing mainly tomato phenolics), i.e. gastric digestion caused 30% and 28% reduction, while gastrointestinal digestion caused 34% and 42% reduction, respectively.

The results of antioxidant activity by BCB test after digestion showed highest value in encapsulate with pea protein as carrier (30.99 mmol TE/100 g encapsulate), since its antioxidant activity increased by 127.27% in comparison to the antioxidant activity determined before *in vitro* gastrointestinal digestion. The increase in antioxidant activity (by 25.96%) was also found in encapsulate with inulin. With gum arabic as a carrier for encapsulation, the antioxidant activity of the BCB test was reduced by 29.66%, and with soy protein as a carrier by 10.98%. It is important to note that by BCB test estimation of antioxidant properties of polar compounds (such as ascorbic acid, known as excellent antioxidant compound) could not be estimated according to phenomenon formulated as the "polar paradox" (38). This is explained

APTEFF, 52, 1-273 (2021) UDC: 635.64:547.56+547.979.8]:616.34-002
DOI: https://doi.org/10.2298/APT2152239S BIBLID: 1450-7188 (2021) 52, 239-252
BY-NC-ND
Original scientific paper

by the fact that polar antioxidants remaining in the aqueous phase of the emulsion are more diluted in lipid phase and are thus less effective in protecting the linoleic acid in BCB test (38). Differently to this, authors have reported that the substrate polarity does not affect DPPH scavenging activity (39).

The impact of variation of the used encapsulation materials on the oxidation stability during storage of powders were investigated in this study, in order to estimate the potential of different wall materials to produce shelf-stable encapsulates with functional compounds extracted from tomato waste. Previous findings reported that the phenolic compounds remain quite stable during storage of encapsulates (19, 40). In contrast, carotenoids are more prone to degradation, precisely to isomerisation, especially at high temperature, in daylight, and oxidation (19). Under these conditions, isomerization of *trans* carotenoids, their usual configuration, is promoted to the *cis* forms, which are much more susceptible to oxidation (41). Therefore, carotenoid retention of tomato waste encapsulates was monitored during four weeks of storage under ambient (25 ± 5 °C) light and dark conditions. When carotenoid retention (%) versus storage time was plotted on a natural logarithmic scale, it followed first-order kinetics (Figure 3).

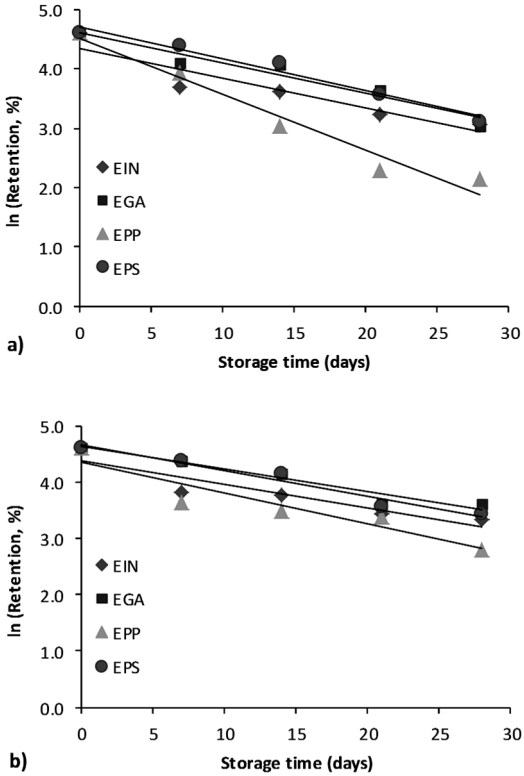

Figure 3. Regression of ln (Retention, %) versus storage time for carotenoids in encapsulates (EIN, EGA, EPP and EPS) under ambient light (a) and dark (b) conditions

APTEFF, 52, 1-273 (2021) UDC: 635.64:547.56+547.979.8]:616.34-002
DOI: https://doi.org/10.2298/APT2152239S BIBLID: 1450-7188 (2021) 52, 239-252
BY-NC-ND
Original scientific paper

The first-order reaction rate constant (k) and half-life time ($t_{1/2}$) values, indicating the degradation rate and stability of the pigments, respectively, were compared (Table 1). Linear correlation coefficients (R^2) ranged from 0.85 to 0.97. As can be seen, carotenoids were susceptible to degradation in the light and dark conditions. The somewhat lower half-life values both in the light and dark conditions were observed for encapsulates with protein than with carbohydrate wall materials, which indicates that encapsulation with carbohydrate carriers slightly increased pigment retention during storage. The half-life values observed for EGA and EIN encapsulates stored in the dark conditions were 17.77 and 16.90 days, and under the light were 13.59 and 13.86 days, respectively. As expected, under the light conditions, all encapsulates retained smaller amount of carotenoids. In the encapsulates stored under the light a greater loss of the total carotenoid content from 6.85% to 15.84% depending on the carrier, in comparison to encapsulates stored in the dark was observed.

Table 1. Kinetic parameters of carotenoid degradation in tomato waste encapsulates (EIN, EAG, EPP and EPS) during four weeks of storage under ambient (25 ± 5 °C) light and dark conditions

Encapsulates	k (day^{-1})	$t_{1/2}$ (day)	R^2
	Light condition		
EIN	0.050	13.86	0.87
EAG	0.051	13.59	0.94
EPP	0.094	7.37	0.96
EPS	0.054	12.83	0.97
	Dark condition		
EIN	0.041	16.90	0.85
EAG	0.039	17.77	0.94
EPP	0.055	12.60	0.87
EPS	0.045	15.40	0.96

In agreement with our results of carotenoid retention in encapsulates prepared on the basis of carbohydrate wall materials, Haas et al. (42) found carotenoid retention of ~30% after four weeks of storage of carotenoid encapsulates prepared with maltodextrin by freeze drying. In the study of Desobry et al. (43), degradation kinetics of encapsulated β-carotene initially followed first order kinetics with an initial fast first order reaction followed by a second much slower first order reaction period. They found that the retention of β-carotene encapsulated in a maltodextrin 25 DE by freeze-drying was about 38% after 15 weeks. In the study of Kulthe et al. (44), β-carotene microcapsules were prepared by spray drying using potato starch, maltodextrin and gelatin as wall materials and after storage for 60 days at ambient conditions the retention of β-carotene was 63-73 %. Wagner and Warthesen (45) found that, after 8 weeks incubation of the spray-dried encapsulated carrot powder in either light or dark conditions at 45°C, total degradation was 90% for both α- and β-carotene in the 4DE hydrolyzed starch powder compared to 70% loss of both α- and β-carotene in the 36.5DE hydrolyzed starch powder. In the study of Przybysz et al. (46), carotenes (α- and β-carotene) isolated from carrot was encapsulated by spray-drying with maltodextrin - arabic gum matrix, and after 3 months of storage the total degradation of pigments was 54.2 %.

BY-NC-ND

CONCLUSIONS

The presented results indicated that the release behavior of bioactive compounds and antioxidant activity after digestion of encapsulates was dependent to the type of wall material. Stronger ability for preservation of phenolic compounds through *in vitro* gastrointestinal digestion was determined in encapsulates prepared with protein carriers. Pea protein showed best carrier properties for the delivery of carotenoid compounds, while differently to other used carriers, gum arabica showed minor ability to release carotenoids after *in vitro* gastrointestinal digestion. Encapsulates produced with carbohydrate wall materials in comparison to protein carriers had somewhat higher half-life values, which indicates that encapsulation with carbohydrate carriers increased pigment retention during storage. The results showed that investigation of release and stability of bioactive compounds in encapsulates during simulated gastrointestinal digestion and storage is obligatory for preparation of functional ingredients and their application in diverse food matrices, including functional food products. Further research would be beneficial to evaluate the influence of the different wall material combinations on the encapsulation of bioactive compounds extracted from tomato waste. This could be of importance since interactions between wall materials may give the improvement of encapsulation process efficiency. Also, response surface methodology can be applied to perform the optimization of the composition of wall materials mixture used in encapsulation according to the preferred responses.

Acknowledgements

This research is part of the Project Project No. 451-03-9/2021-14/200134 which is financially supported by the Ministry of Education, Science and Technological Development of the Republic of Serbia.

REFERENCES

1. Perea-Domínguez, X.P.; Hernández-Gastelum, L.Z.; Olivas-Olguin, H.R.; Espinosa-Alonso, L.G.; Valdez-Morales, M.; Medina-Godoy, S. Phenolic composition of tomato varieties and an industrial tomato by-product: free, conjugated and bound phenolics and antioxidant activity. *J. Food Sci. Technol.* **2018,** *55*(9), 3453-3461.
2. Tommonaro, G.; Speranza, G.; De Prisco, R.; Iodice, C.; Crudele, E.; Abbamondi, G.R.; Nicolaus, B. Antioxidant activity and bioactive compound contents before and after *in vitro* digestion of new tomato hybrids. *J. Sci. Food Agric.* **2017,** *97*(15), 5241-5246.
3. Silva, Y.P.A.; Borba, B.C.; Pereira, V.A.; Reis, M.G.; Caliari, M.; Brooks, M.S.-L.; Ferreira, T.A. P.C. Characterization of tomato processing by-product for use as a potential functional food ingredient: nutritional composition, antioxidant activity and bioactive compounds. *Int. J. Food Sci. Nutr.* **2019,** *70*(2), 150-160.
4. Baaka, N.; El Ksibi, I.; Mhenni, M.F. Optimisation of the recovery of carotenoids from tomato processing wastes: application on textile dyeing and assessment of its antioxidant activity. *Nat. Prod. Res.* **2017,** *31*(2), 196-203.
5. Nour, V.; Ionica, M.E.; Trandafir, I. Bread enriched in lycopene and other bioactive compounds by addition of dry tomato waste. *J. Food Sci. Technol.* **2015,** *52*(12), 8260-8267.
6. Gul, K.; Tak, A.; Singh, A.K.; Singh, P.; Yousuf, B.; Wani, A.A. Chemistry, encapsulation, and health benefits of β-carotene - A review. *Cogent Food & Agric.* **2015,** *1*, 1018696.

BY-NC-ND

7. Shi, J.; Qu, Q.; Kauda, Y.; Yeung, D.; Jiang, Y. Stability and synergistic effect of antioxidative properties of lycopene and other active components. *Crit. Rev. Food Sci. Nutr.* **2004,** *44*, 559-573.
8. Fang, Z.; Bhandari, B. Encapsulation of polyphenols - a review. *Trends Food Sci. Tech.* **2010,** *21*, 510-523.
9. Ahmadian, Z.; Niazmand, R.; Pourfarzad, A. Microencapsulation of saffron petal phenolic extract: their characterization, *in vitro* gastrointestinal digestion, and storage stability. *J. Food Sci.* **2019,** *84*(10), 2745-2757.
10. Harnkarnsujarit, N.; Charoenrein, S.; Roos, Y.H. Porosity and water activity effects on stability of crystalline β-carotene in freeze-dried solids. *J. Food Sci.* **2012,** *77*, 313-320.
11. Stajčić, S.M.; Ćetković, G.S.; Čanadanović-Brunet, J.M.; Tumbas Šaponjac, V.T.; Vulić, J.J.; Šeregelj, V.N. Encapsulation of carotenoids extracted from tomato waste. *Acta periodica technologica*. **2020,** *51*, 149-161.
12. Vaštag, Ž.; Popović, L.; Popović, S.; Krimer, V.; Peričin, D. Production of enzymatic hydrolysates with antioxidant and angiotensin-I converting enzyme inhibitory activity from pumpkin oil cake protein isolate. *Food Chem.* **2011,** *124*, 1316-1321.
13. Singleton, V.L.; Rossi, J.A. Colorimetry of total phenolics with phosphomolybdic-phosphotungstic acid reagents. *Am. J. Enol.Viticult.***1965,** *16*, 144158.
14. Nagata, M.; Yamashita, I. Simple method for simultaneous dermination of chlorophyll and carotenoids in tomato fruit. *J. Jap. Soci. Food Sci. Tehnol.* **1992,** *39*, 925-928.
15. Girones-Vilaplana, A.; Mena, P.; Moreno, D.A.; Garcia-Viguera, C. Evaluation of sensorial, phytochemicaland biological properties of new isotonic beverages enriched with lemon and berries during shelf life. *J. Sci. Food Agric.* **2014,** *94*, 1090-1100.
16. Oyaizu, M. Studies on product of browning reaction prepared from glucose amine. *Japanese Journal of Nutrition.* **1986,** *44*, 307-315.
17. Al-Saikhan, M.S.; Howard, L.R.; Miller, J.J.C. Antioxidant activity and total phenolics in different genotypes of potato (*Solanum tuberosum*, L.). *J Food Sci.* **1995,** *60*(2), 341-343.
18. Cai, Y.Z., Corke, H. Production and properties of spray-dried *Amaranthus* betacyanin pigments. *J. Food Sci.* **2000,** *65*(7), 1248-1252.
19. Šeregelj, V.; Ćetković, G.; Čanadanović-Brunet, J.; Tumbas Šaponjac, V.; Vulić, J.; Stajčić, S. Encapsulation and degradation kinetics of bioactive compounds from sweet potato peel during storage. *Food Technol. Biotechnol.* **2020,** *58*(3), 314-324.
20. McClements, D.J. Encapsulation, protection, and delivery of bioactive proteins and peptides using nanoparticle and microparticle systems: A review. *Adv. Colloid. Interface Sci.* **2018,** *253*, 1-22.
21. Betanzo, J.C.: Betanzo, J.C., Evaluation of food matrix interactions and *in vitro* gastrointestinal digestion on the bioefficacy of polyphenols from blueberries (*Vaccinium* sp.). Ph.D. Thesis, University of Guelph, Ontario, Canada, 2013.
22. Jain, S.; Winuprasith, T.; Suphantharika M. Encapsulation of lycopene in emulsions and hydrogel beads using dual modified rice starch: Characterization, stability analysis and release behaviour during *in-vitro* digestion. *Food Hydrocoll.* **2020,** *104*, 105730.
23. Zhang, Z.; Zhang, R.; McClements, D.J. Encapsulation of β-carotene in alginate-based hydrogel beads: Impact on physicochemical stability and bioaccessibility. *Food Hydrocoll.* **2016,** *61*, 1-10.
24. Flores, F.P.; Singh, R.K.; Kerr, W.L.; Pegg, R.B.; Kong, F. Total phenolics content and antioxidant capacities of microencapsulated blueberry anthocyanins during *in vitro* digestion. *Food Chem*. **2014,** *153*, 272-278.
25. Szabo, K.; Teleky, B.E.; Ranga, F.; Simon, E.; Pop, O.L.; Babalau-Fuss, V.; Kapsalis, N.; Vodnar, D.C. Bioaccessibility of microencapsulated carotenoids, recovered from tomato processing industrial by-products, using *in vitro* digestion model. *LWT - Food Sci. Technol*. **2021,** *152*, 112285.
26. de Boer, F.Y.; Imhofa, A.; Velikov K.P. Encapsulation of colorants by natural polymers for food applications. *Coloration Technology*. **2019,** *135*(1), 183-194.
27. Deng, X.-X.; Zhang, N.; Tang, C.-H. Soy protein isolate as a nano carrier for enhanced water dispersibility, stability and bioaccessibility of β-carotene. *J. Sci. Food Agric.* **2017,** *97*(7), 2230-2237.

BY-NC-ND

28. Kopec, R.E; Gleize, B.; Borel, P.; Desmarchelierd, C., Caris-Veyrat, C. Are lutein, lycopene, and β-carotene lost through the digestive process? *Food Funct.* **2017,** *8*, 1494-1503.
29. Berni, P.; Pinheiro, A.C.; Bourbon, A.I.; Guimarães, M.; Canniatti-Brazaca, S.G.; Vicente, A.A. Characterization of the behavior of carotenoids from pitanga (*Eugenia uniflora*) and buriti (*Mauritia flexuosa*) during microemulsion production and in a dynamic gastrointestinal system. *J. Food Sci. Technol.* **2020,** *57*(2), 650-662.
30. Toor, R.K.; Savage, G.P.; Lister, C.E.; Release of antioxidant components from tomatoes determined by an *in vitro* digestion method. *International Journal of Food Sciences and Nutrition*. **2009**, *60*(2), 119-129.
31. Li, H.; Deng, Z.; Liu, R.; Loewen, S.; Tsao, R. Bioaccessibility, *in vitro* antioxidant activities and *in vivo* anti-inflammatory activities of a purple tomato (*Solanum lycopersicum* L.). *Food Chem.* **2014,** *159*, 353-360.
32. Ydjedd, S.; Bouriche, S.; López-Nicolás, R.; Sánchez-Moya, T.; Frontela-Saseta, C.; Ros-Berruezo, G.; Rezgui, F.; Louaileche, H.; Kati, D.-E. Effect of *in vitro* gastrointestinal digestion on encapsulated and nonencapsulated phenolic compounds of carob (*Ceratonia siliqua* L.) pulp extracts and their antioxidant capacity. *J. Agric. Food Chem.* **2017,** *65*, 827-835.
33. Flores, F.P.; Singh, R.K.; Kerr, W.L.; Phillips, D.R.; Kong, F. *In vitro* release properties of encapsulated blueberry (*Vaccinium ashei*) extracts. *Food Chem*.**2015,** *168*, 225-232.
34. Saikia, S.; Mahnot, N.K.; Mahanta, C.L. Optimisation of phenolic extraction from *Averrhoa carambola* pomace by response surface methodology and its microencapsulation by spray and freeze drying. Food Chem. **2015,** *171*, 144-152.
35. Pasli, A.A.; Yavuz-Düzgün, M.; Altuntas, U.; Altin, G.; Özçelik, B.; Firatligil, E. *In vitro* bioaccessibility of phenolics and flavonoids in various dried vegetables, and the determination of their antioxidant capacity via different spectrophotometric assays. *International Food Research Journal.* **2019,** *26*(3), 793-800.
36. Gullon, B.; Pintado, M.E.; Fernández-López, J.; Pérez-Álvarez, J.A.; Viuda-Martos, M. *In vitro* gastrointestinal digestion of pomegranate peel (*Punica granatum*) flour obtained from co-products: Changes in the antioxidant potential and bioactive compounds stability. *J. Funct. Foods*. **2015,** *19*, 617-628.
37. Rice-Evans, C.A.; Miller, N.J.; Paganga, G. Structure antioxidant activity relationships of flavonoids and phenolic acids. *Free Radical Biol. Med.* **1996,** *20*, 933-956.
38. Kulisic, T.; Radonic, A.; Katalinic, V.; Milos, M. Use of different methods for testing antioxidative activity of oregano essential oil. *Food Chem*. **2004,** *85*, 633-640.
39. Koleva, I.I.; van Beek, T.A.; Linssen, J.P.H.; de Groot, A.; Evstatieva, L.N. Screening of plant extracts for antioxidant activity: a comparative study on three testing methods. *Phytochemical Analysis*. **2002,** 13, 8-17.
40. Moser, P.; Telis, V.; de Andrade Neves, N.; García-Romero, E.; Gómez-Alonso, S.; Hermosín-Gutiérrez, I. Storage stability of phenolic compounds in powdered BRS Violeta grape juice microencapsulated with protein and maltodextrin blends. *Food Chem.* **2017,** *214*, 308-318.
41. Rodriguez-Amaya, D.B. *A guide to carotenoid analysis in foods*. OMNI Research, ILSI Human Nutrition Institute: Washington, DC, 2001.
42. Haas, K.; Obernberger, J.; Zehetner, E.; A.; Kiesslich, Volkert, M.; Jaeger H. Impact of powder particle structure on the oxidation stability and color of encapsulated crystalline and emulsified carotenoids in carrot concentrate powders. *J. Food Eng.* **2019,** *263*, 398-408.
43. Desobry, S.A.; Netto, F.M.; Labuza, T.P. Comparison of spray-drying, drum-drying and freeze-drying for β-carotene encapsulation and preservation. *J. Food Sci.* **1997,** *62*(6), 1158-1162.
44. Kulthe, A.A.; Thorat, S.S.; Mhalaskar, S.R. Physical stability of β-carotene encapsulated with different wall materials. *Bioscan*. **2016,** *11*(3), 1577-1581.
45. Wagner, L.A.; Warthesen, J.J. Stability of spray-dried encapsulated carrot carotenes. *J. Food Sci.* **1995,** *60*, 1048-1053.
Przybysz, M.; Szterk. A.; Symoniuk, E.; Gqszczyk, M.; Dluzevska. E. α- and β-carotene stability during storage of microspheres obtained from spray-dried microencapsulation technology. *Pol. J. Food Nutr. Sci*. **2018,** *68*(1), 45-55.

APTEFF, 52, 1-273 (2021) UDC: 662.754+547.262]:633.11:532.13
DOI: https://doi.org/10.2298/APT2152253S BIBLID: 1450-7188 (2021) 52, 253-263
BY-NC-ND
Original scientific paper

INFLUENCE OF PHYSICOCHEMICAL PARAMETERS OF THE ALKALINE PRETREATMENT ON THE VISCOSITY OF WHEAT STRAW SLURRIES

Vitalii SYDORENKO[1], Oleksandr OBODOVYCH[1], Tetyana GRABOVA[1], Olena PODOBII[2]*

[1] Institute of Engineering Thermophysics of the National Academy of Sciences of Ukraine 2, Akademika Bulakhovskoho St., Kyiv, Ukraine, 03164
[2] National University of Food Technologies, 68, Volodymyrska St., Kyiv, Ukraine, 01601

Received: 20 July 2021. **Revised: 13 September 2021** **Accepted: 24 September 2021**

The paper presents the results of the influence of physicochemical parameters of the alkaline pretreatment on the viscosity of wheat straw slurries on its rheological properties. The authors consider the coefficient of apparent viscosity as a complex indicator of wheat straw slurries pretreatment process which depends on the structure and physicochemical properties of system components, thermal parameters of the process (temperature, dispersion, and concentration of dispersed phase, shear flow rate).

A wheat straw slurries with a solids content of 10…15% were chosen as the object of research. As a result of research, rheological viscosity and fluidity were constructed for these slurries in the range of shear rates from 1 to 437.4 s-1. The value of viscosity as a function of shear rate for a solids concentration of 10, 12, and 15% w. is given. It has been determined that in a certain range of shear rates the slurries show the behavior of viscoelastic fluids with yield stress, and with increasing of the solids concentration the rate of decrease of viscosity increases with increasing shear rate. A study of the effect of alkali concentration on apparent viscosity was performed. It is determined that an increase in the concentration of alkali leads to an increase in the apparent viscosity of the slurry, and with increasing alkali concentration, the rate of decrease in viscosity decreases with increasing shear rate. The value of the apparent viscosity of the suspension as a function of temperature is given.

Keywords: bioethanol, wheat straw, pretreatment, viscosity, temperature.

INTRODUCTION

Bioethanol obtaining from lignocellulosic biomass, compared with sugar or starch-containing raw materials, is more expensive (1).

The stage of lignocellulosic biomass pretreatment before hydrolysis is the most energy-consuming in the process of bioethanol (2). The aim of pretreatment is to destroy the structure of cellulosic biomass, make cellulose more accessible to enzymes that convert carbohydrate polymers into fermenting sugars (3).

The reason for the high energy consumption of biomass pretreatment for hydrolysis is that the process occurs at elevated temperatures and pressures (4).

One way to reduce the cost of processing biomass is by increasing the insoluble solids concentration can reduce the cost of processing biomass. Decreasing the water content reduces operating costs (e.g., heating, water handling) as well as capital costs (5, 6).

* Corresponding author: Vitalii Sydorenko, Institute of Engineering Thermophysics of the National Academy of Sciences of Ukraine 2, Akademika Bulakhovskoho St., Kyiv, Ukraine, e-mail: tdsittf@ukr.net

APTEFF, 52, 1-273 (2021)
DOI: https://doi.org/10.2298/APT2152253S
BY-NC-ND
UDC: 662.754+547.262]:633.11:532.13
BIBLID: 1450-7188 (2021) 52, 253-263
Original scientific paper

However, biomass suspensions are very viscous, non-Newtonian, complex fluids, which make mixing reactants and conveying the biomass challenging (7). Also, an additional task is the subsequent washing of highly concentrated slurries.

It should be noted that the mixing of materials and mass transfer plays a significant role in the physicochemical processing of raw materials and are clear areas for improvement through the application of engineering principles (8).

Biomass slurries consist of solid and liquid phases. The liquid phase is an aqueous solution of alkalis or acids; the solid phase consists of biomass particles. The particles of the biomass suspension are porous, anisotropic, deformable, and, as a rule, not Brownian (9).

The thermal exposure and action of catalysts change the structural properties of raw materials. Water-soluble components such as salts, proteins, sugars, dyes, etc. pass into the solution. During alkaline pretreatment, lignin is released into the alkaline solution, exposing the cellulose fibers (10).

Undiluted pretreated corn stover (PCS) (~ 20% insoluble solids by mass) is a suspension paste: it can easily be formed into a shape that remains when the applied forces are removed (11).

At low concentrations (<4% (v/v)), particles in a Newtonian fluid form suspension where the solid elements are far from each other and have negligible mutual interactions. In such dilute slurries, theoretical viscosity calculations predict a Newtonian fluid behavior as long as the particles are isotropic spheres. However, if the particles are non-spherical, the suspensions can exhibit non-Newtonian behavior even at low concentrations (12).

There are a number of studies on the rheological properties of biomass suspensions, namely corn stover (8, 12-14), marine microalgae suspensions Nannochloropsis sp. (15), cereal straw (16).

Rheological properties were determined both for untreated slurries and slurries after pretreatment.

For example, the corn stover, previously ground and sieved with a 5.1-cm (2 in) screen, was treated with dilute sulfuric acid at a loading of 0.048 g/g (acid per dry biomass) and a temperature of 190 ºC for 1 min was studied (8). The total biomass solids concentration during the reaction was 30% by mass. It was found that undiluted pretreatment corn stover with a concentration of 20% insoluble solids was found to have the rheological properties of a thick, stiff paste. At this concentration, the elastic modulus was measured to be almost an order of magnitude larger than the viscous modulus, and yield stress values were measured on the order of 1,000 Pa. The high yield stress and shear-thinning behavior of the concentrated pretreated biomass indicate that traditional tanks stirred with impellers are not adequate as reaction vessels for enzymatic hydrolysis of the biomass, at least not for the start of the reaction.

The rheological properties of corn stover slurries in a wide range of concentrations (5-30%) were investigated using Brookfield viscometers with a cone and plate instrument and a helical impeller (17).

Corn stover was pretreated with 1.4% sulfuric acid solution for 2-3 minutes. The authors determined that the viscosity of the suspension increased with increasing fiber loading. The resulting relationship between shear stress and the shear rate was linear for only 5% of the suspension. The rest showed non-Newtonian behavior. At other concentrations (>5%) the degree of linearity decreased with increasing mass concentration.

BY-NC-ND

This corn stover was pretreated in a 1.4% sulfuric acid solution for 3–12 min. The authors determined that the viscosity of the suspension increased as the fiber loading increased.

Later the rheological characteristics of untreated and dilute acid pretreated corn stover slurries at high solid concentrations were studied under continuous shear using plate–plate type measurements. Slurry rheological behavior was examined as a function of insoluble solids concentration (10–40%), the extent of pretreatment (0–75% removal of xylan), and particle size (- 20 and -80 mesh). The negative slope of the curves in the dependences of the viscosity on the shear rate implies that these slurries exhibit pseudoplastic or shear-thinning behavior in the range of shear rates tested.

The authors determined that with the increase of the insoluble solid concentration, the viscosity of the suspension increases in the whole range of shear rates, but at high concentrations of the solid phase (30-32 m% of the mass) the curves almost overlap. This behavior is associated by the authors with the fact that available water is absorbed/entrained within the biomass resulting in the transformation of the mixture from slurry to wet granular material. In such granular solids, in the presence of an external shear, frictional interactions among particles would be expected to predominate. Moreover, since it is likely that the frictional forces do not change significantly after the slurry becomes unsaturated, a constant apparent viscosity would be measured at such high solid concentrations.

Klingenberg et al. (7) presented a new device that can measure the rheological properties of lignocellulosic biomass slurries with high solids concentrations (>25%) containing large particles (>10 mm), and that can operate at high temperatures (>230 ºC), high pressures (>2.8 MPa), and low pH (<1.0).

The material was corn stover, chopped, dried to 8% moisture and size-reduced on a 5 mm screen (chopped and milled corn stover) and corn straw, ground with a hammer crusher, additionally ground Wiley mill using a 3 mm and dried to moisturize content of 5% mm (milled corn stover). As a result of testing the device, the dependences of the apparent viscosity on the apparent shear rate for both chopped and milled corn stover (mass fraction of insoluble solids 15%) and milled corn stover (mass of insoluble solids 20%) were obtained in a range of shear rate 0…50 c-1 for temperatures from 95 to 150 ºC. The effect of sulfuric acid on the rheological properties of biomass was also determined, where the apparent viscosity is constructed as a function of temperature for one sample of corn stover (insoluble solids mass fraction ¼ 20%) with 1.0% H_2SO_4. Biomass was heated from 55 to 166 ºC. As the temperature is increased, the viscosity decreases. When the temperature reached 166 ºC, the biomass was then cooled (cooling rate less than 1 K/min). In this case, the viscosity subsequently remained small, much less than that measured before the sample was heated to 166 ºC. Visual inspection of the biomass after the experiment revealed that the biomass solids average particle size and overall concentration had decreased significantly because of the acid-catalyzed hydrolysis of the solids.

Since the removal of lignin during pretreatment is a key point for further hydrolysis, treatment of lignocellulosic raw materials with alkalis is also considered by many authors as a step in the process of bioethanol production (18-20).

Thorough mixing during the biochemical deconstruction of biomass is crucial for achieving maximum process yields and economic success. However, due to the complex morphology and surface chemistry of biomass particles, biomass mixing is challenging, and currently, it is not well understood (21). An understanding of the rheology of feedstock

APTEFF, 52, 1-273 (2021)
DOI: https://doi.org/10.2298/APT2152253S
BY-NC-ND
UDC: 662.754+547.262]:633.11:532.13
BIBLID: 1450-7188 (2021) 52, 253-263
Original scientific paper

(pulp) is essential for designing appropriate reaction processes and equipment (8). This is particularly important for the design and modeling of fluid dynamics and heat transfer in rotor-pulsation apparatus (22).

In industrial technologies, rheological processes are predominant and apply to such heat and mass transfer and physicochemical processes of biomass processing as dispersion, homogenization, hydrotransportation, conversion, etc. As the structural viscosity decreases, the productivity of the plants increases and the energy consumption decreases accordingly.

For the development and operation of technological equipment, obtaining the target product of high quality with minimal energy consumption requires knowledge of the rheological structural and mechanical properties of suspensions.

The mechanism of the viscous flow of the biomass suspension depends on the structural features of the system, which in turn depend on the degree of dispersion and kinetic properties of the dispersed phase and the intensity of the interphase interaction of the components of the biomass suspension. The change in viscosity can also be used to judge the depth of structural transformation of biomass in the pretreatment process.

Given the above, the aim of the work is to determine the influence of physicochemical parameters of the alkaline pretreatment on the viscosity of wheat straw slurries.

Based on the aim it was necessary to solve the following tasks:

- to determine the dependence of the apparent viscosity of the wheat straw aqueous suspension on the weight fraction of solids;
- to determine the dependence of the apparent viscosity of the wheat straw aqueous suspension on the amount of catalyst;
- to determine the dependence of the apparent viscosity of the wheat straw aqueous suspension on temperature.

EXPERIMENTAL

BIOMASS FEEDSTOCK

Wheat straw was harvested in August 2020 in the Kyiv region of Ukraine. From the beginning, the straw was coarsely ground at the Rozumnytsia electric chopper to a fraction of 1 cm. The resulting chop was crushed on a disintegrator DZ 300-2. The particle size distribution of biomass was determined by sieve analysis. Figure 1 shows the obtained wheat straw particle distribution after sieving on sieves.

BIOMASS PRETREATMENT

Distilled water was used to prepare the aqueous suspension of straw.

Straw was gradually added to the pre-weighed water, stirring, in an amount determined by the experimental conditions. Stirring was performed until visual homogeneity of the mixture, but not less than 5 minutes. The resulting mixture was heated in an oil bath to a temperature determined by the experimental conditions.

The influence of alkali concentration on the viscosity of the aqueous straw dispersion was performed in the same way as the aqueous straw suspension, but with a few differences. An alkali solution was prepared at a concentration determined by the experimental con-

APTEFF, 52, 1-273 (2021)
DOI: https://doi.org/10.2298/APT2152253S
BY-NC-ND
UDC: 662.754+547.262]:633.11:532.13
BIBLID: 1450-7188 (2021) 52, 253-263
Original scientific paper

ditions. The solution was brought to the required temperature and the straw was added in the amount determined by the experiment.

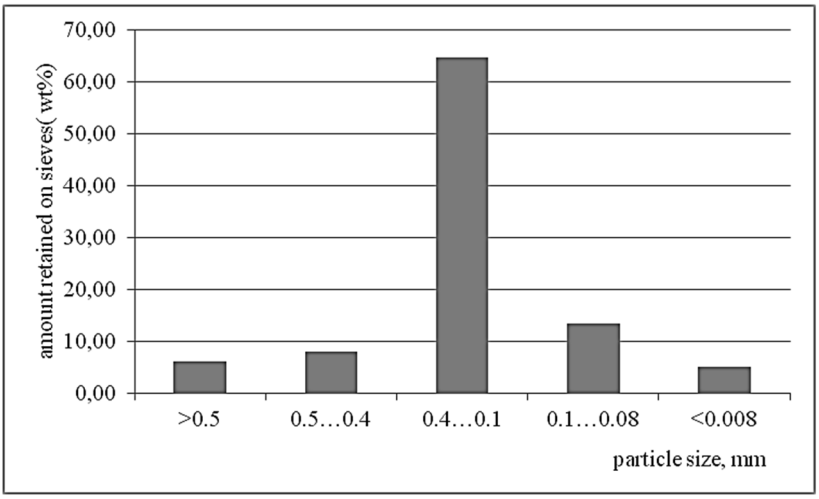

Figure 1. Wheat straw particles distribution retained on sieves

RHEOLOGICAL MEASUREMENTS

Measurements of the apparent viscosity of the obtained suspension were performed on a rotary viscometer REOTEST-2.0 (Germany). with a cylindrical measuring device (viscosity measurement range 1…1.8 · 10^7 mPa·s). To maintain the set temperature during the measurement, the device is equipped with a thermostatic vessel. Spindle S3 (for average viscosity values) was used for measurements.

The measurements were performed according to the method described in the operating instructions of the device REOTEST-2.0. Shear rate, shear stress, apparent viscosity and temperature were collected for all tests. Each flow test was repeated between 3 and 10 times depending on the coefficient of variation, which did not exceed 33%. According to the results in each group of experiments, the average value was determined, according to which the dependencies of the change of rheological parameters were built.

RESULTS AND DISCUSSION

Figure 2 shows the obtained curves of the apparent viscosity for straw concentrations of 10, 12, 15% at a temperature of 20 ºC and 1% NaOH concentration in the load mode. Determination of the viscosity of aqueous slurries of straw without a catalyst is not acceptable for the chosen method of measurement, because such suspensions do not exhibit the properties of structured systems and quickly delaminate (17).

The shape of the curves indicates the non-Newtonian nature of the flow inherent in viscoelastic fluids with yield stress. All curves, both shown in the figure and others obtained during the experiment, are well approximated by the Herschel-Bulkley equation.

APTEFF, 52, 1-273 (2021)
DOI: https://doi.org/10.2298/APT2152253S
BY-NC-ND
UDC: 662.754+547.262]:633.11:532.13
BIBLID: 1450-7188 (2021) 52, 253-263
Original scientific paper

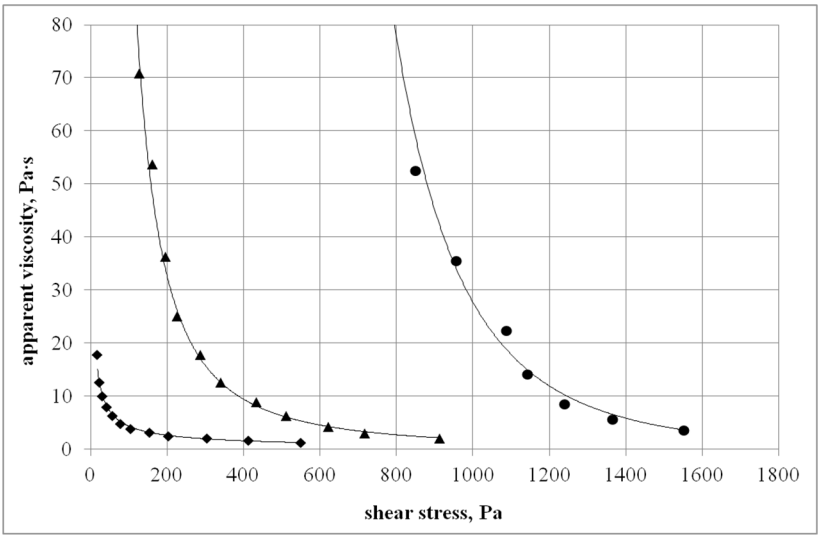

Figure 2a. Rheological curves of viscosity of wheat straw suspension in alkaline solution (1% NaOH) at a temperature of 20 ºC at a solid concentration: ♦ - 10%; ▲ - 12%; ● - 15%.

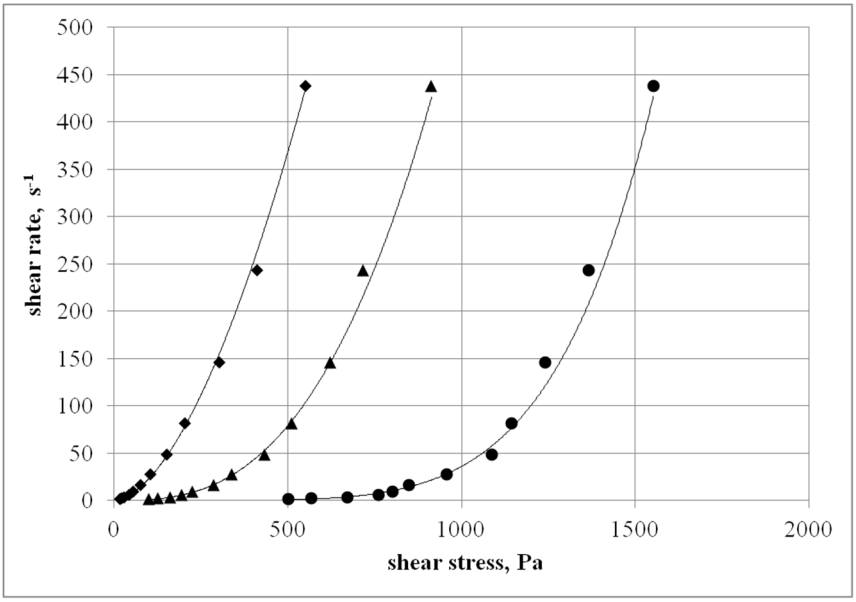

Figure 2b. Rheological fluidity curves of straw slurry in alkaline solution (1 % NaOH) at a temperature of 20 ºC at a solid concentration: ♦ - 10%; ▲ - 12%; ● - 15%.

APTEFF, 52, 1-273 (2021)
DOI: https://doi.org/10.2298/APT2152253S
BY-NC-ND
UDC: 662.754+547.262]:633.11:532.13
BIBLID: 1450-7188 (2021) 52, 253-263
Original scientific paper

The viscosity curves (Fig. 3) presented in double logarithmic coordinates tend to increase the value of the structural viscosity coefficient with increasing concentration of the solid phase in the suspension. Thus, with an increase in concentration by 2% - almost an order of magnitude, with a further increase - slightly lower. In addition, with increasing solid concentration viscosity of the suspension is more sensitive to increasing the rate of deformation, i.e. relaxation processes prevail over the thixotropic restoration of structural bonds in suspension.

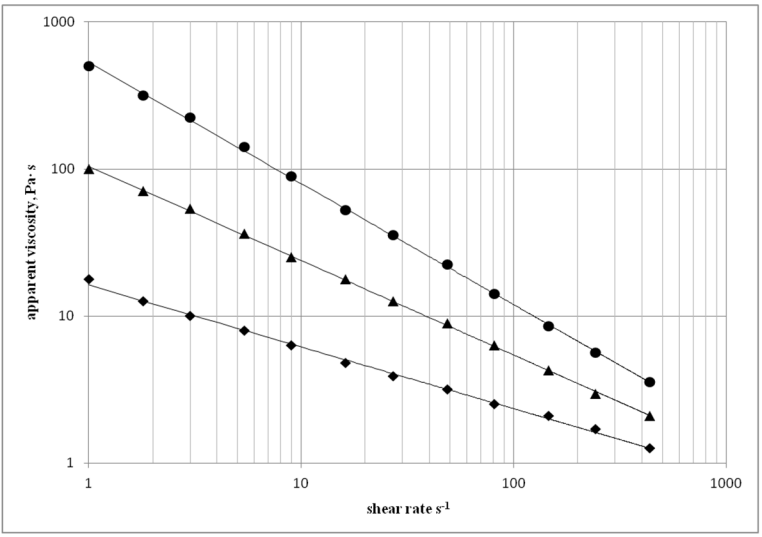

Figure 3. Apparent viscosity as a function of shear rate for the wheat straw slurry (1% NaOH) at a temperature of 20 ºC at a solid concentration: ♦ - 10%; ▲ - 12%; ● - 15%.

Under the action of alkali and shear deformations, there are complex physicochemical processes in the structure of biomass particles: the destruction of the structural framework of biomass particles, reduction of particle size, splitting into fibrillar structures with increasing interfacial surface, swelling and hydration of particles. With increasing pH, the connections between individual fibrillar structures weaken and break down, their surface becomes rough due to the intense release of various lyophilic colloids (e.g., lignin and hemicelluloses). The development of the specific surface of the dispersed particles leads to improved penetration of molecules of the dispersion medium into the interfibrillar space. All this leads to an increase in the suspension viscosity.

Figure 4 shows the effect of alkali concentration on apparent viscosity at 20 ºC at 10% solids concentration. As can be seen from the graph, an increase in alkali concentration leads to a more intense process of releasing lignin derivatives into the solution and, as a result, an increase in apparent viscosity.

APTEFF, 52, 1-273 (2021)
DOI: https://doi.org/10.2298/APT2152253S
BY-NC-ND
UDC: 662.754+547.262]:633.11:532.13
BIBLID: 1450-7188 (2021) 52, 253-263
Original scientific paper

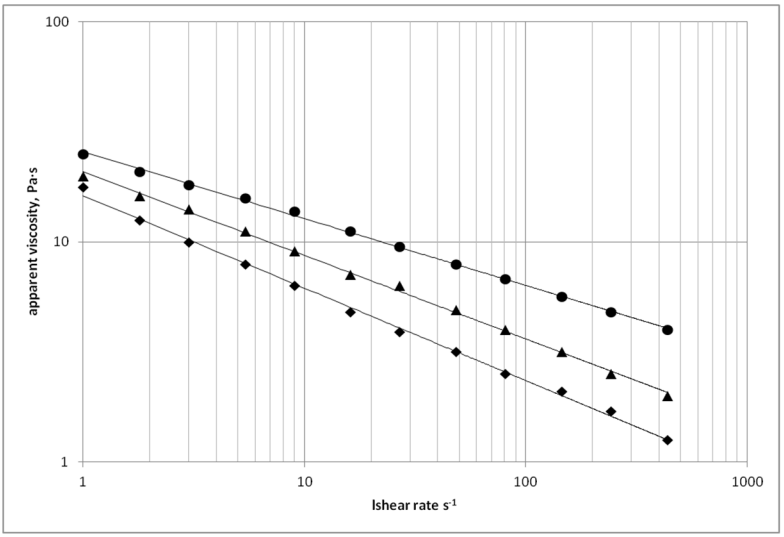

Figure 4. Apparent viscosity as a function of shear rate for the wheat straw slurry (10% solids) at a temperature of 20°C at an alkali concentration: ♦ - 1%; ▲ - 2%; ● - 5%.

The effect of temperature on the apparent viscosity of the wheat straw slurry (1% NaOH) for different concentrations of solids at a shear rate of 16.2 s^{-1} is presented in Table 1.

Table 1. The dependence of the apparent viscosity of the wheat straw slurry (1% NaOH) at a shear rate of 16.2 s^{-1} for the solids concentration of 10, 12, 15 %.

Temperature, °C	**Solid concentration, %**		
	10	12	15
	apparent viscosity, Pa·s		
20	4.78	17.80	52.50
30	3.90	13.00	35.55
40	3.22	10.85	26.10
50	2.78	9.05	20.05
60	2.51	7.5	17.11
70	2.22	6.92	14.51
80	2.10	6.00	12.50

These table indicate that the apparent viscosity of the wheat straw slurry decreases with increasing temperature at all given solids concentrations. As the temperature of the suspension increases, the intermolecular interaction (interaction between the dispersed particles) decreases due to the thermal expansion of the dispersion medium and the increase in the distance between the dispersed particles.

APTEFF, 52, 1-273 (2021)
DOI: https://doi.org/10.2298/APT2152253S
BY-NC-ND
UDC: 662.754+547.262]:633.11:532.13
BIBLID: 1450-7188 (2021) 52, 253-263
Original scientific paper

The effect of alkali concentration on the apparent viscosity of the wheat straw slurry at solids concentration of 10% is given in Table 2.

Table 2. The dependence of the apparent viscosity of the of the wheat straw slurry (10% solids concentration) at a shear rate of 16.2 s^{-1} for the alkali concentration of 1, 2, and 5%.

Temperature, ºC	alkali concentration, %		
	1	2	5
	apparent viscosity, Pa·s		
20	4.78	7.10	11.2
30	3.90	6.00	9.25
40	3.22	5.35	7.95
50	2.78	4.90	7.15
60	2.51	4.38	6.89
70	2.22	4.20	6.11
80	2.10	4.00	6.80

As you can see, as the alkali concentration increases, the apparent viscosity values decrease over the entire temperature range, and the decrease in viscosity in this case is slower than in the case of a change in solids concentration. This is probably due to the fuller release of lignin and hemicelluloses into solution.

CONCLUSIONS

During the work, the value of the apparent viscosity of aqueous suspensions of wheat straw in the range of solids concentrations of 10…15%, alkali concentration of 1…4% by weight was obtained. Visible viscosity values were determined at temperatures from 20 to 80 ºC. The constructed rheological curves allowed to determine the behavior of suspensions in the shear field and to refer the investigated systems to viscoplastic fluids with yield stress. The obtained data give an idea of the degree of influence of each of the above parameters on the viscosity of aqueous suspensions of wheat straw during the process of pretreatment for hydrolysis and the corresponding change in the nature of the flow of these systems in the shear field.

REFERENCES

1. Cheng, M. H.; Huang, H.; Dien, B. S. & Singh, V. The costs of sugar production from different feedstocks and processing technologies. *Biofuels Bioproducts and Biorefining*. **2019**, 13(3), 723–739. DOI: https://doi.org/10.1002/bbb.1976
2. Tsegaye, B.; Balomajumder, C.; Roy, P. Alkali pretreatment of wheat straw followed by microbial hydrolysis for bioethanol production. *Environmental Technology*, **2017**, 1–9, 1203-1211. DOI:10.1080/09593330.2017.1418911

BY-NC-ND

3. Xu, Z.; Huang, F. Pretreatment Methods for Bioethanol Production. *Applied Biochemistry and Biotechnology*, **2014**, 174(1), 43–62. DOI:10.1007/s12010-014-1015-y
4. Nauman Aftab, M.; Iqbal, I.; Riaz, F.; Karadag, A.; Tabatabaei, M. (2019). Different Pretreatment Methods of Lignocellulosic Biomass for Use in Biofuel Production. Biomass for Bioenergy - Recent Trends and Future Challenges. DOI:10.5772/intechopen.84995
5. Lynd, L. R. Overview and evaluation of fuel ethanol from cellulosic biomass: Technology, Economics, the Environment, and Policy. *Annual Review of Energy and the Environment*, **1996**, 21(1), 403–465. DOI:10.1146/annurev.energy.21.1.403
6. Wingren, A.; Galbe, M.; Zacchi, G. Techno-Economic Evaluation of Producing Ethanol from Softwood: Comparison of SSF and SHF and Identification of Bottlenecks. *Biotechnology Progress*, **2008**, 19(4), 1109–1117. DOI:10.1021/bp0340180
7. Klingenberg, D. J.; Root, T. W.; Burlawar, S.; Scott C.T. Rheometry of coarse biomass at high temperature and pressure. *Biomass and Bioenergy*, **2017,** 99, 69-78. https://doi.org/10.1016/j.biombioe.2017.01.031.
8. Stickel, J. J.; Knutsen, J. S.; Liberatore, M. W. Rheology measurements of a biomass slurry: an inter-laboratory study. *Rheologica Acta*, **2009**, 48, 1005–1015. https://doi.org/10.1007/s00397-009-0382-8
9. Crawford, N. C.; Sprague, M. A.; Stickel, J. J. Mixing behavior of a model cellulosic biomass slurry during settling and resuspension. *Chemical Engineering Science*, **2016**, 144, 2, 310-320. https://doi.org/10.1016/j.ces.2016.01.028
10. Kucharska, K.; Rybarczyk, P.; Hołowacz, I.; Łukajtis, R.; Glinka, M.; Kamiński, M. Pretreatment of Lignocellulosic Materials as Substrates for Fermentation Processes. *Molecules*, **2018,** 23(11), 2937. DOI: 10.3390/molecules23112937.
11. Coussot, P. Rheophysics of pastes: a review of microscopic modelling approaches. *Soft Matter*, **2007**, 3(5), 528. DOI:10.1039/b611021p
12. Viamajala, S.; McMillan, J. D.; Schell, D. J.; Elander, R. T. Rheology of corn stover slurries at high solids concentrations -Effects of saccharification and particle size, *Bioresource Technology*, **2009**, 100(2), 925–934. DOI:10.1016/j.biortech.2008.06.070.
13. Ehrhardt, M. R.; Monz, T. O.; Root, T. W.; Connelly, R. K.; Scott, C. T.; Klingenberg, D. J. Rheology of Dilute Acid Hydrolyzed Corn Stover at High Solids Concentration. *Applied Biochemistry and Biotechnology*, **2009**, *160*(4), 1102–1115. DOI:10.1007/s12010-009-8606-z
14. Samaniuk, J. R.; Wang, J.; Root, T. W.; Scott, C. T.; Klingenberg, D. J. Rheology of concentrated biomass. *Korea-Australia Rheology Journal*, **2011**, 23(4), 237–245. DOI:10.1007/s13367-011-0029-z
15. Mettu, S.; Yao, S.; Law, S. Q. K.; Sun, Z.; Scales, P. J.; Ashokkumar, M.; Martin, G. J. O. Rheological properties of concentrated slurries of harvested, incubated and ruptured Nannochloropsis sp. cells. *BMC Chemical Engineering,* **2019**, 1(1). https://doi.org/10.1186/s42480-019-0011-y
16. Tian, S.-Q.; Zhao, R.-Y.; Chen, Z.-C. Review of the pretreatment and bioconversion of lignocellulosic biomass from wheat straw materials. *Renewable and Sustainable Energy Reviews*, **2018**, 91, 483-489. https://doi.org/10.1016/j.rser.2018.03.113.
17. Pimenova, N. V.; Hanley, T. R. Effect of Corn Stover Concentration on Rheological Characteristics. *Applied Biochemistry and Biotechnology*, **2004**, *114*(1-3), 347–360. DOI:10.1385/abab:114:1-3:347
18. Zheng, Q.; Zhou, T.; Wang, Y. Pretreatment of wheat straw leads to structural changes and improved enzymatic hydrolysis. *Scientific Reports*, **2018**, 8(1). DOI:10.1038/s41598-018-19517-5
19. Li, M.; Wang, J.; Yang, Y.; Xie, G. Alkali-based pretreatments distinctively extract lignin and pectin for enhancing biomass saccharification by altering cellulose features in sugar-rich Jerusalem artichoke stem. *Bioresource Technology*, **2016**, 208, 31–41. DOI:10.1016/j.biortech.2016.02.053

BY-NC-ND

20. Gupta, R.; Lee, Y.Y. Investigation of biomass degradation mechanism in pretreatment of switchgrass by aqueous ammonia and sodium hydroxide. *Bioresource Technology*, **2010**, 101(21), 8185–8191. DOI:10.1016/j.biortech.2010.05.039
21. Crawford, N. C.; Sprague, M. A.; Stickel, J. J. Mixing behavior of a model cellulosic biomass slurry during settling and resuspension. *Chemical Engineering Science*, **2018**, 144, 310-320. https://doi.org/10.1016/j.ces.2016.01.028
22. Basok, B.I.; Pirozhenko, I.A.; Davidenko, B.V.; Obodovich, A.N. Strukturno-mehanicheskie svojstva soevoj pasty, poluchennoj pri obrabotke v rotorno-pul'sacionnom apparate. *Promyshlennaja teplotehnika*, **2009**, 31(2), 31-36.

APTEFF, 52, 1-273 (2021) UDC: 669-1:621.9.048
DOI: https://doi.org/10.2298/APT2152265R BIBLID: 1450-7188 (2021) 52, 265-273
BY-NC-ND
Original scientific paper

ULTRASOUND-ASSISTED CREEP DEFORMATION OF METALS

Andrew Rusinko[1], Ali H. Alhilfi[2]*

[1] Obuda University, Nepszinhaz St. 8, Budapest, Hungary, H-1081
[2] Misan University, Amarah, Maysan, Iraq

Received: 15 September 2021 **Revised: 09 October 2021** **Accepted: 11 October 2021**

This paper aims to develop a mathematical model to calculate the creep deformation of metals in the ultrasonic field. Experimental data recording that acoustic energy leads to an increase of primary and secondary creep has become the impetus for this research. The model is constructed in terms of the synthetic theory of irrecoverable deformation. To catch the phenomena caused by sonication, we introduce a new term reflecting the nucleation and development of the crystalline grid's defects in the ultrasonic field. By inserting this term into the basic relationships of the synthetic theory that define the deformation state of the material, we have derived the formulae describing the development of time-dependent deformation coupled with ultrasound. As a result, since the analytic solutions fit good the experimental data, we have elaborated an analytical instrument to predict the increase in the creep deformation of metals due to acoustic energy.

Keywords: ultrasonic softening, creep deformation, synthetic theory

INTRODUCTION

Since the thirty years of the last century, ultrasonic technology has been widely applied in biomedicine, chemistry and chemical engineering, and the metallurgical industry. Due to the high efficiency and simple adaptation of acoustic energy, ultrasonic vibration is a promising assistant technology to improve the microforming processes, for example, decreasing friction, enhancing surface finishing, and reducing forming load/stress.

Researchers record the following phenomena related to the deformational properties of metals in the ultrasonic field:

i. Sonication of annealed materials increases their yield strength; this phenomenon is termed ultrasonic hardening (1, 2).
ii. Deforming materials under simultaneous unidirectional and ultrasonic load; numerous researchers record a drastic decrease in the stress needed to produce the same deformation compared to static loading – ultrasonic softening (3-6).
iii. With the ultrasound-assisted creep deformation, the ultrasonic softening manifests itself in increasing both primary and secondary portions of creep deformation (2, 7).

Despite abundant experimental and theoretical research on ultrasonic technology, the ultrasound mechanism is still controversial and requires further investigation. It can be summarized as:

i. A stress superimposition mechanism proposed by Malygin (8) implies that ultrasonic waves activate anchored dislocations hardened under ordinary deformation.

* Corresponding author: Andrew Rusinko, Obuda University, Nepszinhaz St. 8, Budapest, Hungary, H-1081, e-mail: ruszinko.endre@bgk.uni-obuda.hu

APTEFF, 52, 1-273 (2021) UDC: 669-1:621.9.048
DOI: https://doi.org/10.2298/APT2152265R BIBLID: 1450-7188 (2021) 52, 265-273
BY-NC-ND
Original scientific paper

However, according to Daud et al. (6), one should avoid the simple addition of unidirectional and oscillatory stresses.

ii. Deshpande et al. (3) draw an analogy between the effects of hot deformation and ultrasound action. They indicate microstructure evolution similar to that when thermal energy is replaced with ultrasonic energy. As a result, numerous investigators suggest that ultrasonic vibration induces sufficient heat input to the sample to soften the microstructure (3, 5).

iii. The investigations upon the effect of ultrasound on creep in copper and germanium found that the acceleration in creep rate is attributable to the nucleation of vacancy-type point defects (2).

Based on the preceding, we explain the creep's increase in the acoustic field by the combined action of the factors proposed above, namely (i) the activation of blocked and hindered dislocation via the inflow of ultrasound-nucleated-vacancies, (ii) sonication boosts slips in the active slip systems and involve new ones, and (iii) ultrasound softens the material, similarly to heat energy.

The present work aims to model how ultrasonic vibration affects the creep deformation of metals. For a mathematical apparatus describing phenomena of ultrasound-assisted creep, we take the Synthetic theory of irrecoverable deformation, which turns out to be an effective tool for modeling various problems related to the deformation coupled with acoustic energy (1).

The first steps towards modeling the creep superimposed by ultrasonic vibration were taken in work (9), where we considered the primary creep of metals alone. Here we expand the results obtained in (9) to describe the whole ultrasound-assisted creep diagram. Therefore our goal is to complete the formation of a mathematical model that covers both primary and secondary creep of metals in the presence of ultrasound. Based on the experimental results explaining the physical nature of ultrasound impact upon the microstructural state of sonicated material, we introduce an average measure of crystalline grid's defects induced by acoustic energy into the relationships of the synthetic theory governing the deformation state of the material. As a result, we derive relationships to calculate both primary and secondary creep in the ultrasonic field.

THE SYNTHETIC THEORY OF IRRECOVERABLE DEFORMATION

The synthetic theory (10) incorporates the Budiansky slip concept and the Sanders flow theory. This theory, being two-level, determines an inelastic deformation at a point of deformed material (macrolevel) as a sum of plastic shifts developed in active slip systems (microlevel):

$$e_k = \iiint_V \varphi_N N_k dV\,, \quad k = 1,2,3 \qquad [1]$$

In the formula above, e_k are strain deviator vector components in the Ilyushin three-dimensional deviatoric subspace S^3; φ_N - plastic strain intensity, which is treated as an average measure of plastic deformation within one slip system whose orientation is given by unit vector components N_k; dV symbolizes an elementary set of slip systems involved in

APTEFF, 52, 1-273 (2021) UDC: 669-1:621.9.048
DOI: https://doi.org/10.2298/APT2152265R BIBLID: 1450-7188 (2021) 52, 265-273
BY-NC-ND
Original scientific paper

plastic flows. To provide a physical sense to our manipulations, we relate the φ_N to an average measure of the carriers of plastic/creep deformations, defects of the crystalline grid (dislocations, twins, point defects), as:

$$d\psi_N = rd\varphi_N - K\psi_N dt, \quad [2]$$

where ψ_N defect intensity, t time; K is a function of the acting stress and temperature (10).

The defect intensity is defined as:

$$\psi_N = H_N^2 - I_N^2 - S_P^2 = \begin{cases} \left(\vec{\boldsymbol{S}} \cdot \vec{\boldsymbol{N}}\right)^2 - I_N^2 - S_P^2 & \textit{for planes reached by } \vec{\boldsymbol{S}}: H_N = \vec{\boldsymbol{S}} \cdot \vec{\boldsymbol{N}} \\ 0 & \textit{for planes not reached by } \vec{\boldsymbol{S}}: H_N > \vec{\boldsymbol{S}} \cdot \vec{\boldsymbol{N}} \end{cases} \quad [3]$$

where H_N is the plane distance in the direction $\vec{\boldsymbol{N}}$. In the formula [3], I_N is a rate-integral (10):

$$I_N = B \int_0^t \dot{\vec{\boldsymbol{S}}} \cdot \vec{\boldsymbol{N}}\, e^{-p(t-s)} ds, \quad [4]$$

Where B and p are model constants. The rate-integral increases during active loading ($\dot{\vec{\boldsymbol{S}}} > 0$) and decreases as $\dot{\vec{\boldsymbol{S}}} = 0$, i.e., in the course of primary creep. The condition $I_N \to 0$ symbolizes the transition to the secondary creep.

Since Rusinko's papers (1) mainly focused on ultrasound-assisted plastic deformation, where the second term on the right-hand side in [2] was ignored, special attention must be paid to how this equation works in its full form.

Consider the case of uniaxial tension when the stress vector components are (S_1, 0,0), $S_1 = \sqrt{2/3}\,\sigma$, Eq [3] takes the following form (10):

$$\psi_N = (S_1^2 - I^2)\Omega^2 - S_P^2 = S_P^2\left(\frac{\Omega^2}{b^2} - 1\right), \quad [5]$$

where $\Omega = \sin\beta\cos\lambda$, $I = B\int_0^t \dot{S}_1\, e^{-p(t-s)} ds$,

$$b = \frac{S_P}{\sqrt{S_1^2 - I^2}} = \frac{\sigma_P}{\sigma\sqrt{1 - B^2 e^{-2pt}}}. \quad [6]$$

The incremental form of [5] is:

$$\Delta\psi_N = 2(S_1\Delta S_1 - I\Delta I)\Omega^2. \quad [7]$$

Here we use symbol Δ to distinguish the increments due to the acting stress and time from d in integral [1]. Eq. [2] gives:

$$r\Delta\varphi_N = 2(S_1\Delta S_1 - I\Delta I)\Omega^2 + KS_P^2\left(\frac{\Omega^2}{b^2} - 1\right)\Delta t \quad [8]$$

Simple manipulations lead to:

$$r\Delta\varphi_N = S_P^2\Delta\left(\frac{\Omega^2}{b^2} - 1\right) + KS_P^2\left(\frac{\Omega^2}{b^2} - 1\right)\Delta t. \quad [9]$$

APTEFF, 52, 1-273 (2021) UDC: 669-1:621.9.048
DOI: https://doi.org/10.2298/APT2152265R BIBLID: 1450-7188 (2021) 52, 265-273
BY-NC-ND
Original scientific paper

Integration in [1] with [9] gives the irrecoverable strain vector increment as:

$$\Delta e = \frac{1}{r}\iiint_{\alpha\beta\lambda}\left[S_P^2\Delta\left(\frac{\Omega^2}{b^2}-1\right)+KS_P^2\left(\frac{\Omega^2}{b^2}-1\right)\Delta t\right]\Omega\cos\beta\, d\alpha d\lambda d\beta = a_0(\Delta\Phi + K\Phi\Delta t), \quad [10]$$

$$a_0 = \frac{\pi\sigma_P^2}{9r},\ \ \Phi(b) = \frac{1}{b^2}\left[2\sqrt{1-b^2} - 5b^2\sqrt{1-b^2} + 3b^4\ln\frac{1+\sqrt{1-b^2}}{b}\right]. \quad [11]$$

Finally, creep deformation in uniaxial tension is:

$$\varepsilon = \sqrt{\frac{2}{3}}a_0\left[\Phi(b) + \int_{t_S}^{t} K\Phi(b)dt\right], \quad [12]$$

where t_S the instant of the start of plastic deformation. To model the creep deformation alone (ε_C), we subtract from the formula above the value of plastic deformation:

$$\varepsilon_C = \sqrt{\frac{2}{3}}a_0\left[\Phi(b) - \Phi(b_M) + \int_{t_M}^{t} K\Phi(b)dt\right], \quad [13]$$

where b_M is from [6] at the end of active loading, $t = t_M$. We can write the formula above as:

$$\varepsilon_C = \sqrt{\frac{2}{3}}a_0\left[\Phi(b) - \Phi(b_M) + K\int_{t_M}^{t}\left(\Phi(b) - \Phi\left(\frac{S_P}{S_1}\right)\right)dt + K\Phi\left(\frac{S_P}{S_1}\right)(t-t_M)\right], \quad [14]$$

where fraction S_P/S_1 is obtained from b as $I \to 0$, i.e., it corresponds to the secondary creep. So, we decompose the creep deformation on two portions, primary and secondary:

$$\varepsilon_C = \varepsilon_{C\mathrm{I}} + \varepsilon_{C\mathrm{II}} = \sqrt{\frac{2}{3}}a_0\left[\Phi(b) - \Phi(b_M) + K\int_{t_M}^{\tilde{t}}\left(\Phi(b) - \Phi\left(\frac{S_P}{S_1}\right)\right)dt\right] + a_0K\Phi\left(\frac{S_P}{S_1}\right)(t-t_M), \quad [15]$$

where $\tilde{t}$ is the moment of the transition to the stationary creep. Since the active loading and primary creep accounts for a small portion of the whole duration of creep experiments, we simplify the above equation as follows:

$$\varepsilon_C = \sqrt{\frac{2}{3}}a_0\left[\Phi(b) - \Phi(b_M) + K\Phi\left(\frac{S_P}{S_1}\right)t\right]. \quad [16]$$

As seen from formulae [16], it is the function K that determines the secondary creep rate (10). Although generally, K is defined as a function of stress and temperature, it is enough to take it as a constant when modeling creep diagrams at a given value of stress and temperature.

By utilizing formulae [16] and [11], we plot the strain~time diagram for aluminum at tensile stress σ = 10 MPa (line **1** in Figure 1) with the following set of model parameters: σ_P = 5 Mpa, $B = 2.31 \times 10^{-1}$, $p = 2.5 \times 10^{-4}\mathrm{s}^{-1}$, $K = 1.0 \times 10^{-5}$, and $r = 1.0 \times 10^3$ MPa^2. As seen in Figure 1, the analytical result demonstrates good agreement with the experimental one. At the same time, ultrasound-assisted creep shows significantly greater values than those obtained in the ordinary case (compare curves 1 and 2-4 from Figure 1). It is this fact that motivates us to the extension of the synthetic theory considered below.

APTEFF, 52, 1-273 (2021) UDC: 669-1:621.9.048
DOI: https://doi.org/10.2298/APT2152265R BIBLID: 1450-7188 (2021) 52, 265-273
BY-NC-ND
Original scientific paper

EXTENSION OF THE SYNTHETIC THEORY TO THE CASE OF ULTRASOUND-ASSISTED CREEP

To extend the synthetic theory for the case of ultrasound-assisted creep, we enter time-dependent and time-independent terms reflecting the influence of ultrasound upon the primary and secondary creep, respectively. Firstly, we add to the defects nucleated due to the static load the defects induced by acoustic energy:

$$\psi_N = H_N^2 - I_N^2 - S_P^2 + U_C^2. \quad [17]$$

We define U_C as:

$$U_C = \vec{\boldsymbol{U}} \cdot \vec{\boldsymbol{N}}, \qquad \vec{\boldsymbol{U}} = \psi_{NU}\vec{\boldsymbol{u}}, \quad [18]$$

where ψ_{NU} is ultrasound-induced defect intensity proposed by Rusinko as (1):

$$\psi_{NU} = A_1 {S_m}^{A_2}(1 - e^{-wt}). \quad [19]$$

In the formula above, S_m is an oscillating stress amplitude, and $\vec{\boldsymbol{u}}$ is a unit vector indicating the vibration mode (longitudinal, torsional, etc.). For longitudinal sonication, the $\vec{\boldsymbol{u}}$ vector has $(1,0,0)$ coordinates in S^3. A_1, A_2, w are model constants to be chosen to fit the theoretical results to experimental ones. The scalar product in formulae [18] clearly indicates that the ultrasound effect depends on the slip system orientation.

The term U_C from Eq. [17]-[19] symbolizes the change in the defect structure of the deformed material caused by the nucleation and development of the ultrasound-induced defects. To avoid misunderstanding that the increasing number of defects would harden the material, we address Kulemin's explanation: "When external loading couples with ultrasonic irradiation, both hardening and softening occur. The softening, however, is more intensive, and we observe the phenomenon of acoustic softening" (2). Therefore, Eq. [17] is dual; on the one hand, the ultrasound defects harden the material, but, on the other hand, they become centers of softening processes.

We substantiate the composition of ψ_{NU} as follows. The power function ${A_1 S_m}^{A_2}$ in Eq. [19] reflects numerous studies on zinc, cadmium, aluminum, copper, and steel (2-8, 11, 12). They report that the number of ultrasound-induced defects and, therefore, the magnitude of ultrasonic softening depends on the ultrasonic energy/oscillating stress amplitude. Further, the function $(1 - e^{-wt})$ governs the evolution of the softening effect in time. As $e^{-\mathrm{w}t}$ tends to zero, ψ_{NU} stabilizes at a constant value, reflecting the well-known fact that the number of ultrasound defects increases with time and then reaches a plateau.

Our next step is to increase the function K which is responsible for the steady-state creep. We propose to introduce a linear term of oscillating stress amplitude:

$$K_U = K + A_3 S_m. \quad [20]$$

Therefore, we enhance the K in a way similar to [19] but without a time-dependent portion, since the function K_U reflects the effect of ultrasound upon the steady-state creep.

APTEFF, 52, 1-273 (2021) UDC: 669-1:621.9.048
DOI: https://doi.org/10.2298/APT2152265R BIBLID: 1450-7188 (2021) 52, 265-273
BY-NC-ND
Original scientific paper

If to do similar manipulations as in Eq. [5]-[16] with the defect intensity given by Eq. [17]-[19] and K_U from Eq. [20], we arrive at the following result:

$$\varepsilon_{CU} = \sqrt{\frac{2}{3}} a_0 \left[\Phi(b_U) - \Phi(b_{UM}) + (K + A_3 S_m) \Phi\left(\frac{S_P}{\sqrt{S_1^2 + \left(A_1 {S_m}^{A_2}\right)^2}} \right) t \right], \quad [21]$$

$$b_U = \frac{\sigma_p}{\sqrt{\sigma^2 (1 - B^2 e^{-2pt}) + \left(A_1 {\sigma_m}^{A_2} (1 - e^{-wt})\right)^2}} \quad [22]$$

b_{UM} corresponds to the start of creep deformation, which is supposed to be $t = 0$:

$$b_{UM} = \frac{\sigma_p}{\sigma \sqrt{(1 - B^2)}}. \quad [23]$$

The value of b_U for the steady steady-state creep is obtained from [4.2] as the exponential functions tend to zero:

$$b_U = \frac{\sigma_p}{\sqrt{\sigma^2 + (A_1 {\sigma_m}^{A_2})^2}} \quad [24]$$

Comparing Eq. [22] to [6], it is easy to conclude that $b_U < b$ and thus $e_{CU} > e_C$ due to the terms reflecting the action of ultrasound. This inequality holds for both the time-dependent and linear portions of the creep. The appearance of the term $A_1 {\sigma_m}^{A_2} (1 - e^{-wt})$ in the denominator of Eq. [22] means that the acoustic energy coupled with the unidirectional loading manifests itself in:

i. the intensification of plastic flow within the active slip systems;
ii. the increase of the number of active slip systems.

RESULTS AND DISCUSSION

This point aims in terms of the synthetic theory to plot ultrasound-assisted strain~time curves for aluminum and compare the model results to experimental observations. The experiments (2) were conducted in two regimes: (**i**) ordinary creep under the action of tensile stress $\sigma = 10$ MPa and (**ii**) simultaneous action of tensile stress $\sigma = 10$ MPa and longitudinal oscillating stress of various amplitudes: $\sigma_{m1} = 0.6$ MPa, $\sigma_{m2} = 1.3$ MPa, and $\sigma_{m3} = 2.0$ Mpa (Fig. 1).

By formulae [20]-[22] with model constants A_1=1.28 MPa^{1-A_2}, A_2=2.0, A_3=1.5×10^{-5} $(MPa \times s)^{-1}$, and w=2.1×10^{-3} s^{-1} we plot analytical creep diagrams in the presence of ultrasound; they demonstrate good agreement between the theoretical and experimental results. It must be stressed that the model constants used for Line **1** in Fig. 1 remain actual here as well.

APTEFF, 52, 1-273 (2021)
DOI: https://doi.org/10.2298/APT2152265R
BY-NC-ND
UDC: 669-1:621.9.048
BIBLID: 1450-7188 (2021) 52, 265-273
Original scientific paper

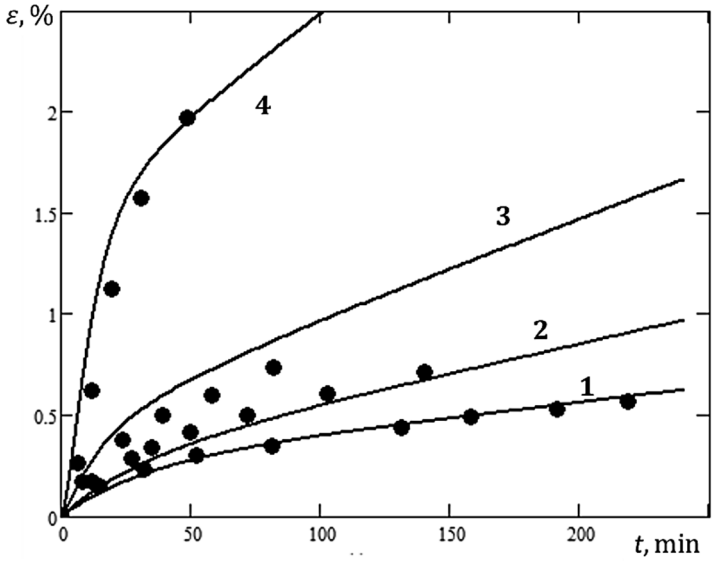

Figure 1. Creep diagrams of aluminum in uniaxial tension (σ=10 MPa, T=40℃), **1** – ordinary creep, **2**-**4** ultrasound-assisted creep with oscillating stress amplitudes of 0.6 MPa (**2**), 1.3 MPa (**3**), and 2.0 MPa (**4**); • – experiment (2).

A question may arise as to whether the term $A_3 S_m$ in Eq. [21] is needed to model the ultrasound-assisted secondary creep because the term $A_1 {S_m}^{A_2}$ leads to the increase of Φ as well. To answer this question, let us plot strain~time diagrams via formulae [20]-[22] at $A_3 = 0$ (Fig. 2).

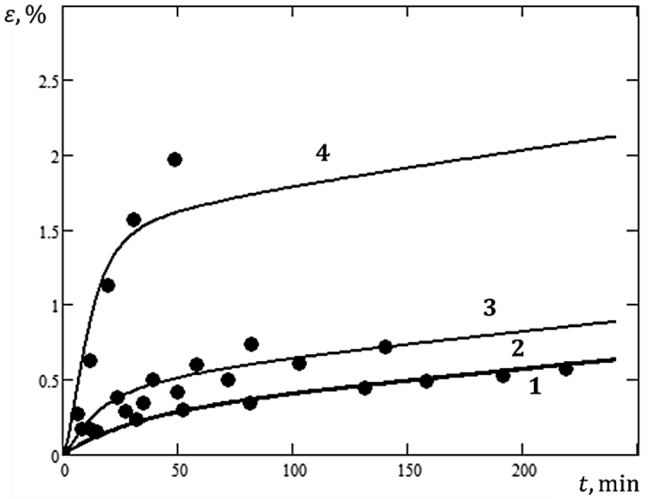

Figure 2. Creep diagrams plotted via the model relationships at $A_3 = 0$ (nomenclature is the same as in Fig. 1)

APTEFF, 52, 1-273 (2021)
DOI: https://doi.org/10.2298/APT2152265R
BY-NC-ND
UDC: 669-1:621.9.048
BIBLID: 1450-7188 (2021) 52, 265-273
Original scientific paper

As one can see, the result is unsatisfactory; the linear portion's slope increase is much less than that from the experiment. Therefore, the addition of $A_3 S_m$ to K, which is responsible for the growth of secondary creep rate in the ultrasonic field, is vital. In confirmation, Fig. 3 shows the deformations' linear portions at various values of oscillating stress amplitudes. It is pretty clear that the ignoring of A_3 results in a small increase in the slope angle, while the lines with $A_3 \neq 0$ show much greater angle increments.

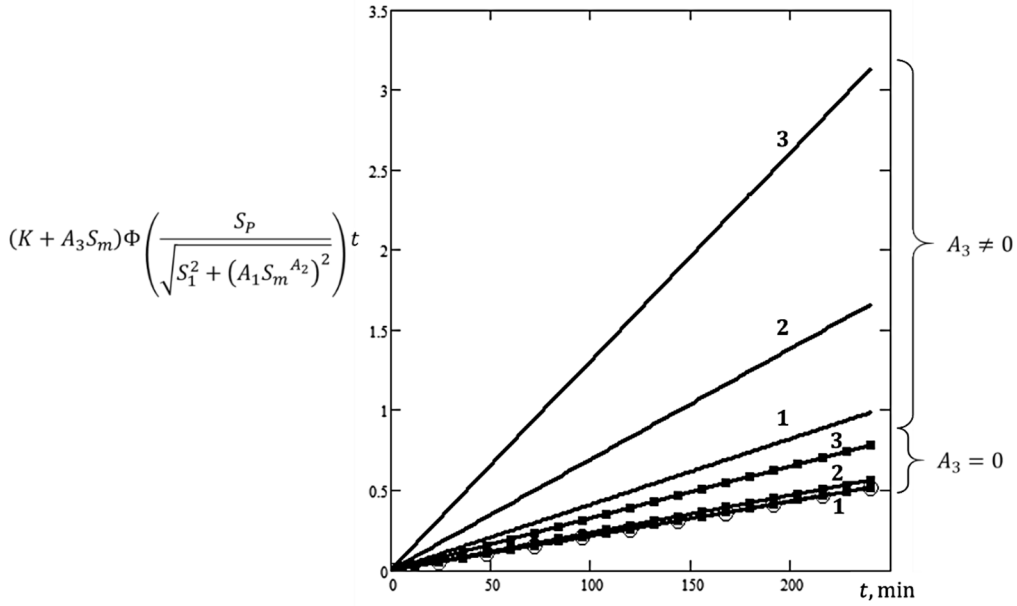

Figure 3. Linear portions from Eq. [21] at amplitudes $\sigma_{m1} = 0.6$ MPa (**1**), $\sigma_{m2} = 1.3$ MPa (**2**), and $\sigma_{m3} = 2.0$ MPa (**3**); circle-dotted line – ordinary creep ($\sigma_m = 0$).

Summarizing, formulae [20]-[22] correctly predict the increase in both portions of creep coupled with ultrasound, primary and secondary (compare line **1** for ordinary creep to lines **2-4** obtained for creep in the acoustic field). The analysis of the non-linear and linear portions of creep deformation from Figs. 2 and 3 substantiates that the presentation of function K in the form of Eq. [20] is vital.

CONCLUSION

Here, we developed a mathematical model to calculate the creep deformation of metals coupled with ultrasonic energy. The model based on the Synthetic theory of irrecoverable deformation catches the increase in the primary creep and steady-state creep rate caused by the ultrasound imposed on the static load. All this was made possible by introducing a term accounting for the nucleation and development of the ultrasound-induced defects. We define their time-dependent behavior relying on experimental observations on the kinetics of

APTEFF, 52, 1-273 (2021) UDC: 669-1:621.9.048
DOI: https://doi.org/10.2298/APT2152265R BIBLID: 1450-7188 (2021) 52, 265-273
BY-NC-ND
Original scientific paper

the increase in crystalline grid defects caused by sonication. By inserting the ultrasound defect intensity into the synthetic theory's constitutive equation governing the material's deformation state, we derived the relationships relating deformation in both stages of creep to the amplitude of oscillating stresses. As a result, we plotted strain~time diagrams for aluminum creep in uniaxial tension under the simultaneous action of unidirectional stress and oscillating stress of various amplitudes. The model results show good agreement with experimental data, making it possible to utilize the synthetic theory as a reliable mathematical apparatus to predict metals' ultrasound-assisted creep deformation.

Since ultrasonic vibrations is an effective mechanism to enhance the performance of metal forming, for example, achieving increased production speeds, less tool wear, reduced forming forces, and better surface finish, understanding processes in ultrasound-assisted inelastic deformations –plastic and/or creep –and ability to model them is of inevitable and crucial importance.

REFERENCES

1. Rusinko, A. Analytical description of ultrasonic hardening and softening. *Ultrasonics*, **2011**, *51*, 709–714.
2. Kulemin, A. *Ultrasound and Diffusion in Metals*. Metallurgia, Moscow, 1978.
3. Deshpande, A.; Tofangchi, A.; Hsu, K. Microstructure evolution of Al6061 and copper during ultrasonic energy-assisted compression. *Materials Characterization*. **2019**, *153*, 240-250.
4. Zhou, H.; Cui, H.; Qin, Q. Influence of ultrasonic vibration on the plasticity of metals during compression process. *J. Mater. Process. Technol*. **2018**, *251*, 146-159.
5. Lum, I.; Huang, H.; Chang, B.; Mayer, M.; Du, D.; Zhou, Y. Effects of superimposed ultrasound on deformation of gold. *Journal of Applied Physics*. **2009**, *105*, 024902.
6. Daud, Y.; Lucas, M.; Huang, Z. Modelling the effects of superimposed ultrasonic vibrations on tension and compression tests of aluminium. *J. Mater. Process. Technol.* **2007**, *186*, 179-190.
7. Graff, K. Ultrasonic metal forming: processing. In *Power Ultrasonics*, Woodhead Publishing 2015, pp. 377-438.
8. Malygin, G. Acoustoplastic effect and the stress superimposition mechanism. *Physics of the Solid State*. **2000**, *42*, 72-78.
9. Rusinko, A; Alhilfi, A.H.; Rusinko, M. An analytic description of the creep deformation of metals in the ultrasonic field. *Mech Time-Depend Mater* https://doi.org/10.1007/s11043-021-09505-0 (accessed: 02 June 2021).
10. Rusinko, A.; Rusinko, K. *Plasticity and Creep of Metals*, Berlin, Springer, 2011.
11. Bagherzadeh, S.; Abrinia, K. Effect of ultrasonic vibration on compression behavior and microstructural characteristics of commercially pure aluminum. *Journal of Materials Engineering and Performance*. **2015**, *24*, 4364-4376.
12. Yao, Z.; Kim, G.; Wang, Z.; Faidley, I.; Zou, Q.; Mei, D.; Chen, Z. Acoustic softening and residual hardening in aluminum: modeling and experiments. *International Journal of Plasticity*, **2012**, *38*, 75-87.

EDITORIAL POLICY

The journal ***Acta Periodica Technologica*** (formerly *Proceedings of Faculty of Technology*) publishes reviews and original scientific papers covering from all branches of technology (food, chemical, biochemical, and pharmaceutical), process engineering and related scientific fields.

Acta Periodica Technologica is an Open Access journal.

Contributions to journal shall be submitted in English, with summaries in English and Serbian which is closely defined with Instruction for manuscript preparation.

The Journal is issued once a year.

The journal is indexed in Chemical Abstracts, Columbus, Ohio, Referativnyi zhurnal -Khimija, VINITI, Moscow, Ulrich's International Periodical Directory, and Elsevier Bibliographic databases - SCOPUS.

Editorial responsibilities

The Editorial Board is responsible for deciding which articles submitted to ***Acta Periodica Technologica*** will be published. The Editorial Board is guided by the Editorial Policy and constrained by legal requirements in force regarding libel, copyright infringement and plagiarism.

The Editor-in-Chief reserves the right to decide not to publish submitted manuscripts in case it is found that they do not meet relevant standards concerning the content and formal aspects. The Editorial Staff will inform the authors whether the manuscript is accepted for publication within 60-90 days from the date of the manuscript submission.

Editor-in-Chief must hold no conflict of interest with regard to the articles they consider for publication. If an Editor feels that there is likely to be a perception of a conflict of interest in relation to their handling of a submission, the selection of reviewers and all decisions on the paper shall be made by the Editorial Board.

Editor-in-Chief and Editorial Board shall evaluate manuscripts for their intellectual content free from any racial, gender, sexual, religious, ethnic, or political bias.

The Editor and the Editorial Staff must not use unpublished materials disclosed in submitted manuscripts without the express written consent of the authors. The information and ideas presented in submitted manuscripts shall be kept confidential and must not be used for personal gain.

Editors and the Editorial Staff shall take all reasonable measures to ensure that the reviewers remain anonymous to the authors before, during and after the evaluation process.

Authors' responsibilities

Authors warrant that their manuscript is their original work, that it has not been published before and are not under consideration for publication elsewhere. Parallel submission of the same paper to another journal constitutes a misconduct and eliminates the manuscript from consideration by ***Acta Periodica Technologica.***

The Authors also warrant that the manuscript is not and will not be published elsewhere after the publication in ***Acta Periodica Technologica*** in any language without the consent of the Publisher.

In case a submitted manuscript is a result of a research project, or its previous version has been presented at a conference in the form of an oral presentation (under the same or similar

title), detailed information about the project, the conference, etc. shall be provided in *Acknowledgements* at the end of paper, and before List of references. A paper that has already been published in another journal cannot be reprinted in ***Acta Periodica Technologica.***

It is the responsibility of each author to ensure that papers submitted to ***Acta Periodica Technologica*** are written with ethical standards in mind. Authors affirm that the article contains no unfounded or unlawful statements and does not violate the rights of third parties. The Publisher will not be held legally responsible should there be any claims for compensation.

Reporting standards. A submitted manuscript should contain sufficient detail and references to permit reviewers and, subsequently, readers to verify the claims presented in it. The deliberate presentation of false claims is a violation of ethical standards.

Authors are exclusively responsible for the contents of their submissions and must make sure that they have permission from all involved parties to make the data public.

Authors wishing to include figures, tables or other materials that have already been published elsewhere are required to obtain permission from the copyright holder(s). Any material received without such evidence will be assumed to originate from the authors.

Authorship. Authors must make sure that all only contributors who have significantly contributed to the submission are listed as authors and, conversely, that all contributors who have significantly contributed to the submission are listed as authors. If persons other than authors were involved in important aspects of the research project and the preparation of the manuscript, their contribution should be acknowledged in a Acknowledgements section.

Acknowledgment of Sources. Authors are required to properly cite sources that have significantly influenced their research and their manuscript. Information received in a private conversation or correspondence with third parties, in reviewing project applications, manuscripts and similar materials, must not be used without the express written consent of the information source.

Plagiarism. Plagiarism, where someone assumes another's ideas, words, or other creative expression as one's own, is a clear violation of scientific ethics. Plagiarism may also involve a violation of copyright law, punishable by legal action.

Plagiarism includes the following:

- Word for word, or almost word for word copying, or purposely paraphrasing portions of another author's work without clearly indicating the source or marking the copied fragment (for example, using quotation marks);
- Copying equations, figures or tables from someone else's paper without properly citing the source and/or without permission from the original author or the copyright holder.

Please note that all submissions are thoroughly checked for plagiarism.

Any paper which shows obvious signs of plagiarism will be automatically rejected and authors will be temporarily forbidden to publish in the journal.

In case plagiarism is discovered in a paper that has already been published by the journal, it will be retracted in accordance with the procedure described below under Retraction policy, and authors will be temporarily forbidden to publish in the journal.

Conflict of interest. Authors should disclose in their manuscript any financial or other substantive conflict of interest that might have influenced the presented results or their interpretation.

Fundamental errors in published works. When an author discovers a significant error or inaccuracy in his/her own published work, it is the author's obligation to promptly notify the journal Editor or publisher and cooperate with the Editor to retract or correct the paper.

By submitting a manuscript, the authors agree to abide by the Acta Periodica Technologica's editorial Policies.

Reviewers' responsibilities

Reviewers are required to provide written, competent and unbiased feedback in a timely manner on the scholarly merits and the scientific value of the manuscript.

The reviewers assess manuscript for the compliance with the profile of the journal, the relevance of the investigated topic and applied methods, the originality and scientific relevance of information presented in the manuscript, the presentation style and scholarly apparatus.

Reviewers should alert the Editor to any well-founded suspicions or the knowledge of possible violations of ethical standards by the authors. Reviewers should recognize relevant published works that have not been cited by the authors and alert the Editor to substantial similarities between a reviewed manuscript and any manuscript published or under consideration for publication elsewhere, in the event they are aware of such. Reviewers should also alert the Editor to a parallel submission of the same paper to another journal, in the event they are aware of such.

Reviewers must not have conflict of interest with respect to the research, the authors and/or the funding sources for the research. If such conflicts exist, the reviewers must report them to the Editor without delay.

Any selected referee who feels unqualified to review the research reported in a manuscript or knows that its prompt review will be impossible should notify the Editor without delay.

Reviews must be conducted objectively. Personal criticism of the author is inappropriate. Reviewers should express their views clearly with supporting arguments.

Any manuscripts received for review must be treated as confidential documents. Reviewers must not use unpublished materials disclosed in submitted manuscripts without the express written consent of the authors. The information and ideas presented in submitted manuscripts shall be kept confidential and must not be used for personal gain.

Peer review

The submitted manuscripts are subject to a peer review process. The purpose of peer review is to assists the Editor-in-Chief and Editorial Board in making editorial decisions and through the editorial communications with the author it may also assist the author in improving the paper.

All papers submitted to the journal will be reviewed by at least two independent referees who will be asked to complete the refereeing job within 2-4 weeks. Final decision on publication will be made by the Editorial Board.

The choice of reviewers is at the Editors' discretion. The reviewers must be knowledge able about the subject area of the manuscript; they must not be from the authors' own institution and they should not have recent joint publications with any of the authors.

In a main phase of peer review process, the reviewers must fill reviewer's form which indicates which aspects to be covered in order to make decision about manuscript publication. In the final part of the form, reviewers must submit their observations and suggestions on how to submitted manuscript improve.

All of the reviewers of a paper act independently and they are not aware of each other's identities. If the decisions of the two reviewers are not the same (accept/reject), the Editor may assign additional reviewers.

During the review process Editor may require authors to provide additional information (including raw data) if they are necessary for the evaluation of the scholarly merit of the manuscript. These materials shall be kept confidential and must not be used for personal gain.

The Editorial team shall ensure reasonable quality control for the reviews. With respect to reviewers whose reviews are convincingly questioned by authors, special attention will be paid to ensure that the reviews are objective and high in academic standard. When there is any doubt with regard to the objectivity of the reviews or quality of the review, additional reviewers will be assigned.

Procedures for dealing with unethical behaviour

Anyone may inform the editors and/or Editorial Board at any time of suspected unethical behaviour or any type of misconduct by giving the necessary information/evidence to start an investigation.

Investigation. Editor-in-Chief will consult with the Editorial Board on decisions regarding the initiation of an investigation.

During an investigation, any evidence should be treated as strictly confidential and only made available to those strictly involved in investigating.

The accused will always be given the chance to respond to any charges made against them.

If it is judged at the end of the investigation that misconduct has occurred, then it will be classified as either minor or serious.

Minor misconduct. Minor misconduct will be dealt directly with those involved without involving any other parties, e.g.:

- Communicating to authors/reviewers whenever a minor issue involving misunderstanding or misapplication of academic standards has occurred.
- A warning letter to an author or reviewer regarding fairly minor misconduct.

Major misconduct. The Editor-in-Chief, in consultation with the Editorial Board, and, when appropriate, further consultation with a small group of experts should make any decision regarding the course of action to be taken using the evidence available. The possible outcomes are as follows (these can be used separately or jointly):

- Publication of a formal announcement or editorial describing the misconduct.
- Informing the author's (or reviewer's) head of department or employer of any misconduct by means of a formal letter.
- The formal, announced retraction of publications from the journal in accordance with the Retraction Policy (see below).
- A ban on submissions from an individual for a defined period.
- Referring a case to a professional organization or legal authority for further investigation and action.

When dealing with unethical behaviour, the Editorial Board will rely on the guidelines and recommendations provided by the Committee on Publication Ethics (COPE): http://publicationethics.org/resources/.

Retraction policy

Legal limitations of the publisher, copyright holder or author(s), infringements of professional ethical codes, such as multiple submissions, bogus claims of authorship, plagiarism, fraudulent use of data or any major misconduct require retraction of an article. Occasionally a retraction can be used to correct errors in submission or publication. The main reason for withdrawal or retraction is to correct the mistake while preserving the integrity of science; it is not to punish the author.

Standards for dealing with retractions have been developed by a number of library and scholarly bodies, and this practice has been adopted for article retraction by ***Acta Periodica Techno-***

***logica*:** in the electronic version of the retraction note, a link is made to the original article. In the electronic version of the original article, a link is made to the retraction note where it is clearly stated that the article has been retracted. The original article is retained unchanged, save for a watermark on the PDF indicating on each page that it is "retracted."

Open access policy

Acta Periodica Technologica is an Open Access Journal. All articles can be downloaded free of charge from:

http://www.doiserbia.nb.rs/journal.aspx?issn=1450-7188 or

https://www.tf.uns.ac.rs/en/science-and-research/publications.html and used with terms defined with Creative Commons licence (http://creativecommons.org/licenses/by-nc-nd/3.0/rs).

The journal does not charge any fees at submission, reviewing, and production stages.

Self-archiving Policy

The journal ***Acta Periodica Technologica*** allows authors to deposit Publisher's version/PDF in an institutional repository and non-commercial subject-based repositories, such as PubMed Central, Europe PMC or arXiv, or to publish it on Author's personal website (including social networking sites, such as ResearchGate, Academia.edu, etc.) and/or departmental website, at any time after publication. Full bibliographic information (authors, article title, journal title, volume, issue, pages) about the original publication must be provided and a link must be made to the article's DOI.

Copyright

Once the manuscript is accepted for publication, authors shall transfer the copyright to the Publisher. If the submitted manuscript is not accepted for publication by the journal, all rights shall be retained by the author(s).

Authors grant to the Publisher the following rights to the manuscript, including any supplemental material, and any parts, extracts or elements thereof:

- the right to reproduce and distribute the Manuscript in printed form, including print-on-demand;
- the right to produce prepublications, reprints, and special editions of the Manuscript;
- the right to translate the Manuscript into other languages;
- the right to reproduce the Manuscript using photomechanical or similar means including, but not limited to photocopy, and the right to distribute these reproductions;
- the right to reproduce and distribute the Manuscript electronically or optically on any and all data carriers or storage media - especially in machine readable/digitalized form on data carriers such as hard drive, CD-Rom, DVD, Blu-ray Disc (BD), Mini-Disk, data tape - and the right to reproduce and distribute the Article via these data carriers;
- the right to store the Manuscript in databases, including online databases, and the right of transmission of the Manuscript in all technical systems and modes;
- the right to make the Manuscript available to the public or to closed user groups on individual demand, for use on monitors or other readers (including e-books), and in printable form for the user, either via the internet, other online services, or via internal or external networks.

The authors and third parties who wish use the article in a way not covered by the Creative Common licence (http://creativecommons.org/licenses/by-nc-nd/3.0/rs) must obtain a written consent of the publisher. Contact e-mail for written consent is: apteff@tf.uns.ac.rs.

Authors grant to the publisher the right to publish the article, to be cited as its original publisher in case of reuse, and to distribute it in all forms and media.

Disclaimer

The views expressed in the published works do not express the views of the Editor-in-Chief and Editorial Board. The authors take legal and moral responsibility for the ideas expressed in the articles. Publisher shall have no liability in the event of issuance of any claims for damages. The Publisher will not be held legally responsible should there be any claims for compensation.

INSTRUCTION FOR MANUSCRIPT PREPARATION

Acta Periodica Technologica publishes reviews and scientific papers covering all branches of food, chemical, biochemical, and pharmaceutical technologies, as well as process engineering and related scientific fields.

Acta Periodica Technologica is published in English. The journal may include supplements from congresses, meetings or symposiums.

SUBMISSION OF PAPERS

All correspondence, including submission of the manuscript, notification of the Editor's decision and requests for revision, takes place by e-mail apteff@tf.uns.ac.rs or apteff.tf.uns@gmail.com.

Authors are expected to propose the category of manuscript (review or original scientific paper) and three potential reviewers. Reviewers should be experts in the field of the paper, and not associated with the institution with which the authors are affiliated. The final choice of referees will remain entirely with the Editor. Also, optionally, the authors should state any person that is not desired as a reviewer.

Submission of paper implies that:

- it is prepared according to this Instructions,
- it has not been published previously (except in the form of an abstract or as a whole in the proceedings of papers of a scientific meeting, or as part of a published lecture or academic thesis),
- it is not under consideration for publication elsewhere, and
- it will not be published elsewhere in the same form, in English or any other language, without the written consent of the publisher.

PREPARATION OF MANUSCRIPT

Language: Manuscript should be written in English.

Typing: Manuscript must be written in Word with a font size 10 pt, 1.5 lines spaced, with 2.5 cm margins, on A4 pages (maximum 15 pages for scientific papers and 25 pages for review papers). All lines of the manuscript should be numbered restarting on each page. Also, all pages must be numbered. Import tables and figures into the text. Abbreviations and symbols-notation should be explained at first appearing, or on a separate list at the end of the manuscript.

General format. The manuscript should contain the following in this order: Title page, ABSTRACT and KEYWORDS, INTRODUCTION, EXPERIMENTAL, RESULTS and DISCUSSION, CONCLUSIONS, ACKNOWLEDGEMENTS and REFERENCES.

Title page: On the first page should be the title without symbols, formulae or abbreviations (capital bold letters). The title should be concise and explanatory of the content of the paper. Full name (name, initial and surname) of authors (without degrees, professional or official titles) should be given under the title, written in italic. Clearly indicate (with an asterisk) who is responsible for correspondence at all stages of refereeing and publication. Ensure that e-mail address and the full postal address are provided. Affiliation of authors should be given after the author's name. Indicate all affiliations with the superscript number

immediately after authors name and in front of the appropriate address. If the paper was given, wholly or in part, at a scientific meeting, this should be stated in a footnote on the title page.

Abstract of the paper (100-250 words, written in italic) should be given under the title and authors. Abstracts should contain the aim of investigated work, methods, results and conclusion.

Keywords (normal letters, max. 5 keywords) should be listed afterward.

Introduction should state previous relevant work with appropriate references, the problem investigated and the aim of work.

Experimental. The materials and methods used should be stated clearly in sufficient detail to permit the work to be repeated by others. Only new techniques should be described in detail; known methods must have adequate references.

Results and Discussion. Results should be presented concisely, with tables or illustrations for clarity. The significance of the findings should be discussed without repetition of the material in the Introduction. The adequate number of illustrations, graphs and chemical formulae used must be kept on a minimum.

Conclusions. This section should present the main conclusions of the study. Also, conclusions should indicate the significance of contribution and application possibilities of the obtained results.

Acknowledgements: These should be kept to a minimum.

References cited should be indicated in the text using Arabic numerals in round brackets ( ), in the order of appearing. All publications cited in the text should be presented in a list of references given on a separate page. Abbreviations of journal titles should be given according to the Chemical Abstracts Service (CASSI Search Tool; http://cassi.cas.org). The list of references should be presented according to the *ACS citation style* and their appearance in the text. Give names of all authors (do not use „et. al."), with their initials after respective surnames. Include article titles in journals. The abbreviated titles should be followed by the year (**bold**), volume (*italic*), number (in round brackets if exists), and first and last page numbers.

Examples:

Journals: Pascual, E.C.; Goodman, B.A; Yeretzian, C. Characterisation of Free Radicals in Solubile Coffee by Electron Paramagnetic Resonance Spectroscopy. *J. Agric. Food Chem.* **2002,** *50* (21), 6114-6122.

Books: Morris, R. *The Last Sorcerers: The Path from Alchemy to the Periodic Table;* Joseph Henry Press: Washington, DC, 2003; pp 145-158.

Book with more chapters: Puls, J.; Saake, B. Industrially Isolated Hemicelluloses. In *Hemicelluloses: Science and Technology;* Gatenholm, P., Tenkanen, M., Eds.; ACS Symposium Series 864; American Chemical Society: Washington, DC, 2004; pp 24-37.

Book of Abstracts: Noe, W.; Howaldt, M.; Ulber, R.; Scheper, T. Immunobase elution assay for process control, 8th European Congress on Biotechnology, Budapest, 17-21 August 1997, Book of Abstracts WE 163, p. 246.

Thesis: Linstead, J.B.: Linstead, J.B. Effects of adding natural antioxidants on colour stability of paprika. Ph.D. (or M.S.) Thesis, University of Glasgow, November 2006.

Patent: Lenssen, K. C.; Jantscheff, P.; Kiedrowski, G.; Massing, U. Cationic Lipids with Serine Backbone for Transfecting Biological Molecules. Eur. Pat. Appl. 1457483, 2004.

Unpublished data: Should be cited with one of the following comments: *in press*, *unpublished work* or *personal communication*.

Online citations: Should include the author, title, website and date of access.
Example: Wright, N.A. The Standing of UK Histopathology Research 1997-2002. http://pathsoc.org.uk (accessed 7 October 2004).

Chemical nomenclature and units. Authors are requested to use SI units and chemical nomenclature following the rules of Chemical Abstracts whenever possible.

Tables. Each Table is numbered with an Arabic numeral, followed by the title (**Table 1.** The result...). The table width must be 12.5 cm max.

Figures. Each drawing or figure should also be numbered with Arabic numerals followed by the title (**Figure 1.** Chromatogram of...). Graphs and charts must be prepared by Microsoft Excel or Origin. Schemes must be prepared by Microsoft Visio or Corel Draw. *It is necessary to submit them as separate files in the original extension* (xls, xlsx, vdr, cdr). Scanned black & white schemes should be submitted in tiff, wmf, or bmp form. Photographs should be submitted in jpg form.

Formulae and Equations. Type formulas and mathematical equations clearly, accurately placing superscripts and subscripts. Equations should be indicated in the text using Arabic numerals in square brackets [ ].

Review process. All papers submitted to the journal will be reviewed by at least two independent referees who will be asked to complete the refereeing job within 2-4 weeks. The final decision on publication will be made by the Editorial Board. Manuscripts may be sent back to authors for revision if necessary. Revised manuscript submissions should be made as soon as possible (within 2 weeks) after the receipt of the referees' comments.

Proofs. One set of page proofs will be sent by e-mail to the corresponding author. Please use this proof only for checking the typesetting, editing, completeness and correctness of the manuscript. The author may list the corrections and return to the journal in an e-mail within 48 hours of receipt.

Author service. For inquiries relating to the submission of the manuscript, please send an e-mail to the Editor’s office (apteff@tf.uns.ac.rs or apteff.tf.uns@gmail.com). Postal address: *Acta Periodica Technologica*, Editorial Board, Bulevar cara Lazara 1, 21000 Novi Sad, Serbia.

THIS ISSUE OF ACTA PERIODICA TECHNOLOGICA IS FINANCIALLY SUPPORTED BY:

Ministry of Education, Science and Technological Development of Republic of Serbia

FORMER EDITORS-IN-CHIEF

Prof. Dr. Adalbert Šenborn (1967-1970)
Prof. Dr. Radivoj Žakula (1972-1975)
Prof. Dr. Miroslava Todorović (1976-1994)
Prof. Dr. Biljana Škrbić (1995-1998)
Prof. Dr. Sonja Đilas (1999-2016)

Editorial:

University of Novi Sad, Faculty of Technology Novi Sad,
Bulevar Cara Lazara 1, 21000 Novi Sad, Serbia

Phone: +381 21 485 3693
Fax: +381 21 450 413
e-mail: apteff@tf.uns.ac.rs, apteff.tf.uns@gmail.com

Prepress: Branislav S. Bastaja
Printed by BIROGRAF COMP d.o.o., Atanasija Pulje 22, 11080 Zemun
Copies: 200

Articles published in the Acta Periodica Technologica are Open-Access articles distributed under a license Creative Commons BY-NC-ND 3.0 Serbia (http://creativecommons.org/licenses/by-nc-nd/3.0/rs)